THE UNIVERSITY
of EDINBURGH

Cardiac Magnetic Resonance Imaging Assessment of Aortic Stenosis to Improve Clinical Care

Dr Russell J Everett

MBBS BSc MRCP

THE UNIVERSITY *of* EDINBURGH

A Thesis Presented for the Degree of Doctor of Philosophy

The University of Edinburgh
2018

To Emily

Contents

Figures Index

Tables Index

Abstract

Background

Aortic stenosis is the commonest valve disease requiring intervention in the developed world. Current guideline-based management strategies are based on historical observational data or expert opinion and may leave many patients with irreversible myocardial damage and adverse outcomes following valve intervention. The aims of this thesis are to investigate novel cardiac magnetic resonance techniques and how they can be applied to improve our decision making around the timing of valve intervention.

Methods and Results

Cardiac magnetic resonance imaging can detect two forms of myocardial fibrosis non-invasively; diffuse fibrosis using T1 mapping and replacement fibrosis with the late gadolinium enhancement technique. I devised a novel measure of diffuse fibrosis, the indexed extracellular volume (iECV) and showed that these techniques can be used to divide patients into three categories according to the type and amount of fibrosis present: no fibrosis, diffuse fibrosis and replacement fibrosis. Moreover, I demonstrated that there was evidence of increasing left ventricular decompensation across these three groups.

How fibrosis and left ventricular hypertrophy change over time has not been well studied in patients with aortic stenosis. Using serial imaging scans, I showed that hypertrophy and diffuse fibrosis gradually progress over time,

whilst replacement fibrosis accumulates rapidly once first established. Following valve replacement, cellular hypertrophy regresses faster than diffuse fibrosis, but replacement fibrosis appears permanent and irreversible.

I then proceeded to investigate T1 mapping measures in a large international multicentre cohort of patients with aortic stenosis scheduled for valve replacement. I showed that extracellular volume-based T1 mapping measures were comparable across centres and therefore confirmed that multicentre studies are feasible. Extracellular volume fraction was associated with a decompensating ventricle and emerged as a powerful independent predictor of all-cause mortality in this group.

Finally, I investigated the use of novel hybrid magnetic resonance and positron emission tomography imaging in patients with aortic stenosis, showing that this technique is feasible and well-tolerated. I tested novel attenuation correction and motion correction methods and showed that this technique can offer multiparametric imaging of valve, myocardium and coronary arteries in a single scan.

Conclusion

I have defined the longitudinal changes in hypertrophy and myocardial fibrosis in aortic stenosis and validated extracellular volume measures as prognostic markers in this group. Moreover, I have described novel magnetic resonance and positron emission tomography techniques and their potential to aid the clinical assessment of patients with aortic stenosis.

Lay Summary

Aortic stenosis is the narrowing of the main outlet heart valve that controls blood flowing out of the heart and around the body. This narrowing increases the pressure load of the heart leading to thickening of the heart muscle over time. Working out when is the best time to offer surgery to replace the narrowed valve can be challenging. MRI scans of the heart can pick up scarring of the heart muscle, which is not seen with other tests. We know that finding a discrete area of heart muscle scarring in patients is associated with a higher risk of death and having symptoms, but we are less clear on the importance of finding a diffuse pattern of scarring.

I investigated the importance of patterns of scarring in patients recruited to a research study in Edinburgh. I found that patients with discrete areas of scar had the highest chance of dying, and those with a diffuse scarring pattern had an intermediate chance of dying compared with those with no scarring.

I also performed multiple MRI scans in patients with aortic stenosis to see how thickening and scarring of the heart muscle changed over time. I found that heart muscle thickening and diffuse scarring increased slowly over time, but if a discrete scar formed, accelerated new scar formation was observed on the next MRI scan. After valve surgery, both heart muscle thickening and diffuse scarring got better, but the discrete scars did not, meaning this type of scarring is permanent.

I then looked at diffuse scars in a large study of 400 patients with aortic stenosis who were waiting for valve replacement operations from several hospitals around the world. I found that the measurements of diffuse scarring from different MRI scanners could be compared, and that patients with diffuse heart muscle scarring were at a higher risk of dying regardless of their age, gender and overall heart pump function.

Finally, I tested a new type of MRI scanner that is combined with a PET (positron emission tomography) camera, where an injection of low-dose radioactivity is given, allowing us to track where the injection has travelled to in the body. I showed that this type of scanner gives us good images and measurements in people with aortic stenosis, but more research is needed.

In summary I have developed several new and powerful imaging techniques for assessing patients with aortic stenosis that hold promise in optimising the timing of aortic valve replacement.

Declaration

This thesis represents the research I performed at the Clinical Research Facility, Edinburgh Imaging at the Queens Medical Research Institute, Little France Campus and the Royal Infirmary of Edinburgh between August 2015 and August 2018.

I personally performed the final follow-up visits of patients in the CMRAS study and supervised the cardiovascular magnetic resonance (CMR) scans. For the Progression Analysis (Chapter 4) I reanalysed all of the CMR scans from both Edinburgh and Quebec cohorts. I had not recruited or collected any data from the Quebec patients. I was not involved in patient recruitment for the ECV400 study (Chapter 5) but did collate the data from the international centres and performed CMR analysis of all of the scans. I recruited all participants in the PASS study (Chapter 6) and supervised the MR/PET scans. I performed the statistical analyses for all included data.

Chapters 3 and 4 have been published in high-impact peer reviewed journals. I was the first co-author for both of these papers. Chapters 5 and 6 are in the process of submission for publication at the time of thesis submission. In all chapters, I performed the primary statistical analysis and drafted the manuscripts.

I have also set up (as Principal Investigator) the EVOLVED (Early Valve Replacement guided by Biomarkers of Left Ventricular Decompensation in

Asymptomatic Patients with Severe Aortic Stenosis) clinical trial. This is a multicentre randomised controlled blinded end-point trial investigating whether early valve intervention leads to improved clinical outcomes in patients with asymptomatic severe AS and evidence of mid-wall late gadolinium enhancement on CMR. I personally drafted the protocol with assistance from Edinburgh Clinical Trials Unit, obtained Research Ethics Committee and NHS R&D approval and have set up over ten U.K. sites. I have screened and recruited patients in Edinburgh over the last 12 months of my PhD. The EVOLVED trial is detailed in Chapter 7 and the protocol included as an appendix.

This thesis has not been accepted in any previous applications for a degree and all sources of information have been acknowledged. The research was undertaken in accordance with the Declaration of Helsinki and the regulations of the South East Scotland Ethics Committee.

Dr Russell Everett 18th October 2018

Acknowledgements

This programme of research was undertaken under the supervision of Professor David Newby (Professor of Cardiology and Consultant Cardiologist) and Dr Marc Dweck (BHF Reader and Consultant Cardiologist). I wish to thank them for their tireless support and remain consistently astounded by their commitment to both academic cardiology and the plethora of research students they nurture. I would also like to acknowledge the British Heart Foundation and Sir Jules Thorn Charitable Trust who have funded my PhD training and the studies with which I have been involved.

The staff at the Edinburgh Imaging Facility at the Queens Medical Research Institute have been instrumental in the conduct of my studies and subsequent data analysis. In particular, Scott Semple (Reader and MR Physicist) and Gillian MacNaught (MR Physicist) have helped me explore the murky world of MR physics and inspired me to pursue MR imaging as a long-term career. I would also like to thank Tom MacGillivray, Calum Gray and Giorgos Papanastasiou for their support with the often-frustrating task of image analysis and Annette Cooper and David Brian (MRI research radiographers) for accommodating my scans. I am extremely grateful for the support of the Wellcome Trust Clinical Research Facility at the Royal Infirmary of Edinburgh in aiding in the conduct of study visits and Audrey White (Research sonographer) for maintaining her tireless enthusiasm for performing my scans.

I have also had the pleasure of working with the Edinburgh Clinical Trials Unit and in particular would like to thank Christopher Tuck for helping me navigate the complex process of setting up a multicentre clinical trial and providing excellent company on many a site initiation visit.

Much of this work has been made possible by our network of collaborators both in the UK and overseas. They are too numerous to name individually but Calvin Chin, Vass Vassiliou, Lionel Tastet, Anvesha Singh, Thomas Treibel, Petra Biljsterveld, Marzia Rigolli and Miho Fuhui have been particularly supportive of my research efforts.

Finally, I would like to thank my wife Emily for her love, support and ceaseless (yet possibly feigned) interest in hearing about both magnetic resonance imaging and aortic stenosis, all whilst pursuing her own doctoral studies.

Abbreviations

^{18}F-NaF – ^{18}F sodium fluoride

AS – Aortic stenosis

AVA – Aortic valve area

AVR – Aortic valve replacement

BNP – Brain natriuretic peptide

CMR – Cardiac magnetic resonance

CMRA – Coronary magnetic resonance angiography

cTNI – Cardiac troponin I

ECG – Electrocardiogram

EF – Ejection fraction

MOLLI – Modified Look-Locker inversion-recovery

MR/PET – Magnetic resonance / positron emission tomography

LV – Left ventricle

LVH – Left ventricular hypertrophy

ShMOLLI – Shortened modified Look-Locker inversion recovery

SUV – Standardised uptake value

TAVI – Transcatheter aortic valve insertion

TBR – Tissue-to-background ratio

V Max – Peak aortic-jet velocity

Chapter 1: Introduction

Extracts from this chapter have been published in:

Everett, R. J. Clavel, M.A., Pibarot, P. Dweck, M.R. Timing of Intervention in Aortic Stenosis: A Review of Current and Future Strategies. *Heart* 2018

Everett, R. J., Newby, D. E., Jabbour, A., Fayad, Z. A. & Dweck, M. R. The Role of Imaging in Aortic Valve Disease. *Curr Cardiovasc Imaging Rep* **9,** 21–14 (2016).

Everett, R. J. *et al.* Assessment of myocardial fibrosis with T1 mapping MRI. *Clin Radiol* **71,** 768–778 (2016).

OVERVIEW

Aortic stenosis is the most common valve disease requiring surgical intervention in high-income countries (1). It is characterised by progressive thickening, fibrosis and calcification of the leaflets leading to restriction and valve obstruction (2). The consequent increase in left ventricular afterload leads to a hypertrophic response of the left ventricle, normalising wall tension and maintaining cardiac output. However, with progressive valvular stenosis, this hypertrophic response eventually decompensates resulting in symptom development, heart failure and death.

With no medications proven to attenuate or reverse stenosis progression, the only available treatment is valve replacement. This should ideally be performed when the risks of the disease process (i.e. sudden cardiac death, irreversible functional impairment and heart failure) outweigh those of intervention (i.e. procedural risk, long-term complications and potential need for reoperation). However, we frequently lack robust evidence to make accurate assessments of such risk. Deciding on the timing of valvular intervention is therefore difficult in many patients and contemporary clinical guidelines are often underpinned by historical observational data rather than high-quality randomised controlled trials. I will review our current understanding of the pathophysiology of aortic stenosis, describe and examine the evidence behind current guideline recommendations, and explore potential future strategies to optimise the timing of valve intervention, focussing on the

assessment of left ventricular decompensation using cardiac magnetic resonance imaging.

PATHOPHYSIOLOGY OF VALVULAR STENOSIS AND THE HYPERTROPHIC RESPONSE

Since the original description of aortic stenosis by Mönckeberg in 1904, the decline in rheumatic fever and ageing population have led to a demographic transition towards fibrocalcific disease. For many years, fibrocalcific aortic stenosis was viewed as a degenerative disease where progressive “wear and tear” led to structural damage and passive valvular calcification. However, contemporary thinking is that fibrocalcific aortic stenosis develops as part of a series of intricate and highly regulated inflammatory, fibrotic and osteogenic processes. The pathophysiological processes driving aortic valve stenosis can be divided into two phases (2). The initiation phase is characterised by endothelial injury accompanied by infiltration of lipids, lipid oxidation and pro-inflammatory response. Despite the clear similarities with atherosclerosis, three large randomised trials have failed to show any effect of statins on disease progression or clinical outcome. The second phase, or propagation phase, is characterised by the appearance of osteoblast-like cells which co-ordinate progressive valvular calcium and bone matrix deposition. This osteogenic phenotype involves many signalling molecules involved in bone formation and is both self-perpetuating and highly regulated (2). Advances in imaging now allow for non-invasive assessment of both the burden and activity of calcification in the valve (3,4). However the severity of aortic valve obstruction is still best assessed using echocardiography (5).

Myocardial response

The traditional focus of aortic stenosis assessments has been on the valve. However, the left ventricular myocardial response to pressure overload is equally important (6), particularly as the correlation between echocardiographic measures of aortic stenosis severity and the degree of myocardial hypertrophy is moderate at best (7). Whilst left ventricular hypertrophy maintains wall stress and cardiac output for many years, it eventually decompensates, with cell death and myocardial fibrosis identified as key processes (8). Many imaging and biomarker surrogates of these processes have been investigated providing significant prognostic information that will be discussed later in this chapter.

CURRENT GUIDELINE RECOMMENDED TREATMENT STRATEGIES AND THEIR LIMITATIONS

Broadly speaking, contemporary clinical guidelines recommend aortic valve intervention when stenosis severity is deemed severe *and* there is evidence of left ventricular decompensation, using either direct objective or surrogate symptomatic measures (Figure 1.1 and Table 1.1) (9,10). Haemodynamic severity is best assessed using echocardiography but can be challenging when measures of severity are discordant or low-flow states exist. New recommendations for confirming AS severity are given in the 2017 ESC/EACTS guideline update (5). Detailed discussion of low-flow states is beyond the scope of this thesis but can be found elsewhere (11).

Presence of Aortic Stenosis-related Symptoms

It is universally accepted that the development of patient symptoms (exertional dyspnoea, angina or syncope, Table 1.2) serves as an indicator of left ventricular decompensation and a dismal prognosis without intervention. This was first described in the seminal paper by Braunwald and Ross in 1968 and forms the underlying framework of how we manage patients today. However, this finding was based on retrospective data from just 12 patients with a mixture of bicuspid and rheumatic valve disease and a mean age of death of 63 years. The changing demographics of aortic stenosis make it difficult to interpret the current relevance of these historical data to the patients seen in current practice who are frequently in their eighth or ninth decades. Symptom

assessment can be highly challenging in these patients due to the high prevalence of both co-morbidity, which may cause symptoms to be falsely attributed to aortic stenosis, and physical inactivity, which can conceal exertion-related problems.

Exercise testing may help unmask symptoms in many patients and is safe when performed in stable patients (12). ESC guidelines recommend surgery in patients with severe aortic stenosis and typical symptoms on exercise test (class I, level C) or a fall in systolic blood pressure at peak exercise (class IIa, level C). This recommendation is based largely on observational data demonstrating that a positive exercise test is a strong predictor of sudden death or symptom development (13). However, these data are limited, consisting of a series of relatively small observational studies with inherent risk of bias and heterogeneity as to what constituted an abnormal test. According to a recent meta-analysis, whilst the negative predictive value of stress testing for subsequent cardiac events is reasonable (79%), the positive predictive value is modest (66%) (12). Exercise testing has other major limitations, up to 20% of patients will be unable to perform the test due to poor mobility, whilst pre-existing ECG abnormalities are present in up to 50% of patients confounding test interpretation (14). It is worth noting that exercise testing may also detect abnormalities caused by co-existent coronary disease which is an important determinant of both management and prognosis (15).

Impaired Left Ventricular Ejection Fraction

Development of left ventricular systolic impairment, as identified by a reduced left ventricular ejection fraction, is an inevitable consequence of progressive and untreated valvular stenosis, assuming sudden death does not occur. Although the risk of perioperative mortality is elevated in the setting of reduced ejection fraction, these patients have a dismal prognosis without intervention and improved long-term outcomes with valve replacement earning a class I, level C recommendation in clinical guidelines (9,10).

In clinical practice, patients with aortic stenosis can develop a reduction in ejection fraction for a variety of reasons and it remains important to consider the mechanism of this reduction and whether it is reversible. Reductions in ejection fraction occur as a direct response to increases in afterload and will reverse following valve replacement. By contrast the ejection fraction does not improve in approximately 25% of patients (9,10,16,17) who are more likely to remain symptomatic and who have adverse long term outcomes (twice as likely to die over 5 years follow-up) (18). In these patients, persistent systolic dysfunction appears related to the development of irreversible scar due to either myocardial infarction or decompensation of the hypertrophic response (19). In sick, frail patients such information may govern whether valve intervention is likely to be of benefit.

Very Severe Aortic Stenosis

Patients with critical aortic stenosis appear to have a particularly poor prognosis, similar to that of symptomatic severe aortic stenosis (20). Indeed patients with peak aortic jet velocities of >5.0 and >5.5 m/s demonstrate a 2-year event free survival of 43% and 25% respectively compared with 70% in those with Vmax 4.0-4.9 m/s (21). The ESC/EACTS guidelines therefore recommend consideration of aortic valve replacement in patients with Vmax >5.5 m/s if the estimated surgical risk is low (class IIa, level C). However, these observational studies mostly examined the composite endpoint of mortality and referral for aortic valve intervention with a strong risk of referral bias and event rates mainly driven by decisions to perform surgery.

Rapid Haemodynamic Progression

Although the average rate of progression (measured by peak aortic-jet velocity) is 0.24±0.30 m/s/year, this rate is highly variable (22). Moreover, it is subject to scan-rescan variation in peak velocity measurements, which can be high in clinical practice. Patients with rapid progression (>0.3 m/s/year) and significant valve calcification have a rate of symptom development or mortality of 79% at 2 years (23). As a result, referral for surgical intervention in these patients is given a class IIa, level C recommendation in the latest guidelines. However again this is based on limited observational data and this strategy requires standardised high-quality echocardiography over several years to confidently determine rate of progression.

Elevation of Brain Natriuretic Peptide Levels

Brain natriuretic peptide (BNP) is the first cardiac biomarker to be included in the decision-making algorithm for aortic valve replacement. Early studies investigating natriuretic peptides in aortic stenosis showed promise but were criticised for their small size, observational nature and use of softer outcome endpoints (24,25). In addition, many patients were symptomatic and the variation in normal BNP with age and sex were not accounted for. A more recent study of 565 patients with asymptomatic moderate-to-severe aortic stenosis identified that a BNP ratio (measured BNP value divided by upper limit of normal for patient's age and sex) of >1 was independently predictive of mortality and a ratio of >3 had a hazard ratio of 7.3 for survival in patients with asymptomatic severe aortic stenosis (26). As such the latest clinical guidelines reflect these data with a level IIa, class C recommendation for aortic valve replacement if the BNP ratio is persistently above 3 and overall surgical risk is low. However, BNP is a non-specific marker of cardiac dysfunction and its utility, like each of the other measures, has yet to be tested in a randomised controlled trial.

The recently published ESC clinical guidelines also removed two previous IIb indications for AVR in asymptomatic patients; an increase in mean aortic gradient of >20 mmHg with exercise, or the finding of excessive LV hypertrophy in the absence of hypertension.

Figure 1.1: ESC/EACTS algorithm for management of severe aortic stenosis (2017 guidelines)

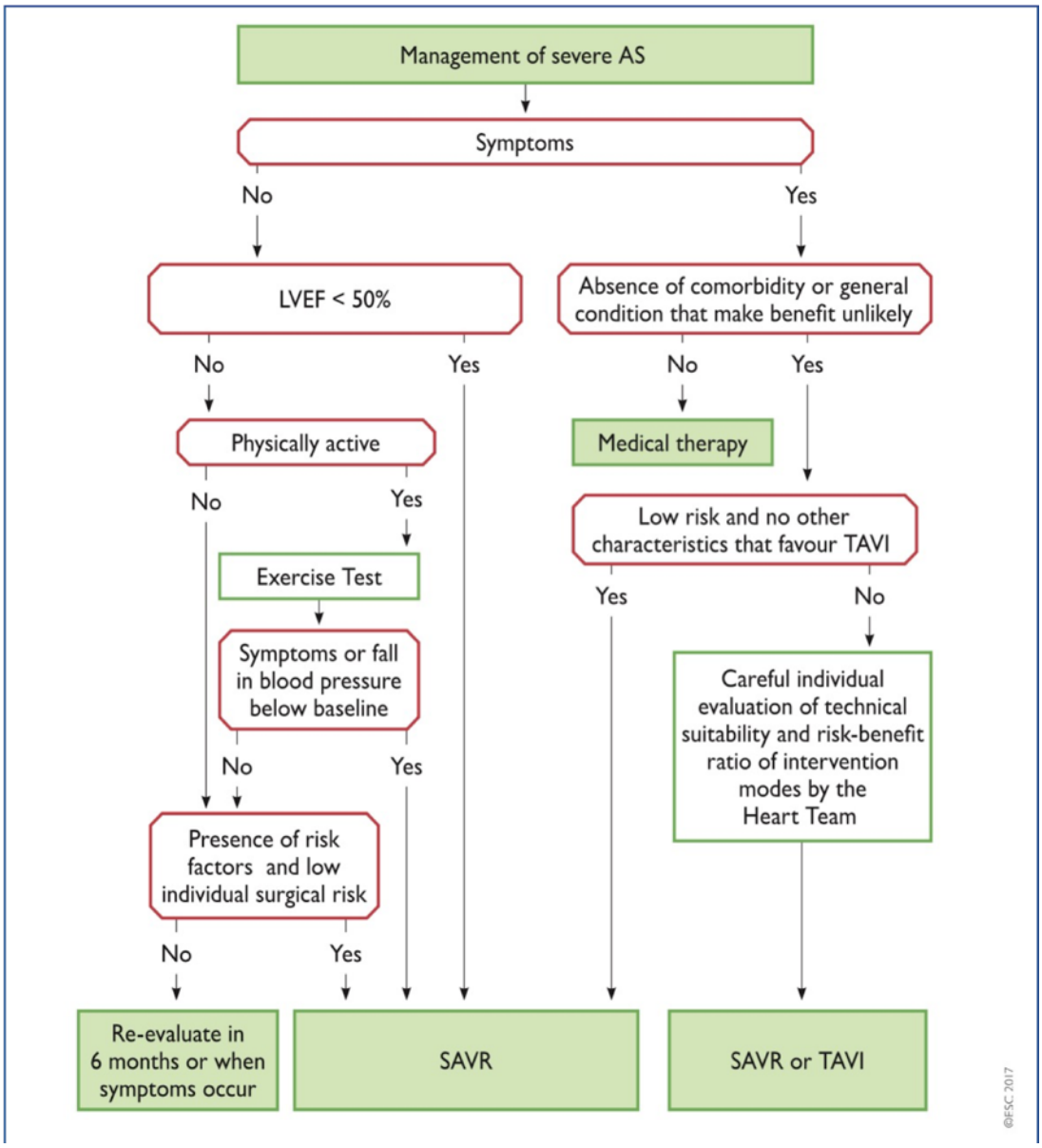

AS, aortic stenosis; LVEF, left ventricular ejection fraction; SAVR, surgical aortic valve replacement; TAVI, transcatheter aortic valve implantation.

Table 1.1: Recommendations for Intervention in patients with severe aortic stenosis (ESC/EACTS guidelines 2017)

Symptomatic Severe AS (surgical AVR or TAVI)	Class	Level
Indicated in severe high gradient aortic stenosis (AV Vmax >4m/s or mean gradient >40mmHg)	I	B
Indicated in patients with low-flow low-gradient severe AS with reduced ejection fraction and evidence of contractile reserve excluding pseudosevere AS	I	C
Should be considered in patients with low-flow low-gradient severe AS with preserved ejection fraction after careful confirmation of severe AS.	IIa	C
Should be considered in patients with low-flow low-gradient severe AS with reduced ejection fraction without evidence of contractile reserve especially where CT calcium scoring confirms severe AS	IIa	C
Should NOT be performed in patients with severe comorbidities where the intervention is unlikely to improve quality of life or survival	III	C
Asymptomatic Severe AS (surgical AVR only)		
Indicated in patients with severe AS and left ventricular systolic dysfunction (LVEF <50%) not due to another cause	I	C
Indicated in patients with abnormal exercise test showing symptoms on exercise clearly related to aortic stenosis	I	C
Should be considered in patients with abnormal exercise test showing a decrease in blood pressure below baseline	IIa	C
Should be considered if the surgical risk is low and one of the following abnormalities is present: • Very severe aortic stenosis (AV Vmax >5.5m/s) • Severe valve calcification with a rate of progression ≥0.3m/s/year • Markedly elevated BNP (> threefold above age- and sex– corrected normal range) confirmed by repeated measurements without other explanations • Severe pulmonary hypertension (systolic pulmonary artery pressure >60mmHg at rest confirmed by invasive measurement) without other explanation	IIa	C

AS, aortic stenosis; AV, aortic valve; BNP, b-type natriuretic peptide; CT, computed tomography; LVEF, left ventricular ejection fraction

Table 1.2: Symptomatology of Severe Aortic Stenosis

Symptom:	Aetiology:	Potential questions to ask:
Angina	Supply-demand imbalance: co-existent coronary disease and fixed cardiac output versus hypertrophied myocardium	"do you get chest pain or discomfort when walking or doing other activities?"
Breathlessness /reduced exercise capacity	Reduced LV compliance increased left ventricular end-diastolic and pulmonary capillary pressures	"can you walk ask many stairs as this time last year?" "can you keep up with your friends?"
Presyncope / syncope *(important to elicit any exertional component)*	Fixed cardiac output, skeletal muscle vasodilation on exertion and resultant cerebral hypoperfusion	"have you felt lightheaded like you might faint? "have you had any fainting or blackout episodes?"
Palpitation	Development of atrial or ventricular arrhythmia, myocardial scarring	"are you aware of your heart racing?"

BALANCING COMPETING RISKS

There are clear limitations with many of our guideline-advocated strategies. Most are based upon limited observational data and supported by level C recommendations. There is therefore a need for randomised controlled trials assessing the optimal timing of surgery and novel objective methods to guide this major clinical decision. Ideally, intervention would be performed in patients just as the left ventricle is starting to decompensate but before substantial irreversible damage has accrued and at a time when the short and long-term risks of the intervention are outweighed by the risks of not intervening (Figure 1.2 and Table 1.3). An understanding of these competing risks is therefore critical.

1. Risks of valve intervention

Surgical aortic valve replacement remains the standard of care for valvular intervention, with improvements in surgical and post-operative care driving peri-operative mortality down to ~1-3%. Other important perioperative complications include conduction disease requiring permanent pacemaker insertion (1.5-8.6% (27)) and cerebrovascular accidents (2.4-8.1% (28-30)). There is also the risk of cognitive decline (due to peri-operative cerebral hypoperfusion, microemboli or anaesthetic agent neurotoxicity (30)). An individual's risk of these complications can be estimated using surgical risk calculators such as EUROSCORE II and the Society of Thoracic Surgeons score. An argument in favour of early surgery is that operative risk is lower in

younger patients that are asymptomatic, have less co-morbidity and normal left ventricular function.

The emergence of minimally invasive transcatheter aortic valve insertion (TAVI) over the last 10 years has completely changed the landscape for decision making regarding valve intervention in symptomatic patients. Current trials show non-inferiority of this percutaneous technique compared with surgical intervention in both high and intermediate-risk patients (29,31-34) and procedural risk may further reduce with increasing clinical experience and advances in prosthesis design and delivery. Indeed, major vascular complications have decreased substantially (from >10% to <5% (35)) as have stroke rates which are between 2-3% in contemporary cohorts (35). However the requirement for permanent cardiac pacing following the procedure remains consistently higher than surgical intervention at >10% (35) and whilst TAVI allows for rapid patient recovery and mobilisation, the long term durability of these bioprostheses has not been demonstrated (36). This will be key before their widespread use in younger or asymptomatic patient groups can be recommended.

Performing valve intervention introduces small but significant annual risks associated with the presence of a prosthetic valve. These risks are heavily influenced by valve type, with both anticoagulant-related major bleeding (1.8-2.6% per year) and thromboembolism (0.7-1.0% per year) more frequent with mechanical valves (37). In addition, there is an increased risk of endocarditis

(1-3% during the first year then <0.5% per year (38)) which has a high associated morbidity and mortality. Whereas structural valve degeneration is exceedingly rare in mechanical valves, bioprosthetic valves have a limited lifespan which can be difficult to predict. In these patients, valve degeneration usually starts to occur 10 years following implantation (39), and occurs more rapidly in younger patients (40). This is an extremely important issue if bioprosthetic valves are to be utilised in younger asymptomatic patients. Ongoing research into decellularisation techniques and tissue engineering may lead to improved bioprosthetic valve longevity, whilst advances in mechanical valve design might eventually eliminate the need for anticoagulation and associated bleeding risk. In addition, the use of a transcatheter valve inside a surgical bioprosthetic valve (so called valve-in-valve TAVI) may reduce the risk of future procedures should valve degeneration occur.

2. Risks of not intervening

The risk of sudden cardiac death in patients with asymptomatic severe aortic stenosis managed conservatively is ~1% per year and occurs without preceding symptoms in 70% of cases (41-43). Once symptoms develop, further clinical deterioration can be rapid with a significant risk of sudden death whilst awaiting intervention (4% at 1 month, 12% at 6 months)(44).

Delaying aortic valve intervention until there is evidence of advanced left ventricular decompensation results in greater perioperative risks (43).

Observational studies have quoted increased perioperative mortality (9-19% (9,18,45)) in patients who have developed left ventricular systolic impairment and advanced myocardial fibrosis (46). Further risk stratification can be performed using stress echocardiography to assess myocardial contractile reserve, with lower perioperative risks if contractile reserve is present (5% versus 22-32% (10,47)). However, given the dismal prognosis of untreated AS, even patients without contractile reserve have improved long-term survival if they survive the perioperative period (9,10).

The highest burden in mortality and morbidity related to delaying valve intervention appears to occur in the months and years following AVR, particularly in those patients who have evidence of left ventricular decompensation. As discussed, patients with an impaired ejection fraction prior to AVR have a poor long term prognosis (18), whilst in a recent study of aortic stenosis patients with a high probability of LV decompensation, more than half were either dead or admitted to hospital with heart failure within 2 years (48). Both these observations may reflect the development of irreversible scarring in the myocardium whilst patients are waiting for surgery.

Figure 1.2: Optimising the timing of aortic valve intervention in progressive aortic stenosis

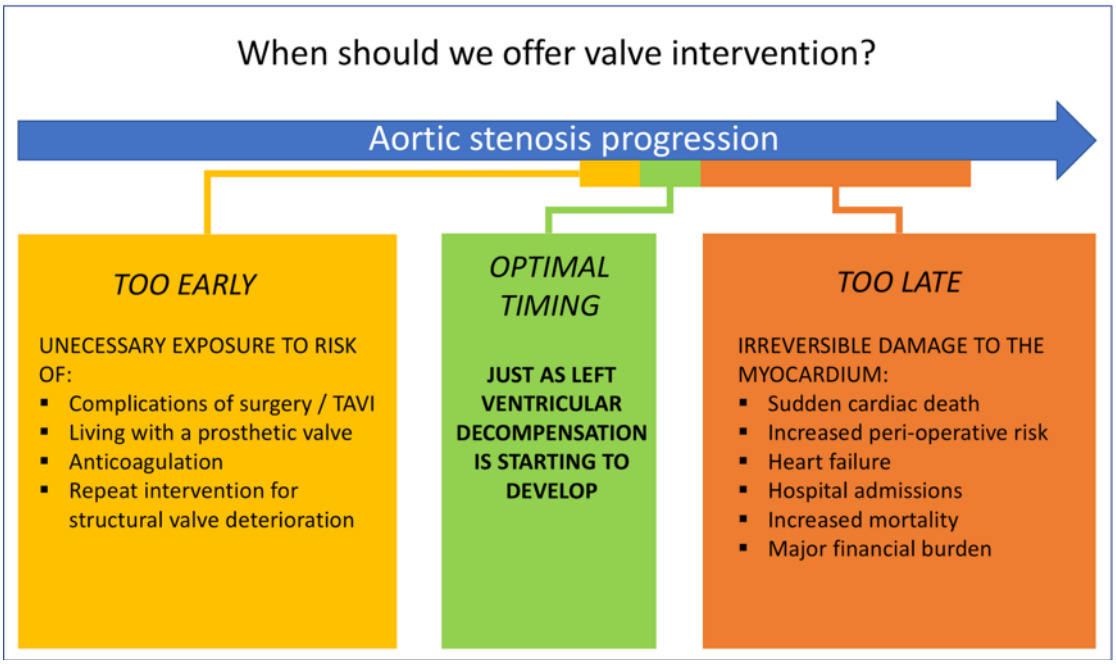

Table 1.3: Estimates of clinical risks associated with watchful waiting or early intervention strategies

Risks associated with watchful waiting	Risk estimate	Risks associated with early intervention	Risk estimate
Sudden cardiac death	1.0-1.5% per year (41-43)	Peri-operative mortality	1-3% (refine using validated risk calculator)
Death whilst awaiting elective intervention once symptoms develop	4% at 1 month, 12% at 6 months (44)	Peri-operative complications (SAVR) -stroke -pacemaker requirement -major bleeding -new atrial fibrillation	 2.4-8.1% (28-30) 1.5-8.6% (27) 9-26% (31,34) 17–43% (29,31,34)
Increased peri-operative mortality -impaired left ventricular function -no contractile reserve	9-19% (9,18,45) 22-32% (10,47)	Peri-procedural complications (TAVI) -stroke -pacemaker requirement -major vascular complications -major bleeding -new atrial fibrillation	 2.2-2.6% (35) 7-25% (33-35) 2.0-4.5% (35) 12-15% (31,34) 10-13% (29,31,34)
Lack of improvement in ejection fraction following intervention	25-50% (9,10)	Long term prosthetic valve complications -thromboembolism -major bleeding with anticoagulation	 0.7-1.0% per year (37) 1.8-2.6% per year (37)
Incomplete resolution of symptoms	Approximately 50% (45)	Prosthetic valve endocarditis	1-3% in first year then <0.5% per year (38)
Increased late post-intervention mortality -impaired ejection fraction -myocardial fibrosis	Hazard ratio 2.0 (18) Hazard ratio 1.25-5.25 (19,46,49)	Reoperation for structural valve degeneration -<65 years of age ->65 years of age	 46-55% at 20 years 8-15% at 20 years (40)

POTENTIAL FUTURE STRATEGIES FOR DECIDING ON TIMING OF AORTIC VALVE INTERVENTION

Several different strategies for optimising the timing of valve replacement in aortic stenosis have been proposed, many of which are currently being evaluated within the context of randomised controlled trials (Figure 1.3 and Table 1.4). Many of these target asymptomatic patients and it should be recognised that many patients who feel otherwise fit and healthy might not want to undergo major heart surgery.

1. All-comers with severe aortic stenosis

Historical teaching has been that “aortic valve replacement is the most common cause of death in patients with asymptomatic severe aortic stenosis”. However, improving outcomes following surgical and transcatheter valve interventions are challenging this doctrine. Performing valve intervention on all asymptomatic patients with severe aortic stenosis is a simple and pragmatic solution that does not seek to identify the point at which left ventricular decompensation occurs. Although some patients will undergo intervention earlier than they may have required (and therefore be exposed unnecessarily to the problems associated with prosthetic valves), the risks associated with contemporary intervention techniques are low and no patient should be left with irreversible left ventricular decompensation. This strategy is supported by evidence from the Japanese Contemporary outcomes after sURgery and medical tREatmeNT in patients with severe Aortic Stenosis (CURRENT AS)

registry. Propensity-score matching was used to compare 291 asymptomatic patients who underwent early surgery with 291 patients who were managed conservatively. Those who received early AVR had a reduced all-cause mortality at 5 years (15%) compared with those who were initially managed conservatively (26%). Heart failure hospitalisation was also reduced in the early intervention group (4% versus 20%). However, propensity matching may not have accounted for all potential influences on outcomes and a significant proportion of the conservatively managed patients who developed symptoms were not referred for intervention, undoubtedly contributing to the worse observed survival in this group: confounding by indication. Three randomized controlled trials (AVATAR, ESTIMATE and EARLY-TAVR, Table 1.4) are currently recruiting which will examine whether valve intervention in unselected asymptomatic severe aortic stenosis patients can improve clinical outcomes.

2. Refined assessment of valve structure and function

An alternative strategy is to operate only in asymptomatic patients with very high peak aortic-jet velocities. Peak velocities >4.5 m/s are associated with increased referral for surgical intervention (21) but also increased rates of peri-operative death and cardiac death in a prospective cohort study with propensity matching (42). The RECOVERY randomised controlled trial will examine whether early aortic valve replacement in asymptomatic patients with velocities >4.5 m/s and a negative exercise test leads to improved patient outcomes compared to watchful waiting (Table 1.4).

The total haemodynamic load seen by the left ventricle can also be quantified by calculating the valvuloarterial impedence (ZVa= (systolic blood pressure + mean AV gradient) / indexed LV stroke volume). This measure is an independent marker of adverse outcome in asymptomatic patients (50) and warrants further study for its use in determining the timing of intervention.

Another approach is to quantify valvular calcium burden using CT calcium scoring. Validated sex-specific thresholds for severe aortic stenosis have been proposed (2000 Agatston units [AU] for men, 1300 AU for women) (5), which provide powerful prediction of clinical events of incremental value to echocardiographic assessments (3). Performing valve intervention on the basis of severe valvular calcification on CT might therefore represent an attractive alternative strategy.

3. Imaging and biomarkers of left ventricular decompensation

The two broad strategies listed above largely ignore any detailed assessment of the left ventricular response to pressure overload beyond assessment of LV ejection fraction. Reductions in ejection fraction are a late, non-specific and often irreversible feature in aortic stenosis, and this has led to interest in alternative methods for detecting left ventricular decompensation (Figure 1.4) (7,51-53). These will now be discussed in more detail.

Figure 1.3: Comparison of EARLY-TAVR and EVOLVED randomised-controlled trial designs

Currently recruiting randomised controlled trials generally fall into two groups; those investigating valve intervention in all asymptomatic patients with severe aortic stenosis (e.g. EARLY-TAVR) and those looking to target intervention based on measures of left ventricular decompensation (e.g. EVoLVeD).

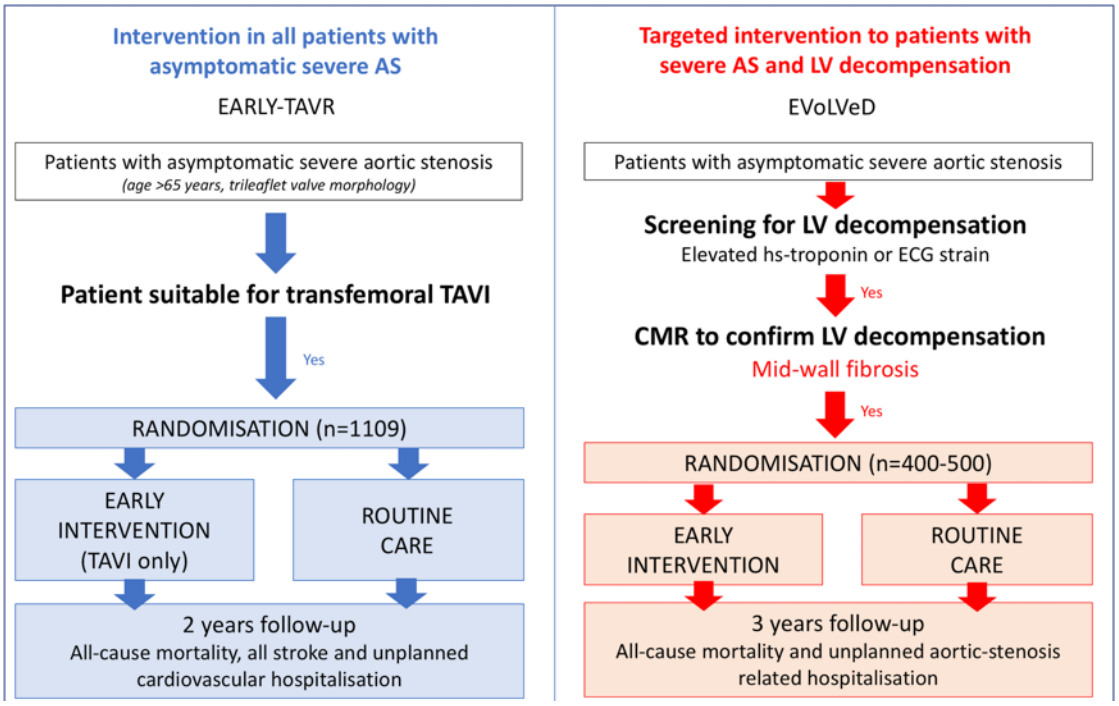

AS, aortic stenosis; CMR, cardiac magnetic resonance; hs, high-sensitivity; LV, left ventricular; TAVI, transcatheter aortic valve insertion

Figure 1.4: Imaging and biomarker assessments of stage of valvular stenosis and myocardial response to increased afterload

Progressive haemodynamic obstruction as a result of aortic leaflet restriction is assessed using echocardiography. However, specific valvular pathologies such as fibrosis and calcification can be assessed using computed tomography methods. Ejection fraction is a poorly sensitive marker of myocardial decompensation with abnormalities in Doppler measures, longitudinal strain and systolic function all detectable prior to this. However, these measures, along with biomarkers such as troponin and BNP, are non-specific and may be abnormal as a result of co-existent myocardial pathology such as coronary heart disease. T1 mapping methods and late gadolinium enhancement are more specific for decompensation as a result of pressure overload.

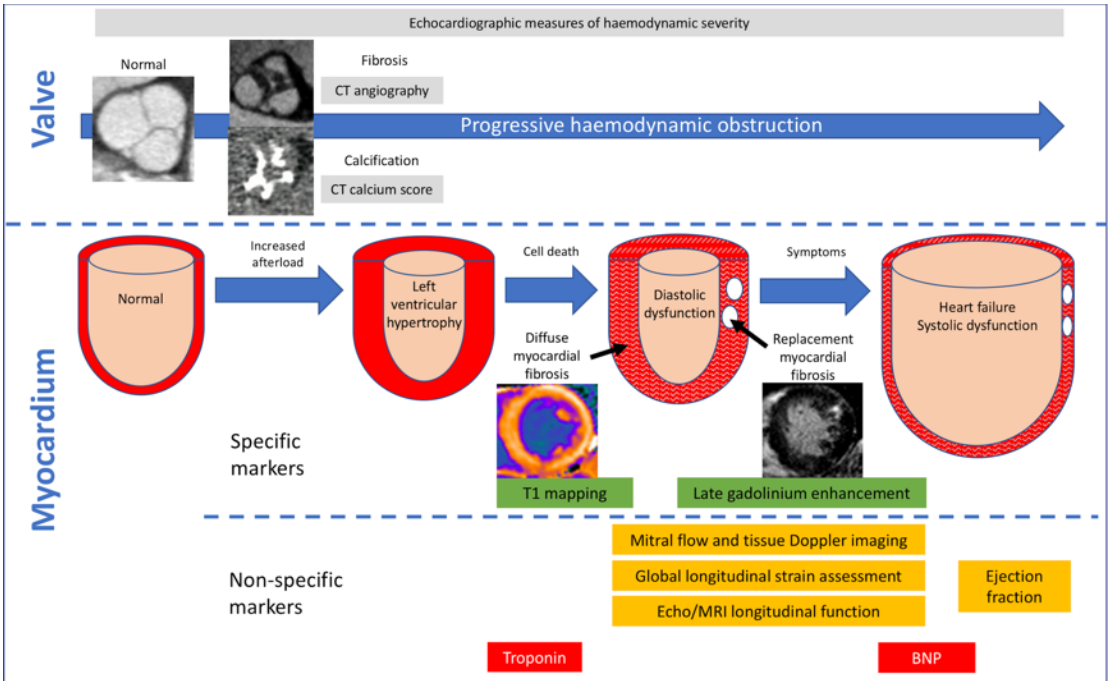

Table 1.4: Current and planned randomised-controlled trials investigating timing of aortic valve intervention

Strategy	Proposed or ongoing trials	Population	Intervention	Primary outcome	Trial status / unique identifier	Country	Estimated completion
All-comers with asymptomatic severe AS	AVATAR (Aortic Valve Replacement Versus Conservative Treatment in Asymptomatic Severe Aortic Stenosis)	312 patients with asymptomatic severe AS and STS score <8%.	SAVR or Routine care	All-cause mortality and MACE at 3 years	Recruiting NCT02436655	Serbia	2020
	ESTIMATE (Early Surgery for Patients with Asymptomatic Aortic Stenosis)	360 patients with asymptomatic severe AS, normal ETT and low surgical risk	SAVR or Routine care	All-cause mortality and MACE at 1 year	Recruiting NCT02627391	France	2019
	EARLY TAVR (Evaluation of Transcatheter Aortic Valve Replacement Compared to SurveilLance for Patients with AsYmptomatic Severe Aortic Stenosis)	1109 patients aged >65 with asymptomatic severe AS, trileaflet valve morphology and favourable ileo-femoral arterial anatomy	Transfemoral TAVI (Edwards SAPIEN 3) or Routine care	All-cause mortality, all stroke, and unplanned cardiovascular hospitalization at 2 years	Recruiting NCT03042104	United States	2021
Refined assessment of valve function - higher peak velocity threshold	RECOVERY (Early Surgery Versus Conventional Treatment in Very Severe Aortic Stenosis)	145 patients with very severe AS (Vmax >4.5m/s, AVA <0.75cm) and a negative ETT	SAVR or Routine care	Cardiac mortality at 4 years	Recruiting NCT01161732	South Korea	2022
Assessment of myocardial decompensation -multiple biomarker assessment of LV decompensation	EVoLVeD (Early Valve Replacement Guided by Biomarkers of LV Decompensation in Asymptomatic Patients with Severe AS)	400 patients with asymptomatic severe AS, normal LVEF and mid-wall fibrosis on cardiac MRI	SAVR / TAVI or Routine care	All-cause mortality and unplanned AS-related hospitalisation at 3 years	Recruiting NCT03094143	UK	2020

ETT, exercise tolerance test; LV, left ventricle; MACE, major adverse cardiovascular events; SAVR, surgical aortic valve replacement; STS, Society of Thoracic Surgeons; TAVI, transcatheter aortic valve insertion

ASSESSMENT OF LEFT VENTRICULAR DECOMPENSATION

Cardiac biomarkers

Simple cardiac biomarkers beyond BNP are being investigated in aortic stenosis as markers of LV decompensation. Cardiac troponin is a structural protein present in cardiomyocytes which is released into the bloodstream during myocardial injury and can now be detected at very low plasma concentrations using high-sensitivity assays. In aortic stenosis, troponin I concentrations are associated with a more advanced left ventricular hypertrophic response, diffuse and replacement myocardial fibrosis and worse long-term clinical outcomes (AVR or cardiovascular death) in patients with aortic stenosis (54,55). They are thought to reflect the cardiomyocyte death that drives progressive left ventricular decompensation alongside myocardial fibrosis (8). Elevation in cardiac troponin is not however specific to aortic stenosis.

Electrocardiogram

The 12-lead electrocardiogram (ECG) is useful in the assessment of patients with AS. Although unable to directly detect valve stenosis, the secondary left ventricular hypertrophy leads to characteristic ECG changes, which are specific but poorly sensitive for the presence of significant left ventricular hypertrophy. These include left axis deviation, increasing QRS voltage in both chest and limb leads, change in ST or T wave vector, and broadening of the QRS duration. Furthermore, the presence of ST depression in the lateral

leads, representing LV strain, has been shown to correlate with an increased LV mass, high-sensitivity troponin value, and both diffuse interstitial and mid-wall replacement fibrosis (positive predictive value of ECG strain for mid-wall fibrosis was 100%) (56). The ECG-strain pattern is also a powerful independent predictor of AVR or cardiovascular death (56). Although highly specific, the poor sensitivity of ECG measures for detecting LV decompensation limit use as a lone screening tool.

Echocardiographic measures

Prior to reduction in global LV ejection fraction, echocardiography can detect alteration in various measures of diastolic and longitudinal systolic function in patients with aortic stenosis which appear related to the presence of myocardial fibrosis (7). Reduced left ventricular global longitudinal strain (GLS) can be observed in asymptomatic patients with aortic stenosis, acting as an independent predictor of mortality (52). However, several of these measures still require standardisation across vendor platforms and all suffer from significant overlap between results in healthy individuals and those with aortic stenosis. Moreover, these imaging markers are not specific to valvular heart disease and, like symptoms, might equally reflect co-morbidity such as ischaemic heart disease.

CARDIAC MAGNETIC RESONANCE IMAGING IN AORTIC STENOSIS

Echocardiography is the first line imaging tool used to investigate patients with known or suspected aortic stenosis as it is low-cost, readily available in most secondary care settings and provides important information on valve function by use of Doppler flow assessment. However, advanced imaging techniques are increasingly being used to provide a more detailed assessment of the left ventricle itself. Cardiac magnetic resonance (CMR) imaging provides gold-standard measurements of LV mass, volume and ejection fraction due to superior spatial resolution. It also provides detailed views of the AV and can reliably identify anatomical variants such as congenitally bicuspid valves. This is particularly valuable in patients with poor acoustic windows, prohibiting adequate assessment by echocardiography (Figure 1.5).

Although pressure overloaded states such as hypertension and AS induce concentric LV remodelling and hypertrophy, several studies using CMR have suggested that asymmetric phenotypes (defined as left ventricular wall thickness >1.5 times the opposing segment) are present in up to 25% of patients (57). While the exact mechanism is unknown, it is possible that increased wall stress could exacerbate a pre-existing genetic tendency towards a hypertrophic cardiomyopathy phenotype. Regardless, LV mass is most accurately calculated using CMR where the entire volumetric data of the LV is quantified.

There is also heterogeneity in the range of the LV hypertrophic response, which individual patients develop for a given severity of valve stenosis. Several studies have shown a poor correlation between the degree of LV hypertrophy and the severity of valvular stenosis (as assessed on echocardiography using aortic valve area, peak or mean gradient) (57-59). This variation is partly explained by sex differences and clinical factors such as co-existent hypertension, age, obesity, metabolic syndrome and polymorphisms in the angiotensin-converting enzyme gene. Importantly, LV mass index, whether calculated using echocardiography or CMR, is an independent predictor of adverse cardiovascular events or all-cause mortality (57,60,61). This emphasizes the importance to assess both the valve and myocardium independently.

CMR is able to assess potentially more sensitive measures of left ventricular dysfunction. Although reduced LVEF is strongly associated with a poor prognosis in patients with AS, this is a late finding and is preceded by impairment of diastolic function, longitudinal strain and longitudinal systolic function (subendocardial myocardial fibres oriented in a longitudinal direction are affected first by pressure overload). Although no standardised method yet exists, longitudinal systolic function can be measured using CMR by assessing the mitral valve annular excursion between systole and diastole (62). In addition, CMR is able to assess regional and global myocardial strain, using

techniques such as myocardial tissue tagging, velocity encoding or tagged cine displacement encoding with simulated echoes (DENSE) (63).

Importantly, CMR provides a crucial advantage over other imaging techniques in that it offers tissue characterisation and assessment of myocardial fibrosis. The gold-standard assessment of fibrosis is invasive endomyocardial biopsy but this is susceptible to sampling error and associated with a small but significant risk of complications (64). Cardiac magnetic resonance can provide non-invasively whole-heart detection and quantification of myocardial fibrosis using two methods: late gadolinium enhancement (LGE) which detects replacement fibrosis, and T1 mapping for diffuse fibrosis.

Figure 1.5: Multiparametric cardiac imaging with cardiac magnetic resonance

Cardiac magnetic resonance offers high spatial resolution imaging of the left ventricle and aortic valve (3 chamber cine and short axis cines) in addition to providing tissue characterisation. The late gadolinium enhancement (LGE) method can detect replacement myocardial fibrosis in a mid-wall pattern (red arrows) and native and post-contrast T1 mapping can identify diffuse fibrosis by estimating the T1 time of tissues which is altered in the presence of fibrosis. Focal replacement fibrosis is also detectable on these T1 mapping sequences (white arrows).

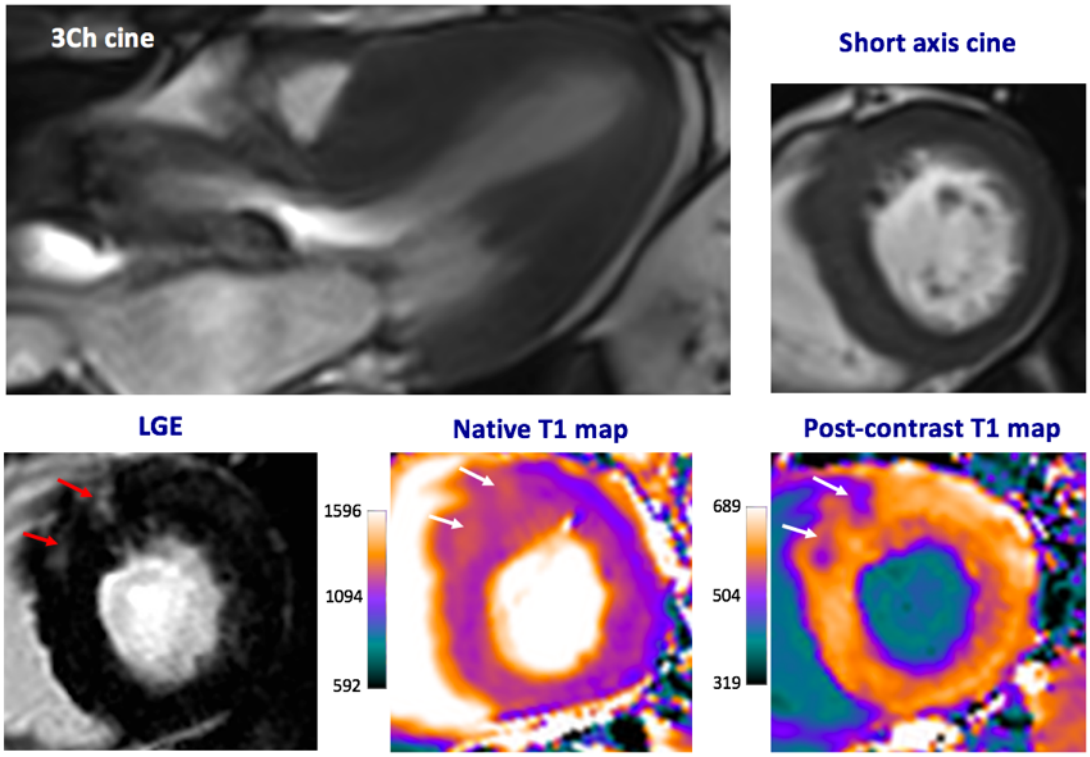

3Ch, 3-chamber; LGE, late gadolinium enhancement

LATE GADOLINIUM ENHANCEMENT TECHNIQUE

The late gadolinium enhancement (LGE) technique is now well established in clinical practice and is often used for both diagnostic and prognostic purposes in both ischaemic and non-ischaemic cardiomyopathies, particularly in cases of diagnostic uncertainty. This method uses T1-weighted imaging sequences performed 10-20 min following an intravenous bolus of gadolinium-based contrast agent. Gadolinium chelate complexes are too large to cross cell membranes and therefore distribute in the extracellular space where they accumulate in areas of extracellular volume expansion. The inversion time of the sequence is manually set to so that there is minimal or no signal generated from normal myocardium (so called “nulling”). A qualitative difference can be appreciated between “nulled” normal myocardium, which appears black, and areas of extracellular matrix expansion as seen in focal replacement fibrosis, which then appear bright on T1-weighted sequences. These focal areas of replacement fibrosis are likely a consequence of increased coronary flow resistance and repeated ischaemia in the regions of left ventricular hypertrophy and tend to occur in a mid-wall distribution (65). This can usually be differentiated from myocardial infarction, which is another common cause of focal replacement fibrosis that characteristically occurs in a subendocardial distribution.

Mid-wall replacement fibrosis is detectable on CMR in 29-62% of patients with AS (46,49,66) depending on the population studied. Subendocardial LGE,

suggesting previous myocardial infarction, is also commonly seen in patients with AS (10 to 28% (46)) as patients are often elderly with vascular risk factors and, therefore, have co-existent ischemic heart disease. Interestingly, the presence of mid-wall LGE appears more closely related to the degree of left ventricular hypertrophy rather than the severity of valve narrowing. Importantly, several studies have shown no regression in replacement fibrosis following relief of LV pressure overload associated with AV replacement (19,67,68), suggesting that this type of fibrosis is irreversible. As well as being a potential substrate for re-entrant arrhythmias, mid-wall fibrosis also correlates with myocardial injury as measured by high-sensitivity cardiac troponin I (54) and predicts functional recovery following surgery. Perhaps most importantly, the presence of mid-wall fibrosis has been shown to be a strong independent predictor of all–cause mortality in three separate studies (19,46,49,69), underlining its utility as an objective marker of LV decompensation in AS.

One notable disadvantage of the late gadolinium enhancement technique is the inability to detect diffuse interstitial myocardial fibrosis as this relatively homogeneous process provides no normal myocardium for visual contrast. Therefore, a considerable interest exists in the use of T1 mapping methods to quantify fibrosis burden in AS patients (Figure 1.6). This may potentially identify the optimal time-point to perform aortic valve intervention before the development of irreversible pressure overload-induced pathological changes to the ventricle.

Figure 1.6: T1 mapping and Late Gadolinium Enhancement in Aortic Stenosis

Left column: a healthy control patient with normal myocardium, extracellular volume values and no late gadolinium enhancement. Middle column: a patient with severe aortic stenosis with raised extracellular volume indicating diffuse fibrosis. Right column: a patient with severe aortic stenosis with asymmetrical anteroseptal left ventricular hypertrophy, a raised extracellular volume and mid-wall late gadolinium enhancement (white arrows).

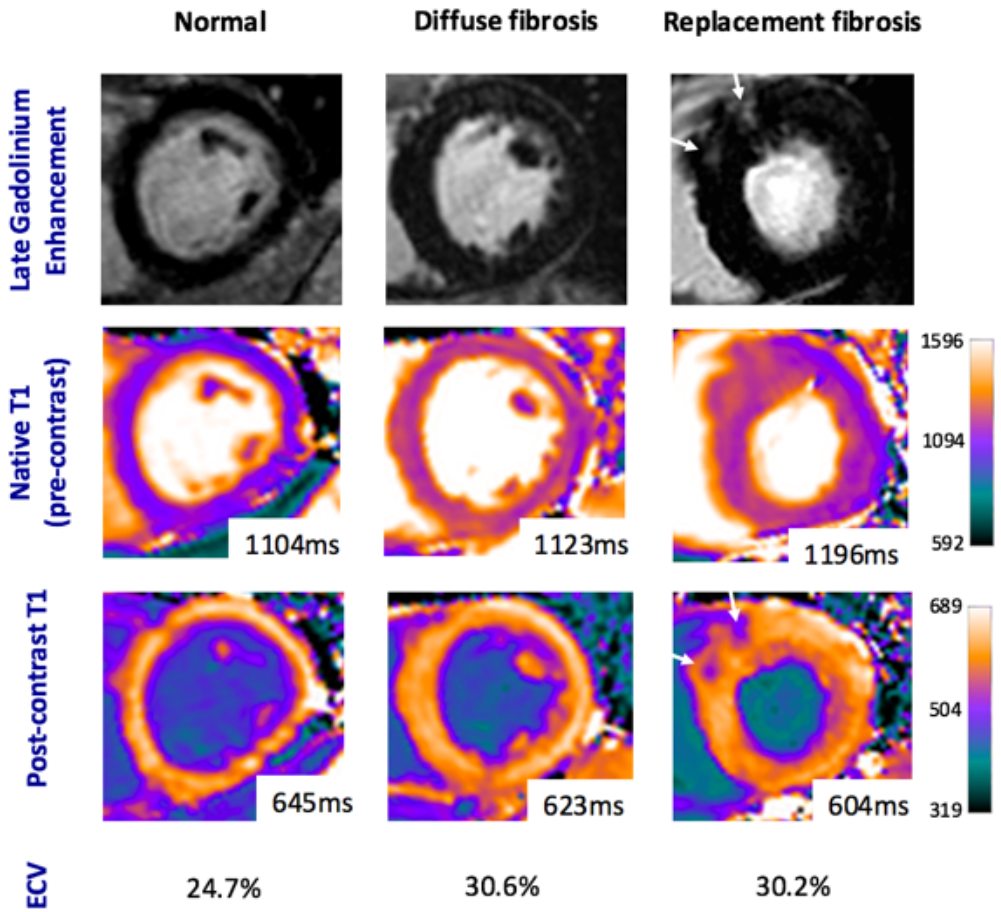

ECV, extracellular volume fraction; ms, millisecond

T1 MAPPING

T1 mapping techniques enable the detection and quantification of diffuse myocardial fibrosis, an earlier form thought to precede replacement myocardial fibrosis. This process is characterised by collagen deposition and associated expansion of the extracellular volume (ECV). This progressive change may occur due to an increased requirement for extracellular matrix to support the hypertrophied myocytes as a consequence of an increased LV afterload, likely triggering increased myofibroblast collagen synthesis.

A variety of T1 mapping sequences exist, being based on either inversion recovery or saturation recovery sequences. The sequence most commonly used is the MOdified Look-Locker Inversion recovery (MOLLI) which samples the T1 recovery curve following inversion pulses over multiple consecutive heart beats (70). This allows the T1 value (the time taken to recover 63% of longitudinal magnetisation following inversion, a property of different tissues) to be estimated (Figure 1.7). A Shortened MOLLI (ShMOLLI) sequence has also been developed which does not allow for complete recovery of longitudinal magnetisation following each inversion pulse and can therefore be acquired over fewer heartbeats. This means the breathhold duration is significantly shorter and ShMOLLI may also give more accurate T1 estimation at higher heart rates (71). The SAturation recovery single-sHot Acquisition (SASHA) sequence is less commonly used (72). Importantly, the T1 values generated will vary by sequence and magnetic field strength and this has led

to difficulties conducting clinical trials over multiple research centres especially given the ongoing iterative development of T1 mapping sequences.

A variety of T1 mapping measures exist that have been studied in literature. The evidence for and utility of each of these measurements in the assessment of patients with AS will be examined in detail.

Native T1

Native T1 describes the use of T1 mapping sequences to estimate tissue T1 values without the use of gadolinium contrast. The sole use of native T1 has many advantages; it has good reproducibility in some studies involving patients with AS (73) and scanning times are shorter than the equivalent contrast-based approaches. Native T1 is particularly attractive in patients with advanced renal impairment (estimated glomerular filtration rate <30 mL/min/1.73 m^2) in whom gadolinium-based contrast is contraindicated.

T1 values vary according to the molecular composition and water content in any of the tissue compartments of imaged tissue. In some conditions such as hypertrophic cardiomyopathy, the most significant changes are intracellular with sarcomeric and myocyte disarray. Much of the current literature regarding AS focuses on the extracellular compartment where extracellular matrix expansion with collagen deposition (myocardial fibrosis) causes an increase in native T1 values. Deposition of other proteins, such as those causing amyloidosis can show marked increase in native T1 values. However, water

content, whether intra or extravascular, is an important determinant of native T1. For example, patients with myocarditis have raised native T1 values in areas of myocardial inflammation due to the presence of myocardial oedema. The intravascular compartment is often overlooked as highlighted in a study using adenosine stress CMR. Patients with severe AS have increased resting coronary flow volume and reduced flow reserve (74). Native T1 values were greater in AS patients compared with controls, but both increased to a similar level during pharmacological stress. The authors suggest this demonstrates increased resting coronary flow volume in AS patients with consequent reduced flow reserve and may partially explain higher resting native T1 values in AS patients (67). However this explanation contradicts our current understanding of the pathophysiology of LV decompensation that vascular bed expansion is insufficient to supply the hypertrophied myocardium leading to ischaemia (75-77).

In general, native T1 has demonstrated a good correlation with diffuse myocardial fibrosis on histological analysis (as assessed by collagen volume fraction (78-80)) although this has not been a universal finding (81). Moreover, histological analysis has only been performed on myocardial biopsy samples obtained at the time of surgical valve replacement and therefore T1 mapping measures in less advanced aortic stenosis have not been histologically validated.

Bull and colleagues first investigated the use of native T1 in 109 patients with moderate or severe aortic stenosis. Native T1 values were raised in patients with aortic stenosis compared to 33 age and sex matched controls. Both AV area and indexed LV mass were independently associated with native T1 values. (78). Several other studies have shown that native T1 is able to differentiate patients with AS from controls albeit with considerable overlap in values between the two groups (73,82,83). Chin and colleagues investigated various T1 mapping measures at 3 tesla (3T) in 20 patients with AS and 20 healthy volunteers. While native T1 had excellent intra and inter–observer variability and acceptable scan-rescan reproducibility, it was unable to discriminate between AS and control subjects (82). This finding may have been due to a wider spectrum of AS severity in this study (mild to severe) compared to the previous studies, which involved patients with more severe disease.

The accumulation of diffuse myocardial fibrosis leads to progressive impairment in LV function. Although no studies have yet shown a link between native T1 and reduced ejection fraction in aortic stenosis, native T1 has been associated with these earlier measures of left ventricular dysfunction. Lee and colleagues assessed 80 asymptomatic patients with moderate or severe aortic stenosis using 3T cardiac magnetic resonance and included echocardiographic speckle tracking imaging. Native T1 values showed a good correlation with measures of impaired global longitudinal strain and diastolic dysfunction (mean e' and left atrial volume) (79).

The immediate priority for introducing native T1 in clinical practice will be to establish normal native T1 values in healthy hearts and, therefore, to define cut-off values of abnormal levels of fibrosis in cardiac pathology. To date, two studies have attempted to do this in patients with AS. Lee and colleagues showed that at 3T, a cut off of 1190 ms could discriminate between moderate and severe AS with c-statistic of 0.704 (79). However, given the poor correlation between AS severity and the LV remodelling response, it may be more useful to identify native T1 cut-offs that predict future adverse events. In another recent study of 40 patients undergoing AV replacement (AS 77.5% and aortic regurgitation 15%) or root replacement (7.5%) with concurrent myocardial biopsies, Kockova and colleagues defined an optimum native T1 cut-off value of 1010 ms, generating a sensitivity of 90%, specificity of 73% and c-statistic of 0.82 to detect severe diffuse fibrosis on histology (defined as collagen volume fraction of >30%) (80).

A recent study has demonstrated the prognostic power of native T1. One hundred and twenty-seven patients with moderate or severe aortic stenosis were imaged with native T1 mapping at 3T. When split into tertiles of native T1, there was an increasing event rate (all-cause mortality and hospitalisation for heart failure) across the tertiles with an increase in events both pre and post valve replacement. Native T1 predicted events independent of Euroscore II and presence of LGE on the multivariable analysis (83).

The major limitation of native T1 is that the values obtained are specific to the sequence, scanner and magnetic field strength. As such, a reliable comparison between the clinical centres is challenging and has limited the development of validated reference ranges to define health and disease states, which in turn limits clinical applicability.

Post-contrast T1 and the Partition Coefficient

Intravenous gadolinium shortens the T1 values and localizes the extracellular space. These behaviours can be utilized in conjunction with T1 mapping to aid further in the assessment of diffuse myocardial fibrosis. The use of equilibrium CMR (where a constant intravenous gadolinium-based contrast media infusion is used to create contrast equilibrium) have been supplanted by dynamic equilibrium techniques (where imaging is performed at a set time following bolus administration when it is assumed to be a dynamic equilibrium between myocardial and blood gadolinium concentrations). However, the isolated post-contrast T1 values are highly dependent on an individual's gadolinium kinetics and the varying time to image post contrast administration results in poor scan-rescan reproducibility, limiting its clinical use (82).

Correction to post-contrast T1 values can be performed by calculating the partition coefficient (λ), which calculates the ratio of myocardial T1 to blood T1 and corrects for the variation caused by an individual's gadolinium contrast kinetics. It has a much improved scan-rescan variability compared to the isolated post-contrast T1 and differentiates AS from control subjects (82).

Extracellular Volume Fraction

The further use of the haematocrit to calculate the blood volume in turn allows the myocardial volume to be estimated (assuming contrast equilibrium between these two compartments). As gadolinium is purely extracellular, its distribution in the myocardial volume is equal to the extracellular volume (ECV) and this measure is termed ECV fraction (ECV%, Figure 1.8). Although the extracellular space contains not just collagen but other extracellular matrix components, including myocardial capillaries, the ECV% measure has been shown to correlate well with histological collagen volume fraction on myocardial biopsy samples in multiple studies of AS patients undergoing aortic valve replacement (80,84-86).

Extracellular volume fraction was first validated in AS in 2010 by Flett and colleagues who used equilibrium contrast CMR at 1.5T to investigate 18 patients with severe AS who underwent myocardial biopsy at the time of AV replacement. Extracellular volume fraction strongly correlated (r^2=0.86) with collagen volume fraction as assessed by picrosirius red quantification on histology (85). Equilibrium contrast CMR involved a highly complex protocol, requiring an extra 30-90 minutes of patient time in the radiology department.

Flett and colleagues went on to examine further the utility of ECV% using similar methods in 63 patients with severe AS undergoing AV replacement and 30 healthy controls (87). Diffuse myocardial fibrosis was estimated using a line

of best fit correlation between histological fibrosis (collagen volume fraction) and CMR obtained ECV% values from their previous study (85). Patients with AS had more diffuse myocardial fibrosis compared to control subjects (18 versus 13%) although these values overlapped significantly. Diffuse fibrosis was associated with diastolic dysfunction and impaired functional status as measured by 6-minute walk test independent of age, sex, LVEF, AV area and presence of LGE (87).

ECV% has excellent reproducibility and appears to have superior inter-observer, intra-observer and scan-rescan reproducibility compared to other T1 measures at 3T (82). This study used simplified dynamic equilibrium sequences using a contrast bolus injection with imaging performed 10-20 min post administration, which have been shown to give comparable results to the more complex equilibrium contrast infusion techniques. These bolus techniques have, therefore, almost universally been adopted. ECV% was also found to be significantly greater in patients with AS compared to healthy controls although a large degree of overlap was observed. Similar findings have been observed in other studies (87,88); however, the control populations in these studies were younger and common co-morbidities such as hypertension or diabetes were excluded. In another study, ECV% was unable to differentiate between patients with asymptomatic moderate or severe aortic stenosis in age, gender and co-morbidity matched controls; nevertheless, this study may have been under-powered (73).

As with native T1, establishing the normal range of ECV% values in healthy controls and disease specific cut-offs is essential for clinical utility. ECV% is much less dependent on scanning sequence and magnetic field strength but some variability may remain (84). The study by Kockova and colleagues showed that a cut-off ECV% of ≥0.32 was able to detect severe myocardial fibrosis (defined as >30% by histology) with a sensitivity of 80%, specificity of 90% and c-statistic of 0.85. The clinical utility of this cut-off and long-term prognostic value are unknown. Defining the clinically relevant cut-off values remains key. Overall, a higher ECV% has been shown to be predictive of all-cause mortality and heart failure admissions in heterogeneous populations with cardiac disease (excluding hypertrophic cardiomyopathy and amyloidosis); (89) however, this has not been examined in an aortic stenosis population to date.

Indexed Extracellular Volume

The limitation of current T1 measurement is that they universally show a substantial overlap between AS patients and healthy controls, limiting their clinical application. Although ECV% is conceptually a particularly attractive measure, it assesses diffuse fibrosis as a percentage of the left ventricular myocardial volume and, therefore, a measure of relative fibrosis. Compared to other myocardial pathology, this may be of less use in AS which is characterised by a reactive increase in both LV mass and diffuse myocardial fibrosis in response to sustained pressure overload. As such, the relative fibrosis may not change as disease progresses. An absolute measure of whole

heart fibrosis, such as the indexed extracellular volume (extracellular volume fraction x end-diastolic myocardial volume) may therefore be more useful in staging disease and tracking changes in fibrosis over time.

Figure 1.7: T1 mapping using a 3(3)-3(3)-5 MOdified Look-Locker Inversion recovery sequence

A T1 map is generated using a MOdified Look-Locker Inversion recovery (MOLLI) sequence. The sequence description denotes the number of heartbeats over which consecutive readouts occur with no readouts occurring for the number of heartbeats in brackets which allows for magnetisation recovery. Following a 180-degree inversion pulse, T1 readouts are performed at the same point in the cardiac cycle on consecutive heartbeats (usually end-diastole). Two further inversion recovery experiments are performed with different inversion times (TI) and the raw images are ordered by inversion time. The signal is then plotted against TI for each voxel and a best-fit curve is generated. The T1 value for each voxel (time taken to recover 63% of longitudinal magnetisation) is the estimated and displayed visually as a T1 map.

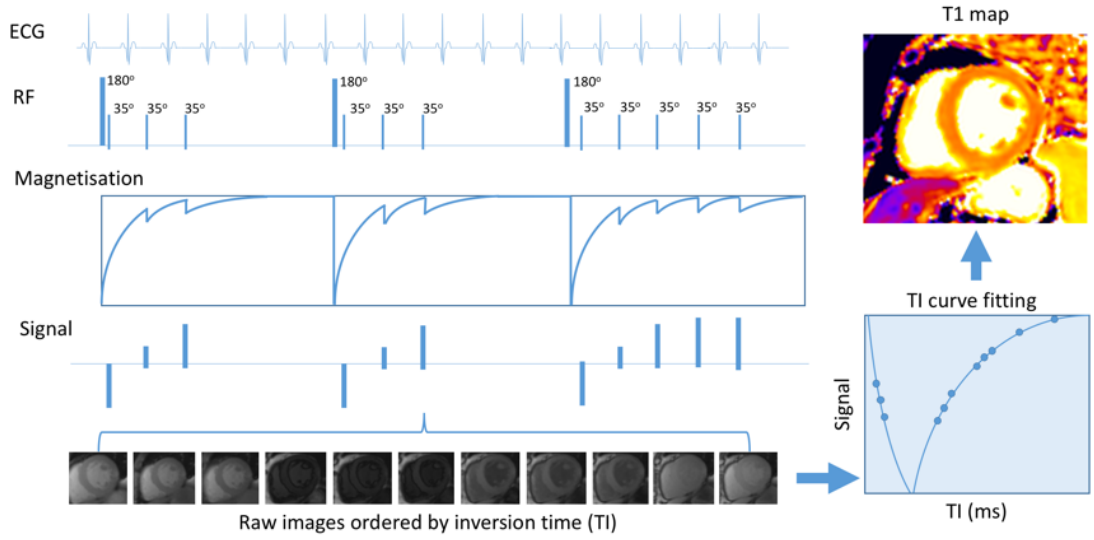

ECG, electrocardiogram; RF, radiofrequency; TI, inversion time

Figure 1.8: Different forms of T1 mapping available

Native T1 maps are produced as detailed above (Figure 1.7). This process can then be repeated 10-20 minutes following intravenous contrast administration to generate post-contrast T1 maps. Note that T1 is shortened in the presence of gadolinium. Extracellular volume fraction can be calculated either using regions of interest drawn onto myocardium and blood pool on pre and post contrast maps (shown below, red endocardial contour, green epicardial contour, orange blood pool region of interest) or by combining the native and post contrast maps to generate an ECV map where the ECV for each voxel is demonstrated. Myocardial regions of interest are usually offset to avoid signal contamination by either blood pool or epicardial fat (10% contour offset shown below).

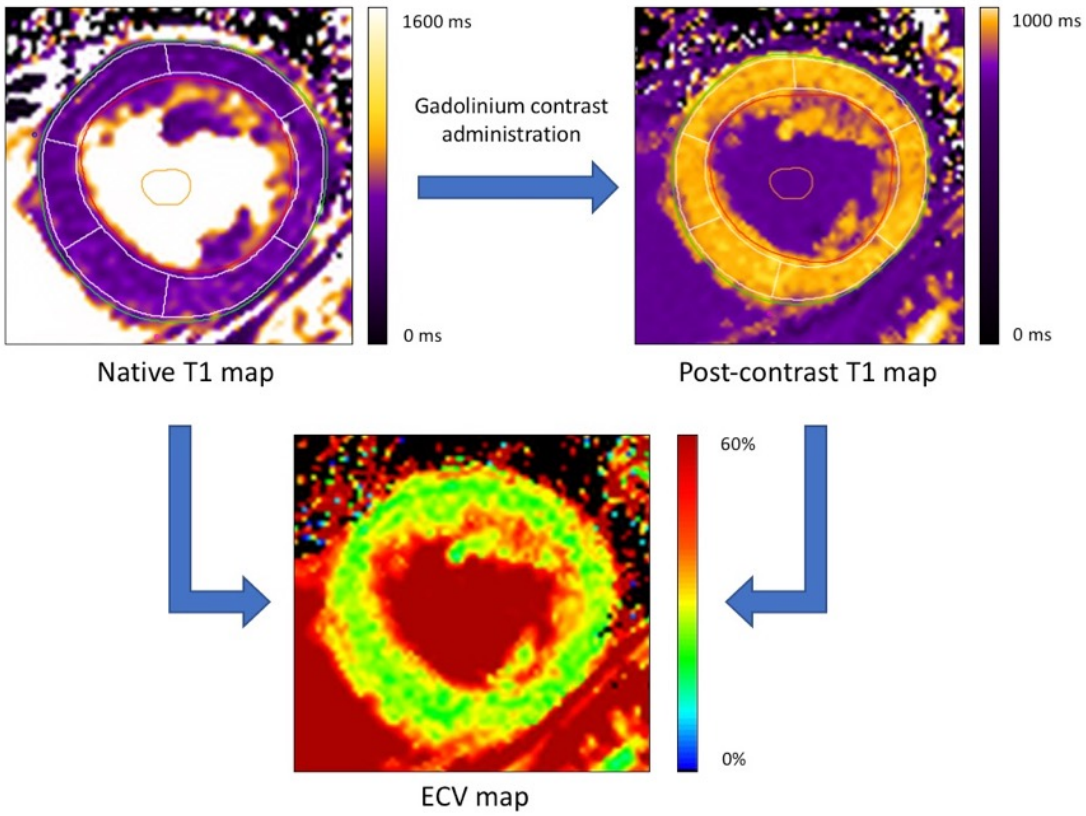

ECV, extracellular volume fraction; ms, millisecond

HYBRID MAGNETIC RESONANCE IMAGING / POSITRON EMISSION TOMOGRAPHY TECHNIQUES

Positron emission tomography in aortic stenosis

Positron emission tomography involves the intravenous administration of radioactive tracer compounds that allow the activity of specific disease processes to be measured *in-vivo*. This technique has been previously investigated in aortic stenosis using two radiotracers to measure inflammation (^{18}F-fluorodeoxyglucose [^{18}F-FDG]) and calcification activity (^{18}F-sodium fluoride [^{18}F-NaF) in the aortic valve. Hybrid PET/CT scanners then allow the activity of these two key processes to be compared with macroscopic findings such as the presence of established regions of macrocalcification on CT.

^{18}F-Fluorodeoxyglucose

^{18}F-FDG PET is widely used to image vascular inflammation. This PET tracer is a glucose analogue, which accumulates in metabolically active cells such as vascular macrophages. Indeed an excellent correlation between macrophage burden on histology (CD68 staining on immunohistochemistry) in carotid atheroma (90) and the ^{18}F-FDG signal has been observed. In aortic stenosis, ^{18}F-FDG activity is higher in patients compared with control subjects, demonstrating a modest correlation with severity of valvular disease (91). Of interest, no correlation with CD68 staining of explanted valves was observed suggesting that ^{18}F-FDG uptake is occurring in other metabolically active cells, although this study was limited by a low sample size (4). Perhaps the biggest

limitation of this technique is the effect of physiological myocardial ^{18}F-FDG uptake, which frequently contaminates signal originating from the aortic valve.

^{18}F-Fluoride

^{18}F-Fluoride has been used as a bone tracer for 50 years as it binds to hydroxyapatite and reflects regions of increased bone activity. In the vasculature it binds preferentially to regions of newly developing microcalcification because the surface area of hydroxyapatite in these nanocrystalline regions is at its highest. By contrast, in regions of macrocalcification, much of the hydroxyapatite is internalised and not available for binding (92). In aortic stenosis, ^{18}F-fluoride acts as a marker of calcification activity correlating with histological staining for alkaline phosphatase (r=0.65) and osteocalcin (r=0.68)(4) and predicts where novel regions of macroscopic calcium are going to form. Tracer uptake increases with more advanced aortic stenosis (91), offers powerful prediction of disease progression at 1 and 2 years, has some incremental value to computed tomography (4,93) and acts as an independent predictor of adverse clinical events (93). This technique holds promise in better understanding the role of calcification in aortic stenosis, for example a recent PET study demonstrated that, whilst calcification activity in aortic stenosis is greater than inflammation, the reverse is true in atherosclerosis, potentially explaining the differential effects of statins in these two conditions (94). With further research, ^{18}F-fluoride PET may prove of clinical utility in identifying patients likely to progress rapidly towards surgery

and as an efficacy end-point in clinical trials of novel therapies (e.g. SALTIRE 2: NCT02132026).

Hybrid MR/PET imaging

Although PET/CT offers excellent anatomical resolution, it is associated with a substantial radiation dose. Hybrid MR/PET imaging offers numerous advantages over PET/CT; simultaneous acquisition of PET and MR data for more accurate co-registration, reduction in radiation exposure, additional functional imaging and myocardial tissue characterisation. Commercial MR/PET platforms have recently become available; the key technological advancement making this possible has been the development of semi-conductor based PET detectors, which are not affected by a strong magnetic field unlike the photo-multiplier tubes historically used in PET scanners (95). However other technical challenges to optimise image quality and accuracy remain.

Attenuation correction

PET activity is detected and localised by deriving the line of response from the detection of two photons by the ring of PET detectors that correspond to a single annihilation event (coincidence event). However, coincidence events can be missed by attenuation of photons in radiodense tissues or scatter outside the field of view, and this may result in underestimation of PET activity from tissues deep within the body or next to radiodense structures. As such, attenuation maps (μ-maps) that contain the radiodensity for 511 keV photons

(the energy of photons produced by an 18F positron-electron annihilation event) of each voxel within the PET field-of-view must be produced. This has historically been performed using an external source ^{68}Germanium transmission scan or more recently with a CT μ-map (using 80-140 keV where a correction factor must be applied to convert to the radiodensity for 511 keV photons) (96). The μ-map is then used in the MR attenuation correction (MRAC) process during post-processing to produce a valid representation of regional PET activity.

Attenuation correction in MR/PET poses additional challenges as no external ionising radiation source is present to generate the μ-map. Instead the most common approach has been using a multi-point Dixon sequence for segmentation of the imaged field of view into four classes: air (background), lung, fat and soft tissue. A separate linear attenuation coefficient (LAC, which estimates the attenuation for 511 keV photons) for each tissue class is then applied to each voxel as appropriate. Of note, this sequence does not segment calcium or bone into a separate class. Potential solutions to this include ultrashort echo time (UTE) sequences and the addition of major bones as a separate tissue class using a patient-specific atlas (97).

MRAC μ-maps are usually acquired during breath-held expiration which do not correspond well with the average position of intrathoracic organs during 50-60 min of free-breathing PET acquisition and can result in significant image artefact on the final co-registered images. MRAC using a free-breathing

golden angle radial spoiled GRE acquisition has been proposed as a solution and initial experience suggests this results in improved image quality with a reduction in PET artefacts (98).

Identification of co-existent myocardial pathology

One further advantage of hybrid MR/PET techniques is the identification and characterisation of coexistent myocardial pathology. Transthyretin cardiac amyloidosis is an increasingly recognised condition in the elderly due to the availability of more advanced imaging methods in clinical practice. Transthyretin (TTR) is a 127-amino acid plasma protein predominantly produced by the liver that exists as a tetramer of four identical subunits and acts as a binding protein for thyroxine and retinol-binding protein (99). Although several gene mutations have been identified that lead to destabilisation of the TTR tetramer, amyloid fibril assembly and cardiac deposition occurs most frequently in individuals with non-mutated “wild-type” TTR (wtTTR, also called senile systemic amyloidosis). Why some individuals with wtTTR develop clinically significant cardiac deposition of amyloid fibrils is not understood, but this process is associated with advancing age and appears more common in men (100). Over time, ongoing amyloid deposition leads to ventricular thickening, progressive diastolic dysfunction and cardiac rhythm disturbance eventually resulting in systolic dysfunction, symptomatic heart failure and death. A novel disease-modifying treatment for TTR cardiac amyloidosis has recently become available (101) and other agents are currently undergoing phase 2/3 clinical trials (102).

Cardiac amyloidosis has historically been suspected when concentric LV hypertrophy with a speckled appearance to the myocardium is visualised on echocardiography (103). However, this speckled-appearance is much less specific to amyloidosis using modern echocardiography machines that utilise harmonic imaging. Other imaging findings of pericardial effusion and thickened interatrial septum and AV valves, have poor sensitivity and specificity for amyloidosis, particularly in patients with aortic stenosis (104).

Whilst historically requiring invasive myocardial biopsy for confirmation, the variety of modern imaging techniques now available enable a diagnosis of cardiac amyloidosis to be made non-invasively in most patients. Histological confirmation of subtype (TTR versus AL amyloid) is still important as both treatment and prognosis are different. Global longitudinal strain, as measured using transthoracic echocardiography is significantly reduced in cardiac amyloidosis, with characteristic sparing of the apex giving a “bull’s eye” appearance (105). In addition to providing more accurate measures of LV volumes, mass and ejection fraction, CMR also offers tissue characterisation with LGE and T1 mapping techniques. Two LGE patterns are recognised in patients with cardiac amyloidosis, circumferential subendocardial and transmural, with increasing burden portending a worse survival (106). Phase-sensitive inversion recovery (PSIR) techniques are superior to magnitude only imaging in this setting as the tissue with the longest TI is always nulled ensuring diagnostic images where transmural involvement is present (106).

T1 mapping techniques are of particular interest in the diagnosis of cardiac amyloidosis as gross extracellular deposition of amyloid usually results in dramatic increases in both native T1 and ECV% which overlap minimally with other pathologies. In one recent study, both native T1 (area under curve (AUC) 0.87) and ECV% (AUC 0.91) were able to differentiate cardiac amyloidosis from hypertrophic cardiomyopathy with high diagnostic accuracy. Moreover, ECV% predicted all-cause mortality independent of measures including BNP, LV ejection fraction and LGE (107).

Bone scintigraphy has also proven a powerful tool in diagnosing cardiac amyloidosis. Although the underlying mechanisms are unclear, ^{99m}Technicium-3,3-diphosphono-1,2-propanodicarboxylic acid (^{99m}Tc-DPD), along with other bone radiotracers has high diagnostic sensitivity and specificity for the presence of TTR cardiac amyloidosis (108). Uptake is qualitatively assessed by the Perugini score (0-3, 0= no cardiac uptake, 1= cardiac uptake less than bone uptake, 2= cardiac uptake equal to or greater than bone uptake, 3= cardiac uptake with attenuation or absence of bone uptake). Although a score of 2 or 3 is considered diagnostic for cardiac involvement, DPD scan grading offers no further prognostic information (109). This test is highly specific for TTR amyloidosis, although one study suggested that minor cardiac uptake could be seen in up to a third of patients with AL amyloid (110).

Prevalence of co-existent TTR amyloidosis and aortic stenosis

Given that the imaging features on standard echocardiography are similar to that seen in advanced aortic stenosis, a diagnosis of amyloidosis is often not considered in these patients. In fact, the prevalence of coexistent amyloidosis has been estimated at between 6 and 16% of severe AS populations (104,111). Interestingly in one recent study, of the 6 aortic stenosis patients with confirmed TTR amyloid deposition on histological analysis of myocardial biopsies, only two had clear imaging features diagnostic of CMR whereas the other four had features that were compatible with a sole diagnosis of severe aortic stenosis (104). All patients who survived to ^{99m}Tc-DPD imaging (4 out of 6) had positive scans (although 50% of these were only Perugini grade 1). This suggests that the sensitivity of CMR in the early diagnosis of cardiac TTR amyloidosis may be improved by the addition of a PET with a bone radiotracer such as ^{18}F-NaF. One small study demonstrated this proof-of-concept; 4 patients with biopsy proven TTR cardiac amyloidosis, along with 3 AL-amyloid and 7 healthy control subjects were imaged with MR/PET using 386 megabequerels (MBq) 18F-NaF. Myocardial target-to-background-ratio (TBR) was significantly greater in the TTR group (1.14±0.24) compared with AL (0.77±0.06) or healthy controls (0.68±0.04, Figure 1.9) (112). Importantly, 18F-NaF appears to discriminate between TTR and AL amyloidosis which would be another incremental advantage over standard CMR imaging.

Figure 1.9: Hybrid MR/PET with 18F-sodium fluoride in a patient with familial TTR amyloidosis

Short axis LGE image fused with PET data showing increased 18F-NaF uptake in the inferolateral wall co-localising to areas of LGE (white arrows). Maximum myocardial target to background ratios (TBR) were 48% greater than AL amyloid and 68% higher than control subjects (A), both of whom demonstrated TBR values below 1. Dynamic imaging assessing TBR mean values (B) showed optimal separation of values ≥ 60 minutes.

Images reproduced from Trivieri et al, JACC 2016 (112)

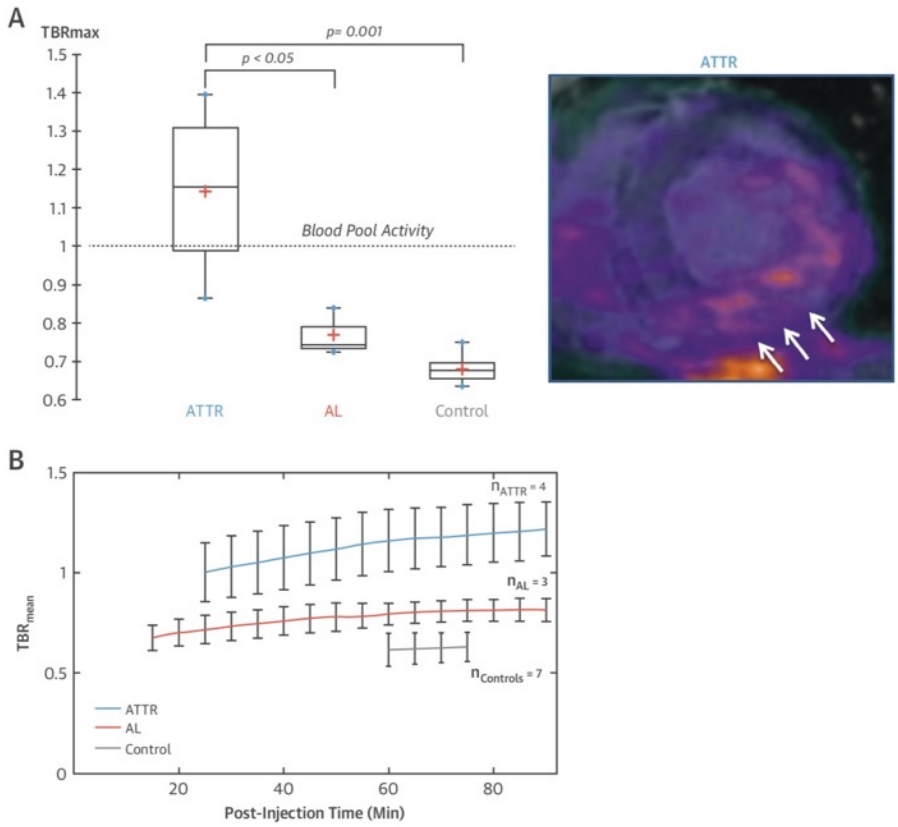

SUMMARY

Aortic stenosis is characterised by both valvular stenosis and the resultant left ventricular response, namely myocyte hypertrophy eventually leading to cell death, myocardial fibrosis and systolic dysfunction. Valve intervention can alleviate the dismal clinical course of advanced aortic stenosis, but the optimal timing of intervention is controversial, based on historical observational data and expert opinion. Risks of valve intervention must be balanced against the risks of sudden death or long-term complications due to ventricular decompensation. The ideal time to intervene is just before the onset of irreversible left ventricular pathological changes.

CMR imaging provides non-invasive multiparametric assessment of the left ventricle which can identify focal replacement fibrosis using late gadolinium enhancement and diffuse fibrosis with T1 mapping methods. The addition of PET imaging using hybrid MR/PET scanners also provides added information about metabolic processes and may be able to identify co-existent myocardial pathology. Further work is required to explore how these novel imaging modalities can be integrated into clinical practice.

THESIS AIMS AND HYPOTHESES

The aims of this thesis are:

1. To explore the utility of T1 mapping measures as surrogate markers of diffuse fibrosis burden, left ventricular decompensation and predictors of adverse outcomes

2. To characterise the progression of myocardial hypertrophy, diffuse and replacement fibrosis over time in asymptomatic severe AS and how these processes are influenced by relief of pressure overload with valve replacement

3. To assess the prognostic utility of T1 mapping measures and their associations with other markers of LV decompensation in a large multicentre cohort of symptomatic patients with severe aortic stenosis undergoing aortic valve replacement procedures

4. To investigate MR/PET imaging in aortic stenosis patients for assessment of AS severity, disease activity and the presence of LV decompensation and co-existent myocardial pathology

The hypotheses of this thesis are:

1. T1 mapping can identify a group of patients with abnormally increased diffuse fibrosis who have an intermediate measures of LV decompensation between normal levels of fibrosis and those with advanced replacement fibrosis (Chapter 3).

2. In the natural history of aortic stenosis, both cellular hypertrophy and diffuse fibrosis progress at a steady rate and new areas of late enhancement develop between interval scans. Following valve replacement, cellular hypertrophy and diffuse fibrosis regress but replacement fibrosis is irreversible (Chapter 4).

3. Extracellular volume-based T1 mapping measures are independently associated with measures of disease severity and worse clinical outcome in a large cohort of patients undergoing valve intervention (Chapter 5).

4. MR/PET imaging with free-breathing attenuation correction is feasible and reproducible in aortic stenosis and may be able to quantify calcification activity in the aortic valve and identify cases of co-existent TTR amyloidosis (Chapter 6).

Chapter 2: Methodology

PATIENT POPULATIONS

Patients with mild to severe aortic stenosis were recruited to an observational research study (Role of Fibrosis in Aortic Stenosis, NCT01755936, "CMRAS study"). These patients were prospectively recruited at the Edinburgh Heart Centre, United Kingdom. Written informed consent was provided by all participants and the ethical approval was obtained from the South East Scotland Research Ethics Committee. The study was conducted in accordance with the Declaration of Helsinki.

The exclusion criteria were: (1) moderate or severe other valve disease; (2) significant comorbidities with a predicted life expectancy of less than 1 year; (3) contraindications to CMR imaging (such as implantable cardiac devices); (4) significant renal impairment precluding intravenous gadolinium contrast administration (estimated glomerular filtration rate <30 mL/min/1.73m^2) and (5) inherited or acquired cardiomyopathy. The presence of coronary heart disease was defined as clinical symptoms of angina (in non-severe aortic stenosis), previous myocardial infarction, obstructive coronary artery disease on anatomical imaging or evidence of significant ischaemia on functional imaging.

Patient populations from other centres were included for specific analyses (Chapters 4 and 5) as detailed below:

Chapter 4: To investigate the progression of hypertrophy and myocardial fibrosis, only those patients with repeat CMR from the CMRAS study were included. These were combined with similar patients from an observational study in Quebec, Canada (PROGRESSA, NCT01679431).

Chapter 5: In order to investigate the prognostic utility of ECV-based T1 mapping measures, a large international multicentre cohort was formed. Inclusion criteria were patients with severe aortic stenosis scheduled for aortic valve intervention who underwent CMR imaging prior to their procedure. This included patients from the Edinburgh CMRAS cohort, as well as additional data from Leeds, Leicester, Oxford and London. Further patients meeting the inclusion criteria from Berlin (Germany), Quebec (Canada), Pittsburgh (U.S.A) and Seoul (South Korea) were included. All patients were enrolled in observational studies in accordance with local research ethics governance and conforming to the Declaration of Helsinki. Appropriate legal agreements were produced to cover the international transfer of anonymised data.

A separate cohort of patients and healthy volunteers were recruited to investigate the utility of PET/MRI in aortic stenosis ("PASS" study, Chapter 6). These participants were aged 70 or over and the aortic stenosis patients had been referred for aortic valve intervention. The exclusion criteria were (1) moderate of severe other valve disease; (2) contraindications to CMR imaging (such as implantable cardiac devices); (3) significant renal impairment precluding intravenous gadolinium contrast administration (estimated

glomerular filtration rate <30 mL/min/1.73m2); (4) acute valvular heart disease and (5) acute pulmonary oedema or cardiogenic shock.

Further details concerning each cohort are available within each results chapter.

ECHOCARDIOGRAPHY

Transthoracic echocardiography is the primary non-invasive imaging method for assessment of valvular stenosis. This modality uses ultrasonography to produce 2D cardiac images in a variety of imaging planes with high temporal and spatial resolution. In addition, the use of colour flow mapping alongside both pulsed and continuous wave Doppler techniques enables detailed assessment of severity of valve stenosis (113). Both peak and mean valvular gradient can be measured using continuous wave Doppler aligned to the blood flow through the aortic valve, and effective aortic valve area can then be calculated using the continuity equation (aortic valve area = Doppler stroke volume / aortic valve velocity-time integral; Doppler stroke volume = left ventricular outflow tract velocity-time integral x left ventricular outflow tract area).

Comprehensive transthoracic echocardiography was performed in all patients (iE33, Philips Medical Systems, The Netherlands). Careful attention was given in the assessment of aortic stenosis severity. The left ventricular (LV) outflow tract diameter was measured in the parasternal long-axis view, at the insertion of the aortic cusps from the inner edge of the septal endocardium to the inner edge of the anterior mitral leaflet in mid-systole. Left ventricular outflow tract velocity-time integral was measured in the apical 5-chamber view using pulsed-wave Doppler just proximal to the aortic valve, with care taken to obtain a laminar spectral tracing. The peak aortic jet velocity and mean transvalvular gradient were derived from the aortic valve velocity-time integral,

using continuous-wave Doppler. The highest aortic jet velocity and mean transvalvular gradient were determined in multiple acoustic windows using both standard and standalone doppler probes. The mean of 3 readings (5 if the patient had atrial fibrillation) was recorded. Aortic valve area was calculated using the continuity equation.

Trans-mitral early (E) and late diastolic velocities, as well as, deceleration time of early filling velocity were measured at the tips of the mitral valve leaflets using pulsed-wave Doppler. The mean early diastolic velocities of the medial and lateral mitral annulus (e') were measured using pulsed-wave tissue Doppler imaging. Diastolic function was assessed as recommended in recent guidelines (114).

Echocardiography is highly reproducible when performed by experienced operators. We have previously demonstrated excellent intraobserver (4.9%) and interobserver (6.9%) variability of aortic valve area measurement in our centre (115).

CARDIOVASCULAR MAGNETIC RESONANCE

Magnetic resonance imaging utilises a strong static magnetic field, variable gradient magnetic fields and radiofrequency energy to produce highly detailed 3-dimensional images. Protons (most abundantly found in biological tissue as part of water molecules) will align their magnetic moments in the presence of a strong magnetic field producing a net magnetisation. This magnetisation can be altered (excitation) by the use of radiofrequency energy applied at the correct frequency, following which the excited tissue returns to equilibrium in a process called relaxation. This signal can be detected by radiofrequency receiver coils and is spatially localised and encoded by the application of variable gradient magnetic fields. Decoding of the signal is then performed to generate an MR image. This technology is increasingly being used in cardiac imaging where a combination of ECG gating with patient breath-holding or respiratory navigated sequences can produce high-resolution images in spite of cardiac and respiratory motion.

Cardiovascular magnetic resonance (CMR) imaging in Edinburgh was performed at 3T (MAGNETOM Verio, Siemens AG, Erlangen, Germany) in the Edinburgh Imaging Facility at the Queen's Medical Research Institute. Localiser views were first obtained to determine the position and orientation of the heart within the thorax. Multiple cine acquisitions were performed a balanced steady-state free precession sequence to obtain both long and short-axis cine images. Short axis cines were acquired extending from the mitral

valve to the left ventricular apex (8-mm parallel slices with 2-mm spacing; temporal resolution ≤45 ms) and used to determine left ventricular volumes, mass and systolic function.

Focal replacement and diffuse interstitial myocardial fibrosis were assessed in all patients using late gadolinium enhancement (LGE) and myocardial T1 mapping, respectively. Late gadolinium enhancement was performed 15 min following gadobutrol (Gadovist, Bayer Pharma AG, Germany, 0.1 mmol/kg) using an inversion-recovery fast gradient-echo sequence performed in two phase-encoding directions to differentiate true late enhancement from artefact. The inversion time was optimized to achieve satisfactory nulling of the myocardium.

Diffuse myocardial fibrosis was assessed using Modified Look-Locker Inversion-recovery with built-in motion correction. A heart beat acquisition scheme of 3(3)-3(3)-5 was used (flip angle 35°; minimum TI 100 ms; TI increment of 80 ms; time delay of 150 ms) (70,116,117). A gradient echo field map and associated shim were performed to minimize off-frequency artefact.

For the analysis in Chapter 4, included patients from Quebec were scanned locally at either 1.5 or 3T (ACHIEVA and INGENIA, Philips Healthcare, Best, the Netherlands). All patients were rescanned using standardised imaging protocols (Short axis cine imaging: 8 mm parallel slices with no gap. Typical parameters at 1.5T were FOV 380 mm, TR/TE 3.2/1.6 ms, flip angle 60º and

NEX of 1, in-plane spatial resolution of 1.6 x 2 mm. Equivalent acquisition parameters at 3T were FOV 380 mm, TR/TE 2.8/1.3 ms, flip angle 45º, and NEX of 1, in-plane spatial resolution of 1.7 mm x 2 mm, 7-mm slice thickness, 0-mm gap.). Late enhancement was performed using 0.2 mmol/kg gadobutrol contrast. T1 mapping was performed using a MOLLI acquisition scheme of 5(3)-3 pre-contrast and either 5(3)-3 (1.5T) or 4(1)-3(1)-2 (3T) post-contrast (118).

For the international multicentre analysis in Chapter 5, patients were imaged using local scanners and protocols which are summarised in Table 2.1. Further details are contained within Chapter 5.

CMR offers superior accuracy and reproducibility when assessing left ventricular volume and mass compared with echocardiography (119). In particular, excellent intra- and inter-observer variability has been demonstrated for left and right ventricular volume and mass measurements, with slightly worse values for ejection fraction, where potential measurement errors from multiple measurements are compounded (Table 2.2) (120).

Both native T1 and extracellular volume fraction (ECV%) have excellent intra- and inter-observer reproducibility at 3T as demonstrated at our centre, with ECV% having superior scan-rescan reproducibility compared to other T1 mapping measures (Table 2.3) (82).

Table 2.1: ECV400 study - cardiac magnetic resonance technical details by study centre

Site	Scanner	T1 mapping pre	T1 mapping post	Time to PC imaging	Contrast agent and dose
Edinburgh Heart Centre, UK	Siemens Verio 3T	MOLLI 3(3)-3(3)-5	MOLLI 3(3)-3(3)-5	20 mins	Gadobutrol 0.1 mmol/kg
Leeds Teaching Hospitals NHS Trust, UK	Phillips Achieva 1.5T	MOLLI 5(3)-3	MOLLI 4(1)-3(1)-2	15 mins	Gadoteric acid 0.2 mmol/kg
Glenfield Hospital, Leicester, UK	Siemens 1.5T Skyra 3T	MOLLI 3(3)-3(3)-5	MOLLI 3(3)-3(3)-5	20 mins	Gadobutrol 0.15 mmol/kg
Barts Heart Centre, London, UK	Siemens Avanto 1.5T	MOLLI 5(3)-3 ShMOLLI 5(1)-1(1)-1	MOLLI 4(1)-3(1)-2 ShMOLLI 5(1)-1(1)-1	15 mins	Gadoteric acid 0.10 mmol/kg
John Radcliffe Hospital, Oxford, UK	Siemens Trio 3T	ShMOLLI 5(1)-1(1)-1	ShMOLLI 5(1)-1(1)-1	15 mins	Gadodiamide 0.03 mmol/kg Gadoteric acid 0.10 mmol/kg
HELIOS Hospital Berlin-Buch, Berlin, Germany	Siemens Verio 3T	MOLLI 3(3)-3(3)-5	MOLLI 3(3)-3(3)-5	10 mins	Gadobutrol 0.20 mmol/kg
University of Pittsburgh Medical Centre, Pittsburgh, PA, U.S.A.	Siemens Espree 1.5T	MOLLI 5(3)-2	MOLLI 4(1)-3(1)-2	20 mins	Gadobutrol 0.20 mmol/kg Gadoteridol 0.20 mmol/kg
Quebec Heart and Lung Institute, Quebec, Canada	Phillips Achieva 1.5T Ingenia 3T	MOLLI 5(3)-3 MOLLI 5(3)-3	MOLLI 5(3)-3 MOLLI 4(1)-3(1)-2	15 mins	Gadobutrol 0.20 mmol/kg
Seoul National University Hospital, Seoul, South Korea	Siemens Trio 3T	MOLLI 3(3)-3(3)-5	MOLLI 3(3)-3(3)-5	10 mins	Gadopentetic acid 0.20 mmol/kg

Table 2.2: Reproducibility of Cardiovascular Magnetic Resonance Imaging Measures of Left and Right Ventricular Size and Function (n=60)

Measure	Coefficient of variability	Repeatability coefficient	Intraclass correlation coefficient	
			Intra-observer	Inter-observer
Indexed left ventricular end-diastolic volume, mL/m^2	3.6	8.2	0.993	0.989
Indexed left ventricular end-systolic volume, mL/m^2	10.5	8.4	0.967	0.939
Indexed left ventricular stroke volume mL/m^2	6.6	8.0	0.976	0.973
Left ventricular ejection fraction, %	5.8	9.4	0.824	0.789
Indexed left ventricular mass, g/m^2	5.3	7.7	0.985	0.981
Indexed right ventricular end-diastolic volume, mL/m^2	6.4	24.4	0.991	0.977
Indexed right ventricular end-systolic volume, mL/m^2	13.0	19.2	0.982	0.950
Indexed right ventricular stroke volume, mL/m^2	11.8	19.2	0.969	0.947
Right ventricular ejection fraction, %	8.0	10.7	0.874	0.810

Adapted from Mooij et al, J Magn Reson Imaging, 2008 (120)

Table 2.3: Reproducibility of T1 mapping measures at 3 Tesla (n=40)

Measure	Intraclass correlation coefficient		
	Intra-observer	Inter-observer	Scan-rescan
Blood pool native T1, ms	1.00	1.00	0.65
Myocardial native T1, ms	0.99	0.99	0.72
Blood pool post-contrast T1, ms	1.00	1.00	0.58
Myocardial post-contrast T1, ms	1.00	1.00	0.56
Partition coefficient	0.99	0.94	0.93
Extracellular volume fraction, %	1.00	0.97	0.96

Adapted from Chin et al, Eur Heart J Cardiovasc Imaging 2014 (82).

HYBRID MAGNETIC RESONANCE IMAGING / POSITION EMISSION TOMOGRAPHY

Positron emission tomography (PET) allows for the localization and assessment of activity of functional metabolic processes. For example, the radioactive isotope fluorine-18 decays via positron emission to oxygen-18 with a half-life of 109.8 mins. This positron travels a short distance (usually <1 mm, maximum 2-3 mm (121)) before interacting with an electron in an annihilation event that creates two gamma ray photons travelling in opposite (180 degrees) directions. When multiple positron decays occur in this way inside a ring of detectors, the emission source can be spatially localised with a high degree of accuracy (4-6 mm (121,122)). PET is an extremely sensitive technique requiring only very small amounts of radiotracer (10^{-6} – 10^{-9} g) which have essentially no pharmacological effects, allowing the measurement of metabolic processes without disturbing these processes (123). As discussed in chapter 1, integration of PET with magnetic resonance imaging (MR/PET) allows accurate co-registration of PET data but optimizing methods of attenuation correction and cardiac and respiratory motion correction require further research.

MR/PET imaging was performed at 3T using a Siemens Biograph mMR scanner (Siemens AG, Erlangen, Germany). The body transmission coil, a flexible 6-channel body arrayed receiver, and a 6-channel spine arrayed receiver mounted in the scanner table were used to acquire MR data. PET

data were acquired in list-mode 60 min after intravenous injection of 250 MBq of ^{18}F-sodium fluoride. Both 3D Dixon VIBE (124) and free-breathing radial gradient echo (GRE, Siemens work-in-progress #793F) sequences were acquired for MR attenuation correction (MRAC). MRAC maps were generated using the method described by Robson et al (98). The MR protocol included standard long- and short-axis cine imaging. Coronary magnetic resonance angiography (CMRA) was performed using a non-contrast ECG-gated respiratory-navigated motion corrected (MC) proprietary sequence (iNAV-based MC CMRA, Kings College London, UK (125)) to achieve a high-resolution isotropic 3D data volume encompassing proximal coronary arteries, aortic valve and left ventricular myocardium which could be fused with the PET dataset. T1 mapping was performed using a MOLLI sequence (native 5(3)-3, post contrast 4(1)-3(1)-2, MyoMaps product, Siemens) using a single 4-chamber slice both before and 15-20 minutes after 0.1 mmol/kg of intravenous gadobutrol contrast (Gadovist, Bayer Pharma AG, Germany). Late gadolinium enhancement was performed approximately 10 min following contrast injection using phase-sensitive inversion recovery sequences (short axis stack and 4 chamber views).

The Biograph mMR scanner has a spatial resolution of 4.3 mm (full-width-at-half-maximum) (126). We have previously demonstrated excellent intra- and inter-observer variability for aortic valve standardized uptake values (SUV_{max}) using PET/CT (intraclass correlation coefficients 1.00 and 0.99 respectively (91)) but this has not been assessed to date using MR/PET.

ELECTROCARDIOGRAM

In all patients recruited at Edinburgh Royal Infirmary, a standard 12-lead electrocardiogram was performed (10 mm/mV, 25 mm/s) using the same machine (Philips Pagewriter TC50, Philips Medical Systems, Massachusetts, U.S.A). An electrocardiographic diagnosis of left ventricular hypertrophy was determined by a Romhilt-Estes system score of greater than or equal to 5 (127). Left ventricular strain was defined as down-sloping ST-segment depression $\geq$1 mm with asymmetrical T-wave inversion in the lateral ECG leads.

CARDIAC BIOMARKERS

Plasma cardiac troponin I concentrations were determined in the CMRAS study using the ARCHITECT STAT high-sensitivity cTnI assay (Abbot Laboratories, Abbott Park, Il, USA) (54). The lower limit of detection of this assay is 1.2 ng/L with a 10% inter-assay coefficient of variation at 4.7 ng/L.

The brain natriuretic peptide (BNP) concentration was determined with Triage BNP assay (Biosite Inc., San Diego, CA, USA) for the CMRAS patients detailed in Chapter 3.

INTRA-OPERATIVE MYOCARDIAL BIOPSY AND HISTOLOGICAL ANALYSIS

All patients who were enrolled in either CMRAS or PASS studies who underwent surgical aortic valve replacement were approached regarding intra-operative myocardial biopsy at the time of surgery. Biopsies were obtained from the basal muscular septum 2 cm below the outflow tract using a 14-gauge coaxial needle (BD Carefusion, Tru-cut needle) and samples were then fixed in 10%-buffered formalin and embedded in paraffin.

Processed samples were stained with picrosirius red and analysed using an automated segmentation tool (Image-pro plus 7, Rockville, MD, USA, an average eight regions per sample) to quantify myocardial fibrosis by calculated the area stained with picrosirius red as a percentage of the total myocardial area.

For samples from the PASS study, histological analysis to determine the presence of amyloidosis was performed at the National Amyloidosis Centre, Royal Free Hospital, London, UK. All samples were staining with Congo red and analysed using bright-field and cross-polarised light. If a diagnosis of cardiac amyloidosis was suggested by the presence of apple-green birefringence, immunohistochemistry was then performed using a TTR antibody (PA5-35315, ThermoFisher Scientific).

IMAGE ANALYSIS

Cardiovascular magnetic resonance

For the original baseline CMRAS data (Chapter 3), the left ventricular volumes mass and function were analysed using Argus Ventricular Function software (Siemens AG Healthcare Sector, Erlangen, Germany). Both papillary muscles and minor trabeculations were included in the LV intracavity volume measurement (and therefore excluded from the mass measurement). The presence of myocardial late gadolinium enhancement was determined by two experienced cardiologists (Dr Marc Dweck and Dr Calvin Chin). Quantitative analysis using a threshold of >2 standard deviations above the mean value in a region of normal myocardium was performed using QMASS software (Medis Medical Imaging Systems, Leiden, the Netherlands). Areas of inversion artefact were excluded as were areas of partial voluming with blood pool or epicardial fat. The motion-corrected scanner generated short-axis T1 maps at mid-ventricular level were used for the quantitative T1 mapping analysis (OsiriX version 4.1.1, Geneva, Switzerland). Placement of regions of interest were standardised so as to avoid partial voluming effects with blood pool or epicardial fat. These regions were then copied onto the post-contrast maps with adjustment to allow for artefacts (Figure 2.1).

All image analysis in Chapters 4 through 6 were performed using CVI42 software (Circle Cardiovascular Imaging Inc., Calgary, Canada). This involved reanalysis of the relevant baseline CMR scans from the CMRAS cohort

included in Chapters 4 and 5. Volumetric image analysis was performed by a single reporter (RJE) in two studies (Chapters 4 and 6) and for the final study (ECV400 study, Chapter 5) was performed by several reporters. All scans were analysed in line with an image analysis protocol (see appendix) and was performed according to Society for Cardiovascular Magnetic Resonance (SCMR) guidelines (128). Basal ventricular slices were included if >50% of the LV blood pool was surrounded by myocardium. Papillary muscles and minor trabeculations were included in the left ventricular mass measurements and excluded from the intracavity volume measurements again as per SCMR guidelines (128).

The left ventricular wall thickness was measured in each of the 16 myocardial segments (excluding the LV apex) and the maximum value recorded. No standardised measure of left ventricular longitudinal function has been recommended in current literature. In these studies, it was determined by measuring the difference in the distance between the mitral valve plane and the epicardial left ventricular apex in end-systole and end-diastole. The final value was calculated as the mean value of the recorded measurements in both 4-chamber and 2-chamber views. Left atrial volume was calculated using the bi-plane area-length method by tracing the endocardial LA contour in end-ventricular systole in both 2 and 4 chamber long-axis views (129).

The presence of mid-wall myocardial fibrosis was determined qualitatively by two independent and experienced operators (MRD and RJE) in Chapters 4

and 6 and by a single observer in Chapter 5 (RJE). The distribution of mid-wall fibrosis was described according to the standard 17-segment model recommended by the American College of Cardiology/American Heart Association. A variety of recommended semi-automated LGE quantification methods were used, including signal intensity thresholds (of >2, 3 or 5 standard deviations above the mean value in a region of normal myocardium) and the full-width half-maximum technique (128,130). Areas of inversion artefact, infarct pattern LGE or signal contamination by epicardial fat or blood pool were manually excluded. Sub-endocardial LGE was also identified and quantified using the same analysis technique.

T1 mapping analysis was performed on basal and mid-ventricular short axis images (Chapter 4), a single mid-ventricle short axis image (Chapters 5) or a 4-chamber image (Chapter 6). Analysis of the short axis slices was performed using manually drawn endocardial and epicardial contours on the native motion-corrected myocardial T1 maps with 10% offsetting applied to avoid partial volume effects. The right ventricular insertion points were identified leading to automatic segmentation as per the 17 segment AHA/ACC model (131). No analysis was performed on the apical myocardial segments as these are most susceptible to partial volume effects. These contours were subsequently copied onto corresponding 20-min post-contrast maps with minor adjustments made to avoid partial volume effects and artefact (Figure 2.2). Segments demonstrating mid-wall late enhancement were included in

the overall T1 analysis whereas those containing infarct pattern LGE were excluded as per recent post-processing guidelines (132).

Analysis of the 4-chamber T1 maps was performed by drawing a region of interest (ROI) in the mid-ventricular septum, again taking care to offset the contours to avoid partial voluming with blood pool. Another ROI was drawn in the centre of the blood pool. These ROIs were copied onto the post contrast maps.

The extracellular volume fraction (ECV%) was then calculated according to: ECV% = partition coefficient x [1 - haematocrit], where partition coefficient = [ΔR1myocardium / ΔR1blood-pool] and ΔR1 = (1/post-contrast T1) - (1 / pre-contrast T1). Haematocrit was sampled at the time of cardiovascular magnetic resonance imaging (87,133). The indexed extracellular volume (iECV) in each patient was derived using the following: ECV% x left ventricular end-diastolic myocardial volume indexed to body surface area (using the Mosteller formula), where left ventricular myocardial volume = left ventricular mass /1.05 g/mL (7).

Positron emission tomography

Analysis of the PET was performed using FusionQuant software (Cedars-Sinai Medical Center, Los Angeles, U.S.A). The full list mode acquisition was reconstructed using an Ordered Subsets Expectation Maximization (OSEM) algorithm with the following parameters: 256x256 field of view, 4 iterations, 21 subsets, 5mm Gaussian filter, zoom 1. No ECG gating was applied. PET data

was first reconstructed applying the standard 3D Dixon VIBE MRAC method (4 tissue class segmentation; air, lung, soft tissue and fat). PET data was also reconstructed when applying a custom MRAC map derived from the free-breathing radial GRE sequence (2 tissue classes: background [air and lung] and soft tissue [soft tissue and fat] (98)). PET reconstructions were fused with the iNAV-based MC CMRA sequence (Kings College London, UK (125)). As the MR and PET data was acquired simultaneously and co-registered, in theory no manual correction was required. However, in cases where co-registration was imperfect, small manual corrections were performed by aligning PET uptake in the ventricular cavities, aorta and aortic valve with these structures on the MR angiogram. Radiotracer uptake was analysed using a standardised protocol (see appendix). In brief, regions of interest (ROI) were drawn on the co-registered image around the perimeter of the aortic valve on co-axial short-axis views. Standardised uptake values (SUV, mean and maximum) were then calculated for these ROIs and were corrected for blood pool activity (measured in the right atrium (134)) to generate tissue-to-background ratios (TBR). Myocardial SUV values were also measured in the septal myocardium at mid cavity level.

Figure 2.1: T1 mapping using Osirix software

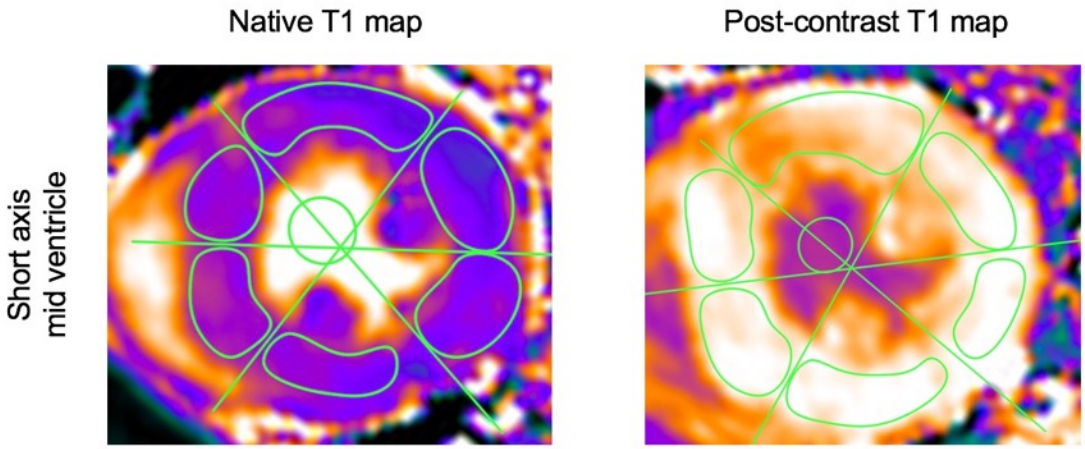

Regions of interest (outlines in green) were drawn in each of the six myocardial segments, taking care to avoid partial voluming with blood pool or epicardial fat. A separate region was drawn in the blood pool, avoid papillary muscles. These regions were copied onto the post contrast maps with minor adjustments to avoid artefact. These values were then used to calculate extracellular volume fraction (ECV%, Chapter 3).

Figure 2.2: T1 mapping analysis using CVI42 software

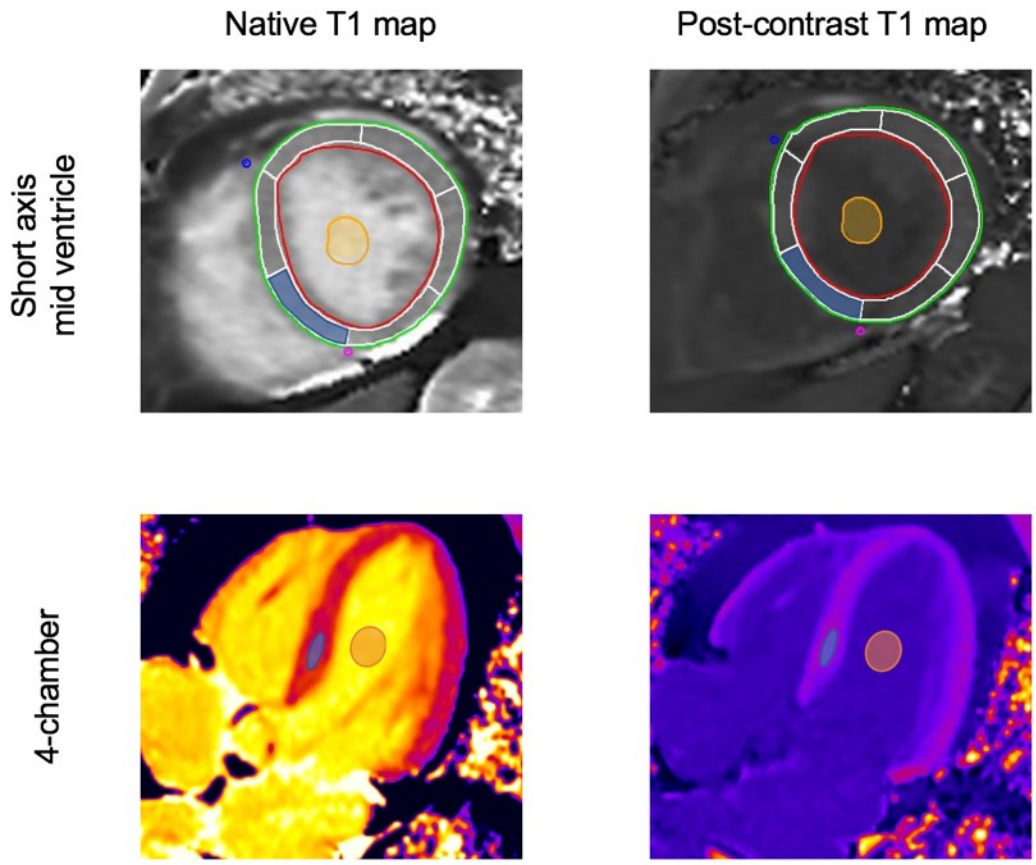

Analysis of short-axis T1 maps was performed by contouring the endocardial (red) and epicardial (green) borders. A 10% contour offset was then applied (white contours), and the right ventricle insertion points marked (blue and purple circles) resulting in automatic segmentation into 6 myocardial segments). The average T1 value from 6 segments (Chapter 4) or 1 segment (segment 9, blue area, Chapter 5) was used for reporting native and post-contrast T1 values and for calculation of ECV% and iECV. 4-chamber T1 maps were analysed by drawing a manual region of interest (ROI) in the septal myocardium taking care to avoid partial volume effects (blue oval, Chapter 6). In both cases, blood pool T1 was taken as the average of a ROI (orange circles), taking care to exclude papillary muscles.

STATISTICAL ANALYSIS

All statistical analyses were performed using GraphPad Prism Version 7.0 and SPSS Version 23. A two-sided $P<0.05$ was considered statistically significant. The distribution of all continuous variables using the Shapiro-Wilk test and visual analysis of histograms. Data was then presented as mean ± standard deviation or median [interquartile range]. Comparisons were made using the 2-sample t-test and the Mann-Whitney test (or for paired data, the paired *t*-test or Wilcoxon matched pairs signed-rank test) where appropriate. Annualised change in Chapter 4 was assessed using a one sample *t*-test or Wilcoxon signed-rank test where appropriate to compare with a hypothetical mean (or median) of zero. Comparisons between three or more groups were made using the one-way analysis of variance (ANOVA) or Kruskal-Wallis tests where appropriate.

We presented all categorical variables as percentages and used the $\chi 2$ test for comparison. The relationship between two continuous variables was assessed using either Pearson's r or Spearman's ρ, as appropriate. Potential confounders were adjusted using multivariable linear regression analyses. Time-to-first event survival curves were estimated using the Kaplan-Meier method and compared with the log-rank test. Univariable and multivariable Cox regression models were used to determine clinical and imaging factors associated with events. Further details regarding specific statistical methods are found in the corresponding results chapter.

Chapter 3: Myocardial Fibrosis and Cardiac Decompensation in Aortic Stenosis

Published in:

Everett, R.J.*, Chin, C. W. L.* *et al.* Myocardial Fibrosis and Cardiac Decompensation in Aortic Stenosis. *JACC Cardiovasc Imaging* (2016).

*joint contribution as first author

SUMMARY

Objectives

We used cardiovascular magnetic resonance (CMR), to investigate the extracellular compartment and myocardial fibrosis in patients with aortic stenosis and their association with other measures of left ventricular decompensation and mortality.

Background

Progressive myocardial fibrosis drives the transition from hypertrophy to heart failure in aortic stenosis. Diffuse fibrosis is associated with extracellular volume expansion detectable using T1-mapping, whilst late gadolinium enhancement (LGE) detects replacement fibrosis.

Methods

In a prospective observational cohort study, 203 subjects (166 with aortic stenosis [69 years, 69% male]; 37 healthy volunteers [68 years, 65% male]) underwent comprehensive phenotypic characterisation with clinical, imaging and biomarker evaluation. On CMR we quantified the total extracellular volume of the myocardium indexed to body surface area (iECV). The iECV upper limit of normal from the control group (22.5 mL/m^2) was used to define extracellular compartment expansion. Areas of replacement mid-wall LGE were also identified. All-cause mortality was determined over 2.9±0.8 years of follow up.

Results

iECV demonstrated a good correlation with diffuse histological fibrosis on myocardial biopsies (r=0.87, P<0.001, n=11) and was increased in patients with aortic stenosis (23.6±7.2 *versus* 16.1±3.2 mL/m^2 in control subjects, P<0.001). iECV was used alongside LGE to categorize patients: *normal myocardium* (iECV <22.5 mL/m^2, 51% of patients), *extracellular expansion* (iECV ≥22.5 mL/m^2, 22%) and *replacement fibrosis* (presence of mid-wall LGE, 27%). Across these groups, there was evidence of increasing hypertrophy, myocardial injury, diastolic dysfunction and longitudinal systolic dysfunction consistent with progressive left ventricular decompensation (all P<0.05). Moreover this categorisation was of prognostic value with step-wise increases in unadjusted all-cause mortality (8 *versus* 36 *versus* 71 deaths/1000 patient-years respectively, P=0.009).

Conclusion

CMR detects ventricular decompensation in aortic stenosis through the identification of myocardial extracellular expansion and replacement fibrosis. This holds major promise in tracking myocardial health in valve disease and optimising the timing of valve replacement.

INTRODUCTION

Calcific aortic stenosis is the most common valvular heart condition in the western world and a major public health burden (135). In recent years, the role of left ventricular (LV) remodelling in disease progression, symptom development and adverse cardiovascular events in aortic stenosis has been increasingly appreciated (6). In the initial phases, the increased afterload imposed by aortic valve narrowing induces adaptive LV hypertrophy that acts to maintain wall stress and cardiac output. Ultimately, this process decompensates and patients transition from hypertrophy to heart failure and the development of symptoms and adverse cardiovascular events (6,136). This transition often correlates poorly with the severity of aortic valve narrowing and is predominantly driven by myocardial fibrosis and myocyte cell death (8) perhaps as a consequence of supply-demand mismatch and myocardial ischemia in the hypertrophied myocardium (6). There is therefore considerable interest in developing novel biomarkers to detect the early signs of left ventricular decompensation.

Cardiovascular magnetic resonance imaging (CMR) provides the non-invasive gold standard method for measuring left ventricular wall thickness, mass, volumes, and ejection fraction. Moreover, it is able to detect structural changes in the left ventricular myocardium including replacement fibrosis with the late gadolinium technique and expansion of the extracellular volume using T1 mapping (85). The latter in part reflects increases in diffuse myocardial fibrosis (a reversible early form of fibrosis) (137) and potentially changes in the

intravascular compartment. Early studies have suggested that CMR-derived measures of LV mass and replacement myocardial fibrosis are of prognostic significance (46,49). However, these studies have largely been conducted in small cohorts of patients with end-stage aortic stenosis referred for CMR on clinical grounds. Findings may therefore have been confounded by referral bias, limiting their applicability and generalizability to the broad population of patients with aortic stenosis. Moreover comparisons with age- and sex-matched control populations and prognostic T1 mapping studies have been lacking.

We here report the largest prospective study to evaluate systematically the utility of CMR in patients with aortic stenosis. In particular, we investigated its ability to detect expansion of the extracellular volume and replacement myocardial fibrosis, and how these are related to other markers of left ventricular decompensation, functional capacity and clinical outcomes.

METHODS

Study Population

All stable patients with at least mild aortic stenosis (aortic jet velocity ≥2 m/s) attending the Edinburgh Heart Centre between March 2012 and August 2014 were invited to participate in this prospective observational cohort study. The exclusion criteria were other forms of valvular heart disease (≥moderate severity), significant co-morbidities with limited life expectancy, contraindications to gadolinium-enhanced CMR, and acquired or inherited non-ischaemic cardiomyopathies (assessed by clinical history or ultimately on CMR). In addition, we recruited healthy volunteers from the community with a similar demographic profile in terms of age and sex but no history or clinical features consistent with current cardiovascular disease. The study was conducted in accordance with the Declaration of Helsinki and approved by the local research committee. Written informed consent was obtained from all participants.

Subject Characterization

All subjects underwent detailed clinical evaluation including history, physical examination and electrocardiogram. In addition, venous blood samples were obtained for evaluation of biochemistry and cardiac biomarkers of interest.

Cardiac Biomarkers

Plasma cardiac troponin I concentrations (cTnI) were determined by the ARCHITECT STAT high-sensitivity cTnI assay (Abbot Laboratories, Abbott Park, Il, USA) (54). The brain natriuretic peptide (BNP) concentration was determined with Triage BNP assay (Biosite Inc., San Diego, CA, USA).

Six-Minute Walk Test

A six-minute walk test was performed in 156 (94%) patients as an objective measure of functional capacity in our predominantly elderly cohort many of whom could not perform an exercise tolerance test. Explicit instructions were given to patients asking them to walk as far as possible for six minutes.

Echocardiography

Comprehensive transthoracic echocardiography was performed in all patients (iE33, Philips Medical Systems, The Netherlands) by a dedicated research ultrasonographer (ACW) and a cardiologist certified in echocardiography (CWLC). The severity of aortic stenosis and diastolic function were assessed according to American Society of Echocardiography (ASE) guidelines.

Cardiovascular Magnetic Resonance

Cardiovascular magnetic resonance was performed using a 3T scanner (MAGNETOM Verio, Siemens AG, Erlangen, Germany). Short-axis cine images were acquired and used to calculate ventricular volumes, mass and function. Left ventricular hypertrophy (LVH) was defined as left ventricular

mass (indexed to body surface area, using the Du Bois formula) >95th centile using age- and sex-specific reference ranges (138). Left ventricular longitudinal function was determined by measuring the difference in mitral annular displacement between end-systole and end-diastole.

Focal replacement fibrosis and extracellular volume (ECV) expansion were assessed in all patients using late gadolinium enhancement and myocardial T1 mapping respectively. Late gadolinium enhancement was performed 15 min following 0.1 mmol/kg of gadobutrol (Gadovist, Bayer Pharma AG, Germany). The presence of mid-wall myocardial fibrosis was determined qualitatively by two independent and experienced operators (MRD and CWLC) and its distribution recorded (46,54).

T1 mapping was performed using the Modified Look-Locker Inversion-recovery (116) and a standardised image analysis approach (82). In the short-axis mid-cavity myocardium, 6 standard segments were defined on native T1 maps and these regions were then copied onto the corresponding 20-min post-contrast maps (OsiriX version 4.1.1, Geneva, Switzerland). Analysis of mid-ventricle segments has been shown to correlate well with analysis of all 17 myocardial segments, is simpler to perform and avoids partial volume effects in apical segments (82). Segments with mid-wall LGE present were included in this analysis whereas segments containing subendocardial, infarct-pattern LGE were excluded. Four commonly used T1 approaches were assessed: native and post-contrast myocardial T1, partition coefficient (λ) and

extracellular volume (ECV) fraction. We have recently reported the reproducibility of these measures at 3T (82).

We also investigated a novel marker, the indexed extracellular volume (iECV) that modifies the ECV fraction to act as a measure of the *total volume of the extracellular compartment* in the left ventricle. It was derived using the formula: ECV fraction x left ventricular end-diastolic myocardial volume normalised to body surface area.

Histological Validation of Myocardial Fibrosis

All patients who underwent surgical aortic valve replacement were approached regarding intra-operative myocardial biopsy at the time of surgery. Biopsies were obtained from the basal muscular septum 2 cm below the outflow tract using a Tru-Cut needle, stained with picrosirius red and analysed using an automated segmentation tool. Two blinded and independent observers (ATV and GE) analysed all the specimens, and the inter-observer reproducibility was 4.1±2.6%.

Clinical Outcomes

We examined the prognostic value of the different patterns of fibrosis on all-cause mortality as our primary outcome. Patients were followed between March 2012 and September 2015. All deaths were identified through the General Register of Scotland. We also assessed AS-related mortality. This

was established from the official death certificate and defined as any death where aortic stenosis was listed as either the primary cause or a contributing factor to that death by the clinical care team.

Statistical analysis

We assessed the distribution of all continuous variables using the Shapiro-Wilk test, and presented them as mean ± standard deviation or median [interquartile range]. Comparisons were made using the 2-sample *t*-test and the Mann-Whitney test where appropriate. We presented all categorical variables as percentages and used the χ^2 test for comparison. The relationship between two continuous variables was assessed using either Pearson's *r* or Spearman's ρ, as appropriate. Potential confounders were adjusted using multivariable linear regression analyses. Time-to-first event survival curves associated with the categories of LV decompensation were estimated using the Kaplan-Meier method and compared with the log-rank test. All statistical analyses were performed using SPSS Version 20 and GraphPad Prism Version 6.0. A two-sided $P<0.05$ was considered statistically significant.

RESULTS

Study Population

A total of 203 subjects were recruited: 166 patients with aortic stenosis (peak aortic valve velocity 3.8±0.90 m/s) and 37 healthy volunteers. These two groups were well matched for age, sex, chronic renal impairment and diabetes. Although a history of hypertension was more common in the AS group, blood pressure was well-controlled and similar between the two groups at enrolment (Table 3.1).

Table 3.1. Baseline Characteristics of Patients with Aortic Stenosis and Healthy Volunteers

	Healthy Volunteers (n=37)	Aortic Stenosis (n=166)	P value
Clinical Characteristics			
Age, years	68 [63, 74]	69 [63,75]	0.44
Males, n (%)	24 (65)	115 (69)	0.57
Hypertension, n (%)	10 (27)	112 (67)	<0.001
Diabetes Mellitus, n (%)	0	25 (15)	-
Coronary artery disease, n (%)	3 (8)	62 (37)	-
- CCTA assessment, n (%) - Invasive coronary angiography, n (%) - Previous PCI, n (%) - Previous CABG, n (%)	13 (35) 3 (8) 2 (5) 0	21 (13) 78 (47) 11 (6) 8 (5)	- - - -
Atrial fibrillation, n (%)	0	4 (2)	-
Body mass index, kg/m^2	27.0±3.6	28.9±4.8	0.02
Body surface area (m^2)	1.86±0.16	1.88±0.19	0.54
NYHA Class, n (%)			
I	36 (97)	74 (45)	
II	1 (3)	56 (34)	<0.001
III	-	32 (19)	
IV	-	4 (2)	
Six-minute walk test, m	430 [400,475]	400 [340, 450]	0.001
Systolic blood pressure, mmHg	148±16	151±21	0.53
Biomarkers			
High sensitivity troponin I concentration, ng/L	3.1 [1.2, 7.1]	6.6 [3.8, 12.4]	<0.001
Brain natriuretic peptide concentration, pg/mL	9.5 [5.1, 20.6]	26.1 [10.7, 54.3]	0.001
Echocardiography			
Aortic valve area, cm^2	2.4±0.6	1.0±0.4	<0.001
Peak aortic jet velocity, m/s	1.4±0.2	3.8±0.9	<0.001
Mean pressure gradient, mmHg	4.2±1.4	35±19	<0.001
Dimensionless index	0.71 [0.67, 0.81]	0.26 [0.22, 0.32]	<0.001
Valvulo-arterial impedance, mmHg/ml/m^2	4.0 [3.6, 4.7]	4.3 [3.6, 5.1]	0.38
Mean e', cm/s	7.3 [6.2, 8.1]	5.9 [4.9, 7.5]	<0.001
Mean E/e' ratio	8.5 [7.0, 10.4]	12.6 [10.3, 16.9]	<0.001
Mean diastolic dysfunction grade	0.5±0.8	2.0±0.9	<0.001

Cardiovascular Magnetic Resonance			
End-diastolic volume (indexed) (EDVi), mL/m^2	66 [60, 80]	69 [61, 78]	0.52
End-systolic volume (indexed), mL/m^2	23 [19, 29]	23 [18, 27]	0.40
Stroke volume (indexed), mL/m^2	44 [40, 50]	47 [40, 54]	0.16
Systolic ejection fraction, %	65 [62, 68]	67 [63, 71]	0.02
Longitudinal function, mm	14.8±2.7	12.2±2.9	<0.001
Left ventricular mass (indexed) (LVMi), g/m^2	62 [54, 71]	88 [73, 99]	<0.001
LVMi/EDVi, g/mL	0.92 [0.84, 0.99]	1.24 [1.04, 1.44]	<0.001
Maximal myocardial wall thickness, mm	7.5 [6.8, 8.7]	11.4 [8.8, 14.2]	<0.001
Mean myocardial wall thickness, mm	5.6 [5.0, 6.3]	7.4 [6.3, 9.0]	<0.001
Indexed left atrial volume, ml/m^2	28±11	36±15	0.01
Mid-wall late gadolinium enhancement, n (%)	0	44 (27)	-
Native myocardial T1, ms	1166±27	1184±42	0.02
20-min post-contrast myocardial T1, ms	645±51	638±46	0.47
Partition coefficient	0.45±0.02	0.46±0.04	0.06
Extracellular volume (ECV) fraction, %	26.5±1.3	27.7±2.6	0.005
Extracellular volume, mL	29.9±7.3	44.4±15.1	<0.0001
Indexed extracellular volume (iECV), mL/m^2	16.1±3.2	23.6±7.2	<0.0001

CCTA: coronary computed tomography angiography, PCI: percutaneous coronary intervention, CABG: coronary artery bypass graft, NYHA: New York Heart Association,

Coronary artery disease was defined by previous myocardial infarction, clinical symptoms of angina with documented evidence of myocardial ischemia in the absence of severe aortic stenosis, a >50 % luminal stenosis in a major epicardial coronary artery or previous coronary revascularisation. All patients with clinical symptoms of angina underwent coronary angiography.

Left Ventricular Hypertrophy

Although the severity of aortic stenosis correlated positively with left ventricular hypertrophy (left ventricular mass index r=0.48, P<0.001), it accounted for less than a quarter (r^2=0.23) of the variance observed (Figure 3.1). Male sex and aortic stenosis severity were the only independent predictors of left ventricular mass (P<0.001 for both), independent of systolic blood pressure, age and coronary artery disease status.

Figure 3.1: Factors Governing the Magnitude of the Hypertrophic Response in Aortic Stenosis.

Only a modest correlation between the severity of valve narrowing and the magnitude of the hypertrophic response was observed. The other predictor of left ventricular mass index on multivariate analysis was sex with males having more hypertrophy than females.

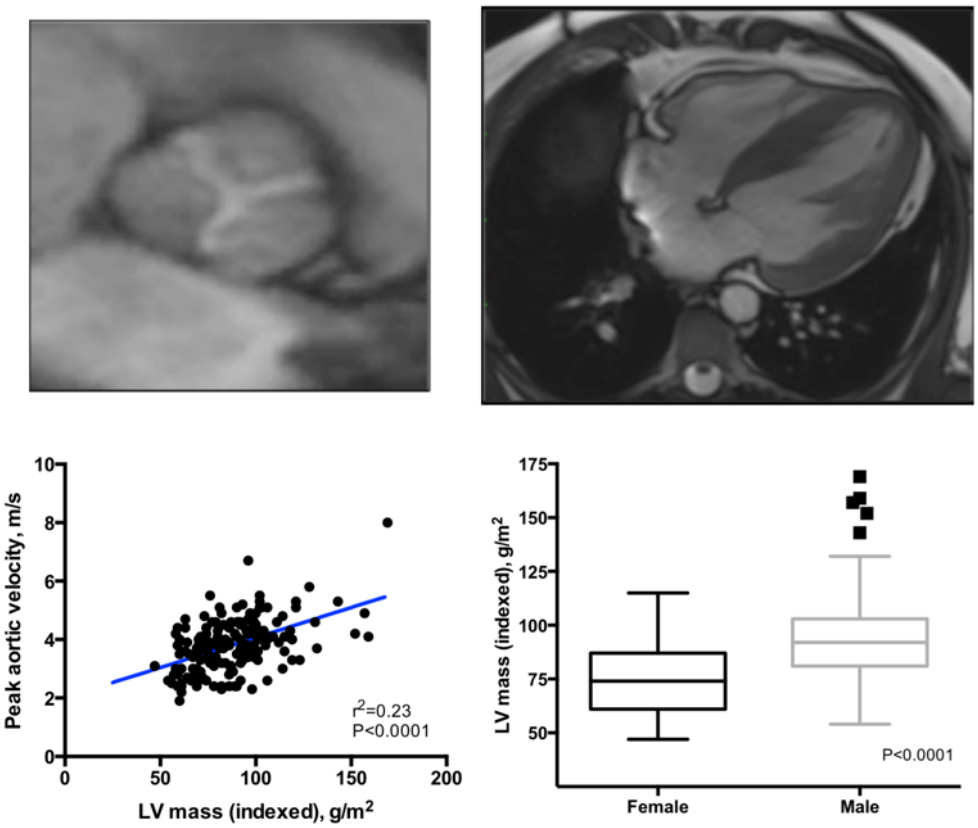

T1 Mapping and Extracellular Expansion

Myocardial biopsies were obtained in 11 out of 37 patients who underwent surgical aortic valve replacement. Strong correlations were observed between the amount of myocardial fibrosis on histology and T1 mapping parameters (native T1 r=0.76, P=0.007; λ r=0.82, P=0.002; ECV fraction r=0.70, P=0.016; iECV r=0.87, P<0.001; Figure 3.2) with the exception of post-contrast myocardial T1 (r=0.01, P=0.98). Indexed LV mass also correlated well with histological fibrosis (r=0.83, P<0.001).

Compared to the healthy volunteers, patients with aortic stenosis had increased diffuse myocardial fibrosis with iECV providing the best discrimination between cases and controls (23.6$\pm$7.2 *versus* 16.1$\pm$3.2 mL/m^2, P<0.0001; Table 3.1, Figure 3.2). Moreover, of all the T1-measures, only the iECV demonstrated a progressive increase across patients with mild, moderate and severe aortic stenosis (19.6±4.6 versus 22.9±5.4 versus 25.5±8.1 mL/m^2 respectively, P<0.001; Table 3.2). Notably ECV fraction did not vary with aortic stenosis severity (as measured by AV Vmax, P=0.30, Table 3.2) and showed a high degree of overlap between cases and controls (26.5±1.4% versus 27.7±2.6%, P=0.007).

We explored iECV in greater detail, dividing our entire patient cohort into tertiles of iECV (Table 3.3). Using this approach, a steady increase across the tertiles was observed for each of the following markers of disease severity and LV decompensation: indexed LV mass, peak aortic valve velocity, plasma high

sensitivity cardiac troponin I concentrations, serum BNP concentrations, diastolic dysfunction, longitudinal systolic dysfunction and the proportion of patients with mid-wall fibrosis ($P<0.05$ for all). Similar results were obtained using tertiles of ECV fraction (Table 3.4) but by comparison, tertiles of LV mass index were less discriminatory with no differences in diastolic function nor serum BNP concentrations across these groups (both $P>0.05$, Table 3.5).

Figure 3.2: Indexed Extracellular Volume (iECV) as a Marker of Extracellular Expansion in the Myocardium

A. Regions of interest manually drawn onto native and post-contrast T1 maps are used to calculate iECV. B. Histology from a patient with aortic stenosis with areas of diffuse fibrosis stained with picrosirus red. C. Excellent correlation between iECV and diffuse myocardial fibrosis on histology. D. iECV provided good discrimination between disease states. E. iECV values were higher in patients with replacement fibrosis than patients with normal myocardium or extracellular expansion.

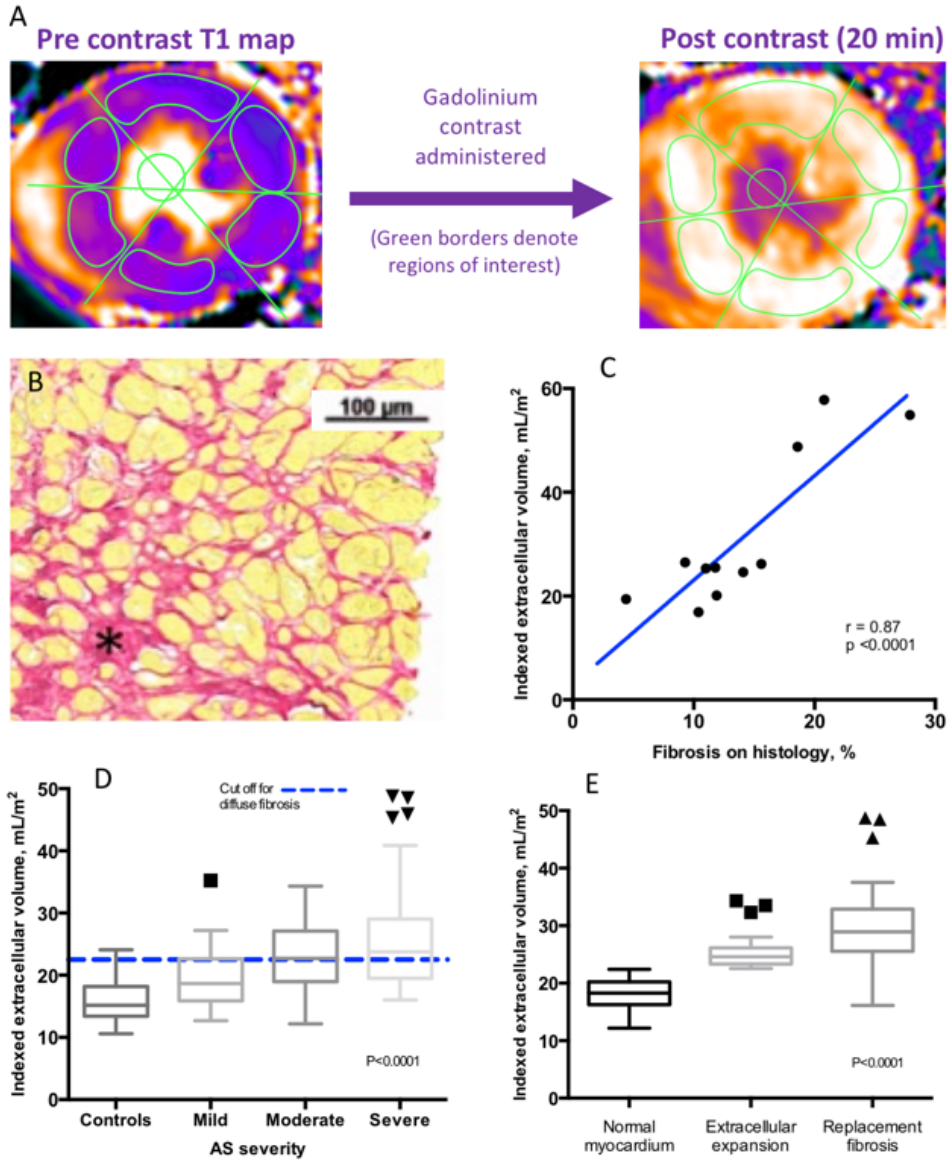

Table 3.2: Cardiovascular Magnetic Resonance Measures of Myocardial Fibrosis and Functional Status by Severity of Aortic Stenosis

	Mild (n=34)	Moderate (n=45)	Severe (n=87)	P value
Age	67 [56, 75]	72 [66, 77]	71 [65, 76]	0.048
Male gender (%)	20 (59)	32 (71)	63 (72)	0.33
End-diastolic volume (indexed) (EDVi), mL/m^2	69 [60, 77]	68 [64, 81]	69 [61, 79]	0.72
End-systolic volume (indexed), mL/m^2	24 [19, 26]	23 [20, 27]	22 [17, 27]	0.87
Stroke volume (indexed), mL/m^2	47 [39, 52]	47 [42, 56]	47 [40, 54]	0.56
Systolic ejection fraction, %	67 [63, 69]	66 [63, 70]	67 [63, 72]	0.65
Longitudinal function, mm	13.6±2.4	13.2±2.9	11.2±2.8	<0.001
Left ventricular mass (indexed) (LVMi), g/m^2	71 [61. 86]	87 [74, 98]	93 [80, 104]	<0.001
LVMi/EDVi, g/mL	1.08±0.20	1.21±0.23	1.36±0.28	<0.001
Maximal myocardial wall thickness, mm	8.2±2.1	11.1±3.3	13.4±3.4	<0.001
Mean myocardial wall thickness, mm	5.9±1.1	7.3±1.6	8.7±1.9	<0.001
Number of patients with LVH, (%)	6 (17)	24 (53)	59 (68)	<0.001
Native myocardial T1, ms	1170±30	1180±37	1192±46	0.02
20-min post-contrast myocardial T1, ms	637±45	643±48	636±45	0.73
Partition coefficient	0.466±0.03	0.466±0.04	0.466±0.05	0.07
Extracellular volume (ECV) fraction, %	27.8±2.5	27.5±2.0	27.8±3.0	0.79
Indexed extracellular volume (iECV), mL/m^2	19.6±4.6	22.9±5.4	25.5±8.1	<0.001
Extracellular expansion (iECV>22.5 mL/m^2, %)	9 (26)	23 (51)	47 (54)	0.021
Mid-wall late gadolinium enhancement, n (%)	2 (5.9)	14 (31)	28 (32)	0.008
Diastolic function (E/e')	11.1 [8.0, 14.2]	12.2 [10.1, 16.4]	13.5 [11.4, 18.6]	0.009
Natural log (hs troponin I)	1.25 [0.72, 1.55]	1.76 [1.33, 2.34]	2.16 [1.59, 2.81]	<0.0001
Six-minute walk test, m	420 [363, 448]	400 [340, 450]	390 [320, 440]	0.05

Table 3.3: Progressive increase in markers of LV hypertrophy and decompensation with increasing Indexed Extracellular Volume (iECV) stratified in to tertiles

	Tertile 1 (n=54)	Tertile 2 (n=54)	Tertile 3 (n=53)	P value
Age	70 [63, 75]	70 [65, 70]	72 [64, 78]	0.30
Male gender, n (%)	27 (50)	42 (78)	43 (81)	0.0006
Echo				
Peak aortic jet velocity, m/s	3.45±0.78	3.77±0.81	4.25±0.96	<0.0001
Aortic valve area, cm^2	1.01±0.37	0.95±0.36	0.90±0.35	0.32
Mean AV pressure gradient, mmHg - Mild aortic stenosis, n - Moderate aortic stenosis, n - Severe aortic stenosis, n	27.6 ±12.7 19 13 22	32.7±15.0 12 17 25	42.6±23.7 3 15 35	<0.0001
Valvulo-arterial impedance, $mmHg/ml/m^2$	4.4±1.1	4.0±1.0	3.8±1.0	0.019
Mean e' (cm/s)	6.9±2.0	6.4±1.7	5.4±1.8	<0.0001
Mean E/e' ratio	11.6 [9.8, 14.4]	12.4 [9.3, 16.5]	14.3 [11.9, 19.2]	0.02
Mean diastolic dysfunction grade	1.5±1.0	2.0±0.8	2.5±0.7	<0.0001
CMR				
Left ventricular mass (indexed), g/m^2	68±9	88±9	110±19	<0.0001
Ejection fraction, %	68 [63, 71]	67 [64, 73]	66 [61, 71]	0.44
Longitudinal function, mm	13.0±2.7	12.8±2.7	11.0±3.0	0.0004
Mid wall fibrosis, n (%)	2 (4)	6 (11)	36 (68)	0.0001
Indexed left atrial volume, ml/m^2	29±13	36±14	38±13	0.004
Biomarkers				
Natural log (hs troponin I)	1.3 [0.8, 1.6]	2.1 [1.5, 2.4]	2.5 [1.9, 3.3]	<0.0001
Natural log (BNP)	2.8 [1.9, 3.5]	3.1 [2.4, 3.9]	4.0 [2.8, 4.7]	<0.0001
Functional Status				
Six minute walk test, m	410 [345, 445]	410 [358, 453]	385 [295, 443]	0.09
NYHA class (%) 1 2 3 4	 27 (50) 20 (37) 6 (11) 1 (2)	 23 (43) 19 (35) 12 (22) 0 (0)	 24 (45) 15 (28) 11 (21) 3 (6)	
OUTCOMES				
All-cause mortality, n	2	2	10	-
Mortality rate (per 1000 patient-years)	12	12	72	0.005
Aortic-stenosis related mortality, n	0	2	8	-

5 patients had insufficient data to calculate iECV
AV; Aortic valve, BNP; Brain natriuretic peptide

Table 3.4. Aortic stenosis population stratified into tertiles of ECV fraction.

Although significant differences exist across the tertiles for most measures, ECV fraction was unrelated to aortic stenosis severity.

	Tertile 1 (n=54)	Tertile 2 (n=53)	Tertile 3 (n=54)	P value
Age	68 [61, 72]	71 [65, 75]	73 [66, 78]	0.025
Male gender, n (%)	43 (80)	37 (70)	32 (60)	0.07
Echo				
Peak aortic jet velocity, m/s	3.74±0.84	3.73±0.77	3.98±1.1	0.30
Aortic valve area, cm^2	0.96±0.35	1.00±0.41	0.91±0.31	0.58
Mean AV pressure gradient, mmHg	33±15	32±14	38±25	0.29
- Mild aortic stenosis, n	11	12	11	
- Moderate aortic stenosis, n	14	17	14	
- Severe aortic stenosis, n	29	24	29	
Mean E/e' ratio	12.2±4.7	13.7±5.5	17.8±10.3	0.0003
CMR				
Longitudinal function, mm	12.7±2.8	12.7±2.8	11.4±3.1	0.025
Ejection fraction, %	67 [63, 71]	68 [63, 72]	67 [63, 71]	0.87
Left ventricular mass (indexed), g/m^2	82±14	87±20	97±26	0.002
Mid wall fibrosis, n (%)	1 (2)	13 (25)	30 (56)	<0.0001
Biomarkers				
Natural log (hs troponin I)	1.6 [1.3, 2.2]	1.7 [1.3, 2.3]	2.4 [1.4, 3.4]	0.002
Natural log (BNP)	2.7 [1.6, 3.7]	3.3 [2.4, 3.8]	4.0 [2.9, 4.8]	<0.0001
Functional Status				
Six-minute walk test, m	420 [360, 455]	390 [340, 450]	380 [290, 430]	0.02
OUTCOMES				
All-cause mortality, n	2	1	11	-
Mortality rate (per 1000 patient-years)	12	6	78	0.0006
Aortic stenosis-related mortality, n	0	1	9	-

AV; Aortic valve, BNP; Brain natriuretic peptide, hs; high sensitivity

Table 3.5. Aortic stenosis population stratified into tertiles of LV mass index.

Unlike the tertiles of iECV there was no significant differences in diastolic function, BNP or all-cause mortality across these groups

	Tertile 1 (n=55)	Tertile 2 (n=56)	Tertile 3 (n=55)	P value
Age	70 [63, 77]	70 [65, 74]	71 [63, 77]	0.44
Male gender, n (%)	25 (45)	43 (77)	47 (85)	<0.0001
Echo				
Peak aortic jet velocity, m/s	3.39±0.77	3.77±0.74	4.35±0.92	<0.001
Aortic valve area, cm^2	1.02±0.37	0.95±0.36	0.88±0.33	0.12
Mean AV pressure gradient, mmHg	26.8 ±13.6	32.3±13.0	44.8±23.1	<0.0001
- Mild aortic stenosis, n - Moderate aortic stenosis, n - Severe aortic stenosis, n	23 14 18	8 19 29	3 12 40	
Mean E/e' ratio	12.2 [10.1, 15.0]	12.6 [9.5, 17.0]	13.6 [10.8, 18.0]	0.28
CMR				
Longitudinal function, mm	13.1±2.9	12.1±3.1	11.5±2.6	0.016
Ejection fraction, %	68 [63, 71]	66 [63, 70]	66 [62, 71]	0.54
Extracellular volume (ECV) fraction, %	27.3±2.0	27.1±2.3	28.8±3.1	0.0008
Mid wall fibrosis, n (%)	4 (7)	10 (18)	30 (55)	<0.0001
Biomarkers				
Natural log (hs troponin I)	1.3 [0.7, 1.6]	2.2 [1.5, 2.5]	2.3 [1.8, 3.1]	<0.0001
Natural log (BNP)	3.1 [2.1, 3.7]	3.1 [2.5, 4.0]	3.8 [2.6, 4.5]	0.060
Functional Status				
Six-minute walk test, m	400 [340, 440]	390 [340, 430]	400 [320, 460]	0.74
OUTCOMES				
All-cause mortality, n	2	5	7	-
Mortality rate (per 1000 patient-years)	12	32	47	0.23
Aortic stenosis-related mortality, n	0	5	5	-

AV; Aortic valve, BNP; Brain natriuretic peptide, hs; high sensitivity

Replacement Myocardial Fibrosis

Replacement mid-wall fibrosis assessed by late gadolinium enhancement was present in 44 (27%) patients with aortic stenosis but none of the healthy volunteers. We examined the association between mid-wall myocardial fibrosis and the severity of aortic stenosis (Table 3.2). Although patients with mid-wall fibrosis had more severe aortic stenosis compared to those without (AV Vmax 4.1 [3.7, 4.6] versus 3.8 [3.4, 4.6] m/s respectively, P=0.001), this difference was small and unlikely to be of any clinical significance. By contrast, patients with mid-wall fibrosis demonstrated a marked 30% increase in left ventricular mass indicative of an advanced hypertrophic response (left ventricular mass index 107±24 *versus* 82±16 g/m^2 respectively; P<0.001). Indeed, left ventricular mass index was independently associated with mid-wall myocardial fibrosis in those with hypertrophy (odds ratio 1.09, 95% confidence interval 1.04 to 1.14; P<0.001) after adjusting for aortic stenosis severity, age, sex and systolic blood pressure.

Relationship Between Myocardial Extracellular Volume and Replacement Fibrosis

It has been suggested that replacement fibrosis represents the irreversible final stage of diffuse interstitial fibrosis and extracellular expansion. Consistent with this hypothesis, patients with replacement mid-wall fibrosis had evidence of increased extracellular volume on T1 mapping compared to patients without (iECV 32.0 [29.1 34.9] *versus* 21.5 [20.6 22.4] mL/m^2, P<0.0001; ECV fraction 29.1±2.4 *versus* 26.9±2.1 %, P<0.001). Indeed, the

iECV was independently associated with mid-wall fibrosis after adjusting for age, sex, severity of aortic stenosis and even left ventricular mass (odds ratio 1.22; 95% confidence interval 1.11 to 1.35; P<0.001). Similar associations were observed using ECV fraction.

Categorisation of Left Ventricular Decompensation

We proceeded to categorise patients into three groups according to our CMR measures of myocardial fibrosis: normal myocardium, extracellular expansion and replacement mid-wall fibrosis (Figure 3.3). The upper limit of normal for iECV in the healthy volunteers (defined by two standard deviations above the mean, 22.5 mL/m^2) was used to define expansion of the extracellular myocardium. Values below this threshold defined normal myocardium. This categorisation was then validated in the 11 patients who underwent myocardial biopsy, with the percentage fibrosis on histology increasing progressively across the three groups (*normal myocardium* 8.9%±4.0 vs. *extracellular expansion* 12.4±2.5% vs *replacement fibrosis 22*.4±4.9%, P<0.004; Table 3.6).

In the larger imaging cohort of patients with aortic stenosis (after exclusion of patients with an infarct pattern of LGE n=22, or incomplete T1 mapping data n=5), 71 patients had *normal myocardium* (iECV <22.5 mL/m^2). These patients had largely mild-to-moderate aortic stenosis, a mild hypertrophic response, minimal cardiac injury and good left ventricular performance (Table 3.6, Figures 3.3 & 3.4). Thirty-one patients had *extracellular expansion* (iECV

≥22.5 mL/m^2) with values for aortic stenosis severity, left ventricular mass, myocardial injury, diastolic function, and longitudinal systolic function that were intermediate between patients with normal myocardium and replacement fibrosis. Finally, 37 patients had evidence of *replacement myocardial fibrosis* on late gadolinium enhancement. These patients were confirmed as having the most severe aortic stenosis, left ventricular hypertrophy, myocardial injury and impairment in left ventricular performance (Table 3.6). Compared to patients with extracellular expansion, they had even greater iECV values (30.4±8.2 *versus* 25.4±3.1 mL/m^2, P<0.0001, Figure 3.2) whilst compared to patients with normal myocardium they had increased serum BNP concentrations (16.7 [6.1, 36.0] versus 34.4 [10.5, 76.2] pg/mL respectively, P=0.026) and impaired functional capacity (6-minute walk test 405±74 versus 359±138 m respectively, P=0.03). Indeed, both mid-wall fibrosis and ECV fraction were predictors of functional capacity independent of age, gender, LV mass and peak velocity (Table 3.7). These findings were unchanged when patients with mild aortic stenosis were excluded from the analysis (Table 3.8).

Figure 3.3: CMR Categorisation of Myocardial Fibrosis in Aortic Stenosis

Patients with aortic stenosis were categorized into three groups based upon CMR assessments of fibrosis.

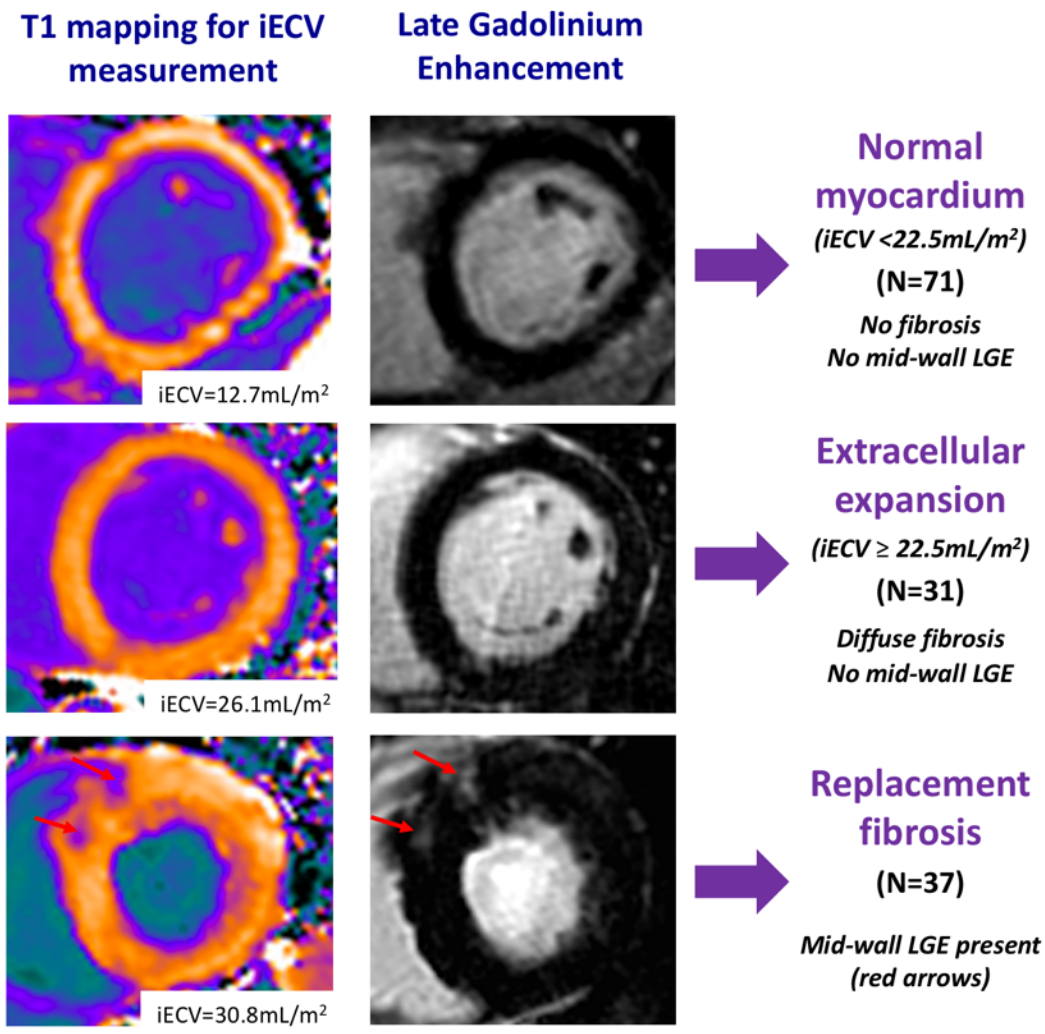

Table 3.6: Characteristics of Patients Stratified According to Indexed Extracellular Volume (iECV) Thresholds and Presence of Mid-Wall Late Gadolinium Enhancement

	Normal myocardium N=71	Extracellular expansion N=31	Replacement fibrosis N=37	P value
Age	70 [63, 75]	70 [63, 75]	71 [65, 78]	0.59
Gender (male=1)	0.56 [0.44, 0.68]	0.81 [0.67, 0.96]	0.76 [0.62, 0.90]	0.023
Hypertension (%)	48 (68)	20 (65)	22 (59)	0.70
Diabetes (%)	8 (11)	7 (23)	2 (5)	0.09
Body mass index, kg/m^2	28.2±4.5	28.9±4.6	29.3±4.3	0.44
Echo				
Peak aortic jet velocity, m/s	3.53±0.82	3.79±1.0	4.23±0.92	<0.001
Aortic valve area, cm^2	0.98 [0.73, 1.18]	0.88 [1.2, 0.7]	0.83 [0.73, 0.91]	0.049
Mean AV pressure gradient, mmHg	29.1±14.2	34.8±21.1	41.1±23.5	0.007
- Mild aortic stenosis, n	24	7	2	
- Moderate aortic stenosis, n	18	10	11	
- Severe aortic stenosis, n	29	14	24	
Valvulo-arterial impedance, mmHg/ml/m^2	4.1±1.0	3.9±0.9	4.0±1.0	0.46
Mean e' (cm/s)	6.7±2.0	6.5±1.8	5.2±1.4	0.0004
Mean E/e' ratio	13.1±7.7	13.2±4.8	16.5±6.5	0.04
Mean diastolic dysfunction grade	1.5±0.9	2.0±0.9	2.7±0.5	<0.0001
CMR				
Left ventricular mass (indexed), g/m^2	73±11	96±11	107±25	<0.0001
Relative wall thickness	0.60±0.12	0.61±0.09	0.67±0.11	0.018
Indexed extracellular volume, mL/m^2	18.3±2.5	25.4±3.1	30.4±8.2	<0.0001
Ejection fraction, %	68 [63, 71]	66 [64, 71]	67 [64, 72]	0.94
Longitudinal systolic function, mm	13.2±2.6	12.5±2.4	11.2±3.1	0.002
Indexed left atrial volume, ml/m^2	31±13	37±11	38±15	0.027
Biomarkers				
Natural log (hs troponin I)	1.43±0.96	2.02±0.93	2.60±0.90	<0.0001
Natural log (BNP)	2.95±1.00	3.06±0.96	3.41±1.10	0.12
Functional Status				
Six minute walk test, m	406±74	385±95	359±138	0.08

NYHA class (%) 1 2 3 4	 33 (46) 27 (38) 11 (15) 0 (0)	 18 (58) 6 (19) 7 (23) 0 (0)	 17 (46) 12 (32) 5 (14) 3 (8)	
OUTCOMES				
All-cause mortality, n	2	4	8	-
All-cause mortality rate (per 1000 patient-years)	8	36	71	0.009
Aortic stenosis-related mortality, n	0	4	6	-
AS-related mortality rate (per 1000 patient-years)	0	36	52	0.0045
Patients undergoing myocardial biopsy	**Normal myocardium on CMR N=3**	**Extracellular expansion on CMR N=5**	**Replacement fibrosis on CMR N=3**	**P value**
Histological fibrosis (%)	8.9±4.0	12.4±2.5	22.4±4.9	0.004
Aortic valve area, cm^2	0.57±0.10	0.94±0.29	0.81±0.44	0.29
Peak aortic jet velocity, m/s	4.6 [4.4, 5.1]	4.5 [4.0, 5.9]	4.9 [4.1, 8.0]	0.63
Left ventricular mass (indexed), g/m^2	76±15	98±4	162±6	<0.0001
Native myocardial T1, ms	1189±23	1183±16	1277±15	0.0002
Post-contrast myocardial T1, ms	676±45	615±24	672±84	0.22
Partition coefficient	0.43±.0.05	0.47±0.02	0.55±0.02	0.008
Extracellular volume (ECV) fraction, %	25.3±3.1	27.3±1.4	32.2±1.9	0.019
Indexed extracellular volume (iECV), mL/m^2	18.8±1.9	25.6±0.7	49.6±4.8	<0.0001

AS; aortic stenosis, AV; aortic valve, BNP; brain natriuretic peptide, CMR; cardiac magnetic resonance, NYHA; New York Heart Association

Table 3.7: Univariable and Multivariable Linear Regression Analysis to Examine the Association of Fibrosis Assessments with Functional Status

	Univariable Analysis		Multivariable Analysis			
			Model 1 (ECV fraction)		Model 2 (mid-wall fibrosis)	
	Relative change in six minute walk (95% CI)	P value	Relative change in six minute walk (95% CI)	P value	Relative change in six minute walk (95% CI)	P value
Age ≥70, years	- 50.3 [- 83.0 to -17.6]	0.003	- 41.4 [- 74.5 to - 8.36]	0.01	- 50.3 [- 83.0 to – 17.7]	0.003
Sex, males	- 0.81 [- 37.7 to 36.1]	0.97	- 19.9 [- 61.3 to 21.6]	0.35	- 8.88 [- 48.5 to 30.7]	0.66
Peak aortic jet velocity, m/s	- 12.25 [- 30.6 to 6.14]	0.19	- 14.9 [- 35.4 to 5.73]	0.16	- 11.9 [- 32.4 to 8.64]	0.26
Left ventricular mass index, g/m²	- 0.22 [- 1.00 to 0.56]	0.57	0.62 [- 0.44 to 1.68]	0.25	0.45 [- 0.62 to 1.52]	0.41
Extracellular volume (ECV) fraction, %	-9.09 [-15.4 to -2.81]	0.005	- 9.77 [- 17.0 to - 2.58]	0.01	-	-
Presence of mid-wall fibrosis	- 40.9 [- 78.5 to - 3.24]	0.03	-	-	-45.6 [- 89.1 to - 2.11]	0.04

Table 3.8. Characteristics of Patients with Moderate and Severe Aortic Stenosis Only (Mild Aortic Stenosis Excluded) Stratified According to Indexed Extracellular Volume Thresholds and Presence of Mid-Wall Late Gadolinium Enhancement

	Normal myocardium N=47	ECV expansion N=24	Replacement fibrosis N=35	P value
Age	71 [66, 75]	71 [66, 75]	71 [65, 78]	0.94
Male gender, n (%)	27 (57)	19 (79)	28 (80)	0.047
Echo				
Peak aortic jet velocity, m/s	3.99±0.59	4.17±0.80	4.31±0.88	0.17
Mean AV pressure gradient, mmHg	36.6±11.2	41.0±20.0	42.4±23.4	0.32
Aortic valve area, cm^2	0.82±0.21	0.85±0.21	0.83±0.22	0.90
Moderate aortic stenosis, n	18	10	11	
Severe aortic stenosis, n	29	14	24	
Mean E/e' ratio	14.1±9.0	14.1±4.6	16.3±6.5	0.37
CMR				
Left ventricular mass (indexed), g/m^2	76±12	97±12	108±24	<0.0001
Ejection fraction (%)	68 [64, 72]	66 [63, 74]	67 [64, 72]	0.49
Longitudinal systolic function, mm	12.9±3.0	12.1±2.0	11.3±3.1	0.042
Indexed extracellular volume (iECV), mL/m^2	18.7±2.3	25.7±3.3	30.5±8.3	<0.0001
Biomarkers				
Natural log (hs troponin I)	1.68±1.03	2.00±0.81	2.58±0.90	0.0003
Natural log (BNP)	3.08±1.07	3.15±0.84	3.42±1.11	0.39
Functional Status				
Six-minute walk test, m	400±77	383±104	356±142	0.23
NYHA class (%)				
1	17 (36)	11 (46)	15 (43)	
2	21 (45)	6 (25)	12 (34)	
3	9 (19)	7 (29)	5 (14)	
4	0 (0)	0 (0)	3 (9)	
OUTCOMES				
All-cause mortality, n	2	4	8	-
Mortality rate (per 1000 patient-years)	12	46	76	0.047
Aortic-stenosis related mortality, n	0	4	6	-
AS-related mortality rate (per 1000 patient-years)	0	46	57	0.017

AV; Aortic valve, BNP; Brain natriuretic peptide, NYHA; New York Heart Association

Clinical Outcomes

Participants were followed up for an average of 2.9±0.8 years during which a total of 14 patients with aortic stenosis died: 2 with normal myocardium, 4 with extracellular expansion and 8 with replacement fibrosis. Unadjusted all-cause mortality rates rose progressively across the groups (8 versus 36 versus 71 deaths/1000 patient-years, log-rank test P=0.009; Table 3.6, Figure 3.4). AS-related mortality also increased in a stepwise fashion (0 versus 36 versus 52 deaths/1000 patient-years, P=0.0045) with no AS-related deaths in the normal myocardium group. Tertiles of ECV fraction (P=0.0006, Table 3.4) and iECV (P=0.005, Table 3.3) also displayed prognostic ability in this unadjusted analysis but no difference in mortality was observed across tertiles of the indexed LV mass (P=0.23, Table 3.5).

Figure 3.4: Progressive Left Ventricular Decompensation on moving from Normal Myocardium to Extracellular Expansion to Replacement Fibrosis

On moving from normal myocardium to extracellular expansion and then replacement fibrosis there was a step-wise increase in the following measures: the severity of valve narrowing (A); the degree of hypertrophy (B); myocardial injury (C); left ventricular performance (D) and all-cause-mortality (E).

LV; left ventricular, hsTni; high sensitivity Troponin I concentration

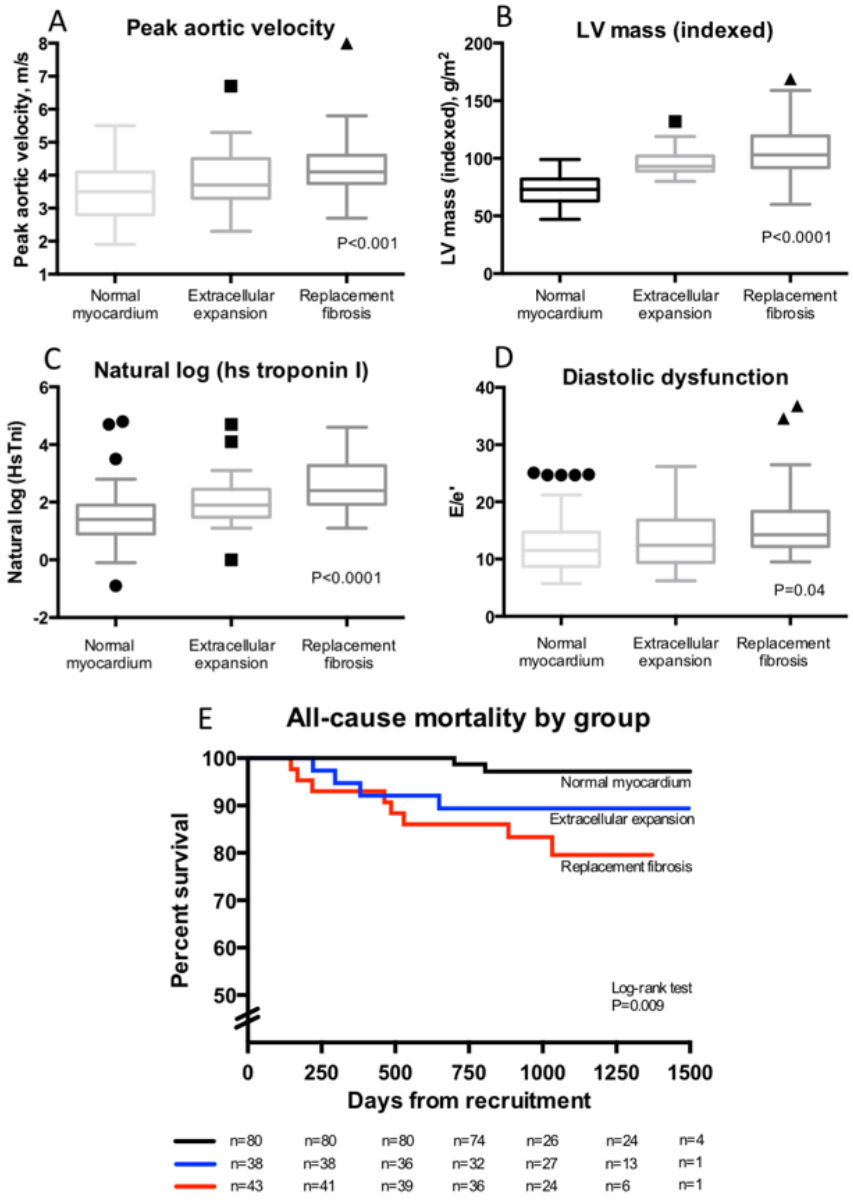

DISCUSSION

This is the largest prospective CMR study to evaluate systematically both extracellular expansion and replacement fibrosis in the myocardium of patients with aortic stenosis and healthy control subjects. Both measures are increased in aortic stenosis but are only weakly associated with the severity of valve narrowing. In contrast, they demonstrate a close association with the magnitude of the hypertrophic response, the presence of left ventricular dysfunction, the functional capacity of the patient and clinical outcome. We believe these findings demonstrate that the structural changes in the left ventricular myocardium are as important a consideration as the severity of the valvular disease itself. Based on these results, we propose that patients with aortic stenosis be categorised into three groups: those with normal myocardium, extracellular expansion and replacement myocardial fibrosis. We believe this classification has major potential in the early detection of subclinical ventricular decompensation in aortic stenosis and ultimately may be able to guide decisions regarding the timing of aortic valve replacement.

As one would expect, our data have demonstrated an association between the severity of valve narrowing and the degree of hypertrophy in aortic stenosis. However, this only explained approximately a quarter of the observed variance in LV mass, confirming that the hypertrophic response in aortic stenosis cannot be accurately predicted from the degree of valve narrowing alone and should be assessed independently.

T1 mapping techniques (ECV fraction and iECV) can provide an assessment of myocardial extracellular volume expansion. Potentially this can reflect increased myocardial fibrosis, myocardial infiltration or expansion in the intravascular compartment (132). In aortic stenosis myocardial fibrosis has been established pathologically as a key process driving the transition from hypertrophy to heart failure (8). Moreover we and others have observed a close correlation between these parameters and histological assessments of myocardial fibrosis (78,79,85,87). However, there is now some debate as to whether T1 mapping can provide direct assessment of myocardial fibrosis with recent evidence indicating that increased intravascular volume may also influence native T1 values (67),(139). Pressure overload conditions such as aortic stenosis are associated with reduced capillary density (75) and myocardial ischemia (77). Mahmod et al recently suggested that this ischemia may result in coronary vasodilatation and increased intravascular volume potentially contributing to increased native T1. Whilst confirmation of this interesting hypothesis is required it may be that T1 values also relate to the closely related myocardial ischemia that is believed to trigger fibrosis and the transition from hypertrophy to heart failure. Regardless, T1 mapping remains at the very least a useful surrogate of myocardial fibrosis and LV decompensation in aortic stenosis.

Controversy remains as to the optimal T1 image analysis strategy (82,132,140). Consistent with previous research (82), both native T1 and ECV fraction demonstrated major overlap with values in control groups and little

difference between patients with mild, moderate and severe aortic stenosis. We sought to tackle this issue by developing a novel parameter, the iECV that provides an assessment of the total extracellular volume in the myocardium. This effectively combines the prognostic information provided by ECV fraction with the improved discrimination between groups associated with indexed LV mass into a single measure.

iECV demonstrated good correlation with histological assessment of fibrosis burden. Moreover, across tertiles of iECV there was a clear step-wise increase in each of the different clinical and imaging measures of LV decompensation as well as clinical outcomes, supporting iECV as a marker of decompensation. Finally, iECV provided the best discrimination between disease states, being the only T1 measure to differentiate between patients with mild, moderate and severe aortic stenosis. In combination iECV would therefore appear to provide the most useful marker of left ventricular decompensation in aortic stenosis with advantages compared to both ECV fraction and LV mass in isolation.

How do extracellular expansion and diffuse fibrosis relate to the development of replacement fibrosis as detected using mid-wall LGE? In agreement with previous studies (46,49), regions of mid-wall LGE were observed in 27% of our patients, with roughly two-thirds having severe aortic stenosis and one-third moderate. Importantly patients with mid-wall replacement fibrosis also had marked increases in iECV, as a surrogate for diffuse fibrosis, in their remote myocardium. Indeed, iECV was an independent predictor of the

presence of mid-wall LGE. This was confirmed by our histological data and suggests that replacement fibrosis does not occur until the end stages of myocardial matrix remodelling and is preceded by an intermediate stage of extracellular expansion reflecting increasing diffuse fibrosis. Longitudinal studies using serial CMR imaging are required to confirm this hypothesis.

Using our CMR assessments of myocardial structure, we categorised our patients into three stages of left ventricular decompensation. We used iECV to differentiate patients with normal myocardium from those with *extracellular expansion* and then late gadolinium enhancement to define *replacement fibrosis* (Figure 3.3). On moving across these groups, patients had advancing left ventricular hypertrophy, histological fibrosis, myocyte cell injury, diastolic dysfunction and longitudinal systolic dysfunction, suggesting progressive, subclinical LV decompensation. Most importantly there was a steady decline in prognosis with unadjusted all-cause mortality rates quadrupling on moving from normal myocardium to the extracellular expansion groups and more than doubling again in those with replacement fibrosis. Moreover these groups also predicted AS-related deaths on unadjusted analysis, with no AS-related deaths occurring in the normal myocardium group. More simple categorisation using LV mass was less discriminatory and not of prognostic value.

Our categorisation holds promise as a mean of monitoring the development of LV decompensation, and helping to optimise the timing of aortic valve replacement. Currently the development of symptoms guides the need for

surgery. However symptoms are frequently difficult to assess in elderly patients with multiple co-morbidities. Objective imaging assessments that monitor the changes in myocardial structure that are themselves responsible for progressive LV decompensation are therefore potentially attractive (6,136). This is the first study to describe iECV in aortic stenosis, so that confirmation of our findings in larger studies with longer follow-up is required. However we here present the fourth separate cohort to demonstrate the adverse prognosis associated with mid-wall LGE in aortic stenosis (19,46,49) as well as demonstrating its association with patient functional capacity, left ventricular performance and multiple other parameters of LV decompensation. This data has now led to the Early Valve Replacement guided by Biomarkers of Left Ventricular Decompensation in Asymptomatic Patients with Advanced Aortic Stenosis (EVoLVeD) study. This multicentre randomised controlled trial will begin enrolment next year and assess whether early valve intervention in patients with asymptomatic advanced aortic stenosis and mid-wall fibrosis on CMR improves clinical outcomes compared with standard care.

Limitations

There were insufficient deaths to perform multivariate analysis. Studies with longer follow up are required to confirm whether iECV is of independent prognostic value and assess the contribution of the intravascular volume to T1 mapping values. Finally, although similar to previous studies (78,79,87), the number of patients agreeing to intraoperative myocardial biopsy was modest perhaps reflecting the invasive nature of this assessment.

CONCLUSIONS

CMR can detect progressive fibrosis in aortic stenosis and can be used to categorise patients as having normal myocardium, extracellular expansion or replacement fibrosis. On moving across these groups, there was a step-wise increase in myocardial injury, fibrosis, left ventricular dysfunction and unadjusted mortality consistent with progressive ventricular decompensation. This categorisation may be able to track the transition of hypertrophy to heart failure in patients with aortic stenosis.

Chapter 4: Progression of Hypertrophy and Myocardial Fibrosis in Aortic Stenosis: A Multicentre Cardiac Magnetic Resonance Study

Published in:

Everett, R.J., Tastet, L.* *et al.* Progression of Hypertrophy and Myocardial Fibrosis in Aortic Stenosis: A Multicenter Cardiac Magnetic Resonance Study. *Circulation Cardiovasc Imaging* (2018).

SUMMARY

Background

Aortic stenosis (AS) is accompanied by progressive left ventricular hypertrophy and fibrosis. We investigated the natural history of these processes in asymptomatic patients and their potential reversal post-aortic valve replacement (AVR).

Methods

Asymptomatic and symptomatic patients with AS underwent repeat echocardiography and magnetic resonance imaging. Changes in peak aortic-jet velocity, left ventricular mass index (LVMi), diffuse fibrosis (indexed extracellular volume [iECV]) and replacement fibrosis (late gadolinium enhancement [LGE]) were quantified.

Results

In 61 asymptomatic patients (43% mild, 34% moderate, 23% severe AS) significant increases in peak aortic-jet velocity, LVMi, iECV and LGE mass were observed after 2.1±0.7 years, with the most rapid progression observed in patients with most severe stenosis. Patients with baseline mid-wall LGE (n=16 (26%); LGE mass 2.5 [0.8 - 4.8] g) demonstrated particularly rapid increases in scar burden (78 [50 -158] % increase in LGE mass per year).

In 38 symptomatic patients (age 66±8 years, 76% male) who underwent AVR there was a 19 [11 - 25] % reduction in LVMi (P<0.0001) and an 11 [4 - 16] %

reduction in iECV (P=0.003) 0.9±0.3 years following surgery. By contrast mid-wall LGE (n=10 (26%); mass 3.3 [2.6 - 8.0] g) did not change post-AVR (n=10; 3.5 [2.1 - 8.0] g, P=0.23), with no evidence of regression even out to 2 years.

Conclusion

In patients with AS, cellular hypertrophy and diffuse fibrosis progress in a rapid and balanced manner but are reversible following AVR. Once established, mid-wall LGE also accumulates rapidly but is irreversible post-valve replacement. Given its adverse long-term prognosis, prompt AVR when mid-wall LGE is first identified may improve clinical outcomes.

Clinical Trial Registration

URL: https://clinicaltrials.gov, Unique Identifiers: NCT01755936 and NCT01679431

INTRODUCTION

Aortic stenosis is the most common valve disease requiring operative intervention in high-income countries (1). Traditional assessments of aortic stenosis severity focus on the degree of hemodynamic obstruction in the valve. However the importance of the myocardial response to pressure overload has been increasingly appreciated, especially when considering the development of symptoms and long-term prognosis following valve intervention (6). Left ventricular hypertrophy (LVH) initially normalises wall stress and maintains cardiac output for many years, if not decades. However, with time, the left ventricle decompensates and the patient transitions towards heart failure, symptoms and adverse events.

Pathological studies have suggested that this transition from hypertrophy to heart failure is driven by a combination of myocyte cell death and myocardial fibrosis (8). Magnetic resonance imaging can detect focal myocardial fibrosis using late gadolinium enhancement (LGE) and estimates diffuse interstitial fibrosis with T1 mapping. A mid-wall pattern of LGE observed in aortic stenosis acts as a marker of left ventricular decompensation and is associated with an adverse prognosis following surgery (7,19,46,49,141). However, to date, we have lacked longitudinal studies to assess how left ventricular hypertrophy and fibrosis progress with time, and how aortic valve replacement (AVR) affects these processes. The aims of this prospective multicentre study were to assess the time course of left ventricular hypertrophy and fibrosis in patients

with asymptomatic aortic stenosis, and to determine how they are affected in symptomatic patients who undergo AVR.

METHODS

Study Population

Patients were recruited from two large prospective observational magnetic resonance imaging studies investigating the natural history of aortic stenosis (NCT01755936; Edinburgh Heart Centre, United Kingdom (7), and NCT01679431; Quebec Heart and Lung Institute, Canada (142)). In both studies, patients underwent comprehensive clinical and echocardiographic assessment including repeat magnetic resonance imaging. Eligible participants had undergone at least two serial magnetic resonance imaging scans. Symptomatic patients had AVR shortly after baseline magnetic resonance imaging allowing us to assess the reverse remodelling effect of surgery on repeat scans. The study was conducted in accordance with the Declaration of Helsinki and approved by the local research committees. Written informed consent was obtained from all participants. Study data can be made available to other researchers on request to the corresponding author.

Echocardiography

Comprehensive transthoracic echocardiography was performed in all patients to assess aortic stenosis severity as per clinical guidelines (see Appendix).

Cardiac Magnetic Resonance

Magnetic resonance imaging was performed using both 1.5T and 3T scanners and standard cine images of the left ventricle were acquired. Late gadolinium enhancement was performed 15 minutes following administration of gadobutrol. T1 mapping was performed using the Modified Look-Locker Inversion-recovery sequence (116) before and 15-20 minutes following gadolinium contrast administration. Although there was variation in the scanners used at the different centres all patients underwent standardised baseline and repeat imaging within their respective institutions (see Appendix). To account for potential inter-scanner variation in T1 measurements (143), extracellular volume (ECV)-derived T1 mapping measures were obtained to normalise myocardial T1 values to blood-pool measurements.

Image analysis

Analysis of all magnetic resonance imaging scans from both centres was performed at the Edinburgh Core Lab using CVI42 (Circle Cardiovascular Imaging Inc., Calgary, Canada) by a single reporter (RJE) blinded to the scan time-point (see Appendix). Short-axis cine images were used to calculate ventricular volumes, mass and function. The presence of mid-wall late gadolinium enhancement was determined both qualitatively and quantitatively by two experienced operators (RJE and MRD), and its distribution recorded. LGE was quantified in a semi-automated manner using a signal intensity threshold of >3 standard deviations above the mean value in a region of normal myocardium (130). Whilst segments with mid-wall late enhancement

were included in the overall T1 calculation, segments with subendocardial infarct pattern LGE were excluded. Extracellular volume fraction (ECV%) and indexed extracellular volume (iECV: ECV% x left ventricular end-diastolic myocardial volume normalised to body surface area) were calculated using the motion-corrected native and post-contrast T1 maps (see Appendix). We have previously reported the reproducibility of these measures at 3T (82), and demonstrated that iECV acts as a marker of left ventricular decompensation in aortic stenosis, correlates with the burden of diffuse fibrosis on histology, and is associated with future clinical events (7). Other groups have also recently used the same parameter (144).

Statistical analysis

All statistical analyses were performed using GraphPad Prism Version 7.0 and SPSS Version 23. A two-sided $P<0.05$ was considered statistically significant. Given heterogeneity in timing of follow-up imaging, changes in the left ventricular remodelling variables were annualised. Annualised change was calculated as the difference between the baseline and final follow-up magnetic resonance imaging scans, divided by the number of days in between time points and multiplied by 365. This approach assumes that progression is linear. In a sensitivity analysis we restricted analysis of progression and reverse remodelling in those patients who had repeat imaging at the same time interval (2 years in the natural history cohort and 1 year in the AVR cohort) and examined absolute change in the left ventricular remodelling variables.

We assessed the distribution of all continuous variables using the Shapiro-Wilk test, and presented them as appropriate using mean ± standard deviation or median [interquartile range]. Annualised change was assessed using a one sample *t*-test or Wilcoxon signed-rank test where appropriate to compare with a hypothetical mean (or median) of zero. Other comparisons were made using the Kruskal-Wallis test where appropriate. We presented all categorical variables as percentages and used the $\chi 2$ test for comparison. Absolute change in the sensitivity analysis was analysed using the paired *t*-test or Wilcoxon matched pairs signed-rank test. Univariate linear regression was performed on both cohorts to investigate the change in indexed LV mass using variables known or suspected to influence LV mass change (including age, gender, history of hypertension and valvulo-arterial impedance). Multivariable linear regression analysis was then performed with change in indexed LV mass as the dependent variable and the same relevant clinical variables included as covariates. RJE had full access to study data and is responsible for data integrity and analysis.

RESULTS

Repeat magnetic resonance imaging was performed in a total of 99 patients (n=63 from UK, n=36 from Canada; Table 4.1), 38 underwent AVR (*AVR Cohort*: age 66±8 years, 76% male, peak aortic-jet velocity 4.70±0.83 m/s) and 61 remained under medical surveillance without intervention (*Natural History Cohort*: age 61±12 years, 66% male, peak aortic-jet velocity 3.24±0.76 m/s).

Table 4.1: Baseline characteristics of Patients in the Natural History and AVR Cohorts

	Natural History Cohort N=61	AVR Cohort N=38
Age, years	61±12	66±8
Male gender n (%)	40 (66)	29 (76)
Body mass index (kg/m^2)	28.3±5.6	27.3±3.6
Body surface area (m^2)	1.88±0.21	1.86±0.16
Past medical history		
Hypertension, n (%)	35 (58)	23 (61)
Diabetes mellitus, n (%)	21 (34)	6 (16)
Hyperlipidemia, n (%)	17 (28)	19 (50)
Obstructive coronary artery disease, n (%)	15 (25)	16 (42)
Previous percutaneous coronary intervention, n (%)	9 (15)	6 (16)
Previous coronary artery bypass graft, n (%)	3 (5)	0 (0)
Systolic blood pressure, mmHg	139±22	146±22
Diastolic blood pressure, mmHg	82±11	85±13
Echocardiography		
Aortic stenosis severity, n (%)		
- Mild	26 (43)	0
- Moderate	21 (34)	0
- Asymptomatic severe	14 (23)	0
- Symptomatic severe	0	38 (100)

Natural History Cohort (LV Remodelling)

At baseline, aortic stenosis was graded as mild in half of the cohort, with the remainder split between moderate (34%) and severe (23%, Table 4.1). No patient had symptoms attributable to valve disease. Follow-up magnetic resonance imaging was performed at 2.1±0.7 years following baseline scan.

As expected, aortic stenosis severity increased (peak aortic-jet velocity 0.15 [0 to 0.29] m/s/yr; mean gradient 3 [1 to 5] mmHg/yr; AVA: -0.05 [-0.08 to -0.01] cm^2/yr; P<0.001 for all, Table 4.2) with concurrent increases in both left ventricular mass index (3 [1 to 5] g/m^2/yr, P<0.001) and maximum left ventricular wall thickness (0.5 [0 to 1] mm/yr, P<0.001). These changes were accompanied by a reduction in longitudinal systolic function (-0.5 [-1.5 to 0.3] mm/yr, P=0.003) and an increase in left ventricular filling pressures (E/e' 0.6 [-0.4 to 1.3] /yr, P=0.006, Table 4.2). There was no significant change in left ventricular stroke volume or ejection fraction over time (both P≥0.20).

When classified by baseline aortic stenosis severity, there was a stepwise increase in the progression of both the valve stenosis severity (change in peak aortic-jet velocity: mild aortic stenosis 0.05 [-0.03 to 0.20], moderate aortic stenosis 0.16 [-0.04 to 0.29], and severe aortic stenosis 0.33 [0.16 to 0.42] m/s/yr, P=0.002) and the hypertrophic response (change in left ventricular mass index: mild aortic stenosis 2 [1 to 4], moderate aortic stenosis 3 [2 to 5], and severe aortic stenosis 5 [2 to 9] g/m^2/yr, P=0.07; Table 4.3, Figure 4.1). Indeed, a moderate correlation was observed between the rate of peak aortic-

jet velocity progression and the rate of LVMi progression (r=0.41, P=0.001) with both baseline and annualised peak aortic-jet velocity change being predictors of the rate of left ventricular mass index progression on univariable analysis. Annualised change in peak aortic-jet velocity was the only independent predictor of left ventricular mass index progression on multivariable analysis (P=0.02, Table 4.4).

Myocardial Fibrosis

Indexed extracellular volume (iECV) increased over time (0.5 [0 to 2.3] mL/m^2/yr; P<0.0001, Table 4.2, Figure 4.1), with progression again appearing to increase in a step-wise manner across patients with mild (0.3 [-0.1 to 0.6] mL/m^2), moderate (0.8 [-0.1 to 2.9] mL/m^2) and severe (2.0 [0.2 to 2.9] mL/m^2) aortic stenosis (P=0.07, Table 4.3). Indeed, iECV increased almost 7-fold faster in those with severe versus mild aortic stenosis (p=0.01, Figure 4.1). By contrast, no progression in ECV% was observed over time either across the cohort as a whole (0 [-1 to 1] %, P=0.80) or within severity subgroups (P=0.61).

Mid-wall LGE was present at baseline in 16 patients (26%) and progressed rapidly with time (change in LGE mass 1.6 [0.4 to 4.1] g/yr, P<0.0001; Table 4.2), equivalent to a relative annual progression of 78 [50 to 158] %. This occurred both at the sites of existing LGE and, in a quarter of patients, at remote sites with the development of new areas of mid-wall LGE (Figures 4.2 and 4.3). Again faster rates of progression were observed in patients with more advanced valve stenosis (P=0.02) and greater levels of diffuse fibrosis

(P=0.019, by tertiles of iECV, Figure 4.2). Moreover patients with the most mid-wall LGE at baseline demonstrated the fastest subsequent progression (tertile 1 baseline LGE: 0.3 [0.1 to 0.9], tertile 2: 1.6 [1.0 to 3.8] and tertile 3: 4.1 [3.4 to 7.2] g/yr, P=0.007; Figure 4.2). Eight patients (13%) had a subendocardial pattern of LGE at baseline. On repeat magnetic resonance imaging there were no new areas of subendocardial LGE and no change in the subendocardial LGE mass (P=0.56, Table 4.2), consistent with these areas representing previous myocardial infarction.

Figure 4.1: Annualised Changes in Aortic Valve Obstruction, Left Ventricular Hypertrophy and Diffuse Fibrosis in the Natural History and AVR Groups.

Annualised progression in peak aortic-jet velocity (A), left ventricular mass (B) and diffuse fibrosis (iECV, C) increased in a step-wise fashion with severity of aortic stenosis. The slowest progression for each parameter was observed in patients with mild aortic stenosis and the fastest progression in those with severe stenosis. ECV% did not change (D) suggesting balanced progression in cellular hypertrophy and interstitial fibrosis.

Following AVR there was significant regression in valve obstruction (A), LVMi (B) and iECV (diffuse fibrosis, C). ECV% increased (D) suggesting more rapid regression in cellular hypertrophy than interstitial diffuse fibrosis (all P values <0.005).

AVR; aortic valve replacement, ECV; extracellular volume, iECV; indexed extracellular volume, LVMi; left ventricular mass index

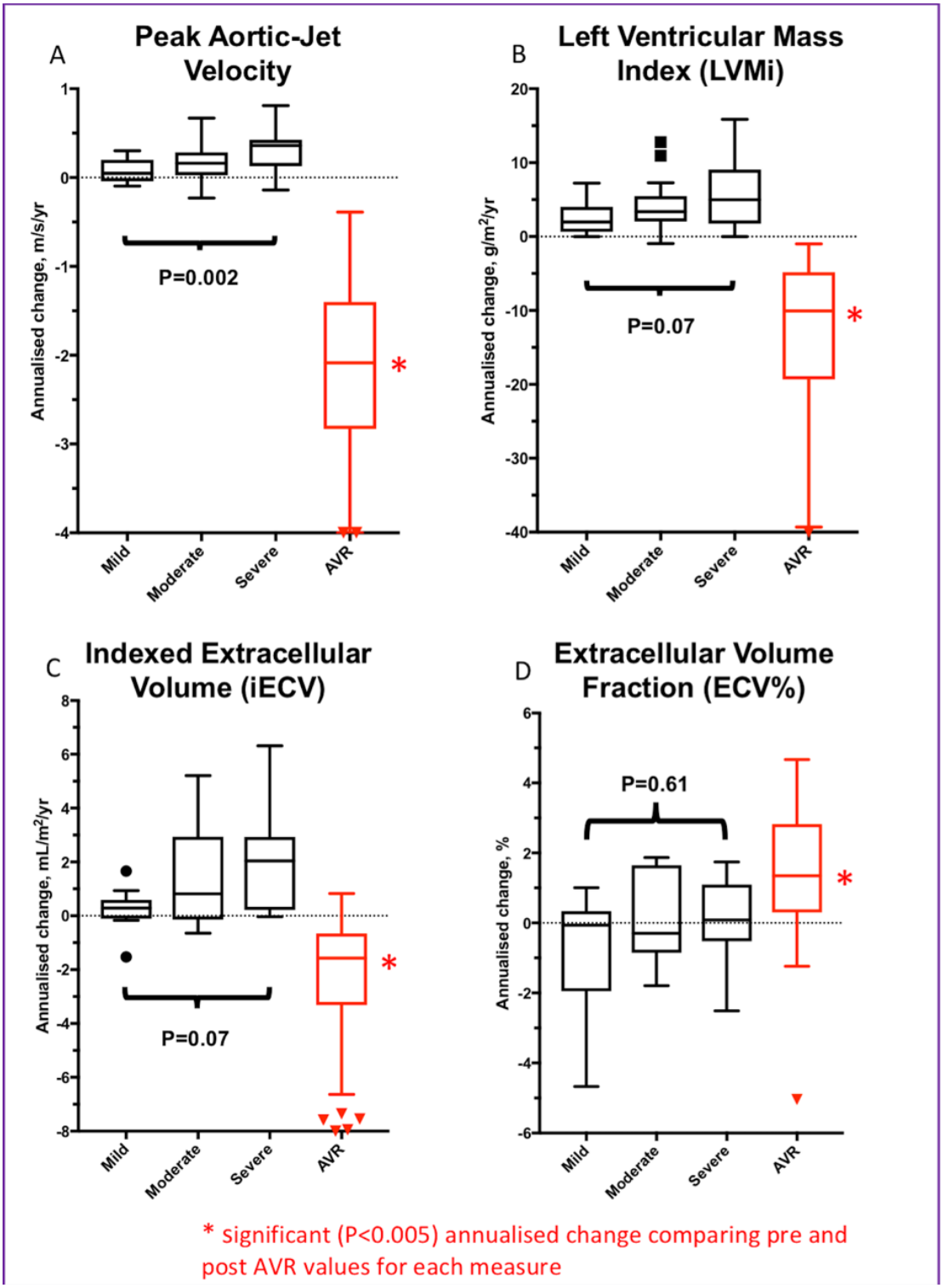

* significant (P<0.005) annualised change comparing pre and post AVR values for each measure

Figure 4.2: Serial Magnetic Resonance Images in a Patient with Severe Aortic Stenosis and Progression of Replacement Fibrosis.

Top Row: Mid-wall LGE is present baseline magnetic resonance imaging (white arrow, baseline image). New areas of LGE can be seen on follow-up magnetic resonance imaging after one year (red arrows). The patient subsequently developed exertional breathlessness and underwent AVR. Repeat imaging 1 year after AVR demonstrated no change in the pattern or volume of LGE.

In patients with established mid-wall LGE, rapid accumulation of further LGE was observed with the fastest progression in those with the most severe aortic stenosis (A), the highest baseline burden of LGE (B) and the most advanced iECV (C). Following AVR there was no change in LGE burden (A).

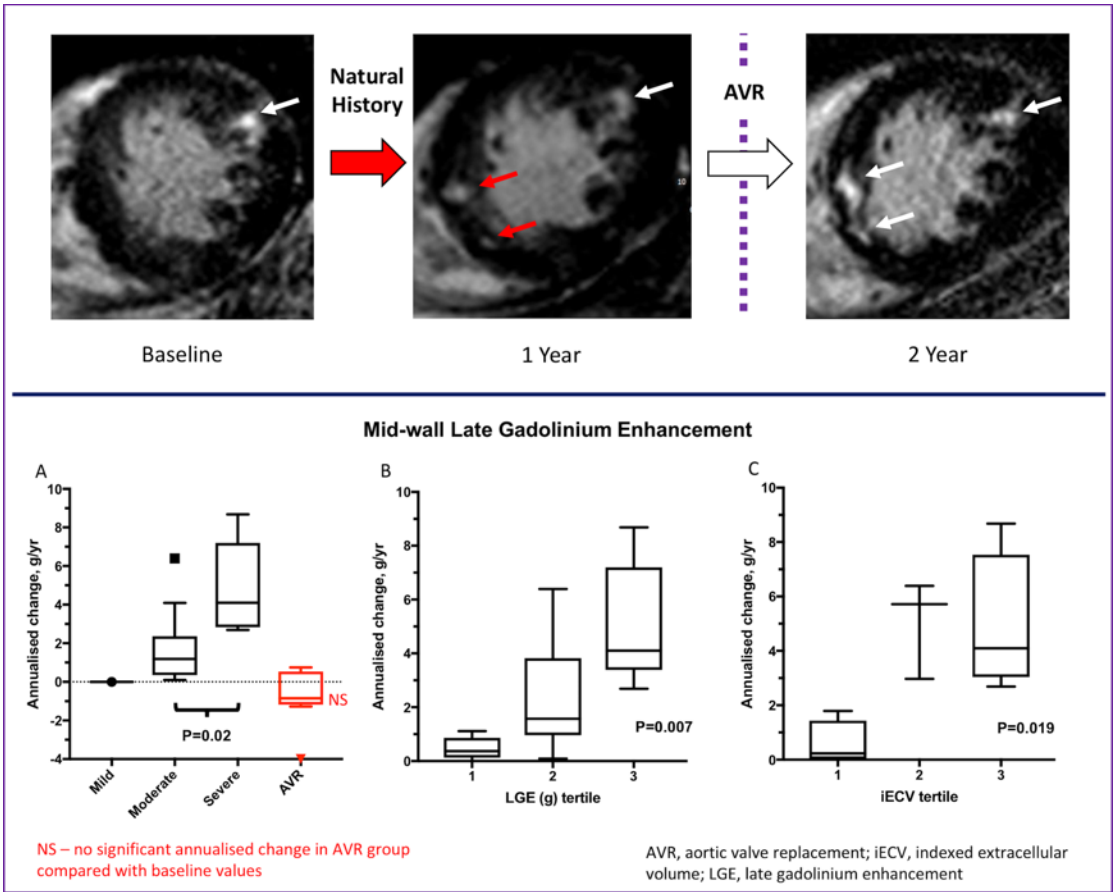

Figure 4.3: Changes in Left Ventricular Mass, Diffuse Fibrosis and Replacement Fibrosis in Aortic Stenosis Before and After Valve Replacement

Longitudinal changes in left ventricular mass (LVMi), diffuse fibrosis (iECV) and replacement fibrosis (LGE) before and after valve replacement (AVR) are illustrated with two example patients (A and B). All three measures increase exponentially as stenosis severity increases (patient A, natural history cohort) and new areas of LGE are seen on follow-up imaging (red arrows). However following AVR, cellular hypertrophy regresses more quickly than diffuse fibrosis and replacement fibrosis appears unchanged (patient B, white arrows).

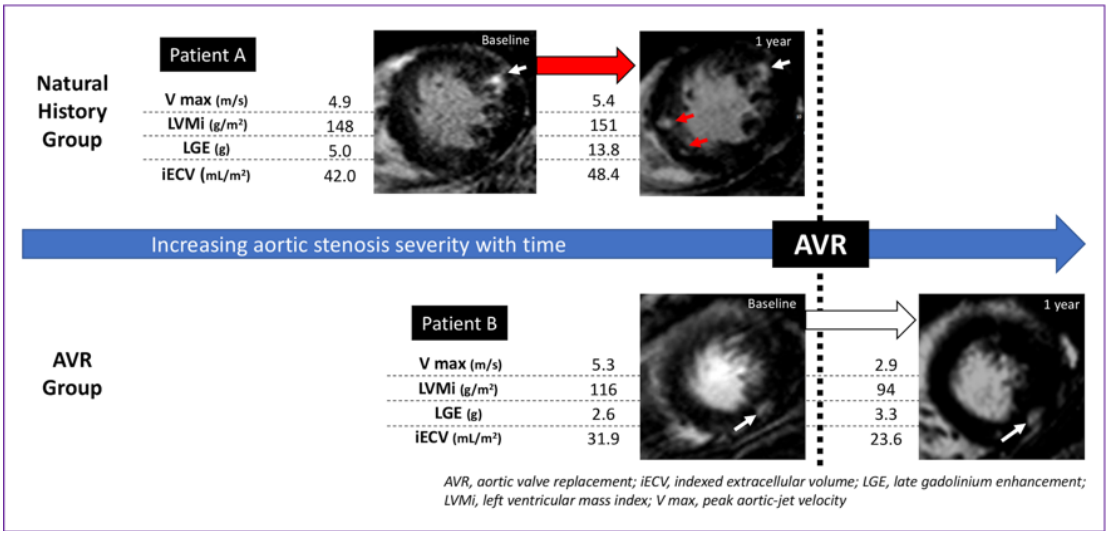

Table 4.2: Baseline and Annualised Change in Markers of Left Ventricular Remodelling Amongst Patients in the Natural History Group

	NATURAL HISTORY GROUP (N = 61) (2.1±0.7 years follow-up)		
LV assessment	**Baseline values**	**Annualised absolute change (units/yr)**	**P value**
Indexed left ventricular-end diastolic volume, mL/m^2	70±12	-1 [-4, 2]	0.015
Indexed left ventricular-end systolic volume, mL/m^2	18±7	-1 [-3, 1]	0.03
Indexed stroke volume, mL/m^2	52±9	0 [-3, 2]	0.31
Ejection fraction, %	75±8	0 [-2, 4]	0.23
Left ventricular mass index, g/m^2	75±20	3 [1, 5]	<0.0001
Maximum left ventricular wall thickness, mm	12±3	0.5 [0, 1]	<0.0001
Mass/volume, g/mL	1.09±0.28	0.08 [0.02, 0.14]	<0.0001
Longitudinal systolic function, mm	14±3	-0.5 [-1.5, 0.3]	0.0003
Indexed left atrial volume, mL/m^2	37±12	0 [-3, 3]	0.99
Infarct late gadolinium enhancement, n (%)	8 (13)	-	-
Infarct late gadolinium enhancement mass, g	7.6±4.5	-0.1 [-1.4, 0.7]	0.56
Mid-wall late gadolinium enhancement, n (%)	16 (26)	-	-
Mid-wall late gadolinium enhancement mass, g	2.5 [0.8, 4.8]	1.6 [0.4, 4.1]	<0.0001
T1 mapping measures			
Extracellular volume fraction, %	26.6±3.1	0 [-1, 1]	0.80
Total extracellular volume, mL	40±13	0.8 [0.1, 4.0]	<0.0001
Indexed extracellular volume, mL/m^2	21±6	0.5 [0, 2.3]	<0.0001
Echocardiography			
Peak aortic-jet velocity, m/s	3.24±0.76	0.15 [0, 0.29]	<0.0001
Mean aortic valve gradient, mmHg	24±12	3 [1, 5]	<0.0001
Aortic valve area, cm^2	1.08±0.31	-0.05 [-0.08, -0.01]	<0.0001
Indexed stroke volume, mL/m^2	42±7	0 [-1, 2]	0.31
Mean systolic blood pressure, mmHg	139±22	-1 [-6, 2]	0.011
Valvuloarterial impedance (Zva), mmHg/mL/m^2	4.06±0.99	-0.01 [-0.15, 0.20]	0.86
E/A ratio	1.1±0.3	0 [-0.1, 0.1]	0.71
Mean e', cm/s	7.47±2.34	-0.10 [-0.59, 0.42]	0.20
E/e' ratio	10.9 [8.7, 12.8]	0.6 [-0.4, 1.3]	0.006

Variables are expressed as mean ± standard deviation or median [IQR] as appropriate
For the annualised changes, the unit is the unit mentioned after the name of the variable per year: e.g. for indexed left ventricular volumes (mL/m^2), the unit for the annualised change is mL/m^2/yr.

Table 4.3: Annualised Change in Markers of Progression and Left Ventricular Remodelling According to Aortic Stenosis Severity in the Natural History Group

	Aortic Valve Stenosis severity			
LV assessment	**Mild N = 26**	**Moderate N = 21**	**Severe N = 14**	**P value**
Indexed left ventricular-end diastolic volume, mL/m^{2}/yr	-1 [-5, 3]	-1 [-4, 2]	-2 [-5, 3]	0.93
Indexed left ventricular-end systolic volume, mL/m^2/yr	-1 [-5, 4]	-1 [-7, 2]	-3 [-5, 3]	0.43
Indexed stroke volume, mL/m^2/yr	-1 [-3, 1]	0 [-3, 3]	0 [-3, 2]	0.55
Ejection fraction, %/yr	0 [-3, 2]	0 [-1, 4]	2 [-2, 4]	0.26
Left ventricular mass index, g/m^2/yr	2 [1, 4]	3 [2, 5]	5 [2, 9]	0.07
Maximum left ventricular wall thickness, mm/yr	0.5 [0.0, 1.0]	0.5 [-0.3, 1.2]	0.5 [0.0, 1.0]	0.91
Mass/volume, g/mL/yr	0.06 [-0.01, 0.11]	0.06 [0.02, 0.12]	0.14 [0.08, 0.27]	0.01
Longitudinal systolic function, mm/yr	-0.5 [-1.1, 0.3]	-1.2 [-2.0, -0.3]	-0.1 [-1.5, 0.5]	0.08
Indexed left atrial volume, mL/m^2/yr	-1 [-3, 2]	1 [-2, 5]	0 [-5, 2]	0.30
Infarct late gadolinium enhancement, n (%)	2 (8)	3 (14)	3 (21)	-
Mid-wall late gadolinium enhancement, n (%)	1 (4)	10 (48)	5 (36)	-
Mid wall late gadolinium enhancement mass, g/yr	0	1.2 [0.3, 2.4]	4.1 [2.8, 7.2]	0.02*
T1 mapping measures				
Extracellular volume fraction, %/yr	0 [-1.9, 0.8]	0 [-0.8. 1.7]	0 [0.5, 0.9]	0.61
Total extracellular volume, mL/yr	0.7 [0.0, 1.0]	1.5 [-0.2, 6.8]	3.7 [0.4, 6.0]	0.08
Indexed extracellular volume, mL/m^2/yr	0.3 [-0.1, 0.6]	0.8 [-0.1, 2.9]	2.0 [0.2, 2.9]	0.07
Echocardiography				
Peak aortic-jet velocity, m/s/yr	0.05 [-0.03, 0.20]	0.16 [-0.04, 0.29]	0.33 [0.16, 0.42]	0.002
Mean aortic valve gradient, mmHg/yr	2 [0, 3]	2 [0, 5]	7 [3, 10]	<0.001
Aortic valve area, cm^2/yr	-0.05 [-0.12, -0.02]	-0.03 [-0.07, 0.00]	-0.06 [-0.09, 0.00]	0.47
Indexed stroke volume, mL/m^2/yr	-1 [-2, 1]	0 [-1, 2]	3 [-2, 5]	0.06
Mean systolic blood pressure, mmHg/yr	-2 [-6, 1]	-1 [-7, 3]	-5 [-15, 1]	0.65
Valvuloarterial impedance (Zva), mmHg/mL/m^2/yr	0 [-0.15, 0.28]	0 [-0.15, 0.49]	0.36 [-0.32, 1.19]	0.50
E/A ratio	0 [-0.1, 0.1]	0 [-0.1, 0.2]	0 [-0.2, 0.1]	0.91
Mean e', cm/s/yr	-0.17 [-0.56, 0.18]	-0.04 [-0.73, 0.58]	-0.15 [-0.78, 0.51]	0.82
E/e' ratio	0.6 [-0.4, 1.2]	-0.1 [-0.9, 1.1]	1.6 [0.9, 2.3]	<0.001

Results expressed as median [IQR]

Table 4.4: Univariable and Multivariable Linear Regression Analysis to Examine the Predictors of Annualised Progression of Left Ventricular Mass Over Time in the Natural History Group.

	Univariable analysis		Multivariable analysis	
	Change in left ventricular mass index, β (95% CI) ($g/m^2/yr$)	**P value**	**Change in left ventricular mass index, β (95% CI) ($g/m^2/yr$)**	**P value**
Age, years	0.03 (-0.05 to 0.10)	0.50	0.05 (-0.04 to 0.13)	0.30
Men	0.66 (-1.33 to 2.64)	0.51	0.95 (-1.16 to 3.05)	0.37
Hypertension	-1.38 (-3.25 to 0.49)	0.14	-1.75 (-3.95 to 0.44)	0.12
Valvuloarterial impedance (Zva)	-0.24 (-1.49 to 1.01)	0.70	-0.08 (-1.35 to 1.20)	0.91
Baseline peak aortic-jet velocity, m/s	1.44 (0.26 to 2.63)	0.02	0.67 (-0.73 to 2.07)	0.34
Annualised peak aortic-jet velocity change, m/s/yr	7.10 (2.90 to 11.30)	0.001	4.98 (0.53 to 9.91)	0.048
Presence mid-wall late gadolinium enhancement	0.45 (-1.67 to 2.56)	0.68	-0.17 (-2.28 to 1.95)	0.88

CI; confidence interval

AVR Cohort (Reverse Remodelling)

Patients underwent AVR for a guideline-based indication 32 [13 to 66] days after baseline imaging with repeat imaging performed 0.9±0.3 years after AVR. Twenty-nine patients received a bioprosthetic AVR and in 9 patients a mechanical prosthesis was utilized. No patient underwent transcatheter valve replacement (TAVR). As expected, echocardiographic assessments of aortic valve obstruction improved after surgery (change in peak aortic-jet velocity -2.05 [-2.70 to 1.56] m/s, change in mean gradient: -32 [-44 to -26] mmHg, change in AVA 0.73 [0.46 to 0.91] cm^2, change in valvulo-arterial impedance ZVa -0.60 [-1.19 to 0.08], all P<0.0001; Table 4.5).

There was a 19% reduction in left ventricular mass index (-10 [-19 to -5] $g/m^2/yr$, P<0.0001, Table 4.5) following AVR, accompanied by a corresponding reduction in maximal left ventricular wall thickness (-2 [-2 to -1] mm/yr, P<0.0001). A moderate correlation was observed between the magnitude of left ventricular mass regression and the reduction in peak aortic-jet velocity following valve intervention (ρ=0.35, P=0.03). On multivariable regression analysis, a high pre-AVR left ventricular mass index and the absence of hypertension were both associated with greater left ventricular mass regression (Table 4.6) as was a lower post-AVR Vmax, although this last variable did not reach statistical significance (P=0.06).

Measures of left ventricular relaxation and filling pressure improved following AVR (mean e' 1.35 [0.26 to 2.91], P=0.0004; E/e' -1.3 [-4.3 to 1.1], P=0.02) and there was an apparent trend towards improved longitudinal left ventricular systolic function (1 [-1 to 3] mm/yr, P=0.10). No change in ejection fraction was observed (P=0.78) although the indexed end-diastolic left ventricular volume did decrease modestly (-3 [-9 to 2] mL/m^2/yr, P=0.009).

Myocardial Fibrosis

There was a 11% reduction in indexed extracellular volume (iECV) on repeat imaging following AVR (-2 [-3 to -1] mL/m^2/yr, P<0.001; Table 4.5, Figure 4.1). In contrast, the ECV% increased (1.2 [0.4 to 2.2] %/yr, P=0.003; Figure 4.1) consistent with faster regression of left ventricular mass than diffuse fibrosis. The type of replacement valve implanted did not influence the degree of LV mass (P=0.61) or iECV (P=0.97) regression.

Upon visual assessment, mid-wall LGE was present in 10 patients (26%) at baseline. No patient went on to develop new areas of LGE on repeat imaging, nor did any patient with existing LGE demonstrate resolution of any established areas post-AVR (Figure 4.3). Quantitatively there was no significant change in LGE mass following AVR (P=0.22, Table 4.5), even in patients rescanned after 2 years. Infarct pattern LGE was observed at baseline in 5 patients (13%). One new infarct was detected on repeat imaging but overall no change was observed in LGE mass in these patients (P=0.72).

Sensitivity analysis was performed in patients who underwent repeat imaging at the same time interval (2 years in the natural history cohort, n=50, 1 year in the AVR cohort, n=27). Our findings were unchanged from those made across the cohort as a whole (Figure 4.4 and Tables 4.7 and 4.8).

Figure 4.4: Absolute Changes in Aortic Valve Obstruction, Left Ventricular Hypertrophy and Diffuse Fibrosis in the Natural History and AVR Groups.

Absolute change in measures was assessed at the time-point with the majority of patient follow-up in the Natural History (2 years, N=50) and the AVR (1 year, N=27) groups. As in the annualised change analysis, there is an increase in rate of progression of aortic-jet velocity, LVMi and iECV with increasing AS severity in the Natural History group. However, ECV fraction does not change at 2 years. Following AVR, there is regression of both LVMi and iECV, and again consistent with the annualised change analysis, we see an increase in ECV fraction, suggesting that cellular hypertrophy regresses more quickly than diffuse fibrosis.

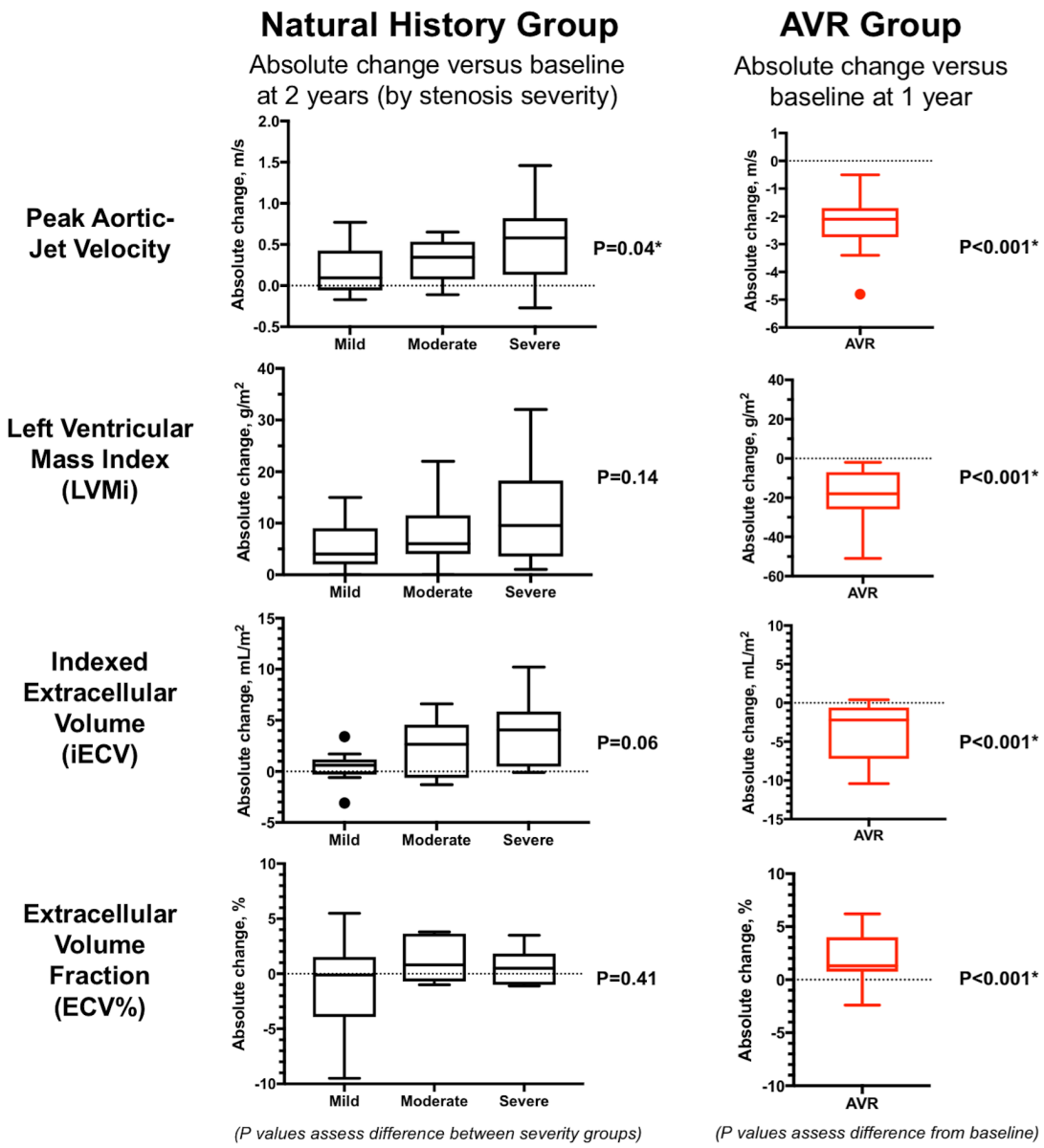
Natural History Group
Absolute change versus baseline at 2 years (by stenosis severity)
AVR Group
Absolute change versus baseline at 1 year
Peak Aortic-Jet Velocity
Absolute change, m/s
Mild
Moderate
Severe
P=0.04*
AVR
P<0.001*
Left Ventricular Mass Index (LVMi)
Absolute change, g/m²
P=0.14
P<0.001*
Indexed Extracellular Volume (iECV)
Absolute change, mL/m²
P=0.06
P<0.001*
Extracellular Volume Fraction (ECV%)
Absolute change, %
P=0.41
P<0.001*
(P values assess difference between severity groups)
(P values assess difference from baseline)

Table 4.5: Baseline and Annualised Change in Markers of Left Ventricular Remodelling Amongst Patients in the AVR Group

	AVR GROUP (N = 38) (0.9±0.3 years follow-up)			
LV assessment	**Baseline values**	**Absolute change**	**Annualised absolute change (units/yr)**	**P value**
Indexed left ventricular-end diastolic volume, mL/m^2	67±15	-	-3 [-9, 2]	0.009
Indexed left ventricular-end systolic volume, mL/m^2	19±13	-	-2 [-5, 1]	0.19
Indexed stroke volume, mL/m^2	49±8	-	-3 [-7, 1]	0.009
Ejection fraction, %	74±8	-	0 [-4, 4]	0.78
Left ventricular mass index, g/m^2	93±21	-	-10 [-19, -5]	<0.0001
Maximum left ventricular wall thickness, mm	15±3	-	-2 [-2, -1]	<0.0001
Mass/volume, g/mL	1.43±0.32	-	-0.08 [-0.19, 0.02]	0.003
Longitudinal systolic function, mm	12±3	-	1 [-1, 3]	0.10
Indexed left atrial volume, mL/m^2	37±11	-	-1 [-8, 4]	0.33
Infarct late gadolinium enhancement, n (%)	5 (13)	-	-	-
Infarct late gadolinium enhancement mass, g	4.8±2.8	-	0 [-0.7, 1.7]	0.72
Mid-wall late gadolinium enhancement, n (%)	10 (26)	-	-	-
Mid-wall late gadolinium enhancement mass, g	3.3 [2.6, 8.0]	-	-0.9 [-1.2, 0.5]	0.22
T1 mapping measures				
Extracellular volume fraction, %	27.2±2.8	-	1.2 [0.4, 2.2]	0.003
Total extracellular volume, mL	47±18	-	-3 [-12, -1]	<0.0001
Indexed extracellular volume, mL/m^2	25±8	-	-2 [-3, -1]	<0.0001
Echocardiography				
Peak aortic-jet velocity, m/s	4.70±0.83	-2.05 [-2.70, 1.56]	-	<0.0001
Mean aortic valve gradient, mmHg	52±22	-32 [-44, -26]	-	<0.0001
Aortic valve area, cm^2	0.79±0.20	0.73 [0.46, 0.91]	-	<0.0001
Indexed stroke volume, mL/m^2	48±10	-	-1 [-9, 4]	0.13
Mean systolic blood pressure, mmHg	146±22	-	-2 [-22, 11]	0.46
Valvuloarterial impedance (Zva), mmHg/mL/m^2	4.29±1.05	-0.60 [-1.19, 0.08]	-	<0.0001
E/A ratio	1.0±0.3	-	0.16 [-0.06, 0.42]	0.004
Mean e', cm/s	6.15±2.04	-	1.35 [0.26, 2.91]	0.0004
E/e' ratio	12.9 [10.2, 18.0]	-	-1.3 [-4.3, 1.1]	0.02

Table 4.6: Univariable and Multivariable Linear Regression Analysis to Examine the Predictors of Annualised Regression of Left Ventricular Mass Over Time in the AVR Group.

	Univariable analysis		Multivariable analysis	
	Change in left ventricular mass index, β (95% CI) ($g/m^2/yr$)	**P value**	**Change in left ventricular mass index, β (95% CI) ($g/m^2/yr$)**	**P value**
Age, years	0.45(0.01 to 0.90)	0.047	-0.11(-0.46 to 0.24)	0.53
Men	-3.0(-12.1 to 6.1)	0.50	5.23(-1.10 to 11.55)	0.10
Hypertension	10.4(3.9 to 16.8)	0.002	5.52(0.29 to 10.75)	0.04
Valvuloarterial impedance (Zva)	1.9(-1.4 to 5.2)	0.26	-0.69(-3.18 to 1.79)	0.57
Pre-AVR left ventricular mass index, g/m^2	-0.37(-0.49 to -0.25)	<0.001	-0.39(-0.53 to -0.26)	<0.001
Peak aortic-jet velocity at 1 year post-AVR, m/s	2.2(-4.3 to 8.8)	0.49	4.33(-0.27 to 8.93)	0.06
Presence mid-wall late gadolinium enhancement	-9.3(-17.5 to -1.1)	0.027	-4.7(-10.5 to 1.12)	0.11

CI; confidence interval

Table 4.7: Baseline and Absolute Change in Markers of Left Ventricular Remodelling at 2 Years in the Natural History Group

	NATURAL HISTORY GROUP N = 50		
LV assessment	**Baseline values**	**2-year absolute change**	**P value**
Indexed left ventricular-end diastolic volume, mL/m^2	69±11	-2 [-8, 5]	0.058
Indexed left ventricular-end systolic volume, mL/m^2	15 [13, 22]	-2 [-5, 3]	0.07
Indexed stroke volume, mL/m^2	52±9	-1 [-6, 4]	0.47
Ejection fraction, %	75±9	0 [-4, 8]	0.15
Left ventricular mass index, g/m^2	72±17	5 [2, 12]	<0.0001
Maximum left ventricular wall thickness, mm	12±3	1 [0, 2]	<0.0001
Mass/volume	1.06±0.28	0.15 [0.02, 0.29]	<0.0001
Longitudinal systolic function, mm	14±3	-1 [-3, 0.5]	0.0005
Indexed left atrial volume, mL/m^2	37±11	-1 [-7, 5]	0.79
Infarct late gadolinium enhancement, n (%)	4 (8)	4 (8)	-
Infarct late gadolinium enhancement mass, g	8.2±4.9	0.6 [-1.8, 1.4]	0.94
Mid-wall late gadolinium enhancement, n (%)	10 (20)	10 (20)	-
Mid-wall late gadolinium enhancement mass, g	1.2 [0.5, 4.5]	2.6 [0.7, 6.0]	0.002
T1 mapping measures			
Extracellular volume fraction, %	26.6±3.4	0.1 [-1.0, 1.5]	0.89
Total extracellular volume, mL	38±11	2 [4, 1]	0.001
Indexed extracellular volume, mL/m^2	20±5	1 [0, 4]	0.001
Echocardiography			
Peak aortic-jet velocity, m/s	3.13±0.73	0.25 [-0.05, 0.51]	<0.0001
Mean aortic valve gradient, mmHg	23±12	4 [1, 9]	<0.0001
Aortic valve area, cm^2	1.12±0.31	-0.09 [-0.16, -0.02]	<0.0001
Indexed stroke volume, mL/m^2	42±7	-1 [-3, 3]	0.73
Mean systolic blood pressure, mmHg	138±20	-3 [-12, 5]	0.06
Valvuloarterial impedance (Zva), mmHg/mL/m^2	3.99±0.97	0.02 [-0.28, 0.44]	0.26
Mean e', cm/s	7.58±2.07	-0.10 [-1.17, 0.96]	0.33
E/e' ratio	10.9 [8.7, 11.9]	1.2 [-0.8, 2.5]	0.019

Table 4.8: Baseline and Absolute Change in Markers of Left Ventricular Remodelling at 1 Year in the AVR Group

	AVR GROUP N=27		
LV assessment	**Baseline values**	**1-year absolute change**	**P value**
Indexed left ventricular-end diastolic volume, mL/m^2	68±16	-4 [-18, 6]	0.047
Indexed left ventricular-end systolic volume, mL/m^2	19 [13, 25]	-3 [-8, 4]	0.22
Indexed stroke volume, mL/m^2	48±9	-3 [-14, 4]	0.08
Ejection fraction, %	73±9	1 [-5, 7]	0.77
Left ventricular mass index, g/m^2	97±23	-18 [-26, -7]	<0.0001
Maximum left ventricular wall thickness, mm	15±3	-2 [-4, -2]	<0.0001
Mass/volume	1.50±0.35	-0.17 [-0.34, -0.07]	0.02
Longitudinal systolic function, mm	11±3	3 [-1, 5]	0.003
Indexed left atrial volume, mL/m^2	36±11	-12 [-26, 0]	0.08
Infarct late gadolinium enhancement, n (%)	3 (11)	4 (15)	-
Infarct late gadolinium enhancement mass, g	4.8±2.8	0 [-0.8, 1.7]	0.72
Mid-wall late gadolinium enhancement, n (%)	10 (37)	10 (37)	-
Mid-wall late gadolinium enhancement mass, g	3.6 [2.6, 9.6]	-1 [-1.4, 0]	0.14
T1 mapping measures			
Extracellular volume fraction, %	26.9±2.5	1.4 [0.8, 4.0]	<0.0001
Total extracellular volume, mL	50±20	-4 [-12, -1]	<0.0001
Indexed extracellular volume, mL/m^2	27±9	-2 [-7, -1]	<0.0001
Echocardiography			
Peak aortic-jet velocity, m/s	4.73±0.91	-2.15 [-2.78, -1.60]	<0.0001
Mean aortic valve gradient, mmHg	54±25	-32 [-48, -26]	<0.0001
Aortic valve area, cm^2	0.79±0.22	0.70 [0.49, 1.06]	<0.0001
Indexed stroke volume, mL/m^2	47±10	-2 [-8, 3]	0.028
Mean systolic blood pressure, mmHg	143±21	-4 [-17, 12]	0.15
Valvuloarterial impedance (Zva), mmHg/mL/m^2	4.33±1.14	-0.56 [-1.39, -0.05]	0.0004
Mean e', cm/s	6.05±2.01	1.38 [-0.12, 3.37]	0.003
E/e' ratio	12.9 [10.1, 18.0]	-1 [-5, 3]	0.56

DISCUSSION

This is the first study to characterise how left ventricular hypertrophy and fibrosis progress in aortic stenosis and how these processes then reverse remodel following AVR. Using a multicentre multi-modality imaging approach with serial echocardiography and magnetic resonance imaging, we have demonstrated that both hypertrophy and fibrosis progress in an increasingly rapid manner as aortic stenosis severity advances. Once mid-wall patterns of replacement fibrosis (LGE) have become established, further scarring appears to accumulate rapidly. Whilst left ventricular hypertrophy and diffuse fibrosis reverse following AVR, mid-wall LGE does not and appears to be irreversible. Given the adverse prognosis associated with mid-wall fibrosis burden, our data suggest prompt AVR at the first sign of mid-wall LGE or just before its development might improve long-term patient outcomes.

In the Natural History Cohort we observed a slow and steady progression in each of the echocardiographic measures of valvular stenosis as anticipated.(14) This valve progression was strongly influenced by baseline aortic stenosis severity, with the slowest progression in patients with mild stenosis and the most rapid progression in those with severe obstruction. This was mirrored by a similar pattern of increasing left ventricular mass progression. Indeed a moderate correlation was observed between valve stenosis progression and left ventricular mass progression, with the annualised increase in peak aortic-jet velocity the only independent predictor

of left ventricular mass progression on multi-variable analysis. Consistent with this, AVR resulted in a substantial reduction in aortic valve obstruction that was accompanied by a ~20% reduction in the left ventricular mass. Again there was a strong correlation between the reduction in trans-valvular gradient and left ventricular mass regression, with the former emerging as an independent predictor of reverse remodelling on multivariable analysis. One surprising finding was a small but significant reduction in stroke volume following AVR. This may relate to accompanying reductions in LV end-diastolic volume but requires further study.

What about myocardial fibrosis? Magnetic resonance imaging is the only non-invasive imaging technique capable of assessing both diffuse interstitial (T1 mapping techniques) and replacement fibrosis (LGE). T1 mapping provides multiple different measurements that demonstrate close agreement with collagen volume fraction on histology and therefore act as surrogates of interstitial myocardial fibrosis.(7,85) We here investigated the ECV% and iECV because of the advantages these measures hold when comparing values acquired in a multi-centre setting on different scanners and at different field strengths. Whilst ECV% gives an indication of the proportion of the myocardium made up of fibrosis, iECV is a surrogate of the total fibrosis burden in the left ventricle. Together these two measures can provide unique insights into how the extracellular and intracellular compartments of the myocardium change in aortic stenosis and in response to AVR. Like peak aortic-jet velocity and left ventricular mass index, the iECV increased with time

suggesting progressive expansion of the extracellular compartment and diffuse interstitial fibrosis. Once again this progression appeared to occur quickest in those with the most advanced valvular stenosis. By comparison, ECV% did not demonstrate any evidence of progression suggesting balanced increases in the size of the cellular and extracellular compartments as left ventricular remodelling advances.

Following AVR, reductions in iECV were observed similar to those observed in peak aortic-jet velocity and left ventricular mass, confirming that diffuse interstitial fibrosis is indeed reversible. However the accompanying rise in ECV% suggests that regression in cellular hypertrophy occurs faster and to a greater degree than this reduction in diffuse fibrosis. These novel imaging findings are in keeping with historical data from myocardial biopsies performed following AVR showing an initial increase of percentage interstitial fibrosis on histology at 18 months.(137)

Mid-wall LGE represents a more advanced stage of focal replacement fibrosis(55) in the myocardium and has been described in numerous aortic stenosis populations.(46,49,66) Mid-wall LGE is a marker of left ventricular decompensation demonstrating a close association with myocardial injury, left ventricular diastolic function, left ventricular systolic function and exercise capacity.(7) Moreover multiple different studies from multiple centres have confirmed mid-wall LGE as a powerful prognostic marker of long-term all-cause and cardiovascular mortality.(7,19,46,49) Most of these adverse events

occur after AVR(145) and there appears to be a proportionate relationship: the more myocardial LGE, the worse the clinical outcomes.(19,46)

For the first time, we have demonstrated that the burden of mid-wall LGE increases whilst asymptomatic patients are being monitored in the clinic. Indeed, once mid-wall LGE has become established then further accumulation of such scarring is relatively rapid, increasing on average by 75% each year especially in patients with a high baseline fibrosis burden. Importantly, we go on to demonstrate that whilst this progressive scarring is arrested by AVR, it does not reverse even out to 2 years after AVR. This is consistent with smaller short-term studies and implies that the scar patients develop whilst waiting for surgery remains with them for the rest of their life, contributing to their poorer long-term prognosis. These findings could have important clinical implications for optimising patient care and the timing of aortic valve replacement. For example, based on our data, prompt AVR could be undertaken when mid-wall LGE is first identified, in order to prevent the accumulation of further scarring and to improve long-term patient outcomes. This strategy requires prospective confirmation and is currently being tested in the Early Valve Replacement guided by Biomarkers of Left Ventricular Decompensation in Asymptomatic Patients with Severe Aortic Stenosis (EVOLVED) randomised controlled trial (NCT03094143).

Our study does have some limitations. Given the heterogeneity in the timing of follow-up imaging we used annualised change for our primary analysis. This

assumes linear progression or regression of variables which may not be the case. In the sensitivity analysis, we repeated our analysis of the data using absolute change in the subgroup of patients who underwent repeat imaging after the same time interval (2 years in the natural history cohort (n=50) and 1 year in the AVR cohort (n=27)). Our results were consistent with the annualised analysis. Further studies are still required to investigate how LV remodelling and reverse remodelling progress over multiple time points in individual patients. The ECV measurements (ECV%, iECV) reflect the size of the extracellular compartment and therefore potentially represent multiple different factors including the intravascular space and myocardial infiltration. However, in patients with aortic stenosis (and in the absence of associated cardiac amyloidosis), there is a close association between these ECV measurements and histological markers of interstitial fibrosis, confirming that they provide a useful surrogate measure of interstitial fibrosis, as here presented.

CONCLUSION

We have used echocardiography and magnetic resonance imaging to characterise the structural changes in the myocardium that occur in patients with aortic stenosis both during routine surveillance and following AVR. In patients with aortic stenosis, cellular hypertrophy and diffuse interstitial fibrosis increase in a balanced and exponential manner before reversing at different rates following AVR. Once established, mid-wall replacement fibrosis accumulates rapidly but appears irreversible following AVR. The myocardial scar burden that patients develop whilst waiting for surgery therefore persists into the long-term along with prognostic implications that this entails. Prompt valve replacement as soon as mid-wall fibrosis develops holds promise in improving clinical outcomes in patients with aortic stenosis.

Chapter 5: Myocardial Extracellular Volume in Patients with Aortic Stenosis Undergoing Valve Intervention

SUMMARY

Background

Myocardial fibrosis is a key mechanism of left ventricular decompensation in advanced aortic stenosis and can be quantified using cardiac magnetic resonance (CMR) imaging T1 mapping techniques. We assessed T1 mapping measures of fibrosis in patients with severe aortic stenosis referred for aortic valve intervention, and determined their associations with clinical characteristics, disease severity and long-term clinical outcome.

Methods

In this international prospective cohort study, patients with severe aortic stenosis underwent CMR with T1 mapping prior to aortic valve intervention. Image analysis was performed by a single core laboratory and three T1 mapping measures (native T1, extracellular volume fraction [ECV%] and indexed extracellular volume [iECV]) were determined.

Results

Four-hundred patients (70±10 years, 60% male) from nine international centres were enrolled. Native T1 was higher in patients imaged at 3 T compared to 1.5 T (1213±57 versus 1050±48 ms, $P<0.001$), whereas ECV% did not vary by CMR scanner manufacturer, magnetic field strength or T1 mapping sequence (all $P>0.30$).

Unadjusted native T1 did not show clear associations with clinical or imaging variables. ECV% correlated with increasing age, Society of Thoracic Surgeons Predicted Risk of Mortality score, known coronary artery disease, reduced peak velocity, increasing left ventricular mass, presence of late gadolinium enhancement and reduced ejection fraction ($P<0.05$ for all). Following adjustment for all clinical variables, ECV% remained associated with both left ventricular ejection fraction ($P<0.001$) and mass index ($P=0.043$). Similar associations were seen with iECV.

Aortic valve intervention was performed 19 [4, 61] days following CMR imaging, with median of 3.8 [1.7, 4.5] years follow-up in 391 patients and 40 deaths recorded. No prognostic association for native T1 was observed, even after adjustment for magnetic field strength. A progressive increase in all-cause mortality was seen across tertiles of ECV% (14.0, 28.5 and 53.7 deaths per 1000 patient-years; log-rank test, $P=0.003$). ECV% was independently associated with all-cause mortality following adjustment for age, sex, peak velocity, impaired ejection fraction and presence of late gadolinium enhancement (hazard ratio per unit increase in ECV%: 1.13, 95%, (1.04 to 1.24), $P=0.006$). iECV was associated with all-cause mortality following adjustment for age and sex (hazard ratio 1.03 [1.00 to 1.06], $P=0.04$) but not following adjustment for other clinical variables.

Conclusion

In patients with severe aortic stenosis scheduled for aortic valve intervention, extracellular volume-based T1 mapping measures are robust, track with left ventricular decompensation, and independently predict all-cause mortality.

INTRODUCTION

Aortic stenosis is a disease of both valve and myocardium. Progressive myocardial hypertrophy occurs over time in response to sustained pressure overload restoring wall stress and maintaining cardiac performance. However, this hypertrophic response eventually decompensates, and patients transition to heart failure, symptoms and adverse events.

Myocardial fibrosis is a key pathological process driving left ventricular decompensation (8). Two patterns of fibrosis are observed; focal replacement fibrosis and diffuse interstitial fibrosis (55). Both forms of fibrosis can be detected non-invasively using cardiac magnetic resonance (CMR) imaging; replacement fibrosis with the late gadolinium enhancement (LGE) technique and diffuse interstitial fibrosis with newer T1 mapping approaches. While replacement fibrosis appears irreversible, regression of diffuse fibrosis is observed following relief of pressure overload with aortic valve intervention (137,144,146). Accurate and robust assessment of diffuse fibrosis burden is therefore desirable to identify early left ventricular decompensation at a stage where pathological left ventricular changes are largely reversible and targeted early valve intervention may improve patient outcomes.

Several T1 mapping measures have been proposed to date. Native T1 mapping produces a voxel-based map of the myocardium which estimates absolute myocardial T1 values (70). Extracellular volume (ECV)-based

measures utilise gadolinium contrast to calculate the relative (extracellular volume fraction [ECV%]) or absolute (indexed extracellular volume [iECV]) extracellular volume of the myocardium (7,85). Although these measures have been validated against histology (7,78-81,84-86,147), the optimal T1 mapping approach in aortic stenosis remains unclear and robust multicentre outcome data are lacking.

In the present study, we investigated T1 mapping in a large international multicentre study of patients with severe aortic stenosis scheduled for aortic valve intervention. In particular, we analysed the technical factors affecting measurement variability and explored the association of native T1, ECV% and iECV with markers of disease severity and clinical outcomes.

METHODS

Patient populations

Patients with AHA/ACC/ESC criteria (5,148) for severe aortic stenosis who were awaiting aortic valve intervention were recruited as part of prospective observational cohorts from several centres across Europe, North America and Asia: the UK (Edinburgh, Leeds, Leicester, Oxford, Barts Heart Centre - London), Germany (Berlin), U.S.A. (Pittsburgh), Canada (Quebec) and South Korea (Table 5.1). All patients underwent CMR with T1 mapping performed both prior to and following intravenous gadolinium contrast administration. Exclusion criteria were the presence of an implantable cardiac device, major renal dysfunction (estimated glomerular filtration rate <30 mL/min/1.73m^2) and presence of another co-existent myocardial pathology such as cardiac amyloidosis, hypertrophic cardiomyopathy or myocarditis. The study was conducted according to the Declaration of Helsinki and approved by local research ethics committees. Written informed consent was obtained from all participants. All patients underwent comprehensive medical history and physical examination. Transthoracic echocardiography was performed according to international clinical guidelines and within accredited tertiary echocardiographic units. Particular focus was placed upon measurement of aortic stenosis severity, which was assessed on the basis of the peak velocity, mean gradient and aortic valve area (149).

Table 5.1: Cardiac magnetic resonance technical details and T1 mapping results by study centre

Site	Scanner	Pulse sequence (pre)	Pulse sequence (post)	Contrast agent, dose and timing	N	Mean native T1, ms	Mean ECV%
Edinburgh Heart Centre, UK	Siemens Verio 3T	MOLLI 3(3)-3(3)-5	MOLLI 3(3)-3(3)-5	Gadovist 0.1 mmol/kg 20 mins	28	1184±52	26.4±2.6
Leeds Teaching Hospitals NHS Trust, UK	Phillips Achieva 1.5T	MOLLI 5(3)-3	MOLLI 4(1)-3(1)-2	Dotarem 0.2 mmol/kg 15 mins	24	1071±53	27.7±3.0
Glenfield Hospital, Leicester, UK	Siemens 1.5T Skyra 3T	MOLLI 3(3)-3(3)-5	MOLLI 3(3)-3(3)-5	Gadovist 0.15 mmol/kg 20 mins	5 10	997±80 1118±31	26.2±4.0
Barts Heart Centre, London, UK	Siemens Avanto 1.5T	MOLLI 5(3)-3 ShMOLLI 5(1)-1(1)-1	MOLLI 4(1)-3(1)-2 ShMOLLI 5(1)-1(1)-1	Dotarem 0.10 mmol/kg 15 mins	131 3	1053±45 1002±59	28.6±3.1
John Radcliffe Hospital, Oxford, UK	Siemens Trio 3T	ShMOLLI 5(1)-1(1)-1	ShMOLLI 5(1)-1(1)-1	Omniscan 0.03 mmol/kg 15 mins Dotarem 0.10 mmol/kg 15 mins	17 26	1224±52	28.1±3.4
HELIOS Hospital Berlin-Buch, Berlin, Germany	Siemens Verio 3T	MOLLI 3(3)-3(3)-5	MOLLI 3(3)-3(3)-5	Gadovist 0.20 mmol/kg 10 mins	2	1207±11	25.9±7.1
University of Pittsburgh Medical Centre, Pittsburgh, PA, U.S.A.	Siemens Espree 1.5T	MOLLI 5(3)-2	MOLLI 4(1)-3(1)-2	Gadovist 0.20 mmol/kg 20 mins Prohance 0.20 mmol/kg 20 mins	33 33	1045±45	26.6±5.0
Quebec Heart and Lung Institute, Quebec, Canada	Phillips Achieva 1.5T Ingenia 3T	MOLLI 5(3)-3 MOLLI 5(3)-3	MOLLI 5(3)-3 MOLLI 4(1)-3(1)-2	Gadovist 0.20 mmol/kg 15 mins	9 2	1013±45 1238±19	26.1±3.1
Seoul National University Hospital, Seoul, South Korea	Siemens Trio 3T	MOLLI 3(3)-3(3)-5	MOLLI 3(3)-3(3)-5	Magnevist 0.20 mmol/kg 10 mins	77	1232±47	28.3±3.6

Cardiac magnetic resonance

CMR was performed on local platforms employing a range of different scanners, T1 mapping sequences and field strengths (Table 5.1). Standard long-axis cine images were acquired as well as a short-axis cine stack of the left ventricle. LGE imaging with both a short-axis left ventricular stack and standard long-axis views was performed 10-15 min following gadolinium contrast medium administration. T1 mapping data were acquired in a short-axis mid-ventricular view of the left ventricle both prior and 10-20 min following gadolinium contrast medium administration.

Image post-processing and analysis

CMR image analysis was performed by a core lab according to a standardized analysis protocol (see appendix) using CVI42 software (Circle Cardiovascular Imaging Inc., Calgary, Canada). Patients with CMR features consistent with a diagnosis of an alternative myocardial pathology were excluded from the final analysis. Body surface area was calculated using the Mosteller formula. The short-axis stack was contoured to calculate left and right ventricular volumes, ejection fraction and left ventricular mass which were indexed to body surface area. Values were compared to age and sex specific normal ranges in order to define the presence of left ventricular hypertrophy (138). Left ventricular trabeculations and papillary muscles were included in the myocardial mass and excluded from the cavity volumes as per Society of Cardiovascular Magnetic Resonance (SCMR) recommendations(128). Left atrial volume was

calculated via the biplane area-length method and indexed to body surface area (129).

The presence of non-infarct (mid-wall) and infarct patterns of LGE were recorded together and quantitative analysis performed using the full-width-at-half-maximum technique (128), with the extent of LGE expressed as a percentage of total left ventricular mass. Areas of inversion artefact or signal contamination by epicardial fat or blood pool were manually excluded.

Core lab T1 mapping analysis was performed using a standardized pre-specified analysis protocol. Epicardial and endocardial contours were manually drawn in the mid-inferoseptum (segment 9 of the standard 17-segment model (131) on scanner-generated, short-axis, native and post-contrast T1 maps at the mid-ventricular level. A 10% offset was applied to minimize the influence of signal from the adjacent blood pool and epicardial fat. A septal segment was chosen because improved reproducibility has previously been demonstrated using septal regions of interest compared with analysis of all mid-ventricular segments on short-axis images (150). Segments containing non-infarct LGE were included in the T1 mapping analysis whereas those with infarct LGE were excluded according to SCMR guidelines (132). Extracellular volume fraction (ECV%) and indexed extracellular volume (iECV) were then calculated (see appendix). Interobserver reproducibility of each of the T1 mapping measures was determined from independent analysis of 15 randomly selected scans. ECV% and iECV were pre-specified as the

predominant T1 mapping measures for comparison because of the potential advantages these measures offer when comparing values acquired at different magnetic field strengths (151) and with different pulse sequences (84). The variability of native T1, ECV% and iECV were investigated to explore the effect of imaging centre, scanner manufacturer, magnetic field strength and pulse sequence (Shortened [ShMOLLI] versus standard MOdified Look-Locker Inversion-recovery [MOLLI]).

Longitudinal follow-up and clinical events

The primary outcome measure was all-cause mortality. The secondary outcome measure was cardiovascular mortality, which was defined as death attributable to myocardial ischaemia or infarction, heart failure, cardiac arrest (due to arrhythmia or unknown cause) or cerebrovascular accident. Cause of death was adjudicated by three observers (PB, JPG, MRD). Amongst the centres in the United Kingdom, official death certificates were available in all patients. Deaths occurring at international sites outside of the United Kingdom were adjudicated using a combination of medical record review, reports from family members and death certificates where available.

Statistical analysis

The distribution of all continuous variables was assessed using the Shapiro-Wilk test, which were presented using mean ± standard deviation or median [interquartile range]. Comparisons between groups were performed using the independent two-sample *t*-test or Mann-Whitney test as appropriate. We presented all categorical variables as counts and percentages and used the

Fishers exact test or χ2 test for comparison. The relationship between two continuous variables were assessed using Pearson's r and Spearman's rho as appropriate. Comparisons between ECV% and iECV tertiles were performed with one-way analysis of variance (ANOVA) or Kruskal-Wallis test as appropriate.

The influence of imaging centre, CMR scanner manufacturer, magnetic field strength and pulse sequence on T1 mapping values was analysed using independent two-sample *t*-tests and linear regression analysis. Univariable linear regression was also performed to determine associations between clinical and imaging variables with T1 mapping measures. Multivariable linear regression was then performed using variables significantly associated with T1 measures as well as important variables (e.g. age and sex) regardless of strength of univariable association. Univariable Cox-regression analysis was performed to determine which variables were associated with the primary outcome measure (all-cause mortality). Time to event or final status check was taken from the date of valve intervention. Variables with a significant association, as well as any variables not significantly associated but thought to potentially have an effect on outcome were included in the multivariable Cox regression model. The hazard ratio (HR) per unit increase in the variable of interest and 95% confidence intervals (CI) were expressed as HR, 95% CI.

All statistical analyses were performed using SPSS Version 23 and GraphPad Prism Version 7.0. A two-sided $P<0.05$ was considered statistically significant.

RESULTS

A total of 400 patients across 9 sites in 5 countries were included in the final analysis (70±10 years, 60% male; Figure 5.1) with a large proportion having hypertension (65%), diabetes mellitus (20%), and coronary heart disease (40%) (Table 5.2 and Table 5.3). Overall 237 (59%) patients were imaged on 1.5 T and 163 (41%) patients on 3 T magnetic resonance scanners.

Figure 5.1: Flow diagram of study participants

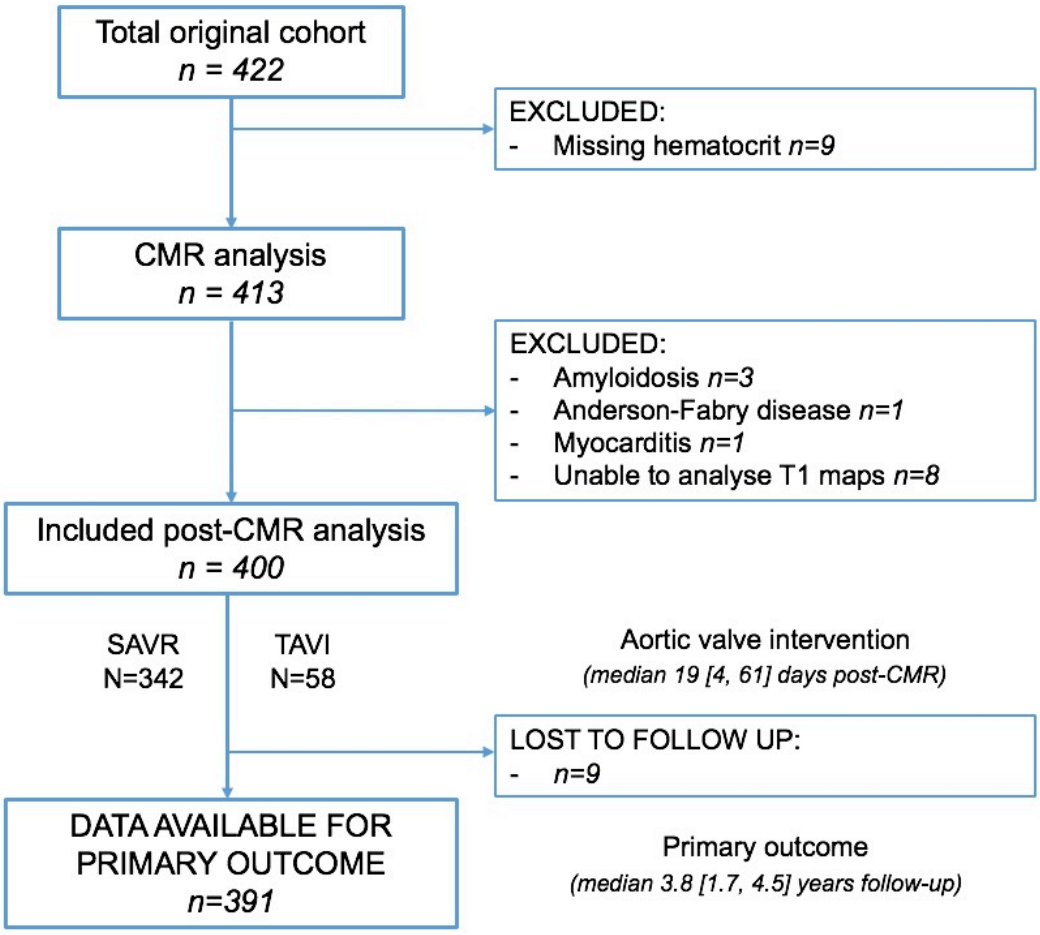

CMR; cardiovascular magnetic resonance, SAVR; surgical aortic valve replacement, TAVI; transcatheter aortic valve insertion

Table 5.2: Baseline characteristics, echocardiography and cardiac magnetic resonance imaging results by centre

Site	Age, yrs	Male gender, n (%)	Coronary disease, n (%)	STS-PROM score, %	Peak aortic-jet velocity, m/s	AVAi, cm^2/m^2	Reduced EF <50%, n (%)	LGE, n (%)	iECV, mL/m^2
Edinburgh Heart Centre, UK N=28	67±8	23 (82)	6 (21)	1.40 [0.85, 2.28]	4.67 ±0.93	0.43 ±0.12	8 (29)	10 (36)	16.7 [13.9, 21.2]
Leeds Teaching Hospitals NHS Trust, UK N=24	71±12	9 (38)	12 (50)	2.17, [1.40, 3.27]	4.92 ±0.52	0.31 ±0.08	5 (21)	15 (63)	22.0 [18.2, 27.5]
Glenfield Hospital, Leicester, UK N=15	75±13	8 (53)	1 (7)	1.28 [0.79, 2.45]	4.40 ±0.53	0.41 ±0.12	2 (13)	5 (33)	17.1 [13.7, 19.8]
Bart's Heart Centre, London, UK N=134	71±9	74 (55)	52 (39)	1.45 [1.00, 2.42]	4.38 ±0.58	0.38 ±0.11	21 (16)	78 (58)	22.1 [17.8, 28.0]
John Radcliffe Hospital, Oxford, UK N=43	71±9	30 (70)	19 (44)	0.87 [0.76, 1.19]	4.56 ±0.74	0.38 ±0.11	2 (5)	28 (67)	24.5 [19.7, 28.2]
HELIOS Hospital Berlin-Buch, Berlin, Germany N=2	69±7	2 (100)	0 (0)	2.76	5.04 ±0.81	0.34 ±0.05	0 (0)	2 (100)	24.4
University of Pittsburgh Medical Centre, Pittsburgh, PA, U.S.A. N=66	69±12	38 (58)	50 (76)	2.12 [1.29, 3.91]	3.96 ±0.86	0.39 ±0.14	15 (23)	35 (53)	22.9 [17.8, 31.5]
Quebec Heart and Lung Institute, Quebec, Canada N=11	62±9	8 (73)	1 (9)	0.81 [0.69, 1.07]	3.79 ±0.65	0.44± 0.07	0 (0)	6 (55)	16.8 [14.1, 19.2]
Seoul National University Hospital, Seoul, South Korea N=77	70±7	48 (62)	18 (23)	1.64 [1.14, 2.38]	4.60 ±0.90	0.46± 0.17	7 (9)	30 (39)	26.6 [21.6, 36.0]

Table 5.3: Baseline characteristics and imaging results in all study participants and by ECV% tertile

		Extracellular volume fraction (ECV%)			
	All patients N=400	**Tertile 1 (<25.9%) N=133**	**Tertile 2 (25.9-29.3%) N=134**	**Tertile 3 (>29.3%) N=133**	**P value**
Age, years	70±10	69±9	70±10	71±10	0.28
Male sex, n (%)	240 (60)	81 (61)	82 (61)	77 (58)	0.83
Body mass index, kg/m^2	27.9±5.1	28.2±5.1	28.1±5.6	27.4±4.6	0.45
Body surface area, m^2	1.87±0.23	1.86±0.26	1.86±0.25	1.83±0.26	0.41
Past medical history					
Hypertension, n (%)	258 (65)	83 (62)	84 (63)	91 (70)	0.42
Diabetes mellitus, n (%)	81 (20)	21 (16)	23 (17)	36 (28)	0.04
Atrial fibrillation, n (%)	46 (12)	9 (7)	13 (10)	24 (18)	0.01
Previous myocardial infarction, n (%)	38 (10)	4 (3)	13 (10)	21 (16)	0.002
Known coronary artery disease*, n (%)	159 (40)	42 (32)	47 (35)	70 (53)	0.001
Clinical factors					
NYHA functional class III or IV, n (%)	143 (36)	29 (25)	54 (48)	60 (54)	<0.001
Systolic blood pressure, mmHg	132±19	133±17	135±21	129±18	0.04
Diastolic blood pressure, mmHg	73±12	73±12	73±11	72±14	0.75
STS-PROM score, %	1.52 [1.00, 2.48]	1.51 [0.88, 2.31]	1.36 [0.98, 2.12]	1.91 [1.17, 3.33]	<0.001
EuroSCORE II, %	1.47 [0.96, 2.56]	1.24 [0.82, 2.16]	1.44 [0.99, 2.22]	2.16 [1.05, 4.41]	<0.001
Echocardiographic measures					
Peak aortic-jet velocity, m/s	4.41±0.78	4.42±0.65	4.50±0.75	4.30±0.91	0.13
Peak aortic valve gradient, mmHg	80±28	80±23	83±27	77±33	0.25
Mean aortic valve gradient, mmHg	49±18	49±16	50±17	47±21	0.39
Aortic valve area, cm^2	0.74±0.25	0.74±0.19	0.77±0.31	0.72±0.24	0.21
Indexed aortic valve area, cm^2/m^2	0.40±0.13	0.40±0.11	0.41±0.16	0.40±0.13	0.38
Valvuloarterial impedance, mmHg/mL/m^2	3.93±1.11	3.93±1.14	3.96±1.18	3.92±1.02	0.96
Bicuspid aortic valve, n (%)	129 (32)	41 (33)	43 (35)	45 (36)	0.82
Cardiac magnetic resonance					
Indexed left ventricular end-diastolic volume, mL/m^2	77±27	68±19	77±26	86±31	<0.001
Indexed left ventricular end-systolic volume, mL/m^2	24 [14, 43]	19 [11, 33]	20 [12, 43]	34 [21, 55]	<0.001
Indexed left ventricular stroke volume, mL/m^2	48±13	48±11	50±14	47±13	0.26
Left ventricular ejection fraction, %	66±16	72±12	68±15	59±17	<0.001

Left ventricular ejection fraction <50%, n (%)	60 (15)	8 (6)	18 (13)	34 (26)	<0.001
Left ventricular mass index, g/m^2	92±31	84±24	91±29	100±36	0.001
Maximum left ventricular wall thickness, mm	15±3	15±3	15±3	15±3	0.42
Mass/volume, g/mL	1.26±0.40	1.28±0.36	1.26±0.48	1.22±0.36	0.51
Indexed right ventricular end-diastolic volume	65±17	63±14	64±15	68±20	0.067
Indexed right ventricular end-systolic volume, mL/m^2	21 [15, 29]	20 [15, 25]	20 [14, 28]	25 [17, 31]	0.15
Indexed right ventricular stroke volume, mL/m^2	41±10	41±10	41±10	41±10	>0.99
Right ventricular ejection fraction, %	64±11	66±9	65±10	62±13	0.019
Indexed left atrial volume, mL/m^2	53±22	46±16	54±22	59±25	<0.001
Late gadolinium enhancement, n (%)	208 (52)	53 (40)	68 (51)	87 (66)	<0.001
LGE as a percentage of myocardial mass (full-width-at-half-maximum method), %	3.57 [1.92, 6.79]	2.89 [1.60, 4.53]	3.77 [1.88, 6.63]	4.48 [2.19, 8.33]	0.069
Extracellular volume fraction (ECV%), %	27.8±3.7	23.9±1.6	27.5±1.0	31.9±2.4	-
Indexed extracellular volume (iECV), mL/m^2	22.5 [18.0, 29.1]	18.1 [15.1, 22.2]	22.2 [18.3, 28.3]	27.9 [22.4, 35.8]	<0.001
Clinical events					
All-cause mortality, rate / 1000 patient years	-	14.0	28.5	53.7	0.003

LGE; late gadolinium enhancement, NYHA; New York Heart Association, STS-PROM; Society of Thoracic Surgeons Predicted Risk of Mortality

**known coronary artery disease defined as history of previous myocardial infarction, obstructive disease on angiography (stenosis >50% left main stem or >70% proximal epicardial coronary artery) or previous coronary intervention*

Consistency of T1 Mapping

In keeping with previous work (151,152), substantial variation in native T1 values was observed between the different centres (Figure 5.2). In particular, native T1 values were higher in patients imaged at 3 T compared to 1.5 T (1213±57 versus 1050±48 ms, P<0.001). However, there was no association between native T1 and either scanner manufacturer or the pulse sequence used (such as ShMOLLI or MOLLI) when adjusted for magnetic field strength (model 1, Table 5.4). In contrast, ECV% values were relatively consistent across the different centres (Figure 5.2), with no differences between ECV% values in patients imaged at 1.5 T and 3 T (27.9±3.9% versus 27.7±3.5%, P=0.55). On univariable linear regression analysis, there was no association between ECV% values and either magnetic field strength (P=0.571), scanner manufacturer (P=0.379) or the pulse sequence used (P=0.307).

Figure 5.2: Multiparametric cardiac magnetic resonance assessment

Cardiac magnetic resonance (CMR) short axis cine images were contoured to provide ventricular volume, mass and ejection fraction measurements (A). Areas of late gadolinium enhancement (LGE, B, red arrows) were quantified using the 5-standard-deviation technique. Native (C) and post-contrast (D) T1 maps were analysed and the mean value from segment 9 (shaded blue) and blood pool (orange contour) were used to calculate the extracellular volume fraction (ECV%). Native T1 values varied significantly by centre (G) mainly due to the effect of magnetic field strength (black = 1.5T, blue = 3T). Less variation was observed with ECV% values (H) which did not vary by field strength (P=0.55, F).

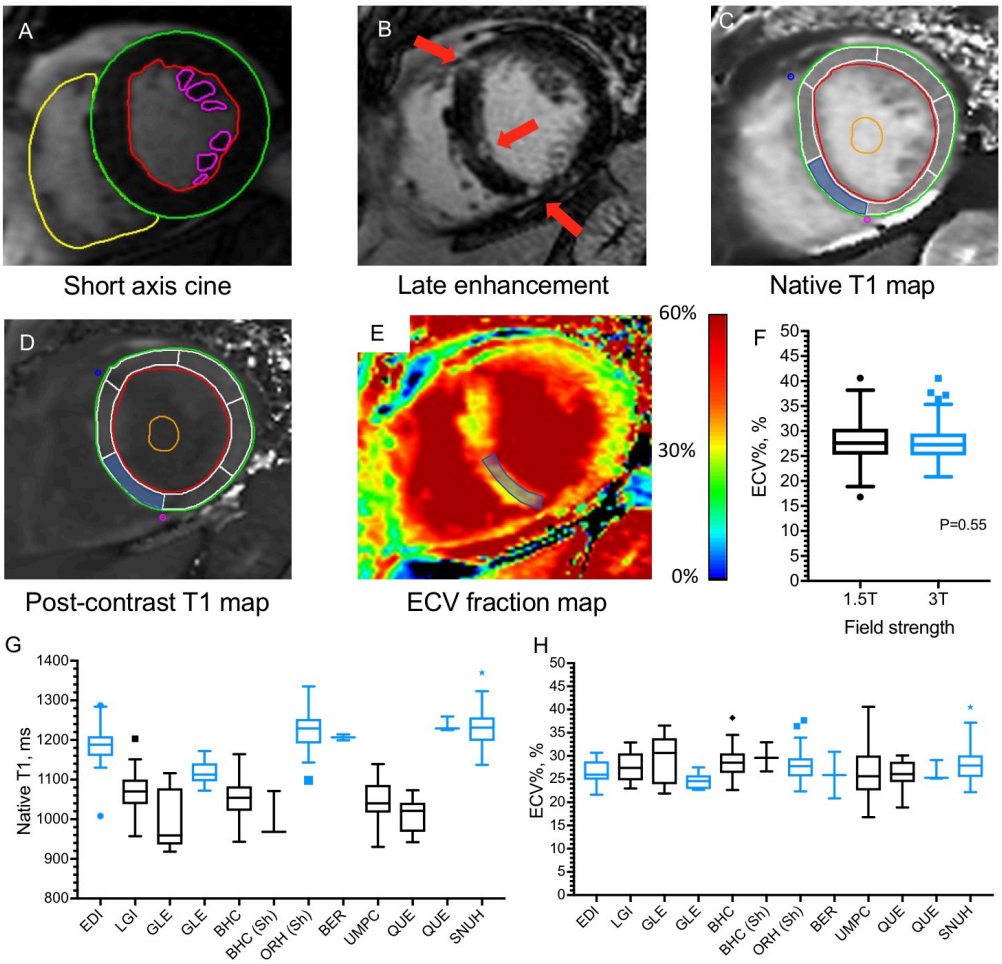

EDI; Edinburgh, LGI; Leeds, GLE; Leicester, BHC; Barts Heart Centre, ORH; Oxford, BER; Berlin, UPMC; Pittsburgh, QUE; Quebec, SNUH; Seoul, Sh; ShMOLLI T1 mapping sequence used

T1 Mapping and Clinical Factors

Native T1 displayed good interobserver reproducibility (1.5±1.4%, intraclass correlation coefficient = 0.923). After adjustment for magnetic field strength on multivariable analysis, higher native T1 values were associated with female sex, presence of coronary artery disease, reduced left ventricular ejection fraction, higher peak aortic valve velocity and presence of LGE (Tables 5.4 and 5.5).

The mean ECV% was 27.8±3.7, with low interobserver variability for this measurement (4.4±3.4%, intraclass correlation coefficient = 0.961). To explore associations between ECV% and clinical variables further, the total cohort was divided into tertiles (tertile 1: <25.9%, tertile 2: 25.9-29.3%, tertile 3: >29.3%; Figure 5.3 and Table 5.3). Across the tertiles, there was a progressive increase in patients with established coronary heart disease ($P<0.05$), and both Society of Thoracic Surgeons Predicted Risk of Mortality (STS-PROM) and EuroSCORE II risk scores (both $P<0.001$). More patients were classified as NYHA functional status III or IV ($P<0.001$), and both indexed left ventricular volumes and mass increased progressively (all $P\leq0.001$; Table 5.3) as did the proportion of patients with LGE ($P<0.001$). In contrast, there was a fall in both left and right ventricular ejection fraction across the tertiles, albeit largely within the normal range (both $P<0.001$; Table 5.3). Although similar associations with ECV% were observed in the univariable analysis (Table 5.6), only lower left ventricular ejection fraction ($P<0.001$) and greater

left ventricular mass index (P=0.043) remained independently associated with ECV% on multivariable analysis.

Median iECV was 22.5 [18.0 to 29.1] mL/m^2. Analysis by iECV tertile (tertile 1, <19.3 mL/m^2; tertile 2, 19.3-26.5 mL/m^2; tertile 3, >26.5 mL/m^2; Table 5.7) demonstrated a progressive increase in the proportion of males, subjects with known coronary heart disease and surgical risk scores (EuroSCORE II; P<0.01 for all). Similar to ECV%, imaging markers of left ventricular decompensation (LV mass, LV volumes, presence of LGE, reduction in ejection fraction) also progressed across the tertiles (Table 5.7). Associations with iECV on univariable analysis were similar to the tertiles analysis (Table 5.8). On multivariable analysis, clinical measures independently associated with iECV were age, male sex, known coronary heart disease, presence of LGE and reduction in left ventricular ejection fraction (P<0.02 for all, Table 5.8).

Figure 5.3: Progression of clinical and imaging variables across ECV% and iECV tertiles

When comparing clinical and imaging variables across ECV% tertiles, there was a progressive increase in left ventricular mass (A), left ventricular end-diastolic volume (C) and proportion of patients with late gadolinium enhancement (E), with a reduction in left ventricular ejection fraction (G). A similar pattern was seen when comparing across iECV tertiles (B,D,F,H).

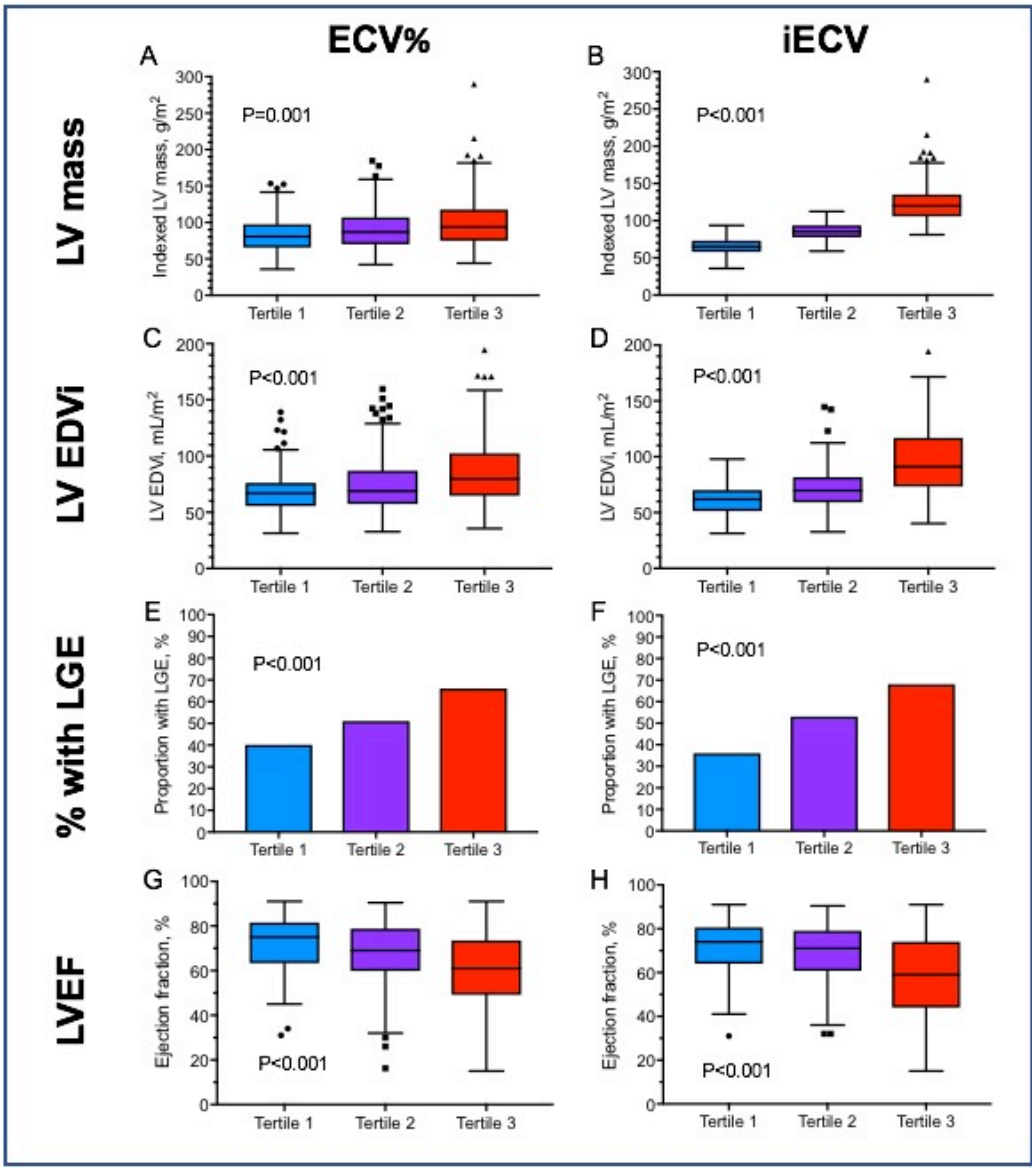

EDVi; indexed end-diastolic volume, LGE; late gadolinium enhancement, LV; left ventricle, LVEF; left ventricular ejection fraction

Table 5.4: Baseline characteristics and imaging results by native T1 tertile

	Tertile 1 (<1057 ms) N=133	Tertile 2 (1056 – 1167 ms) N=134	Tertile 3 (>1167 ms) N=133	P value
Age, years	71±10	71±11	70±8	0.53
Male sex, n (%)	78 (59)	74 (55)	88 (66)	0.18
Body mass index, kg/m^2	29.1±5.0	28.5±5.7	26.2±4.0	<0.001
Body surface area, m^2	1.94±0.22	1.88±0.24	1.79±0.22	<0.001
Past medical history				
Hypertension, n (%)	89 (67)	95 (72)	74 (56)	0.016
Diabetes mellitus, n (%)	30 (23)	24 (18)	26 (20)	0.66
Atrial fibrillation, n (%)	19 (14)	20 (15)	7 (5)	0.022
Previous myocardial infarction, n (%)	11 (8)	23 (17)	4 (3)	<0.001
Known coronary artery disease*, n (%)	61 (46)	61 (46)	37 (28)	0.003
Clinical factors				
NYHA functional class III or IV, n (%)	48 (36)	63 (49)	32 (40)	0.092
Systolic blood pressure, mmHg	132±18	132±19	132±20	0.99
Diastolic blood pressure, mmHg	73±12	73±13	73±13	0.83
STS-PROM score, %	1.60 [1.02, 2.31]	2.08 [1.03, 3.32]	1.40 [0.93, 2.20]	0.009
EuroSCORE II, %	1.67 [1.03, 2.49]	1.93 [0.99, 4.02]	1.19 [0.87, 1.83]	<0.001
Echocardiographic measures				
Peak aortic-jet velocity, m/s	4.19±0.68	4.42±0.71	4.63±0.89	<0.001
Peak aortic valve gradient, mmHg	72±22	80±25	89±34	<0.001
Mean aortic valve gradient, mmHg	45±15	48±17	53±21	0.001
Aortic valve area, cm^2	0.75±0.27	0.72±0.23	0.76±0.27	0.31
Indexed aortic valve area, cm^2/m^2	0.39±0.12	0.38±0.11	0.43±0.16	0.004
Valvuloarterial impedance, mmHg/mL/m^2	3.98±1.08	4.05±1.02	3.77±1.21	0.095
Bicuspid aortic valve, n (%)	33 (25)	41 (32)	55 (50)	<0.001
Cardiac magnetic resonance				
Indexed left ventricular end-diastolic volume, mL/m^2	70±25	82±26	80±29	<0.001
Indexed left ventricular end-systolic volume, mL/m^2	18 [11, 26]	30 [16, 52]	20 [12, 33]	<0.001
Indexed left ventricular stroke volume, mL/m^2	46±11	46±10	53±15	<0.001
Left ventricular ejection fraction, %	70±14	60±17	70±15	<0.001
Left ventricular ejection fraction <50%, n (%)	13 (10)	34 (25)	13 (10)	<0.001

Left ventricular mass index, g/m^2	82±24	92±27	102±37	<0.001
Maximum left ventricular wall thickness, mm	14±2	15±3	16±3	<0.001
Mass/volume, g/mL	1.23±0.32	1.19±0.44	1.34±0.42	0.006
Indexed right ventricular end-diastolic volume	64±18	66±17	65±15	0.35
Indexed right ventricular end-systolic volume, mL/m^2	22 [16, 27]	21 [15, 30]	22 [16, 28]	0.75
Indexed right ventricular stroke volume, mL/m^2	40±10	42±10	41±10	0.52
Right ventricular ejection fraction, %	64±10	64±11	64±12	0.90
Indexed left atrial volume, mL/m^2	50±21	57±26	52±16	0.04
Late gadolinium enhancement, n (%)	66 (50)	79 (59)	63 (48)	0.15
LGE as a percentage of myocardial mass (full-width-at-half-maximum method), %	3.30 [2.10, 6.23]	3.23 [1.51, 6.75]	4.88 [2.21, 7.87]	0.22
Extracellular volume fraction, %	26.3±3.5	28.9±3.8	28.3±3.3	<0.001
Indexed extracellular volume (iECV), mL/m^2	19.2 [15.6, 23.2]	23.5 [19.3, 30.5]	25.1 [19.6, 33.3]	<0.001
Clinical events				
All-cause mortality, rate / 1000 patient years	28.6	35.6	30.9	0.85

LGE; late gadolinium enhancement, NYHA; New York Heart Association, STS-PROM; Society of Thoracic Surgeons Predicted Risk of Mortality

Table 5.5: Univariable and multivariable associations with native T1

		Analysis of associations with native T1			
		Unstandardised coefficients		Standardised coefficients	
	Univariable analysis	**B**	**SE**	**Beta**	**P value**
Technical factors	Magnetic field strength (3 T v 1.5 T)	163.0	5.308	0.839	<0.001
	T1 mapping sequence (ShMOLLI v MOLLI)	98.83	14.17	0.330	<0.001
	Scanner vendor (Phillips v Siemens)	-48.48	16.77	-0.143	0.004
Clinical factors	Age	-0.683	0.494	-0.069	0.167
	Male sex	9.302	9.762	0.048	0.341
	Hypertension	-19.36	10.06	-0.096	0.055
	Diabetes mellitus	4.802	12.00	0.020	0.689
	Atrial fibrillation	-36.34	14.90	-0.121	0.015
	STS-PROM score	-4.108	2.927	-0.074	0.161
	EuroSCORE II	-5.736	1.738	-0.171	0.001
	Known coronary disease	-26.75	9.691	-0.137	0.006
	NYHA functional class III or IV	5.221	9.513	0.030	0.584
	Peak aortic-jet velocity, m/s	24.89	6.023	0.204	<0.001
	Indexed aortic valve area, cm^2/m^2	100.4	35.72	0.142	0.005
	Left ventricular ejection fraction, %	0.019	0.301	0.003	0.950
	Indexed left atrial volume, mL/m^2	0.117	0.219	0.027	0.595
	Right ventricular ejection fraction, %	0.061	0.438	0.007	0.888
	Presence of LGE	-1.911	9.585	-0.010	0.842
	LGE as a percentage of myocardial mass (full-width-at-half-maximum method), %	2.340	1.600	0.104	0.145
	Multivariable analysis				
Model 1	Magnetic field strength (3 T v 1.5 T)	163.6	5.852	0.841	<0.001
	T1 mapping sequence (ShMOLLI v MOLLI)	9.48	9.443	0.028	0.316
	Scanner vendor (Phillips v Siemens)	2.33	8.882	0.008	0.793
Model 2	Magnetic field strength (3 T v 1.5 T)	169.5	5.518	0.871	<0.001
	Age	-0.205	0.276	-0.021	0.457
	Male sex	-14.23	5.322	-0.073	0.008
	Atrial fibrillation	5.816	8.418	0.019	0.490
	Known coronary disease	11.04	5.559	0.057	0.048
	Peak aortic-jet velocity, m/s	8.55	3.360	0.070	0.011
	Left ventricular ejection fraction, %	-0.75	0.170	-0.126	<0.001
	Presence of LGE	11.38	5.486	0.060	0.039

Table 5.6: Univariable and multivariable associations with ECV%

		Analysis of associations with ECV%			
		Unstandardised coefficients		Standardised coefficients	
	Univariable analysis	**B**	**SE**	**Beta**	**P value**
Scanning factors	Magnetic field strength (3 T v 1.5 T)	-0.213	0.376	-0.028	0.571
	T1 mapping sequence (ShMOLLI v MOLLI)	0.511	0.579	0.044	0.379
	Scanner vendor (Phillips v Siemens)	-0.669	0.654	-0.051	0.307
Clinical factors	Age, per 10 years	0.430	0.190	1.120	0.025
	Male sex	-0.198	0.378	-0.026	0.601
	Hypertension	0.222	0.389	0.029	0.570
	Diabetes mellitus	1.039	0.460	0.113	0.024
	Atrial fibrillation	1.537	0.575	0.133	0.008
	STS-PROM score	0.622	0.111	0.283	<0.001
	EuroSCORE II	0.427	0.066	0.323	<0.001
	Known coronary disease	0.990	0.375	0.131	0.009
	NYHA functional class III or IV	1.609	0.396	0.216	<0.001
	Peak aortic-jet velocity, m/s	-0.521	0.237	-0.110	0.029
	Indexed aortic valve area, cm^2/m^2	0.921	1.403	0.033	0.512
	Left ventricular ejection fraction, %	-0.080	0.011	-0.345	<0.001
	Left ventricular mass index, g/m^2	0.030	0.006	0.247	<0.001
	Indexed left atrial volume, mL/m^2	0.040	0.008	0.238	<0.001
	Right ventricular ejection fraction, %	-0.037	0.017	-0.112	0.027
	Presence of LGE	1.681	0.360	0.228	<0.001
	LGE as a percentage of myocardial mass (full-width-at-half-maximum method), %	0.135	0.062	0.154	0.031
	Multivariable analysis				
Model 1	Age, per 10 years	0.290	0.210	0.790	0.171
	Male sex	-0.746	0.415	-0.100	0.073
	Diabetes mellitus	0.459	0.469	0.050	0.329
	Atrial fibrillation	0.633	0.637	0.058	0.321
	Known coronary disease	0.473	0.404	0.064	0.242
	NYHA functional class III or IV	0.660	0.400	0.089	0.100
	Peak aortic-jet velocity, m/s	-0.243	0.268	-0.050	0.364
	Left ventricular ejection fraction, %	-0.064	0.015	-0.281	<0.001
	Left ventricular mass index, g/m^2	0.018	0.009	0.125	0.043
	Indexed left atrial volume, mL/m^2	0.014	0.011	0.082	0.199
	Right ventricular ejection fraction, %	0.022	0.022	0.065	0.308
	Presence of LGE	0.666	0.403	0.091	0.099

LGE; late gadolinium enhancement, LV; left ventricle, NYHA; New York Heart Association, STS-PROM; Society of Thoracic Surgeons Predicted Risk of Mortality

Table 5.7: Baseline characteristics and imaging results by iECV tertile

	Tertile 1 (<19.3 mL/m^2) N=133	Tertile 2 (19.3-26.5 mL/m^2) N=134	Tertile 3 (>26.5 mL/m^2) N=133	P value
Age, years	70±9	71±10	70±10	0.41
Male sex, n (%)	57 (43)	85 (63)	98 (74)	<0.001
Body mass index, kg/m^2	28.7±5.2	28.2±4.4	26.8±5.4	0.10
Body surface area, m^2	1.87±0.21	1.88±0.23	1.85±0.26	0.53
Past medical history				
Hypertension, n (%)	89 (67)	88 (66)	81 (62)	0.65
Diabetes mellitus, n (%)	22 (17)	29 (22)	29 (22)	0.46
Atrial fibrillation, n (%)	14 (11)	15 (11)	17 (13)	0.84
Previous myocardial infarction, n (%)	10 (8)	11 (8)	17 (13)	0.30
Known coronary artery disease*, n (%)	45 (34)	49 (37)	65 (49)	0.028
Clinical factors				
NYHA functional class III or IV, n (%)	49 (39)	43 (38)	51 (50)	0.18
Systolic blood pressure, mmHg	135±17	134±19	128±20	0.006
Diastolic blood pressure, mmHg	75±11	74±13	70±13	0.016
STS-PROM score, %	1.42 [0.98, 2.28]	1.62 [1.07, 2.62]	1.80 [0.98, 2.76]	0.075
EuroSCORE II, %	1.29 [0.87, 2.00]	1.64 [0.96, 2.79]	1.88 [1.00, 3.53]	0.001
Echocardiographic measures				
Peak aortic-jet velocity, m/s	4.26±0.62	4.50±0.68	4.46±0.99	0.03
Peak aortic valve gradient, mmHg	74±21	83±25	83±36	0.012
Mean aortic valve gradient, mmHg	45±14	50±16	50±23	0.015
Aortic valve area, cm^2	0.77±0.24	0.73±0.23	0.74±0.29	0.47
Indexed aortic valve area, cm^2/m^2	0.41±0.12	0.39±0.12	0.40±0.16	0.40
Valvuloarterial impedance, mmHg/mL/m^2	4.22±1.16	3.95±0.99	3.63±1.10	<0.001
Bicuspid aortic valve, n (%)	40 (32)	42 (34)	47 (38)	0.55
Cardiac magnetic resonance				
Indexed left ventricular end-diastolic volume, mL/m^2	61±14	73±19	97±32	<0.001
Indexed left ventricular end-systolic volume, mL/m^2	17 [10, 23]	23 [15, 35]	39 [21, 66]	<0.001
Indexed left ventricular stroke volume, mL/m^2	44±9	49±10	52±16	<0.001
Left ventricular ejection fraction, %	72±11	69±13	58±19	<0.001
Left ventricular ejection fraction <50%, n (%)	6 (5)	11 (8)	43 (32)	<0.001
Left ventricular mass index, g/m^2	65±11	86±11	124±29	-
Maximum left ventricular wall thickness, mm	13±2	15±2	17±3	<0.001
Mass/volume, g/mL	1.11±0.28	1.25±0.33	1.40±0.51	<0.001
Indexed right ventricular end-diastolic volume	60±13	64±15	71±20	<0.001
Indexed right ventricular end-systolic volume, mL/m^2	18 [14, 25]	21 [15, 28]	24 [18, 33]	<0.001
Indexed right ventricular stroke volume, mL/m^2	39±9	42±10	43±12	0.009

Right ventricular ejection fraction, %	65±9	66±8	61±14	<0.001
Indexed left atrial volume, mL/m^2	45±17	53±25	64±27	<0.001
Late gadolinium enhancement, n (%)	48 (36)	70 (53)	90 (68)	<0.001
LGE as a percentage of myocardial mass (full-width-at-half-maximum method), %	2.21 [1.19, 3.95]	3.74 [2.21, 7.02]	5.47 [2.23, 8.12]	0.001
Extracellular volume fraction, %	25.6±2.9	27.8±3.1	30.0±3.7	<0.001
Indexed extracellular volume (iECV), mL/m^2	16.4 [14.0, 18.0]	22.3 [20.6, 24.1]	32.7 [28.9, 39.5]	-
Clinical events				
All-cause mortality, rate / 1000 patient years	22.9	36.0	36.0	0.34

LGE; late gadolinium enhancement, NYHA; New York Heart Association, STS-PROM; Society of Thoracic Surgeons Predicted Risk of Mortality

*known coronary artery disease defined as history of previous myocardial infarction, obstructive disease on angiography (stenosis >50% left main stem or >70% proximal epicardial coronary artery) or previous coronary intervention

Table 5.8: Univariable and multivariable associations with iECV

		Analysis of associations with iECV			
		Unstandardised coefficients		Standardised coefficients	
	Univariable analysis	**B**	**SE**	**Beta**	**P value**
Clinical factors	Age, per 10 years	-0.570	0.510	-0.550	0.269
	Male sex	5.523	0.977	0.273	<0.001
	Hypertension	-0.746	1.043	-0.036	0.475
	Diabetes mellitus	2.376	1.234	0.096	0.055
	Atrial fibrillation	0.430	1.560	0.014	0.783
	STS-PROM score	1.118	0.311	0.186	<0.001
	EuroSCORE II	0.971	0.183	0.268	<0.001
	Known coronary disease	2.287	1.010	0.113	0.024
	NYHA functional class III or IV	2.085	0.945	0.119	0.028
	Peak aortic-jet velocity, m/s	0.930	0.638	0.073	0.145
	Indexed aortic valve area, cm^2/m^2	2.022	3.776	0.027	0.593
	Left ventricular ejection fraction, %	-0.222	0.029	-0.356	<0.001
	Indexed left atrial volume, mL/m^2	0.132	0.022	0.297	<0.001
	Right ventricular ejection fraction, %	-0.214	0.043	-0.242	<0.001
	Presence of LGE	5.126	0.965	0.258	<0.001
	LGE as a percentage of myocardial mass (full-width-at-half-maximum method), %	0.409	0.170	0.170	0.017
	Multivariable analysis				
Model 1	Age, per 10 years	-2.540	0.460	-3.050	<0.001
	Male sex	4.620	0.826	0.270	<0.001
	Diabetes mellitus	0.502	0.975	0.024	0.607
	Known coronary disease	1.496	0.285	0.313	<0.001
	NYHA functional class III or IV	1.132	0.839	0.066	0.179
	Peak aortic-jet velocity, m/s	0.361	0.822	0.021	0.661
	Left ventricular ejection fraction, %	-0.160	0.030	-0.305	<0.001
	Indexed left atrial volume, mL/m^2	0.086	0.020	0.224	<0.001
	Right ventricular ejection fraction, %	0.064	0.042	0.084	0.130
	Presence of LGE	2.020	0.814	0.120	0.014

LGE; late gadolinium enhancement, NYHA; New York Heart Association, STS-PROM; Society of Thoracic Surgeons Predicted Risk of Mortality

Clinical Outcomes

Aortic valve intervention was performed in all patients 19 [4 to 61] days following magnetic resonance imaging. This was either isolated surgical aortic valve replacement (n=283, 71%), combined coronary artery bypass grafting with surgical aortic valve replacement (n=59, 15%), or transcatheter aortic valve insertion (n=58, 14%). Clinical outcome data were collected from 391 patients after a median of 3.8 [1.7 to 4.5] years (9 patients were lost to follow-up). Over this time, 40 deaths were observed (10%), of which five occurred within 30 days of valve intervention. No information on cause of death was available at the time of thesis writing for 19 individuals. Of the 21 deaths where the cause of death was established, 12 (57%) were classified as cardiac deaths. Secondary analysis of associations with cardiovascular death was therefore not performed due to missing data, although these data should be available shortly.

Similar rates of all-cause mortality were observed across native T1 tertiles (P=0.85, Table 5.9) and native T1 showed no association with all-cause mortality on univariable Cox regression analysis (P=0.74). Similarly, no association with the primary outcome measure was seen when native T1 values were adjusted for differences in scanner magnetic field strength (P=0.88) or when additional correction for age, sex, peak aortic-jet velocity and presence of LGE was performed (P=0.84, model 2, Table 5.9).

All-cause mortality progressively increased across the ECV% tertiles, being nearly 4 times higher in the top versus the bottom tertile (tertile 1, 14.0; tertile 2, 28.5; tertile 3, 53.7 deaths per 1000 patient-years log-rank test, P=0.003; Figure 5.4). Univariable Cox regression analysis showed a positive association between ECV% and mortality (hazard ratio 1.18, 95% confidence interval 1.09 to 1.28, P<0.0001); other univariate predictors included age, male sex, STS-PROM score, EuroSCORE II, atrial fibrillation, indexed left atrial volume, and established coronary heart disease (all P<0.05, Table 5.10). Whilst there was an apparent trend for LGE to be associated with mortality, this did not reach statistical significance (hazard ratio 1.60, 95% confidence interval 0.84 to 3.03, P=0.15). Inclusion of variables in the multivariable models was limited to prevent overfitting. In the first model, ECV% remained predictive of the primary outcome independent of age and sex. In the second model, it remained predictive independent of age, sex, LGE, peak velocity, and left ventricular ejection fraction (hazard ratio 1.13, 95% confidence interval 1.04 to 1.24, P=0.006; Figure 5.4 and Table 5.11). In the third model, ECV% was predictive of outcome independent of age, sex and STS-PROM risk score (hazard ratio 1.12, 95% confidence interval 1.03 to 1.23, P=0.013).

There was no difference between all-cause mortality rates when the cohort was analysed by iECV tertile (P=0.34, Figure 5.4). However, univariable Cox regression analysis demonstrated a positive association between iECV and all-cause mortality (hazard ratio 1.03, 95% confidence interval 1.01 to 1.06, P=0.018). Multivariable cox-regression analysis was then performed using the

same models as employed for ECV% (Table 5.11). iECV remained associated with the primary outcome when adjusted for age and sex (model 1: hazard ratio 1.03, 95% confidence interval 1.00 to 1.06, P=0.033) but was no longer an independent predictor when adjusted for age, sex, peak aortic valve velocity, impaired left ventricular ejection fraction and presence of LGE (model 2, P=0.092, Figure 5.4) or in the final model adjusting for age, sex and STS-PROM risk score (model 3, P=0.34).

Figure 5.4: Distribution of ECV fraction and iECV values and relationship with clinical events

Extracellular volume fraction (ECV%) is normally distributed (A). When divided into tertiles, the all-cause mortality rate progressively increased across the tertiles (red squares). Indexed extracellular volume (iECV) presents with a positively skewed distribution (B). All-cause mortality similarly increases across tertiles of iECV (red squares, B). When the cohort was divided into tertiles of ECV% a progressive worsening of prognosis was seen across the tertiles (C). Greater overlap was seen between tertiles of iECV (D, P=0.34). ECV% remained an independent predictor of adverse outcome on multivariable analysis (E, hazard ratio: 1.13, P=0.006) however iECV did not (F, hazard ratio: 1.03, P=0.103).

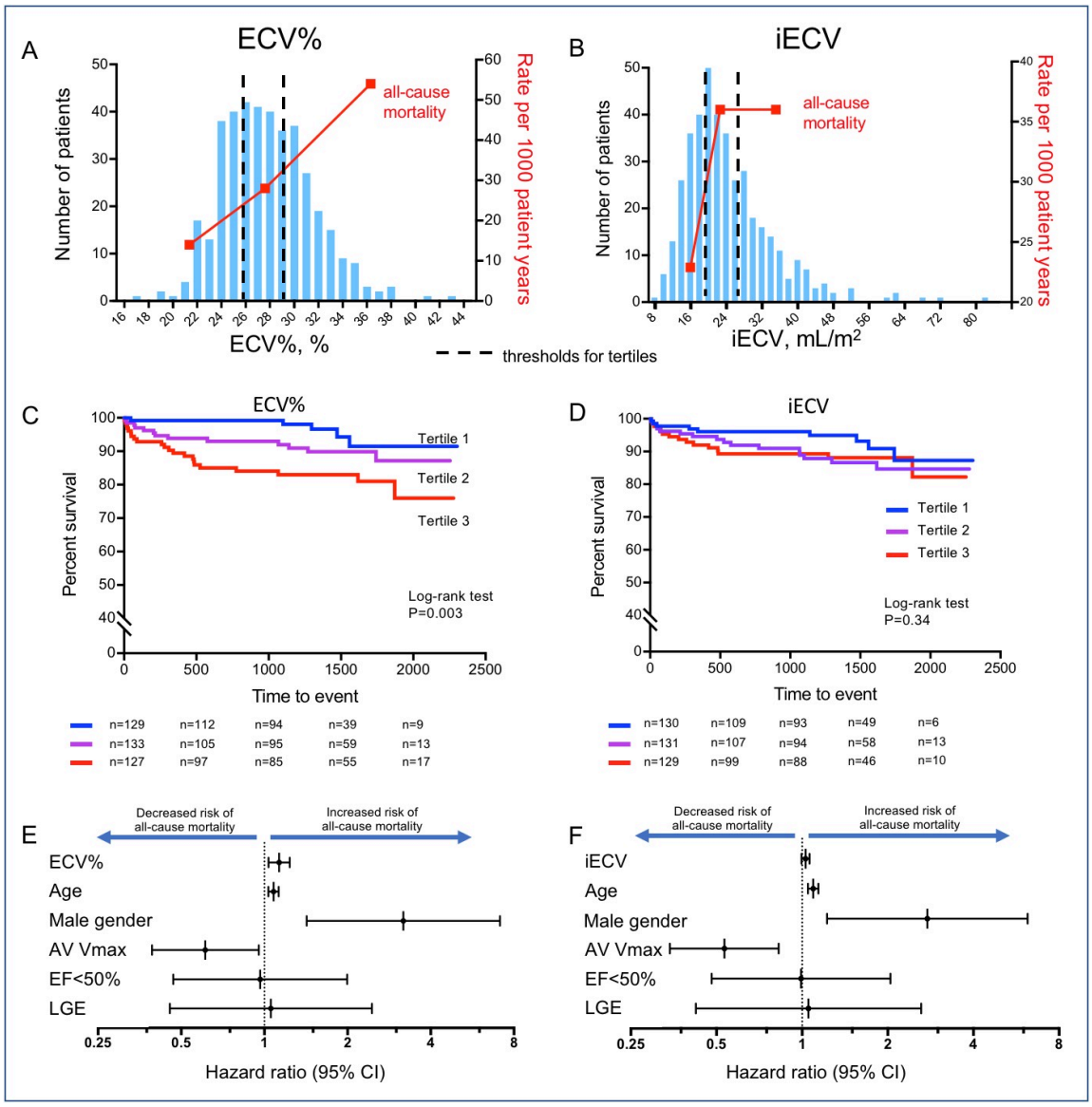
A
ECV%
Number of patients
Rate per 1000 patient years
all-cause mortality
ECV%, %
B
iECV
Number of patients
Rate per 1000 patient years
all-cause mortality
iECV, mL/m2
thresholds for tertiles
C
ECV%
Percent survival
Tertile 1
Tertile 2
Tertile 3
Log-rank test P=0.003
Time to event
n=129 n=112 n=94 n=39 n=9
n=133 n=105 n=95 n=59 n=13
n=127 n=97 n=85 n=55 n=17
D
iECV
Percent survival
Tertile 1
Tertile 2
Tertile 3
Log-rank test P=0.34
Time to event
n=130 n=109 n=93 n=49 n=6
n=131 n=107 n=94 n=58 n=13
n=129 n=99 n=88 n=46 n=10
E
Decreased risk of all-cause mortality
Increased risk of all-cause mortality
ECV%
Age
Male gender
AV Vmax
EF<50%
LGE
Hazard ratio (95% CI)
F
Decreased risk of all-cause mortality
Increased risk of all-cause mortality
iECV
Age
Male gender
AV Vmax
EF<50%
LGE
Hazard ratio (95% CI)

Table 5.9: Univariable and multivariable cox regression analysis of associations between native T1 value and all-cause mortality

						95% CI for HR	
	Variable	**β**	**SE**	**P value**	**HR**	**Lower**	**Upper**
Univariable	Native T1	-0.0001	0.002	0.743	0.999	0.996	1.003
Model 1	Native T1	0.000	0.003	0.876	1.000	0.994	1.006
	Magnetic field strength (3 T v 1.5 T)	-0.019	0.599	0.975	0.982	0.304	3.175
Model 2	Native T1	0.001	0.003	0.837	1.001	0.995	1.006
	Magnetic field strength (3 T v 1.5 T)	-0.139	0.641	0.828	0.870	0.248	3.054
	Age, yrs	0.088	0.022	<0.001	1.092	1.046	1.141
	Male sex	1.125	0.417	0.007	3.081	1.360	6.983
	Peak aortic-jet velocity, m/s	-0.651	0.219	0.003	0.522	0.340	0.801
	Presence of LGE	0.164	0.352	0.642	1.178	0.591	2.348

CI; confidence interval, HR; hazard ratio, LGE; late gadolinium enhancement, SE; standard error

Table 5.10: Univariable cox regression analysis for all-cause mortality

	Univariable analysis	
Variable	**Hazard ratio (95% CI)**	**P value**
Age, years	1.08 (1.04 to 1.13)	<0.001
Male sex	2.73 (1.26 to 5.92)	0.011
STS-PROM Score, %	1.35 (1.19 to 1.53)	<0.001
EuroSCORE II, %	1.14 (1.08 to 1.20)	<0.001
Known coronary disease	2.25 (1.20 to 4.22)	0.011
NYHA functional class III or IV	2.46 (1.24 to 4.88)	0.01
Atrial fibrillation	4.20 (2.13 to 8.28)	<0.001
Peak aortic-jet velocity, m/s	0.55 (0.37 to 0.82)	0.003
Mean aortic valve gradient, mmHg	0.97 (0.95 to 0.99)	0.002
Indexed aortic valve area, cm^2/m^2	1.67 (0.20 to 14.24)	0.64
Bicuspid aortic valve	0.63 (0.31 to 1.30)	0.21
LV ejection fraction < 50%	1.73 (0.85 to 3.56)	0.27
Indexed LV end-diastolic volume, mL/m^2	1.00 (1.00 to 1.01)	0.57
Indexed LV stroke volume, mL/m^2	0.98 (0.95 to 1.00)	0.078
Indexed LV mass, g/m^2	1.00 (1.00 to 1.01)	0.39
Indexed left atrial volume, mL/m^2	1.02 (1.00 to 1.03)	0.007
Valvuloarterial impedance	1.04 (0.79 to 1.37)	0.78
Late gadolinium enhancement	1.60 (0.84 to 3.03)	0.15
Right ventricular ejection fraction, %	0.98 (0.95 to 1.00)	0.052
Native T1 (per 10 ms change)	0.99 (0.96 to 1.03)	0.74
ECV%, %	1.18 (1.09 to 1.28)	<0.001
iECV, mL/m^2	1.03 (1.01 to 1.06)	0.018

CI; confidence interval, ECV; extracellular volume, iECV; indexed extracellular volume, LV; left ventricular, NYHA; New York Heart Association, STS-PROM; Society of Thoracic Surgeons Predicted Risk of Mortality

Table 5.11: Multivariable cox regression analysis of association between ECV% and iECV and predictors of all-cause mortality

		Extracellular volume fraction (ECV%)						Indexed extracellular volume (iECV)					
						95% CI for HR						95% CI for HR	
	Variable	β	SE	P value	HR	Lower	Upper	β	SE	Sig.	HR	Lower	Upper
Univariable	ECV%	0.168	0.042	<0.001	1.183	1.091	1.284	-	-	-	-	-	-
	iECV, mL/m^2	-	-	-	-	-	-	0.029	0.013	0.021	1.030	1.004	1.056
Model 1	ECV%	0.149	0.041	<0.001	1.161	1.072	1.257	-	-	-	-	-	-
	iECV, mL/m^2	-	-	-	-	-	-	0.029	0.014	0.038	1.029	1.002	1.058
	Age, yrs	0.074	0.020	<0.001	1.077	1.036	1.120	0.089	0.021	<0.001	1.093	1.049	1.138
	Male sex	1.203	0.399	0.003	3.331	1.524	7.283	1.002	0.405	0.013	2.721	1.231	6.029
Model 2	ECV%	0.123	0.045	0.006	1.131	1.035	1.236	-	-	-	-	-	-
	iECV, mL/m^2	-	-	-	-	-	-	0.027	0.017	0.103	1.028	0.995	1.062
	Age, yrs	0.076	0.022	<0.001	1.079	1.034	1.126	0.089	0.021	<0.001	1.093	1.049	1.140
	Male sex	1.157	0.411	0.005	3.182	1.422	7.120	1.014	0.414	0.014	2.755	1.223	6.205
	Peak aortic-jet velocity, m/s	-0.492	0.227	0.030	0.611	0.392	0.954	-0.629	0.224	0.005	0.533	0.343	0.827
	Presence of LGE	-0.035	0.369	0.925	0.966	0.468	1.992	-0.009	0.369	0.981	.991	0.481	2.044
	LVEF <50%	0.054	0.430	0.901	1.055	0.455	2.449	0.051	0.465	0.912	1.053	0.423	2.621
Model 3	ECV%	0.114	0.046	0.013	1.120	1.025	1.225	-	-	-	-	-	-
	iECV, mL/m^2	-	-	-	-	-	-	0.015	0.016	0.354	1.015	0.984	1.047
	Age, yrs	0.063	0.023	0.007	1.065	1.018	1.115	0.065	0.024	0.007	1.067	1.018	1.119
	Male sex	1.425	0.431	0.001	4.157	1.786	9.677	1.334	0.447	0.003	3.797	1.581	9.119
	STS-PROM score, %	.141	0.097	0.149	1.151	0.951	1.393	0.205	0.097	0.035	1.227	1.015	1.484

CI; confidence interval, SE; standard error, HR; hazard ratio, LVEF; left ventricular ejection fraction, LGE; late gadolinium enhancement; STS-PROM; Society of Thoracic Surgeons Predicted Risk of Mortality

DISCUSSION

We present the largest T1 mapping study in aortic stenosis and the first to adopt a pragmatic multicentre protocol using a range of different magnetic resonance imaging scanners, pulse sequences and magnetic field strengths. We have demonstrated the feasibility of this generalisable approach and that, in this setting, ECV-based T1 mapping measures are robust across centres, scanner manufacturers and field strengths. Moreover, we have shown that both ECV% and iECV demonstrate clear associations with multiple different clinical and imaging measures of left ventricular decompensation, and that ECV% in particular provides powerful and independent long-term prognostic information. ECV-based T1 mapping indices hold major promise as fully quantitative markers of myocardial fibrosis and left ventricular decompensation in aortic stenosis.

Native T1 has some considerable advantages as a marker of diffuse myocardial fibrosis. In particular, it requires only a single measurement and avoids the need for gadolinium-based contrast medium administration. However, in this pragmatic multicentre setting, native T1 was hampered by the considerable variation in values at different field strengths and was not of prognostic value. Recent studies have demonstrated that standardisation of native T1 values acquired in different centres at different field strengths can be achieved with phantom testing (153). This was not performed in our study design but should be explored in future multi-centre studies.

The ECV-based techniques explored in our study offer important advantages over native T1 mapping. First, gadolinium chelates do not cross cell membranes, and therefore distribute throughout the extracellular space following intravenous administration. Whereas native T1 combines signal from both intra and extracellular compartments, the potent T1-shortening effect of gadolinium allows the myocardial extracellular space to be specifically interrogated (85). Second, the calculation of ECV% corrects myocardial T1 for values in the blood pool on the same scan thereby potentially correcting for many between scanner differences (84,151) and enabling comparison between ECV% values across centres. Accordingly, we observed no difference in ECV% values between patients imaged on Siemens or Phillips platforms, at 1.5 or 3 T, or using different pulse sequences (shortened versus standard Modified Look-Locker Inversion-recovery).

The two ECV-based measures examined in this study provide complementary information regarding diffuse myocardial fibrosis in the left ventricle. The ECV% provides an assessment of relative diffuse fibrosis burden and has been extensively validated against histological fibrosis (84-86,147). Our experience to date suggests that whilst ECV% offers an accurate point assessment of diffuse fibrosis in aortic stenosis, serial ECV% measurements are less sensitive in detecting alterations in fibrosis content over short-term follow-up due to balanced increases in myocyte mass and extracellular volume. (146) In contrast, the indexed extracellular volume (iECV) provides a

measure of absolute fibrosis burden, indexed to body surface area (7) that can better track changes in diffuse fibrosis over time and in response to intervention such as valve replacement (146). In our cohort, both greater ECV% and iECV were associated with multiple features of a decompensating ventricle; higher left ventricular mass, volumes, left atrial volumes, atrial fibrillation, surgical risk scores, presence and amount of LGE and worsening left ventricular ejection fraction. As such both measures hold great promise as fully quantitative markers of left ventricular decompensation in aortic stenosis.

Prognostic data on T1 mapping in aortic stenosis has been limited to date, with preliminary data only available from small single centre studies.(7,83) For the first time, we have shown a strong association between ECV% and all-cause mortality in patients with aortic stenosis on both univariable and multivariable models. Indeed, after correction for a variety of other well-established prognostic markers, a 14% increase in risk of all-cause mortality was seen for every 1% increase in ECV%. iECV performed less well in the multivariable models compared with ECV%, predicting adverse outcome independent of age and sex but not when adjusted for other imaging findings. This is an interesting observation. iECV relates not only to the percentage fibrosis but also the volume (and therefore mass) of the left ventricle. The more powerful association of outcomes with ECV% than iECV suggests that fibrosis is more closely associated with prognosis than left ventricular size.

One unexpected finding was the lack of an association between late gadolinium enhancement and the primary outcome in this cohort. A positive association between LGE and all-cause mortality has been repeatedly demonstrated in multiple observational studies (7,19,46,49) including the recent large AS700 multicentre study (69). The hazard ratio associated with the presence of LGE in our study was 1.60 (95% confidence interval 0.84 to 3.03), which is in fact similar to that previously reported in AS700 (e.g. AS700 (HR 2.21 (95% CI 1.34 to 3.36), P=0.002 (69)) although this particular study resulted in twice the number of deaths. This apparent discrepancy is therefore most likely to reflect insufficient statistical power, although it is of interest that ECV% was able to demonstrate a clear independent association in the same data set. Further data comparing the prognostic value of LGE and ECV% is warranted in aortic stenosis and indeed other cardiovascular conditions.

Limitations

We observed no prognostic utility of native T1 in this cohort. Whilst we performed a simple statistical adjustment to account for differences in magnetic field strength, it is possible that more complex statistical modelling may yet alter this finding. Whilst we demonstrated no effect of T1 mapping pulse sequence on ECV%, this result cannot be extrapolated to saturation recovery-based T1 mapping techniques, which were not examined and may produce a lower ECV% value compared to inversion recovery sequences (154). In addition, analysis of associations with cardiovascular mortality was not possible due to missing data in a significant proportion of events.

Conclusions

Extracellular volume-based T1 mapping measures in aortic stenosis are comparable across different magnetic resonance imaging scanners, pulse sequences and magnetic field strengths, and associated with multiple measures of left ventricular decompensation. ECV% is a strong independent predictor of long-term adverse events in patients scheduled for aortic valve replacement, with further work now required to determine how these measures can be used to optimise the timing of aortic valve intervention.

Chapter 6: Combined Magnetic Resonance / Positron Emission Tomography Imaging in Aortic Stenosis

SUMMARY

Background

Hybrid magnetic resonance / positron emission tomography (MR/PET) offers combined functional metabolic imaging with advanced tissue characterisation. This technique has not yet been investigated in aortic stenosis (AS). In addition, the radiotracer ^{18}F sodium fluoride (^{18}F-NaF) may be able to detect co-existent cardiac transthyretin (TTR) amyloidosis.

Methods

Patients with severe AS awaiting aortic valve replacement (AVR) and age and sex matched healthy volunteers underwent hybrid MR/PET imaging using ^{18}F-NaF. Multiparametric MR examination included late gadolinium enhancement and T1 mapping sequences. Magnetic resonance attenuation correction (MRAC) maps were acquired using both standard Dixon and free breathing radial gradient echo (GRE) sequences and used to reconstruct the list-mode PET data, which were then fused with a novel non-contrast image navigator (iNAV) based coronary magnetic resonance angiography (CMRA) sequence with inline motion correction (MC). Aortic valve and septal myocardial radiotracer uptake were analysed using standardised uptake values (SUV) and target-to-background ratios (TBR). Septal myocardial biopsy was performed in patients undergoing AVR to examine for evidence of cardiac TTR amyloidosis.

Results

Sixteen patients with severe AS were recruited (80±5 years, 63% male) along with six healthy volunteers (78±5 years, 66% male). Overall the scan was well tolerated, with 95% of participants completing the full imaging protocol. MRAC using radial GRE sequence was superior to the Dixon method with significant reduction in bright artefact. Analysis of valvular and myocardial ^{18}F-NaF uptake was possible in all patients, with significantly greater radiotracer activity in the aortic valve in AS patients compared with controls (SUV_{max}: 2.57±0.60 versus 1.32±0.18, P<0.0001). No increased septal myocardial ^{18}F-NaF uptake or MR evidence of cardiac amyloidosis was seen in any patient, with no evidence of TTR deposition on any myocardial biopsy specimen (n=7). MR image quality allowed for detailed assessment of the aortic valve and annulus in 82% of participants. The iNAV MC CMRA sequence provided good views of the proximal coronary arteries in most participants (64%) and an excellent anatomical reference for fusion with PET data, with minor adjustments required to coregistration in only three (14%) participants.

Conclusion

MR/PET is feasible and well-tolerated in AS populations and can provide a comprehensive “one stop” assessment of valve, annulus, myocardium and coronary arteries. Future work should concentrate on improved motion correction of both PET and MR datasets. Further studies are required to investigate the ability of 18F-NaF to detect co-existent cardiac TTR amyloidosis.

INTRODUCTION

Aortic stenosis (AS) is a major public health burden with an increasing prevalence linked to the aging population. Current management involves watchful waiting for patient-reported symptoms or the detection of a reduction in left ventricular ejection fraction (LVEF) which is a late and often irreversible finding (9). There is therefore considerable interest in novel methods of assessment of both the LV myocardium and aortic valve that could more accurately stage disease progression, plan interventional valve strategies and be used to monitor response to novel therapies.

Positron emission tomography (PET) offers functional metabolic imaging allowing the activity of specific disease processes to be assessed *in-vivo*. Radiolabelled ^{18}F-sodium fluoride (^{18}F-NaF) binds preferentially to newly developing regions of microcalcification (92) and has therefore been used as a marker of calcification activity in the aortic valve using PET/CT imaging (4). Greater aortic valve tracer uptake is seen in more advanced AS (6) and appears to predict both disease progression and future clinical events (93). In addition, recent work suggests that ^{18}F-NaF PET may be able to detect cardiac transthyretin (TTR) amyloidosis (112), which is observed in up to 16% of patients being considered for transcatheter aortic valve implantation (TAVI) (111).

Cardiac magnetic resonance imaging (MRI) has to date been used primarily in a research capacity in aortic stenosis patients. It not only provides more accurate estimates of LV volume, mass and ejection fraction (155) but also offers non-invasive tissue characterisation, being able to detect both focal replacement and diffuse interstitial myocardial fibrosis using late gadolinium enhancement (LGE) and T1 mapping techniques respectively. Mid-wall late enhancement is a common finding in advanced aortic stenosis (29-62% depending on the population studied) and is well established as a strong independent predictor of adverse clinical outcomes (7,19,46,49,69). Importantly mid-wall fibrosis appears to accumulate rapidly prior to valve replacement in some individuals and is irreversible following valve intervention (144,146). T1 mapping methods still require further investigation and optimisation however both native T1 (83) and extracellular volume (ECV)-based measures (7) have shown a close association with histological fibrosis assessments and other markers of LV decompensation in patients with aortic stenosis. Importantly, both of these techniques may be able to identify early evidence of LV decompensation and therefore help optimise the timing of valve intervention.

Hybrid MR/PET technology is now available potentially combining the strengths of these two imaging modalities. Moreover MR/PET holds important advantages over PET/CT including reduced radiation exposure, advanced myocardial tissue characterisation and improved co-registration and motion correction. Given the complex nature of heart valve disease an imaging

modality that can assess multiple aspects of the disease process in both the valve and myocardium in a single scan is potentially attractive. To our knowledge, only a single case using MR/PET in aortic stenosis has been published to date (156). We here report our early experience with combined MR/PET in the assessment of patients with severe AS, providing comprehensive single stop imaging of the valve and myocardium as well as the aorta and coronary arteries.

METHODS

Patients with severe aortic stenosis referred for valve intervention were recruited from cardiology and cardiothoracic clinics at a single centre between September 2017 and August 2018. Healthy volunteers with no history or symptomatology to suggest current cardiovascular disease were also recruited. The study was approved by South East Scotland Research Ethics Committee 01 (17/SS/0066) and was conducted in accordance with the Declaration of Helsinki. All participants provided written consent prior to participation. Patients underwent comprehensive clinical assessment including 12-lead electrocardiogram and blood sampling for haematocrit and renal function. Participants with severe aortic stenosis underwent clinical transthoracic echocardiography at an accredited department with comprehensive assessment of aortic valve haemodynamics.

MR/PET

All participants underwent simultaneous ^{18}F-NaF PET and MR imaging using a hybrid MR/PET system (Biograph mMR, Siemens, Erlangen, Germany). In the aortic stenosis group this occurred within 4 weeks prior to a planned date of valve intervention. PET data was acquired for 50 min in list-mode, starting 60 min after intravenous injection of 250 MBq of ^{18}F-NaF. Both 3D Dixon VIBE (124) and free-breathing radial gradient echo (GRE, Siemens work-in-progress #793F) sequences were acquired for MR attenuation correction (MRAC). MRAC maps were generated using the method described by Robson

et al (98). protocol included standard long- and short-axis cine imaging. Coronary magnetic resonance angiography (CMRA) was performed using a non-contrast ECG-gated image-navigator (iNAV) based motion corrected (MC) proprietary sequence with 100% respiratory scan efficiency (iNAV-based CMRA with in-line 2D translational motion correction, Kings College London, UK (125)) to achieve a high-resolution isotropic 3D data volume encompassing proximal coronary arteries, aortic valve and left ventricular myocardium which could be fused with the PET dataset. T1 mapping was performed using MOLLI (native 5(3)-3, post contrast 4(1)-3(1)-2, MyoMaps product, Siemens) on a single 4-chamber slice both before and 15-20 minutes after 0.1 mmol/kg of intravenous gadobutrol contrast (Gadovist, Bayer Pharma AG, Germany). Late gadolinium enhancement (LGE) was performed approximately 10 minutes following contrast injection using phase-sensitive inversion recovery sequences (2D short-axis, 10 slices). The total MRI scan duration was approximately 60 minutes.

MR post-processing and analysis

Image analysis was performed by a single reporter (RE) using CVI42 (Circle Cardiovascular Imaging Inc., Calgary, Canada). Short-axis cine images were used to calculate ventricular volumes, mass and function as per SCMR guidelines (128). Longitudinal systolic function was assessed as previously described (146). The presence of mid-wall LGE was determined both qualitatively and quantitatively in a semi-automated manner using signal intensity thresholds of >3 and >5 standard deviations above the mean value

in a region of normal myocardium (130). Native and post-contrast T1 mapping analysis was performed using manually drawn regions of interest in the basal septum on the motion corrected scanner-generated T1 maps and used to calculate both extracellular volume fraction (ECV%) and indexed extracellular volume (iECV: ECV% x left ventricular end-diastolic myocardial volume normalised to body surface area). Whilst segments with mid-wall late enhancement were included in the overall T1 calculation, segments with subendocardial infarct pattern LGE were excluded (132). Aortic valve annulus and coronary height measurements were performed using OsiriX software (Pixemo, Bernex, Switzerland).

PET post-processing and analysis

Off-line PET reconstructions were carried out using e7tools (Siemens Healthcare). The full list mode acquisition was reconstructed using an Ordered Subsets Expectation Maximization (OSEM) algorithm with the following parameters: 256x256 field of view, 4 iterations, 21 subsets, 5mm Gaussian filter, zoom 1. No ECG gating was applied. PET data was first reconstructed applying the standard 3D Dixon VIBE MRAC method (4 tissue class segmentation; air, lung, soft tissue and fat). PET data was also reconstructed when applying a custom MRAC map derived from the free-breathing radial GRE sequence (2 tissue classes: background [air and lung] and soft tissue [soft tissue and fat] (98)). PET reconstructions were fused with the iNAV-based MC CMRA sequence (125). As the MR and PET data is acquired simultaneously and co-registered, in theory no manual correction is required.

However, all images were reviewed for discrepancies and in cases where co-registration was imperfect, small manual corrections were performed by aligning PET uptake in the ventricular cavities, aorta and aortic valve with these structures on the MR angiogram.

PET image analysis was performed using FusionQuant software (Cedars-Sinai Medical Center, Los Angeles, U.S.A). Radiotracer uptake was analysed using a standardised protocol (see appendix). In brief, regions of interest (ROI) were drawn on the co-registered image around the perimeter of the aortic valve on co-axial short-axis views. Standardised uptake values (SUV, mean and maximum) were then calculated for these ROIs and were corrected for blood pool activity (measured in the right atrium (134)) to generate tissue-to-background ratios (TBR). Myocardial SUV values were also measured in the septal myocardium at mid cavity level.

Myocardial biopsies and histological analysis

All patients undergoing surgical aortic valve replacement consented to intraoperative septal myocardial biopsy which was performed under direct vision by the surgical team using a 14-gauge coaxial needle (BD Carefusion, Tru-cut needle) from the basal interventricular septum 2 cm below the left ventricular outflow tract (LVOT). Samples were then fixed in 10%-buffered formalin and embedded in paraffin. The presence of cardiac amyloidosis was assessed using Congo red staining and both bright field and cross-polarised light. If amyloidosis was suggested by the presence of apple-green

birefringence under cross-polarised light, immunohistochemistry was to be performed using a TTR antibody.

Statistical Analysis

All statistical analyses were performed using GraphPad Prism Version 7.0 and SPSS Version 23. A two-sided $P<0.05$ was considered statistically significant. The distribution of all continuous variables was assessed using the Shapiro-Wilk test, which were presented using mean ± standard deviation or median [interquartile range]. Comparisons between groups were performed using the two-sample *t*-test or Mann-Whitney test as appropriate. We presented all categorical variables as percentages and used the Fishers exact test or $\chi 2$ test for comparison. The relationship between two continuous variables were assessed using Pearson's r and Spearman's rho as appropriate.

RESULTS

In total, 16 patients with severe aortic stenosis (80±5 years, 63% male) and 6 healthy volunteers (78±5 years, 66% male) were recruited to the study. Patients and healthy volunteers were well matched for age and sex with similar prevalence of non-cardiac comorbidities (Table 6.1). Recorded blood pressures were similar between volunteers and patients with AS (P>0.35).

Table 6.1: Baseline characteristics

	Healthy volunteers N=6	Severe aortic stenosis N=16	P-value
Age, years	78±5	80±5	0.59
Male gender, n (%)	4 (66)	10 (63)	>0.99
Hypertension, n (%)	2 (33)	10 (63)	0.35
Hypercholesterolaemia, n (%)	3 (50)	7 (44)	>0.99
Diabetes mellitus, n (%)	1 (17)	3 (19)	>0.99
Cerebrovascular accident, n (%)	0 (0)	2 (13)	>0.99
Previous myocardial infarction, n (%)	-	2 (13)	-
Percutaneous coronary intervention, n (%)	-	2 (13)	-
Coronary artery bypass grafting, n (%)	-	1 (6)	-
Known coronary artery disease*, n (%)	-	11 (69)	-
NYHA, n • 1 • 2 • 3 • 4	-	 2 12 2 0	-
Body mass index, kg/m^2	25.7±3.0	28.6±4.9	0.18
Body surface area, m^2	1.90±0.21	1.95±0.18	0.54
Systolic blood pressure, mmHg	147±7	144±20	0.71
Diastolic blood pressure, mmHg	77±6	74±8	0.35
ECG			
Atrial fibrillation, n (%)	0 (0)	1 (6)	-
Heart rate, bpm	63±9	66±10	0.59
QRS duration, ms	99±31	103±18	0.69
ECG criteria for left ventricular hypertrophy, n (%)	1 (17)	13 (81)	0.01
ECG strain pattern, n (%)	0 (0)	9 (56)	0.046

*known coronary artery disease defined as history of previous myocardial infarction, obstructive disease on angiography (stenosis >50% left main stem or >70% proximal epicardial coronary artery) or previous coronary intervention

Healthy volunteers

All volunteers completed the study protocol uneventfully. None had symptoms suggestive of cardiac disease. One patient had an incidental finding of right bundle branch block and another thin patient had ECG criteria for left ventricular hypertrophy. Neither patient had a detectable cardiac structural abnormality on MRI.

Aortic stenosis patients

All patients had severe AS on echocardiography (peak aortic-jet velocity 4.63±0.60 m/s, mean gradient 52±15 mmHg, aortic valve area 0.78±0.27 cm^2). Most patients (n=14) had high-gradient severe AS, with two patients exhibiting low-gradient subtypes (Table 6.2). All valves were tricuspid in morphology when assessed using MRI, although this was indeterminate on echocardiography in 3 (19%) patients.

All but one patient was symptomatic awaiting valve intervention at enrolment. One patient was asymptomatic but was due to undergo early surgery as part of the EVOLVED randomised controlled (NCT03094143). Most patients had ECG criteria for LVH and half had the LV strain pattern (Table 6.1). One AS patient (age 89, scheduled for TAVI) requested early termination of the scan due to general discomfort just prior to gadolinium contrast administration. In this case, all acquired MRI data (including approximately 30 minutes of PET acquisition) were included in the analysis. All other participants completed the entire imaging protocol.

Table 6.2: Echocardiographic characteristics of the aortic stenosis group

	Severe aortic stenosis N=16
Peak aortic-jet velocity, m/s	4.63±0.60
Mean aortic valve gradient, mmHg	53±15
Aortic valve area, cm^2	0.80±0.25
Indexed aortic valve area, cm^2/m^2	0.40±0.10
Left ventricular outflow tract area, cm^2	3.32±0.47
Left ventricular outflow tract area (planimetered on CMRA), cm^2	4.57±0.78
Aortic valve area (continuity equation using planimetered MRI LVOT area), cm^2	1.01±0.30
Indexed aortic valve area (continuity equation using planimetered MRI LVOT area), cm^2/m^2	0.52±0.16
Aortic regurgitation, n (%) • None • Trivial or mild • Moderate or severe	 4 10 2
Indexed stroke volume (SVi), mL/m^2	44±12
Low flow state (SVi $\leq$35mL/m^2), n (%)	4 (25)
Left ventricular systolic function, n (%) • Normal • Mild impairment • Moderate impairment • Severe impairment	 13 1 2 0
Aortic stenosis subtype, n (%)	
• High-gradient	14
• Low-flow low-gradient impaired EF	1
• Low-flow low-gradient preserved EF	1
E/A ratio	1.03±0.66
Mean e', cm/s	6.3±1.6
E/e' ratio	14.8 [9.5, 18.9]
Deceleration time, ms	251±80

EF; ejection fraction, LVOT; left ventricular outflow tract, CMRA; coronary magnetic resonance angiography, SVi; stroke volume index, VTI; velocity-time integral

Technical aspects of MR/PET

The average administered dose of ^{18}F-NaF was 239±12 MBq. Upon review of the fused PET reconstructions with the iNAV-based MC CMRA sequence, minor manual adjustments to registration were only required in 3 patients. Significant artefacts affecting image interpretation were present in all study participants when the images were reconstructed using the standard Dixon MRAC. This consisted of increased tracer activity around the heart-lung and liver-lung borders and also in the bronchial tree (due to mis-segmentation of bronchi as soft tissue). In two participants, there was reduced activity in both lung bases. Artefact was successfully eliminated in all patient images when the PET data was reconstructed using the free-breathing radial GRE MRAC rather than the 3D Dixon VIBE MRAC (Figure 6.1). Subsequent quantification of PET uptake was therefore performed on the free-breathing radial GRE PET reconstruction. Detailed analysis of PET uptake in the valve, and myocardium was possible in all patients. Analysis of coronary PET uptake was possible in all but 1 patient due to failure to optimise the angiogram sequence (Table 6.3).

Figure 6.1: Magnetic resonance attenuation correction using free-breathing radial gradient echo reconstruction reduces artefact.

Positron emission tomography (PET) reconstructions in the coronal plane fused with the non-contrast angiogram sequence are shown in three patients (A, C and D). The left-hand column applied the MR attenuation correction (MRAC) map derived from the standard 3D Dixon VIBE MRAC and the right column applied the MRAC map from the radial gradient echo (GRE) acquisition. Examples of the MRAC maps for each sequence are shown (B). The radial GRE improves the segmentation of tissues along the heart-lung borders and bronchial tree (blue arrows) compared with the Dixon attenuation correction map. Bright artefacts are seen around the heart-lung and liver-lung borders (red arrows) as well as the main bronchi (white arrows) in the Dixon reconstruction but these artefacts are eliminated using the radial GRE map to reconstruct the PET data.

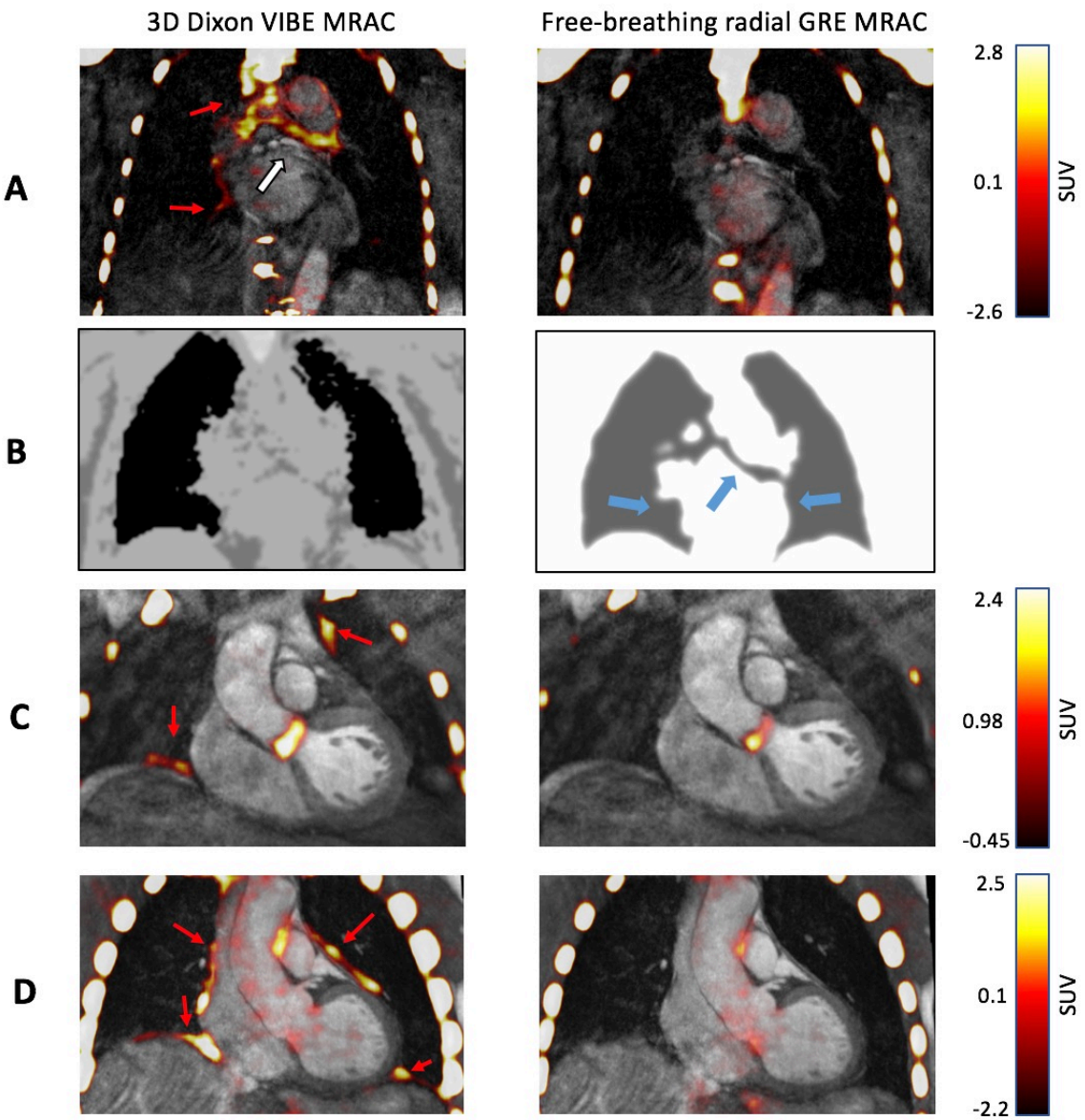
3D Dixon VIBE MRAC
Free-breathing radial GRE MRAC
A
B
C
D
2.8
0.1
-2.6
SUV
2.4
0.98
-0.45
SUV
2.5
0.1
-2.2
SUV

Table 6.3: Quality of hybrid magnetic resonance imaging / positron emission tomography assessments

Number of participants with diagnostic image quality, n (%)	Healthy volunteers N=6	Severe aortic stenosis N=16
Aortic valve		
Valve morphology	6 (100)	16 (100)
Annulus measurements	6 (100)	12 (75)
^{18}F-NaF uptake	6 (100)	16 (100)
Myocardium		
LV volumes, mass and ejection fraction	6 (100)	16 (100)
Late gadolinium enhancement	6 (100)	16 (100)
T1 mapping	6 (100)	16 (100)
^{18}F-NaF uptake	6 (100)	16 (100)
Coronary arteries		
Proximal arteries visualised	5 (83)	9 (56)
Mid arteries visualised	5 (83)	4 (25)
Distal arteries visualised	5 (83)	1 (6)
Coronary ostia height	6 (100)	12 (75)
^{18}F-NaF uptake	6 (100)	15 (94)

Aortic valve measurements

High intensity ^{18}F-fluoride was observed in the aortic valves of all the aortic stenosis patients. AS patients had greater ^{18}F-fluoride uptake in the aortic valve compared with controls whether defined using SUV_{max} (2.57±0.60 versus 1.32±0.18, P<0.0001) or TBR_{max} (2.57±0.62 versus 1.66±0.23, P<0.0001, Figure 6.2 and Table 6.4). No correlation was observed between SUV_{max} and aortic valve peak jet velocity (r=0.05, P=0.86).

CMRA image quality was considered sufficient to measure aortic annulus / LVOT dimensions in 18 (82%) participants. Two patients underwent TAVI and had a pre-procedure cardiac CT available for comparison. Measurements were similar on CMRA and CT in these patients for aortic annulus area (mean absolute and percentage difference between measurements = 0.2 cm^2, 4%), annular perimeter (1.2 mm, 1%)), circular diameter (0.5 mm, 2%), maximum annular diameter (0.7 mm, 3%) and minimum annular diameter (1.75 mm, 8%). In the AS cohort, LVOT measurements were greater when using planimetered values from the CMRA compared with standard echocardiographic assessment (CMRA LVOT area: 4.57±0.78 cm^2, echo LVOT area: 3.32±0.47 cm^2, P<0.0001, Table 6.2). This resulted in increased AVA valve using the continuity equation when the CMRA LVOT area was substituted for the echo LVOT area (CMRA: 1.01±0.30 cm^2, echo: 0.73±0.15 cm^2, P=0.0004).

Figure 6.2: 18F-sodium fluoride uptake in the aortic valve in a patient with severe aortic stenosis

Aortic valve leaflet thickening is clearly visualised on the non-contrast iNAV-based motion-corrected coronary magnetic resonance angiogram sequence (orthogonal views a, b and c). ^{18}F-sodium fluoride (^{18}F-NaF) activity localises to all three valve leaflets (orthogonal view d, e and f). Aortic valve SUV_{max} was 2.01 and TBR_{max} was 3.35. Overall, both aortic valve SUV_{max} (g) and TBR_{max} (h) were greater in aortic stenosis patients compared with healthy volunteers (both $P<0.003$).

SUV; standardised uptake value, TBR; tissue-to-background ratio

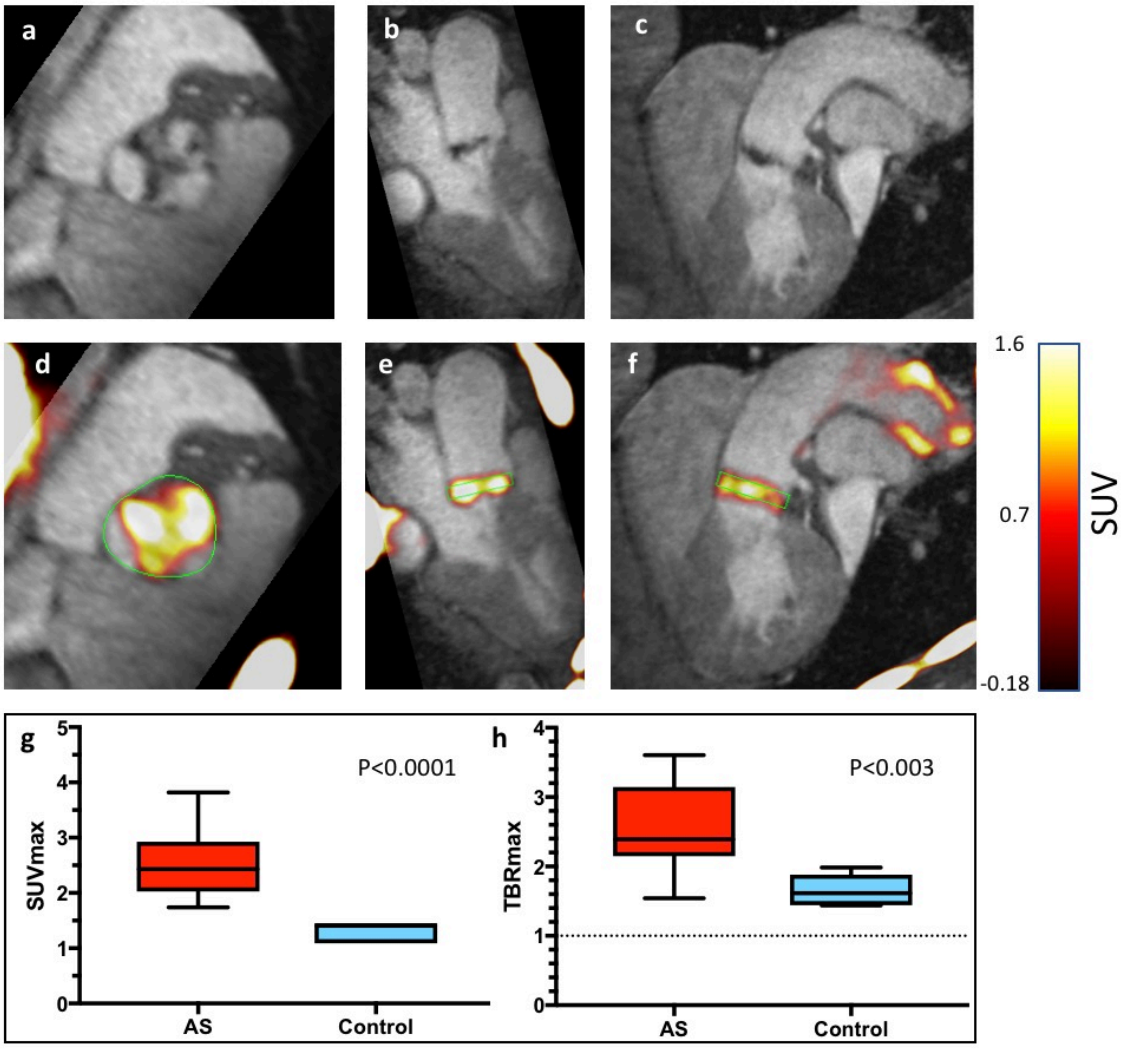
a
b
c
d
e
f
1.6
0.7
-0.18
SUV
g
SUVmax
P<0.0001
AS
Control
h
TBRmax
P<0.003
AS
Control

Table 6.4: Hybrid magnetic resonance imaging / positron emission tomography results from aortic stenosis and control groups

	Healthy volunteers N=6	Severe aortic stenosis N=16	P-value
Indexed left ventricular-end diastolic volume, mL/m^2	72±20	74±26	0.88
Indexed left ventricular-end systolic volume, mL/m^2	20 [13, 21]	17 [10, 31]	0.76
Indexed stroke volume, mL/m^2	55±17	51±12	0.56
Ejection fraction, %	75±6	73±16	0.72
Ejection fraction < 50%, n (%)	0(0)	1 (6)	-
Left ventricular mass index, g/m^2	64±8	105±27	0.002
Maximum left ventricular wall thickness, mm	11±1	17±3	0.0007
Mass/volume, g/mL	0.9 [0.7, 1.1]	1.3 [1.1, 1.6]	0.008
Myocardial contraction fraction, %	84±17	52±20	0.002
Longitudinal systolic function, mm	15.3±3.3	8.3±3.6	0.0005
Indexed left atrial volume, mL/m^2	38±3	51±16	0.13
Infarct late gadolinium enhancement, n (%)	0 (0)	1 (6)	-
Mid-wall late gadolinium enhancement, n (%)	0 (0)	8 (50)	-
Mid-wall late gadolinium enhancement mass (3 standard deviation method), g	-	8.2±5.2	-
Mid-wall late gadolinium enhancement mass (5 standard deviation method), g	-	1.5±1.3	-
T1 mapping			
Native T1 (mid-inferoseptum), ms	1241±39	1285±49	0.06
Post-contrast T1 (mid-inferoseptum), ms	656±45	654±30	0.92
Extracellular volume fraction, %	27.6±2.4	27.5±2.0	0.94
Indexed extracellular volume, mL/m^2	17±2	28±8	0.003
Standardised uptake values (SUV)			
Aortic valve SUV_{max}	1.32+0.18	2.57±0.60	<0.0001
Aortic valve SUV_{mean}	1.07±0.16	1.81±0.35	<0.0001
Septal myocardium SUV_{max}	0.86±0.13	0.92±0.23	0.53
Septal myocardium SUV_{mean}	0.74±0.09	0.78±0.21	0.61
Right atrium SUV_{mean}	0.81±0.18	1.05±0.32	0.10
Tissue-to-Background Ratio (TBR)*			
Aortic valve TBR_{max}	1.66±0.23	2.57±0.62	0.003
Aortic valve TBR_{mean}	1.34±0.14	1.80±0.34	0.005
Septal myocardium TBR_{max}	1.08±0.19	0.90±0.13	0.014
Septal myocardium TBR_{mean}	0.93±0.15	0.76±0.12	0.01

*TBR calculated using right atrial ^{18}F-NaF uptake as background uptake

Myocardial assessment

Assessment of left ventricular volumes and ejection fraction was possible in all participants and values were similar between AS patients and controls (Table 6.3). Most AS patients (n=15) had preserved LVEF as measured on MRI with one patient found to have an ejection fraction less than 50%. This patient (81-year-old, male) was assessed as moderate LV dysfunction on echocardiography but had a severely reduced LVEF (30%) on MRI in the context of previous myocardial infarction. One further patient (89-year-old, female, atrial fibrillation, TAVI referral) had suboptimal image quality on transthoracic echocardiography with moderate LV systolic impairment by visual assessment but an MRI LVEF measured above 50%.

Indexed left ventricular mass was greater in AS patients compared to controls (105±27 g/m^2 versus 64±8 g/m^2, P=0.02) as was maximum left ventricular wall thickness (17±3 mm versus 11±1 mm, P=0.0007, Table 6.4). Myocardial contraction fraction was significantly reduced in AS patients compared with controls (52±20% versus 84±17%, P=0.002) as was longitudinal systolic function (8.3±3.6 mm versus 15.3±3.3 mm, P=0.0005). Although the mean indexed LV stroke volume was similar between modality (MR: 51±12 mL/m^2, echo: 43±12 mL/m^2, P=0.08), echocardiography consistently underestimated indexed stroke volume compared with MR (Bland-Altman analysis; bias -7.4 mL/m^2) with wide limits of agreement (-37.2 to 22.4 mL/m^2, Figure 6.3).

Mid-wall late gadolinium enhancement was seen in eight AS patients (50%) and none of the healthy volunteers (Figure 6.4). One AS patient had subendocardial late enhancement consistent with previous anteroapical myocardial infarction. No patient had echocardiographic or MRI features suggestive of a diagnosis of cardiac amyloidosis. Of interest, there was a trend towards greater septal native T1 between AS patients compared with controls (1285±49 ms versus 1241±39 ms) but this did not reach statistical significance (P=0.06, Table 6.4). ECV% was similar between groups (patients with AS: 27.5±2.0%, control subjects: 27.6±2.4%, P=0.94) but iECV was greater in patients with AS (28±8 mL/m^2 versus 17±2 mL/m^2, P=0.003).

No ^{18}F-NaF uptake in the myocardium was observed in any patient on visual analysis (Figure 6.4). There was no difference in SUV_{max} of the septal myocardium between patients with AS and control subjects (P=0.53). Across all participants, ^{18}F-NaF septal myocardial uptake did not correlate with native T1 (SUV_{max}: r=0.37, P=0.09) or ECV% (SUV_{max}: r=-0.28, P=0.22).

All patients who underwent surgical aortic valve replacement consented to intraoperative myocardial biopsy (n=14) from the interventricular septum. At the time of writing, nine biopsy samples had been collected and analysed. Samples were not collected from patients who underwent TAVI (n=2) or surgical AVR via mini-sternotomy (n=1), and in one patient the sample was not sufficient for analysis. No complications from biopsy collection were observed. Samples were analysed at the National Amyloid Centre (Royal Free

Hospital, London, UK); Congo red staining was negative for the presence of amyloid deposits in all samples. As such, TTR immunohistochemistry was not performed.

Figure 6.3: Bland-Altman analysis of echocardiography and magnetic resonance imaging in the measurement of left ventricular indexed stroke volume

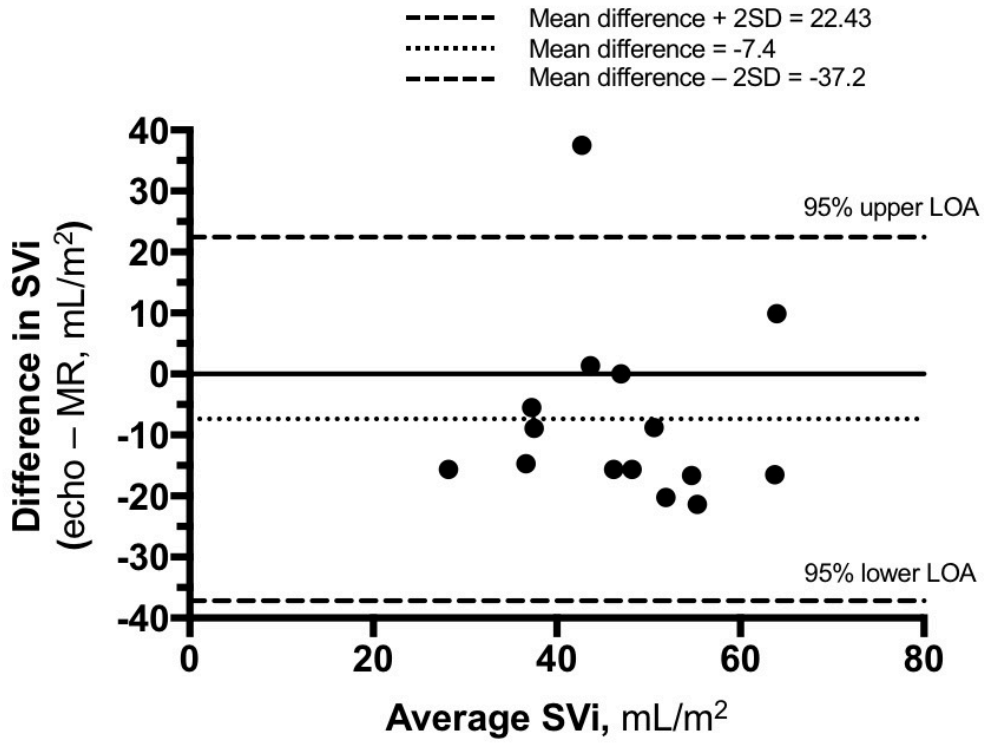

Figure 6.4: Multiparametric assessment of the left ventricular myocardium using hybrid magnetic resonance imaging / positron emission tomography

Late gadolinium enhancement imaging (a and phase-swap, b) can detect focal replacement fibrosis (red arrow). Cine imaging (c) provides gold-standard assessment of LV volumes, mass, stroke volume and ejection fraction. Both native T1 mapping (d) and extracellular volume fraction (ECV%, combination of native and post-contrast (e) T1 mapping) can detect and quantify diffuse fibrosis and look for the presence of cardiac amyloidosis. The absolute fibrosis burden can be quantified with the indexed extracellular volume (iECV) by combining ECV% and left ventricular mass (c). Myocardial ^{18}F-sodium fluoride activity can be assessed using a region of interest in the interventricular septum again to look for evidence of cardiac TTR amyloidosis (f-i).

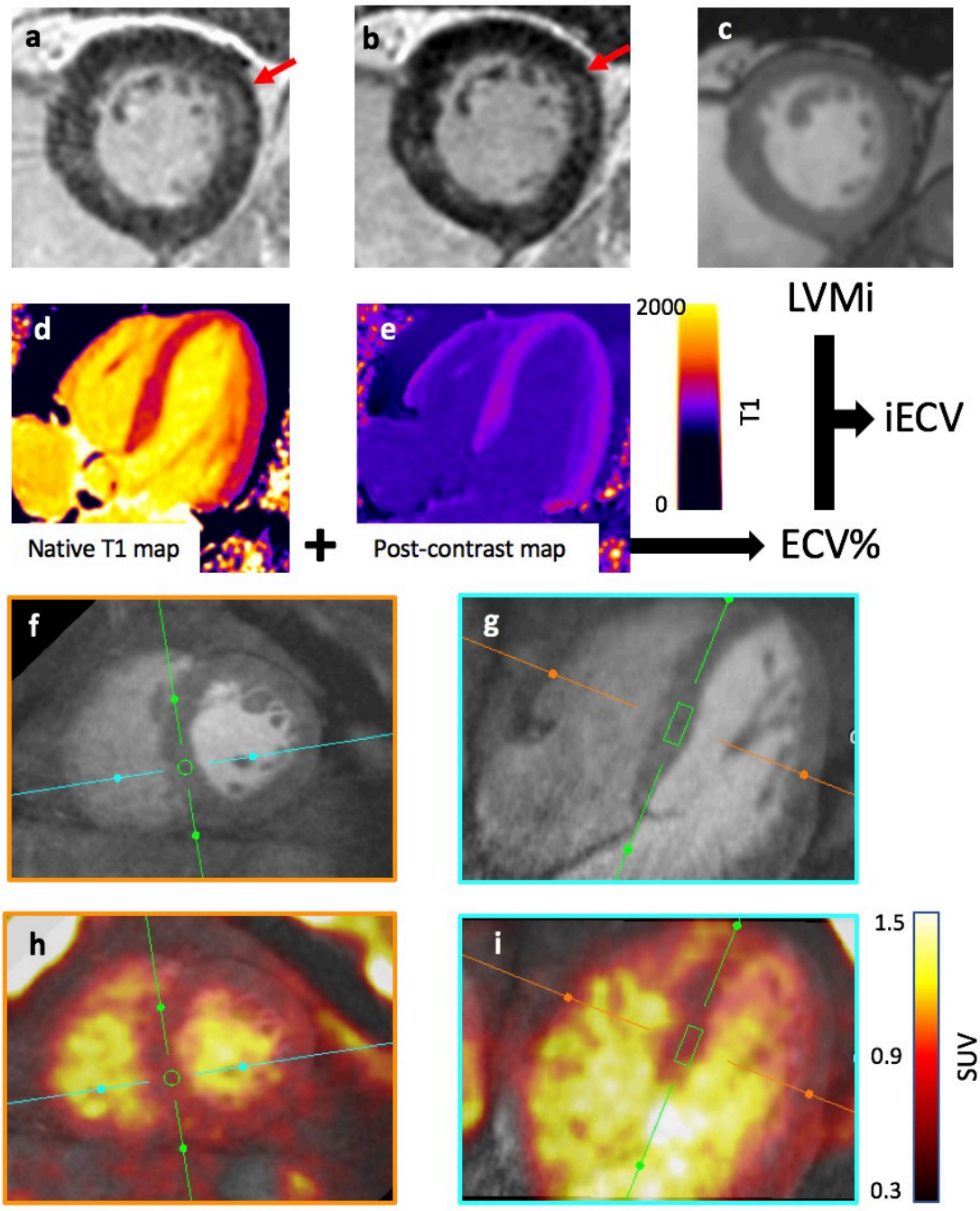
a
b
c
d
e
2000
T1
0
LVMi
iECV
Native T1 map
Post-contrast map
ECV%
f
g
h
i
1.5
0.9
0.3
SUV

Coronary arteries

The coronary ostia height could be measured in 18 (81%) participants. There was reasonable agreement in measurements between MR/PET and CT in the two patients who underwent pre-operative CT TAVI (mean absolute and percentage difference in left coronary ostia height: 1.1 mm, 7%), right coronary ostia height: 1.6 mm, 8%).

Excellent resolution of the proximal coronary arteries was possible with the iNAV-based MC CMRA sequence in 14 (64%) of participants. In 9 individuals, good image quality was also available of the mid-vessels, with the lumen of more distal vessels such as the posterior descending artery clearly seen in four participants (Table 6.3 and Figure 6.5). Detailed analysis of the CMRA for presence and degree of coronary stenosis was not performed, as the sequence was not optimised for this purpose in these scans.

Coronary ^{18}F-NaF uptake could be assessed in 21 individuals (95%), with uptake noted in 3 participants (all with aortic stenosis, Figure 6.5). In total, five high-uptake areas were identified (3 left anterior descending artery, 2 left circumflex artery) with a mean SUV_{max} of 1.54±0.27.

Figure 6.5: Hybrid magnetic resonance imaging / positron emission tomography of the coronary arteries

Excellent resolution of the proximal coronary arteries was possible with the iNAV-based motion-corrected coronary magnetic resonance angiogram sequence in most participants. The left anterior descending (LAD, white arrows), left circumflex (green arrows) and right coronary (blue arrow) arteries are clearly visible in one of the healthy volunteers (a-e). In a separate patient with aortic stenosis, a lesion is seen (red arrows) in the proximal LAD (f). There is co-localised ^{18}F-sodium fluoride activity (g) was an SUV_{max} of 1.85. The corresponding invasive angiogram confirmed an obstructive proximal LAD stenosis in the same location (red arrows)

SUV; standardised uptake value

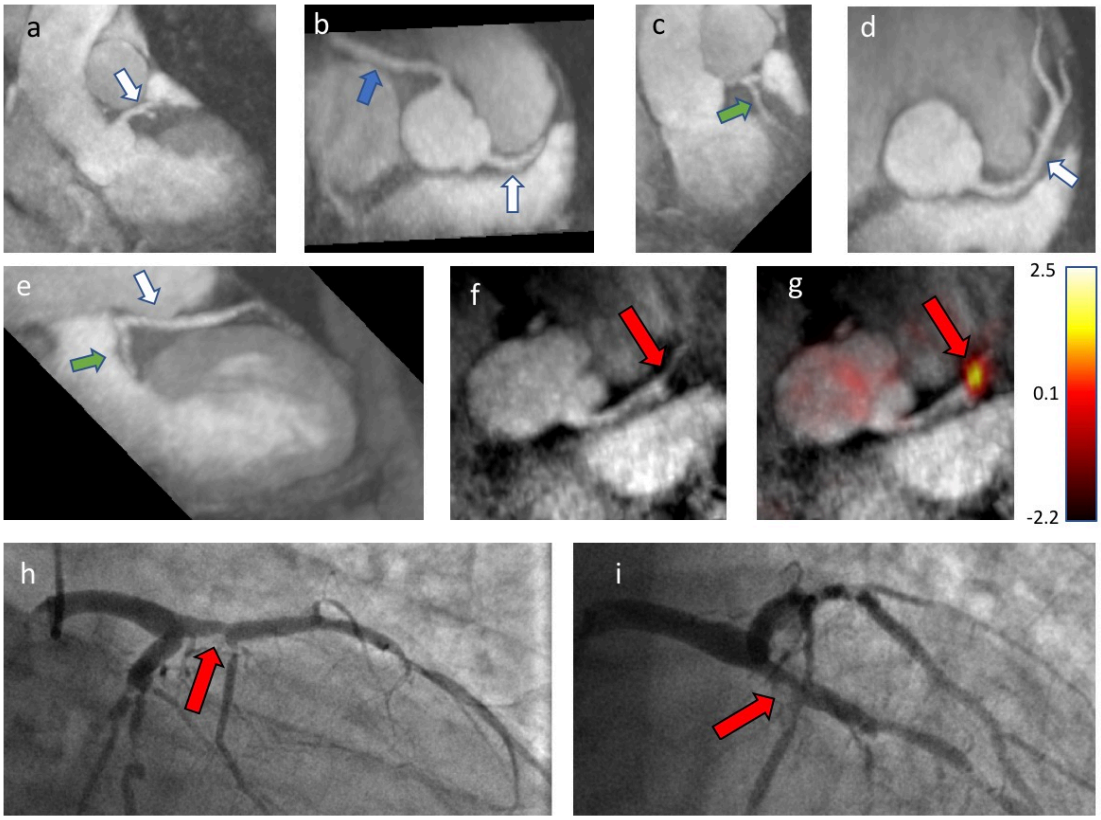

DISCUSSION

This is the first description of cardiac MR/PET imaging in a cohort of patients with severe aortic stenosis with age and gender-matched healthy volunteers. We have demonstrated that MR/PET imaging is feasible and well tolerated in these cohorts, and offers a multiparametric assessment of the valve, myocardium and coronary arteries. In particular, we have shown that MRAC with a free-breathing radial GRE sequence is superior to the standard Dixon approach, and that novel non-contrast iNAV-based MC CMRA with 100% respiratory scan efficiency provides excellent visualisation of the valve, myocardium and proximal coronary arteries in the majority of imaged patients.

Hybrid MR/PET platforms offer considerable advantages over PET/CT in that functional metabolic information can be acquired with considerable reduction in radiation exposure whilst simultaneously offering high resolution functional assessment of both the valve and myocardium with added myocardial tissue characterisation. Two specific technical issues related to MR/PET imaging that require further optimisation are attenuation correction and motion correction.

Accurate quantification and localisation of PET activity requires application of attenuation correction maps (MRAC map) to account for the radiodensity of tissues that PET photons must traverse from their source at an annihilation event to the PET detector. In PET/CT, the CT source can be used to generate a MRAC map that can be used to correct the PET data. In a MR/PET scanner,

alternative approaches use MRI sequences to segment the acquired volume into different tissue types. A correction factor (or linear attenuation coefficient, LAC) unique to each tissue type is then applied to the PET data (124). The standard Dixon MRAC map provides poor resolution particularly along the heart-lung and liver-lung interfaces which are subject to respiratory motion and usually mis-segments the bronchi as soft tissue, leading to significant artefact due to inaccurate correction of the PET counts. MRAC using a novel free-breathing radial GRE sequence has been shown to reduce these artefacts in a coronary disease population (98). We have here confirmed the superiority of this method of attenuation correction for cardiac purposes demonstrating that it eliminates these reported artefacts.

Regional analysis of PET data in different structures within the heart requires fusion with a 3D anatomical MR dataset. In our study, this was provided by a novel non-contrast CMRA sequence. This ECG-gated and respiratory translational motion corrected sequence produces a high-resolution isotropic volume encompassing LV, aortic valve and proximal coronary arteries without the need for gadolinium contrast administration and in a predictable scan time. This meant that only a single bolus dose of gadolinium was required for late enhancement imaging, avoiding staggered contrast doses which might confound image interpretation. Whilst co-registration of PET and MRI datasets is generally good as they are acquired simultaneously, manual registration adjustment was sometimes required in this study and enabled by the acquisition of the CMRA images. A simultaneous motion corrected PET-

CMRA approach has been recently proposed to correct for both PET and CMRA data leading to co-registered MRAC, PET and CMRA images. This approach has been demonstrated in a small cohort of patients with total coronary occlusion (157) and will be investigated in patients with severe aortic stenosis in future work.

The valve

Hybrid MR/PET imaging allowed detailed anatomical assessment of the aortic valve in most participants. As previously noted using PET/CT (6), intense aortic valve uptake was noted in all the aortic stenosis patients. Previous studies have established that this activity indicates increased calcification activity within the valve and serves as a method to predict future valve disease progression and when patients are likely to require valve replacement. Aortic annulus measurements could also be performed showing good agreement with CT in two cases where both modalities were available for comparison. Accurate annulus area measurements are of potential utility in valve sizing prior to TAVI, and also for more accurate estimation of the aortic valve area (AVA) using the continuity equation. Indeed, substantial underestimation of the annulus / LVOT area and therefore the AVA was observed with echocardiographic measurements compared with MR. Substituting MR measurements in deriving AVA has previously been shown to reduce the inconsistency in the relationship between mean gradient and AVA, and the number of patients with discordant haemodynamic assessments of disease severity (158). MR is also considered the gold-standard method for assessing

LV volumes, including LV stroke volume (155). We showed a systematic underestimation and poor agreement between echocardiography and MR in LV stroke volume assessment, which not only influenced calculation of aortic valve area but also assessment of flow status. Using MR in the assessment of both AS severity and flow status may therefore prove useful to confirm AS severity and subtype (e.g. low-flow low-gradient) in borderline cases, particularly when considering high-risk intervention.

The myocardium

We have shown that comprehensive multiparametric assessment of the myocardium is feasible within a single scan. T1 mapping and LGE assessment can detect and quantify diffuse and replacement myocardial fibrosis respectively, both of which are associated with an adverse prognosis and have been proposed as early markers of LV decompensation (7,46,49,83). There is considerable interest in using these as objective markers of LV decompensation prior to the development of symptoms or impaired ejection fraction in order to optimise the timing of valve intervention. Whether a strategy of targeted early valve replacement in asymptomatic patients with preserved LVEF but evidence of mid-wall LGE on MR imaging can improve long-term clinical outcomes is being tested in the Early Valve Replacement guided by Biomarkers Of LV Decompensation in Asymptomatic Patients with Severe Aortic Stenosis (EVOLVED, NCT03094143) randomised controlled trial.

One further advantage of hybrid techniques is the identification and characterisation of co-existent pathology. Transthyretin (TTR) cardiac amyloidosis is an increasingly recognised condition in the elderly but given that the imaging features on transthoracic echocardiography are similar to those seen in advanced AS, a diagnosis of concomitant amyloidosis is often not considered. In fact, the prevalence of coexistent myocardial TTR amyloid deposition has been estimated at between 6 and 16% of severe AS populations (104,111) and up to 25% in the general population over 85 (100). Not only can MRI identify overt cardiac amyloidosis using LGE and T1 mapping, but early studies show that the addition of ^{18}F-NaF PET may be able to discriminate between TTR and AL subtypes without the need for further investigations (112). This is important as patients with co-existent TTR amyloidosis have a mortality rate approaching 50% regardless of interventional strategy (104,159) and this diagnostic information could be used to inform decision making about approach or even appropriateness of valve intervention.

In spite of recruiting an elderly cohort (mean age 80 years), no patient in our study had typical MRI imaging features of cardiac amyloidosis. Septal myocardial SUV_{max} values in our cohort were consistently less than blood pool, as described in the control patients of the previous report by Trivieri et al (112). Importantly, cardiac amyloid deposition was excluded in all patients where myocardial biopsy samples were available for histological analysis. The potential for ^{18}F-NaF PET to detect co-existent TTR amyloidosis in this

population therefore remains unproven and requires a study with a larger sample size.

Coronary imaging

Coronary imaging using MRI has traditionally been challenging given the small size and complex motion of the coronary arteries. We have demonstrated that novel ECG-gated, free-breathing MR sequences with inline 2D translational respiratory motion correction can provide high quality imaging of the proximal coronary arteries in most cases, without the need for contrast administration and in a predictable scan time (no data rejection due to respiratory motion). Whilst detailed coronary analysis remains challenging scan quality was sufficient for localisation of coronary PET data to the coronary vasculature and also for accurate and detailed measurement of the height of the coronary arteries above the plane of the aortic valve: another key measurement used in the work up of patients being considered for TAVI. Further improvements in motion correction, including non-rigid respiratory motion compensation, have been shown to lead to better visualization of the coronaries (160) and will be investigated as future work.

Where might this hybrid MR/PET technique find future clinical use in aortic stenosis? Undoubtedly for the foreseeable future MR/PET will remain a research tool but in time may become attractive as a “one-stop” assessment of valve, myocardium and coronary arteries prior to considering an interventional strategy. We have demonstrated that most aspects of the TAVI

CT can be replicated using MRI, which might be particularly useful in patients with renal impairment or proven contrast allergy where non-contrast MR angiography sequences could be used. Whilst not performed in this study MR also provides excellent assessment of the peripheral vasculature. MR assessment of LVOT area and stroke volume may be able to clarify AS severity in borderline case and to more accurately identify reductions in ejection fraction. Moreover, the ability of MR/PET to detect presence of mid-wall LGE and co-existent cardiomyopathy such as TTR amyloidosis may play a future role in deciding on when best to replace the valve, although further work in this area is required.

Further improvements to this technique are possible, particularly in the area of motion correction. MR allows for monitoring of both cardiac and respiratory motion which can be used to apply non-rigid motion correction to both the MR and PET data as shown in recent studies (125,157). This results in a reduced acquisition time, increased visible length and sharpness of coronary arteries and improved PET signal-to-noise ratio. In addition, ultrashort echo time MR imaging could potentially be used to detect vascular and valvular calcification which would be desirable for pre-TAVI imaging.

CONCLUSION

Hybrid MR/PET imaging in aortic stenosis is feasible and well-tolerated, offering a multiparametric assessment of aortic valve, LV myocardium and coronary arteries. Compared with PET/CT, advantages include reduced radiation dose, simultaneous acquisition of PET and MR data, added myocardial tissue characterisation and potential avoidance of intravenous iodinated contrast. Further research is required to optimise motion correction techniques and assess the ability of ^{18}F-NaF to detect co-existent TTR amyloidosis in larger cohorts.

Acknowledgements

We would like to thank Siemens Healthcare for allowing us to use their Radial Selfgating package (Work-In-Progress #793F). This sequence is based on contributions from Simon Bauer, Robert Grimm and Matthias Fenchel.

Chapter 7: Conclusions and Future Directions

SUMMARY OF FINDINGS

Aortic stenosis is a condition of both valve and myocardium. Cardiac magnetic resonance assessment of the left ventricular myocardium can detect both diffuse and replacement myocardial fibrosis. In this thesis, I have applied a novel T1 mapping marker of diffuse fibrosis, the indexed extracellular volume (iECV) and shown that patients with aortic stenosis can be classified into three groups depending on the amount and type of myocardial fibrosis. In addition, this classification is able to detect early evidence of decompensation of the LV hypertrophic response. I have also characterised the progression and regression of cellular hypertrophy and different types of myocardial fibrosis over time using cardiac magnetic resonance. I then proceeded to further demonstrate the association of extracellular-volume based measures with various measures of LV decompensation and adverse clinical outcomes following aortic valve intervention in a large multicentre cohort. Finally, I explored the utility of novel hybrid positron emission tomography / magnetic resonance imaging technology in patients with aortic stenosis.

Myocardial Fibrosis and Cardiac Decompensation in Aortic Stenosis

Aortic stenosis is now well-recognised as a disease both of the valve and the myocardium (6). Cardiac magnetic resonance (CMR) offers distinct and complementary advantages to echocardiographic assessment: namely gold standard assessments of ventricular volumes, mass and ejection fraction (161) but also tissue characterisation and the detection and quantification of myocardial fibrosis. Focal replacement fibrosis is detected using late gadolinium enhancement techniques and has been shown to be a powerful independent predictor of adverse prognosis in several cohorts (19,46,49,141). Newer T1 mapping methods can identify extracellular volume expansion and diffuse fibrosis (85) which appear to be an early, reversible form of fibrosis (137). The utility of T1 mapping in the assessment of patients with aortic stenosis requires further study.

Using CMR assessment of myocardial fibrosis, I have shown that patients with aortic stenosis can be classified into three groups depending on the amount and type of fibrosis - normal ventricle, extracellular volume expansion (diffuse fibrosis) and mid-wall late gadolinium enhancement (replacement fibrosis). I found that a novel marker, the indexed extracellular volume (or iECV), an absolute marker of burden of diffuse fibrosis, was better able to differentiate patients according to AS severity and correlated well with collagen volume fraction on myocardial biopsy. Markers of both systolic and diastolic LV function, as well as cardiac biomarkers worsened across these three groups suggesting that this classification can detect early evidence of

decompensation of the LV hypertrophic response. More importantly there was a stepwise worsening of both all-cause and aortic stenosis related mortality across the three groups. This is the first study showing the potential prognostic utility of ECV-based measures in aortic stenosis.

Progression and Regression of Hypertrophy and Fibrosis in Aortic Stenosis

Although cardiovascular magnetic resonance can accurately assess both cellular hypertrophy and extracellular volume (a widely used surrogate measure of diffuse myocardial fibrosis), how these processes change over time both in the natural history of aortic stenosis and in response to relief of pressure overload following aortic valve intervention has not been described. In addition, although focal replacement fibrosis is thought to be irreversible following valve replacement (68), how this process evolves over time in the natural history of AS is unknown.

In order to further investigate longitudinal changes in these processes, I have analysed a multicentre cohort of almost 100 patients who underwent serial echocardiography and CMR imaging at multiple time points. By examining the novel marker iECV, along with ECV% and LV mass I was able to provide a comprehensive assessment of both myocardial intra and extracellular compartments. Whilst some patients underwent valve replacement surgery during the interval between imaging timepoints, others did not, allowing me to study both the natural history of hypertrophy and fibrosis in AS and also how these processes remodel following valve intervention. In the natural history group, there was steady progression in both myocyte volume and diffuse fibrosis / extracellular volume over time, resulting in no change in the relative extracellular volume (ECV%). In patients with focal mid-wall fibrosis there was

rapid accumulation over time with new areas visible in remote myocardial segments in several patients.

Following valve replacement, there was regression of diffuse fibrosis but much faster fall in myocyte volume, leading to an initial increase in ECV%. I also confirmed findings in previous studies that replacement fibrosis (mid-wall LGE) is irreversible and although valve replacement appeared to arrest progression, no regression of replacement fibrosis was seen during the study follow-up. This provides insights into the rapid progression of replacement fibrosis in the natural history of AS, which appears to confer a worse prognosis the more fibrosis is present (46) and suggests that valve replacement limits further scarring from forming. Thus, a strategy of early valve replacement when replacement fibrosis is detected might lead to improved clinical outcomes compared with standard watchful waiting until symptoms develop.

Further investigation of the utility of T1 mapping assessments of diffuse fibrosis in aortic stenosis requires larger multicentre studies for adequate statistical power and to demonstrate the feasibility of techniques over multiple vendor platforms and sequences.

Gathering patient data internationally from 400 individuals enrolled in prospective observational cohort studies I analysed the largest cohort to date of severe aortic stenosis patients scheduled for valve replacement surgery who underwent T1 mapping CMR prior to their procedures. As expected, there was significant variation in native T1 values across different centres, mainly related to differing magnetic field strength. In contrast, I showed that extracellular volume-based measures did not significantly vary with the above technical factors.

Native T1 was not clearly associated with measures of disease severity. In particular, native T1 did not predict clinical outcomes, even after adjusting for technical factors. However, both ECV% and the novel marker iECV were associated with several markers of LV decompensation and more importantly with patient outcomes. I observed a 14% increase in all-cause mortality for every 1% rise in ECV% independent of age, sex, peak velocity, presence of LGE and reduced ejection fraction. I found that iECV predicted all-cause

mortality independent of age and sex but not when other clinical factors were considered.

In patients with severe aortic stenosis awaiting valve replacement, I have demonstrated that ECV-based T1 mapping techniques are robust across different scanner platforms and field strengths, correlate well with measures of LV decompensation and independently predict all-cause mortality.

Feasibility and Utility of Hybrid Magnetic Resonance Imaging / Positron Emission Tomography in Aortic Stenosis

Positron emission tomography (PET) offers functional metabolic imaging allowing the activity of specific disease processes to be measured *in vivo*. Previous work has demonstrated that 18F-sodium fluoride (18F-NaF) radiotracer binds to hydroxyapatite in newly developing areas of calcification in the aortic valve is activity appears to predict valve disease progression and future clinical events when combined with computed tomography (PET/CT) (6,93). Hybrid MR/PET technology offers significant advantages; reduced overall radiation dose and improved tissue characterisation, co-registration and motion correction.

I investigated the novel use MR/PET in aortic stenosis in 16 patients scheduled for valve replacement procedures and 6 healthy volunteers. I showed that MR/PET is feasible and well-tolerated in this patient group and offered excellent image quality in the majority of patients. In particular, detailed assessments of the aortic valve, annulus, proximal coronary arteries and LV myocardium were possible. I also investigated the use of novel methods of attenuation correction and motion correction, which allow simultaneous assessment of calcification activity in the aortic valve along with CMR assessments of myocardial health.

FUTURE DIRECTIONS

Investigating the clinical utility of CMR mid-wall fibrosis assessment

There is now a significant body of observational evidence identifying mid-wall replacement myocardial fibrosis as a marker of early LV decompensation in aortic stenosis. Multiple single centre observational studies (19,46,49) as well as a large multicentre study (69) have found the presence of mid-wall LGE to be a strong independent risk factor for adverse outcomes. I have shown that once present in AS patients, mid-wall fibrosis accumulates rapidly (146) and previous work suggests that increasing LGE mass is associated with a higher risk of adverse events (46). In addition, although valve replacement arrests further LGE development (146), no regression of existing LGE is seen out to two years following intervention (68,144,146) indicating that this type of fibrosis is permanent and once developed patients are left with poor long-term outcomes with conventional management strategies (48). Given the accumulated evidence it is now time for a randomised controlled trial to determine if an early valve replacement procedure in patients without conventional indication for surgery but with evidence of mid-wall fibrosis could improve clinical outcomes.

To that end, we have designed and implemented the Early Valve Replacement guided by Biomarkers of Left Ventricular Decompensation in Asymptomatic Patients with Severe Aortic Stenosis (EVOLVED, NCT03094143) clinical trial. EVOLVED is a parallel-group multicentre prospective randomised open-label

blinded endpoint (PROBE) controlled trial of early aortic valve intervention in asymptomatic patients with severe AS and evidence of LV decompensation (mid-wall fibrosis) on CMR imaging. There is an additional observation arm of patients without evidence of LV decompensation on cardiac MRI. During my PhD I was instrumental in designing and writing the study protocol, acted as Principal Investigator in Edinburgh and was responsible for setting up remote study sites along with the EVOLVED trial manager.

Patients with severe aortic stenosis (aortic valve peak velocity ≥4.0 m/s, or aortic valve area indexed to body surface area <0.6 cm^2/m^2 with aortic valve peak velocity ≥3.5 m/s) are eligible to be enrolled if they are asymptomatic. This is a pragmatic definition, that requires the treating cardiologist to determine they have no symptoms that would warrant consideration of aortic valve intervention. Key exclusion criteria are 1) planned cardiac surgery or previous valve replacement, 2) co-existent severe valvular regurgitation, 3) LV ejection fraction <50%, 4) any contraindication to MRI scanning (e.g. pacemaker), 5) any contraindication to gadolinium contrast (e.g. egfr <30mL/min/1.73m^2) and 6) patient deemed unfit to be considered for valve intervention. Full exclusion criteria are listed in the appendix (EVOLVED study protocol).

Patients meeting the inclusion criteria are initially screened with high sensitivity troponin (if Abbott architect high sensitivity assay available locally) and 12-lead ECG. Patients are deemed higher risk if they have a troponin level ≥6

ng/L or ECG left ventricular hypertrophy plus strain pattern (≥1mm concave downsloping ST segment depression with asymmetrical T wave inversion in at least two contiguous lateral leads). In the ECG-only sites (where the Abbott troponin assay is not available) patients are considered higher risk if they meet ECG criteria for left ventricular hypertrophy, regardless of presence of the strain pattern.

Patients who are lower risk are not eligible for further study participation. Those deemed higher risk are invited back for a baseline assessment (see study protocol in Appendix for further details). This includes a CMR scan with gadolinium contrast and late gadolinium enhancement imaging. Several LGE sequences are performed (short-axis stack, phase swap stack and long-axis views) to optimise the ability to interpret the images for the presence of mid-wall fibrosis.

Following CMR, final eligibility check is performed. If patients meet all criteria, they are randomised using a web-based system with minimisation criteria. If mid-wall fibrosis is present patients undergo randomisation 1 (1:1 between early valve intervention and routine clinical care, Figure 7.1). If mid-wall fibrosis is not present, patients undergo randomisation 2 (1:2 randomisation between routine clinical care with study follow-up and routine clinical care without study follow-up).

Figure 7.1: Summary of EVOLVED study protocol

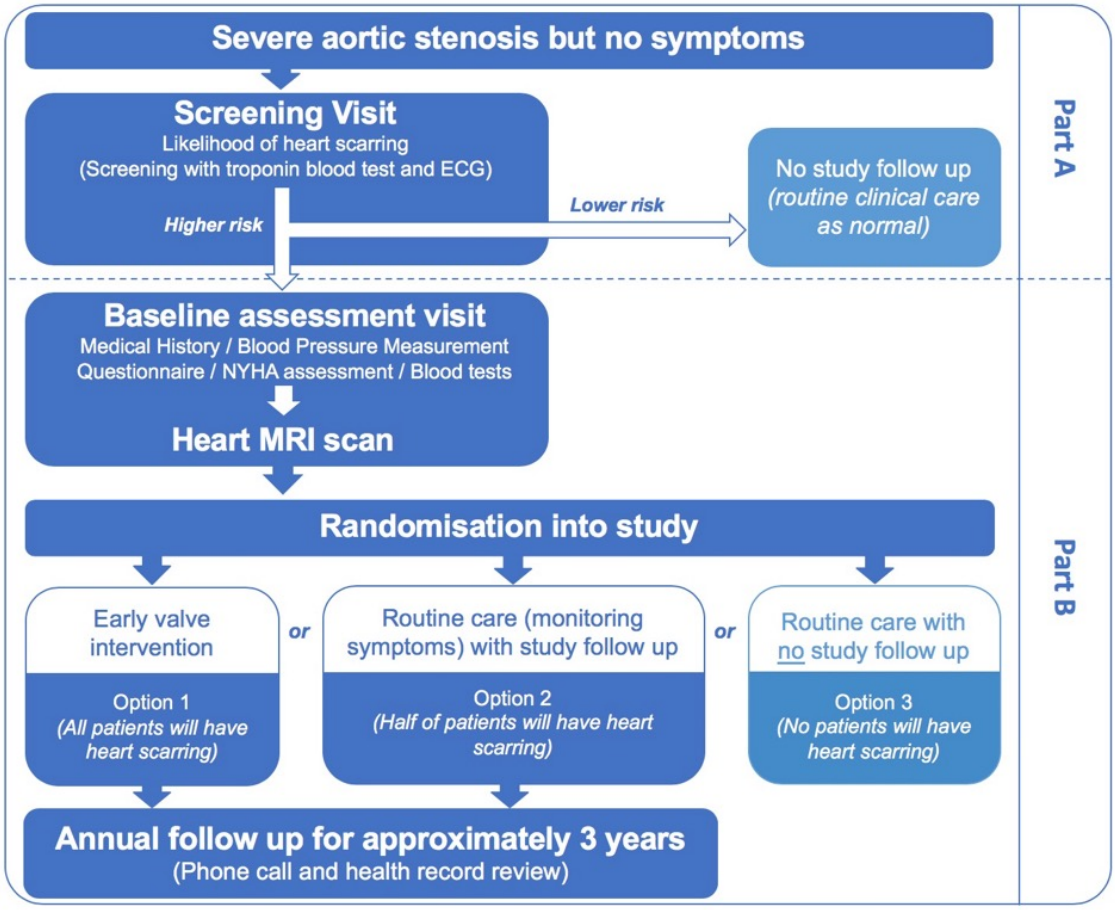

If randomised to early valve intervention this should be performed as per local NHS processes. The trial protocol does not mandate an interventional strategy (AVR versus TAVI) and concomitant coronary bypass grafting or aortic root surgery may also be performed. If possible, intervention should be performed within 2 months of randomisation. Patients randomised to routine clinical care will have any decisions about timing of future valve intervention made by their usual cardiologist.

Study follow-up is annual, with a telephone call and medical records check. The primary outcome is a composite of all-cause mortality and unplanned aortic stenosis related hospitalisation. The study end-point is event driven with an expected mean follow-up time of 2-3 years.

In total across the sites we plan to screen approximately 1600 patients of whom approximately 1000 higher risk patients will be invited to attend baseline visit including CMR imaging. We expect this to identify 400 patients with mid-wall fibrosis for the primary study randomisation. The study has a 90% power at the 5% significance level once 88 events are reached assuming an event rate of 25% in the routine care arm and 13.4% in the early intervention arm.

One key aspect of the study design was introducing blinding of the CMR result to patients, clinicians and the study investigators. This is to avoid bias that might be introduced by patients randomised to routine care being aware they have mid-wall fibrosis. To this end, a proportion of patients without mid-wall

fibrosis will also receive study follow-up, and the cohort of patients receiving routine care with study follow-up will contain patients both with and without mid-wall fibrosis and will appear as a single group to all those except the CMR reviewers (Figure 7.2). The CMR review result (presence of absence of mid-wall fibrosis) is logged in the trial database so that the appropriate randomisation step and group allocation is performed if a patient meets eligibility criteria.

Figure 7.2: Blinding of CMR result in the EVOLVED trial

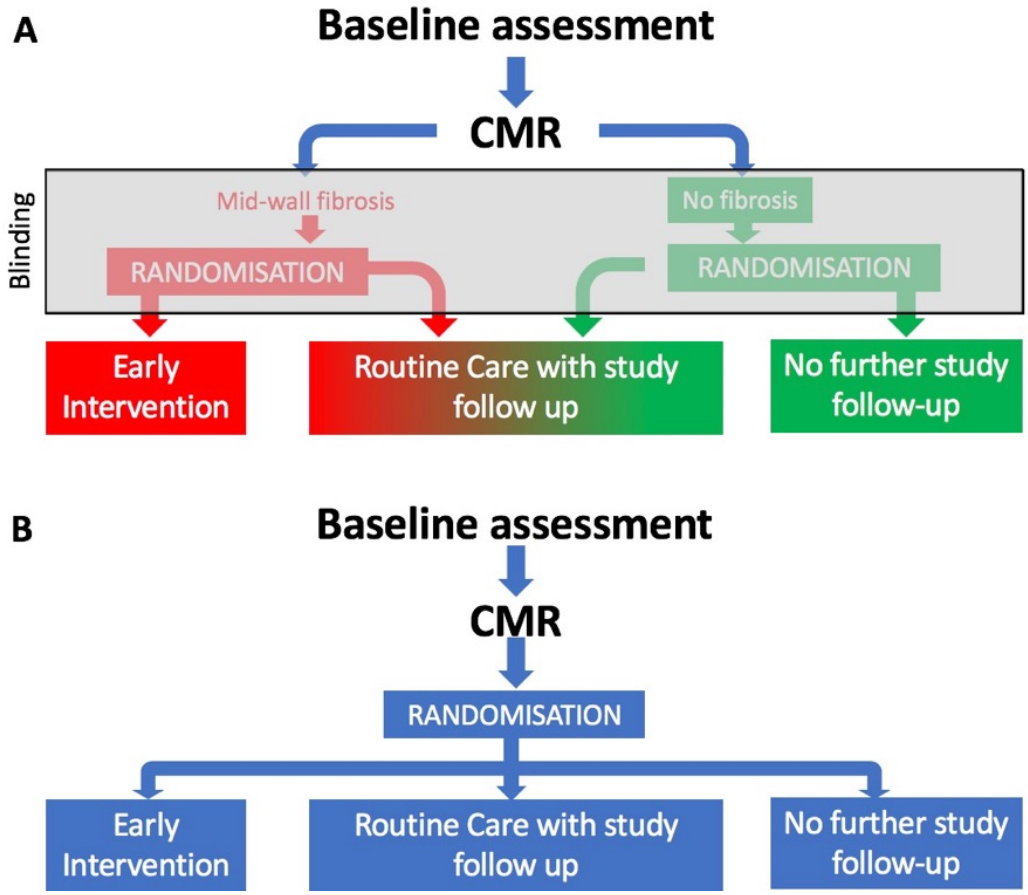

Patients, researchers and clinicians are blinded to the results of the CMR review (A). As a result, patients are placed into one of three groups as a result of the two randomisation processes depending on the presence of mid-wall fibrosis on CMR review. The middle group has a mixture of patients with and without mid-wall fibrosis. However, to blinded individuals this appears as a single randomisation step into one of three groups (B).

Research ethics committee approval was obtained on 12th May 2017 (17/SS/0052) and recruitment in Edinburgh commenced on 27th July 2017. To date, 12 sites are open to recruitment with another 12 planned to open (Figure 7.3). Provisional end-date for recruitment is August 2020.

It is hoped that the strategy explored in EVOLVED will target valve intervention to those patients who will derive greatest benefit and we await the trial results with great interest.

Figure 7.3: EVOLVED study sites

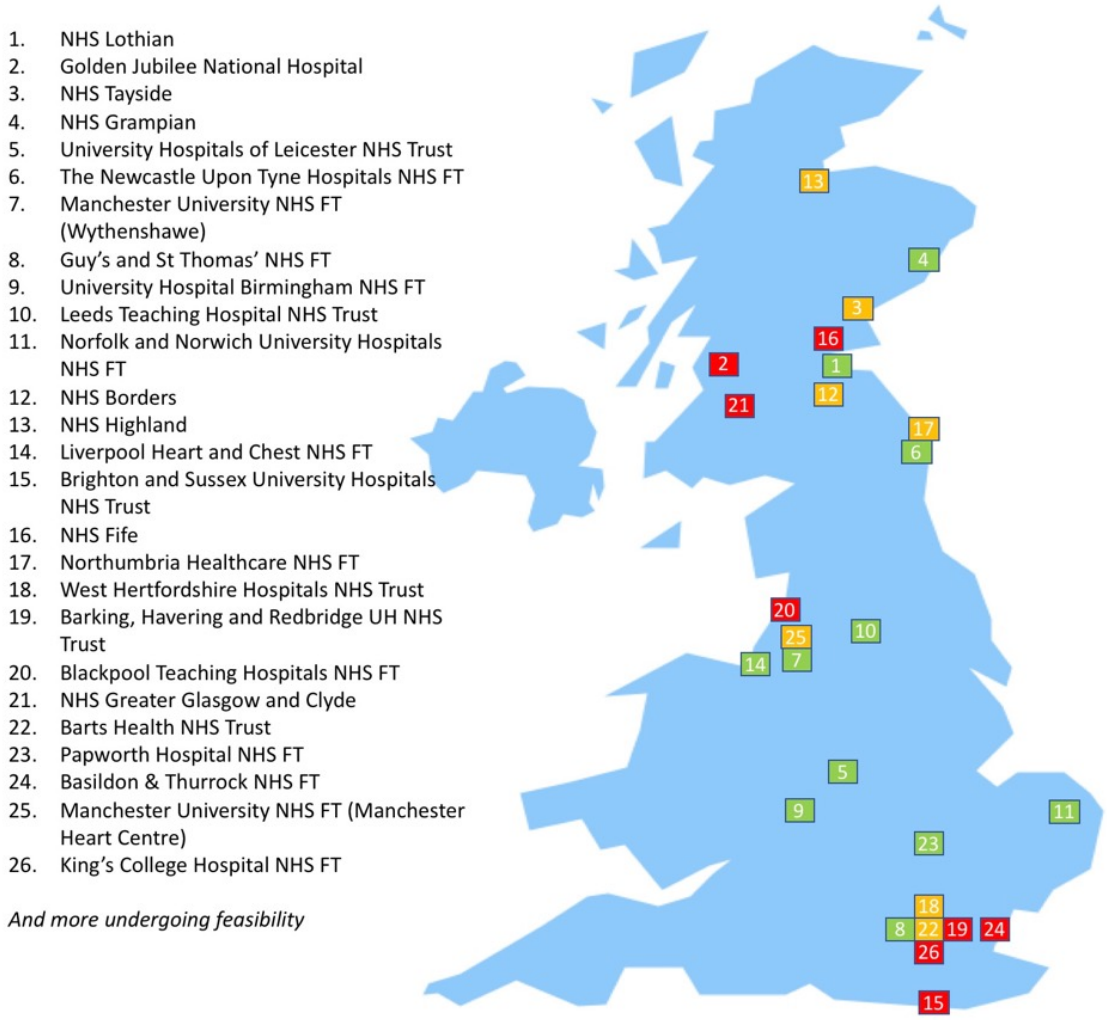

Sites in green are open to recruitment, yellow; awaiting sponsors authorisation to open, red; awaiting capability and capacity assessment.

Diffuse fibrosis as a marker of risk / threshold for intervention

Although mid-wall fibrosis is now well established as a marker of early LV decompensation it appears to be permanent (68,144,146) meaning that such patients are still left with an elevated risk of adverse events following valve replacement (48). It would clearly be advantageous to utilise an earlier reversible marker of LV decompensation, such as T1 mapping assessments of diffuse fibrosis (137,144,146), in future decision-making pathways. I have demonstrated the prognostic importance of ECV-based T1 mapping measures in patients with severe aortic stenosis undergoing valve replacement and the feasibility of conducting multicentre studies using this technique. As such, future research should concentrate on developing and validating thresholds for abnormal diffuse fibrosis that could be investigated in randomised prospective trials.

MR/PET in aortic stenosis

I have demonstrated that MR/PET is feasible as a one-stop assessment of aortic valve, myocardium and coronary arteries in AS patients. Excellent image quality was obtained in most patients but could potentially be improved upon. For example, further application of advanced motion correction techniques for both MRA and PET datasets may significantly improve image clarity, PET signal-to-noise ratio and reduce acquisition time (125). With novel therapies for TTR amyloidosis now becoming available (101), MR/PET could be used to identify patients eligible for treatment and to monitor response to therapy.

CLINICAL PERSPECTIVES

Aortic stenosis is the most common valve disease requiring intervention in the developed world however no randomised evidence exists to help determine treatment decisions. Clinical guidelines currently recommend valve intervention for severe aortic stenosis in the presence of classical symptoms or findings of an impaired ejection fraction (5,148). However, improvements in surgical technique, peri-operative care, replacement valve technology and the advent of transcatheter procedures, along with a not insignificant rate of sudden death (approximately 1-1.5% per year whilst symptom free (41-43)) mean that the balance of risks and benefits is likely shifting towards offering earlier valve intervention in the asymptomatic phase. How we as doctors are able to identify those patients who will benefit most from an earlier procedure is critical. Although many novel biomarkers such as troponin, diastolic dysfunction and assessments of myocardial strain may be able to identify earlier evidence of decompensation, assessments of myocardial fibrosis appear the most promising.

Myocardial fibrosis appears to be a consequence of direct pressure-overload and repeated myocardial ischaemia (8). Although the mechanism of sudden cardiac death in aortic stenosis is poorly understood it is likely that myocardial fibrosis may contribute as a substrate for life-threatening arrhythmia. Offering early valve replacement to those with evidence of replacement myocardial fibrosis on CMR imaging is being investigated in the ongoing EVOLVED trial

which will be the first randomised controlled trial of targeted early intervention in asymptomatic patients with severe aortic stenosis.

Furthermore, advanced imaging techniques such as T1 mapping are able to detect and quantify diffuse fibrosis, a precursor to replacement fibrosis which is reversible following valve intervention (144,146). Further work to identify clinically relevant thresholds for abnormal levels of diffuse fibrosis which could then be examined as triggers for valve intervention in prospective randomised trials is warranted. In addition, T1 mapping provides fully quantitative, accurate and reproducible assessment of whole-heart fibrosis, meaning this technique may be used as an end-point for future clinical trials assessing novel anti-fibrotic therapies.

Finally, as decision-making surrounding intervention becomes more complex, “one-stop” multiparametric imaging using MR/PET to assess the aortic valve, ventricular myocardium, coronary arteries and aorta is attractive. Such an assessment could provide information on activity of calcification in the valve, presence and extent of myocardial fibrosis and identify co-existent amyloidosis that enables clinicians to make a fully informed decision about the method or even appropriateness of valve intervention. In addition, this assessment could provide valuable technical information about the aortic annulus, aorta, coronary arteries and peripheral vasculature to determine the optimum approach for valve replacement.

References

1. Iung B, Baron G, Butchart EG, Delahaye F, Gohlke-Bärwolf C, Levang OW, et al. A prospective survey of patients with valvular heart disease in Europe: The Euro Heart Survey on Valvular Heart Disease. European Heart Journal. 2003 Jul;24(13):1231–43.

2. Pawade TA, Newby DE, Dweck MR. Calcification in Aortic Stenosis: The Skeleton Key. Journal of the American College of Cardiology. 2015 Aug 4;66(5):561–77.

3. Clavel M-A, Pibarot P, Messika-Zeitoun D, Capoulade R, Malouf J, Aggarval S, et al. Impact of aortic valve calcification, as measured by MDCT, on survival in patients with aortic stenosis: results of an international registry study. Journal of the American College of Cardiology. 2014 Sep 23;64(12):1202–13.

4. Dweck MR, Jenkins WSA, Vesey AT, Pringle MAH, Chin CWL, Malley TS, et al. 18F-sodium fluoride uptake is a marker of active calcification and disease progression in patients with aortic stenosis. Circ Cardiovasc Imaging; 2014 Mar;7(2):371–8.

5. Baumgartner H, Falk V, Bax JJ, De Bonis M, Hamm C, Holm PJ, et al. 2017 ESC/EACTS Guidelines for the management of valvular heart disease: The Task Force for the Management of Valvular Heart Disease of the European Society of Cardiology (ESC) and the European Association for Cardio-Thoracic Surgery (EACTS). European Heart Journal. 2017 Aug 26.

6. Dweck MR, Boon NA, Newby DE. Calcific aortic stenosis: a disease of the valve and the myocardium. Journal of the American College of Cardiology. 2012 Nov 6;60(19):1854–63.

7. Chin CWL, Everett RJ, Kwiecinski J, Vesey AT, Yeung E, Esson G, et al. Myocardial Fibrosis and Cardiac Decompensation in Aortic Stenosis. JACC Cardiovasc Imaging. 2016 Dec 8.

8. Hein S, Arnon E, Kostin S, Schönburg M, Elsässer A, Polyakova V, et al. Progression from compensated hypertrophy to failure in the pressure-overloaded human heart: structural deterioration and compensatory mechanisms. Circulation. 2003 Feb 25;107(7):984–91.

9. Connolly HM, Oh JK, Orszulak TA, Osborn SL, Roger VL, Hodge DO, et al. Aortic valve replacement for aortic stenosis with severe left ventricular dysfunction. Prognostic indicators. Circulation. 1997 May 20;95(10):2395–400.

10. Tribouilloy C, Levy F, Rusinaru D, Guéret P, Petit-Eisenmann H, Baleynaud S, et al. Outcome after aortic valve replacement for low-flow/low-gradient aortic stenosis without contractile reserve on dobutamine stress echocardiography. Journal of the American College of Cardiology. 2009 May 19;53(20):1865–73.

11. Clavel M-A, Magne J, Pibarot P. Low-gradient aortic stenosis. European Heart Journal. 2016 Sep 7;37(34):2645–57.

12. Rafique AM, Biner S, Ray I, Forrester JS, Tolstrup K, Siegel RJ. Meta-analysis of prognostic value of stress testing in patients with asymptomatic severe aortic stenosis. Am J Cardiol. 2009 Oct 1;104(7):972–7.

13. Das P, Rimington H, Chambers J. Exercise testing to stratify risk in aortic stenosis. European Heart Journal. 2005 Jul;26(13):1309–13.

14. Otto CM, Burwash IG, Legget ME, Munt BI, Fujioka M, Healy NL, et al. Prospective study of asymptomatic valvular aortic stenosis. Clinical, echocardiographic, and exercise predictors of outcome. Circulation. 1997 May 6;95(9):2262–70.

15. Paradis J-M, Fried J, Nazif T, Kirtane A, Harjai K, Khalique O, et al. Aortic stenosis and coronary artery disease: what do we know? What don't we know? A comprehensive review of the literature with proposed treatment algorithms. European Heart Journal. 2014 Aug 14;35(31):2069–82.

16. Fairbairn TA, Steadman CD, Mather AN, Motwani M, Blackman DJ, Plein S, et al. Assessment of valve haemodynamics, reverse ventricular remodelling and myocardial fibrosis following transcatheter aortic valve implantation compared to surgical aortic valve replacement: a cardiovascular magnetic resonance study. Heart; 2013 Aug;99(16):1185–91.

17. Dauerman HL, Reardon MJ, Popma JJ, Little SH, Cavalcante JL, Adams DH, et al. Early Recovery of Left Ventricular Systolic Function After CoreValve Transcatheter Aortic Valve Replacement. Circ Cardiovasc Interv; 2016 Jun;9(6):e003425.

18. Vaquette B, Corbineau H, Laurent M, Lelong B, Langanay T, de Place C, et al. Valve replacement in patients with critical aortic stenosis and depressed left ventricular function: predictors of operative risk, left ventricular function recovery, and long term outcome. Heart; 2005 Oct;91(10):1324–9.

19. Azevedo CF, Nigri M, Higuchi ML, Pomerantzeff PM, Spina GS, Sampaio RO, et al. Prognostic Significance of Myocardial Fibrosis Quantification by Histopathology and Magnetic Resonance Imaging

in Patients With Severe Aortic Valve Disease. JACC. 2010;56(4):278–87.

20. Kitai T, Honda S, Okada Y, Tani T, Kim K, Kaji S, et al. Clinical outcomes in non-surgically managed patients with very severe versus severe aortic stenosis. Heart; 2011 Dec;97(24):2029–32.

21. Rosenhek R, Zilberszac R, Schemper M, Czerny M, Mundigler G, Graf S, et al. Natural history of very severe aortic stenosis. Circulation. American Heart Association, Inc; 2010 Jan 5;121(1):151–6.

22. Rosenhek R, Klaar U, Schemper M, Scholten C, Heger M, Gabriel H, et al. Mild and moderate aortic stenosis. Natural history and risk stratification by echocardiography. European Heart Journal. The Oxford University Press; 2004 Feb;25(3):199–205.

23. Rosenhek R, Binder T, Porenta G, Lang I, Christ G, Schemper M, et al. Predictors of outcome in severe, asymptomatic aortic stenosis. N Engl J Med. 2000 Aug 31;343(9):611–7.

24. Bergler-Klein J, Mundigler G, Pibarot P, Burwash IG, Dumesnil JG, Blais C, et al. B-type natriuretic peptide in low-flow, low-gradient aortic stenosis: relationship to hemodynamics and clinical outcome: results from the Multicenter Truly or Pseudo-Severe Aortic Stenosis (TOPAS) study. Circulation; 2007 Jun 5;115(22):2848–55.

25. Weber M, Arnold R, Rau M, Elsaesser A, Brandt R, Mitrovic V, et al. Relation of N-terminal pro B-type natriuretic peptide to progression of aortic valve disease. European Heart Journal. 2005 May;26(10):1023–30.

26. Clavel M-A, Malouf J, Michelena HI, Suri RM, Jaffe AS, Mahoney DW, et al. B-type natriuretic peptide clinical activation in aortic stenosis: impact on long-term survival. Journal of the American College of Cardiology. 2014 May 20;63(19):2016–25.

27. Hwang YM, Kim J, Lee JH, Kim M, Hwang J, Kim JB, et al. Conduction disturbance after isolated surgical aortic valve replacement in degenerative aortic stenosis. J Thorac Cardiovasc Surg. 2017 Jun 15.

28. Chaker Z, Badhwar V, Alqahtani F, Aljohani S, Zack CJ, Holmes DR, et al. Sex Differences in the Utilization and Outcomes of Surgical Aortic Valve Replacement for Severe Aortic Stenosis. J Am Heart Assoc. American Heart Association, Inc; 2017 Sep 21;6(9)

29. Leon MB, Smith CR, Mack MJ, Makkar RR, Svensson LG, Kodali SK, et al. Transcatheter or Surgical Aortic-Valve Replacement in

Intermediate-Risk Patients. N Engl J Med; 2016 Apr 28;374(17):1609–20.

30. Auensen A, Hussain AI, Bendz B, Aaberge L, Falk RS, Walle-Hansen MM, et al. Morbidity outcomes after surgical aortic valve replacement. Open Heart. Archives of Disease in childhood; 2017;4(1):e000588.

31. Smith CR, Leon MB, Mack MJ, Miller DC, Moses JW, Svensson LG, et al. Transcatheter versus surgical aortic-valve replacement in high-risk patients. N Engl J Med. ; 2011 Jun 9;364(23):2187–98.

32. Leon MB, Smith CR, Mack M, Miller DC, Moses JW, Svensson LG, et al. Transcatheter aortic-valve implantation for aortic stenosis in patients who cannot undergo surgery. N Engl J Med. ; 2010 Oct 21;363(17):1597–607.

33. Thourani VH, Kodali S, Makkar RR, Herrmann HC, Williams M, Babaliaros V, et al. Transcatheter aortic valve replacement versus surgical valve replacement in intermediate-risk patients: a propensity score analysis. Lancet. 2016 May 28;387(10034):2218–25.

34. Reardon MJ, Van Mieghem NM, Popma JJ, Kleiman NS, Søndergaard L, Mumtaz M, et al. Surgical or Transcatheter Aortic-Valve Replacement in Intermediate-Risk Patients. N Engl J Med; 2017 Apr 6;376(14):1321–31.

35. Ludman P. Transcatheter Aortic Valve Implantation: UK TAVI Audit 2016. BCIS TAVI Audit.

36. Mack MJ, Leon MB, Smith CR, Miller DC, Moses JW, Tuzcu EM, et al. 5-year outcomes of transcatheter aortic valve replacement or surgical aortic valve replacement for high surgical risk patients with aortic stenosis (PARTNER 1): a randomised controlled trial. Lancet. 2015 Jun 20;385(9986):2477–84.

37. Cannegieter SC, Rosendaal FR, Briët E. Thromboembolic and bleeding complications in patients with mechanical heart valve prostheses. Circulation. 1994 Feb;89(2):635–41.

38. Glaser N, Jackson V, Holzmann MJ, Franco-Cereceda A, Sartipy U. Prosthetic Valve Endocarditis After Surgical Aortic Valve Replacement. Circulation. American Heart Association, Inc; 2017 Jul 18;136(3):329–31.

39. Hammermeister K, Sethi GK, Henderson WG, Grover FL, Oprian C, Rahimtoola SH. Outcomes 15 years after valve replacement with a mechanical versus a bioprosthetic valve: final report of the Veterans Affairs randomized trial. JACC. 2000 Oct;36(4):1152–8.

40. Johnston DR, Soltesz EG, Vakil N, Rajeswaran J, Roselli EE, Sabik JF, et al. Long-term durability of bioprosthetic aortic valves: implications from 12,569 implants. Ann Thorac Surg. 2015 Apr;99(4):1239–47.

41. Pellikka PA, Sarano ME, Nishimura RA, Malouf JF, Bailey KR, Scott CG, et al. Outcome of 622 adults with asymptomatic, hemodynamically significant aortic stenosis during prolonged follow-up. Circulation; 2005 Jun 21;111(24):3290–5.

42. Kang D-H, Park S-J, Rim JH, Yun S-C, Kim D-H, Song J-M, et al. Early surgery versus conventional treatment in asymptomatic very severe aortic stenosis. Circulation; 2010 Apr 6;121(13):1502–9.

43. Taniguchi T, Morimoto T, Shiomi H, Ando K, Kanamori N, Murata K, et al. Initial Surgical Versus Conservative Strategies in Patients With Asymptomatic Severe Aortic Stenosis. Journal of the American College of Cardiology. 2015 Dec 29;66(25):2827–38.

44. Malaisrie SC, McDonald E, Kruse J, Li Z, McGee EC, Abicht TO, et al. Mortality while waiting for aortic valve replacement. Ann Thorac Surg. 2014 Nov;98(5):1564–70–discussion1570–1.

45. Flores-Marín A, Gómez-Doblas JJ, Caballero-Borrego J, Cabrera-Bueno F, Rodríguez-Bailón I, Melero JM, et al. Long-term predictors of mortality and functional recovery after aortic valve replacement for severe aortic stenosis with left ventricular dysfunction. Rev Esp Cardiol. 2010 Jan;63(1):36–45.

46. Dweck MR, Joshi S, Murigu T, Alpendurada F, Jabbour A, Melina G, et al. Midwall Fibrosis Is an Independent Predictor of Mortality in Patients With Aortic Stenosis. Journal of the American College of Cardiology. 2011 Sep;58(12):1271–9.

47. Monin J-L, Quéré J-P, Monchi M, Petit H, Baleynaud S, Chauvel C, et al. Low-gradient aortic stenosis: operative risk stratification and predictors for long-term outcome: a multicenter study using dobutamine stress hemodynamics. Circulation; 2003 Jul 22;108(3):319–24.

48. Chin CWL, Messika-Zeitoun D, Shah ASV, Lefevre G, Bailleul S, Yeung ENW, et al. A clinical risk score of myocardial fibrosis predicts adverse outcomes in aortic stenosis. European Heart Journal. 2016 Feb 21;37(8):713–23.

49. Barone-Rochette G, Piérard S, de Meester de Ravenstein C, Seldrum S, Melchior J, Maes F, et al. Prognostic significance of LGE by CMR in aortic stenosis patients undergoing valve replacement.

Journal of the American College of Cardiology. 2014 Jul 15;64(2):144–54.

50. Hachicha Z, Dumesnil JG, Pibarot P. Usefulness of the valvuloarterial impedance to predict adverse outcome in asymptomatic aortic stenosis. Journal of the American College of Cardiology. 2009 Sep 8;54(11):1003–11.

51. Cramariuc D, Cioffi G, Rieck AE, Devereux RB, Staal EM, Ray S, et al. Low-flow aortic stenosis in asymptomatic patients: valvular-arterial impedance and systolic function from the SEAS Substudy. JACC Cardiovasc Imaging. 2009 Apr;2(4):390–9.

52. Kusunose K, Goodman A, Parikh R, Barr T, Agarwal S, Popovic ZB, et al. Incremental prognostic value of left ventricular global longitudinal strain in patients with aortic stenosis and preserved ejection fraction. Circ Cardiovasc Imaging. 2014 Nov;7(6):938–45.

53. Lund O, Flø C, Jensen FT, Emmertsen K, Nielsen TT, Rasmussen BS, et al. Left ventricular systolic and diastolic function in aortic stenosis. Prognostic value after valve replacement and underlying mechanisms. European Heart Journal. 1997 Dec;18(12):1977–87.

54. Chin CWL, Shah ASV, McAllister DA, Joanna Cowell S, Alam S, Langrish JP, et al. High-sensitivity troponin I concentrations are a marker of an advanced hypertrophic response and adverse outcomes in patients with aortic stenosis. European Heart Journal. 2014 Sep 7;35(34):2312–21.

55. Treibel TA, López B, González A, Menacho K, Schofield RS, Ravassa S, et al. Reappraising myocardial fibrosis in severe aortic stenosis: an invasive and non-invasive study in 133 patients. European Heart Journal. 2017.

56. Shah ASV, Chin CWL, Vassiliou V, Cowell SJ, Doris M, Kwok TC, et al. Left ventricular hypertrophy with strain and aortic stenosis. Circulation; 2014 Oct 28;130(18):1607–16.

57. Dweck MR, Joshi S, Murigu T, Gulati A, Alpendurada F, Jabbour A, et al. Left ventricular remodeling and hypertrophy in patients with aortic stenosis: insights from cardiovascular magnetic resonance. Journal of Cardiovascular Magnetic Resonance; 2012 Jul 28;14(1):1–1.

58. Gunther S, Grossman W. Determinants of ventricular function in pressure-overload hypertrophy in man. Circulation. 1979 Apr;59(4):679–88.

59. Salcedo EE, Korzick DH, Currie PJ, Stewart WJ, Lever HM, Goormastic M. Determinants of left ventricular hypertrophy in patients with aortic stenosis. Cleve Clin J Med. 1989 Sep;56(6):590–6.

60. Cioffi G, Faggiano P, Vizzardi E, Tarantini L, Cramariuc D, Gerdts E, et al. Prognostic effect of inappropriately high left ventricular mass in asymptomatic severe aortic stenosis. Heart; 2011 Feb;97(4):301–7.

61. Gerdts E, Rossebø AB, Pedersen TR, Cioffi G, Lønnebakken MT, Cramariuc D, et al. Relation of Left Ventricular Mass to Prognosis in Initially Asymptomatic Mild to Moderate Aortic Valve Stenosis. Circ Cardiovasc Imaging. 2015 Nov;8(11).

62. Dobson LE, Musa TA, Fairbairn TA, Uddin A, Blackman DJ, Ripley DP, et al. CMR assessment of longitudinal left ventricular function following transcatheter aortic valve implantation (TAVI) for severe aortic stenosis. Journal of Cardiovascular Magnetic Resonance; 2015 Feb 3;17(1):P180.

63. Ibrahim E-SH. Myocardial tagging by cardiovascular magnetic resonance: evolution of techniques--pulse sequences, analysis algorithms, and applications. Journal of Cardiovascular Magnetic Resonance; 2011 Jul 28;13(1):36.

64. Yilmaz A, Kindermann I, Kindermann M, Mahfoud F, Ukena C, Athanasiadis A, et al. Comparative evaluation of left and right ventricular endomyocardial biopsy: differences in complication rate and diagnostic performance. Circulation.; 2010 Aug 31;122(9):900–9.

65. Debl K, Djavidani B, Buchner S, Lipke C, Nitz W, Feuerbach S, et al. Delayed hyperenhancement in magnetic resonance imaging of left ventricular hypertrophy caused by aortic stenosis and hypertrophic cardiomyopathy: visualisation of focal fibrosis. Heart; 2006 Oct;92(10):1447–51.

66. Rudolph A, Abdel-Aty H, Bohl S, Boyé P, Zagrosek A, Dietz R, et al. Noninvasive detection of fibrosis applying contrast-enhanced cardiac magnetic resonance in different forms of left ventricular hypertrophy relation to remodeling. Journal of the American College of Cardiology. 2009 Jan 20;53(3):284–91.

67. Mahmod M, Piechnik SK, Levelt E, Ferreira VM, Francis JM, Lewis A, et al. Adenosine stress native T1 mapping in severe aortic stenosis: evidence for a role of the intravascular compartment on myocardial T1 values. Journal of Cardiovascular Magnetic Resonance; 2014;16(1):92.

68. Weidemann F, Herrmann S, Störk S, Niemann M, Frantz S, Lange V, et al. Impact of myocardial fibrosis in patients with symptomatic severe aortic stenosis. Circulation; 2009 Aug 18;120(7):577–84.

69. Musa TA, Treibel TA, Vassiliou VS, Captur G, Singh A, Chin C, et al. Myocardial Scar and Mortality in Severe Aortic Stenosis: Data from the BSCMR Valve Consortium. Circulation. American Heart Association, Inc; 2018 Jul 12;

70. Messroghli DR, Radjenovic A, Kozerke S, Higgins DM, Sivananthan MU, Ridgway JP. Modified Look-Locker inversion recovery (MOLLI) for high-resolution T1 mapping of the heart. Magn Reson Med; 2004 Jul;52(1):141–6.

71. Piechnik SK, Ferreira VM, Dall'Armellina E, Cochlin LE, Greiser A, Neubauer S, et al. Shortened Modified Look-Locker Inversion recovery (ShMOLLI) for clinical myocardial T1-mapping at 1.5 and 3 T within a 9 heartbeat breathhold. Journal of Cardiovascular Magnetic Resonance. BioMed Central Ltd; 2010 Nov 19;12(1):69.

72. Chow K, Flewitt JA, Green JD, Pagano JJ, Friedrich MG, Thompson RB. Saturation recovery single-shot acquisition (SASHA) for myocardial T(1) mapping. Magn Reson Med. 2014 Jun;71(6):2082–95.

73. Singh A, Horsfield MA, Bekele S, Khan JN, Greiser A, McCann GP. Myocardial T1 and extracellular volume fraction measurement in asymptomatic patients with aortic stenosis: reproducibility and comparison with age-matched controls. European Heart Journal - Cardiovascular Imaging. Oxford University Press; 2015 Jul;16(7):763–70.

74. Eberli FR, Ritter M, Schwitter J, Bortone A, Schneider J, Hess OM, et al. Coronary reserve in patients with aortic valve disease before and after successful aortic valve replacement. European Heart Journal. 1991 Feb;12(2):127–38.

75. Rakusan K, Flanagan MF, Geva T, Southern J, Van Praagh R. Morphometry of human coronary capillaries during normal growth and the effect of age in left ventricular pressure-overload hypertrophy. Circulation. 1992 Jul;86(1):38–46.

76. Rajappan K, Rimoldi OE, Dutka DP, Ariff B, Pennell DJ, Sheridan DJ, et al. Mechanisms of coronary microcirculatory dysfunction in patients with aortic stenosis and angiographically normal coronary arteries. Circulation. 2002 Jan 29;105(4):470–6.

77. Galiuto L, Lotrionte M, Crea F, Anselmi A, Biondi-Zoccai GGL, De Giorgio F, et al. Impaired coronary and myocardial flow in severe

aortic stenosis is associated with increased apoptosis: a transthoracic Doppler and myocardial contrast echocardiography study. Heart; 2006 Feb;92(2):208–12.

78. Bull S, White SK, Piechnik SK, Flett AS, Ferreira VM, Loudon M, et al. Human non-contrast T1 values and correlation with histology in diffuse fibrosis. Heart; 2013 Jul;99(13):932–7.

79. Lee S-P, Lee W, Lee JM, Park E-A, Kim H-K, Kim Y-J, et al. Assessment of diffuse myocardial fibrosis by using MR imaging in asymptomatic patients with aortic stenosis. Radiology; 2015 Feb;274(2):359–69.

80. Kockova R, Kacer P, Pirk J, Maly J, Sukupova L, Sikula V, et al. Native T1 Relaxation Time and Extracellular Volume Fraction as Accurate Markers of Diffuse Myocardial Fibrosis in Heart Valve Disease - Comparison With Targeted Left Ventricular Myocardial Biopsy. Circ J. 2016 Apr 25;80(5):1202–9.

81. de Meester de Ravenstein C, Bouzin C, Lazam S, Boulif J, Amzulescu M, Melchior J, et al. Histological Validation of measurement of diffuse interstitial myocardial fibrosis by myocardial extravascular volume fraction from Modified Look-Locker imaging (MOLLI) T1 mapping at 3 T. Journal of Cardiovascular Magnetic Resonance. 2015;17(1):48.

82. Chin CWL, Semple S, Malley T, White AC, Mirsadraee S, Weale PJ, et al. Optimization and comparison of myocardial T1 techniques at 3T in patients with aortic stenosis. European Heart Journal - Cardiovascular Imaging. 2014 May;15(5):556–65.

83. Lee H, Park J-B, Yoon YE, Park E-A, Kim H-K, Lee W, et al. Noncontrast Myocardial T1 Mapping by Cardiac Magnetic Resonance Predicts Outcome in Patients With Aortic Stenosis. JACC Cardiovasc Imaging. 2017 Nov 10.

84. Fontana M, White SK, Banypersad SM. Comparison of T1 mapping techniques for ECV quantification. Histological validation and reproducibility of ShMOLLI versus multibreath-hold T1 quantification J Cardiovasc Magn 2012.

85. Flett AS, Hayward MP, Ashworth MT, Hansen MS, Taylor AM, Elliott PM, et al. Equilibrium contrast cardiovascular magnetic resonance for the measurement of diffuse myocardial fibrosis: preliminary validation in humans. Circulation. Lippincott Williams & Wilkins; 2010 Jul 13;122(2):138–44.

86. White SK, Sado DM, Fontana M, Banypersad SM, Maestrini V, Flett AS, et al. T1 mapping for myocardial extracellular volume

measurement by CMR: bolus only versus primed infusion technique. JACC Cardiovasc Imaging. 2013 Sep;6(9):955–62.

87. Flett AS, Sado DM, Quarta G, Mirabel M, Pellerin D, Herrey AS, et al. Diffuse myocardial fibrosis in severe aortic stenosis: an equilibrium contrast cardiovascular magnetic resonance study. European Heart Journal - Cardiovascular Imaging. The Oxford University Press; 2012 May 25;13(10):jes102–826.

88. Sado DM, Flett AS, Banypersad SM, White SK, Maestrini V, Quarta G, et al. Cardiovascular magnetic resonance measurement of myocardial extracellular volume in health and disease. Heart. BMJ Publishing Group Ltd and British Cardiovascular Society; 2012 Oct;98(19):1436–41.

89. Schelbert EB, Piehler KM, Zareba KM, Moon JC, Ugander M, Messroghli DR, et al. Myocardial Fibrosis Quantified by Extracellular Volume Is Associated With Subsequent Hospitalization for Heart Failure, Death, or Both Across the Spectrum of Ejection Fraction and Heart Failure Stage. J Am Heart Assoc. 2015 Dec 18;4(12).

90. Tawakol A, Migrino RQ, Bashian GG, Bedri S, Vermylen D, Cury RC, et al. In vivo 18F-fluorodeoxyglucose positron emission tomography imaging provides a noninvasive measure of carotid plaque inflammation in patients. Journal of the American College of Cardiology. 2006 Nov 7;48(9):1818–24.

91. Dweck MR, Jones C, Joshi NV, Fletcher AM, Richardson H, White A, et al. Assessment of valvular calcification and inflammation by positron emission tomography in patients with aortic stenosis. Circulation. Lippincott Williams & Wilkins; 2012 Jan 3;125(1):76–86.

92. Irkle A, Vesey AT, Lewis DY, Skepper JN, Bird JLE, Dweck MR, et al. Identifying active vascular microcalcification by (18)F-sodium fluoride positron emission tomography. Nat Commun. Nature Publishing Group; 2015;6:7495.

93. Jenkins WSA, Vesey AT, Shah ASV, Pawade TA, Chin CWL, White AC, et al. Valvular (18)F-Fluoride and (18)F-Fluorodeoxyglucose Uptake Predict Disease Progression and Clinical Outcome in Patients With Aortic Stenosis. Journal of the American College of Cardiology. 2015 Sep 8;66(10):1200–1.

94. Dweck MR, Khaw HJ, Sng GKZ, Luo ELC, Baird A, Williams MC, et al. Aortic stenosis, atherosclerosis, and skeletal bone: is there a common link with calcification and inflammation? European Heart Journal. The Oxford University Press; 2013 Jun;34(21):1567–74.

95. Nensa F, Bamberg F, Rischpler C, Menezes L, Poeppel TD, la Fougère C, et al. Hybrid cardiac imaging using PET/MRI: a joint position statement by the European Society of Cardiovascular Radiology (ESCR) and the European Association of Nuclear Medicine (EANM). Eur Radiol. Springer Berlin Heidelberg; 2018 May 2;55:2614–6.

96. Carney JPJ, Townsend DW, Rappoport V, Bendriem B. Method for transforming CT images for attenuation correction in PET/CT imaging. Med Phys. Wiley-Blackwell; 2006 Apr;33(4):976–83.

97. Paulus DH, Quick HH, Geppert C, Fenchel M, Zhan Y, Hermosillo G, et al. Whole-Body PET/MR Imaging: Quantitative Evaluation of a Novel Model-Based MR Attenuation Correction Method Including Bone. J Nucl Med. Society of Nuclear Medicine; 2015 Jul;56(7):1061–6.

98. Robson PM, Dweck MR, Trivieri MG, Abgral R, Karakatsanis NA, Contreras J, et al. Coronary Artery PET/MR Imaging: Feasibility, Limitations, and Solutions. JACC Cardiovasc Imaging. 2017 Jan 13.

99. Dungu JN, Anderson LJ, Whelan CJ, Hawkins PN. Cardiac transthyretin amyloidosis. Heart. BMJ Publishing Group Ltd and British Cardiovascular Society; 2012 Nov;98(21):1546–54.

100. Tanskanen M, Peuralinna T, Polvikoski T, Notkola I-L, Sulkava R, Hardy J, et al. Senile systemic amyloidosis affects 25% of the very aged and associates with genetic variation in alpha2-macroglobulin and tau: a population-based autopsy study. Ann Med. 2008;40(3):232–9.

101. Maurer MS, Schwartz JH, Gundapaneni B, Elliott PM, Merlini G, Waddington-Cruz M, et al. Tafamidis Treatment for Patients with Transthyretin Amyloid Cardiomyopathy. N Engl J Med. Massachusetts Medical Society; 2018 Sep 13;379(11):1007–16.

102. Dahm CN, Cornell RF, Lenihan DJ. Advances in Treatment of Cardiac Amyloid. Curr Treat Options Cardio Med. Springer US; 2018 Apr 7;20(5):37.

103. Falk RH, Plehn JF, Deering T, Schick EC, Boinay P, Rubinow A, et al. Sensitivity and specificity of the echocardiographic features of cardiac amyloidosis. Am J Cardiol. 1987 Feb 15;59(5):418–22.

104. Treibel TA, Fontana M, Gilbertson JA, Castelletti S, White SK, Scully PR, et al. Occult Transthyretin Cardiac Amyloid in Severe Calcific Aortic Stenosis: Prevalence and Prognosis in Patients Undergoing Surgical Aortic Valve Replacement. Circ Cardiovasc Imaging. American Heart Association, Inc; 2016 Aug;9(8):e005066.

105. Sun JP, Stewart WJ, Yang XS, Donnell RO, Leon AR, Felner JM, et al. Differentiation of hypertrophic cardiomyopathy and cardiac amyloidosis from other causes of ventricular wall thickening by two-dimensional strain imaging echocardiography. Am J Cardiol. 2009 Feb 1;103(3):411–5.

106. Fontana M, Pica S, Reant P, Abdel-Gadir A, Treibel TA, Banypersad SM, et al. Prognostic Value of Late Gadolinium Enhancement Cardiovascular Magnetic Resonance in Cardiac Amyloidosis. Circulation. American Heart Association, Inc; 2015 Oct 20;132(16):1570–9.

107. Martinez-Naharro A, Kotecha T, Norrington K, Boldrini M, Rezk T, Quarta C, et al. Native T1 and Extracellular Volume in Transthyretin Amyloidosis. JACC Cardiovasc Imaging. 2018 Mar 12.

108. Gillmore JD, Maurer MS, Falk RH, Merlini G, Damy T, Dispenzieri A, et al. Nonbiopsy Diagnosis of Cardiac Transthyretin Amyloidosis. Circulation. American Heart Association, Inc; 2016 Jun 14;133(24):2404–12.

109. Hutt DF, Fontana M, Burniston M, Quigley A-M, Petrie A, Ross JC, et al. Prognostic utility of the Perugini grading of 99mTc-DPD scintigraphy in transthyretin (ATTR) amyloidosis and its relationship with skeletal muscle and soft tissue amyloid. European Heart Journal - Cardiovascular Imaging. 2017 Dec 1;18(12):1344–50.

110. Rapezzi C, Quarta CC, Guidalotti PL, Pettinato C, Fanti S, Leone O, et al. Role of (99m)Tc-DPD scintigraphy in diagnosis and prognosis of hereditary transthyretin-related cardiac amyloidosis. JACC Cardiovasc Imaging. 2011 Jun;4(6):659–70.

111. Castaño A, Narotsky DL, Hamid N, Khalique OK, Morgenstern R, DeLuca A, et al. Unveiling transthyretin cardiac amyloidosis and its predictors among elderly patients with severe aortic stenosis undergoing transcatheter aortic valve replacement. European Heart Journal. 2017 Oct 7;38(38):2879–87.

112. Trivieri MG, Dweck MR, Abgral R, Robson PM, Karakatsanis NA, Lala A, et al. (18)F-Sodium Fluoride PET/MR for the Assessment of Cardiac Amyloidosis. Journal of the American College of Cardiology. 2016 Dec 20;68(24):2712–4.

113. Baumgartner H, Hung J, Bermejo J, Chambers JB, Evangelista A, Griffin BP, et al. Echocardiographic assessment of valve stenosis: EAE/ASE recommendations for clinical practice. Vol. 22, Journal of the American Society of Echocardiography : official publication of the American Society of Echocardiography. 2009. pp. 1–23–quiz101–2.

114. Nagueh SF, Appleton CP, Gillebert TC, Marino PN, Oh JK, Smiseth OA, et al. Recommendations for the evaluation of left ventricular diastolic function by echocardiography. Eur J Echocardiogr. The Oxford University Press; 2009 Mar;10(2):165–93.

115. Smith LA, Cowell SJ, White AC, Boon NA, Newby DE, Northridge DB. Contrast agent increases Doppler velocities and improves reproducibility of aortic valve area measurements in patients with aortic stenosis. J Am Soc Echocardiogr. 2004 Mar;17(3):247–52.

116. Messroghli DR, Greiser A, Fröhlich M, Fr o hlich M, Dietz R, Schulz-Menger J. Optimization and validation of a fully-integrated pulse sequence for modified look-locker inversion-recovery (MOLLI) T1 mapping of the heart. J Magn Reson Imaging [Internet]. 2007;26(4):1081–6.

117. Xue H, Shah S, Greiser A, Guetter C, Littmann A, Jolly M-P, et al. Motion correction for myocardial T1 mapping using image registration with synthetic image estimation. Magn Reson Med. Wiley Subscription Services, Inc., A Wiley Company; 2012 Jun;67(6):1644–55.

118. Kellman P, Hansen MS. T1-mapping in the heart: accuracy and precision. Journal of Cardiovascular Magnetic Resonance. 2014;16(1):2.

119. Bottini PB, Carr AA, Prisant LM, Flickinger FW, Allison JD, Gottdiener JS. Magnetic resonance imaging compared to echocardiography to assess left ventricular mass in the hypertensive patient. Am J Hypertens. 1995 Mar;8(3):221–8.

120. Mooij CF, de Wit CJ, Graham DA, Powell AJ, Geva T. Reproducibility of MRI measurements of right ventricular size and function in patients with normal and dilated ventricles. J Magn Reson Imaging. Wiley-Blackwell; 2008 Jul;28(1):67–73.

121. Shukla AK, Kumar U. Positron emission tomography: An overview. J Med Phys. 2006 Jan;31(1):13–21.

122. Moses WW. Fundamental Limits of Spatial Resolution in PET. Nucl Instrum Methods Phys Res A. 2011 Aug 21;648 Supplement 1:S236–40.

123. Kwee TC, Torigian DA, Alavi A. Overview of positron emission tomography, hybrid positron emission tomography instrumentation, and positron emission tomography quantification. Journal of Thoracic Imaging. 2013 Jan;28(1):4–10.

124. Martinez-Möller A, Souvatzoglou M, Delso G, Bundschuh RA, Chefd'hotel C, Ziegler SI, et al. Tissue classification as a potential approach for attenuation correction in whole-body PET/MRI: evaluation with PET/CT data. J Nucl Med. Society of Nuclear Medicine; 2009 Apr;50(4):520–6.

125. Munoz C, Neji R, Cruz G, Mallia A, Jeljeli S, Reader AJ, et al. Motion-corrected simultaneous cardiac positron emission tomography and coronary MR angiography with high acquisition efficiency. Magn Reson Med. Wiley-Blackwell; 2018 Jan;79(1):339–50.

126. Delso G, Fürst S, Jakoby B, Ladebeck R, Ganter C, Nekolla SG, et al. Performance measurements of the Siemens mMR integrated whole-body PET/MR scanner. J Nucl Med. Society of Nuclear Medicine; 2011 Dec;52(12):1914–22.

127. Romhilt DW, Estes EH. A point-score system for the ECG diagnosis of left ventricular hypertrophy. Am Heart J. 1968 Jun;75(6):752–8.

128. Schulz-Menger J, Bluemke DA, Bremerich J, Flamm SD, Fogel MA, Friedrich MG, et al. Standardized image interpretation and post processing in cardiovascular magnetic resonance: Society for Cardiovascular Magnetic Resonance (SCMR) board of trustees task force on standardized post processing. Vol. 15, Journal of Cardiovascular Magnetic Resonance. BioMed Central; 2013. p. 35.

129. Kawel-Boehm N, Maceira A, Valsangiacomo-Buechel ER, Vogel-Claussen J, Turkbey EB, Williams R, et al. Normal values for cardiovascular magnetic resonance in adults and children. Journal of Cardiovascular Magnetic Resonance. 3rd ed. BioMed Central; 2015;17(1):29.

130. Mikami Y, Kolman L, Joncas SX, Stirrat J, Scholl D, Rajchl M, et al. Accuracy and reproducibility of semi-automated late gadolinium enhancement quantification techniques in patients with hypertrophic cardiomyopathy. Journal of Cardiovascular Magnetic Resonance. BioMed Central; 2014 Oct 7;16(1):85.

131. Hundley WG, Bluemke D, Bogaert JG, Friedrich MG, Higgins CB, Lawson MA, et al. Society for Cardiovascular Magnetic Resonance guidelines for reporting cardiovascular magnetic resonance examinations. Vol. 11, Journal of Cardiovascular Magnetic Resonance. BioMed Central; 2009. p. 5.

132. Moon JC, Messroghli DR, Kellman P, Piechnik SK, Robson MD, Ugander M, et al. Myocardial T1 mapping and extracellular volume quantification: a Society for Cardiovascular Magnetic Resonance (SCMR) and CMR Working Group of the European Society of

Cardiology consensus statement. Journal of Cardiovascular Magnetic Resonance. BioMed Central Ltd; 2013;15(1):92.

133. Doltra A, Messroghli D, Stawowy P, Hassel J-H, Gebker R, Leppänen O, et al. Potential reduction of interstitial myocardial fibrosis with renal denervation. J Am Heart Assoc. Lippincott Williams & Wilkins; 2014 Dec;3(6):e001353–3.

134. Pawade TA, Cartlidge TRG, Jenkins WSA, Adamson PD, Robson P, Lucatelli C, et al. Optimization and Reproducibility of Aortic Valve 18F-Fluoride Positron Emission Tomography in Patients With Aortic Stenosis. Circ Cardiovasc Imaging. American Heart Association, Inc; 2016 Oct;9(10):e005131.

135. Nkomo VT, Gardin JM, Skelton TN, Gottdiener JS, Scott CG, Enriquez-Sarano M. Burden of valvular heart diseases: a population-based study. The Lancet. 2006 Sep;368(9540):1005–11.

136. Chin CWL, Pawade TA, Newby DE, Dweck MR. Risk Stratification in Patients With Aortic Stenosis Using Novel Imaging Approaches. Circ Cardiovasc Imaging. Lippincott Williams & Wilkins; 2015 Aug;8(8):e003421.

137. Krayenbeuhl HP, Hess OM, Monrad ES, Schneider J, Mall G, Turina M. Left-Ventricular Myocardial Structure in Aortic-Valve Disease Before, Intermediate, and Late After Aortic-Valve Replacement. Circulation. 1989 Apr;79(4):744–55.

138. Maceira A, Prasad S, Khan M, Pennell D. Normalized Left Ventricular Systolic and Diastolic Function by Steady State Free Precession Cardiovascular Magnetic Resonance. Journal of Cardiovascular Magnetic Resonance [Internet]. 2006 Jul 1;8(3):417–26.

139. Liu A, Wijesurendra RS, Francis JM, Robson MD, Neubauer S, Piechnik SK, et al. Adenosine Stress and Rest T1 Mapping Can Differentiate Between Ischemic, Infarcted, Remote, and Normal Myocardium Without the Need for Gadolinium Contrast Agents. JACC Cardiovasc Imaging. 2016 Jan;9(1):27–36.

140. Everett RJ, Stirrat CG, Semple SIR, Newby DE, Dweck MR, Mirsadraee S. Assessment of myocardial fibrosis with T1 mapping MRI. Clin Radiol. 2016 Mar 19;71(8):768–78.

141. Vassiliou VS, Perperoglou A, Raphael CE, Joshi S, Malley T, Everett R, et al. Midwall Fibrosis and 5-Year Outcome in Moderate and Severe Aortic Stenosis. Journal of the American College of Cardiology. 2017 Apr 4;69(13):1755–6.

142. Capoulade R, Mahmut A, Tastet L, Arsenault M, Bédard E, Dumesnil JG, et al. Impact of plasma Lp-PLA2 activity on the progression of aortic stenosis: the PROGRESSA study. JACC Cardiovasc Imaging. 2015 Jan;8(1):26–33.

143. Lee JJ, Liu S, Nacif MS, Ugander M, Han J, Kawel N, et al. Myocardial T1 and extracellular volume fraction mapping at 3 tesla. Journal of Cardiovascular Magnetic Resonance. BioMed Central; 2011 Nov 28;13(1):75.

144. Treibel TA, Kozor R, Schofield R, Benedetti G, Fontana M, Bhuva AN, et al. Reverse Myocardial Remodeling Following Valve Replacement in Patients With Aortic Stenosis. Journal of the American College of Cardiology. 2018 Feb 27;71(8):860–71.

145. Quarto C, Dweck MR, Murigu T, Joshi S, Melina G, Angeloni E, et al. Late gadolinium enhancement as a potential marker of increased perioperative risk in aortic valve replacement. Interactive CardioVascular and Thoracic Surgery [Internet]. 2012 Jul;15(1):45–50.

146. Everett RJ, Tastet L, Clavel M-A, Chin CWL, Capoulade R, Vassiliou VS, et al. Progression of Hypertrophy and Myocardial Fibrosis in Aortic Stenosis: A Multicenter Cardiac Magnetic Resonance Study. Circ Cardiovasc Imaging. American Heart Association, Inc; 2018 Jun;11(6):e007451.

147. Miller CA, Naish JH, Bishop P, Coutts G, Clark D, Zhao S, et al. Comprehensive validation of cardiovascular magnetic resonance techniques for the assessment of myocardial extracellular volume. Circ Cardiovasc Imaging. Lippincott Williams & Wilkins; 2013 May 1;6(3):373–83.

148. Nishimura RA, Otto CM, Bonow RO, Carabello BA, Erwin JP, Guyton RA, et al. 2014 AHA/ACC Guideline for the Management of Patients With Valvular Heart Disease: executive summary: a report of the American College of Cardiology/American Heart Association Task Force on Practice Guidelines. Lippincott Williams & Wilkins; 2014. pp. 2440–92.

149. Baumgartner H, Hung J, Bermejo J, Chambers JB, Edvardsen T, Goldstein S, et al. Recommendations on the Echocardiographic Assessment of Aortic Valve Stenosis: A Focused Update from the European Association of Cardiovascular Imaging and the American Society of Echocardiography. J Am Soc Echocardiogr. 2017 Apr;30(4):372–92.

150. Rogers T, Dabir D, Mahmoud I, Voigt T, Schaeffter T, Nagel E, et al. Standardization of T1 measurements with MOLLI in differentiation

between health and disease--the ConSept study. Journal of Cardiovascular Magnetic Resonance. BioMed Central; 2013 Sep 11;15(1):78.

151. Kawel N, Nacif M, Zavodni A, Jones J, Liu S, Sibley CT, et al. T1 mapping of the myocardium: intra-individual assessment of the effect of field strength, cardiac cycle and variation by myocardial region. Journal of Cardiovascular Magnetic Resonance. BioMed Central; 2012 May 1;14(1):27.

152. Dabir D, Child N, Kalra A, Rogers T, Gebker R, Jabbour A, et al. Reference values for healthy human myocardium using a T1 mapping methodology: results from the International T1 Multicenter cardiovascular magnetic resonance study. Journal of Cardiovascular Magnetic Resonance. BioMed Central Ltd; 2014;16(1):69.

153. Captur G, Gatehouse P, Keenan KE, Heslinga FG, Bruehl R, Prothmann M, et al. A medical device-grade T1 and ECV phantom for global T1 mapping quality assurance-the T1 Mapping and ECV Standardization in cardiovascular magnetic resonance (T1MES) program. Journal of Cardiovascular Magnetic Resonance. BioMed Central; 2016 Sep 22;18(1):58.

154. Rosmini S, Bulluck H, Captur G, Treibel TA, Abdel-Gadir A, Bhuva AN, et al. Myocardial native T1 and extracellular volume with healthy ageing and gender. European Heart Journal - Cardiovascular Imaging. Oxford University Press; 2018 Jun 1;19(6):615–21.

155. Myerson SG. Heart valve disease: investigation by cardiovascular magnetic resonance. Journal of Cardiovascular Magnetic Resonance. BioMed Central Ltd; 2012;14(1):7.

156. Doris MK, Rubeaux M, Pawade T, Otaki Y, Xie Y, Li D, et al. Motion-corrected imaging of the aortic valve with (18)F-NaF PET/CT and PET/MR: a feasibility study. J Nucl Med. 2017 May 25;58(11):jnumed.117.194597–1814.

157. Munoz C, Kunze KP, Neji R, Vitadello T, Rischpler C, Botnar RM, et al. Motion-corrected whole-heart PET-MR for the simultaneous visualisation of coronary artery integrity and myocardial viability: an initial clinical validation. Eur J Nucl Med Mol Imaging. Springer Berlin Heidelberg; 2018 May 12;54:402–12.

158. Chin CWL, Khaw HJ, Luo E, Tan S, White AC, Newby DE, et al. Echocardiography underestimates stroke volume and aortic valve area: implications for patients with small-area low-gradient aortic stenosis. Can J Cardiol. 2014 Sep;30(9):1064–72.

159. Galat A, Guellich A, Bodez D, Slama M, Dijos M, Zeitoun DM, et al. Aortic stenosis and transthyretin cardiac amyloidosis: the chicken or the egg? European Heart Journal. The Oxford University Press; 2016 Dec 14;37(47):3525–31.

160. Cruz G, Atkinson D, Henningsson M, Botnar RM, Prieto C. Highly efficient nonrigid motion-corrected 3D whole-heart coronary vessel wall imaging. Magn Reson Med. Wiley-Blackwell; 2017 May;77(5):1894–908.

161. Myerson SG, Bellenger NG, Pennell DJ. Assessment of left ventricular mass by cardiovascular magnetic resonance. Hypertension. 2002 Mar 1;39(3):750–5.

Appendix

Contents

Supplemental Methods

Chapter 4: Progression of Hypertrophy and Myocardial Fibrosis in Aortic Stenosis: A Multicentre Cardiac Magnetic Resonance Study

Echocardiography

A comprehensive transthoracic echocardiographic assessment was performed in all patients (Edinburgh: iE33, Philips Medical Systems, The Netherlands. Quebec: iE33 or EPIQ, Philips Healthcare, Ontario, Canada) by dedicated research ultrasonographers. Careful attention was given in the assessment of aortic stenosis severity. The left ventricular (LV) outflow tract diameter was measured in the parasternal long-axis view, at the insertion of the aortic cusps from the inner edge of the septal endocardium to the inner edge of the anterior mitral leaflet in mid-systole. Left ventricular outflow tract velocity-time integral was measured in the apical 5-chamber view using pulsed-wave Doppler just proximal to the aortic valve, with care taken to obtain a laminar spectral tracing. The peak aortic jet velocity and mean transvalvular gradient were derived from the aortic valve velocity-time integral, using continuous-wave Doppler. The highest aortic jet velocity and mean transvalvular gradient were determined in multiple acoustic windows using both standard S51 and D2cwc probes (Philips Medical Systems, Best, the Netherlands). The mean of 3 readings (5 if the patient had atrial fibrillation) was recorded. Aortic valve area was calculated using the continuity equation. The severity of aortic stenosis was assessed and classified according to the European Association of Echocardiography/American Society of Echocardiography guidelines.[1]

Trans-mitral early (E) and late diastolic velocities, as well as, deceleration time of early filling velocity were measured at the tips of the mitral valve leaflets using pulsed-wave Doppler. The mean early diastolic velocities of the medial and lateral mitral annulus (e') were measured using pulsed-wave tissue Doppler imaging. Diastolic function was assessed as recommended in recent guidelines.[2]

Magnetic resonance imaging

Magnetic resonance imaging was performed using both 1.5 and 3T scanners (Edinburgh: MAGNETOM Verio, Siemens AG, Erlangen, Germany; Quebec: ACHIEVA and INGENIA, Philips Healthcare, Best, the Netherlands or, Erlangen, Germany). Repeat imaging was performed using the same standardized protocols at each site. Short-axis cine images extending from the mitral valve to the left ventricular apex were obtained using a balanced steady-state free precession sequence (Edinburgh: 8-mm parallel slices with 2-mm spacing; temporal resolution ≤45ms. Quebec: 8 mm parallel slices with no gap). Typical parameters at 1.5T were FOV 380 mm, TR/TE 3.2/1.6 ms, flip angle 60º and NEX of 1, in-plane spatial resolution of 1.6 x 2 mm. Equivalent acquisition parameters at 3T were FOV 380 mm, TR/TE 2.8/1.3 ms, flip angle 45º, and NEX of 1, in-plane spatial resolution of 1.7 mm x 2 mm, 7-mm slice thickness, 0-mm gap.

Focal replacement and diffuse interstitial myocardial fibrosis was assessed in all patients using late gadolinium enhancement (LGE) and myocardial T1 mapping, respectively. Late gadolinium enhancement was performed 15 min following gadobutrol (Gadovist, Bayer Pharma AG, Germany, 0.1 mmol/kg [Edinburgh], 0.2 mmol/kg [Quebec]) using an inversion-recovery fast gradient-echo sequence

performed in two phase-encoding directions to differentiate true late enhancement from artefact. The LGE imaging parameters at 1.5T were FOV 350 mm, TR/TE 4.5/1.3 ms, flip angle 15 º, 8-mm slice thickness, in-plane resolution of 1.9 mm x 3.1 mm with an inversion time of 200 to 300 ms adjusted to null normal myocardium following gadolinium contrast administration. Equivalent acquisition parameters at 3T were FOV 350 mm, TR/TE 6.1/3 ms, flip angle 25 º, 8 mm slice thickness, in-plane resolution of 1.6 mm x 2 mm. The inversion time was optimized to achieve satisfactory nulling of the myocardium.

Diffuse myocardial fibrosis was assessed using Modified Look-Locker Inversion-recovery with built-in motion correction. A heart beat acquisition scheme of 3(3)-3(3)-5 was used in Edinburgh (flip angle 35°; minimum TI 100 ms; TI increment of 80 ms; time delay of 150 ms)[3,4,5] whilst an acquisition scheme of 5(3)-3 was used in Quebec (with a post-contrast acquisition scheme of 4(1)3(1)2 used in patients scanned at 3T).[6] A gradient echo field map and associated shim were performed to minimize off-frequency artefact.

Image analysis

Ventricular volumes, mass and function were quantified using dedicated software (CVI42 (Circle Cardiovascular Imaging Inc., Calgary, Canada) by a single reporter (RJE) blinded to the scan time-point. Basal ventricular slices were included if >50% of the LV blood pool was surrounded by myocardium. Papillary muscles and minor trabeculations were included in the left ventricular mass measurements and excluded from the intracavity volume measurements as per Society for Cardiovascular Magnetic Resonance guidelines.[7]

The left ventricular wall thickness was measured in each of the 16 myocardial segments (excluding the LV apex) and the maximum value recorded. Left ventricular longitudinal function was determined by measuring the difference in the distance between the mitral valve plane and the epicardial left ventricular apex in end-systole and end-diastole. The final value was calculated as the mean value of the recorded measurements in both 4-chamber and 2-chamber views. Left atrial volume was calculated using the bi-plane area-length method by tracing the endocardial LA contour in end-ventricular systole in both 2 and 4 chamber long-axis views.

The presence of mid-wall myocardial fibrosis was determined qualitatively by two independent and experienced operators (MRD and RJE). The distribution of mid-wall fibrosis was described according to the standard 17-segment model recommended by the American College of Cardiology/American Heart Association.[8] LGE was quantified in a semi-automated manner using a signal intensity threshold of >3 standard deviations above the mean value in a region of normal myocardium.[9] Areas of inversion artefact, infarct pattern LGE or signal contamination by epicardial fat or blood pool were manually excluded. Sub-endocardial LGE was also identified and quantified using the same analysis technique.

T1 mapping analysis was performed using CVI42 (Circle Cardiovascular Imaging Inc., Calgary, Canada). Endocardial and epicardial contours were manually contoured on the native motion-corrected myocardial T1 maps with manual offsetting of the contours to avoid partial volume effects. The right ventricular insertion points were identified leading to automatic segmentation of the basal and mid-ventricular slices. No analysis was performed on the apical myocardial segments as these are most susceptible to partial volume effects. These contours were subsequently copied onto

corresponding 20-minute post-contrast maps with minor adjustments made to avoid partial volume effects and artefact. Segments demonstrating mid-wall late enhancement were included in the overall T1 analysis whereas those containing infarct pattern LGE were excluded as per recent post-processing guidelines.[10] The extracellular volume fraction (ECV%) was calculated according to: ECV% = partition coefficient x [1-haematocrit], where partition coefficient = [$\Delta R1_{myocardium}/\Delta R1_{blood\text{-}pool}$] and $\Delta R1$ = (1/post-contrast T1-1/pre-contrast T1). This was calculated based on the average of the values obtained from the basal and mid ventricular segments. Hematocrit was sampled at the time of cardiovascular magnetic resonance imaging. The indexed extracellular volume (iECV) in each patient was derived using the following: ECV% x left ventricular end-diastolic myocardial volume indexed to body surface area (using the Dubois formula), where left ventricular myocardial volume = left ventricular mass /1.05 g/mL.[11,12]

References

1. Baumgartner H, Hung J, Bermejo J, Chambers JB, Edvardsen T, Goldstein S, Lancellotti P, LeFevre M, Miller F, Otto CM. Recommendations on the Echocardiographic Assessment of Aortic Valve Stenosis: A Focused Update from the European Association of Cardiovascular Imaging and the American Society of Echocardiography. *J Am Soc Echocardiogr*. 2017;30:372–392.

2. Nagueh SF, Smiseth OA, Appleton CP, Byrd BF, Dokainish H, Edvardsen T, Flachskampf FA, Gillebert TC, Klein AL, Lancellotti P, Marino P, Oh JK, Alexandru Popescu B, Waggoner AD, Houston, Texas; Oslo, Norway; Phoenix, Arizona; Nashville, Tennessee; Hamilton, Ontario, Canada; Uppsala, Sweden; Ghent and Liège, Belgium; Cleveland, Ohio; Novara, Italy; Rochester, Minnesota; Bucharest, Romania; and St. Louis, Missouri. Recommendations for the Evaluation of Left Ventricular Diastolic Function by Echocardiography: An Update from the American Society of Echocardiography and the European Association of Cardiovascular Imaging. *Eur Heart J - Cardiovasc Imaging*. 2016;17:1321–1360.

3. Messroghli DR, Radjenovic A, Kozerke S, Higgins DM, Sivananthan MU, Ridgway JP. Modified Look-Locker inversion recovery (MOLLI) for high-resolution T1 mapping of the heart. *Magn Reson Med*. 2004;52:141–146.

4. Messroghli DR, Greiser A, Fröhlich M, Fr o hlich M, Dietz R, Schulz-Menger J. Optimization and validation of a fully-integrated pulse sequence for modified look-locker inversion-recovery (MOLLI) T1 mapping of the heart. *J Magn Reson Imaging*. 2007;26:1081–1086.

5. Xue H, Shah S, Greiser A, Guetter C, Littmann A, Jolly M-P, Arai AE, Zuehlsdorff S, Guehring J, Kellman P. Motion correction for myocardial T1 mapping using image registration with synthetic image estimation. *Magn Reson Med*. 2012;67:1644–1655.

6. Kellman P, Hansen MS. T1-mapping in the heart: accuracy and precision. *J Cardiovasc Magn Reson* 2014;16:2.

7. Schulz-Menger J, Bluemke DA, Bremerich J, Flamm SD, Fogel MA, Friedrich MG, Kim RJ, Knobelsdorff-Brenkenhoff von F, Kramer CM, Pennell DJ, Plein S, Nagel E. Standardized image interpretation and post processing in cardiovascular magnetic resonance: Society for Cardiovascular Magnetic Resonance (SCMR) board of trustees task force on standardized post processing. *J Cardiovasc Magn Reson*. 2013;15:35.

8. Cerqueira MD, Cerqueira M. Standardized Myocardial Segmentation and Nomenclature for Tomographic Imaging of the Heart: A Statement for Healthcare Professionals From the Cardiac Imaging Committee of the Council on Clinical Cardiology of the American Heart Association. *Circulation*. 2002;105:539–542.

9. Mikami Y, Kolman L, Joncas SX, Stirrat J, Scholl D, Rajchl M, Lydell CP, Weeks SG, Howarth AG, White JA. Accuracy and reproducibility of semi-automated late gadolinium enhancement quantification techniques in patients

with hypertrophic cardiomyopathy. *J Cardiovasc Magn Reson*. 2014;16:85.

10. Messroghli DR, Moon JC, Ferreira VM, Grosse-Wortmann L, He T, Kellman P, Mascherbauer J, Nezafat R, Salerno M, Schelbert EB, Taylor AJ, Thompson R, Ugander M, van Heeswijk RB, Friedrich MG. Clinical recommendations for cardiovascular magnetic resonance mapping of T1, T2, T2* and extracellular volume: A consensus statement by the Society for Cardiovascular Magnetic Resonance (SCMR) endorsed by the European Association for Cardiovascular Imaging (EACVI). *J Cardiovasc Magn Reson*. 2017;19:75.

11. Flett AS, Sado DM, Quarta G, Mirabel M, Pellerin D, Herrey AS, Hausenloy DJ, Ariti C, Yap J, Kolvekar S, Taylor AM, Moon JC. Diffuse myocardial fibrosis in severe aortic stenosis: an equilibrium contrast cardiovascular magnetic resonance study. *Eur Heart J - Cardiovasc Imaging*. 2012;13:jes102–826.

12. Doltra A, Messroghli D, Stawowy P, Hassel J-H, Gebker R, Leppänen O, Gräfe M, Schneeweis C, Schnackenburg B, Fleck E, Kelle S. Potential reduction of interstitial myocardial fibrosis with renal denervation. *J Am Heart Assoc*. 2014;3:e001353–e001353.

ECV400: Image analysis protocol

(adapted from BSCMR valve consortium guidance for AS700 study, Musa, Treibel et al, Circulation 2018)

1. **Left and right ventricular volume and mass quantification**
    a. **The left ventricle**
    b. **The right ventricle**
2. **Left atrial volume**
3. **Late gadolinium enhancement**
4. **T1 mapping**

1. Left and right ventricular volume and mass quantification

(adapted from Schulz-Menger et al. Journal of Cardiovascular Magnetic Resonance 2013, 15:35)

- For each study, LV and RV volumes and LV mass are to be contoured by the same one individual using the dedicated LV short axis cine stack.
- If no intra- or extracardiac shunts are present, the RV and LV stroke volumes should be nearly equal (small differences are seen as a result of bronchial artery supply). Since the LV stroke volume is more reliably determined than the RV stroke volume, the LV data can be used to validate RV data.
- Manual contouring performed in cvi42 using the Bezier tool is the suggested method of analysis; the fully automated contour detection option is to be avoided.

1a. The left ventricle

- The LV end-diastolic and end-systolic image should be chosen as the images with the largest and smallest LV blood volumes respectively (for their identification, the full image stack should be evaluated).
- Deviations may occur, and extra care should be taken in the setting of LV dyssynchrony or severe mitral regurgitation. Aortic valve closure defines end-systole.
- If a slice is uninterpretable (e.g. degraded by triggering/breathing artefact) it should be excluded from systolic and diastolic measurements of both the LV and RV.
- The LV outflow tract is included as part of the LV blood volume. When aortic valve cusps are identified on the basal slice(s) the contour is drawn to include the outflow tract to the level of the aortic valve cusps.
- Care must be taken with the one or two most basal slices. A slice that contains blood volume at end-diastole may include only left atrium (LA) without LV blood volume at end-systole. The LA can be identified when less than 50% of the blood volume is surrounded by myocardium and the blood volume cavity is seen to be expanding during systole.
- Papillary muscles are to be **EXCLUDED** from the LV cavity for the purpose of analysis and **INCLUDED** within the LV mass (thus do require specific delineation).

- Epicardial borders should be drawn on the middle of the chemical shift artefact line (when present).
- Absolute LV mass is derived from diastolic epicardial and endocardial delineation; systolic epicardial contours are NOT required.
- Maximal LV wall thickness is measured as the thickest portion of the interventricular septum in short axis at end diastole (mm)
- When the most basal slice contains only a small crescent of basal lateral myocardium and no discernible ventricular blood pool, an epicardial contour for the visible myocardium is included for LV mass only.
- Similarly, when the most apical slice contains only a circle of myocardium without cavity blood pool, an epicardial contour without an endocardial contour should be drawn for LV mass calculations

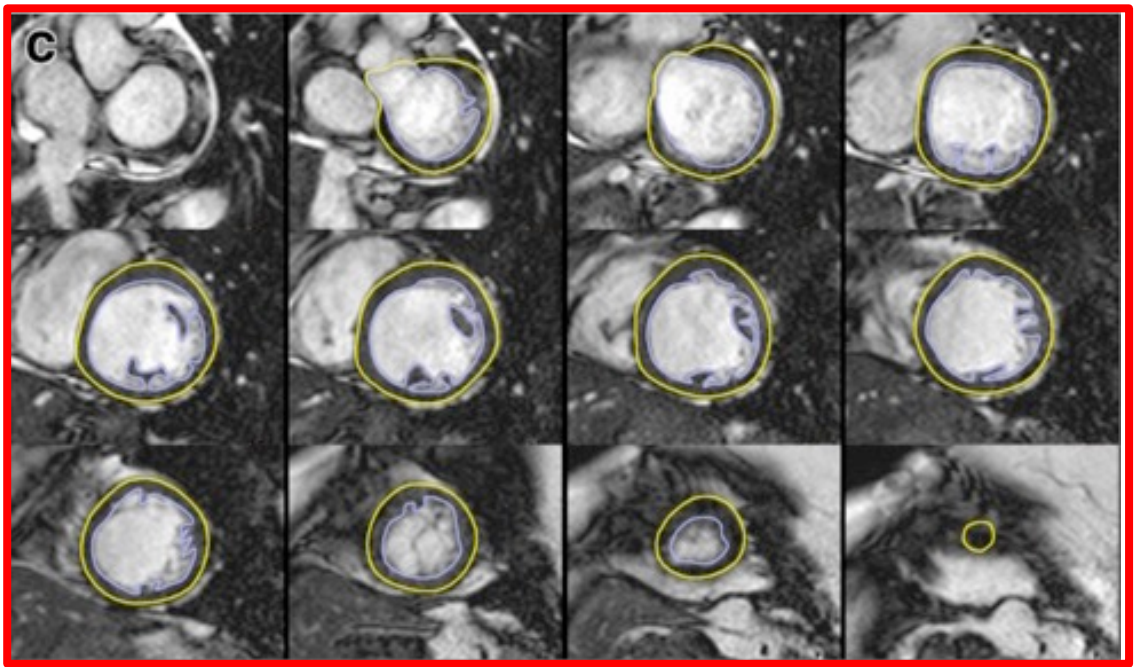

Left ventricular (LV) chamber quantification. For LV chamber quantification, the endocardial (blue) and epicardial (yellow) contours are delineated in diastole in a stack of short axis slices that cover the whole left ventricle. c) illustrates the approach with Exclusion of the papillary muscles as part of the LV volume.

1b. The right ventricle

- As for the LV, it may be necessary to review all image slices in the stack to define end-diastole and end-systole for the RV.
- Trabeculations of the RV should be ignored, and a smooth endocardial border drawn to improve reader reproducibility (RV trabeculae and papillary muscles are typically included in RV volumes).
- Again, if no intra- or extracardiac shunts are present, the RV and LV stroke volumes should be nearly equal (small differences are seen as a result of bronchial artery supply).

- Since the LV stroke volume is more reliably determined than the RV stroke volume, the LV data can be used to validate RV data.
- The pulmonary valve may be visualized, and contours are included just up to, but not superior to this level.

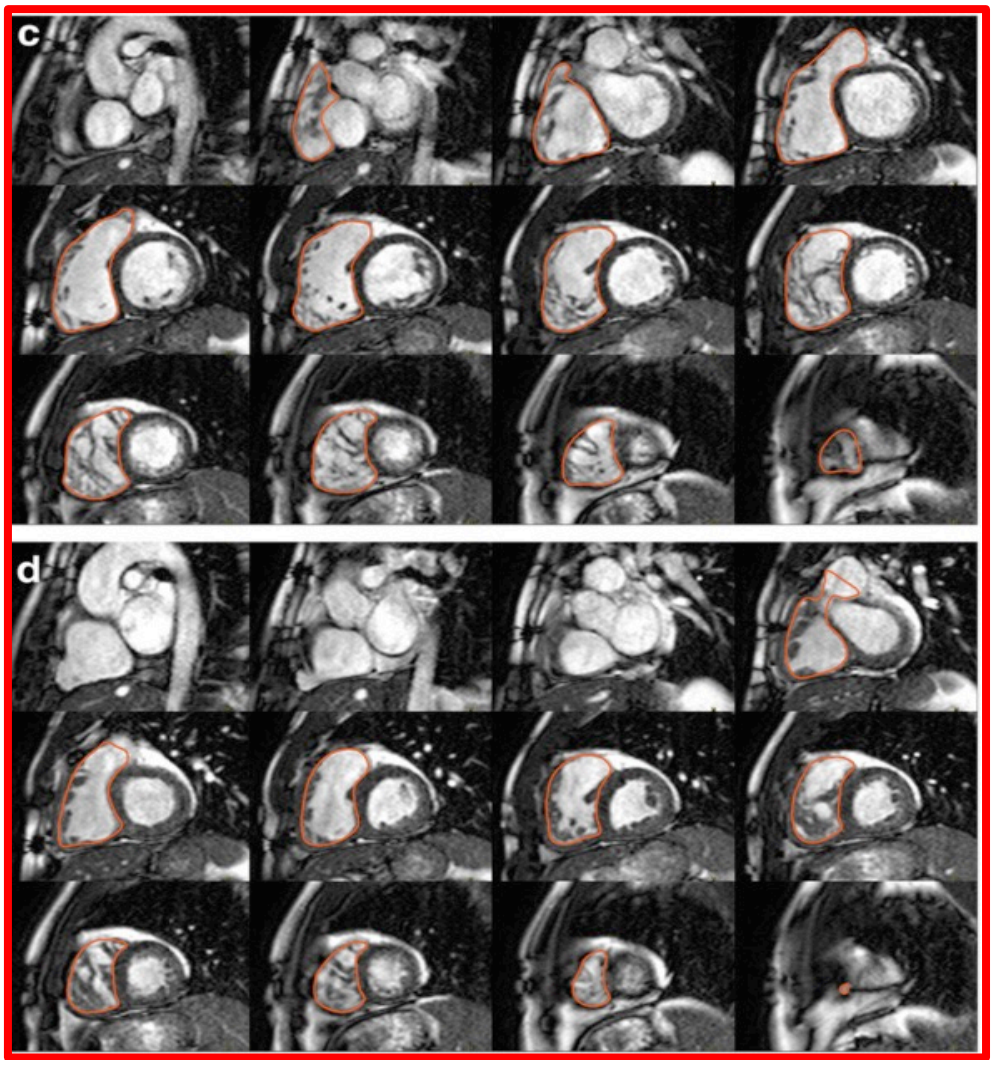

Right ventricular (RV) chamber quantification. For RV volume quantification, the endocardial (red) contours are delineated in diastole (top) and systole (bottom) or short-axis (c and d) slices that cover the whole RV.

2. Left atrial volume quantification

-
- Measurement of left atrial (LA) volume is by the biplane area–length method.
- Images are analysed in the viewer module of cvi42 with a dual panel display selected to permit synchronisation of HLA and VLA by phase.
- All measurements are taken from the two-chamber (A) and four-chamber (B) views at end-ventricular systole, ensuring maximal LA size.

- The atrial endocardial border is traced to determine LA area with exclusion of the pulmonary veins, LA appendage, and mitral valve recess.
- LA length is measured from the midpoint of the mitral annulus plane to the posterior aspect of the left atrium. Left atrial volume (LAV) was calculated using the formula:

$$LAV = 8 \times (A2Ch) \times (A4Ch) / 3\pi L$$

- where A2Ch and A4Ch refer to the LA area in the two-chamber and four-chamber views,
  respectively, and L is the shorter of the two LA length measurements (L2Ch, L4Ch) from these views.

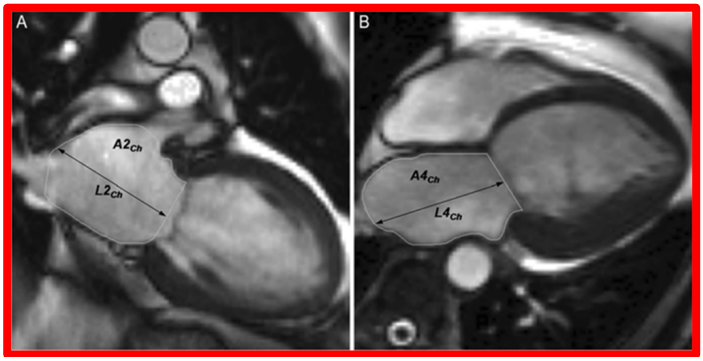

Gulati et al. 2013. European Journal of Heart Failure; 15(6); 660-670.

3. Late gadolinium enhancement quantification

- All images are to be quantified using CVI 42.
- The short axis LV stack acquired 10-15 minutes following gadolinium contrast administration is used for the purposes of late gadolinium quantification.
- Each slice is visually inspected by an experienced CMR reader for the presence or absence of gadolinium enhancement. Phase swap and other geometry images were used in order to assist in decision making where required.
- In only those slices deemed to have LGE present, epi and endocardial contours should be manually drawn, with care take to exclude artefact, blood pool, fat and pericardium.
- The auto-identification tool is then applied, and an area of normal remote myocardium defined alongside identification of areas with increased signal intensity.
- Any hyperintense regions felt to be related to artefact are manually excluded.
- The 5SD technique should be used to determined LGE mass.
- LGE mass is then divided by absolute LV mass as determined from the SA cine measurements to arrive at the %LGE mass.

4. T1 mapping analysis

- All T1 mapping analysis should be performed using the T1 mapping module of CVI42
- The mid-ventricular short axis native T1 map should be loaded into the viewer (scanner generated motion-corrected T1 maps are preferred).
- The endocardial and epicardial contours should be drawn using the Bezier tool ('click-draw' icon displayed).

- Anterior and posterior RV insertion points should be marked with the appropriate tool.
- The manual epicardial and epicardial offsets should both be set to "10%" and the number of segments per slice changed to "6". This should result in automatic segmentation in the right-hand display into the 6 mid-ventricular myocardial segments (segments 7-12 of the AHA/ACC model).
- The blood pool contour should be drawn in the centre of visible blood pool with care taken to avoid papillary muscles within the region of interest.
- The above process should be repeated using the post-contrast T1 map at the same slice position (again, scanner-generated map is preferred). The blood pool contour should be copied from the native T1 map with adjustments applied as needed to avoid papillary muscles or artefact.
- The mean native and post-contrast T1 values for segment 9 are then recorded along with the mean blood pool native and post-contrast T1 values. If mid-wall LGE is present in segment 9 this is included in the analysis, however if subendocardial infarct LGE is present then this area is manually excluded (as per SCMR post-processing guidance). In the case of extensive infarction LGE in segment 9, a separate unaffected mid-ventricular myocardial segment may be selected for T1 analysis.

- **Extracellular volume fraction (ECV%)** is then calculated using the following equations:
    - ECV% = partition coefficient x [1-hematocrit] x 100
      (to give a percentage value from 0-100)
    - Partition coefficient = [ΔR1myocardium / ΔR1blood-pool]
    - ΔR1 = (1 / post-contrast T1) - (1 / native T1)

- **Indexed extracellular volume (iECV)** is calculated using the following equation:
    - iECV = (ECV% x indexed LV mass) / (myocardial density x 100)
    - Myocardial density = 1.05 g/mL

PET/MRI in Aortic Stenosis (PASS) – PET Analysis Protocol
Version 1.0, January 2018

Open FusionQuant software
Load caspr motion- corrected non-contrast angiogram sequence as “background”

Load MRAC-corrected PET data as “overlay”:
- Gate 1: Siemens 3D Dixon VIBE
- Gate 2: NYC radial GRE VIBE

1. Find aortic valve plane (CT method)
   Draw polygon ROI in short axis view
   Depth 6mm (similar to CT method) centred on valve
   Record:
   - **AV SUV max**
   - **AV SUV mean**

2. Reorientate views to show 4Ch, 2Ch and short axis at mid-ventricle level, centre image on LV cavity
   Draw cylinder ROI (3mm radius x 15mm depth) at mid-myocardial level parallel to LV long axis. Ensure ROI is as far away from endo / epicardial surface as possible
   Record
   - **Septal Myo SUV max**
   - **Septal Myo SUV mean**

3. Keeping with same SA plane:
   Draw spherical ROI in middle of LV cavity (6mm radius, approx. 1cm^3 volume)
   Record
   - **LV background SUV mean**

   Draw spherical ROI in middle of RV cavity (6mm radius, approx. 1cm^3 volume)
   Record
   - **RV background SUV mean**

4. Keeping in same 4Ch plane:
   Draw spherical ROI in middle of LA cavity (6mm radius, approx. 1cm^3 volume)
   Record
   - **LA background SUV mean**

   Draw spherical ROI in middle of RV cavity (6mm radius, approx. 1cm^3 volume)
   Record
   - **RA background SUV mean**

5. Save contours within patient study folder

Lothian NHS Board

South East Scotland Research Ethics Committee 02

Waverley Gate
2-4 Waterloo Place
Edinburgh
EH1 3EG
Telephone 0131 536 9000

www.nhslothian.scot.nhs.uk

Date 12 May 2017
Your Ref
Our Ref

Enquiries to: Joyce Clearie
Extension: 35674
Direct Line: 0131 465 5674
Email: Joyce.Clearie@nhslothian.scot.nhs.uk

Please note: This is the favourable opinion of the REC only and does not allow you to start your study at NHS sites in England until you receive HRA Approval

12 May 2017

Dr Marc Dweck
University of Edinburgh, Centre for Cardiovascular Sciences
Chancellors Building
49 Little France Crescent
EH16 4SB

Dear Dr Dweck

Study title:	**Early Valve Replacement guided by Biomarkers of Left Ventricular Decompensation in Asymptomatic Patients with Severe Aortic Stenosis**
REC reference:	**17/SS/0052**
Protocol number:	**AC17024**
IRAS project ID:	**196827**

Thank you for your letter of 11th May 2017, responding to the Committee's request for further information on the above research.

The further information has been considered on behalf of the Committee by the Chair.

We plan to publish your research summary wording for the above study on the HRA website, together with your contact details. Publication will be no earlier than three months from the date of this opinion letter. Should you wish to provide a substitute contact point, require further information, or wish to make a request to postpone publication, please contact hra.studyregistration@nhs.net outlining the reasons for your request.

Confirmation of ethical opinion

On behalf of the Committee, I am pleased to confirm a favourable ethical opinion for the above research on the basis described in the application form, protocol and supporting documentation as revised, subject to the conditions specified below.

Conditions of the favourable opinion

The REC favourable opinion is subject to the following conditions being met prior to the start of the study.

Management permission must be obtained from each host organisation prior to the start of the study at the site concerned.

Management permission should be sought from all NHS organisations involved in the study in accordance with NHS research governance arrangements. Each NHS organisation must confirm through the signing of agreements and/or other documents that it has given permission for the research to proceed (except where explicitly specified otherwise).
Guidance on applying for NHS permission for research is available in the Integrated Research Application System, www.hra.nhs.uk or at http://www.rdforum.nhs.uk.

Where a NHS organisation's role in the study is limited to identifying and referring potential participants to research sites ("participant identification centre"), guidance should be sought from the R&D office on the information it requires to give permission for this activity.

For non-NHS sites, site management permission should be obtained in accordance with the procedures of the relevant host organisation.

Sponsors are not required to notify the Committee of management permissions from host organisations

Registration of Clinical Trials

All clinical trials (defined as the first four categories on the IRAS filter page) must be registered on a publically accessible database within 6 weeks of recruitment of the first participant (for medical device studies, within the timeline determined by the current registration and publication trees).

There is no requirement to separately notify the REC but you should do so at the earliest opportunity e.g. when submitting an amendment. We will audit the registration details as part of the annual progress reporting process.

To ensure transparency in research, we strongly recommend that all research is registered but for non-clinical trials this is not currently mandatory.

If a sponsor wishes to request a deferral for study registration within the required timeframe, they should contact hra.studyregistration@nhs.net. The expectation is that all clinical trials will be registered, however, in exceptional circumstances non registration may be permissible with prior agreement from the HRA. Guidance on where to register is provided on the HRA website.

It is the responsibility of the sponsor to ensure that all the conditions are complied with before the start of the study or its initiation at a particular site (as applicable).

Ethical review of research sites

NHS sites

The favourable opinion applies to all NHS sites taking part in the study, subject to management permission being obtained from the NHS/HSC R&D office prior to the start of the study (see "Conditions of the favourable opinion" below).

Non-NHS sites (if applicable)

The Committee has not yet completed any site-specific assessment (SSA) for the non-NHS research site(s) taking part in this study. The favourable opinion does not therefore apply to any non-NHS site at present. We will write to you again as soon as an SSA application(s) has been reviewed. In the meantime no study

procedures should be initiated at non-NHS sites.

Approved documents

The final list of documents reviewed and approved by the Committee is as follows:

Document	*Version*	*Date*
Evidence of Sponsor insurance or indemnity (non NHS Sponsors only) [Evidence of Insurance (UoE)]		
GP/consultant information sheets or letters [EVOLVED GP Letter]	1.0	21 March 2017
IRAS Checklist XML [Checklist_24032017]		24 March 2017
Letter from funder [Award Letter]		02 November 2015
Other [EVOLVED Screening Result Letter (Higher Risk)]	1.0	21 March 2017
Other [EVOLVED Screening Result Letter (Lower Risk)]	1.0	21 March 2017
Other [Statement of Activities (PIC)]		
Other [Statement of Activities (Recruiting Site)]		
Other [Schedule of Events (PICs)]		
Other [Schedule of Events (Recruiting Sites)]		
Other [EVoLVeD Protocol [tracked changes]]	2.0	11 May 2017
Other [EVoLVeD - Initial Ethics Response Letter]	n/a	11 May 2017
Participant information sheet (PIS) [EVOLVED PISCF (Screening Part A)]	2.0	05 May 2017
Participant information sheet (PIS) [EVOLVED PISCF (Screening Part A) [tracked changes]]	2.0	05 May 2017
Participant information sheet (PIS) [EVOLVED PISCF (Main Study Part B)]	2.0	05 May 2017
Participant information sheet (PIS) [EVOLVED PISCF (Main Study Part B) [tracked changes]]	2.0	05 May 2017
Participant information sheet (PIS) [EVOLVED PISCF (ECG only) [tracked changes]]	2.0	05 May 2017
REC Application Form [REC_Form_24032017]		24 March 2017
Research protocol or project proposal [EVoLVeD Protocol]	2.0	11 May 2017
Summary CV for Chief Investigator (CI) [CV - Marc Dweck]		09 February 2017
Summary CV for student [CV - Russell Everett]		09 February 2017
Summary CV for supervisor (student research) [CV - Dave Newby]		21 March 2017
Validated questionnaire [WHODAS 2.0 (12 item version)]	2.0	
Validated questionnaire [Edmonton Frail Scale]		

Statement of compliance

The Committee is constituted in accordance with the Governance Arrangements for Research Ethics Committees and complies fully with the Standard Operating Procedures for Research Ethics Committees in the UK.

After ethical review

Reporting requirements

The attached document *"After ethical review – guidance for researchers"* gives detailed guidance on reporting requirements for studies with a favourable opinion, including:

- Notifying substantial amendments
- Adding new sites and investigators
- Notification of serious breaches of the protocol
- Progress and safety reports
- Notifying the end of the study

The HRA website also provides guidance on these topics, which is updated in the light of changes in reporting requirements or procedures.

User Feedback

The Health Research Authority is continually striving to provide a high quality service to all applicants and sponsors. You are invited to give your view of the service you have received and the application procedure. If you wish to make your views known please use the feedback form available on the HRA website: http://www.hra.nhs.uk/about-the-hra/governance/quality-assurance/

HRA Training

We are pleased to welcome researchers and R&D staff at our training days – see details at http://www.hra.nhs.uk/hra-training/

17/SS/0052	**Please quote this number on all correspondence**

With the Committee's best wishes for the success of this project.

Yours sincerely

Mr Lindsay Murray
Chair

Email:joyce.clearie@nhslothian.scot.nhs.uk

Enclosures: "After ethical review – guidance for researchers" *[SL-AR2]*

Copy to: *ACCORD, NHS Lothian Research & Development Office*

Study Protocol

EVoLVeD

Early Valve Replacement guided by Biomarkers of Left Ventricular Decompensation in Asymptomatic Patients with Severe Aortic Stenosis

Co-sponsors	University of Edinburgh & NHS Lothian ACCORD The Queen's Medical Research Institute 47 Little France Crescent Edinburgh EH16 4TJ
Sponsor Number	AC17024
Funder	Sir Jules Thorn Charitable Trust
Funding Reference Number	15/JTA
Chief Investigator	Dr Marc Dweck
REC Number	17/SS/0052
NCT ID	NCT03094143
Version Number and Date	Version 4.0 1st May 2018

DOCUMENT HISTORY

Version Number	Version Date	Summary of changes
4.0	01MAY2018	Update of contact details. Addition of screening method as a minimisation variable. Addition of document history section. Addition of PI signature section. Update to ECG LVH criteria. Update to allocation ratio in groups C&D. Minor corrections.
3.0	21AUG2017	Updated screening criteria in ECG only sites from LVH+strain to LVH only. Change in ECG LVH criteria from Romhilt-Estes to Peguero-Lo Presti. Changing the cut off for high sensitivity troponin from >6.0 to ≥6ng/L. Reducing the stated desired maximum interval between randomisation to early intervention and performing the intervention from 4 to 2 months. Inclusion of a participant invitation letter.
2.0	11MAY2017	Clarification of time required to consider consent (section 5.2). Minor corrections.
1.0	21MAR2017	N/A – new document

COORDINATING CENTRE

Chief Investigator Dr Marc Dweck* Centre of Cardiovascular Science Chancellor's Building 51 Little France Crescent Edinburgh EH16 4SB Tel: 07813 619 208 Email: marc.dweck@ed.ac.uk Fax: 0131 242 6379	**Trial Statistician** Professor Steff Lewis* Edinburgh Clinical Trials Unit Level 2, Nine Bioquarter 9 Little France Road Edinburgh EH16 4UX Tel: 0131 651 9956 Email: steff.lewis@ed.ac.uk
Trial Manager Christopher Tuck* Edinburgh Clinical Trials Unit Level 2, Nine Bioquarter 9 Little France Road Edinburgh EH16 4UX Tel: 0131 651 9907 Email: evolved.trial@ed.ac.uk Fax: 0131 537 3851	**Research Fellow** Dr Russell Everett* Centre of Cardiovascular Science Chancellor's Building 51 Little France Crescent Edinburgh EH16 4SB Tel: 07736 927507 Email: russell.everett@ed.ac.uk Fax: 0131 242 6361
Co-sponsor Representative Jo-Anne Robertson ACCORD The Queen's Medical Research Institute 47 Little France Crescent Edinburgh EH16 4TJ Tel: 0131 242 3326 Email: resgov@accord.scot	**Co-sponsor Representative** Kenneth Scott ACCORD The Queen's Medical Research Institute 47 Little France Crescent Edinburgh EH16 4TJ Tel: 0131 242 3325 Email: accord@nhslothian.scot.nhs.uk

* - protocol authors

CONTENTS

PROTOCOL APPROVAL

EVoLVeD: Early Valve Replacement guided by Biomarkers of Left Ventricular Decompensation in Asymptomatic Patients with Severe Aortic Stenosis

Signatures

Dr Marc Dweck Chief Investigator	Signature	Date
Prof Steff Lewis Trial Statistician	Signature	Date
Jo-Anne Robertson Sponsor(s) Representative	Signature	Date
Kenneth Scott Sponsor(s) Representative	Signature	Date
Principal Investigator	Signature	Date

LIST OF ABBREVIATIONS

ACCORD	The Academic and Clinical Central Office for Research & Development
AS	Aortic Stenosis
AVR	Aortic Valve Replacement
BNP	Brain Natriuretic Peptide
BP	Blood Pressure
CHI	Community Health Index
CRF	Case Report Form
CTIMP	Clinical Trial of an Investigational Medicinal Product
ECG	Electrocardiography
ECTU	Edinburgh Clinical Trials Unit
EFS	Edmonton Frail Scale
eGFR	Estimated Glomerular Filtration Rate
GCP	Good Clinical Practice
hsTnI	High Sensitivity Troponin I
HF	Heart Failure
ISF	Investigator Site File
LGE	Late Gadolinium Enhancement
LV	Left Ventricular
LVEF	Left Ventricular Ejection Fraction
LVH	Left Ventricular Hypertrophy
MI	Myocardial Infarction
MRI	Magnetic Resonance Imaging
NHS	National Health Service
NICE	National Institute for Health and Care Excellence
NYHA	New York Heart Association
PMG	Project Management Group
PROBE	Parallel-group multicentre prospective randomised open-label blinded endpoint
RBH	Royal Brompton Hospital
REC	Research Ethics Committee
SAE	Serious Adverse Event

SAR	Serious Adverse Reaction
SIGN	Scottish Intercollegiate Guidelines Network
SOP	Standard Operating Procedure
SPC	Summary of Product Characteristics
SUSAR	Suspected Unexpected Serious Adverse Reaction
TAVI	Transcatheter Aortic Valve Implantation
TMF	Trial Master File
TSC	Trial Steering Committee
WHODAS	World Health Organisation Disability Assessment Schedule

SUMMARY

Professional Summary

Design: A parallel-group multicentre prospective randomised open-label blinded endpoint (PROBE) controlled trial of early aortic valve intervention in asymptomatic patients with severe aortic stenosis (AS) and evidence of left ventricular (LV) decompensation (mid-wall fibrosis) on cardiac magnetic resonance imaging (MRI), with an observation arm of patients without evidence of LV decompensation on cardiac MRI.

Setting: Hospitals in Scotland and England.

Target Population:

Inclusion criteria: 1. Severe aortic stenosis (aortic valve peak velocity ≥4.0 m/s, or aortic valve area indexed to body surface area <0.6cm^2/m^2 with aortic valve peak velocity ≥3.5m/s) 2. Age over 18 years 3. No symptoms attributable to aortic stenosis that require aortic valve replacement

Exclusion criteria: 1. Deemed lower risk for mid-wall fibrosis on screening 2. Planned cardiac surgery 3. Previous valve replacement 4. Severe hypertension (systolic >180 or diastolic >110 mmHg) 5. Acute pulmonary oedema or cardiogenic shock 6. Left ventricular ejection fraction <50% on cardiac MRI 7. Significant abnormalities on cardiac MRI that would prevent enrolment 8. Coexistent severe aortic regurgitation or mitral regurgitation 9. Coexistent mitral stenosis greater than mild in severity 10. Coexistent hypertrophic cardiomyopathy or cardiac amyloidosis 11. Any contraindication to MRI scanning 12. Advanced renal impairment 13. Pregnancy or breast feeding 14. Patient judged to be unfit to be considered for aortic valve replacement or transcatheter aortic valve implantation 15. Patient declines to consider undergoing valve replacement surgery or transcatheter aortic valve implantation 16. Inability to give informed consent 17. Previous randomisation into this study

Health technologies being assessed: Use of aortic valve intervention (surgical aortic valve replacement or transcatheter aortic valve implantation) in patients with asymptomatic severe aortic stenosis with evidence of LV decompensation.

Measurement of outcome

Primary outcome: Composite of all-cause mortality or unplanned aortic stenosis-related hospitalisation between randomisation and final follow up visit for study participants with mid-wall fibrosis.

Secondary outcomes: 1. Mortality: all-cause, cardiovascular, AS-related, and sudden cardiac death. 2. Unplanned aortic-stenosis related hospitalisation. 3. Symptomatic status as assessed by NYHA functional classification. 4. Health and disability status as assessed by the WHODAS 2.0. 5. The development of systolic LV dysfunction. 6. Stroke 7. Permanent pacemaker insertion, cardiac resynchronisation therapy or automated implantable cardioverter defibrillator. 8. Endocarditis 9. 30 day post-operative complications following aortic valve intervention

Sample size: We expect the proportion of primary outcome events (all-cause mortality or unplanned AS-related hospitalisation) to be 25% in the routine care arm of the study, and 13.4% in the early intervention arm (a hazard ratio of 2), over 2 years of follow up (Dweck et al 2011, RBH cohort). We aim to recruit 1000 participants with evidence of

decompensation on screening (ECG and/or troponin) who will then be imaged with cardiac MRI for evidence of LV decompensation (mid-wall fibrosis). We would expect this to result in 400 patients with mid-wall fibrosis being randomised (1:1). Using a logrank approach, we will need to observe 88 primary outcome events to give us 90% power at 5% significance level. We will follow participants up for as long as possible before the end of study, and thus participants will have between 2 and 3.5 years of follow up. We expect mean follow up to be 2.75 years. We are likely to reach 88 events when we have recruited 356 participants (slightly more allowing for drop-out).

Lay Summary

The aortic valve can be thought of as a one-way door through which blood leaves the heart to enter the body. It has to be able to open well to allow blood out and close properly to stop blood leaking back and overloading the heart.

Aortic stenosis is a condition where the aortic valve becomes progressively narrowed (stenosed; i.e. the door doesn't open very well) usually over a number of years or decades. This is usually caused by hardening and thickening of the valve so that it becomes less flexible. This puts a strain on the heart muscle as it has to work harder to "open the door" and pump blood through the narrowed valve. For many years the heart adapts and copes with this increased pressure but eventually it is no longer able to cope and patients develop symptoms (chest pain, breathlessness, collapse) and an increased risk of heart failure and dying. The only treatment currently available for severe aortic stenosis is surgery to replace the narrowed valve. The timing is key: replace the valve too early and patients are put through surgery and the risk of a replacement valve without reason; too late and patients may be left with irreversible symptoms and heart failure. At the moment we replace the valve when patients first develop symptoms but these can be tricky to assess in patients with lots of other health conditions or in those that are inactive. As a consequence the timing of aortic valve operations is often suboptimal.

Fibrosis or scarring of the heart is one of the key processes that causes the heart to fail in this condition. Scarring once formed does not appear reversible, so any scar that forms prior to valve replacement will remain with the patient even after surgery. Using cardiac MRI (a completely safe method of scanning the heart involving strong magnetic fields and lying in a tunnel) we are able to detect the earliest stages of this scarring. We believe this will identify patients whose hearts are starting to fail (even before they develop symptoms) and who therefore need prompt replacement of their valves.

In our study we will use cardiac MRI to look for heart scarring in patients with severe aortic stenosis but no symptoms. Patients with confirmed heart scarring will then be randomised to either early valve replacement surgery or to the current treatment strategy. This consists of continued monitoring of the valve over time waiting for patients to develop symptoms.

We believe that performing aortic valve replacement on patients with severe aortic stenosis with no symptoms but who have evidence of early scarring on cardiac MRI will prevent further scarring from forming, reduce subsequent heart failure and lead to improved long-term symptoms following surgery (e.g. breathlessness) and a reduced chance of dying. The aim of this trial is to find out whether this is correct.

1 INTRODUCTION

1.1 BACKGROUND

Aortic stenosis is the most common form of valve disease in the western world. It is already a major health care burden [1,2] but, with an ageing population, is set to treble by the year 2050. In the initial phases, the increased afterload imposed by aortic valve narrowing induces adaptive LV hypertrophy that acts to maintain wall stress and cardiac output. Ultimately, this process decompensates and patients transition from hypertrophy to heart failure and the development of symptoms and adverse cardiovascular events [3-5].

Yet despite the prevalence of aortic stenosis, we lack effective medical therapies. Indeed, the only treatment option available is replacement of the valve using either surgical or percutaneous techniques. Judicious timing of aortic valve replacement (AVR) is crucial. Too early and patients are exposed unnecessarily to the significant morbidity and mortality associated with prosthetic heart valve replacement surgery. Too late and patients will sustain irreversible damage to their heart muscle that translates in to an increase in post-operative complications, the development of heart failure and an adverse long-term prognosis. Current guidelines recommend AVR in patients with severe stenosis and evidence of left ventricular decompensation. Traditionally the latter is defined by the development of symptoms and/or a fall in ejection fraction. However, both of these criteria are outdated and have major limitations. Symptoms are subjective and frequently difficult to interpret in elderly patients, whilst a reduction in ejection fraction is often a late and irreversible phenomenon [6].

There is therefore a major unmet clinical need for more objective and specific markers of LV decompensation that can more accurately define the optimum timing of AVR. The purpose of this study is to address these key issues and ultimately to improve the care of patients with aortic stenosis.

1.2 RATIONALE FOR STUDY

The development of symptoms and adverse events in aortic stenosis relates to how the left ventricle adapts to the associated increases in afterload. Indeed aortic stenosis triggers a hypertrophic response in the myocardium that initially restores wall stress and maintains cardiac performance, but eventually leads to decompensation, driving the transition to heart failure, symptoms and ultimately death (Figure 1—1). Importantly only a weak association exists between the magnitude of the hypertrophic response and the severity of valve obstruction, making it important that both processes are considered independently.

In conditions associated with left ventricular pressure overload such as aortic stenosis and hypertension, myocyte size and myocardial wall thickness increase to restore wall stress. This hypertrophic response is initially adaptive maintaining cardiac output and systolic function. However as hypertrophy increases, the left ventricle ultimately decompensates, leading to progressive impairment in ventricular performance and the development of symptoms and adverse cardiovascular events. Histological studies have indicated that this pathologic transition from ventricular adaptation to decompensation is driven primarily by two processes: myocyte death and myocardial fibrosis. Myocyte death takes the form of apoptosis and necrosis (cell swelling and loss of membrane integrity sometimes referred to as oncosis in this context), and is accompanied by signs of cellular stress manifest as increased autophagy.

Figure 1—1: Progressive Changes in the Left Ventricle in Aortic Stenosis

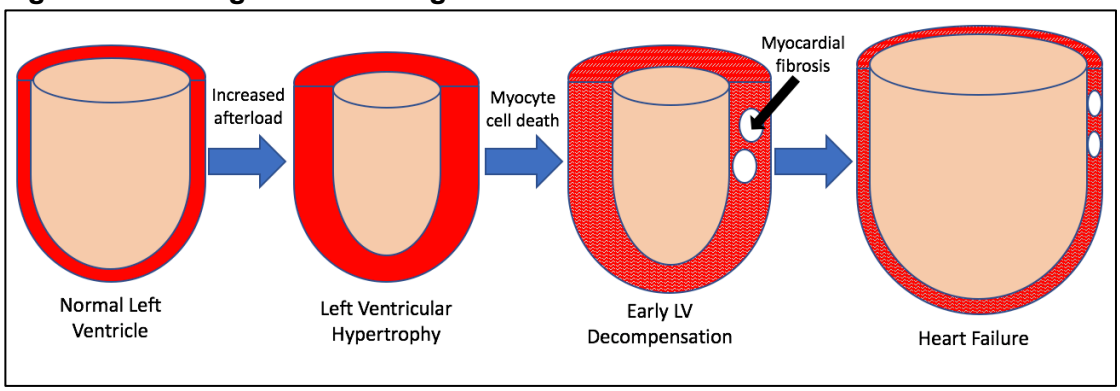

Replacement myocardial fibrosis is believed to occur in response to cell death and the ensuing inflammation. Such fibrosis is irreversible and its accumulation in the ventricle leads to progressive impairment of myocardial relaxation (diastolic dysfunction) and contraction (systolic dysfunction), driving the clinical progression to heart failure.

The presence of myocardial fibrosis can be assessed non-invasively using cardiac MRI and the late gadolinium enhancement (LGE) technique. Following an intravenous bolus, gadolinium partitions and accumulates within the extra-cellular volume. This is particularly prominent where the extracellular volume has expanded, such as areas of replacement myocardial fibrosis, and is detectable on T1-weighted cardiac MRI. Studies examining myocardial biopsy samples have shown a good correlation between histological myocardial fibrosis and LGE on cardiac MRI [7]. Importantly, the presence of LGE in patients with severe aortic stenosis is an independent predictor of all-cause mortality [7-9].

Although cardiac MRI is non-invasive and safe, it is time consuming, expensive and access is still limited in many centres across the United Kingdom. We have recently demonstrated that two routinely used markers, plasma high sensitivity cardiac troponin I (hsTnI) concentration and the ECG (presence of voltage criteria for left ventricular hypertrophy [ECG-LVH] and the ECG-strain pattern) are independently associated with mid-wall myocardial fibrosis on cardiac MRI and adverse cardiovascular events [10,11].

We therefore propose that in a population with severe asymptomatic aortic stenosis, (who currently do not meet guideline indications for surgery) that screening with the ECG and hsTnI will identify patients with an increased probability of mid-wall myocardial fibrosis and LV decompensation as identified on subsequent cardiac MRI. With current management strategies, these patients are at increased risk of adverse cardiovascular events and all-cause mortality. We hypothesise that early aortic valve intervention in this group will limit progression of myocardial fibrosis, halt the transition to heart failure and lead to improved patient outcomes compared to routine clinical management.

2 STUDY OBJECTIVES

2.1 OBJECTIVES

2.1.1 Primary Objective

- To determine whether early aortic valve replacement can reduce death and unplanned AS-related hospital admissions in patients with asymptomatic severe aortic stenosis who have subclinical but objective evidence of LV decompensation.

2.1.2 Secondary Objectives

- To determine whether early aortic valve replacement in patients with asymptomatic severe aortic stenosis who have subclinical but objective evidence of LV decompensation improves other clinical outcomes (see section 2.2.2) including death and unplanned AS considered separately, long-term symptomatic status, post-operative outcomes and reduce the development of LV dysfunction.
- To determine whether amongst patients receiving routine care, those with mid-wall fibrosis develop symptoms more quickly or have worse clinical outcomes compared to those without fibrosis.

2.1.3 Exploratory Objectives

- To explore the association between clinical factors, cardiac biomarkers and cardiac MRI characteristics in patients with aortic stenosis.

2.2 ENDPOINTS

2.2.1 Primary Endpoint

- Composite of all-cause mortality or unplanned aortic stenosis-related hospitalisation between randomisation and final follow up visit for study participants with mid-wall fibrosis.

Unplanned aortic stenosis-related hospitalisation is defined as an unplanned admission with syncope, heart failure, chest pain or arrhythmia (ventricular arrhythmia or second or third degree heart block) attributed to aortic stenosis. This endpoint will be adjudicated by two independent investigators blinded to the details of randomisation (see section 10.5).

2.2.2 Secondary Endpoints

- Mortality: all-cause, cardiovascular, AS related, and sudden cardiac death between randomisation and final follow up visit
- Unplanned aortic-stenosis related hospitalisation between randomisation and final follow up visit
- Health and disability as assessed by the 12-item WHO Disability Assessment Schedule 2.0 (WHODAS) at the final follow up visit.
- The development of LV systolic dysfunction (ejection fraction <45% quantitatively or at least moderate LV dysfunction qualitatively) between randomisation and final follow up visit.
- Symptomatic status as assessed by NYHA functional classification at the final follow up visit.

- Permanent pacemaker insertion, cardiac resynchronisation therapy or automated implantable cardioverter defibrillator between randomisation and final follow up visit
- Stroke between randomisation and final follow up visit
- Endocarditis between randomisation and final follow up visit
- 30 day post-operative complications following aortic valve intervention (safety end-point, appendix A).

Cardiovascular mortality is defined as death due to myocardial infarction, sudden cardiac death, heart failure, stroke, or other cardiovascular causes, death related to cardiovascular procedures, and death due to other cardiovascular causes.

AS-related death is a death where aortic stenosis has been listed as a contributory cause by the clinical care team on the patient's official death certificate.

Sudden cardiac death is defined as any death that occurs unexpectedly and not within 30 days of acute myocardial infarction (MI). This includes unsuccessful resuscitation following an arrhythmia. (see appendix B for full list [12]).

Stroke is defined as any new rapid-onset focal or global neurological deficit (change in conscious level, hemiplegia, hemiparesis, numbness or sensory loss affecting one side of the body, dysphasia, visual loss, or any other sign consistent with a stroke) persisting greater than 24 hours or with brain imaging compatible with new infarction or haemorrhage.

Endocarditis is defined as a clinical diagnosis of endocarditis by the treating physician and have at least one positive blood culture for a typical endocarditis organism (e.g. staphylococcus or streptococcus species).

Secondary endpoints will be analysed in groups A, B and C.

2.2.3 Exploratory Endpoints

Blood samples will be obtained and stored from consented participants to gain a greater understanding of the pathophysiology of aortic stenosis. These will be used to analyse biochemical markers associated with cardiac disease (e.g. Brain Natriuretic Peptide (BNP), hsTnI). Cardiac MRI parameters (such as LV mass, ejection fraction and T1 mapping measures) and their relationship with clinical factors and other biomarkers will also be analysed. In addition, genetic analysis will be performed to assess for gene associations with myocardial fibrosis / LV decompensation.

3 STUDY DESIGN

This will be a parallel-group multi-centre prospective randomised open label blinded endpoint (PROBE) controlled trial with an additional observational arm. Randomisation will be 1: 1 among those with mid-wall fibrosis being randomised into the two arms of the full study, and will use a flexible, adaptive randomisation ratio among those without mid-wall fibrosis being randomised into the observational arm or no further follow up.

Patients with severe aortic stenosis attending outpatient clinics or echocardiogram appointments will be identified and assessed for eligibility. Participants may also be identified by participating centres from local databases – these participants can be invited to take part by sending a letter from their normal care team. Potential participants meeting the inclusion criteria and demonstrating normal left ventricular ejection fraction (LVEF) on routine echocardiography can be approached about participating in study.

Potential participants will undergo an initial screening assessment based upon troponin I measurements and/or the ECG. This will determine whether potential participants

are considered *lower-risk* or *higher-risk* for the presence of mid-wall myocardial fibrosis on cardiac MRI. At sites where the Abbott high sensitivity troponin I assay is available patients will be considered at higher risk if they demonstrate ECG-LVH with strain and/or elevated troponin levels (≥6ng/L). At sites where the Abbott high sensitivity troponin I assay is not available then patients at that site will be screened using the ECG only (ECG only sites). At these sites the presence of voltage criteria for LVH on the ECG (ECG-LVH) with or without strain will be used to define patients at higher risk.

Patients at *lower-risk* (without ECG-LVH with strain and troponin levels <6ng/L; or at the ECG only sites patients without ECG-LVH) will be considered to have a healthy myocardium and no suggestion of LV decompensation. These patients will take no further part in the study but their details will be retained by the research team for future record linkage.

Patients at *higher-risk* will undergo baseline assessments including cardiac MRI.

If a participant is still eligible following baseline assessment and no other exclusion criteria are identified on central cardiac MRI review (see section 5.5.4), then the participant can be enrolled into the study. If the central cardiac MRI review demonstrated mid-wall myocardial fibrosis then the participant will be randomised 1:1 to early treatment or routine care. These patients will be followed up in the study annually.

If no mid-wall fibrosis is detected on central cardiac MRI review then participants will be entered into an observational arm using a flexible, adaptive randomisation ratio, aimed at balancing those in the observational arm and the routine care arm. Those who do not enter the observational arm will have no further study follow up but their data will be retained for future data linkage. Those entered into the observational arm will have the same study follow up schedule to those participants with mid-wall fibrosis. As well as providing key mechanistic insight this approach will also maintain the patient and physician blinding as to the presence or absence of mid-wall fibrosis on cardiac MRI in patients undergoing follow up who are not randomised to early valve intervention.

Figure 3—1: Study Design Overview (screening with ECG and hsTnI)

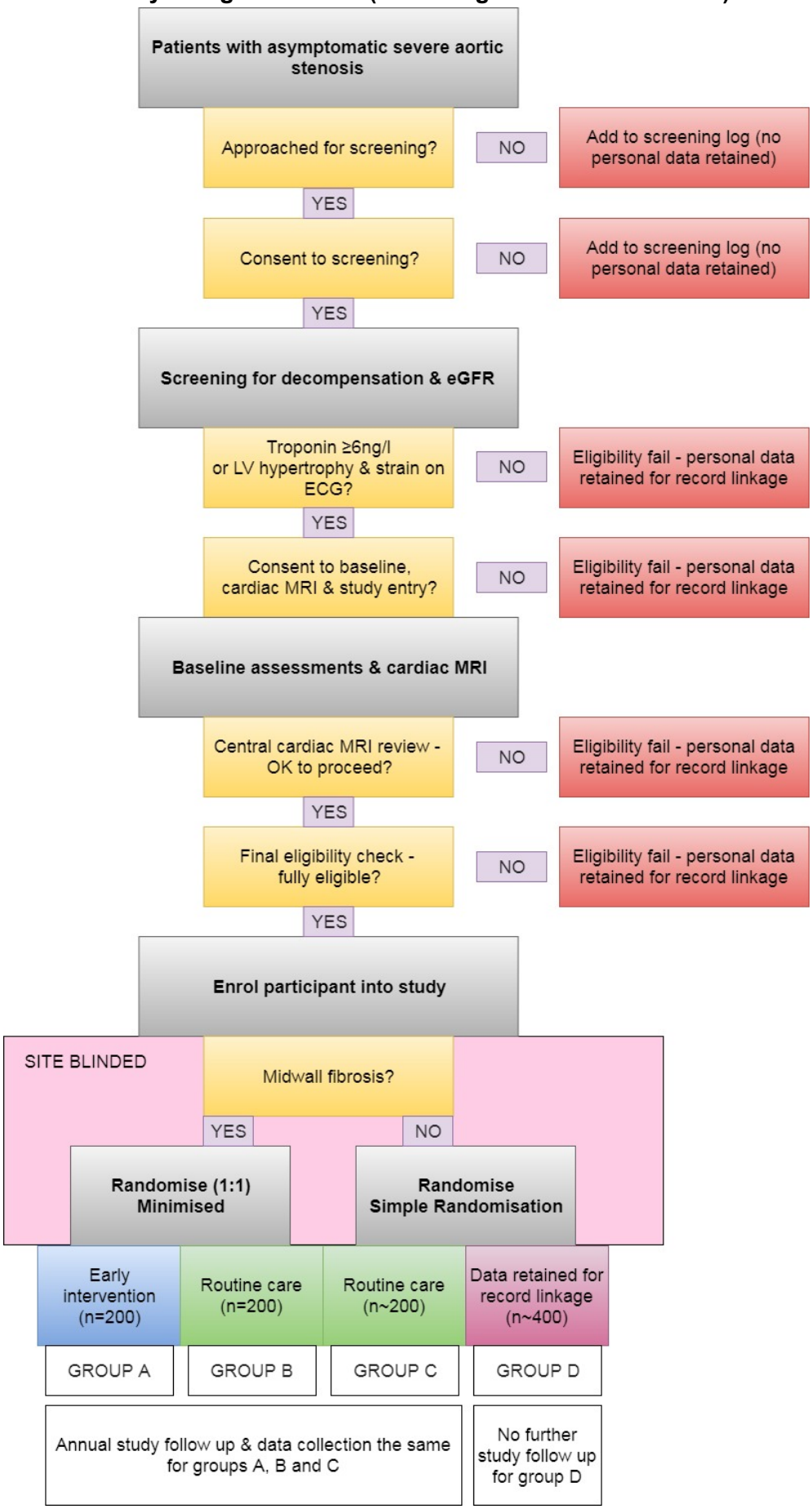

Figure 3—2: Study Design Overview (screening with ECG only)

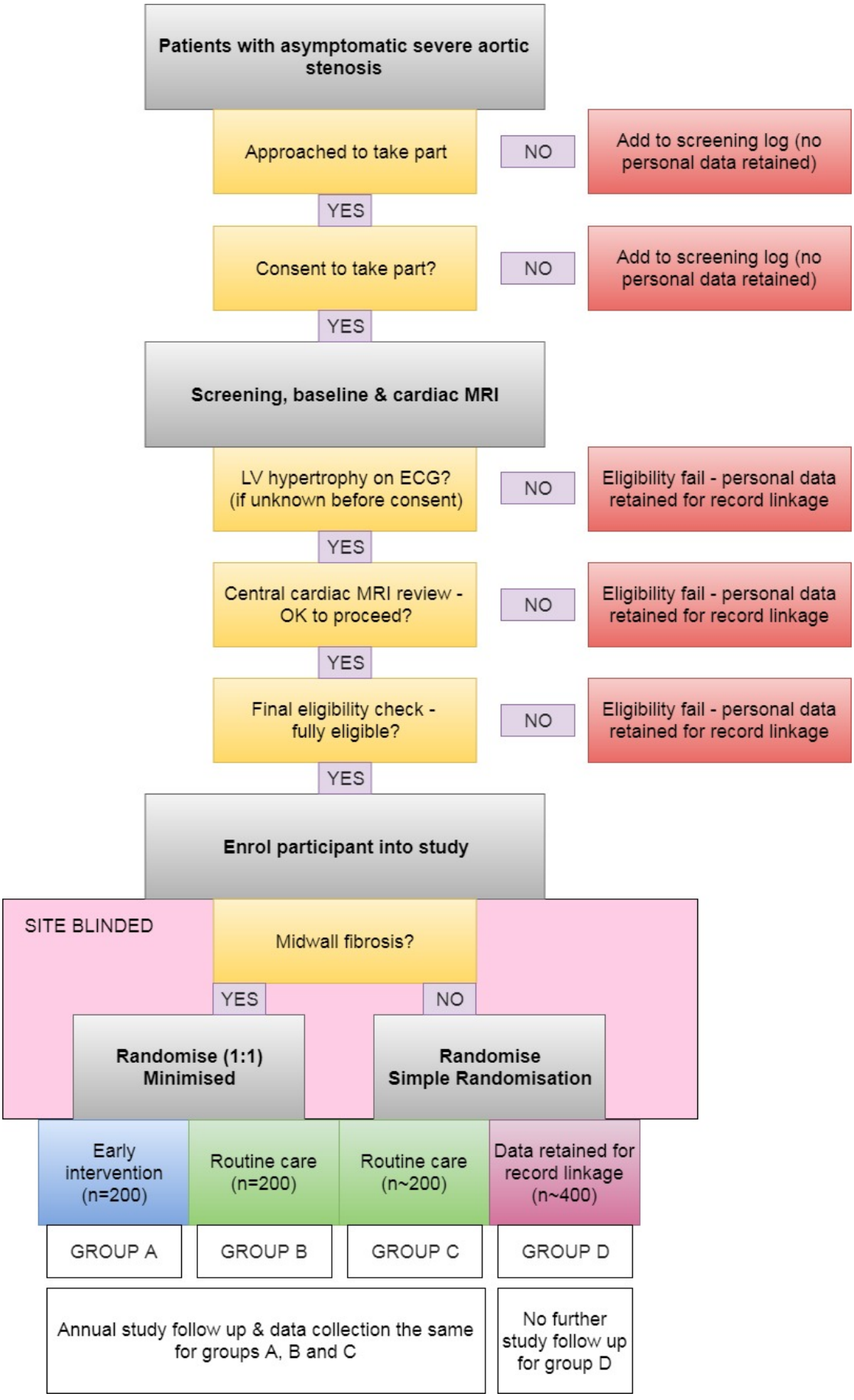

4 STUDY POPULATION

4.1 NUMBER OF PARTICIPANTS

The sites taking part in this study are listed in the Participating Sites document.

We aim to screen patients with asymptomatic severe aortic stenosis (aortic valve peak velocity ≥4.0 m/s on Doppler echocardiography or aortic valve area indexed to body surface area <0.6cm^2/m^2 with aortic valve peak velocity ≥3.5 m/s) and preserved LV systolic function to identify approximately 1000 patients with evidence of LV decompensation to proceed to cardiac MRI. Those meeting the eligibility criteria will be enrolled into the study. 400 participants with mid-wall fibrosis will be randomized 1:1 to receive early valve intervention or routine care. Amongst those without mid-wall fibrosis (approximately 600), 200 participants will enter an observation arm and 400 will not be followed up but their data will be retained for future data linkage. The planned recruitment period is 18 months.

4.2 INCLUSION CRITERIA

For inclusion in the study, participants should fulfil the following criteria:

1. Severe aortic stenosis (aortic valve peak velocity ≥4.0 m/s, or aortic valve area indexed to body surface area <0.6cm^2/m^2 with aortic valve peak velocity ≥3.5m/s)
2. Age over 18 years
3. No symptoms attributable to aortic stenosis that require aortic valve replacement

4.3 EXCLUSION CRITERIA

Participants cannot be enrolled into the study if any of the following criteria are fulfilled:

1. Deemed lower risk for mid-wall fibrosis on screening
2. Planned cardiac surgery
3. Previous valve replacement
4. Severe hypertension (systolic >180 or diastolic >110 mmHg)
5. Acute pulmonary oedema or cardiogenic shock
6. Left ventricular ejection fraction <50% on cardiac MRI
7. Significant abnormalities on cardiac MRI that would prevent enrolment (see section 5.5.4)
8. Coexistent severe aortic regurgitation or mitral regurgitation
9. Coexistent mitral stenosis greater than mild in severity
10. Coexistent hypertrophic cardiomyopathy or cardiac amyloidosis
11. Any contraindication to MRI scanning (such as permanent pacemaker)
12. Advanced renal impairment (glomerular filtration rate <30 mL/min/1.73 m^2)

13. Pregnancy or breast feeding
14. Patient judged to be unfit to be considered for aortic valve replacement or transcatheter aortic valve implantation
15. Patient declines to consider undergoing valve replacement surgery or transcatheter aortic valve implantation
16. Inability to give informed consent
17. Previous randomisation into this study

4.4 CO-ENROLMENT

Co-enrolment will be considered on a case-by-case basis and will consider the extra burden being placed on the study participants and the likelihood of study assessments or interventions influencing the outcomes of either study. The Sponsor's representatives require Investigators from all studies involved in co-enrolment to be aware of the co-enrolment plans and provide documented permission for co-enrolment to be undertaken in their study.

The acceptability of co-enrolment with some specific trials are now considered:

- SALTIRE 2 (a randomised controlled trial of bisphosphonates/denosumab versus placebo on the progression of mild to moderate aortic stenosis) – co-enrolment will not be permitted as both studies could directly affect outcome measures of the other. No wash out time is required following the end of a participant's involvement in SALTIRE 2.
- MODE-AS (observational study of patients undergoing AVR with intraoperative myocardial biopsy) – co-enrolment is permitted as there is significant overlap in study assessments leading to minimal extra burden on patients.
- COMPASS (observational study of patients with asymptomatic moderate to severe aortic stenosis) – co-enrolment will be permitted on a case-by-case basis following discussion between investigators.

5 PARTICIPANT SELECTION AND ENROLMENT

5.1 IDENTIFYING PARTICIPANTS

Participants will be identified and recruited from the cardiology outpatient clinics or echocardiogram lists at participating centres with the aid of local databases (participants can be invited by sending a letter from their normal care team). When identifying potential participants for screening an echocardiogram demonstrating severe aortic stenosis performed within the previous three years is acceptable. However, if a patient proceeds to baseline assessment and no echocardiogram result is available dated within the previous 6 months, an echocardiogram should be performed at the baseline visit.

5.2 CONSENTING PARTICIPANTS

Potential participants will be approached for consent by the site Principal Investigator or appropriate qualified individual to whom this task has been delegated. This will include research nurses and practitioners if compatible with local policy. Once participants have had adequate time to consider the information and ask questions written consent will be sought. Potential participants can be consented on the same day for screening, but should be given at least 24 hours to consider entering the main trial.

The consent process will vary depending on access to the Abbott high sensitivity troponin I assay. When screening with ECG and the Abbott high sensitivity troponin I assay there will be two-step consenting process:

- **Consent to screening for risk of mid-wall fibrosis**
  Potential participants who meet the inclusion criteria and have preserved LV systolic function will be supplied with the Screening Participant Information Sheet (Part A) and Consent Form. If consent is given, this will allow for demographic data to be collected and screening procedures including venepuncture to take place to determine risk of mid-wall fibrosis (see section 5.3).

- **Consent to Baseline, Cardiac MRI and trial entry**
  Those patients deemed to be at *higher-risk* for mid-wall myocardial fibrosis following screening will be invited to attend for baseline assessment. Written informed consent will be obtained before any study related procedures are performed. Details of the baseline assessments can be found in section 6.2.

This 2-step consent process will allow us to screen patients with troponin quickly and efficiently in the clinic. In those found to be eligible, a more detailed second stage consent process will then ensue before participation in the main part of the clinical trial.

When screening without the Abbott high sensitivity troponin I assay (i.e. ECG only), consent will be simplified to a single step and any study-specific activities will be carried out after this consent.

5.3 SCREENING FOR MID-WALL FIBROSIS RISK

The following investigations will be carried out for screening:

1. A standard **12-lead electrocardiogram (ECG)**,

    - If the participant's most recent ECG is within 6 months of screening and is interpretable then there is no requirement to repeat the ECG at screening.

2. **Blood high sensitivity troponin I (hsTnI) concentration**

    - This is a marker of myocardial injury using the Abbott ARCHITECT*STAT* assay. The level of detection of this assay is 1.2 ng/L and the coefficient of variation is <10% at 4.7 ng/L.

    - When screening without the Abbott high sensitivity troponin I assay (i.e. at ECG only sites), a serum sample should still be collected for storage

at ≤-70^{0}C to enable retrospective evaluation of baseline hsTnI concentration. This storage sample can be performed at the baseline assessment.

3. A blood sample will be taken according to local policy to determine eGFR. This is to check suitability for cardiac MRI scanning if the participant proceeds to baseline assessment. If the participant's most recent eGFR result is ≥30 mL/min/1.73 m^2 and within 12 months of screening then there is no requirement to repeat eGFR at screening unless the investigator makes a clinical judgment that a more contemporary result is needed.

The screening process will allow us to stratify patients as *lower risk* or *higher risk* of mid-wall myocardial fibrosis which is defined as the presence of mid-wall late gadolinium enhancement on cardiac MRI. Importantly, there are two methods of screening depending on local availability of the Abbott hsTnI assay. Consequently some sites will screen with troponin/ECG whilst others will screen with the ECG only.

In centres screening with both hsTnI **and** ECG, patients will be deemed at *higher-risk* in the presence of either:

- **A high-sensitivity troponin I concentration** of ≥6 ng/L

- **LV hypertrophy and LV strain pattern on 12-lead electrocardiogram**. LVH will be defined according to standard ECG criteria (including but not limited to the Peguero-Lo Presti criteria [S_D+SV_4 ≥2.8 mV in males, ≥2.3 mV in females][13]; Sokolow-Lyon index; Cornell voltage criteria; and Romhilt-Estes point score system). Patients with left bundle branch block, in whom these criteria cannot be applied, will be assumed to meet ECG criteria for LVH. LV strain will be defined by the presence of LVH with ≥1mm concave downsloping ST segment depression with asymmetrical T wave inversion in at least two contiguous lateral leads.

In centres where local hsTnI testing is not available and **screening is performed using ECG only**, *higher-risk* will be defined as:

- **LV hypertrophy pattern on 12-lead electrocardiogram**, as determined using standard ECG criteria for LVH with or without the strain pattern (see above). Patients with left bundle branch block, in whom these criteria cannot be applied, will be assumed to meet ECG criteria for LVH.

Patients at *higher-risk* for mid-wall myocardial fibrosis and with eGFR ≥30 mL/min/1.73 m^2 will be invited to have baseline assessments and undergo cardiac MRI imaging (see section 6.2).

If the patient does not meet the above higher-risk criteria they will be considered *lower-risk* for mid-wall myocardial fibrosis and will not take further part in the study. Their personal information will be retained for potential future data linkage on the outcomes of those who are considered lower-risk for mid-wall myocardial fibrosis.

If for any reason the screening investigations do not provide a result but the participant is still considered at higher-risk for mid-wall myocardial fibrosis then they can proceed to baseline assessments. Missing results should be repeated at the baseline visit, noting that an eGFR result is needed prior to cardiac MRI.

5.4 INELIGIBLE AND NON-RECRUITED PARTICIPANTS

Potential participants meeting the inclusion criteria and demonstrating normal LVEF on routine echocardiography but who do not consent to any part of the study will be recorded on the study screening log. All patients who consent to any part of the study will be entered into the study database. Ineligible and non-recruited patients will continue to be seen by their cardiologist as part of standard clinical care.

5.5 ENROLMENT AND RANDOMISATION

5.5.1 Enrolment and Randomisation Procedures

Following completion of baseline assessments, cardiac MRI and central MRI review, patients that meet all inclusion/exclusion criteria will be enrolled into the study. A web-based computer-generated randomisation process will be employed. There are two separate randomisations, one for patients with mid-wall fibrosis (Randomisation 1) and another for those without mid-wall fibrosis (Randomisation 2).

5.5.2 Randomisation 1 – Patients with Mid-Wall Fibrosis

We will randomise patients in a 1:1 ratio to either early intervention (group A) or routine clinical care (group B). Minimisation techniques will be employed to ensure balancing of key variables: age, sex, aortic valve peak velocity, ischaemic heart disease and screening method (ECG and hsTnI or ECG only).

Group A: Early intervention (200 patients)

Patients will be referred immediately for aortic valve intervention. The choice of either surgical aortic valve replacement or transcatheter aortic valve implantation (TAVI) will be made by the local clinical team according to local policies. In patients undergoing surgical replacement the choice of surgical technique and type of valve replacement used will be at the discretion of the operating surgeon and the patient. Patients found to have significant coronary artery disease requiring concomitant coronary artery bypass surgery will not be excluded. Similarly the choice of TAVI valve and need for percutaneous coronary intervention will be made by the TAVI heart team. The procedure should be performed as soon as possible and ideally within two months of randomisation and allocation to group A. Participants will be followed up in the study as described in section 6.3.

Group B: Routine care (200 patients)

Patients will be invited back for clinical follow up according to local policy. Decision-making regarding future aortic valve intervention will be taken by the participant's clinical team (cardiologist and cardiac surgeon). Participants will be followed up in the study as described in section 6.3.

5.5.3 Randomisation 2 – Patients without Mid-Wall Fibrosis

We will randomise patients using a flexible, adaptive ratio to either routine clinical care (group C) or no further study follow up (group D). The aim of the randomisation ratio is to balance the number of participants in group C and group B. This will be a simple randomisation. Details of the randomisation ratio value, and dates of change will be recorded.

Group C: Routine care (approximately 200 patients)

Patients will be invited back for clinical follow up according to local policy. Decision-making regarding future aortic valve intervention will be taken by the patient's clinical team (cardiologist and cardiac surgeon). Participants will be followed up in the study as described in section 6.3. Group C will appear identical to Group B (see section 5.5.4).

Group D: No further study follow up (approximately 400 patients)

Patients will be invited back for clinical follow up according to local policy. Decision-making regarding future aortic valve intervention will be taken by the patient's clinical team (cardiologist and cardiac surgeon). No further study follow up will take place but personal data will be retained for future data linkage.

5.5.4 Blinding of the Routine Care Group and Cardiac MRI Result

The patient and clinical team will be blinded to the central cardiac MRI review and result. This is to ensure that this does not influence future treatment for participants with mid-wall fibrosis who are allocated routine care. If mid-wall fibrosis is present, the patient will undergo Randomisation 1. If randomised to early intervention (Group A), the patient will be aware they have mid-wall fibrosis as they will be referred to a surgeon for consideration of valve replacement.

If mid-wall fibrosis is not present, the patient will undergo Randomisation 2. If randomised to no study follow up (Group D), the patient will be aware they do not have mid-wall fibrosis and will have no further follow up in the study.

However if patients are allocated to routine care groups (B or C) the patient and clinical team will simply be told that they have been allocated routine care and not informed if they are in group B or C. Groups A, B and C will have the same follow up which will maintain patient blinding in groups B and C.

The clinical care team will also remain blinded to the cardiac MRI result and allocation to routine care groups ensuring that the presence or absence of fibrosis does not influence clinical decision-making. The cardiac MRI scans will be reviewed centrally prior to enrolment. Any clinically significant cardiac findings that would prevent enrolment or influence patient management will be made available to the clinical team.

This includes but is not limited to:

- Impaired LV ejection fraction <50%
- Intracardiac thrombus
- Intracardiac or extracardiac malignancy
- Significant valve disease not appreciated on echocardiography (e.g. severe eccentric aortic regurgitation)
- Significant aortic pathology likely to require surgical repair.

Any local reporting of the cardiac MRI back to the clinical care team should be limited to non-cardiac findings and should specifically not report on the presence or absence of mid-wall fibrosis.

5.5.5 Withdrawal of Study Participants

Participants are free to withdraw from the study at any point or a participant can be withdrawn by the investigator, but participants are not required to withdraw solely because they have been non-adherent with the randomised treatment or follow up

plan. If withdrawal occurs, the nature and reason for withdrawal will be documented on a change of status form. Any data collected until this point will be retained and analysed unless the participant specifically withdraws consent for this. Participants will be followed up for the primary outcome according to group allocation regardless of their adherence to treatment strategy, unless they withdraw their consent for this.

If a participant, who has given informed consent, loses capacity to consent during the study they should be withdrawn. Identifiable data or tissue already collected with consent can be retained and used in the study. No further data or tissue should be collected or any other research procedures carried out on or in relation to the participant.

Projected dropout of participants is accounted for in the sample size calculation and therefore withdrawn participants will not be replaced.

6 STUDY ASSESSMENTS

6.1 SCREENING ASSESSMENTS

See section 5.3 for details of screening.

6.2 BASELINE ASSESSMENTS

Patients at *higher-risk* of mid-wall myocardial fibrosis on screening tests will be invited back to attend for baseline assessments, where the following investigations will then take place. At ECG-only sites the screening and baseline assessments may be performed at the same visit.

1. **Relevant medical history**
    - Data on medical history, risk factors and current medication will be collected.

2. **Height and weight**
    - The patient's height and weight will be recorded.

3. **Blood pressure measurement**
    - This should be taken using an appropriately sized arm cuff and performed and recorded three times, with the average of the final two readings used to determine eligibility. If the 1st reading shows severe hypertension (systolic BP >180 mmHg or diastolic BP >110 mmHg) the patient should be instructed to lie down in a quiet room for 5 minutes before the 2nd and 3rd BP measurements are performed.

4. **Urine pregnancy test**
    - This is only required if the participant thinks there is a chance they could be pregnant. Given the age of the study population it is unlikely that this will be required.

5. **Edmonton Frail Scale (EFS)**
    - The Edmonton Frail Scale is a brief, valid and reliable tool for measuring frailty, consisting of nine domains and eleven items.

6. **New York Heart Association Functional Classification**

7. **WHODAS, 12-item version**

8. Phlebotomy

- Approximately 20 ml of venous blood will be taken using standard venepuncture equipment **(optional).** This sample will be spun and processed locally for both serum and plasma then frozen below -70°C for future analysis.
- In addition, 10ml venous blood will be taken and stored below -70^{o}C for future genetic analysis **(optional)**.
- Explicit informed consent will be sought for these samples. Provision and/or collection of these samples are optional at both a site and patient level.
- If a site is acquiring the optional T1 mapping cardiac MRI sequences then a further 4.9ml EDTA sample is required to perform haematocrit measurements. This is required in the calculation of the extracellular volume fraction. This sample should be taken on the same day as the cardiac MRI scan.

9. Echocardiogram

- If a clinical echocardiogram report is available from within the previous 6 months then this result can be used for the trial. If not, a standard transthoracic echocardiogram will be performed. The minimum requirement for reporting is:
    i. Aortic valve peak velocity (continuous wave Doppler)
    ii. Mean aortic valve gradient
    iii. Aortic valve area (calculated using continuity equation)
    iv. An assessment of LV systolic function (visual estimation or Simpson's biplane calculation if available)

10. Cardiac Magnetic Resonance Imaging

- Either a 1.5 or 3 tesla (T) MRI scanner will be used according to local availability at the research site. More details regarding technical aspects of the scan are contained within the standardised cardiac MRI scanning guidance. Sites should ensure that there are no absolute contraindications to cardiac MRI before proceeding.
- The cardiac MRI will include late gadolinium enhancement imaging, performed 10-15 min following the administration of gadolinium based contrast agent. Full details can be found in the cardiac MRI scanning guidance.
- The cardiac MRI scan will usually take place at the same time as baseline assessment but can take place on a separate visit if necessary. If the optional T1 mapping sequences are being acquired then a plasma EDTA sample is required on the day of the scan to enable calculation of T1 mapping measures.
- Should the cardiac MRI scan be non-diagnostic then it can be repeated at the investigator's discretion.

6.3 FOLLOW UP ASSESSMENT

Participants in Groups A, B and C will have annual study follow up (linked to the date of randomisation). This will consist of:

1. Annual contact with patient

Participants will be contacted by telephone annually to assess for symptoms or events. At each annual contact NYHA functional classification will be assessed and the WHODAS 2.0 (12-item version) completed. If telephone follow up is unsuccessful, other methods of collecting this information (such as routine clinic appointment, post, email) are acceptable.

2. Medical record review

Participant medical records should be reviewed at least annually to check for study events that require central reporting, however if research teams become aware of an event it should be reported contemporaneously. The following events should be reported until completion of study follow up:

- Death
- Hospitalisation for syncope, heart failure, chest pain or arrhythmia (ventricular arrhythmia or second or third degree heart block)
- Routine echocardiograms
- Stroke
- Insertion of a permanent pacemaker, cardiac resynchronisation therapy device or an automated implantable cardioverter defibrillator
- Endocarditis

It is anticipated that annual follow up will be conducted until 2020. If the event rate is lower or the study needs to be extended then participants will be asked if they are happy to be contacted beyond this date. This will be discussed when the participant consents to take part in the study so written informed consent will not be required to extend follow up.

Long-term follow up of participants will be facilitated by data linkage. Consent will be sought for this.

6.4 AORTIC VALVE INTERVENTION

Patients undergoing aortic valve intervention (regardless of treatment group allocation) will have data collected on post-operative complications within 30 days of surgery. This will be achieved by retrospective examination of participant records.

Table 6—1: Schedule of Assessments

	Screening[1]	Baseline	Surgery	Annually
Informed consent - screening[2]	X			
hsTnI	X[3]			
ECG	X[4]			
eGFR	X[5]			
Demographics	X[6]			
Informed consent – study[2]		X		
Relevant medical history		X		
Height and weight		X		
BP measurement		X		
Urine pregnancy test		X[7]		
Edmonton Frail Scale		X		
NYHA classification		X		X
WHODAS 2.0		X		X
Phlebotomy		X		
Echocardiogram		X[8]		
Cardiac MRI		X		
Inclusion/exclusion criteria		X		
Surgery details & post-operative complications			X	
Annual participant contact				X
Medical record review				X

[1] When screening with ECG only, the screening and baseline assessments may be performed at the same visit
[2] When screening with ECG only, the consent process is simplified to a single consent step
[3] Using Abbott ARCHITECT$_{STAT}$ platform. When screening at ECG only sites, a serum blood sample should be taken and frozen to allow for a retrospective analysis of hsTnI centrally.
[4] If the participant's most recent ECG is within 6 months of screening and is interpretable then there is no requirement to repeat this
[5] If the participant's most recent eGFR result is ≥30 mL/min/1.73 m^2 and within 12 months of screening then there is no requirement to repeat this unless the investigator makes a clinical judgment that a more contemporary result is needed
[6] Demographic data will include a unique identifying number (i.e. CHI or NHS number) for future record linkage
[7] This is only required if the participant thinks there is a chance they could be pregnant.
[8] If the participant's most recent echocardiogram is within 6 months of baseline and the minimum reporting criteria have all been measured then is no requirement to repeat this

7 DATA COLLECTION

Data will be collected from consent until final follow up visit. Site-specific source data plans will be created to indicate where protocol required information will be originally documented. Source data worksheets created by the Edinburgh Clinical Trials Unit (ECTU) will be made available but their use is optional.

Study data will be entered onto an eCRF (case report form) developed by ECTU. Data collected as part of the central cardiac MRI review and endpoint adjudication will be entered directly onto the eCRF.

8 STATISTICS AND DATA ANALYSIS

8.1 SAMPLE SIZE CALCULATION

We expect the proportion of primary outcome events (all-cause mortality or unplanned AS-related hospitalisation) to be 25% in the routine care arm of the study, and 13.4% in the early intervention arm (a hazard ratio of 2), over 2 years of follow up (Dweck et al 2011, RBH cohort). We aim to recruit 1000 participants to be screened with cardiac MRI for evidence of LV decompensation (mid-wall fibrosis). We would expect this to result in 400 patients with mid-wall fibrosis being randomised (1:1). Using a logrank approach, we will need to observe 88 primary outcome events to give us 90% power at 5% significance level. We will follow participants up for as long as possible before the end of study, and thus participants will have between 2 and 3.5 years of follow up, and we expect mean follow up to be 2.75 years. We are likely to reach 88 events when we have recruited 356 participants (slightly more allowing for drop-out).

For further calculations we have assumed that our optimal hsTnI threshold will be ~6 ng/L. This is based upon our preliminary troponin data to date, which demonstrated that 62% of patients with an aortic valve peak velocity ≥4.0 m/s had a troponin >6.0 ng/L. Of these patients, 42% had mid-wall fibrosis on cardiac MRI. On this basis, we will therefore need to screen approximately 1600 patients to identify 1000 patients for cardiac MRI in order to recruit our target of 400 patients with mid-wall fibrosis.

At the time that the required amount of data for the primary analysis of the 2 groups with mid-wall fibrosis has accrued, we should have 90% power to detect a difference in the all-cause mortality between the 2 groups who do not receive early surgery of 15% vs 29% (log rank test, p=0.05, 2 sided test)

8.2 PROPOSED ANALYSES

The primary outcome is defined as first event of all-cause mortality or unplanned AS-related hospital admission, and the primary comparison will be between group A and group B. Time to primary outcome is defined as time from randomisation to primary outcome. Patients withdrawing consent for their data to be collected prospectively prior to reaching primary outcome will have their time to primary outcome censored at the last contact date. The relationship between intervention and the primary outcome will be analysed using Cox proportional hazard regression adjusted for the minimisation variables used in the randomisation algorithm. The results will be expressed as a hazard ratio with the corresponding 95% confidence intervals and 2-sided p-value (which will be considered statistically significant if it is ≤0.05). The individual elements of the composite primary outcome will be reported separately. There are no planned subgroup analyses.

Secondary outcomes will be analysed using appropriate methods: Cox proportional hazards regression for time-to-event outcomes, logistic regression for binary outcomes and linear regression for normally distributed continuous outcomes, adjusted as

described above. Continuous outcomes that are not normally distributed will be analysed using appropriate nonparametric techniques. Secondary outcomes will be presented for groups A, B and C. A first set of secondary analyses will compare groups A and B, and a second set of secondary analyses will compare groups B and C.

For the purpose of analysis, we will retain participants in the treatment groups to which they were originally assigned irrespective of the treatment actually received. Every effort will be made to minimise missing data, analysis will be a complete case analysis. If there is a sufficient level of missing data for it to affect our conclusions, a multiple imputation analysis will be undertaken, using clinically appropriate variables, as a sensitivity analysis. A full statistical analysis plan will be written during the trial, and finalised prior to database lock.

9 ADVERSE EVENTS

The Investigator, or a delegated researcher, is responsible for the detection and documentation of adverse events that may be related to participating in the study and that meet the criteria and definitions detailed below.

9.1 DEFINITIONS

An **adverse event** (AE) is an untoward medical occurrence in a study participant.

An **adverse reaction** (AR), in the context of this study, is any untoward and unintended response which is related to any dose of gadolinium based contrast agent administered to that participant.

A **serious adverse reaction** (SAR) is any AR that:

- results in death of the clinical trial participant; is life threatening*;
- requires in-patient hospitalisation^ or prolongation of existing hospitalisation;
- results in persistent or significant disability or incapacity;
- consists of a congenital anomaly or birth defect;
- results in any other significant medical event not meeting the criteria above.

A **suspected unexpected serious adverse reaction** (SUSAR) is any AR that is classified as serious and is suspected to be caused by the gadolinium contrast agent, that it is not consistent with the information in the Summary of Product Characteristics (SPC).

*Life-threatening in the definition of an SAE or SAR refers to an event where the participant was at risk of death at the time of the event. It does not refer to an event which hypothetically might have caused death if it were more severe.

^Any hospitalisation that was planned prior to randomisation will not meet seriousness criteria. Any hospitalisation that is planned post randomisation will meet the seriousness criteria unless it does not constitute an untoward medical occurrence (e.g. cosmetic elective surgery, social and/or convenience admission, etc.).

9.2 IDENTIFYING AEs AND ARs

All AEs and ARs will be identified from the time a participant signs the consent form to take part in the study until the completion of study follow-up.

9.3 RECORDING AEs AND ARs

AEs, including post-operative complications, potential aortic stenosis related hospitalisations, and mortality, will be recorded as part of the outcome measures in the study CRF. There is no requirement to complete an additional AE form.

When an AE occurs, it is the responsibility of the Investigator to review all documentation (e.g. hospital notes, laboratory and diagnostic reports) related to the event. To the extent the CRF permits, the Investigator will record relevant safety information in the CRF.

Any adverse reaction (AR) to gadolinium contrast that meets seriousness criteria (see section 9.1) will be recorded and reported in the study CRF and will also be recorded on an ACCORD SAE form, which will then be sent to the Sponsor via email (safety@accord.scot).

Pre-existing medical conditions (i.e. existed prior to informed consent) should be recorded as medical history and only recorded as AEs/ARs if medically judged to have unexpectedly worsened during the study. Events that are consistent with the expected progression of underlying disease should not be recorded as adverse events.

9.4 ASSESSMENT OF AEs, SAEs, ARs, SARs and SUSARs

Seriousness, causality, severity and expectedness will be assessed by the PI.

The Investigator is responsible for assessing each adverse event. The CI may not downgrade an event that has been assessed by an Investigator as a SAR or SUSAR, but can upgrade an AR to a SAR or SUSAR if appropriate.

9.4.1 Assessment of Causality

The Investigator will make an assessment of whether an AE is likely to be related to the administration of gadolinium (and therefore be considered an AR) according to the definitions below.

- Unrelated: Where an event is not considered to be related to the administration of gadolinium.
- Possibly Related: The nature of the event, the underlying medical condition, concomitant medication or temporal relationship make it possible that the AE has a causal relationship to the administration of gadolinium in this study.

9.4.2 Assessment of Seriousness

Subsequent to the assessment causality, the Investigator will make an assessment of seriousness as defined in Section 9.1.

9.4.3 Assessment of Severity

The Investigator will make an assessment of severity for each SAR, and record this on the ACCORD SAE form according to one of the following categories:

Mild: an event that is easily tolerated by the participant, causing minimal discomfort and not interfering with every day activities.
Moderate: an event that is sufficiently discomforting to interfere with normal everyday activities.
Severe: an event that prevents normal everyday activities.

Note: the term ‘severe’, used to describe the intensity, should not be confused with ‘serious’ which is a regulatory definition based on participant/event outcome or action criteria. For example, a headache may be severe but not serious, while a minor stroke is serious but may not be severe.

9.4.4 Assessment of Expectedness of SARs

The Investigator will make an assessment of expectedness of any SARs identified following gadolinium administration. The assessment will be based upon the reference safety information available in the most current version of the Summary of Product Characteristics (SPC) for the gadolinium-based contrast agent dosed.

9.5 REPORTING OF SARs/SUSARs

As this trial is a non-CTIMP and involves procedures and interventions that are very well established in the medical community, with extensive information available regarding risks, only serious adverse reactions (SARs) and Suspected Unexpected Serious Adverse Reactions (SUSARs) related to Gadolinium administration, will be onward reported to the Sponsor.

Once the Investigator becomes aware that a gadolinium related SAR/SUSAR, has occurred in a study participant, the information will be reported to the ACCORD Research Governance & QA Office within 24 hours. If the Investigator does not have all information regarding an event, they should not wait for this additional information before notifying ACCORD. The ACCORD SAE report form will be used to submit the event report, and can be updated when the additional information is received.

The SAE form will be transmitted by fax to ACCORD on +44 (0)131 242 9447 or may be submitted by hand to the office or sent via email to Safety.Accord@ed.ac.uk. Only forms in a pdf format will be accepted by ACCORD via email.

Where missing information has not been sent to ACCORD after an initial report, ACCORD will contact the investigator and request the missing information.

All reports sent to ACCORD and any follow up information will be retained by the Investigator in the Investigator Site File.

9.6 REPORTING REQUIREMENTS

The ACCORD Research Governance & QA Office is responsible for pharmacovigilance reporting on behalf of the co-sponsors (Edinburgh University and NHS Lothian).

The Trial Manager will provide the ACCORD Research Governance & QA Office with quarterly safety reports based on the data collected on the CRF.

9.7 FOLLOW-UP PROCEDURES

After initially reporting a gadolinium related SAR/SUSAR, the Investigator will follow each participant until resolution or the completion of study follow-up. Follow-up information will be reported to the ACCORD office.

10 TRIAL MANAGEMENT AND OVERSIGHT ARRANGEMENTS

10.1 TRIAL MANAGEMENT GROUP

ECTU will be responsible for trial management including: organisation of management group meetings, organisation of the steering committee, contracting with other organisations, preparation of REC and R&D applications, standard operating procedures, provision of the randomisation system, database development, data management, and data analysis.

The trial will be led by Christopher Tuck and coordinated by ECTU. An informal project management group (PMG) comprising the Chief Investigator, Research Fellow and relevant members of the ECTU team will be formed. The Academic and Clinical Central Office for Research & Development (ACCORD) in Edinburgh will provide Sponsorship and monitoring oversight for the project and the trial will be conducted in line with the relevant Sponsor SOPs which are available on the Sponsor website.

A Delegation Log will be prepared for each site, detailing the responsibilities of each member of staff working on the trial.

10.2 TRIAL STEERING COMMITTEE

A Trial Steering Committee (TSC) will be established to oversee the conduct and progress of the study. The terms of reference of the Trial Steering Committee, and the names and contact details are detailed in the TSC charter.

10.3 DATA MONITORING COMMITTEE

As this trial involves procedures and interventions that are very well established in the medical community, with extensive information available regarding risks, it was felt that a Data Monitoring Committee is not required.

10.4 INSPECTION OF RECORDS

Investigators and institutions involved in the study will permit trial related monitoring and audits on behalf of the sponsor and REC review. In the event of an audit or monitoring, the Investigator agrees to allow the representatives of the sponsor direct access to all study records and source documentation.

10.5 ENDPOINT ADJUDICATION

Two independent investigators who are blinded to randomisation details will be asked to adjudicate AS-related hospitalisation events from a review of the medical records (relevant sections of the medical records will be anonymized and uploaded to the study database). In the event of disagreement, the opinion of a third independent reviewer will be sought. Causes of death will be established from the death certificate.

11 GOOD CLINICAL PRACTICE

11.1 ETHICAL CONDUCT

The study will be conducted in accordance with the principles of Good Clinical Practice (GCP).

A favourable ethical opinion will be obtained from the appropriate REC and local R&D approval will be obtained prior to commencement of the study.

11.2 INVESTIGATOR RESPONSIBILITIES

The PI is responsible for the overall conduct of the study at the site and compliance with the protocol and any protocol amendments. In accordance with the principles of GCP, the following areas listed in this section are also the responsibility of the PI. Responsibilities may be delegated to an appropriate member of study site staff.

11.2.1 Informed Consent

The Investigator is responsible for ensuring informed consent is obtained before any protocol specific procedures are carried out. The decision of a participant to participate in clinical research is voluntary and should be based on a clear understanding of what is involved.

Participants must receive adequate oral and written information – appropriate Participant Information and Informed Consent Forms will be provided. The oral explanation to the participant will be performed by the Investigator or qualified delegated person, and must cover all the elements specified in the Participant Information Sheet and Consent Form.

The participant must be given every opportunity to clarify any points they do not understand and, if necessary, ask for more information. The participant must be given sufficient time to consider the information provided. It should be emphasised that the participant may withdraw their consent to participate at any time without loss of benefits to which they otherwise would be entitled.

The participant will be informed and agree to their medical records being inspected by representatives of the sponsor(s).

The Investigator or delegated member of the trial team and the participant will sign and date the Informed Consent Form(s) to confirm that consent has been obtained. The participant will receive a copy of this document, with the original filed in the Investigator Site File (ISF) and a copy in the participant's medical notes.

11.2.2 Study Site Staff

The Investigator must be familiar with the intervention, protocol and the study requirements. It is the Investigator's responsibility to ensure that all staff assisting with the study are adequately informed about the intervention, protocol and their trial related duties.

11.2.3 Data Recording

The Principal Investigator is responsible for the quality of the data recorded in the CRF at each Investigator Site. The source data plan identifies which source data correspond to CRF data and states which data are recorded directly into the CRF.

11.2.4 Investigator Documentation

Prior to beginning the study, each Investigator will be asked to provide particular essential documents to the ACCORD Research Governance & QA Office, including but not limited to:

- An original signed Investigator's Declaration (as part of the Clinical Trial Agreement documents);
- Curriculum vitae (CV) signed and dated by the Investigator indicating that it is accurate and current.

The ACCORD Research Governance & QA Office will ensure all other documents required by ICH GCP are retained in a Trial Master File (TMF), where required, and that appropriate documentation is available in local ISFs.

11.2.5 GCP Training

All members of staff involved in study specific activities are strongly encouraged to undertake GCP training in order to understand the principles of GCP.

11.2.6 Confidentiality

All laboratory specimens, evaluation forms, reports, and other records must be identified in a manner designed to maintain participant confidentiality. All records must be kept in a secure storage area with limited access. Clinical information will not be released without the written permission of the participant. The Investigator and study site staff involved with this study may not disclose or use for any purpose other than performance of the study, any data, record, or other unpublished, confidential information disclosed to those individuals for the purpose of the study. Prior written agreement from the sponsor or its designee must be obtained for the disclosure of any said confidential information to other parties.

11.2.7 Data Protection

All Investigators and study site staff involved with this study must comply with the requirements of the Data Protection Act 1998 with regard to the collection, storage,

processing and disclosure of personal information and will uphold the Act's core principles.

Computers used to collate the data will have limited access measures via user names and passwords.

Published results will not contain any personal data and be of a form where it does not identify individuals and re-identification is not likely to take place.

12 STUDY CONDUCT RESPONSIBILITIES

12.1 PROTOCOL AMENDMENTS

Any changes in research activity, except those necessary to remove an apparent, immediate hazard to the participant in the case of an urgent safety measure, must be reviewed and approved by the Chief Investigator.

Amendments to the protocol must be submitted in writing to the appropriate REC and local R&D for approval prior to participants being enrolled into an amended protocol.

12.2 PROTOCOL VIOLATIONS AND DEVIATIONS

Prospective protocol deviations, i.e. protocol waivers, will not be approved by the sponsors and therefore will not be implemented, except where necessary to eliminate an immediate hazard to study participants. If this necessitates a subsequent protocol amendment, this should be submitted to the REC and local R&D for review and approval if appropriate.

Protocol deviations will be recorded in a protocol deviation log and logs will be submitted to the Sponsor every 3 months. Each protocol violation will be reported to the sponsor within 3 days of becoming aware of the violation. All protocol deviation logs and violation forms should be emailed to QA@accord.scot.

12.3 STUDY RECORD RETENTION

All study documentation will be kept for a minimum of 3 years from the protocol defined end of study point. When the minimum retention period has elapsed, study documentation will not be destroyed without permission from the sponsor.

12.4 END OF STUDY

The end of study is defined as the time of database lock.

The Investigators and/or the trial steering committee and/or the co-sponsor(s) have the right at any time to terminate the study for clinical or administrative reasons.

The end of the study will be reported to the REC within 90 days, or 15 days if the study is terminated prematurely. The Investigators will inform participants of the premature study closure and ensure that the appropriate follow up is arranged for all participants involved.

A summary report of the study will be provided to the REC within 1 year of the end of the study.

12.5 INSURANCE AND INDEMNITY

The co-sponsors are responsible for ensuring proper provision has been made for insurance or indemnity to cover their liability and the liability of the Chief Investigator and staff.

- The following arrangements are in place to fulfil the co-sponsors' responsibilities:

- The Protocol has been designed by the Chief Investigator and researchers employed by the University and collaborators. The University has insurance in place (which includes no-fault compensation) for negligent harm caused by poor protocol design by the Chief Investigator and researchers employed by the University.
- Sites participating in the study will be liable for clinical negligence and other negligent harm to individuals taking part in the study and covered by the duty of care owed to them by the sites concerned. The co-sponsors require individual sites participating in the study to arrange for their own insurance or indemnity in respect of these liabilities.
- Sites which are part of the United Kingdom's National Health Service will have the benefit of NHS Indemnity.

13 REPORTING, PUBLICATIONS AND NOTIFICATION OF RESULTS

The protocol for this trial will be submitted for publication and the trial results will be submitted for publication even if this trial stops early. If successfully completed the main paper from this project will be submitted for publication in a leading international general medical journal.

The main outputs will be provided to guideline developing bodies (including NICE, SIGN and the European Society of Cardiology), key professional organisations (such as the College of Emergency Medicine) and patient representative organisations (such as the British Heart Foundation).

13.1 AUTHORSHIP POLICY

Ownership of the data arising from this study resides with the study team. On completion of the study, the study data will be analysed and tabulated, and a study report will be prepared in accordance with the funders requirements. The authors for this project are listed in the trial's writing committee and publication policy document.

13.2 PUBLICATION

The clinical study report will be used for publication and presentation at scientific meetings. Investigators have the right to publish orally or in writing the results of the study.

Summaries of results will also be made available to Investigators for dissemination within their centres (where appropriate and according to their discretion).

13.3 REPRODUCIBLE RESEARCH AND DATA SHARING

Following publication of the primary paper, a deidentified individual participant data set will be submitted to a data archive for sharing purposes. Access to the deidentified dataset will be under a controlled access model in line with ECTU policies at that time.

14 REFERENCES

1. Carabello, B. A. Introduction to aortic stenosis. *Circulation Research* **113,** 179–185 (2013).
2. Nkomo, V. T. *et al.* Burden of valvular heart diseases: a population-based study. *The Lancet* **368,** 1005–1011 (2006).
3. Dweck, M. R., Boon, N. A. & Newby, D. E. Calcific aortic stenosis: a disease of the valve and the myocardium. *Journal of the American College of Cardiology* **60,** 1854–1863 (2012).
4. Chin, C. W. L. *et al.* Markers of left ventricular decompensation in aortic stenosis. *Expert Review of Cardiovascular Therapy* **12,** 901–912 (2014).
5. Elmariah, S. Patterns of Left Ventricular Remodeling in Aortic Stenosis: Therapeutic Implications. *Curr Treat Options Cardio Med* **17,** 1–15 (2015).
6. Connolly, H. M. *et al.* Aortic valve replacement for aortic stenosis with severe left ventricular dysfunction. Prognostic indicators. *Circulation* **95,** 2395–2400 (1997).
7. Azevedo, C. F. *et al.* Prognostic Significance of Myocardial Fibrosis Quantification by Histopathology and Magnetic Resonance Imaging in Patients With Severe Aortic Valve Disease. *JACC* **56,** 278–287 (2010).
8. Dweck, M. R. *et al.* Midwall Fibrosis Is an Independent Predictor of Mortality in Patients With Aortic Stenosis. *Journal of the American College of Cardiology* **58,** 1271–1279 (2011).
9. Barone-Rochette, G. *et al.* Prognostic significance of LGE by CMR in aortic stenosis patients undergoing valve replacement. *Journal of the American College of Cardiology* **64,** 144–154 (2014).
10. Chin, C. W. L. *et al.* High-sensitivity troponin I concentrations are a marker of an advanced hypertrophic response and adverse outcomes in patients with aortic stenosis. *European Heart Journal* **35,** 2312–2321 (2014).
11. Shah, A. S. V. *et al.* Left ventricular hypertrophy with strain and aortic stenosis. *Circulation* **130,** 1607–1616 (2014).
12. Hicks, K. A. *et al.* 2014 ACC/AHA Key Data Elements and Definitions for Cardiovascular Endpoint Events in Clinical Trials: A Report of the American College of Cardiology/American Heart Association Task Force on Clinical Data Standards (Writing Committee to Develop Cardiovascular Endpoints Data Standards). *Journal of the American College of Cardiology* **66,** 403–469 (2015).
13. Peguero, J. G. *et al.* Electrocardiographic Criteria for the Diagnosis of Left Ventricular Hypertrophy. *Journal of the American College of Cardiology* **69,** 1694–1703 (2017).

APPENDIX A

Post-aortic valve intervention complications secondary endpoint

The following post aortic valve intervention complications should be recorded if they occur within 30 days of surgery:

- Death caused by an immediate complication of aortic valve intervention
- Reoperation for any reason (e.g. redo valve replacement, pericardial collection)
- Stroke
- Myocardial infarction
- Diagnosis of infective endocarditis
- Severe paravalvular regurgitation
- Valve thrombosis requiring treatment
- Major vascular complication
    - Access site injury leading to life-threatening bleeding, visceral ischaemia or neurological impairment
- Life threatening bleeding
    - Bleeding in a critical organ (e.g. intracranial, intraspinal, intraocular or intrapericardial requiring treatment)
    - Bleeding causing hypovolaemic shock
    - Drop in haemoglobin >5g/dL or ≥4 units blood transfused
- Wound dehiscence
- Permanent pacemaker implantation
- Still requiring renal replacement therapy at 30 days post surgery

APPENDIX B

Definition of Sudden Cardiac Death

Death that occurs unexpectedly and not within 30 days of an acute myocardial infarction (MI).

Note: Sudden cardiac death includes the following scenarios:

- Death witnessed and occurring without new or worsening symptoms
- Death witnessed within 60 min of the onset of new or worsening cardiac symptoms unless the symptoms suggest acute MI
- Death witnessed and attributed to an identified arrhythmia (e.g., captured on an electrocardiographic recording, witnessed on a monitor, or unwitnessed but found on ICD review)
- Death after unsuccessful resuscitation from cardiac arrest (e.g., ICD unresponsive sudden cardiac death, pulseless electrical activity arrest)
- Death after successful resuscitation from cardiac arrest and without identification of a specific cardiac or non-cardiac aetiology
- Unwitnessed death in a subject seen alive and clinically stable 24 hours before being found dead without any evidence supporting a specific non-cardiovascular cause of death (information about the patient's clinical status preceding death should be provided if available)
- Unless additional information suggests an alternate specific cause of death, if a patient is seen alive 24 hours before being found dead, *sudden cardiac death* should be recorded. For patients who were not observed alive within 24 hours of death, sudden cardiac death should not be recorded. (e.g., a subject found dead in bed but who had not been seen by family members for >24 h).

Adapted from Hicks, K. A. et al. 2014 ACC/AHA Key Data Elements and Definitions for Cardiovascular Endpoint Events in Clinical Trials: A Report of the American College of Cardiology/American Heart Association Task Force on Clinical Data Standards (Writing Committee to Develop Cardiovascular Endpoints Data Standards). Journal of the American College of Cardiology ***66,*** *403–469 (2015).*

Participant Information Sheet and Consent Form
Part A (screening)

The EvoLVed Trial

(Early Valve Replacement guided by Biomarkers of Left Ventricular Decompensation in Asymptomatic Patients with Severe Aortic Stenosis)

You are being invited to take part in screening for a research study. Before you decide whether or not to take part, it is important for you to understand why the research is being done and what it will involve. Please take time to read the following information carefully. Talk to others about the study if you wish. Contact us if there is anything that is not clear or if you would like more information. Take time to decide whether or not you wish to take part.

What is the purpose of the study?
We are doing this study to find out if replacing heart valves earlier in patients with heart narrowing (severe **aortic stenosis**) reduces the chance of the heart failing in the future and helps people to live longer.

Why have I been asked to take part?
You have been asked to take part as you have been previously diagnosed with severe aortic stenosis but do not have symptoms (such as shortness of breath, chest pain or fainting) related to your narrowed valve. At the moment, doctors aren't sure when the best time to replace your valve is – normally we would wait until you have symptoms from your valve before sending you to a surgeon for a valve replacement. Having these symptoms suggests that the heart is struggling to cope with the valve narrowing, but it can be hard to know if these symptoms are from your valve or for another reason.

Some doctors think we would get better results by operating earlier. By doing a heart scan (**MRI**) we can see if there is scarring in the heart, an early sign that the heart is struggling to work properly. Although we don't know yet, replacing the valve when there is scarring but before symptoms develop could lower the chance of the heart failing in the future and help people to live longer. This trial will see which is better - replacing the valve when you have no symptoms but have heart scarring, or replacing the valve when you start to have symptoms.

Before inviting you to take part in the main study and have the MRI scan we need to do some simple tests to see if you are suitable.

Do I have to take part?
No, it is up to you to decide whether or not to take part. If you do decide to take part you will be given this information sheet to keep and be asked to sign a consent form. If you decide to take part you are still free to withdraw at any time and without giving

a reason. Deciding not to take part or withdrawing from the study will not affect the healthcare that you receive, or your legal rights.

What will happen if I take part?
If you decide to take part, you will be invited to confirm your consent in writing by a member of the research team and complete the following screening tests:

- An **ECG** (electrical tracing of the heart using sticky pads). You will only need to do this if you have not had one done in clinic recently.
- A **blood sample**. This will measure the amount of **troponin**, a protein found in heart muscle. We will also use this sample to test your kidney function. This is checked in case you decide to proceed with the main trial as people with poor kidney function cannot receive a special injection that highlights heart scarring.

We do these tests as we have found that a combination of troponin blood test and ECG is good at identifying people who are at lower risk of having heart scarring so we only have to invite those at higher risk of scarring to come back and have an MRI.

What happens following the results of the screening tests?
If the screening tests show you are at lower risk of having heart scarring you will not need any more tests as part of the study. We will contact you to let you know and you will continue to have your follow up with your cardiologist as you would normally.

If the screening tests suggest you are at higher risk of having heart scarring, we will we will contact you to inform you of this. A second information sheet (Part B) containing further details regarding the EVoLVeD trial will have been given to you after your screening tests to read at your leisure. We will offer you an appointment to come and discuss these results in detail and take part in the EVoLVeD trial if you wish.

Undertaking these screening tests may result in us noticing something that could be important to your health. If so, we will contact you to explain what was noticed and support you with information regarding where to go for further advice.

What if there is a problem?
If you have a concern about any aspect of this study please contact Dr Russell Everett on his mobile phone (07736 927507) or via email (russell.everett@ed.ac.uk) who will do their best to answer your questions.

In the unlikely event that something goes wrong and you are harmed during the research and this is due to someone‘s negligence then you may have grounds for a legal action for compensation against your hospital but you may have to pay your legal costs. The normal National Health Service complaints mechanisms will still be available to you (if appropriate).

If you wish to make a complaint about the study please contact **NHS Lothian:**

Patient Experience Team, NHS Lothian
2nd Floor, Waverley Gate, 2-4 Waterloo Place, Edinburgh, EH1 3EG
Tel: 0131 536 3370 Email: feedback@nhslothian.scot.nhs.uk

What happens when the study is finished?
Your study data will be stored indefinitely in a secure manner with access restricted to the research team. With your consent, we will periodically ask central NHS registers to provide information on your health status (you will not be contacted directly for this). This is because it will enable us to find out about any longer-term consequences of aortic stenosis and heart scarring. To help us identify you correctly, we will need to collect your unique patient identifier (CHI number or NHS number) and store it at the University of Edinburgh.

At the end of the study we will make the study data available for other researchers to look at. Before we make it available we will make sure it does not contain any of your personal data.

What will happen to the results of the study?
Once we have completed the study and analysed the results, we will write a paper, which will be submitted for publication in one of the medical journals. You will not be identifiable in any published results. We do not routinely contact participants to inform them of the outcome of the research but once the study has been published a summary of the findings will be available on the Edinburgh Clinical Trials website (http://www.ed.ac.uk/edinburgh-clinical-trials).

Who is organising the research and why?
The study is being sponsored by the University of Edinburgh and NHS Lothian and is being funded by the Sir Jules Thorn Charitable Trust. Your doctors will not be paid for including you in this study.

Who has reviewed the study?
The study proposal has been reviewed by the funder and the Sponsor. All research in the NHS is looked at by an independent group of people, called a Research Ethics Committee. A favourable ethical opinion has been obtained from South East Scotland Research Ethics Committee. NHS management approval has also been obtained.

Will my taking part in the study be kept confidential?
All the information we collect during the course of the research will be kept confidential and there are strict laws which safeguard your privacy at every stage. In the unlikely event that you lose capacity and cannot continue to give consent, no new data would be collected but we would keep any data we have already.

Study researchers will need access to your medical records and data to carry out this research. Information will be stored on secure university/NHS computers, or locked away in secure rooms with restricted access. Access to personal identifiable information will be restricted to the research team.

To ensure that the study is being run correctly, we will ask your consent for responsible representatives from the Sponsor and NHS Institution to access your medical records and data collected during the study, where it is relevant to you taking part in this research. The Sponsor is responsible for overall management of the study and providing insurance and indemnity.

If you have any further questions about the study please contact Dr Russell Everett on his mobile (07736 927507) or via email (russell.everett@ed.ac.uk).

Thank you for taking the time to read this information sheet.

The EVoLVeD trial at a glance

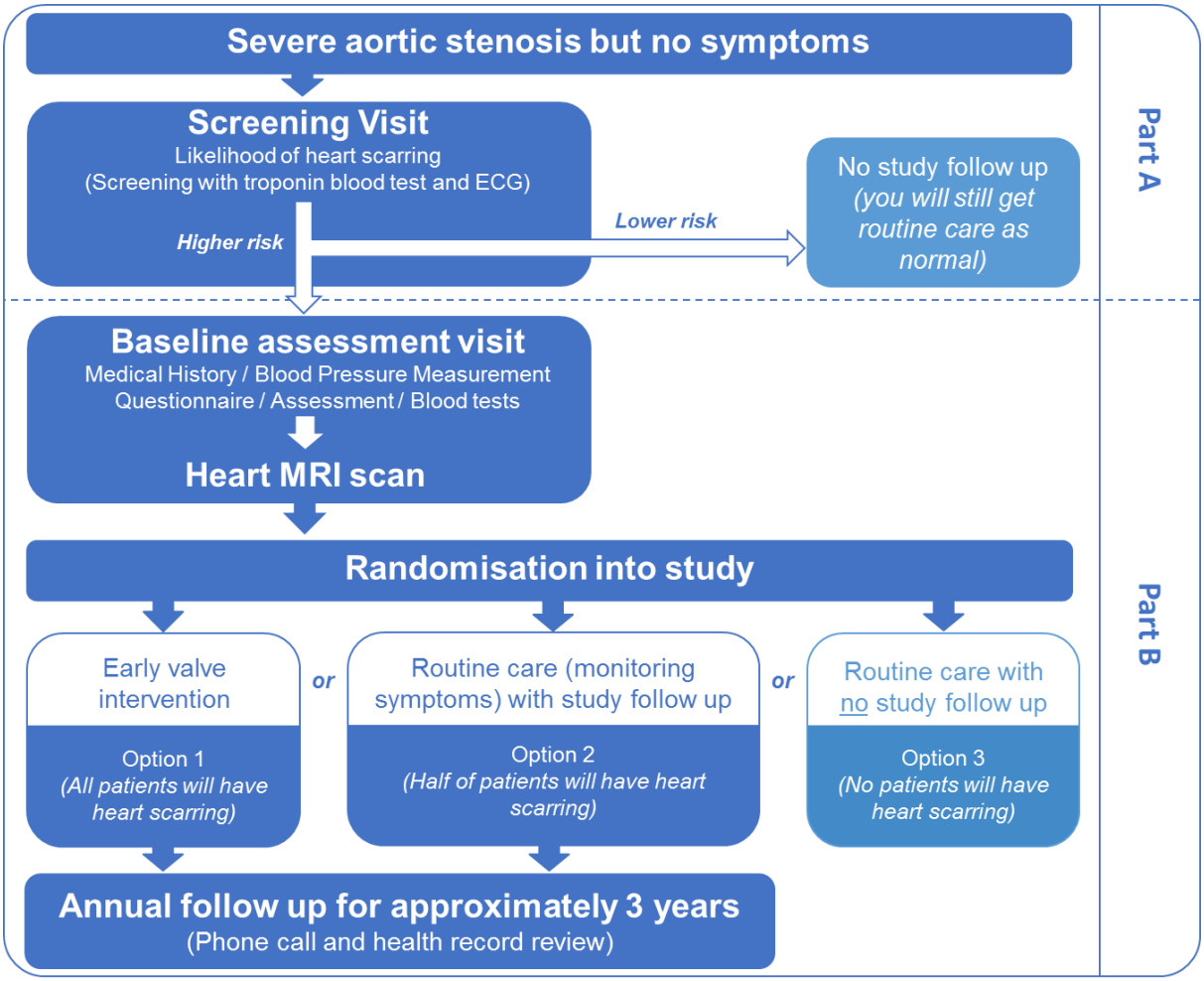

SCREENING CONSENT FORM FOR THE EVOLVED TRIAL

Name of Researcher (PI):	Dr Russell Everett
Site:	Edinburgh (NHS Lothian)
Patient Trial Number:	

Please **initial** each box

1. I confirm that I have read and understand the information sheet (as specified in this document header) for the above study and have had the opportunity to consider the information and ask questions. ☐
2. I understand that my participation is voluntary and that I am free to withdraw at any time, without giving any reason, without my medical care or legal rights being affected. ☐
3. I understand that relevant sections of my medical notes and data collected during the study may be looked at by individuals from the Sponsor, from the NHS organisation or other authorities, where it is relevant to my taking part in this research. I give permission for these individuals to have access to my records. ☐
4. I give permission for my Community Health Index (CHI) or NHS number to be collected and passed to the University of Edinburgh and its Clinical Trials Unit ☐
5. I understand that information held and managed by central UK NHS bodies and NHS Trusts may be used in order to provide information about my health status during and after the study. To do this, I understand that my information will be shared with those bodies. ☐
6. I agree to my data/tissue being used for future ethically approved studies ☐
7. I agree to be screened for the above study ☐

Name of Patient	Signature	Date
Name of Person taking consent	Signature	Date

Original – to Investigator Site File. *First Copy – to participant.* *Second Copy – to hospital notes.*

Participant Information Sheet and Consent Form
Part B (main study)

The EvoLVed Trial

(Early Valve Replacement guided by Biomarkers of Left Ventricular Decompensation in Asymptomatic Patients with Severe Aortic Stenosis)

You are being invited to take part in a research study. Before you decide whether or not to take part, it is important for you to understand why the research is being done and what it will involve. Please take time to read the following information carefully. Talk to others about the study if you wish. Contact us if there is anything that is not clear or if you would like more information. Take time to decide whether or not you wish to take part.

This section of the information sheet follows on from Part A and details what will happen if the screening tests were to find you to be at **higher risk of having heart scarring**. Just because you agreed to take part in the screening does not mean you have to take part in the main study.

What will happen if I take part?
If you decide to take part in the main study, you will be invited to confirm your consent in writing by a member of the research team and attend for the following **baseline assessments**. These assessments will take about 2 to 3 hours (including the MRI scan).

Medical history. We will ask you about your medical history and any symptoms you have. We will also find out what medications you're on.

Blood pressure measurement. This will be performed three times with an automatic cuff.

Questionnaire and Assessment. We will ask you to fill in a short questionnaire and do a 5 minute assessment to get an idea of any symptoms you may have and if you are limited in your day-to-day life.

Blood tests. We will take up to approximately 40ml (8 teaspoons) of blood. We would like to freeze and store some of your blood for future research into heart disease, although you can decide that you would prefer us not to do this.

Echocardiogram (heart ultrasound scan). This will need to be repeated if you have not had a recent scan in clinic.

If you are safe to enter the study we will then perform a heart scan (**MRI**) to confirm the presence of heart scarring:

This will take place at **Clinical Research Imaging Centre** next to the Edinburgh Royal Infirmary**.** We will do our best to perform this scan when you attend for your baseline assessments however if the scanner is particularly busy we may have to invite you back on a separate day for this scan.

The scanner itself involves a strong magnet and uses a combination of magnetic fields and radio waves to create extremely detailed pictures of the heart. No radiation is used and the scan is extremely safe. People who have certain types of metal in their bodies shouldn't enter the magnetic field (e.g. if you have previously had metal fragments in your eyes). It may mean you cannot take part in the study. Most orthopaedic implants (such as hip and knee replacements) are completely safe as are heart artery stents if they were implanted more than 6 weeks before the scan date. It is however usually unsafe to scan patients with pacemakers.

A small plastic tube (cannula) will be inserted into a vein in the arm and you will lie in the scanner for approximately 45 minutes. The scanning tunnel itself is relatively narrow, but you will be given headphones to listen to music during the scan if you wish, and you will also be able to directly speak to the radiographers performing the scan. If you suffer from sever claustrophobia you should discuss this with the research team before agreeing to take part. During the scan you will be asked to hold your breath for several seconds at a time in order to obtain better images. You will also receive an injection of a special dye (gadolinium contrast), which highlights if any heart scarring is present. The contrast itself is extremely safe.

Please let one of the research team know if you have any concerns regarding this scan.

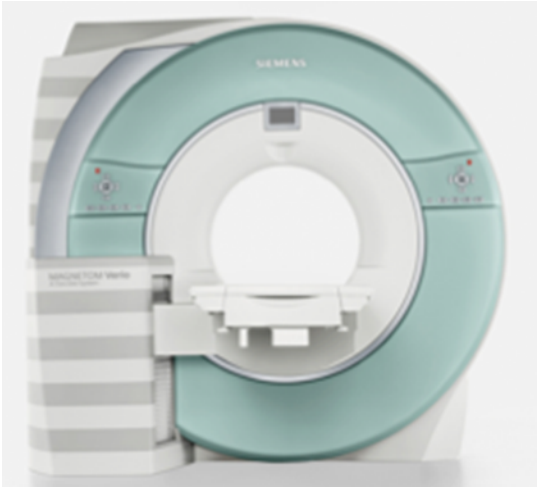	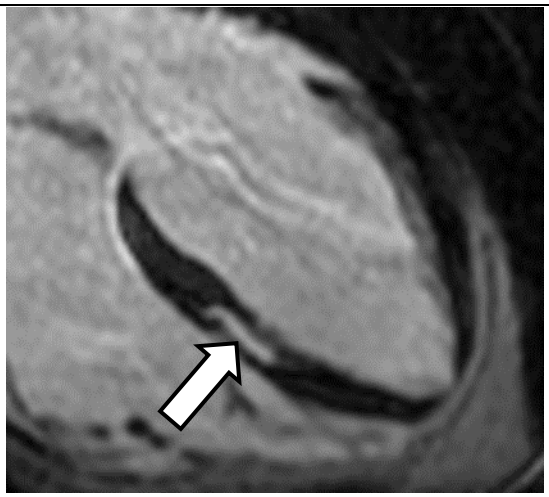
Example MRI scanner	Heart MRI images with white area of heart scarring present (arrow) in the otherwise healthy black heart muscle

Following the baseline assessments, you will be allocated to one of 3 options:

Option 1: *Early Valve Intervention*

You will be referred to a heart surgeon who will assess you for early valve replacement surgery. The surgeon will discuss in detail your options for surgery and any questions you may have. You will only be referred for early valve intervention if the MRI shows that you have heart scarring.

We will also contact you annually as part of the study (see the ***How will I be followed up?*** section).

Option 2: *Routine Clinical Care (with study follow up)*

You will continue to undergo routine follow up with your regular cardiologist. Any decision for heart valve surgery in the future will be based on normal NHS guidelines. This option will contain a mix of people – some will have heart scarring and others will not.

We will also contact you annually as part of the study (see the ***How will I be followed up?*** section).

Option 3: *Routine Clinical Care (without study follow up)*

If allocated to this group, you will continue to be followed up by your regular clinical cardiology team as usual. However you will have no further follow up as part of the EVoLVeD study. Any decision for heart valve surgery in the future will be based on normal NHS guidelines.

You will only allocated this option if the MRI showed you have no heart scarring.

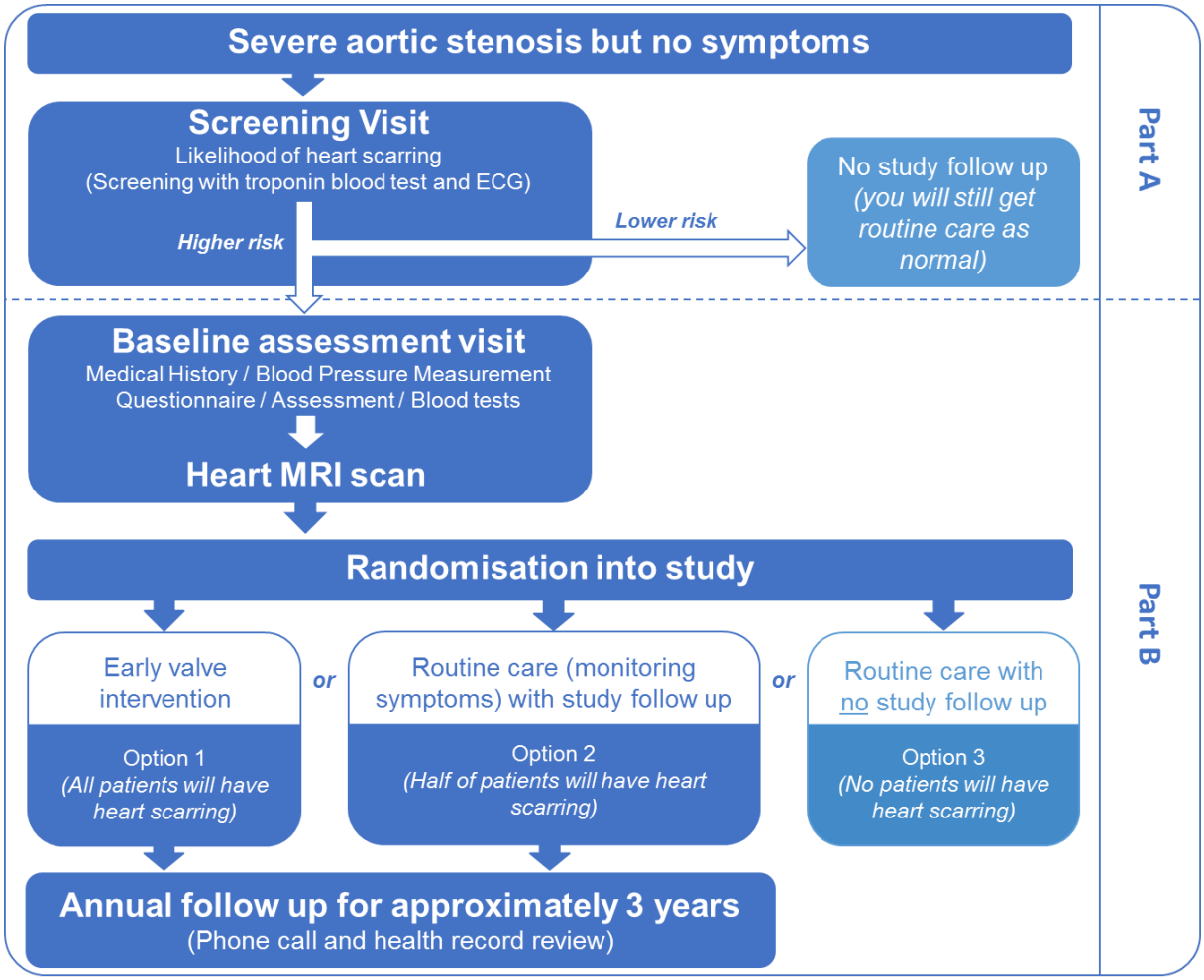

How will my treatment be decided?

Sometimes we don't know the best way to treat patients. To find out, we need to compare different treatments. We put people into groups and give each group a different treatment. The results are compared to see if one is better. To try to make sure the groups are the same to start with, each patient is put into a group by chance (randomly).

In this study, if you have heart scarring you will be randomised to either option 1 or 2. You have an equal chance of getting either option.

If you don't have heart scarring you will be randomised to option 2 or 3. You are twice as likely to be allocated option 3 as option 2.

If you are allocated option 2, neither you nor your doctor will know if you have scarring on your heart. This is known as **blinding**. This is used in all randomised trials wherever possible to make sure the study is fair.

How will I be followed up?

If you are allocated to option 1 or 2, we will phone you as part of the study every year

until the end of the study (approximately 3 years but a maximum of 5 years). This will involve a short discussion about your general health, any symptoms you may have had and we will complete a questionnaire with you. This should take about 10 minutes in total. We will also check your health records for any hospital admissions or new medical problems you may have developed.

If we have to contact you for more than 3 years we will discuss this at one of your study follow up visits and ask for your permission then.

What are the possible benefits of taking part?
You might benefit from the additional procedures and investigations that you will have as part of the study. This will include more contact with medical staff and heart imaging tests that might identify other important problems in the heart or outside the heart that were not previously known about.

What are the possible disadvantages and risks of taking part?
It is not thought that there are many disadvantages. The MRI scanner takes detailed images of a small area of your chest so there is a small chance that we will find another abnormality in this area. If these require further assessment we will let you and your GP know and arrange for you to see a specialist for any further tests that are required. Usually these abnormalities turn out to be of no significance to your health, but they may cause you stress and anxiety whilst they are being investigated.

Valve surgery is generally very successful but, like any other surgery, it is not risk-free. There is a small risk of having a heart attack or stroke, or dying, either during or soon after the operation. Your risk will depend on your age and your current state of health. There are also small risks of living with a replacement heart valve, such as infection, and some types of heart valve wear out gradually over time. Before you agree to take part in the study you should discuss with the research team the risks of surgery for you. These risks will not be increased by taking part in the study but will be brought forward if you enter the study and are selected to have early heart valve surgery. The risk of complications from surgery might be slightly lower if the operation is performed earlier when you and your heart are healthier.

Taking part in a study might affect the insurance cover you get from your insurance provider. Always make sure you know what you need to tell your insurance company and what the insurance policy covers.

Will any genetic research be done?
With your permission, we may ask you to provide some blood for genetic research. This blood sample will be used to find out if certain genes are more common in people with aortic stenosis and for future research into heart disease. You will not know the type of future research your stored sample may be used for and you will not be told of the findings of this future research. You have the right to ask that your blood sample be destroyed at any time by contacting your study doctor. If you do not wish to have the genetic blood sample taken you may still take part in the main study.

What if there is a problem?
If you have a concern about any aspect of this study please contact Dr Russell Everett on his mobile phone (07736 927507) or via email (russell.everett@ed.ac.uk) who will do their best to answer your questions.

In the unlikely event that something goes wrong and you are harmed during the research and this is due to someone's negligence then you may have grounds for a legal action for compensation against your hospital but you may have to pay your legal costs. The normal National Health Service complaints mechanisms will still be available to you (if appropriate).

What happens when the study is finished?
If you have provided research blood samples we will continue to store these samples securely for up to 25 years. When we test these samples in the future we may send them to other academic institutions or commercial companies to help us run those tests.

Your study data will be stored indefinitely in a secure manner with access restricted to the research team. With your consent, we will periodically ask central NHS registers to provide information on your health status (you will not be contacted directly for this). This is because it will enable us to find out about any longer-term consequences of aortic stenosis and heart scarring. To help us identify you correctly, we will need to collect your unique patient identifier (CHI number or NHS number) and store it at the University of Edinburgh.

At the end of the study we will make the study data available for other researchers to look at. Before we make it available we will make sure it does not contain any of your personal data.

What will happen to the results of the study?
Once we have completed the study and analysed the results, we will write a paper, which will be submitted for publication in one of the medical journals. You will not be identifiable in any published results. We do not routinely contact participants to inform them of the outcome of the research but once the study has been published a summary of the findings will be available on the Edinburgh Clinical Trials website (http://www.ed.ac.uk/edinburgh-clinical-trials).

Who is organising the research and why?
The study is being sponsored by the University of Edinburgh and NHS Lothian and is being funded by the Sir Jules Thorn Charitable Trust. Your doctors will not be paid for including you in this study.

Who has reviewed the study?
The study proposal has been reviewed by the funder and the Sponsor. All research in the NHS is looked at by an independent group of people, called a Research Ethics Committee. A favourable ethical opinion has been obtained from South East Scotland Research Ethics Committee. NHS management approval has also been obtained.

Will my taking part in the study be kept confidential?
All the information we collect during the course of the research will be kept confidential and there are strict laws which safeguard your privacy at every stage. In the unlikely event that you lose capacity and cannot continue to give consent, no new data would be collected but we would keep any data we already have.

Study researchers will need access to your medical records and data to carry out this research. Information will be stored on secure university/NHS computers, or locked away in secure rooms with restricted access. Access to personal identifiable information will be restricted to the research team. With your consent we will inform your GP that you are taking part.

To ensure that the study is being run correctly, we will ask your consent for responsible representatives from the Sponsor and NHS Institution to access your medical records and data collected during the study, where it is relevant to you taking part in this research. The Sponsor is responsible for overall management of the study and providing insurance and indemnity.

If you have any further questions about the study please contact Dr Russell Everett on his mobile (07736 927507) or via email (russell.everett@ed.ac.uk).

If you would like to discuss this study with someone independent of the study please contact Dr Neil Grubb (please contact his secretary via the hospital switchboard: 0131 536 1000).

If you wish to make a complaint about the study please contact NHS Lothian:

Patient Experience Team,
NHS Lothian
2nd Floor
Waverley Gate
2-4 Waterloo Place
Edinburgh
EH1 3EG
Tel: 0131 536 3370

Email: feedback@nhslothian.scot.nhs.uk

Thank you for taking the time to read this information sheet.

The study visit schedule at a glance

Visit no.	What will happen
Screening	✓ The study team will ask for your consent to take a blood test (troponin) and perform an ECG (if you've not had one recently) ✓ These results will be used to work out your risk of having heart scarring ✓ Those who are at higher risk will be invited to attend a baseline visit
Baseline	✓ You will be asked to give written consent to enter the study ✓ The study team will then ask you about your general health, ask you to complete a questionnaire and perform a brief assessment ✓ Your blood pressure will be taken. ✓ An echocardiogram heart scan may be repeated if you've not had one recently ✓ We will take some blood
MRI scan	✓ The scan involves lying still inside a tunnel for approximately 45 minutes ✓ A small tube will be inserted into the arm vein to deliver a small amount of contrast needed to highlight heart scarring on the scan ✓ Both the contrast and scan itself are extremely safe
Valve surgery **(Option 1)**	✓ If the MRI scan shows heart scarring you may be randomised to early surgery ✓ The type of surgery that you get will be agreed between you and your local heart surgeon
Routine care **(Options 2 and 3)**	✓ If you are not randomised to early surgery you will continue to have follow up with your usual cardiology team ✓ You will be asked to tell your team if you get any symptoms and your heart will be checked periodically with ultrasound (echocardiogram) scans ✓ You may still receive an operation if or when it is recommended by your cardiologist
Annual contact	✓ The study team will contact you annually to check how you are feeling and will also complete a questionnaire about your symptoms ✓ They will also review your health records to see if you have had any complications or admissions to hospital ✓ This will continue until the end of the study (approximately 3 years but a maximum of 5 years) ✓ You will only be contacted by the study if you are allocated option 1 or 2

CONSENT FORM FOR THE EVOLVED TRIAL

Name of Researcher (PI):	Dr Russell Everett
Site:	Edinburgh (NHS Lothian)
Patient Trial Number:	

Please **initial** each box

1. I confirm that I have read and understand the information sheet (as specified in this document header) for the above study and have had the opportunity to consider the information and ask questions. ☐
2. I understand that my participation is voluntary and that I am free to withdraw at any time, without giving any reason, without my medical care or legal rights being affected. ☐
3. I understand that relevant sections of my medical notes and data collected during the study may be looked at by individuals from the Sponsor, from the NHS organisation or other authorities, where it is relevant to my taking part in this research. I give permission for these individuals to have access to my records. ☐
4. I understand that information held and managed by central UK NHS bodies and NHS Trusts may be used in order to provide information about my health status during and after the study. To do this, I understand that my information will be shared with those bodies. ☐
5. I agree to my data/tissue being used for future ethically approved studies ☐
6. I agree to my General Practitioner being informed of my participation in this study ☐

	Yes	No
7. I agree to give a blood sample which will be frozen and stored for future use (optional – initial the Yes or No box)	☐	☐
8. I agree to give a blood sample which will be used for genetic (DNA) analysis (optional – initial the Yes or No box)	☐	☐

9. I understand my blood samples may be sent to other academic institutions or commercial companies for analysis ☐
10. I agree to take part in the above study ☐

Name of Patient	Signature	Date
Name of Person taking consent	Signature	Date

Original – to Investigator Site File. *First Copy – to participant.* *Second Copy – to hospital notes.*

Cardiac MRI Scanning Guidance

The EvoLVed Trial

This guidance is designed to be used alongside local policies and procedures in the acquisition and processing of cardiac MRI images for the EvoLVeD trial.

Technical considerations

- Either 1.5 or 3 Tesla (T) scanners may be used in image acquisition.
- It is crucial to have a high quality ECG signal to ensure accurate cardiac triggering and optimal image quality.

Patient Positioning

Patients should be imaged using either a dedicated phased array cardiac/body coil with anterior and posterior elements, or alternatively using elements of the spine coil posteriorly and a phased array body coil anteriorly.

The patient should be positioned supine with the heart over the middle of the posterior coil elements being used for imaging.

If the patient is male, the chest may need to be shaved prior to placement of ECG electrodes in order to establish optimal conduction of ECG-gating signal. Electrodes should be placed according to scanner manufacturer specifications. Only MRI-compatible ECG electrodes and gating equipment should be used. Once the electrodes are in place, the technologist should view the ECG signal on the MR patient monitoring system and on the MR scanner console. The technologist should check that the MR system is detecting a gating signal from the ECG. If the MR system is gating reliably and correctly on the R-wave, the anterior cardiac or body coil should be placed over the patient chest, with the heart approximately in the middle of the coil.

The patient should then be moved to the bore aperture and the ECG-gating signal checked again. If the MR system is designed to run through a 'learning' phase for ECG-gating, this procedure should be followed at this stage.

If the ECG-gating signal is still reliable, the middle of the imaging coil (and therefore patient heart) should be moved to magnet isocentre. Once the patient is at isocentre, a final assessment of gating quality should be made. If the MR system is not reliably gating to the patient R-wave, the patient should be removed from the bore and the electrode placement procedure re-started.

Image acquisition

There are three major components to the CMR imaging protocol:

Major components	Structural imaging	Late gadolinium enhancement	T1 mapping (optional)
Pulse sequence	Cine MRI	Fast IR-prepared gradient echo post contrast	MOLLI pre and post contrast
Typical images	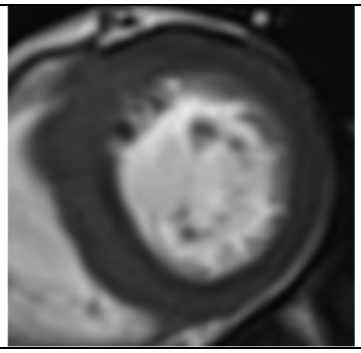	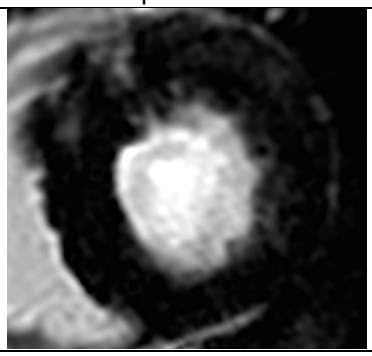	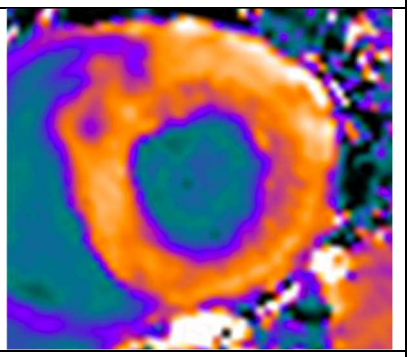
Rationale	Quantify LV size, mass and systolic function	Identify the presence of mid-wall late gadolinium enhancement as a marker of LV decompensation	To assess for extracellular volume expansion / diffuse myocardial fibrosis

In brief the imaging protocol will consist of:

1. Localiser sequences
2. LV imaging I (4 chamber, 3 chamber and 2 chamber long axis cines + LV short axis stack)
3. *Native (pre-contrast) T1 measurements (optional)*
4. Gadolinium contrast administration
5. LV imaging II (LVOT and aortic valve cines)
6. Late gadolinium enhancement imaging
7. *Post-contrast T1 measurements (optional)*

1. Localiser sequences

Note: all breath-holds should be acquired in expiration.

1. Cardiac plane localization
   a) 3-plane localizer: run automatically, untriggered free breathing to localize heart centre position.
   b) 3-plane isocentre localizer: adjust heart to isocentre of bore (run this acquisition in ISOCENTRE mode). Prescribe 3 axial, 3 coronal, 3 sagittal slices, single breath-hold, ECG-trigger on every heartbeat, capture cardiac cycle for diastole.

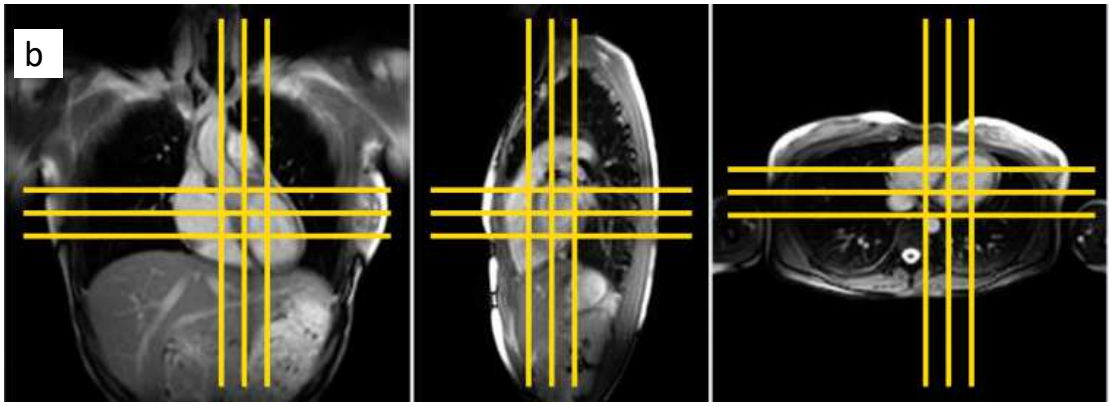

c) Axial dark blood half-fourier localizer: 20 or more slices for coverage prescribed from sagittal and coronal 1b) views, cover from above aortic arch to below apex, multiple breath-holds if required by MR system, trigger on every second heartbeat, capture cycle for diastole. Example image acquired is shown on right.

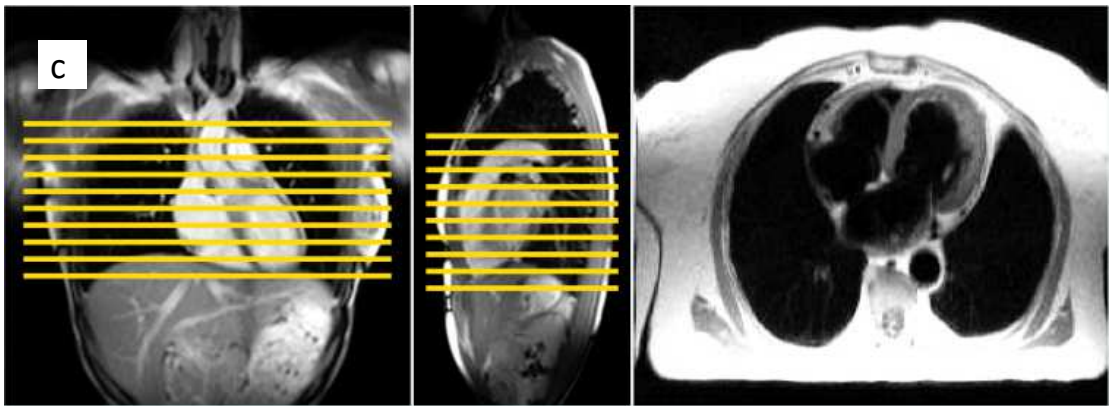

d) 2 chamber localizer: prescribe 1 slice from axial view (1c) parallel to ventricular septum, bisect left ventricle through mitral valve and apex, single breath-hold, trigger on every heartbeat, capture cycle for diastole.

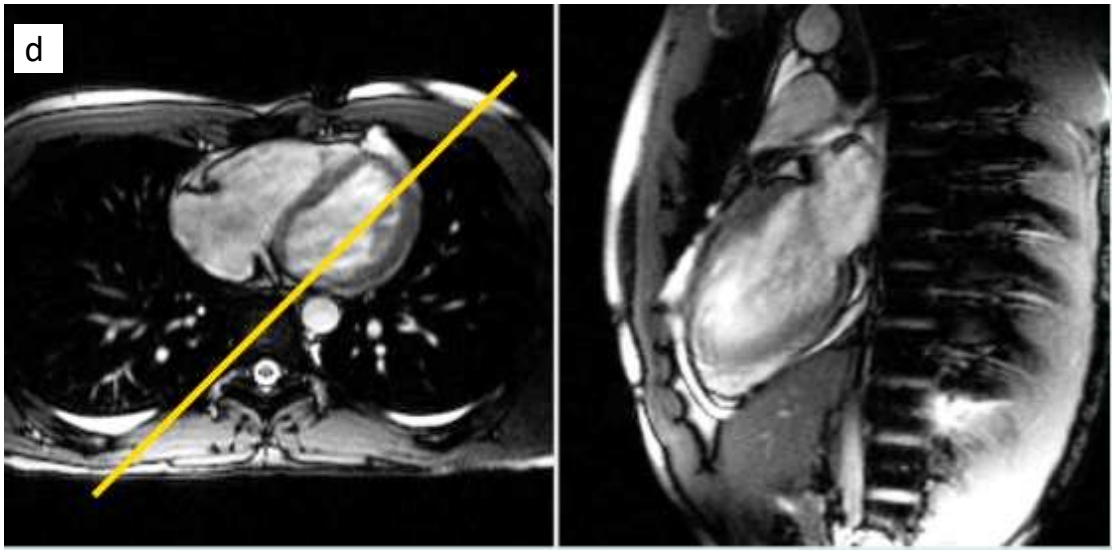

e) 4 chamber localizer: prescribe 1 slice from two chamber view (1d), bisect left ventricle through mitral valve and apex, single breath-hold, trigger on every heartbeat, capture cycle for diastole.

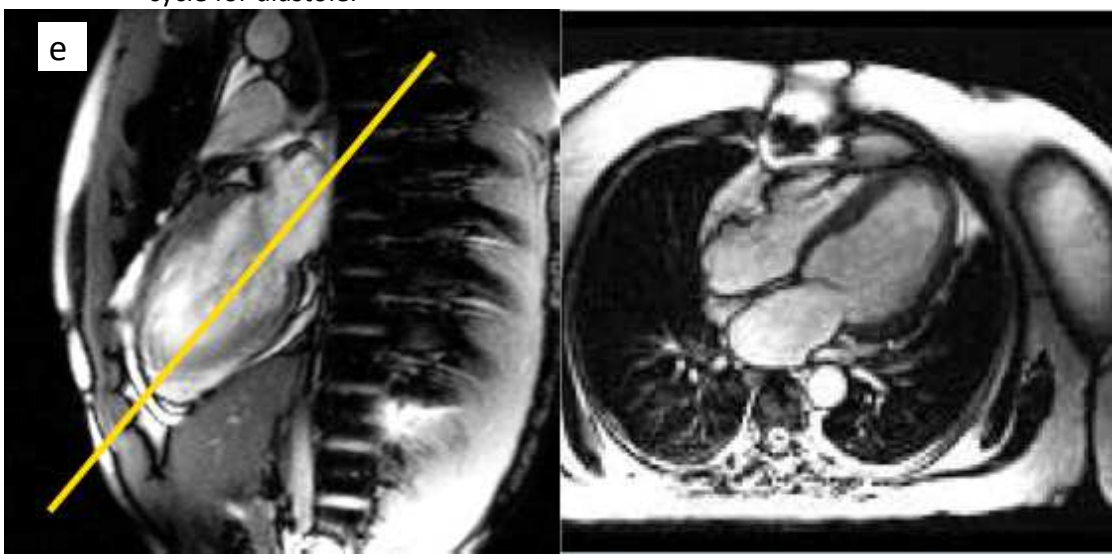

f) Short-axis localizer: prescribe 3 slices from LVOT towards apex (whole stack is shown in image below) from 2 chamber (1d) and 4 chamber (1e) views, perpendicular to long axis of left ventricle, single breath-hold, trigger on every heartbeat, capture cycle for diastole.

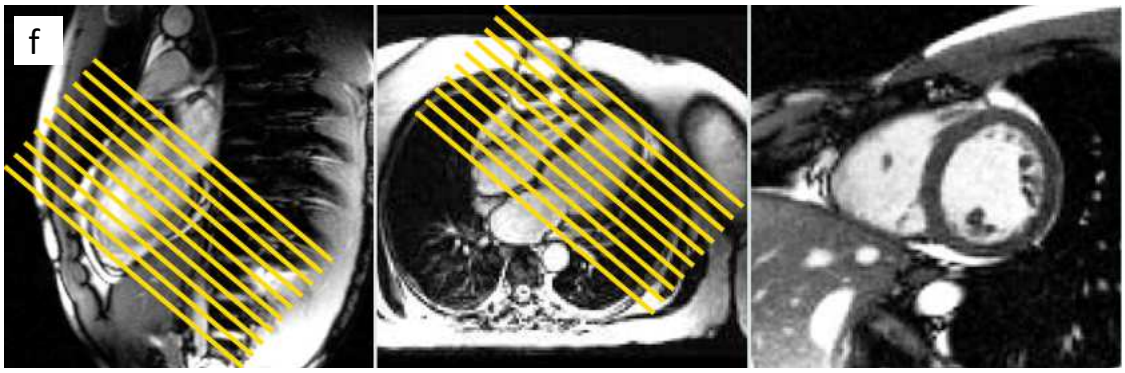

2. LV imaging I

CMR cine imaging will be performed using steady state free-precession (SSFP), breath-hold cines. The following sequences should be acquired:

a) *2-chamber cine:* prescribe 1 slice, parallel to ventricular septum on a mid-ventricle short axis localiser (1f), bisect left ventricle through mitral valve and apex on four chamber localiser (1e), rotate FoV to avoid phase-wrap, single breath-hold, retrospective gating.

b) *3-chamber cine*: prescribe 1 slice, bisect the LVOT and posterolateral LV wall on the most basal short axis localiser (1f), and bisect the LV through the mitral valve and apex on a 4-chamber localiser (1e), rotate FoV to avoid phase-wrap, single breath-hold, retrospective gating.

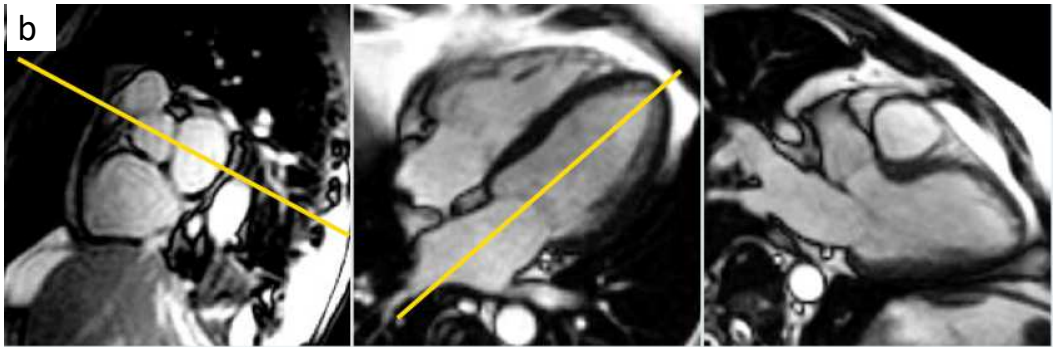

c) *4-chamber cine*: prescribe 1 slice, bisect LV through the mitral valve and apex on 2-chamber localiser (3a), bisect left and right ventricles on between anterior and posterior papillary muscle, mid-ventricle short axis localiser (1f), rotate FoV to avoid phase-wrap, single breath-hold, retrospective gating.

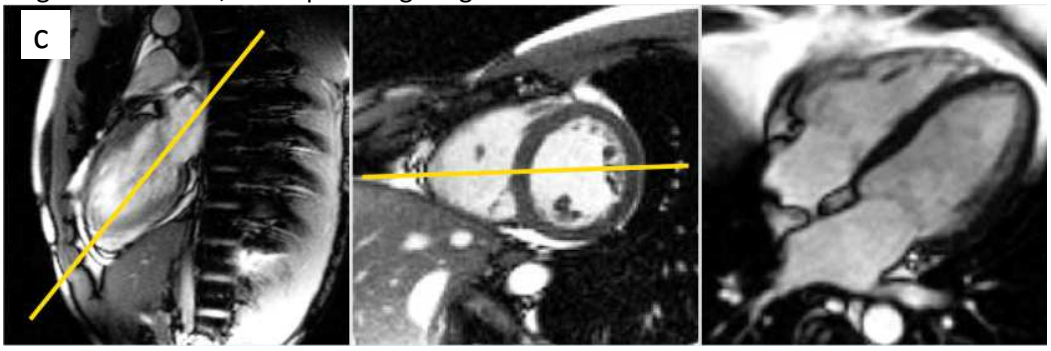

d) Short-axis cine stack: prescribe contiguous slices from 2-chamber cine diastolic view (2a) and 4-chamber cine (2c), perpendicular to long axis of LV, slices should be acquired with 8mm slice thickness and no gap, with enough slices selected to cover from mitral valve to apex. Rotate FoV to avoid phase-wrap, multiple breath-holds (depending on parallel imaging factor used), retrospective gating. Checking each slice for gating artefacts and repeat slice if required.

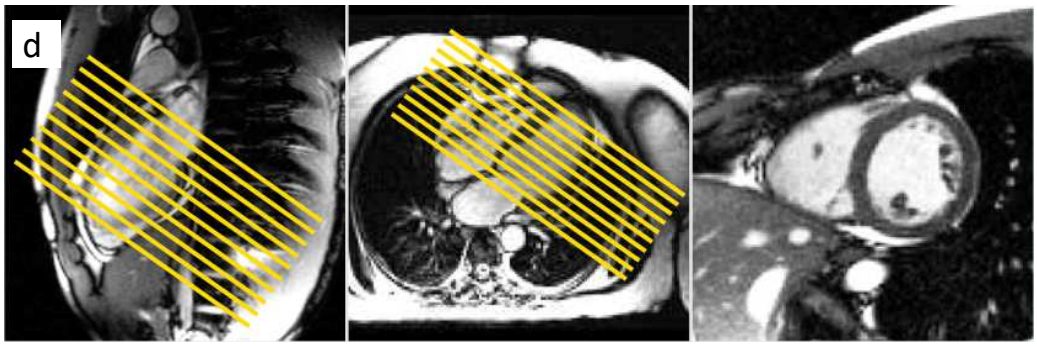

3. Native (pre-contrast) T1 mapping (optional)

If T1 mapping is performed a Modified Look Locker Inversion sequences should be used (3-3-5, start 100ms, increment 80ms, and 160ms).

Two T1 maps should be acquired which correspond to slice positions used during the short axis cine sequences. The two slices to be acquired are the **basal-LV** (the most basal slice with a full circle of myocardium that does not contain the LVOT in mid-diastole) and **mid-LV** (two slices more apically from the basal LV slice, approximately half way from mitral valve to LV apex). This aims to minimise scan time whilst maximising usable data. In our experience, T1 mapping analysis of apical slices is challenging due to partial voluming and therefore we do not intend to acquire T1 mapping images from this area.

Selection of the basal slice is critical to enable image analysis. A complete ring of LV myocardium is necessary for accurate analysis. There should be no hint of LVOT visible on the septal wall to enable accurate T1 values to be calculated from this area (see below).

BASAL-LV SLICE Incomplete ring of myocardium (portion of LVOT is visible). This slice is too basal. **UNACCEPTABLE**	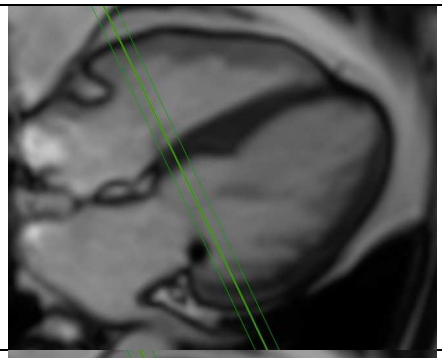	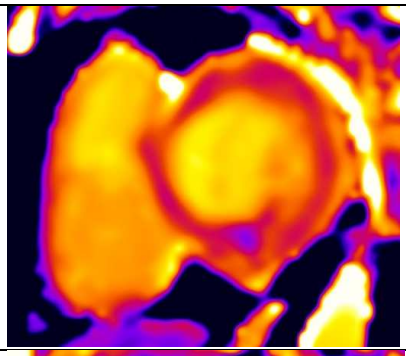
BASAL-LV SLICE First (most basal) slice with complete ring of myocardium visible. **ACCEPTABLE**	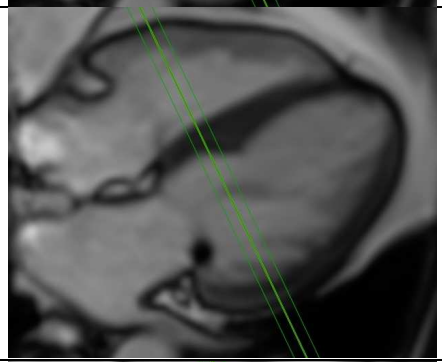	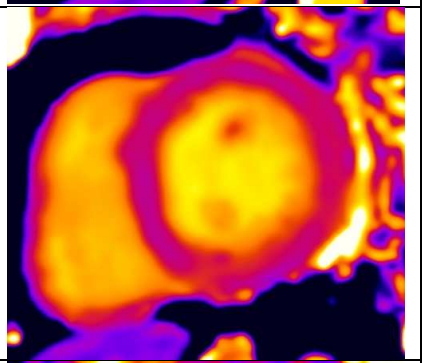
MID-LV SLICE Slice position chosen (from SA cine imaging) 2 slices more apical than selected basal-LV slice. **ACCEPTABLE**	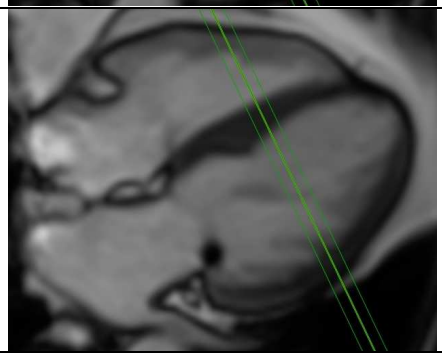	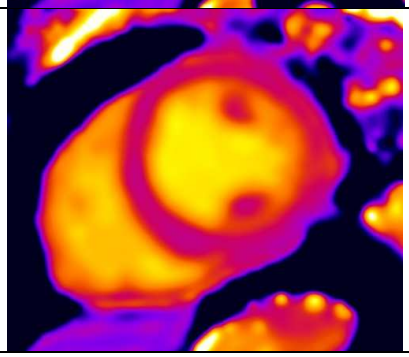

4. Gadolinium contrast administration

A non-linear gadolinium chelate with average (not high) relaxivity should be injected into a peripheral vein via an intravenous cannula. Ideally the cannula should be 20 gauge (pink) or above. The method of injection (power injector or by hand) should be as per local policy. **Gadovist (gadobutrol)** at a dose of **0.15 mmol/kg** is the preferred contrast agent. If other agents are used the dose can be adjusted as per local policy.

Other acceptable contrast agents are:

- Prohance (gadoteridol)
- Dotarem (gadoteric acid)

A single scout image of the LV short axis should be acquired immediately following contrast injection. This image should be labelled as "contrast injection end" and will allow retrospective verification via the time stamps of the timing of the late gadolinium sequences with respect to contrast injection.

5. LV imaging II (LV short axis cines)

Further LV cine imaging will be performed post contrast injection to keep the total scan time as short as possible.

a) LVOT cine (slice perpendicular to the three-chamber view)

b) Aortic valve cross-section sequence (short-axis image of the valve perpendicular to the aortic valve leaflets tips observed on the 3-chamber and LVOT cine views). This should be gradient echo, with low flip angle and short TR (e.g. FLASH)

6. Late gadolinium enhancement imaging

The first images of the late gadolinium enhancement acquisition should be acquired 7 minutes after gadolinium infusion. All late enhancement scans should be acquired with optimal TI selected to null normal myocardial signal as outlined below. Please note that as time progresses TI may need to be adjusted to effectively null normal myocardium.

a) *TI scout:* used to determine the optimal TI for nulling of normal myocardium in subsequent late gadolinium enhancement images. Prescribe as the mid ventricular short axis slice (copied from 2d), rotate FoV to avoid phase-wrap, single breath-hold, trigger on every heartbeat, capture cycle for optimal acquisition window. Please note that repeat T1 scouts should be considered if inadequate nulling it observed on later late gadolinium acquisitions. This should provide an updated optimal TI.

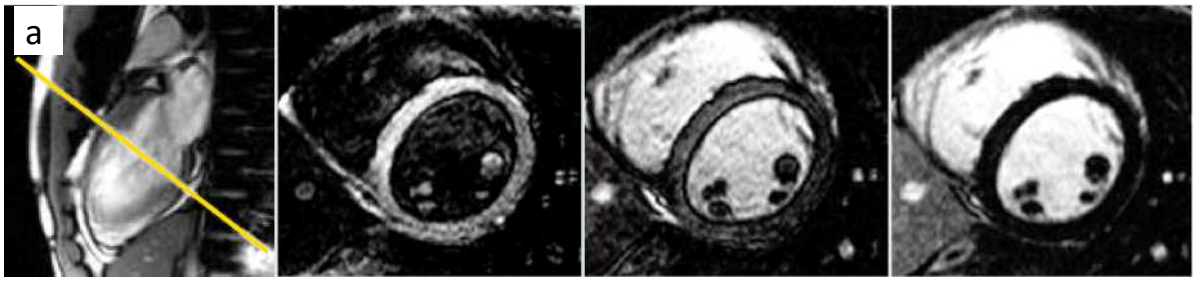

b) *Short-axis gradient echo late gadolinium enhancement (GRE-LGE):* prescribe slices of the breath hold segmented inversion recovery sequence. Copy the exact image position of short-axis cine slices (2d) so that these images can be directly compared to the LGE images. Adjust TI for nulling of normal myocardium (see image on right above), rotate FoV to avoid phase-wrap. Multiple breath-holds, trigger on every second heartbeat, capture cycle for diastolic imaging. Slices should be acquired with 8mm slice width and no slice gap, copied to previously acquired short axis cine slice positions (2d) to image the LV from mitral valve to apex.

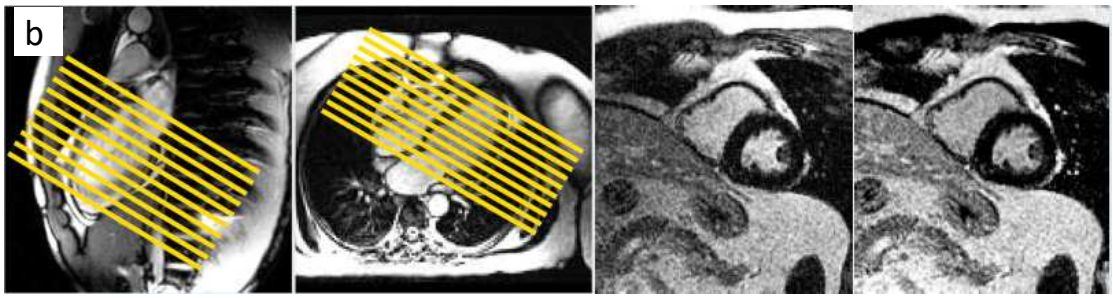

c) *Phase swap short-axis GRE-LGE:* the above (6b) should be repeated using identical settings but with phase swap in order to help distinguish artefact from true LGE.

d) 4-chamber *GRE-LGE*: prescribe 1 slice, breath hold segmented inversion recovery sequence, copy slice position of 4 chamber cine (2c), adjust TI for nulling of normal myocardium, rotate FoV to avoid phase-wrap, single breath-hold, trigger on every second heartbeat, capture cycle for diastole. If regions of LGE are noticed on short-axis images the plane of this long axis image can be altered to capture this area.

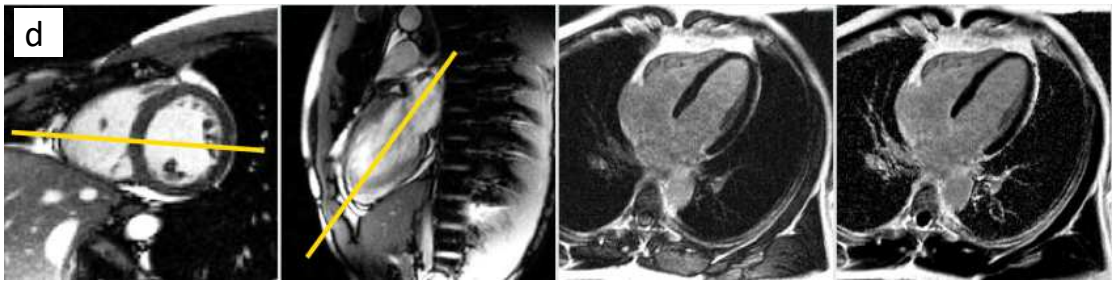

e) 2 chamber late gadolinium enhancement: prescribe 1 slice, breath hold segmented inversion recovery sequence, copy slice position of 2 chamber cine (2a), adjust TI for nulling of normal myocardium, rotate FoV to avoid phase-wrap, single breath-hold, trigger on every second heartbeat, capture cycle for diastole. If regions of LGE are noticed on short-axis images the plane of this long axis image can be altered to capture this area.

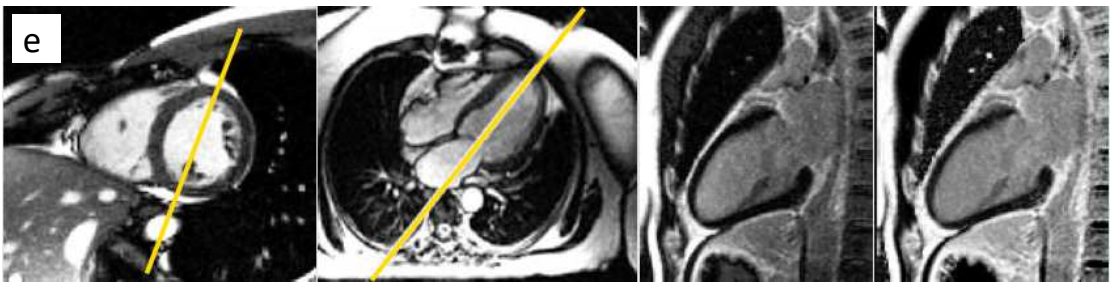

NB. If poor quality GRE-LGE images despite best attempts to null normal myocardium and repeated T1 scouts please switch to phase sensitive inversion recovery (PSIR) imaging. 6abcd should be repeated using a phase sensitive inversion recovery turbo-FLASH technique (select both magnitude and phase images option). Slice position and width should be identical.

7. Post-contrast T1 measurements (optional)

For post-contrast measurements, the same two slice locations should be used as the native T1 map. This image acquisition should be performed at approximately 20 minutes post contrast injection.

8. Acceptable variation:

a. Late gadolinium enhancement

The preferred late gadolinium enhancement sequence is a breath-hold gradient echo as specified above (section 6b). Our primary goal is obtaining **excellent image quality** for the late enhancement imaging as this directly informs study randomisation. If a site has particular experience with other types of LGE sequences (e.g. free breathing PSIR) and these can be performed without sacrificing image quality these may be used instead. Please contact the EVoLVeD trial manager if there are any queries regarding this.

b. Aortic valve cross section

A single short axis cross section view is prescribed in the guidance above (section 5b). Sites that would prefer to perform additional images as part of a stack (e.g. 3 slices, 5mm slice thickness, no gap) may do so providing the quality of the late enhancement images is not compromised.

c. Cross-cutting potential areas of LGE

If areas of mid-wall LGE are observed during the short-axis LGE stack that would not be visible on the 2, 3 or 4 chamber long-axis images, then a long-axis cross-cut view can be acquired. This should be planned on the relevant short axis slice so that the resulting long-axis image intersects both the centre of the LV cavity and the area thought to be LGE. This is useful for the image analysis team to confirm that enhancing areas are true LGE and not artefact.

d. Repeat imaging

In the event that repeat imaging is required, a reduced, targeted scan may be acceptable to minimise participant burden. This would need to be approved by the study team in Edinburgh prior to any repeat scan taking place.

Table of CMR sequences

	Number of acquisitions	Estimated time	Time post-contrast
Position subject within scanner, ensure high quality ECG signal and IV cannula patency		5 mins	
Sequence			
Localiser	1		
Site specific method of localisers to derive appropriate cardiac planes	1-5	1-3 mins	
4 chamber (horizontal long axis) cine	1	2 min	
2 chamber (vertical long axis) cine	1	2 min	
3 chamber cine	1	2 min	
LV short axis stack cine – 8mm slice thickness, no gap	14-15	6 mins	
MOLLI (basal and mid ventricle slices) - OPTIONAL	1	2 mins	
Inject contrast (0.15mmol/kg)			
Single scout – any image, localiser (labelled "contrast injection end"	1	1 min	0-1
LVOT cine (orthogonal to 3 chamber)	1	2 min	1-3
Aortic valve FLASH	1	2 min	3-5
Break – wait until 7 minutes post gadolinium		0-2 mins	5-7
TI scout – to determine optimal TI	1	1 min	7-8
GRE-T1 LGE LV short axis stack – 8mm slice thickness, no gap	14-15	7 mins	8-15
Phase swap GRE-T1 LGE LV short axis stack*	14-15	7 mins	15-22
Long axis GRE-T1 LGE images	3	3 mins	24-27
MOLLI (basal and mid ventricle slices) - OPTIONAL	1	2 mins	22-24
Total scan time			
Standard protocol		45 mins	
Optional T1 mapping included		49 mins	

*PSIR LGE LV short axis stack to be performed instead of phase swap if initial GRE-T1 stack nulling is suboptimal

OPEN ACCESS

Timing of intervention in aortic stenosis: a review of current and future strategies

Russell James Everett,[1] Marie-Annick Clavel,[2] Philippe Pibarot,[2] Marc Richard Dweck[1]

[1]BHF/Centre for Cardiovascular Science, University of Edinburgh, Edinburgh, UK
[2]Department of Medicine, Quebec Heart and Lung Institute, Quebec, Canada

Correspondence to
Dr Russell James Everett, BHF/Centre for Cardiovascular Science, University of Edinburgh, Edinburgh EH16 4SB, UK; russell.everett@ed.ac.uk

Check for updates

To cite: Everett RJ, Clavel M-A, Pibarot P, *et al*. *Heart* Epub ahead of print: [*please include* Day Month Year]. doi:10.1136/heartjnl-2017-312304

INTRODUCTION

Aortic stenosis (AS) is the most common valve disease requiring surgical intervention in high-income countries.[1] It is characterised by progressive thickening, fibrosis and calcification of the leaflets leading to restriction and valve obstruction.[2] The consequent increase in left ventricular afterload leads to a hypertrophic response of the left ventricle, normalising wall tension and maintaining cardiac output. However, with progressive valvular stenosis, this hypertrophic response eventually decompensates resulting in symptom development, heart failure and death.

With no medications proven to attenuate or reverse stenosis progression, the only available treatment is valve replacement. This should ideally be performed when the risks of the disease process (ie, sudden cardiac death, irreversible functional impairment and heart failure) outweigh those of intervention (ie, procedural risk, long-term complications and potential need for reoperation). However, we frequently lack robust evidence to make accurate assessments of such risk. Deciding on the timing of valvular intervention is therefore difficult in many patients, and contemporary clinical guidelines are often underpinned by historical observational data rather than high-quality randomised controlled trials. This article will review our current understanding of the pathophysiology of AS, describe and examine the evidence behind current guideline recommendations and explore potential future strategies to optimise the timing of valve intervention.

Learning objectives

- To review the pathophysiology of fibrocalcific aortic stenosis, the myocardial response to pressure overload and current clinical guidelines concerning the timing of valve intervention.
- To explore and to quantify the risks of earlier intervention in asymptomatic patients compared with the risks of a watchful waiting strategy.
- To detail future potential strategies for deciding on timing of aortic valve intervention and current ongoing randomised controlled trials.

PATHOPHYSIOLOGY OF VALVULAR STENOSIS AND THE HYPERTROPHIC RESPONSE

Since the original description of AS by Mönckeberg in 1904, the decline in rheumatic fever and ageing population have led to a demographic transition towards fibrocalcific disease. For many years, fibrocalcific AS was viewed as a degenerative disease where progressive 'wear and tear' led to structural damage and passive valvular calcification. However, contemporary thinking is that fibrocalcific AS develops as part of a series of intricate and highly regulated inflammatory, fibrotic and osteogenic processes. The pathophysiological processes driving aortic valve stenosis can be divided into two phases.[2] The initiation phase is characterised by endothelial injury accompanied by infiltration of lipids, lipid oxidation and proinflammatory response. Despite the clear similarities with atherosclerosis, three large randomised trials have failed to show any effect of statins on disease progression or clinical outcome. The propagation phase is characterised by the appearance of osteoblast-like cells that coordinate progressive valvular calcium and bone matrix deposition. This osteogenic phenotype involves many signalling molecules involved in bone formation and is both self-perpetuating and highly regulated.[2] Advances in imaging now allow for non-invasive assessment of both the burden and activity of calcification in the valve[3 4]; however, the severity of aortic valve obstruction is still best assessed using echocardiography.[5]

Myocardial response

The traditional focus of AS assessments has been on the valve. However, the left ventricular myocardial response to pressure overload is equally important,[6] particularly as the correlation between echocardiographic measures of AS severity and the degree of myocardial hypertrophy is moderate at best.[7] While left ventricular hypertrophy maintains wall stress and cardiac output for many years, it eventually decompensates, with cell death and myocardial fibrosis identified as key processes.[8] Many imaging and biomarker surrogates of these processes have been investigated providing significant prognostic information that will be discussed later in this article. Gender appears to have an important influence on both the LV remodelling response and patient outcomes,[9] but detailed discussion is beyond the scope of this article.

CURRENT GUIDELINE-RECOMMENDED TREATMENT STRATEGIES AND THEIR LIMITATIONS

Broadly speaking, contemporary clinical guidelines recommend aortic valve intervention when stenosis severity is deemed severe *and* there is evidence of left ventricular decompensation, using either direct objective or surrogate symptomatic

measures (figure 1 and table 1).[10 11] Haemodynamic severity is best assessed using echocardiography but can be challenging when measures of severity are discordant or low-flow states exist. New recommendations for confirming AS severity are given in the 2017 ESC/EACTS guideline update.[5] Detailed discussion of low-flow states is beyond the scope of this article but can be found elsewhere.[12]

Presence of AS-related symptoms

It is universally accepted that the development of patient symptoms (exertional dyspnoea, angina or syncope; table 2) serves as an indicator of left ventricular decompensation and a dismal prognosis without intervention. This was first described in the seminal paper by Braunwald and Ross in 1968[13] and forms the underlying framework of how we manage patients today. However, this finding was based on retrospective data from just 12 patients with a mixture of bicuspid and rheumatic valve disease and a mean age of death of 63 years. The changing demographics of AS make it difficult to interpret the current relevance of these historical data to the patients seen in current practice who are frequently in their eighth or ninth decades. Symptom assessment can be highly challenging in these patients due to the high prevalence of both comorbidity, which may cause symptoms to be falsely attributed to AS, and physical inactivity, which can conceal exertion-related problems.

Exercise testing may help unmask symptoms in many patients and is safe when performed in stable patients.[14] ESC guidelines recommend surgery in patients with severe ASand typical symptoms on exercise test (class I, level C) or a fall in systolic blood pressure at peak exercise (class IIa, level C). This recommendation is based largely on observational data demonstrating that a positive exercise test is a strong predictor of sudden death or symptom development.[15] However, these data are limited, consisting of a series of relatively small observational studies with inherent risk of bias and

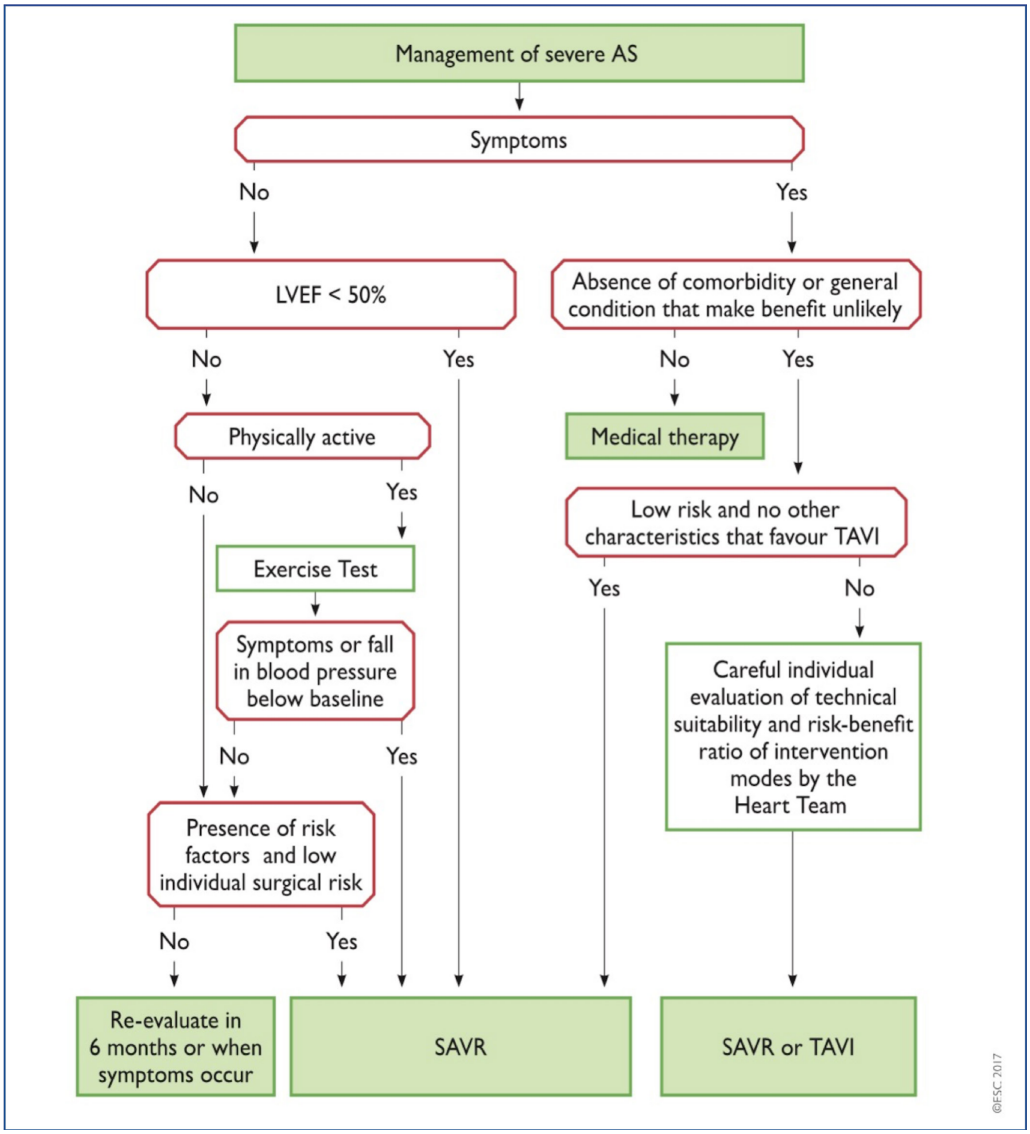

Figure 1 ESC/EACTS algorithm for management of severe AS (2017 guidelines). AS, aortic stenosis; LVEF, left ventricular ejection fraction; SAVR, surgical aortic valve replacement; TAVI, transcatheter aortic valve implantation.

Table 1 Recommendations for Intervention in patients with severe AS (ESC/EACTS guidelines 2017)

Symptomatic severe AS (surgical AVR or TAVI)	Class	Level
Indicated in severe high gradient AS (AV Vmax >4 m/s or mean gradient >40 mm Hg).	I	B
Indicated in patients with low-flow low-gradient severe AS with reduced ejection fraction and evidence of contractile reserve excluding pseudosevere AS.	I	C
Should be considered in patients with low-flow low-gradient severe AS with preserved ejection fraction after careful confirmation of severe AS.	IIa	C
Should be considered in patients with low-flow low-gradient severe AS with reduced ejection fraction without evidence of contractile reserve especially where CT calcium scoring confirms severe AS.	IIa	C
Should NOT be performed in patients with severe comorbidities where the intervention is unlikely to improve quality of life or survival.	III	C
Asymptomatic severe AS (surgical AVR only)		
Indicated in patients with severe AS and left ventricular systolic dysfunction (LVEF <50%) not due to another cause.	I	C
Indicated in patients with abnormal exercise test showing symptoms on exercise clearly related to AS.	I	C
Should be considered in patients with abnormal exercise test showing a decrease in blood pressure below baseline.	IIa	C
Should be considered if the surgical risk is low and one of the following abnormalities is present: ► Very severe AS (AV Vmax >5.5 m/s). ► Severe valve calcification with a rate of progression ≥0.3 m/s/year. ► Markedly elevated BNP (>3-fold above age-corrected and sex-corrected normal range) confirmed by repeated measurements without other explanations. ► Severe pulmonary hypertension (systolic pulmonary artery pressure >60 mm Hg at rest confirmed by invasive measurement) without other explanation.	IIa	C

AS, aortic stenosis; AV, aortic valve; BNP, B-type natriuretic peptide; LVEF, left ventricular ejection fraction; TAVI, transcatheter aortic valve implantation.

heterogeneity as to what constituted an abnormal test. According to a recent meta-analysis, while the negative predictive value of stress testing for subsequent cardiac events is reasonable (79%), the positive predictive value is modest (66%).[14] Exercise testing has other major limitations; up to 20% of patients will be unable to perform the test due to poor mobility, while pre-existing ECG abnormalities are present in up to 50% of patients confounding test interpretation.[16] It is worth noting that exercise testing may also detect abnormalities caused by coexistent coronary disease, which is an important determinant of both management and prognosis.[17]

Impaired left ventricular ejection fraction

Development of left ventricular systolic impairment, as identified by a reduced left ventricular ejection fraction, is an inevitable consequence of progressive and untreated valvular stenosis assuming sudden death does not occur. Although the risk of perioperative mortality is elevated in the setting of reduced ejection fraction, these patients have a dismal prognosis without intervention and improved long-term outcomes with valve replacement earning a class I, level C recommendation in clinical guidelines.[10 11]

In clinical practice, patients with AS can develop a reduction in ejection fraction for a variety of reasons, and it remains important to consider the mechanism of this reduction and whether it is reversible. Reductions in ejection fraction occur as a direct response to increases in afterload and will reverse following valve replacement. By contrast, the ejection fraction does not improve in approximately 25% of patients[10 11 18 19] who are more likely to remain symptomatic and who have adverse long-term outcomes (twice as likely to die over 5 years follow-up).[20] In these patients, persistent systolic dysfunction appears related to the development of irreversible scar due to either myocardial infarction or decompensation of the hypertrophic response.[21] In sick, frail patients, such information may govern whether valve intervention is likely to be of benefit.

Reductions in ejection fraction are therefore a late, non-specific and often irreversible feature in AS, leading to interest in alternative methods for detecting left ventricular decompensation[7 22–24] as will be discussed.

Very severe AS

Patients with critical AS appear to have a particularly poor prognosis, similar to that of symptomatic

Table 2 Symptomatology of severe aortic stenosis

Symptom	Aetiology	Potential questions to ask:
Angina	Supply–demand imbalance: coexistent coronary disease and fixed cardiac output versus hypertrophied myocardium.	'Do you get chest pain or discomfort when walking or doing other activities?'
Breathlessness/reduced exercise capacity	Reduced LV compliance, increased left ventricular end-diastolic and pulmonary capillary pressures.	'Can you walk ask many stairs as this time last year?' 'Can you keep up with your friends?'
Presyncope/syncope *(important to elicit any exertional component)*	Fixed cardiac output, skeletal muscle vasodilation on exertion and resultant cerebral hypoperfusion.	'Have you felt lightheaded like you might faint?' 'Have you had any fainting or blackout episodes?'
Palpitations	Development of atrial or ventricular arrhythmia, myocardial scarring.	'Are you aware of your heart racing?'

LV, left ventricular.

severe AS.[25] Indeed patients with peak aortic jet velocities of >5.0 and >5.5 m/s demonstrate a 2-year event-free survival of 43% and 25%, respectively, compared with 70% in those with Vmax 4.0–4.9 m/s.[26] The ESC/EACTS guidelines therefore recommend consideration of aortic valve replacement in patients with Vmax >5.5 m/s if the estimated surgical risk is low (class IIa, level C). However, these observational studies mostly examined the composite endpoint of mortality and referral for aortic valve intervention with a strong risk of referral bias and event rates mainly driven by decisions to perform surgery.

Rapid haemodynamic progression

Although the average rate of progression (measured by peak aortic-jet velocity) is 0.24±0.30 m/s/year, this rate is highly variable.[27] Moreover, it is subject to scan–rescan variation in peak velocity measurements, which can be high in clinical practice. Patients with rapid progression (>0.3 m/s/year) and significant valve calcification have a rate of symptom development or mortality of 79% at 2 years.[28] As a result, referral for surgical intervention in these patients is given a class IIa, level C recommendation in the latest guidelines. However, again, this is based on limited observational data, and this strategy requires standardised high-quality echocardiography over several years to confidently determine rate of progression.

Elevation of B-type natriuretic peptide (BNP) levels

BNP is the first cardiac biomarker to be included in the decision-making algorithm for aortic valve replacement. Early studies investigating natriuretic peptides in AS showed promise but were criticised for their small size, observational nature and use of softer outcome endpoints.[29 30] In addition, many patients were symptomatic, and the variation in normal BNP with age and sex were not accounted for. A more recent study of 565 patients with asymptomatic moderate-to-severe AS identified that a BNP ratio (measured BNP value divided by upper limit of normal for patient's age and sex) of >1 was independently predictive of mortality and a ratio of >3 had an HR of 7.3 for survival in patients with asymptomatic severe AS.[31] As such, the latest clinical guidelines reflect these data with a level IIa, class C recommendation for aortic valve replacement if the BNP ratio is persistently above 3 and overall surgical risk is low. However, BNP is a non-specific marker of cardiac dysfunction, and its utility, like each of the other parameters, has yet to be tested in a randomised controlled trial.

The recently published ESC clinical guidelines also removed two previous IIb indications for AVR in asymptomatic patients: an increase in mean aortic gradient of >20 mm Hg with exercise, or the finding of excessive LV hypertrophy in the absence of hypertension.

BALANCING COMPETING RISKS

There are clear limitations with many of our guideline-advocated strategies. Most are based on limited observational data and supported by level C recommendations. There is therefore a need for randomised controlled trials assessing the optimal timing of surgery and novel objective methods to guide this major clinical decision. Ideally, intervention would be performed in patients just as the left ventricle is starting to decompensate but before substantial irreversible damage has accrued and at a time when the short-term and long-term risks of the intervention are outweighed by the risks of not intervening (figure 2 and table 3). An understanding of these competing risks is therefore critical.

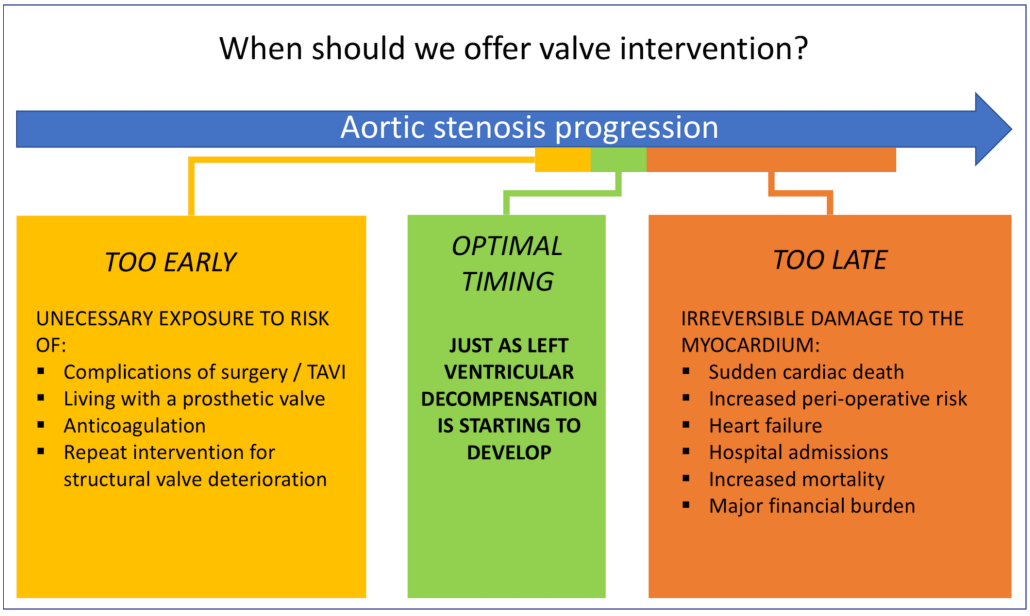

Figure 2 Optimising the timing of aortic valve intervention in progressive aortic stenosis. TAVI, transcatheter aortic valve insertion.

Table 3 Estimates of clinical risks associated with watchful waiting or early intervention strategies

Risks associated with watchful waiting	Risk estimate	Risks associated with early intervention	Risk estimate
Sudden cardiac death	1.0%–1.5% per year [46–48]	Perioperative mortality	1%–3% (refine using validated risk calculator)
Death while awaiting elective intervention once symptoms develop	4% at 1 month, 12% at 6 months [49]	Perioperative complications (SAVR):	
		► Stroke.	2.4%–8.1% [33–35]
		► Pacemaker requirement.	1.5%–8.6% [32]
		► Major bleeding.	9%–26% [36 39]
		► New atrial fibrillation.	17%–43% [34 36 39]
Increased perioperative mortality:	(Refine using validated risk calculator)	Periprocedural complications (TAVI):	
► Impaired left ventricular function.	9%–19% [10 20 50]	► Stroke.	2.2%–2.6%. [40]
► No contractile reserve.	22%–32% [11 52]	► Pacemaker requirement.	7%–25% [38–40]
		► Major vascular complications.	2.0%–4.5% [40]
		► Major bleeding.	12%–15% [36 39]
		► New atrial fibrillation.	10%–13% [34 36 39]
Lack of improvement in ejection fraction following intervention	25%–50% [10 11]	Long-term prosthetic valve complications:	
		► Thromboembolism.	0.7%–1.0% per year [42]
		► Major bleeding with anticoagulation.	1.8%–2.6% per year [42]
Incomplete resolution of symptoms	Approximately 50% [50]	Prosthetic valve endocarditis	1%–3% in first year then <0.5% per year [43]
Increased late postintervention mortality:	HR 2.0 [20]	Reoperation for structural valve degeneration:	
► Impaired ejection fraction.	HR 1.25–5.25 [21 51 57]	► <65 years of age.	46%–55% at 20 years
► Myocardial fibrosis.		► >65 years of age.	8%–15% at 20 years [45]

SAVR, surgical aortic valve replacement; TAVI, transcatheter aortic valve implantation.

Risks of valve intervention

Surgical aortic valve replacement remains the standard of care for valvular intervention, with improvements in surgical and postoperative care driving perioperative mortality down to ~1%–3%. Other important perioperative complications include conduction disease requiring permanent pacemaker insertion (1.5%–8.6% [32]) and cerebrovascular accidents (2.4%–8.1% [33–35]). There is also the risk of cognitive decline (due to perioperative cerebral hypoperfusion microemboli or anaesthetic agent neurotoxicity [35]). An individual's risk of these complications can be estimated using surgical risk calculators such as EUROSCORE II and the Society of Thoracic Surgeons score. An argument in favour of early surgery is that operative risk is lower in younger patients that are asymptomatic, have less comorbidity and have normal left ventricular function.

The emergence of minimally invasive transcatheter aortic valve insertion (TAVI) over the last 10 years has completely changed the landscape for decision making regarding valve intervention in symptomatic patients. Current trials show non-inferiority of this percutaneous technique compared with surgical intervention in both high-risk and intermediate-risk patients, [34 36–39] and procedural risk may further reduce with increasing clinical experience and advances in prosthesis design and delivery. Indeed, major vascular complications have decreased substantially (from >10% to <5% [40]) as have stroke rates, which are between 2% and 3% in contemporary cohorts. [40] However, the requirement for permanent cardiac pacing postprocedure remains consistently higher than surgical intervention at >10% [40] and while TAVI allows for rapid patient recovery and mobilisation, the long-term durability of these bioprostheses has not been demonstrated. [41] This will be key before their widespread use in younger or asymptomatic patient groups can be recommended.

Performing valve intervention introduces small but significant annual risks associated with the presence of a prosthetic valve. These risks are heavily influenced by valve type, with both anticoagulant related major bleeding (1.8%–2.6% per year) and thromboembolism (0.7%–1.0% per year) more frequent with mechanical valves. [42] In addition, there is an increased risk of endocarditis (1%–3% during the first year then <0.5% per year [43]), which has a high associated morbidity and mortality. Whereas structural valve degeneration is exceedingly rare in mechanical valves, bioprosthetic valves have a limited lifespan which can be difficult to predict. In these patients, valve degeneration usually starts to occur 10 years following implantation [44] and occurs more rapidly in younger patients. [45] This is an extremely important issue if bioprosthetic valves are to be used in younger asymptomatic patients. Ongoing research into decellularisation techniques and tissue engineering may lead to improved bioprosthetic valve longevity, while advances in mechanical valve design might eventually eliminate the need for anticoagulation and associated bleeding risk. In addition, the use of a transcatheter valve inside a surgical bioprosthetic valve (so called valve-in-valve TAVI) may reduce the risk of future procedures should valve degeneration occur.

Risks of not intervening

The risk of sudden cardiac death in patients with asymptomatic severe AS managed conservatively is ~1% per year and occurs without preceding symptoms in 70% of cases. [46–48] Once symptoms develop, further clinical deterioration can be rapid with a significant risk of sudden death while awaiting intervention (4% at 1 month, 12% at 6 months). [49]

Delaying aortic valve intervention until there is evidence of advanced left ventricular decompensation results in greater perioperative risks.[48] Observational studies have quoted increased perioperative mortality (9%–19%[10 20 50]) in patients who have developed left ventricular systolic impairment and advanced myocardial fibrosis.[51] Further risk stratification can be performed using stress echocardiography to assess myocardial contractile reserve, with lower perioperative risks if contractile reserve is present (5% vs 22%–32%[11 52]). However, given the dismal prognosis of untreated AS, even patients without contractile reserve have improved long-term survival if they survive the perioperative period.[10 11]

The highest burden in mortality and morbidity related to delaying valve intervention appears to occur in the months and years following AVR, particularly in those patients that have evidence of left ventricular decompensation. As discussed, patients with an impaired ejection fraction prior to AVR have a poor long-term prognosis,[20] while in a recent study of AS patients with a high probability of LV decompensation, more than half were either dead or admitted to hospital with heart failure within 2 years.[53] Both these observations may reflect the development of irreversible scarring in the myocardium while patients are waiting for surgery.

POSSIBLE FUTURE STRATEGIES

Several different strategies for optimising the timing of valve replacement in AS have been proposed, many of which are currently being evaluated within the context of randomised controlled trials (figure 3 and table 4). Many of these target asymptomatic patients, and it should be recognised that many patients that feel otherwise fit and healthy might not want to undergo major heart surgery.

All-comers with severe AS

Historical teaching has been that 'aortic valve replacement is the most common cause of death in patients with asymptomatic severe aortic stenosis'. However, improving outcomes following surgical and transcatheter valve replacement are challenging this doctrine. Performing valve intervention on all asymptomatic patients with severe AS is a simple and pragmatic solution that does not seek to identify the point at which left ventricular decompensation occurs. Although some patients will undergo intervention earlier than they may have required (and therefore be exposed unnecessarily to the problems associated with prosthetic valves), the risks associated with contemporary intervention techniques are low, and no patient should be left with irreversible left ventricular decompensation. This strategy is supported by evidence from the Japanese Contemporary outcomes after sURgery and medical tREatmeNT in patients with severe Aortic Stenosis (CURRENT AS) registry. Propensity-score matching was used to compare 291 asymptomatic patients who underwent early surgery with 291 patients who were managed conservatively. Those who received early AVR had a reduced all-cause mortality at 5 years (15%) compared

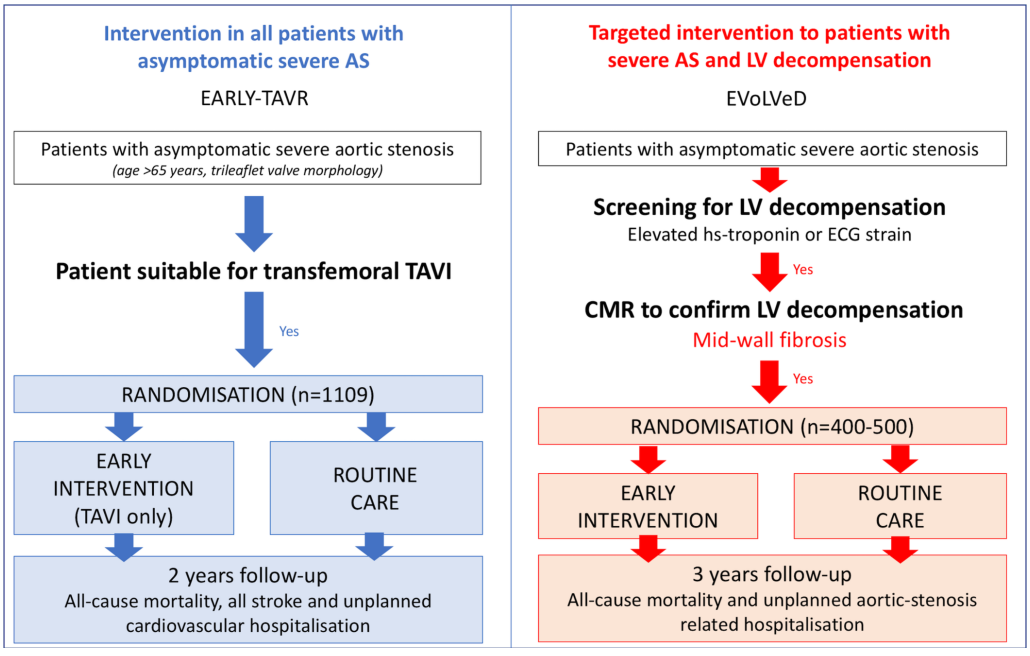

Figure 3 Comparison of EARLY-TAVR and EVoLVeD randomised controlled trial designs. Currently, recruiting randomised controlled trials generally fall into two groups: those investigating valve intervention in all asymptomatic patients with severe AS (eg, EARLY-TAVR) and those looking to target intervention based on measures of left ventricular decompensation (eg, EVoLVeD). AS, aortic stenosis; CMR, cardiac magnetic resonance; EARLY-TAVR, Evaluation of Transcatheter Aortic Valve Replacement Compared to SurveilLance for Patients with AsYmptomatic Severe Aortic Stenosis; EVoLVeD, Early Valve Replacement Guided by Biomarkers of Left Ventricular Decompensation in Asymptomatic Patients with Severe AS; hs, high-sensitivity; LV, left ventricular; TAVI, transcatheter aortic valve insertion.

Table 4 Current and planned randomised controlled trials investigating timing of aortic valve intervention

Strategy	Proposed or ongoing trials	Population	Intervention	Primary outcome	Trial status/ unique identifier	Country	Estimated completion
All-comers with asymptomatic severe AS	Aortic Valve Replacement Versus Conservative Treatment in Asymptomatic Severe Aortic Stenosis (AVATAR)	312 patients with asymptomatic severe AS and STS score <8%.	SAVR or routine care.	All-cause mortality and MACE at 3 years.	Recruiting NCT02436655	Serbia	2020
	Early Surgery for Patients with Asymptomatic Aortic Stenosis (ESTIMATE)	360 patients with asymptomatic severe AS, normal ETT and low surgical risk.	SAVR or routine care.	All-cause mortality and MACE at 1 year.	Recruiting NCT02627391	France	2019
	Evaluation of Transcatheter Aortic Valve Replacement Compared to SurveilLance for Patients with AsYmptomatic Severe Aortic Stenosis (EARLY-TAVR)	1109 patients aged >65 years with asymptomatic severe AS, trileaflet valve morphology and favourable ileofemoral arterial anatomy.	Transfemoral TAVI (Edwards SAPIEN 3) or routine care.	All-cause mortality, all stroke, and unplanned cardiovascular hospitalisation at 2 years.	Recruiting NCT03042104	United States	2021
Refined assessment of valve function – higher peak aortic-jet velocity threshold	Early Surgery Versus Conventional Treatment in Very Severe Aortic Stenosis (RECOVERY)	145 patients with very severe AS (Vmax >4.5 m/s, AVA <0.75 cm) and a negative ETT.	SAVR or routine care.	Cardiac mortality at 4 years.	Recruiting NCT01161732	South Korea	2022
Assessment of myocardial decompensation – multiple biomarker assessment of left ventricular decompensation	Early Valve Replacement Guided by Biomarkers of Left Ventricular Decompensation in Asymptomatic Patients with Severe AS (EVoLVeD)	400 patients with asymptomatic severe AS, normal LVEF and mid-wall fibrosis on cardiac MRI.	SAVR/TAVI or routine care.	All-cause mortality and unplanned AS-related hospitalisation at 3 years.	Recruiting NCT03094143	UK	2020

AS, aortic stenosis; ETT, exercise tolerance test; LVEF, left ventricular ejection fraction; MACE, major adverse cardiovascular events; SAVR, surgical aortic valve replacement; STS, Society of Thoracic Surgeons; TAVI, transcatheter aortic valve insertion.

with those who were initially managed conservatively (26%). Heart failure hospitalisation was also reduced in the early intervention group (4% vs 20%). However, propensity matching may not have accounted for all potential influences on outcomes and a significant proportion of the conservatively managed patients who developed symptoms were not referred for intervention, undoubtedly contributing to the worse observed survival in this group: confounding by indication. Three randomised controlled trials (AVATAR, ESTIMATE and EARLY-TAVR; table 4) are currently recruiting, which will examine whether valve intervention in unselected asymptomatic patients with severe AS can improve clinical outcomes.

Refined assessment of valve structure and function

An alternative strategy is to operate only in asymptomatic patients with very high peak aortic-jet velocities. Peak velocities >4.5 m/s are associated with increased referral for surgical intervention[26] but also increased rates of perioperative death and cardiac death in a prospective cohort study with propensity matching.[47] The RECOVERY randomised controlled trial will examine whether early aortic valve replacement in asymptomatic patients with velocities >4.5 m/s and a negative exercise test leads to improved patient outcomes compared with watchful waiting (table 4).

The total haemodynamic load seen by the left ventricle can also be quantified by calculating the valvuloarterial impedence (ZVa=(systolic blood pressure+mean AV gradient)/indexed LV stroke volume). This measure has consistently been shown to be an independent marker of adverse outcome in asymptomatic patients[54] and warrants further study for its use in determining the timing of intervention.

Another approach is to quantify valvular calcium burden using CT calcium scoring. Validated, sex-specific thresholds for severe AS have been proposed (2000 Agatston units (AU) for men, 1200 AU for women),[5] which provide powerful prediction of clinical events of incremental value to echocardiographic assessments.[3] Performing valve intervention on the basis of severe valvular calcification on CT might therefore represent an attractive alternative strategy.

Imaging and biomarkers of left ventricular decompensation

Simple cardiac biomarkers beyond BNP are being investigated in AS as markers of LV decompensation. Cardiac troponin is a structural protein present in cardiomyocytes, which is released into the bloodstream during myocardial injury and can now be detected at very low plasma concentrations using high-sensitivity assays. In AS, troponin I concentrations are associated with a more advanced left ventricular hypertrophic response, replacement myocardial fibrosis and worse long-term patient outcomes in patients with AS.[55] They are thought to reflect the cardiomyocyte death that drives progressive left ventricular decompensation alongside myocardial fibrosis.[8] Elevation in cardiac troponin is not however specific to AS. By contrast, the presence of LVH and the strain pattern on the 12-lead ECG demonstrate high specificity (but low sensitivity) for left ventricular hypertrophy and myocardial fibrosis, respectively, and also provides prognostic information.[56] As will be discussed, there is interest in using these simple and cheap biomarkers as screening tools to aid the detection of LV decompensation (figure 4).

What about imaging assessment to detect left ventricular decompensation? Despite its limitations, ejection fraction remains the current gold standard; however, several imaging techniques are under early investigation that can detect earlier abnormalities in left ventricular function.

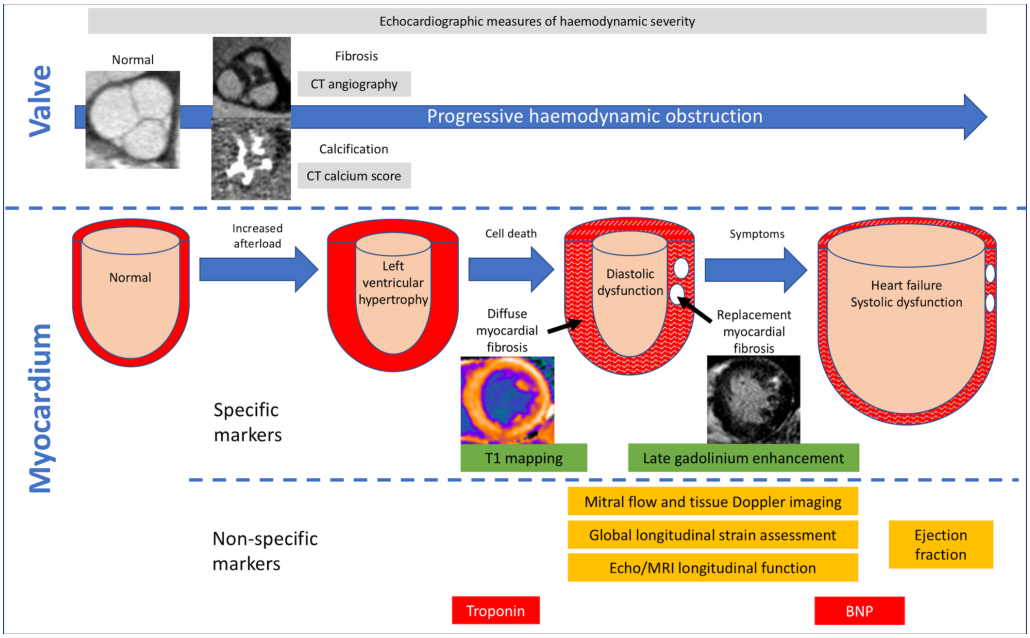

Figure 4 Imaging and biomarker assessments of stage of valvular stenosis and myocardial response to increased afterload. Progressive haemodynamic obstruction as a result of aortic leaflet restriction is assessed using echocardiography. However, specific valvular pathologies such as fibrosis and calcification can be assessed using CT methods. Ejection fraction is a poorly sensitive marker of myocardial decompensation with abnormalities in Doppler measures, longitudinal strain and systolic function, which are all detectable prior to this. However, these measures, along with biomarkers such as troponin and B-type natriuretic peptide (BNP) are non-specific and may be abnormal as a result of coexistent myocardial pathology such as coronary heart disease. T1 mapping methods and late gadolinium enhancement are more specific for decompensation as a result of pressure overload.

Echocardiography can detect alteration in various measures of diastolic and longitudinal systolic function in patients with AS, which appear related to the presence of myocardial fibrosis.[7] Reduced left ventricular global longitudinal strain can be observed in asymptomatic patients with AS, acting as an independent predictor of mortality.[23] However, several of these measures still require standardisation across vendor platforms and all suffer from significant overlap between results in healthy individuals and those with AS. Moreover, these imaging markers are not specific to valve heart disease and like symptoms might equally reflect comorbidity such as ischaemic heart disease.

Perhaps the most promising technique is cardiac MRI, which offers myocardial tissue characterisation and can detect the myocardial fibrosis that drives the development of left ventricular decompensation. Indeed, the late gadolinium enhancement technique allows direct visualisation of this fibrosis in a midwall pattern that can easily be differentiated from prior myocardial infarction. Midwall fibrosis is a direct and specific marker of left ventricular decompensation with close association with measures of left ventricular function, myocardial injury and functional capacity.[7] Furthermore, multiple studies have confirmed that midwall fibrosis is a strong independent predictor of all-cause mortality and cardiovascular death.[21 51 57] Increasing burden of midwall fibrosis correlates with a worse outcome,[21 51] and this fibrosis appears irreversible following valve intervention.[58] Midwall fibrosis therefore appears as a useful tool to identify the early stages of irreversible left ventricular decompensation. T1 mapping is an alternative technique that might allow detection of the preceding stage of reversible diffuse interstitial fibrosis.[59] At present, there are issues with variations in T1 values at different magnetic field strengths and on different scanners and problems caused by the overlap of T1 values between different disease states. Further work is required, although recent studies have shown promising early results for T1 parameters that seek to measure the overall myocardial fibrosis volume.[7]

It is possible that using a multibiomarker strategy to identify LV decompensation may prove superior to any single biomarker in isolation. For example, in the EVoLVeD randomised controlled trial (table 4), patients are initially screened with high sensitivity troponin I and an ECG. Patients with a normal troponin (<6 ng/L) are deemed to have a normal heart with no further imaging required. Patients with an elevated troponin or the ECG-strain pattern proceed to cardiac magnetic resonance (CMR) and those found to have midwall fibrosis then randomised to either early valve intervention or routine clinical care. It is hoped that this strategy will target valve intervention to those patients who will derive greatest benefit.

PRACTICAL RECOMMENDATIONS AND PROCESSES OF CARE

Care of the asymptomatic patient with AS can be complex and challenging. While additional evidence is awaited, we advise detailed clinical and

echocardiographic assessment with exercise testing and advanced imaging (eg, stress echocardiography, TOE, CT and CMR) performed as indicated to clarify symptoms, severity of AS and myocardial health. This should be performed by heart valve specialists working as part of a heart team.[5] Patient involvement in decision making is key where indications for intervention are borderline. Given delays between referral and procedure that are common in most healthcare systems, this could also be discussed with the patient and may inform decision making for earlier intervention. The recent ESC/EACTS guideline update also recommends the establishment of heart valve centres with access to advanced imaging modalities and contemporary interventional techniques supported by robust internal audit processes.[5] Finally, patients managed conservatively should be educated as to the typical symptoms of AS (table 2) and the importance of prompt symptom reporting. Regular clinic surveillance is essential, and current guidelines recommend clinical assessment with echocardiography at least every 6 months.[5]

CONCLUSIONS

AS is a common condition; the only treatment for which is replacement of the aortic valve. The optimal timing of this valve intervention remains unclear with current guidelines based on observational data and expert opinion. However, multiple randomised controlled trials are currently underway investigating whether novel strategies might improve patient outcomes compared with current watchful waiting, heralding a new era of evidence-based medicine for patients with heart valve disease.

Key messages

- Aortic stenosis is a disease of both the valve and the myocardium, characterised by fibrosis and calcification of valve leaflets, progressive left ventricular hypertrophy and myocardial fibrosis.
- Although no randomised controlled trial data exist, current clinical guidelines recommend valve intervention when severe aortic stenosis is accompanied by evidence of left ventricular decompensation.
- Timing of valve intervention is crucial. Too early and the patient will be unnecessarily exposed to risks of intervention and prosthetic valve complications; too late and irreversible myocardial damage can lead to persistent symptoms and risk of adverse events. Ideally valve replacement would be performed just as left ventricular decompensation is starting to develop.
- Improved surgical methods and perioperative care, as well as transcatheter aortic valve implantation techniques have resulted in major reductions in procedural risk. As such, earlier valve intervention in asymptomatic patients could be contemplated, and randomised controlled trials are underway that will help inform our future management.

CME credits for Education in Heart

Education in Heart articles are accredited for CME by various providers. To answer the accompanying multiple choice questions (MCQs) and obtain your credits, click on the 'Take the Test' link on the online version of the article. The MCQs are hosted on BMJ Learning. All users must complete a one-time registration on BMJ Learning and subsequently log in on every visit using their username and password to access modules and their CME record. Accreditation is only valid for 2 years from the date of publication. Printable CME certificates are available to users that achieve the minimum pass mark.

Contributors RJE performed the literature search and drafted the article. Critical revisions were performed by M-AC, PP and MRD. All authors approved the final manuscript and MRD is the guarantor for the overall content.

Funding The work was supported by the British Heart Foundation (FS/14/78/31020 to MRD), the Sir Jules Thorn Charitable Trust (15/JTA to MRD), the Québec Heart and Lung Institute Foundation and Canadian Institutes of Health Research (FDN-143225 and MOP-114997 to PP and M-AC).

Competing interests None declared.

Patient consent Not required.

Provenance and peer review Commissioned; internally peer reviewed.

Data sharing statement Not applicable.

Author note References which include a * have been selected as key references for this paper.

REFERENCES

1 Iung B, Baron G, Butchart EG, *et al*. A prospective survey of patients with valvular heart disease in Europe: The Euro Heart Survey on Valvular Heart Disease. *Eur Heart J* 2003;24:1231–43.
2 Pawade TA, Newby DE, Dweck MR. Calcification in aortic stenosis: the skeleton key. *J Am Coll Cardiol* 2015;66:561–77.
*3 Clavel MA, Pibarot P, Messika-Zeitoun D, *et al*. Impact of aortic valve calcification, as measured by MDCT, on survival in patients with aortic stenosis: results of an international registry study. *J Am Coll Cardiol* 2014;64:1202–13.
4 Dweck MR, Jenkins WS, Vesey AT, *et al*. 18F-sodium fluoride uptake is a marker of active calcification and disease progression in patients with aortic stenosis. *Circ Cardiovasc Imaging* 2014;7:371–8.
*5 Baumgartner H, Falk V, Bax JJ, *et al*. 2017 ESC/EACTS Guidelines for the management of valvular heart disease. *Eur Heart J* 2017;38:2739–91.
6 Dweck MR, Boon NA, Newby DE. Calcific aortic stenosis: a disease of the valve and the myocardium. *J Am Coll Cardiol* 2012;60:1854–63.
*7 Chin CWL, Everett RJ, Kwiecinski J, *et al*. Myocardial fibrosis and cardiac decompensation in aortic stenosis. *JACC Cardiovasc Imaging* 2017;10:1320–33.
8 Hein S, Arnon E, Kostin S, *et al*. Progression from compensated hypertrophy to failure in the pressure-overloaded human heart: structural deterioration and compensatory mechanisms. *Circulation* 2003;107:984–91.
9 Petrov G, Dworatzek E, Schulze TM, *et al*. Maladaptive remodeling is associated with impaired survival in women but not in men after aortic valve replacement. *JACC Cardiovasc Imaging* 2014;7:1073–80.
10 Connolly HM, Oh JK, Orszulak TA, *et al*. Aortic valve replacement for aortic stenosis with severe left ventricular dysfunction. Prognostic indicators. *Circulation* 1997;95:2395–400.
11 Tribouilloy C, Lévy F, Rusinaru D, *et al*. Outcome after aortic valve replacement for low-flow/low-gradient aortic stenosis without

contractile reserve on dobutamine stress echocardiography. *J Am Coll Cardiol* 2009;53:1865–73.
12 Clavel MA, Magne J, Pibarot P, *et al*. Low-gradient aortic stenosis. *Eur Heart J* 2016;37:2645–57.
13 ROSS J, BRAUNWALD E. Aortic Stenosis. *Circulation* 1968;38(1S5) :V-61—-60.
14 Rafique AM, Biner S, Ray I, *et al*. Meta-analysis of prognostic value of stress testing in patients with asymptomatic severe aortic stenosis. *Am J Cardiol* 2009;104:972–7.
15 Das P, Rimington H, Chambers J. Exercise testing to stratify risk in aortic stenosis. *Eur Heart J* 2005;26:1309–13.
16 Otto CM, Burwash IG, Legget ME, *et al*. Prospective study of asymptomatic valvular aortic stenosis. Clinical, echocardiographic, and exercise predictors of outcome. *Circulation* 1997;95:2262–70.
17 Paradis JM, Fried J, Nazif T, *et al*. Aortic stenosis and coronary artery disease: what do we know? What don't we know? A comprehensive review of the literature with proposed treatment algorithms. *Eur Heart J* 2014;35:2069–82.
18 Fairbairn TA, Steadman CD, Mather AN, *et al*. Assessment of valve haemodynamics, reverse ventricular remodelling and myocardial fibrosis following transcatheter aortic valve implantation compared to surgical aortic valve replacement: a cardiovascular magnetic resonance study. *Heart* 2013;99:1185–91.
19 Dauerman HL, Reardon MJ, Popma JJ, *et al*. Early recovery of left ventricular systolic function after corevalve transcatheter aortic valve replacement. *Circ Cardiovasc Interv* 2016;9:e003425.
20 Vaquette B, Corbineau H, Laurent M, *et al*. Valve replacement in patients with critical aortic stenosis and depressed left ventricular function: predictors of operative risk, left ventricular function recovery, and long term outcome. *Heart* 2005;91:1324–9.
21 Azevedo CF, Nigri M, Higuchi ML, *et al*. Prognostic significance of myocardial fibrosis quantification by histopathology and magnetic resonance imaging in patients with severe aortic valve disease. *J Am Coll Cardiol* 2010;56:278–87.
22 Cramariuc D, Cioffi G, Rieck AE, *et al*. Low-flow aortic stenosis in asymptomatic patients: valvular-arterial impedance and systolic function from the SEAS Substudy. *JACC Cardiovasc Imaging* 2009;2:390–9.
23 Kusunose K, Goodman A, Parikh R, *et al*. Incremental prognostic value of left ventricular global longitudinal strain in patients with aortic stenosis and preserved ejection fraction. *Circ Cardiovasc Imaging* 2014;7:938–45.
24 Lund O, Flø C, Jensen FT, *et al*. Left ventricular systolic and diastolic function in aortic stenosis. Prognostic value after valve replacement and underlying mechanisms. *Eur Heart J* 1997;18:1977–87.
25 Kitai T, Honda S, Okada Y, *et al*. Clinical outcomes in non-surgically managed patients with very severe versus severe aortic stenosis. *Heart* 2011;97:2029–32.
26 Rosenhek R, Zilberszac R, Schemper M, *et al*. Natural history of very severe aortic stenosis. *Circulation* 2010;121:151–6.
27 Rosenhek R, Klaar U, Schemper M, *et al*. Mild and moderate aortic stenosis. Natural history and risk stratification by echocardiography. *Eur Heart J* 2004;25:199–205.
28 Rosenhek R, Binder T, Porenta G, *et al*. Predictors of outcome in severe, asymptomatic aortic stenosis. *N Engl J Med* 2000;343:611–7.
29 Bergler-Klein J, Mundigler G, Pibarot P, *et al*. B-type natriuretic peptide in low-flow, low-gradient aortic stenosis: relationship to hemodynamics and clinical outcome: results from the Multicenter Truly or Pseudo-Severe Aortic Stenosis (TOPAS) study. *Circulation* 2007;115:2848–55.
30 Weber M, Arnold R, Rau M, *et al*. Relation of N-terminal pro B-type natriuretic peptide to progression of aortic valve disease. *Eur Heart J* 2005;26:1023–30.
31 Clavel MA, Malouf J, Michelena HI, *et al*. B-type natriuretic peptide clinical activation in aortic stenosis: impact on long-term survival. *J Am Coll Cardiol* 2014;63:2016–25.
32 Hwang YM, Kim J, Lee JH, *et al*. Conduction disturbance after isolated surgical aortic valve replacement in degenerative aortic stenosis. *J Thorac Cardiovasc Surg* 2017;154:1556–65.
33 Chaker Z, Badhwar V, Alqahtani F, *et al*. Sex differences in the utilization and outcomes of surgical aortic valve replacement for severe aortic stenosis. *J Am Heart Assoc* 2017;6:e006370.
34 Leon MB, Smith CR, Mack MJ, *et al*. Transcatheter or surgical aortic-valve replacement in intermediate-risk patients. *N Engl J Med* 2016;374:1609–20.
35 Auensen A, Hussain AI, Bendz B, *et al*. Morbidity outcomes after surgical aortic valve replacement. *Open Heart* 2017;4:e000588.
36 Smith CR, Leon MB, Mack MJ, *et al*. Transcatheter versus surgical aortic-valve replacement in high-risk patients. *N Engl J Med* 2011;364:2187–98.
37 Leon MB, Smith CR, Mack M, *et al*. Transcatheter aortic-valve implantation for aortic stenosis in patients who cannot undergo surgery. *N Engl J Med* 2010;363:1597–607.
38 Thourani VH, Kodali S, Makkar RR, *et al*. Transcatheter aortic valve replacement versus surgical valve replacement in intermediate-risk patients: a propensity score analysis. *Lancet* 2016;387:2218–25.
39 Reardon MJ, Van Mieghem NM, Popma JJ, *et al*. Surgical or transcatheter aortic-valve replacement in intermediate-risk patients. *N Engl J Med* 2017;376:1321–31.
40 Ludman P. Transcatheter Aortic Valve Implantation: UK TAVI Audit 2016. httpswww.bcis.org.ukwp-contentuploadsTAVI-slide-deck-to-data-for-web-as-.pdf
41 Mack MJ, Leon MB, Smith CR, *et al*. 5-year outcomes of transcatheter aortic valve replacement or surgical aortic valve replacement for high surgical risk patients with aortic stenosis (PARTNER 1): a randomised controlled trial. *Lancet* 2015;385:2477–84.
42 Cannegieter SC, Rosendaal FR, Briët E. Thromboembolic and bleeding complications in patients with mechanical heart valve prostheses. *Circulation* 1994;89:635–41.
43 Glaser N, Jackson V, Holzmann MJ, *et al*. Prosthetic valve endocarditis after surgical aortic valve replacement. *Circulation* 2017;136:329–31.
44 Hammermeister K, Sethi GK, Henderson WG, *et al*. Outcomes 15 years after valve replacement with a mechanical versus a bioprosthetic valve: final report of the Veterans Affairs randomized trial. *J Am Coll Cardiol* 2000;36:1152–8.
45 Johnston DR, Soltesz EG, Vakil N, *et al*. Long-term durability of bioprosthetic aortic valves: implications from 12,569 implants. *Ann Thorac Surg* 2015;99:1239–47.
46 Pellikka PA, Sarano ME, Nishimura RA, *et al*. Outcome of 622 adults with asymptomatic, hemodynamically significant aortic stenosis during prolonged follow-up. *Circulation* 2005;111:3290–5.
47 Kang DH, Park SJ, Rim JH, *et al*. Early surgery versus conventional treatment in asymptomatic very severe aortic stenosis. *Circulation* 2010;121:1502–9.
48 Taniguchi T, Morimoto T, Shiomi H, *et al*. Initial surgical versus conservative strategies in patients with asymptomatic severe aortic stenosis. *J Am Coll Cardiol* 2015;66:2827–38.
49 Malaisrie SC, McDonald E, Kruse J, *et al*. Mortality while waiting for aortic valve replacement. *Ann Thorac Surg* 2014;98:1564–71. discussion1570–1.
50 Flores-Marín A, Gómez-Doblas JJ, Caballero-Borrego J, *et al*. Long-term predictors of mortality and functional recovery after aortic valve replacement for severe aortic stenosis with left ventricular dysfunction. *Rev Esp Cardiol* 2010;63:36–45.
51 Dweck MR, Joshi S, Murigu T, *et al*. Midwall fibrosis is an independent predictor of mortality in patients with aortic stenosis. *J Am Coll Cardiol* 2011;58:1271–9.
52 Monin JL, Quéré JP, Monchi M, *et al*. Low-gradient aortic stenosis: operative risk stratification and predictors for long-term outcome: a multicenter study using dobutamine stress hemodynamics. *Circulation* 2003;108:319–24.
53 Chin CW, Messika-Zeitoun D, Shah AS, *et al*. A clinical risk score of myocardial fibrosis predicts adverse outcomes in aortic stenosis. *Eur Heart J* 2016;37:713–23.
54 Hachicha Z, Dumesnil JG, Pibarot P. Usefulness of the valvuloarterial impedance to predict adverse outcome in asymptomatic aortic stenosis. *J Am Coll Cardiol* 2009;54:1003–11.
55 Chin CW, Shah AS, McAllister DA, *et al*. High-sensitivity troponin I concentrations are a marker of an advanced hypertrophic response and adverse outcomes in patients with aortic stenosis. *Eur Heart J* 2014;35:2312–21.
56 Shah AS, Chin CW, Vassiliou V, *et al*. Left ventricular hypertrophy with strain and aortic stenosis. *Circulation* 2014;130:1607–16.
57 Barone-Rochette G, Piérard S, De Meester de Ravenstein C, *et al*. Prognostic significance of LGE by CMR in aortic stenosis patients undergoing valve replacement. *J Am Coll Cardiol* 2014;64:144–54.
58 Weidemann F, Herrmann S, Störk S, *et al*. Impact of myocardial fibrosis in patients with symptomatic severe aortic stenosis. *Circulation* 2009;120:577–84.

59 Krayenbuehl HP, Hess OM, Monrad ES, *et al*. Left ventricular myocardial structure in aortic valve disease before, intermediate, and late after aortic valve replacement. *Circulation* 1989;79:744–55.

Curr Cardiovasc Imaging Rep (2016) 9: 21
DOI 10.1007/s12410-016-9383-z

CARDIAC MAGNETIC RESONANCE (V PUNTMANN AND E NAGEL)

The Role of Imaging in Aortic Valve Disease

Russell J. Everett[1] · **David E. Newby**[1] · **Andrew Jabbour**[2] · **Zahi A. Fayad**[3] · **Marc R. Dweck**[1]

Published online: 7 June 2016

Abstract
Purpose of Review Aortic valve disease is the most common form of heart valve disease in developed countries. Imaging remains central to the diagnosis and risk stratification of patients with both aortic stenosis and regurgitation and has traditionally been performed with echocardiography. Indeed, echocardiography remains the cornerstone of aortic valve imaging as it is cheap, widely available and provides critical information concerning valve hemodynamics and ventricular function.
Recent Findings Whilst diagnostic in the vast majority of patients, echocardiography has certain limitations including operator variability, potential for measurement errors and internal inconsistencies in severity grading. In particular, low-gradient severe aortic stenosis is common and challenging to diagnose. Aortic valve imaging may therefore be improved with alternative and complimentary multimodality approaches.
Summary This review investigates established and novel techniques for imaging both the aortic valve and the myocardial remodelling response including echocardiography, computed tomography, cardiovascular magnetic resonance and positron emission tomography. Moreover, we examine how the complementary information provided by each modality may be used in both future clinical practice and the research arena.

Keywords Valve · Stenosis · Regurgitation · Magnetic resonance imaging · Echocardiography · Computed tomography · Positron emission tomography

This article is part of the Topical Collection on *Cardiac Magnetic Resonance*

✉ Russell J. Everett
russell.everett@ed.ac.uk

[1] BHF/Centre for Cardiovascular Science, University of Edinburgh, Chancellor's Building, 49 Little France Crescent, EH16 4SB Edinburgh, UK

[2] St Vincent's Hospital, Sydney, Australia

[3] Icahn School of Medicine at Mount Sinai, New York, USA

Introduction

Aortic valve disease is the most common valvular heart disease in the developed world [1]. In particular, calcific aortic stenosis is responsible for considerable morbidity and mortality [2]. *Aortic stenosis* (AS) was once thought to be related to simple "wear and tear" as a result of advancing age but is increasingly understood to be a highly regulated process with some similarities to atherosclerosis. An initiating event is believed to cause endothelial damage, inflammatory cell infiltration and initiation of calcification. A progressive cycle of calcium deposition in the valve leaflets then occurs leading to an inexorable march towards severe aortic stenosis and the development of symptoms and heart failure unless aortic valve replacement (AVR) is performed [3]. *Aortic regurgitation* (AR) is common in calcific aortic valve disease but may also be caused by other pathology affecting the valve, such as endocarditis, or the aortic root, causing functional regurgitation as in hypertension, Marfan syndrome, annulo-aortic ectasia, collagen vascular disease and aortic dissection.

In both aortic stenosis and regurgitation, imaging of the aortic valve is critical in establishing a diagnosis, grading severity and informing the timing of valvular intervention. In addition, the importance of the myocardial remodelling response to these forms of valve disease is increasingly appreciated [4]. Aortic stenosis leads to a pressure-overloaded left ventricle, resulting in the left ventricular hypertrophy (LVH),

which normalises wall stress according to Laplace's law. This is initially adaptive, but decompensation eventually occurs leading to the development of heart failure, symptoms and adverse events. Current clinical guidelines suggest valvular intervention in severe aortic stenosis when there is evidence of LV decompensation as indicated by the development of either symptoms or impaired LV ejection fraction (EF) [5, 6]. However, assessment of symptoms in elderly patients who often have multiple comorbidities can be challenging whilst impairment of LV systolic function occurs late in the disease process [7] and is often irreversible [8, 9]. There is therefore a need for more objective assessments of the left ventricular decompensation. Similarly, in aortic regurgitation, the left ventricle dilates in response to chronic volume overload in an eccentric hypertrophic response. With time, this decompensation of this remodelling response also occurs, leading to heart failure, symptoms and adverse events in the absence of treatment. Current guidelines advocate valve replacement in the presence of severe aortic regurgitation and symptoms or when LV dilatation reaches certain thresholds.

In this review, we will describe how modern advances in non-invasive imaging might optimise assessments of aortic valve stenosis and regurgitation as well as how the left ventricular remodels in response to those lesions. In particular, the established role of echocardiography will be explored alongside emerging modalities such as computed tomography (CT), cardiovascular magnetic resonance (CMR) and positron emission tomography (PET).

Aortic Stenosis

Echocardiography

Transthoracic echocardiography (TTE) is the clinical imaging modality of choice for assessing aortic stenosis and has been since in the 1980s when it supplanted invasive catheter-based measurements. It is safe, non-invasive and widely available, allowing direct visualisation of aortic valve anatomy (e.g. bicuspid vs. trileaflet), function and hemodynamics whilst also facilitating measurement of the left ventricular wall thickness, cavity dimensions and both systolic and diastolic function.

Doppler echocardiography provides information on aortic valve hemodynamics that is not readily available using other imaging modalities. Simple assessments of both peak and mean velocities through the aortic valve (Fig. 1) are used to calculate peak and mean pressure gradients using the modified Bernoulli formula as well as the aortic valve area (AVA) using the continuity equation. The latter is flow independent and therefore often essential for diagnostic accuracy particularly in low-flow states [10]. Current guidelines recommend grading haemodynamic severity of aortic stenosis on the basis of

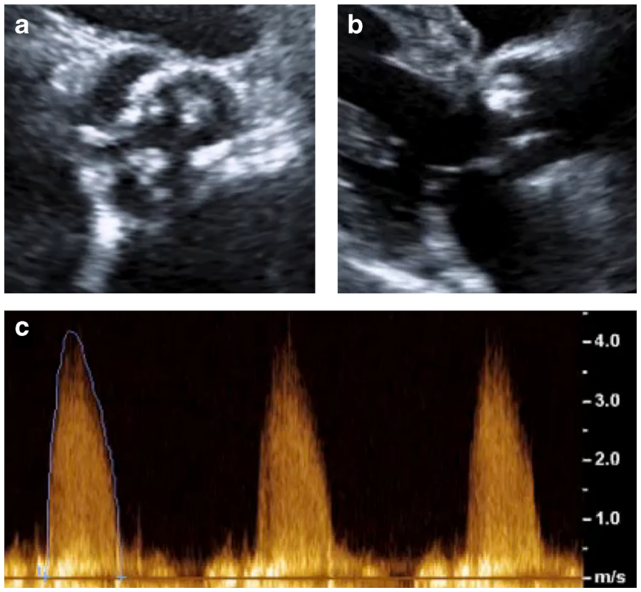

Fig. 1 Echocardiographic assessment of a patient with severe aortic stenosis. **a** Short axis view showing heavily calcified leaflets. **b** Parasternal long axis view showing large calcium deposit on right coronary cusp with restricted valve opening. **c** Right sternal edge continuous-wave Doppler with aortic valve velocity >4 m/s, corresponding with severe stenosis

the combined information provided by the peak velocity (AV Vmax), the mean gradient and the aortic valve area [5, 6].

Whilst this combined approach is effective in the majority of patients, it leads to a wide spectrum of diagnostic categories and the potential for clinical confusion. Other potential limitations of echocardiography are also being increasingly appreciated. Firstly, acquisition of diagnostic acoustic windows can be impossible in certain patients as can perfect alignment of the Doppler probe with the direction of maximal blood flow through the valve. In both circumstances, measurement errors will be introduced. Secondly, echocardiography may have difficulty in measuring the left ventricular outflow tract (LVOT) diameter with accuracy: a key component when using the continuity equation to calculate the aortic valve area. Indeed, echo often underestimates the LVOT diameter due to either calcification or its elliptical shape, and as the measurement is squared, even small errors become magnified substantially. The continuity equation also relies on several geometric assumptions that frequently do not hold true in aortic stenosis (such as a circular outflow tract and laminar flow profile), introducing further error. Finally, internal inconsistencies exist in the severity thresholds established in the clinical guidelines. An AVA of 1.0 cm^2 is sensitive but less specific for severe aortic stenosis and in fact corresponds to a mean pressure gradient of 30–35 mmHg [11], rather than the 40 mmHg cut-off recommended [5, 6]. This in part may explain why between 20 and 30 % of patients with moderate or severe aortic stenosis have discrepant assessments of disease severity depending on the echocardiographic marker assessed [4, 12].

LV Function and Mass

Echocardiography-derived LV ejection fraction is used in clinical guidelines to reflect LV systolic function. Impairment in the EF below 50 % is an indication for valve intervention as these patients have a poor outcome without surgery [8, 13]. However, a fall in ejection fraction is an insensitive measure of LV systolic dysfunction in the presence of concentric remodelling and hypertrophy. Indeed, approximately one third of patients with aortic stenosis and a normal EF have significant evidence of LV systolic impairment when assessed by other methods [14]. These alternative markers include global longitudinal strain measurements, which have been shown to be of prognostic importance in patients with severe aortic stenosis and a normal ejection fraction [15].

Patients with aortic stenosis invariably develop the left ventricular hypertrophy as the LV remodels to normalise wall stress. The degree to which this occurs is not well correlated to the haemodynamic severity of stenosis and is an independent predictor of outcomes [16, 17•]. The LV hypertrophic response should therefore be assessed separately. Concentric remodelling geometry [18] and severe LVH [19] have been associated with mortality following valve replacement whilst increased LV mass is associated with cardiovascular morbidity and mortality in patients with asymptomatic severe AS [17•]. Importantly, recent evidence from 1656 patients in the SEAS trial showed that LV mass index was an independent predictor of cardiovascular events and all-cause mortality [20••].

Low-Flow Low-Gradient Subtypes

The most challenging patients are those with discordant parameters of severity, most commonly characterised by a low AVA and low transvalvular gradient. As discussed, there are several possible explanations for this including measurement error and internal inconsistencies in guideline thresholds. However, in many patients, the discrepancy will not be due to error but instead reflect a low-flow status related to an array of different factors. Low flow is usually defined by a stroke volume (SV) index of <35 ml/m^2 although this cut-off is somewhat arbitrary.

Classical Low-Flow Low-Gradient AS

In patients with severe aortic stenosis and LV systolic dysfunction, the stroke volume is low due to reduced myocardial contractility. As a consequence, the gradient generated over the aortic valve is relatively low (mean gradient <40 mmHg) but the valve area is small <1.0 cm^2 (low-flow low gradient with reduced EF severe AS). It is important to differentiate this condition from "pseudo-severe AS," where the ventricle is severely impaired due to an alternative pathology to the extent that it cannot generate sufficient flow to completely open the aortic valve. Low-dose dobutamine stress echocardiography (DSE), as recommended in clinical guidelines [5, 6], can differentiate between these; if the mean valve gradient increases to >40 mmHg (or AV Vmax >4 m/s) and valve area remains <1.0 cm^2 with dobutamine stress, then severe AS has been identified. These patients have a relatively low operative mortality (5–7 % [21, 22]) and benefit from AVR [23].

Flow Reserve

Those patients who fail to increase their gradient with stress echocardiography likely have no or reduced "flow reserve" which is defined as an increase in stroke volume of less than 20 % [24]. This group of patients has significantly higher operative mortality (22–30 % [13, 21]), but those who survive AVR have outcomes (improvement in EF and mortality) similar to those with flow reserve [13, 25] and an improved prognosis compared to similar patients managed medically [13]. There may be an increased future role for transcatheter aortic valve implantation (TAVI) in this group given their high operative risk.

Paradoxical Low-Flow Low-Gradient AS

These patients have low flow in the context of preserved ejection fraction, again leading to a picture of a reduced AVA (<1.0 cm^2) and low mean gradient (<40 mmHg). It is often referred to as low-flow low-gradient normal EF or paradoxical low-flow low-gradient aortic stenosis and was first identified in 2007 [26]. Commonly, these patients are female and elderly, with a small hypertrophied LV cavity as the cause of their low stroke volume. A recent meta-analysis of 7459 patients and other studies have indicated that mortality is increased in this group [26, 27••, 28, 29] and reduced by valve intervention [28–31]. However, this has not been observed consistently in all trials [32]. Stress echocardiography has not been shown to be helpful in these patients as they often exhibit restrictive physiology due to diastolic dysfunction limiting any increase in SV; however, aortic valve CT calcium scoring may aid in discrimination [12]. Current clinical guidelines recommend aortic valve intervention in this group if the patient is symptomatic and the clinician feels that valve obstruction is the most likely cause of symptoms based on the above parameters [5, 6].

Normal-Flow Low-Gradient AS

Patients with both a low AVA and low mean gradient in the context of preserved EF and normal flow are a common [27••] but under recognised group who are not represented in clinical guidelines. Although this is heterogeneous group that encompasses measurement errors, small body size or inconsistencies in clinical guidelines [11], a significant proportion have severe AS [12] and AVR appears to improve

survival [31]. A recent large meta-analysis has demonstrated that these patients have outcomes similar to high-gradient severe AS which are improved by AVR [27••]. Further research in this area is required.

Dimensionless Index

The dimensionless velocity index is a flow-independent variable calculated by dividing the LVOT velocity-time integral (VTI, or Vmax) by the AV VTI (or Vmax) without a need to measure the LVOT diameter. A ratio of <0.25 indicates severe stenosis and is particularly useful where LVOT measurement is difficult to perform or in cases of inconsistent grading [33].

Advanced Echocardiography

In addition to demonstrating flow reserve in low-flow low-gradient severe AS with a reduced ejection fraction, stress echocardiography has also been shown to improve prognostication in asymptomatic high-gradient severe AS where an increase in mean gradient of >20 mmHg on exercise stress predicts a greater risk of developing symptoms and adverse events [34, 35].

Transoesophageal echocardiography (TOE) can be of use in aortic stenosis with planimetry of the AVA used as an alternative measure of aortic stenosis severity. Whilst planimetry remains difficult on 2D imaging due to extensive calcification and difficulty ensuring position at the leaflet tips, it appears more readily feasible on 3D TOE. A study of 307 patients with severe aortic stenosis compared valve planimetry using 3D TOE with TTE-derived aortic valve area. They showed that valve planimetry was possible in 92 % of patients (in the 8 % where it was not possible, this was due to severe calcification) and that the two measurements showed a good correlation ($r = 0.85$). However, planimetred AVA measurements were consistently higher than those calculated with the continuity equation [36]. Adjudicating disease severity using planimetry can therefore be difficult although in that context, an AVA <1.0 cm^2 is a strong indication of severe aortic stenosis and a potentially useful arbitrator in cases of diagnostic uncertainty.

TOE also offers accurate assessment of the aortic root and annulus dimensions and is frequently performed preoperatively before aortic valve surgery. Similar measurements can be made with CT imaging and the modality used differs between centres. The use of intraoperative TOE is routine in many cardiothoracic centres where it allows accurate assessment of anatomy and optimisation of hemodynamics before establishing cardiopulmonary bypass. Post-procedure, TOE can confirm satisfactory valve function, stable hemodynamics and exclude complications such as outflow tract obstruction. A number of observational studies suggest that intraoperative TOE changes management in 11–18 % of patients may improve outcome [37, 38] and may be cost-effective [39]. Intraoperative TOE has a class lla recommendation from the most recent CC/AHA/ASE 2003 Guideline Update for the Clinical Application of Echocardiography.

Pre-procedural imaging (TOE or CT) is essential prior to TAVI to ensure correct prosthesis sizing, and real-time intra-procedural TOE is often used to aid in device sizing and positioning [40, 41], although this is limited to trans-apical and aortic approaches where the patient is under general anaesthetic. Studies are conflicting but suggest that there is overall a slight overestimation of annulus area with CT and underestimation with TOE [42, 43]. 3D TOE is superior to 2D TOE and offers similar results to CT in some studies [44].

Valvular Calcification

Although the mechanisms underlying valvular calcification remain incompletely determined [3], its importance to disease progression and adverse events was first identified in the seminal studies by Rosenhek and colleagues [45••, 46••]. One hundred and twenty-six patients with asymptomatic severe aortic stenosis were followed up for 22 ± 18 months. Aortic valve calcification was measured on a four-point ordinal scale with moderate or severe calcification (a score of 3 or 4) being the only independent predictor of AVR or mortality, outperforming haemodynamic measures of severity. Significant valve calcification is also associated with faster disease progression, need for AVR and all-cause mortality in patients with mild to moderate stenosis [46••]. Whilst severe aortic valve calcification is considered a lla indication for AVR in asymptomatic patients with severe AS, this technique is in practice difficult to apply because of poor intra-observer agreement as to the severity of calcification [47].

CT

CT Calcium Scoring

Calcium burden in the aortic valve can be more accurately quantified on electrographically gated non-contrast computed tomography (CT). The aortic valve CT calcium score can then be measured using the Agatston score (AU), which accounts for both the density and volume of CT measured calcium and correlates closely with the weight of calcium in explanted aortic valves [47]. Aortic valve CT calcium scoring has demonstrated excellent intra- and inter-observer and scan-rescan reproducibility [47, 48] and correlates closely with echocardiographic measures of haemodynamic severity [47–49]. Importantly, recent data has demonstrated that the aortic valve CT calcium score provides powerful prediction of disease progression and prognosis [50–52].

Severity Cut-Offs

Thresholds in CT calcium score for differentiating moderate from severe aortic stenosis have recently been proposed in a study of 451 patients with concordant grading of AS severity on echocardiography and preserved ejection fraction. Interestingly, these were different for males and females (≥2065 AU for men and ≥1274 AU for women) even after indexing to the aortic annulus area (≥476 AU/cm^2 for men and ≥292 AU/cm^2 for women). These thresholds were then applied to a larger cohort of 794 patients and demonstrated a strong predictive value for all-cause mortality of incremental value to echocardiographic parameters of ejection fraction and stenosis severity [53••] (Fig. 2).

Aortic valve calcium scoring may be of particular use in cases of low-flow low gradient with reduced EF [49, 54], especially in the absence of flow reserve [47] where it can be challenging to determine severity by echocardiography alone. Further work is required to assess the validity of these thresholds in alternative patient populations and to confirm their predictive value. If these prove confirmatory, then we believe CT calcium scoring will emerge as a clinically useful and flow-independent adjuvant to standard echocardiography.

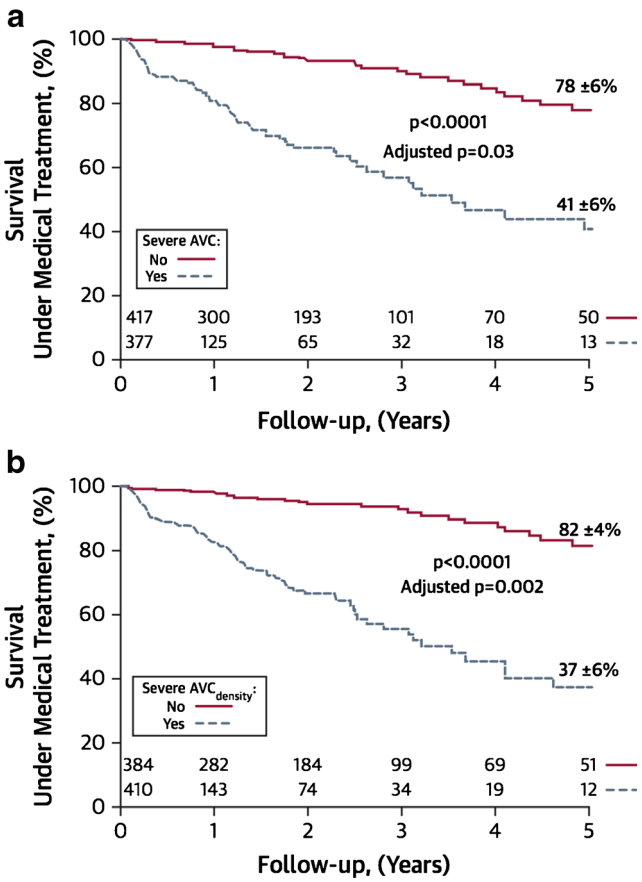

Fig. 2 Survival of patients with aortic stenosis under medical treatment according to valvular calcium score. Patients with severe absolute calcification (**a**) or calcification indexed to body surface area (**b**) had increased all-cause mortality compared to patients with non-severe calcification. Indeed, severe aortic valve calcification (AVC) was an independent predictor of survival following adjustment for age, sex, presence of coronary artery disease or diabetes, indexed aortic valve area and ejection fraction. Reproduced from Clavel et al. [53••] with permission from Elsevier/Journal of the American College of Cardiology

Improved AVA Calculation

The increasing use of CT angiography for valve sizing prior to TAVI procedures has demonstrated that the LVOT is often eccentric not circular. Indeed, a recent study of 269 patients with severe AS undergoing CT demonstrated that the LVOT is eccentric in 93 % of patients [55]. As a consequence, TTE measures of the LVOT diameter can frequently result in underestimation of the true AVA [56]. Using CT, CMR or indeed 3D echo to planimeter the LVOT area could therefore improve the accuracy of AVA calculations.

PET

PET is a novel imaging technique, which allows the activity of specific disease processes to be measured in vivo. Recently, this technique has employed two tracers to measure inflammation (^{18}F-fluorodeoxyglucose (^{18}F-FDG)) and calcification activity (^{18}F-fluoride) in the valves of patients with aortic stenosis. Hybrid PET/CT scanners then allow the activity of these two key processes to be compared with the presence of established regions of macrocalcification on CT.

^{18}F-Fluoride

^{18}F-fluoride has been used as a bone tracer for 50 years binding to hydroxyapatite crystal and detecting regions of increased bone activity. In the vasculature, it binds preferentially to regions of newly developing microcalcification because the surface area of hydroxyapatite in these nanocrystalline regions is at its highest. By contrast in regions of macrocalcification, much of the hydroxyapatite is internalised and not available for binding [57]. In aortic stenosis, ^{18}F-fluoride acts as a marker of calcification activity correlating with histological staining for alkaline phosphatase ($r = 0.65$) and osteocalcin ($r = 0.68$) [52] and predicts where novel regions of macroscopic calcium are going to form (Fig. 3). Tracer uptake increases with more advanced aortic stenosis [58], offers powerful prediction of disease progression at 1 and 2 years, of small incremental value to computed tomography [52, 59], and acts as an independent predictor of adverse clinical events [59]. This technique holds promise in better understanding the role of calcification in aortic stenosis, for example, a recent PET study demonstrated that whilst calcification activity in aortic stenosis is greater than inflammation, the reverse is true in atherosclerosis, potentially explaining the different effects of statins in these two conditions [60]. With further improvement, ^{18}F-fluoride PET may

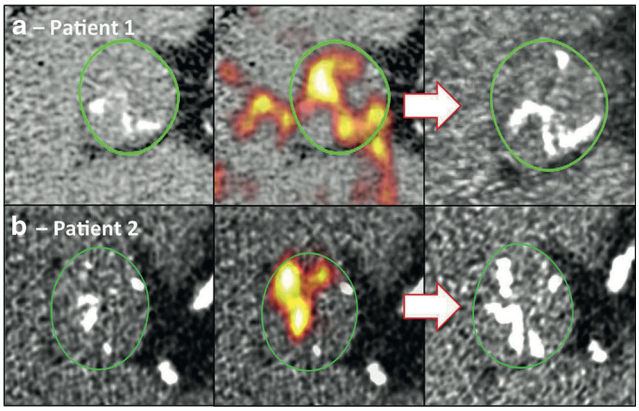

Fig. 3 18F-fluoride PET activity predicts the development of new calcific deposits in the aortic valve on repeat CT imaging performed after 1 year. Example imaging from two patients (a and b) are shown below. Baseline non-contrast CT images (*left*) showed evidence of increased 18F-Fluoride PET activity (*middle*) in areas where subsequent calcification was observed on repeat CT scanning after 1 year (*right*). Reproduced from Pawade et al. [3] with permission from Elsevier/ Journal of the American College of Cardiology

prove of clinical use in identifying patients likely to progress rapidly towards surgery and as a marker of disease activity and efficacy end point in clinical trials of novel therapies (e.g. SALTIRE 2: NCT02132026).

^{18}F-FDG

^{18}F-FDG PET is widely used to image vascular inflammation. This PET tracer is a glucose analogue, which accumulates in metabolically active cells such as vascular macrophages. Indeed, an excellent correlation between macrophage burden on histology (CD68 staining on immunohistochemistry) in carotid atheroma [61] and the ^{18}F-FDG signal has been observed. In aortic stenosis, ^{18}F-FDG activity is higher in patients versus controls, demonstrating a modest correlation with severity of valvular disease [58]. Of interest, no correlation with CD68 staining of explanted valves was observed suggesting that ^{18}F-FDG uptake is occurring in other metabolically active cells, although this study was limited by a low sample size [52]. Perhaps, the biggest limitation of this technique is the effect of physiological myocardial ^{18}F-FDG uptake, which frequently contaminates signal originating from the aortic valve.

CMR

Cardiac magnetic resonance is an emerging technology that offers excellent spatial resolution, functional assessment and the unique ability to provide myocardial tissue characterisation. However, it remains an expensive modality with limited availability for cardiac patients in most centres,

LV Mass and Hypertrophy

CMR provides the gold-standard assessment of LV volumes and mass and allows detailed investigation of both the degree of hypertrophy and the different patterns of the left ventricular adaption. Importantly, the myocardial hypertrophic response is only weakly correlated with the hemodynamic severity of aortic stenosis [16, 62, 63], with males generally display a greater increase in LV mass even after correction for body size [16]. Classically, wall thickening occurs in a concentric pattern, but recent studies have shown that asymmetrical patterns also exist in around a quarter of patients assessed by CMR [16]. The clinical importance of this observation remains unclear.

Myocardial Fibrosis

Myocardial fibrosis is a key mechanism driving the progression from the left ventricular hypertrophy to heart failure and death in aortic stenosis [64]. Historically, it has only been appreciated using invasive endomyocardial biopsy techniques, but this carries a small but significant risk of complications [65] and is susceptible to sampling error. CMR provides a non-invasive assessment of whole-heart fibrosis using two techniques: late gadolinium enhancement (LGE) and T1 mapping (Fig. 4).

LGE

This technique was first described in 1999 [66] and involves the intravenous administration of gadolinium-based contrast agents (GBCA). These agents alter myocardial T1 values and enter healthy myocardium from the blood pool down a concentration gradient within 1–3 min (wash-in phase). Renal excretion of GBCA from the blood pool then produces a reverse concentration gradient with myocardial GBCA concentrations declining over the ensuing 10–30 min (wash-out phase). The large molecular size of gadolinium stops GBCA from crossing cell membranes, so that they effectively label the extracellular space and accumulate in regions of replacement fibrosis due to delayed wash-out [67]. These focal areas can then be detected using T1-weighted sequences 15–20 min after contrast administration. In aortic stenosis, areas of replacement fibrosis appear as bright areas in the mid-wall of the left ventricle in contrast to surrounding healthy myocardium [68]. Areas of previous myocardial infarction, which are common in AS patients, are also detected by this technique but can be differentiated from mid-wall replacement fibrosis by their subendocardial/transmural pattern and their coronary distribution.

Mid-wall replacement fibrosis as detected by LGE is common in aortic stenosis (29–62 % of patients depending on the population studied [69, 70•, 71•]) and seems to be irreversible following valve intervention [72]. The presence of LGE correlates with histological fibrosis [73•] and evidence of

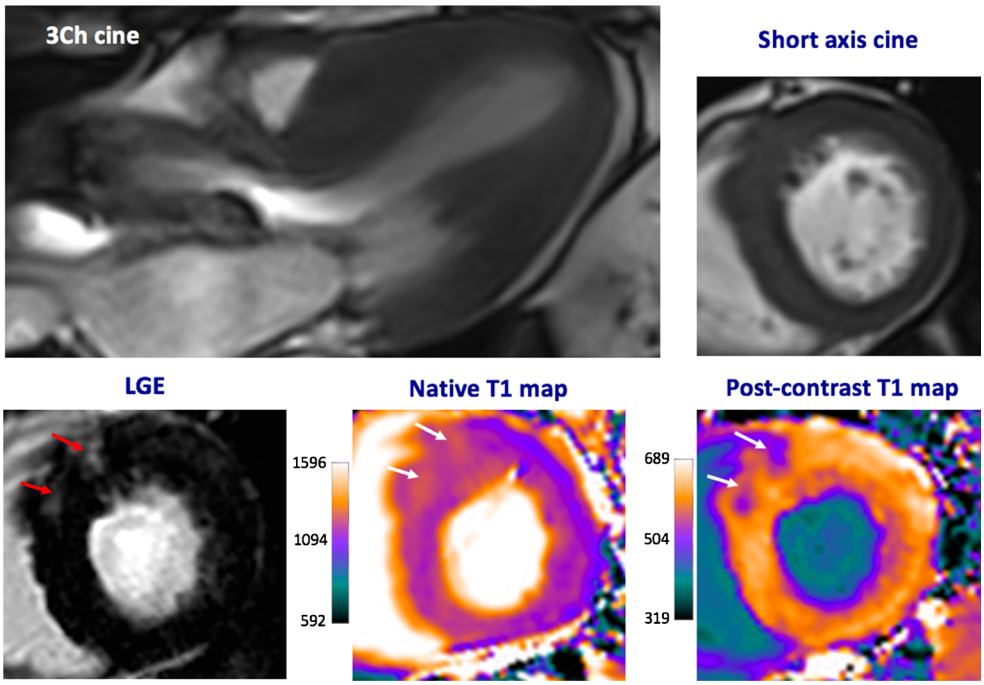

Fig. 4 Cardiac magnetic resonance imaging in a patient with severe aortic stenosis. Predominant asymmetrical hypertrophy of the anteroseptum is seen with associated patchy mid-wall late gadolinium enhancement (LGE, *red arrows*). These areas are also identified visually using native and post-contrast T1 maps (*white arrows*)

myocardial injury (as measured by high sensitivity troponin I concentrations) [74]. Advanced mid-wall fibrosis identifies patients that do not gain improvement in LV systolic function [73•] or overall functional status following AVR [72]. Importantly, three studies have confirmed that the presence of LGE acts as an independent predictor of all-cause mortality [70•, 71•, 73•], increasing the risk of death up to eightfold [70•]. Mid-wall fibrosis therefore appears to be a direct marker of the left ventricular decompensation in aortic stenosis and may be of use in identifying patients whose ventricle are starting to fail and who might benefit from prompt AVR. Further research on this area is needed; indeed, EVoLVeD-AS a multicentre randomised-controlled trial assessing the benefit of early surgery in patients with advanced aortic stenosis and mid-wall fibrosis on CMR is due to the start enrolling patients next year.

Diffuse Fibrosis

The non-invasive assessment of diffuse fibrosis is more challenging. Its homogeneous nature means that it is missed on LGE techniques, which rely on regions of normal myocardium to generate contrast. However, the detection of diffuse fibrosis is important because it is widely believed to be reversible [75] and the precursor to irreversible forms of replacement fibrosis.

Myocardial T1 mapping techniques enable the calculation of a specific T1 relaxation time (native T1) for each CMR voxel which can then be displayed on a 2D map with colour overlays applied for easier visual analysis. Multiple different techniques have been developed (Table 1). Full examination of these techniques is beyond the scope of this article, but further information can be found in this recent review by Moon et al. [76]. In brief, *native T1 measurements* can be made without the need for contrast, an important potential advantage especially in subjects with severe renal dysfunction who are at risk of contrast-induced nephrogenic systemic fibrosis (NSF) [77]. GBCA can also be used to generate *post-contrast T1 maps* as gadolinium shortens T1 relaxation times. In principle, these images provide greater signal but they are influenced by individual variation in gadolinium kinetics and have suffered from poor reproducibility when studied in AS populations [78•]. Importantly, these variations in kinetics can be corrected using several approaches. The partition coefficient (λ) is calculated as a ratio of myocardial to blood post-contrast T1 values, which improves reproducibility and corrects for many confounders. At gadolinium contrast equilibrium, the contrast concentration in the blood and myocardium should be equal. Calculating the blood volume of distribution (1—haematocrit) enables the myocardial volume of distribution to be deduced, also termed the extracellular volume fraction (ECV). Because ECV predominantly comprises collagen and is increased in fibrotic states, it acts as a marker of myocardial fibrosis, correlating closely with the collagen volume fraction on histology [79–82].

Although native T1 and ECV have been extensively studied in the literature, results are mixed and interpretation is confounded by heterogenous studied populations, variations in T1 mapping sequence, CMR scanner, magnetic field strength and analytical technique (e.g. inclusion or exclusion of areas of LGE).

Native T1 values appear to correlate with histological myocardial fibrosis [83, 84] as well as global longitudinal strain

Table 1 T1 mapping measures available for assessment of myocardial fibrosis

Measure	Unit	Calculation	Advantages	Limitations
Native T1	ms	T1 relaxation curve	No gadolinium requirement (can use in severe renal failure)	T1 signal represented a composite of myocardium and extracellular space
Post-contrast T1	ms	T1 relaxation curve following gadolinium administration	Improved sensitivity in identifying myocardial fibrosis	Significant variability due to individual variation in gadolinium kinetics and time to imaging post-contrast injection
Partition coefficient (λ)	Ratio	Ratio of T1 signal change (pre- and post-contrast) in myocardium and blood pool	Excellent scan-rescan reproducibility	Does not account for plasma volume of distribution of gadolinium contrast
Extracellular volume fraction (ECV)	%	ECV = λ × (1—haematocrit)	Excellent scan-rescan reproducibility. Conceptually attractive measure	Gives a measure of relative fibrosis which may not best track changes in aortic stenosis
Fibrosis volume	ml	ECV × end-diastolic volume	Quantitative measure of absolute fibrosis volume	Limited evidence at current time May require indexing to body size to enable comparison between individuals

[84], LV mass, haemodynamic assessments of severity and patient functional status [83]. However, its ability to differentiate healthy patients from controls is dependent on the population studied [78•, 83] with a significant degree of overlap in T1 values between these groups particularly subjects with less advanced stenosis. In a population of non-ischaemic dilated cardiomyopathy patients, native T1 has recently been shown to be an independent predictor of all-cause mortality and heart failure events [85] although this has not been demonstrated in aortic stenosis patients.

ECV

The extracellular volume fraction is used as a surrogate for the extracellular space, which is expanded with collagen deposition in diffuse fibrosis. Our centre has demonstrated superior intra- and inter-observer and scan-rescan variability in aortic stenosis compared to the other T1 measures, and ECV correlates with LV diastolic dysfunction [78•] and functional status [86]. However, prognostic data is currently lacking. There is also significant overlap between ECV values obtained in healthy volunteers and AS patients, and normal ECV values have been observed in a hypertensive population (another condition characterised by LV pressure overload) [87].

Another disadvantage is that ECV measures fibrosis relative to the volume (or mass) of the left ventricle. Balanced increases in both LV mass and diffuse fibrosis with progressive aortic stenosis are therefore not detected using this approach. In fact, an important study by Krayenbeuhl et al. involving serial myocardial biopsies demonstrated that histological myocardial fibrosis as a percentage of the myocardium (which is estimated by ECV calculation on CMR) actually increased early following aortic valve surgery as a result of significant reduction in LV mass with no change in the amount of fibrosis. However, the overall fibrous content (which can be estimated on CMR by fibrosis volume; ECV × end-diastolic myocardial volume) did eventually decrease at a later stage (repeat biopsy an average of 70 months post AVR) [75]. This is partly supported by a recent CMR study which found that ECV did not change at 6 months following AVR, whereas there was significant regression of cellular hypertrophy [86]. There is however no CMR data regarding late regression of diffuse fibrosis measures. We believe the use of the fibrosis volume as a measure of absolute fibrosis may better reflect disease progression and be able to track changes across interval scans, although this requires investigation in prospective studies.

Clinical Risk Score

CMR is an expensive technique with limited availability in many centres. We have devised a clinical risk score [88] based on five readily measured variables: age, sex, peak aortic valve velocity, high sensitivity troponin I concentration and presence of LV strain pattern on ECG, which is highly predictive of the presence of mid-wall replacement fibrosis on CMR and mortality. Ultimately, this could be used clinically in place of CMR imaging or as a screening tool for LV decompensation in aortic stenosis.

Valve Assessment

CT imaging is able to detect macroscopic calcium deposits in the aortic valve but is unable to identify fibrosis or lipid deposition, which are key components in the stenotic valve. CMR offers superior tissue characterisation as demonstrated in a proof of concept study where 30 explanted aortic valves were scanned *ex-vivo* and compared with histological analysis. CMR showed excellent sensitivity and specificity for the identification of both mineralisation (calcification) and fibrosis, with lower accuracy for lipid-rich tissues [89]. Although this is an exciting field for further research, in vivo imaging with this approach is not currently feasible due to leaflet motion.

Aortic Regurgitation

Echocardiography

TTE remains the first-line imaging modality in the investigation of patients with aortic regurgitation, allowing assessment of mechanism, valve morphology and severity of regurgitation as well as measures of LV remodelling and function. Imaging of the aortic root and ascending aorta is essential, although in patients with poor acoustic windows, cross-sectional imaging may be required for accurate assessment.

The assessment of aortic regurgitation severity is more nuanced than aortic stenosis, requiring the integration of different visual, semi-quantitative and quantitative parameters as recommended by clinical guidelines [5, 6]. Visual assessment of the valve leaflets allows appreciation of prolapse or non-coaptation, whilst the length and width of the regurgitant jet on colour Doppler gives a qualitative impression of severity. Whilst useful, these measures correlate only modestly with the following more objective measures of AR severity which also require assessment [90].

Semiquantitative Parameters

Calculating the ratio of the regurgitant jet width to that of the LVOT gives a semiquantitative measure of AR severity (severe if >65 %) [91]. The vena contracta (the narrowest part of the regurgitant jet) can also be measured, and a width of >0.6 cm suggests severe AR. Both these techniques are limited by a single plane of assessment and the assumption of a circular regurgitant orifice. 3D TTE may therefore allow more accurate measurements [92].

Doppler-Based Measures

Although continuous wave AR Doppler jet density is a poor marker of severity, the rate of deceleration (pressure half-time, PHT) is a useful adjunct to other measures. A value of <200 ms is considered severe with measurements critically dependent on obtaining an aligned Doppler signal. PHT is best used in addition to other parameters as it is affected by LV compliance, blood pressure and usually reduced in acute AR of any severity. Doppler assessment of aortic flow direction is highly useful where imaging windows allow. Holodiastolic flow reversal in the descending aorta, especially when associated with an end-diastolic velocity of >20 cm/s, is specific but not sensitive for severe AR [93].

Quantitative Parameters

Calculation of effective regurgitant orifice area (EROA) or regurgitant volume (RV) is possible in some patients using the flow-convergence zone (PISA) method, which is less sensitive to loading conditions than other measures and also useful if the jet is eccentric. It is however less well studied than in mitral regurgitation, assumes a circular orifice (with a hemispheric flow convergence zone) and is impossible to measure in a substantial proportion of patients [90]. An alternative is the regurgitant fraction (RF), which can be calculated by the Doppler volumetric method. This involves comparing the systemic stroke volume (calculated by assessing the flow over either the mitral or pulmonary valves assuming no significant valvular regurgitation) with the total stroke volume (calculated from LVOT flow.) This is time-consuming and the potential for compounding multiple small measurement errors can lead to substantial overall inaccuracies. Again, the use of 3D TTE may be superior in calculating regurgitant fraction [94].

LV Dimensions and Function

The response of the LV to chronic volume overload is chamber dilatation and hypertrophy. Left ventricular end-systolic diameter (LVESd) is an independent predictor of the development of cardiac symptoms or LV dysfunction [95, 96] and the risk of progression or mortality approaches 20 % when LVESd >5.0 cm [97]. LV systolic impairment occurs late in the disease process and is associated with poor prognosis [98] which is improved following AVR [99]. Current clinical guidelines advise valve intervention for asymptomatic severe AR in the presence of significant LV dilatation (LVESd >5.0 cm) or LV systolic impairment [5, 6]. Other measures of LV function such as global strain and strain rate may detect earlier decompensation, and further research on outcomes is needed [100–103].

TOE

As with aortic valve replacement for aortic stenosis, transoesophageal echocardiography is frequently used (with significant variation between centres) both pre- and intraoperatively to aid in prosthesis sizing, confirm satisfactory prosthesis functioning and detect immediate post-operative complications. In centres with appropriate expertise, TOE also allows detailed assessment of valve morphology permitting valve preserving repair procedures in selected patients, particularly those with aortic root aneurysms or regurgitant non-calcified bicuspid valves [104].

CMR

As discussed, CMR provides the gold-standard assessment of LV volumes and ejection fraction [105]. Perhaps unsurprisingly, therefore, left ventricular dilatation detected by CMR (end-diastolic volume (EDV) >246 ml) has shown strong predictive ability for the future development of symptoms and need for valve surgery in AR [106••]. However, CMR is also able to

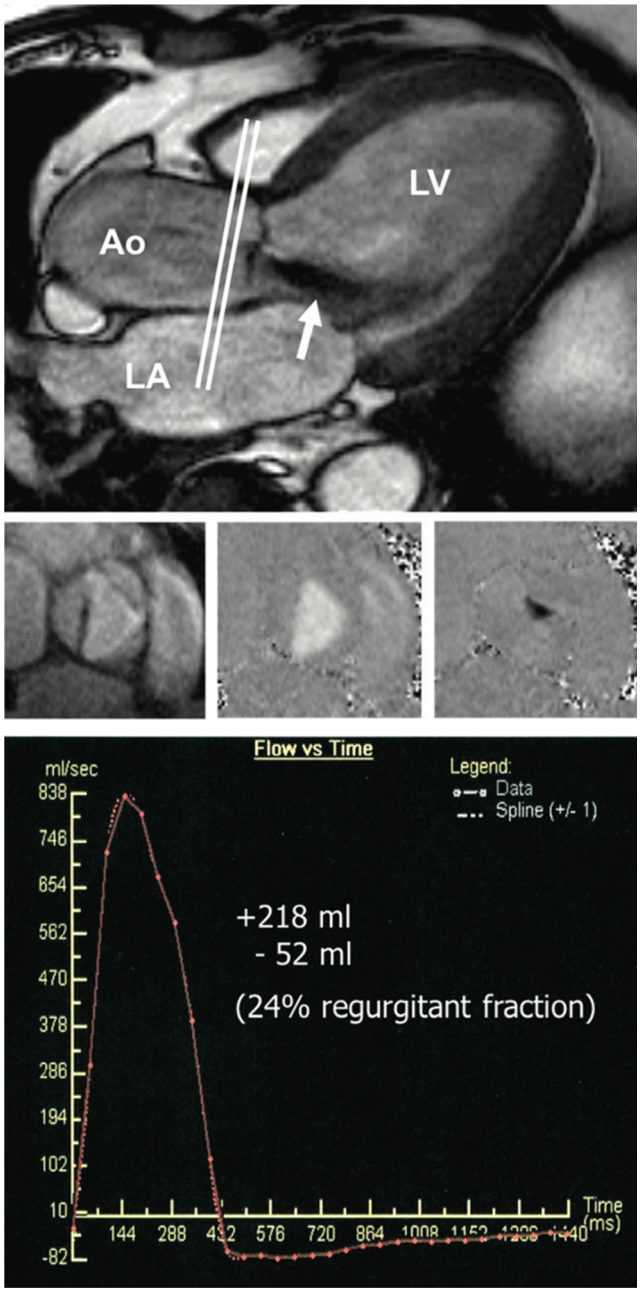

Fig. 5 Phase-contrast velocity mapping for aortic regurgitation quantification. The slice location for through plane measurement is shown on a three chamber still image (*top*) with a jet of aortic regurgitation visible (*white arrow*). Through plane images are shown (*middle*) in systole depicting magnitude (*left*) and flow (*middle*) and diastole showing regurgitation in black (*right*). Regurgitant volume and fraction can then be calculated from a time-flow curve (*bottom*). *LV* left ventricle, *Ao* aorta, *LA* left atrium. Reproduced from Myerson et al. [106••] with permission from Wolters Kluwer Health, Inc./Circulation

determine the aortic regurgitant volume to a high degree of accuracy using phase-contrast velocity mapping. This map, created in an orthogonal plane to that of aortic flow (usually at the level of the sinotubular junction [107]), encodes flow to each voxel and covers the whole cardiac cycle. It can therefore be used to calculate both anterograde and retrograde flow (and ultimately regurgitant volume and fraction, Fig. 5). It shows superior reproducibility to echocardiography [108] and excellent correlation with both TTE assessment [109] and invasive measures of stroke volume [110]. There is some debate as to the optimal cut-off in the regurgitant fraction to define severe regurgitation. A value of 50 % as used in TTE would seem logical, but there is evidence of superior discrimination at a lower value of 30 % [111] and a RF above 33 % strongly predicted the need for surgery within 3 years in a series of 113 patients [106••]. Although there are some technical reasons why a discrepancy may exist, further work is required to corroborate this single centre study and to demonstrate improvement in patient outcomes using this more expensive imaging modality. However, there may be a place for CMR assessment of aortic regurgitation in clinical practice when there is diagnostic uncertainty as to severity of regurgitation.

Conclusions

Aortic valve imaging is a rapidly expanding and exciting field. Although transthoracic echocardiography has limitations, it remains the first-line imaging modality of choice. However, other techniques are emerging which provide complimentary information and may aid clinical decision-making. In particular, CT can quantify the calcium burden in aortic stenosis as an alternative measure of disease severity. CMR can quantify the aortic regurgitant volume and provide detailed assessment of the hypertrophic response whilst PET can directly measure disease activity in the valve. Further research is required to investigate the role that these approaches may play in the future, where incremental clinical benefit to standard echocardiographic approaches will need to be demonstrated.

Compliance with Ethical Standards

Conflict of Interest RJE, DEN, AJ, ZAF and MRD declare that they have no conflicts of interest.

Human and Animal Rights and Informed Consent This article does not contain any studies with human or animal subjects performed by any of the authors.

References

Papers of particular interest, published recently, have been highlighted as:

- • Of importance
- •• Of major importance

1. Nkomo VT, Gardin JM, Skelton TN, Gottdiener JS, Scott CG, Enriquez-Sarano M. Burden of valvular heart diseases: a population-based study. Lancet. 2006;368:1005–11.
2. Carabello BA. Introduction to aortic stenosis. Circulation Research. Lippincott Williams & Wilkins; 2013;113:179–85.
3. Pawade TA, Newby DE, Dweck MR. Calcification in aortic stenosis: the skeleton key. J Am Coll Cardiol. 2015;66:561–77.
4. Dweck MR, Boon NA, Newby DE. Calcific aortic stenosis. JACC. Elsevier Inc; 2012;60:1854–63.
5. Joint task force on the management of valvular heart disease of the European Society of Cardiology (ESC), European Association for Cardio-Thoracic Surgery (EACTS), Vahanian A, Alfieri O, Andreotti F, Antunes MJ, et al. Guidelines on the management of valvular heart disease (version 2012). European Heart Journal. The Oxford University Press; 2012. pp. 2451–96.
6. Nishimura RA, Otto CM, Bonow RO, Carabello BA, Erwin JP, Guyton RA, et al. 2014 AHA/ACC guideline for the management of patients with valvular heart disease: executive summary: a report of the American College of Cardiology/American Heart Association Task Force on Practice Guidelines. Circulation. Lippincott Williams & Wilkins; 2014. pp. 2440–92.
7. Lancellotti P, Donal E, Magne J, Moonen M, O'Connor K, Daubert J-C, et al. Risk stratification in asymptomatic moderate to severe aortic stenosis: the importance of the valvular, arterial and ventricular interplay. Br Heart J. BMJ Publishing Group Ltd and British Cardiovascular Society; 2010;96:1364–71.
8. Connolly HM, Oh JK, Orszulak TA, Osborn SL, Roger VL, Hodge DO, et al. Aortic valve replacement for aortic stenosis with severe left ventricular dysfunction. Prognostic indicators. Circulation. 1997;95:2395–400.
9. Connolly HM, Oh JK, Schaff HV, Roger VL, Osborn SL, Hodge DO, et al. Severe aortic stenosis with low transvalvular gradient and severe left ventricular dysfunction:result of aortic valve replacement in 52 patients. Circulation. 2000;101:1940–6.
10. Rask LP, Karp KH, Eriksson NP. Flow dependence of the aortic valve area in patients with aortic stenosis: assessment by application of the continuity equation. J Am Soc Echocardiogr. 1996;9:295–9.
11. Minners J, Allgeier M, Gohlke-Baerwolf C, Kienzle R-P, Neumann F-J, Jander N. Inconsistent grading of aortic valve stenosis by current guidelines: haemodynamic studies in patients with apparently normal left ventricular function. Heart. BMJ Publishing Group Ltd and British Cardiovascular Society; 2010;96:1463–8.
12. Clavel M-A, Messika-Zeitoun D, Pibarot P, Aggarwal SR, Malouf J, Araoz PA, et al. The complex nature of discordant severe calcified aortic valve disease grading: new insights from combined Doppler echocardiographic and computed tomographic study. J Am Coll Cardiol. 2013;62:2329–38.
13. Tribouilloy C, Levy F, Rusinaru D, Guéret P, Petit-Eisenmann H, Baleynaud S, et al. Outcome after aortic valve replacement for low-flow/low-gradient aortic stenosis without contractile reserve on dobutamine stress echocardiography. J Am Coll Cardiol. 2009;53:1865–73.
14. Cramariuc D, Cioffi G, Rieck AE, Devereux RB, Staal EM, Ray S, et al. Low-flow aortic stenosis in asymptomatic patients: valvular-arterial impedance and systolic function from the SEAS Substudy. JACC Cardiovasc Imaging. 2009;2:390–9.
15. Kusunose K, Goodman A, Parikh R, Barr T, Agarwal S, Popovic ZB, et al. Incremental prognostic value of left ventricular global longitudinal strain in patients with aortic stenosis and preserved ejection fraction. Circ Cardiovasc Imaging. 2014;7:938–45.
16. Dweck MR, Joshi S, Murigu T, Gulati A, Alpendurada F, Jabbour A, et al. Left ventricular remodeling and hypertrophy in patients with aortic stenosis: insights from cardiovascular magnetic resonance. J Cardiovasc Magn Reson. 2012;14:1–1.
17. • Cioffi G, Faggiano P, Vizzardi E, Tarantini L, Cramariuc D, Gerdts E, et al. Prognostic effect of inappropriately high left ventricular mass in asymptomatic severe aortic stenosis. Heart. BMJ Publishing Group Ltd and British Cardiovascular Society; 2011;97:301–7. **This is the first paper suggesting that increased LV mass is an independent predictor of outcome in aortic stenosis**.
18. Duncan AI, Lowe BS, Garcia MJ, Xu M, Gillinov AM, Mihaljevic T, et al. Influence of concentric left ventricular remodeling on early mortality after aortic valve replacement. Ann Thorac Surg. 2008;85:2030–9.
19. Orsinelli DA, Aurigemma GP, Battista S, Krendel S, Gaasch WH. Left ventricular hypertrophy and mortality after aortic valve replacement for aortic stenosis. A high risk subgroup identified by preoperative relative wall thickness. JACC. 1993;22:1679–83.
20. •• Gerdts E, Rossebø AB, Pedersen TR, Cioffi G, Lønnebakken MT, Cramariuc D, et al. Relation of left ventricular mass to prognosis in initially asymptomatic mild to moderate aortic valve stenosis. Circ Cardiovasc Imaging. 2015;8:e003644. **This large prospective study showed that increased LV mass is a predictor of cardiovascular event and all-cause mortality independent of age, sex, ejection fraction and presence of hypertension**.
21. Monin J-L, Quéré J-P, Monchi M, Petit H, Baleynaud S, Chauvel C, et al. Low-gradient aortic stenosis: operative risk stratification and predictors for long-term outcome: a multicenter study using dobutamine stress hemodynamics. Circulation. Lippincott Williams & Wilkins; 2003;108:319–24.
22. Nishimura RA, Grantham JA, Connolly HM, Schaff HV, Higano ST, Holmes DR. Low-output, low-gradient aortic stenosis in patients with depressed left ventricular systolic function: the clinical utility of the dobutamine challenge in the catheterization laboratory. Circulation. 2002;106:809–13.
23. Levy F, Laurent M, Monin J-L, Maillet JM, Pasquet A, Le Tourneau T, et al. Aortic valve replacement for low-flow/low-gradient aortic stenosis operative risk stratification and long-term outcome: a European multicenter study. J Am Coll Cardiol. 2008;51:1466–72.
24. de Filippi CR, Willett DL, Brickner ME, Appleton CP, Yancy CW, Eichhorn EJ, et al. Usefulness of dobutamine echocardiography in distinguishing severe from nonsevere valvular aortic stenosis in patients with depressed left ventricular function and low transvalvular gradients. Am J Cardiol. 1995;75:191–4.
25. Quéré J-P, Monin J-L, Levy F, Petit H, Baleynaud S, Chauvel C, et al. Influence of preoperative left ventricular contractile reserve on postoperative ejection fraction in low-gradient aortic stenosis. Circulation. Lippincott Williams & Wilkins; 2006;113:1738–44.
26. Hachicha Z, Dumesnil JG, Bogaty P, Pibarot P. Paradoxical low-flow, low-gradient severe aortic stenosis despite preserved ejection fraction is associated with higher afterload and reduced survival. Circulation. Lippincott Williams & Wilkins; 2007;115:2856–64.
27. •• Dayan V, Vignolo G, Magne J, Clavel M-A, Mohty D, Pibarot P. Outcome and impact of aortic valve replacement in patients with preserved LVEF and low-gradient aortic stenosis. J Am Coll Cardiol. 2015;66:2594–603. **This meta-analysis provides the strongest evidence to date of increased mortality and survival benefit of AVR in patients with low-flow low-gradient severe aortic stenosis. Similar findings in patients with normal-flow**

low-gradient severe aortic stenosis are novel and require further research.

28. Eleid MF, Sorajja P, Michelena HI, Malouf JF, Scott CG, Pellikka PA. Flow-gradient patterns in severe aortic stenosis with preserved ejection fraction: clinical characteristics and predictors of survival. Circulation. Lippincott Williams & Wilkins; 2013;128:1781–9.
29. Clavel M-A, Dumesnil JG, Capoulade R, Mathieu P, Sénéchal M, Pibarot P. Outcome of patients with aortic stenosis, small valve area, and low-flow, low-gradient despite preserved left ventricular ejection fraction. J Am Coll Cardiol. 2012;60:1259–67.
30. O'Sullivan CJ, Stortecky S, Heg D, Pilgrim T, Hosek N, Buellesfeld L, et al. Clinical outcomes of patients with low-flow, low-gradient, severe aortic stenosis and either preserved or reduced ejection fraction undergoing transcatheter aortic valve implantation. European Heart Journal. The Oxford University Press; 2013;34:3437–50.
31. Ozkan A, Hachamovitch R, Kapadia SR, Tuzcu EM, Marwick TH. Impact of aortic valve replacement on outcome of symptomatic patients with severe aortic stenosis with low gradient and preserved left ventricular ejection fraction. Circulation. Lippincott Williams & Wilkins; 2013;128:622–31.
32. Mehrotra P, Jansen K, Flynn AW, Tan TC, Elmariah S, Picard MH, et al. Differential left ventricular remodelling and longitudinal function distinguishes low flow from normal-flow preserved ejection fraction low-gradient severe aortic stenosis. European Heart Journal. The Oxford University Press; 2013;34:1906–14.
33. Jander N, Hochholzer W, Kaufmann BA, Bahlmann E, Gerdts E, Boman K, et al. Velocity ratio predicts outcomes in patients with low gradient severe aortic stenosis and preserved EF. Br Heart J. BMJ Publishing Group Ltd and British Cardiovascular Society; 2014;100:1946–53.
34. Lancellotti P, Lebois F, Simon M, Tombeux C, Chauvel C, Pierard LA. Prognostic importance of quantitative exercise Doppler echocardiography in asymptomatic valvular aortic stenosis. Circulation. 2005;112:I377–82.
35. Maréchaux S, Hachicha Z, Bellouin A, Dumesnil JG, Meimoun P, Pasquet A, et al. Usefulness of exercise-stress echocardiography for risk stratification of true asymptomatic patients with aortic valve stenosis. European Heart Journal. The Oxford University Press; 2010;31:1390–7.
36. Saura D, de la Morena G, Flores-Blanco PJ, Oliva MJ, Caballero L, González-Carrillo J, et al. Aortic valve stenosis planimetry by means of three-dimensional transesophageal echocardiography in the real clinical setting: feasibility, reliability and systematic deviations. Echocardiography. 2015;32:508–15.
37. Qizilbash B, Couture P, Denault A. Impact of perioperative transesophageal echocardiography in aortic valve replacement. Semin Cardiothorac Vasc Anesth. SAGE Publications; 2007;11:288–300.
38. Michelena HI, Abel MD, Suri RM, Freeman WK, Click RL, Sundt TM, et al. Intraoperative echocardiography in valvular heart disease: an evidence-based appraisal. Mayo Clin Proc. 2010;85:646–55.
39. Ionescu AA, West RR, Proudman C, Butchart EG, Fraser AG. Prospective study of routine perioperative transesophageal echocardiography for elective valve replacement: clinical impact and cost-saving implications. J Am Soc Echocardiogr. 2001;14:659–67.
40. Flachskampf FA, Wouters PF, Edvardsen T, Evangelista A, Habib G, Hoffman P, et al. Recommendations for transoesophageal echocardiography: EACVI update 2014. Eur Heart J - Cardiovasc Imaging. 2014;15:353–65.
41. Hahn RT, Little SH, Monaghan MJ, Kodali SK, Williams M, Leon MB, et al. Recommendations for comprehensive intraprocedural echocardiographic imaging during TAVR. JACC Cardiovasc Imaging. 2015. pp. 261–87.
42. Wang H, Hanna JM, Ganapathi A, Keenan JE, Hurwitz LM, Vavalle JP, et al. Comparison of aortic annulus size by transesophageal echocardiography and computed tomography angiography with direct surgical measurement. Am J Cardiol. 2015;115:1568–73.
43. Tsuneyoshi H, Komiya T, Shimamoto T. Accuracy of aortic annulus diameter measurement: comparison of multi-detector CT, Two- and three-dimensional echocardiography. J Card Surg. 2016;31:18–22.
44. Altiok E, Koos R, Schröder J, Brehmer K, Hamada S, Becker M, et al. Comparison of two-dimensional and three-dimensional imaging techniques for measurement of aortic annulus diameters before transcatheter aortic valve implantation. Heart. BMJ Publishing Group Ltd and British Cardiovascular Society; 2011;97:1578–84.
45.•• Rosenhek R, Binder T, Porenta G, Lang I, Christ G, Schemper M, et al. Predictors of outcome in severe, asymptomatic aortic stenosis. N Engl J Med. 2000;343:611–7. **This seminal paper suggested the strong prognostic importance of aortic valve calcification, outperforming traditional assessment of hemodynamic severity**.
46.•• Rosenhek R, Klaar U, Schemper M, Scholten C, Heger M, Gabriel H, et al. Mild and moderate aortic stenosis. Natural history and risk stratification by echocardiography. Eur Heart J. The Oxford University Press; 2004;25:199–205. **The value of using the above echocardiography-based calcium scoring system was subsequently demonstrated in patients with mild and moderate AS**.
47. Messika-Zeitoun D, Aubry M-C, Detaint D, Bielak LF, Peyser PA, Sheedy PF, et al. Evaluation and clinical implications of aortic valve calcification measured by electron-beam computed tomography. Circulation. Lippincott Williams & Wilkins; 2004;110:356–62.
48. Cowell SJ, Newby DE, Burton J, White A, Northridge DB, Boon NA, et al. Aortic valve calcification on computed tomography predicts the severity of aortic stenosis. Clin Radiol. 2003;58:712–6.
49. Cueff C, Serfaty J-M, Cimadevilla C, Laissy J-P, Himbert D, Tubach F, et al. Measurement of aortic valve calcification using multislice computed tomography: correlation with haemodynamic severity of aortic stenosis and clinical implication for patients with low ejection fraction. Heart. BMJ Publishing Group Ltd and British Cardiovascular Society; 2011;97:721–6.
50. Messika-Zeitoun D, Bielak LF, Peyser PA, Sheedy PF, Turner ST, Nkomo VT, et al. Aortic valve calcification: determinants and progression in the population. Arterioscler. Thromb. Vasc. Biol. Lippincott Williams & Wilkins; 2007;27:642–8.
51. Nguyen V, Cimadevilla C, Estellat C, Codogno I, Huart V, Benessiano J, et al. Haemodynamic and anatomic progression of aortic stenosis. Br Heart J. BMJ Publishing Group Ltd and British Cardiovascular Society; 2015;101:943–7.
52. Dweck MR, Jenkins WSA, Vesey AT, Pringle MAH, Chin CWL, Malley TS, et al. 18F-sodium fluoride uptake is a marker of active calcification and disease progression in patients with aortic stenosis. Circ Cardiovasc Imaging. Lippincott Williams & Wilkins; 2014;7:371–8.
53.•• Clavel M-A, Pibarot P, Messika-Zeitoun D, Capoulade R, Malouf J, Aggarval S, et al. Impact of aortic valve calcification, as measured by MDCT, on survival in patients with aortic stenosis: results of an international registry study. J Am Coll Cardiol. 2014;64:1202–13. **This multicentre observational study showed that previously defined sex-specific values for severe aortic stenosis based on CT assessment of aortic valve calcification provided incremental prognostic information beyond echo-derived measures**.

54. Aksoy O, Cam A, Agarwal S, Ige M, Yousefzai R, Singh D, et al. Significance of aortic valve calcification in patients with low-gradient low-flow aortic stenosis. Clin Cardiol. Wiley Periodicals, Inc; 2014;37:26–31.
55. Clavel M-A, Malouf J, Messika-Zeitoun D, Araoz PA, Michelena HI, Enriquez-Sarano M. Aortic valve area calculation in aortic stenosis by CT and Doppler echocardiography. JACC Cardiovasc Imaging. 2015;8:248–57.
56. Chin CWL, Khaw HJ, Luo E, Tan S, White AC, Newby DE, et al. Echocardiography underestimates stroke volume and aortic valve area: implications for patients with small-area low-gradient aortic stenosis. Can J Cardiol. 2014;30:1064–72.
57. Irkle A, Vesey AT, Lewis DY, Skepper JN, Bird JLE, Dweck MR, et al. Identifying active vascular microcalcification by (18)F-sodium fluoride positron emission tomography. Nat Commun. Nature Publishing Group; 2015;6:7495.
58. Dweck MR, Jones C, Joshi NV, Fletcher AM, Richardson H, White A, et al. Assessment of valvular calcification and inflammation by positron emission tomography in patients with aortic stenosis. Circulation. Lippincott Williams & Wilkins; 2012;125:76–86.
59. Jenkins WSA, Vesey AT, Shah ASV, Pawade TA, Chin CWL, White AC, et al. Valvular (18)F-fluoride and (18)F-fluorodeoxyglucose uptake predict disease progression and clinical outcome in patients with aortic stenosis. J Am Coll Cardiol. 2015;66:1200–1.
60. Dweck MR, Khaw HJ, Sng GKZ, Luo ELC, Baird A, Williams MC, et al. Aortic stenosis, atherosclerosis, and skeletal bone: is there a common link with calcification and inflammation? European Heart Journal. The Oxford University Press; 2013;34:1567–74.
61. Tawakol A, Migrino RQ, Bashian GG, Bedri S, Vermylen D, Cury RC, et al. In vivo 18F-fluorodeoxyglucose positron emission tomography imaging provides a noninvasive measure of carotid plaque inflammation in patients. J Am Coll Cardiol. 2006;48:1818–24.
62. Gunther S, Grossman W. Determinants of ventricular function in pressure-overload hypertrophy in man. Circulation. 1979;59:679–88.
63. Salcedo EE, Korzick DH, Currie PJ, Stewart WJ, Lever HM, Goormastic M. Determinants of left ventricular hypertrophy in patients with aortic stenosis. Cleve Clin J Med. 1989;56:590–6.
64. Hein S, Arnon E, Kostin S, Schönburg M, Elsässer A, Polyakova V, et al. Progression from compensated hypertrophy to failure in the pressure-overloaded human heart: structural deterioration and compensatory mechanisms. Circulation. 2003;107:984–91.
65. Yilmaz A, Kindermann I, Kindermann M, Mahfoud F, Ukena C, Athanasiadis A, et al. Comparative evaluation of left and right ventricular endomyocardial biopsy: differences in complication rate and diagnostic performance. Circulation. Lippincott Williams & Wilkins; 2010;122:900–9.
66. Kim RJ, Fieno DS, Parrish TB, Harris K, Chen EL, Simonetti O, et al. Relationship of MRI delayed contrast enhancement to irreversible injury, infarct age, and contractile function. Circulation. 1999;100:1992–2002.
67. de Jong S, van Veen TAB, de Bakker JMT, Vos MA, van Rijen HVM. Biomarkers of myocardial fibrosis. J Cardiovasc Pharmacol. 2011;57:522–35.
68. Wu E, Judd RM, Vargas JD, Klocke FJ, Bonow RO, Kim RJ. Visualisation of presence, location, and transmural extent of healed Q-wave and non-Q-wave myocardial infarction. Lancet. Elsevier; 2001;357:21–8.
69. Rudolph A, Abdel-Aty H, Bohl S, Boyé P, Zagrosek A, Dietz R, et al. Noninvasive detection of fibrosis applying contrast-enhanced cardiac magnetic resonance in different forms of left ventricular hypertrophy relation to remodeling. J Am Coll Cardiol. 2009;53:284–91.
70.• Dweck MR, Joshi S, Murigu T, Alpendurada F, Jabbour A, Melina G, et al. Midwall fibrosis is an independent predictor of mortality in patients with aortic stenosis. J Am Coll Cardiol. 2011;58:1271–9. **The presence of mid-wall fibrosis on CMR was associated with an eight-fold increase in all-cause mortality**.
71.• Barone-Rochette G, Piérard S, de de Meester Ravenstein C, Seldrum S, Melchior J, Maes F, et al. Prognostic significance of LGE by CMR in aortic stenosis patients undergoing valve replacement. J Am Coll Cardiol. 2014;64:144–54. **Again, mid-wall fibrosis is an independent predictor of all-cause mortality following AVR**.
72. . Weidemann F, Herrmann S, Störk S, Niemann M, Frantz S, Lange V, et al. Impact of myocardial fibrosis in patients with symptomatic severe aortic stenosis. Circulation. Lippincott Williams & Wilkins; 2009;120:577–84.
73.• Azevedo CF, Nigri M, Higuchi ML, Pomerantzeff PM, Spina GS, Sampaio RO, et al. Prognostic significance of myocardial fibrosis quantification by histopathology and magnetic resonance imaging in patients with severe aortic valve disease. JACC. 2010;56:278–87. **A key study showing that mid-wall fibrosis is associated with worse improvement in LV function post-AVR and is an independent predictor of long-term survival**.
74. Chin CWL, Shah ASV, McAllister DA, Joanna Cowell S, Alam S, Langrish JP, et al. High-sensitivity troponin I concentrations are a marker of an advanced hypertrophic response and adverse outcomes in patients with aortic stenosis. Eur Heart J. 2014;35:2312–21.
75. Krayenbeuhl HP, Hess OM, Monrad ES, Schneider J, Mall G, Turina M. Left-ventricular myocardial structure in aortic-valve disease before, intermediate, and late after aortic-valve replacement. Circulation. 1989;79:744–55.
76. Higgins DM, Moon JC. Review of T1 mapping methods: comparative effectiveness including reproducibility issues. Curr Cardiovasc Imaging Rep. Springer US; 2014;7:1–10.
77. Khawaja AZ, Cassidy DB, Shakarchi Al J, McGrogan DG, Inston NG, Jones RG. Revisiting the risks of MRI with gadolinium based contrast agents-review of literature and guidelines. Insights Imaging. Springer Berlin Heidelberg; 2015;6:553–8.
78.• Chin CWL, Semple S, Malley T, White AC, Mirsadraee S, Weale PJ, et al. Optimization and comparison of myocardial T1 techniques at 3T in patients with aortic stenosis. Eur Heart J-Cardiovasc Imaging. 2014;15:556–65. **This paper demonstrated superior intra, inter observer and scan-rescan reproducibility in ECV assessment of patients with aortic stenosis**.
79. Flett AS, Hayward MP, Ashworth MT, Hansen MS, Taylor AM, Elliott PM, et al. Equilibrium contrast cardiovascular magnetic resonance for the measurement of diffuse myocardial fibrosis: preliminary validation in humans. Circulation. Lippincott Williams & Wilkins; 2010;122:138–44.
80. Fontana M, White SK, Banypersad SM. Comparison of T1 mapping techniques for ECV quantification. Histological validation and reproducibility of ShMOLLI versus multibreath-hold T1 quantification …. J Cardiovasc Magn …. 2012.
81. White SK, Sado DM, Fontana M, Banypersad SM, Maestrini V, Flett AS, et al. T1 mapping for myocardial extracellular volume measurement by CMR: bolus only versus primed infusion technique. JACC Cardiovasc Imaging. 2013;6:955–62.
82. Kammerlander AA, Marzluf BA, Zotter-Tufaro C, Aschauer S, Duca F, Bachmann A, et al. T1 mapping by CMR imaging: from histological validation to clinical implication. JACC Cardiovasc Imaging. 2016;9:14–23.
83. Bull S, White SK, Piechnik SK, Flett AS, Ferreira VM, Loudon M, et al. Human non-contrast T1 values and correlation with histology in diffuse fibrosis. Heart. BMJ Publishing Group Ltd and British Cardiovascular Society; 2013;99:932–7.
84. Lee S-P, Lee W, Lee JM, Park E-A, Kim H-K, Kim Y-J, et al. Assessment of diffuse myocardial fibrosis by using MR imaging

in asymptomatic patients with aortic stenosis. Radiology. Radiological Society of North America; 2015;274:359–69.
85. Puntmann VO, Carr-White G, Jabbour A, Yu C-Y, Gebker R, Kelle S, et al. T1-mapping and outcome in nonischemic cardiomyopathy: all-cause mortality and heart failure. JACC Cardiovasc Imaging. 2016;9:40–50.
86. Flett AS, Sado DM, Quarta G, Mirabel M, Pellerin D, Herrey AS, et al. Diffuse myocardial fibrosis in severe aortic stenosis: an equilibrium contrast cardiovascular magnetic resonance study. European Heart Journal - Cardiovascular Imaging. The Oxford University Press; 2012;13:jes102–826.
87. Hinojar R, Varma N, Child N, Goodman B, Jabbour A, Yu C-Y, et al. T1 Mapping in discrimination of hypertrophic phenotypes: hypertensive heart disease and hypertrophic cardiomyopathy: findings from the International T1 Multicenter Cardiovascular Magnetic Resonance Study. Circ Cardiovasc Imaging. Lippincott Williams & Wilkins; 2015;8:e003285.
88. Chin CWL, Messika-Zeitoun D, Shah ASV, Lefevre G, Bailleul S, Yeung ENW, et al. A clinical risk score of myocardial fibrosis predicts adverse outcomes in aortic stenosis. European Heart Journal. The Oxford University Press; 2015;:ehv525.
89. Le Ven F, Tizón-Marcos H, Fuchs C, Mathieu P, Pibarot P, Larose E. Valve tissue characterization by magnetic resonance imaging in calcific aortic valve disease. Can J Cardiol. 2014;30:1676–83.
90. Lancellotti P, Tribouilloy C, Hagendorff A, Popescu BA, Edvardsen T, Pierard LA, et al. Recommendations for the echocardiographic assessment of native valvular regurgitation: an executive summary from the European Association of Cardiovascular Imaging. European Heart Journal - Cardiovascular Imaging. Oxford University Press; 2013;14:611–44.
91. Perry GJ, Helmcke F, Nanda NC, Byard C, Soto B. Evaluation of aortic insufficiency by Doppler color flow mapping. JACC. 1987;9:952–9.
92. Fang L, Hsiung MC, Miller AP, Nanda NC, Yin WH, Young MS, et al. Assessment of aortic regurgitation by live three-dimensional transthoracic echocardiographic measurements of vena contracta area: usefulness and validation. Echocardiography. Blackwell Science Inc; 2005;22:775–81.
93. Tribouilloy C, Avinée P, Shen WF, Rey JL, Slama M, Lesbre JP. End diastolic flow velocity just beneath the aortic isthmus assessed by pulsed Doppler echocardiography: a new predictor of the aortic regurgitant fraction. Br Heart J. BMJ Group; 1991;65:37–40.
94. Choi J, Hong G-R, Kim M, Cho IJ, Shim CY, Chang H-J, et al. Automatic quantification of aortic regurgitation using 3D full volume color doppler echocardiography: a validation study with cardiac magnetic resonance imaging. Int J Cardiovasc Imaging. Springer Netherlands; 2015;31:1379–89.
95. Tornos MP, Olona M, Permanyer-Miralda G, Herrejon MP, Camprecios M, Evangelista A, et al. Clinical outcome of severe asymptomatic chronic aortic regurgitation: a long-term prospective follow-up study. Am Heart J. 1995;130:333–9.
96. Dujardin KS, Enriquez-Sarano M, Schaff HV, Bailey KR, Seward JB, Tajik AJ. Mortality and morbidity of aortic regurgitation in clinical practice. A long-term follow-up study. Circulation. 1999;99:1851–7.
97. Bonow RO, Lakatos E, Maron BJ, Epstein SE. Serial long-term assessment of the natural history of asymptomatic patients with chronic aortic regurgitation and normal left ventricular systolic function. Circulation. 1991;84:1625–35.
98. Turina J, Milincic J, Seifert B, Turina M. Valve replacement in chronic aortic regurgitation. True predictors of survival after extended follow-up. Circulation. 1998;98:II100–6–discussionII106–7.
99. Chaliki HP, Mohty D, Avierinos J-F, Scott CG, Schaff HV, Tajik AJ, et al. Outcomes after aortic valve replacement in patients with severe aortic regurgitation and markedly reduced left ventricular function. Circulation. 2002;106:2687–93.
100. Marciniak A, Sutherland GR, Marciniak M, Claus P, Bijnens B, Jahangiri M. Myocardial deformation abnormalities in patients with aortic regurgitation: a strain rate imaging study. Eur J Echocardiogr. The Oxford University Press; 2009;10:112–9.
101. Smedsrud MK, Pettersen E, Gjesdal O, Svennevig JL, Andersen K, Ihlen H, et al. Detection of left ventricular dysfunction by global longitudinal systolic strain in patients with chronic aortic regurgitation. J Am Soc Echocardiogr. 2011;24:1253–9.
102. Ewe SH, Haeck MLA, Ng ACT, Witkowski TG, Auger D, Leong DP, et al. Detection of subtle left ventricular systolic dysfunction in patients with significant aortic regurgitation and preserved left ventricular ejection fraction: speckle tracking echocardiographic analysis. European Heart Journal - Cardiovascular Imaging. Oxford University Press; 2015;16:992–9.
103. Park SH, Yang YA, Kim KY, Park SM, Kim HN, Kim JH, et al. Left ventricular strain as predictor of chronic aortic regurgitation. J Cardiovasc Ultrasound. 2015;23:78–85.
104. David TE. Surgical treatment of aortic valve disease. Nat Rev Cardiol. Nature Publishing Group; 2013;10:375–86.
105. Bellenger NG, Burgess MI, Ray SG, Lahiri A, Coats AJ, Cleland JG, et al. Comparison of left ventricular ejection fraction and volumes in heart failure by echocardiography, radionuclide ventriculography and cardiovascular magnetic resonance; are they interchangeable? European Heart Journal. The Oxford University Press; 2000;21:1387–96.
106.•• Myerson SG, d'Arcy J, Mohiaddin R, Greenwood JP, Karamitsos TD, Francis JM, et al. Aortic regurgitation quantification using cardiovascular magnetic resonance: association with clinical outcome. Circulation. Lippincott Williams & Wilkins; 2012;126:1452–60. **Regurgitant fraction calculated by phase-encoded velocity mapping can classify AR severity with high accuracy and is strongly predictive of progression to symptoms or AVR within 3 years, although the RV cut-off appeared to be lower that with echocardiography**.
107. Chaturvedi A, Hamilton-Craig C, Cawley PJ, Mitsumori LM, Otto CM, Maki JH. Quantitating aortic regurgitation by cardiovascular magnetic resonance: significant variations due to slice location and breath holding. Eur Radiol. Springer Berlin Heidelberg; 2015:1–10.
108. Cawley PJ, Hamilton-Craig C, Owens DS, Krieger EV, Strugnell WE, Mitsumori L, et al. Prospective comparison of valve regurgitation quantitation by cardiac magnetic resonance imaging and transthoracic echocardiography. Circ Cardiovasc Imaging. Lippincott Williams & Wilkins; 2013;6:48–57.
109. Honda N, Machida K, Hashimoto M, Mamiya T, Takahashi T, Kamano T, et al. Aortic regurgitation: quantitation with MR imaging velocity mapping. Radiology. 1993;186:189–94.
110. Søndergaard L, Lindvig K, Hildebrandt P, Thomsen C, Ståhlberg F, Joen T, et al. Quantification of aortic regurgitation by magnetic resonance velocity mapping. Am Heart J. 1993;125:1081–90.
111. Gabriel RS, Renapurkar R, Bolen MA, Verhaert D, Leiber M, Flamm SD, et al. Comparison of severity of aortic regurgitation by cardiovascular magnetic resonance versus transthoracic echocardiography. Am J Cardiol. 2011;108:1014–20.

Clinical Radiology xxx (2016) 1.e1–1.e11

Contents lists available at ScienceDirect

Clinical Radiology

journal homepage: www.clinicalradiologyonline.net

Review

Assessment of myocardial fibrosis with T1 mapping MRI

R.J. Everett [a,*], C.G. Stirrat [a], S.I.R. Semple [a,b], D.E. Newby [a,b], M.R. Dweck [a], S. Mirsadraee [a,b]

[a] British Heart Foundation/University Centre for Cardiovascular Science, University of Edinburgh, UK
[b] Clinical Research Imaging Centre, University of Edinburgh, UK

ARTICLE INFORMATION

Article history:
Received 10 November 2015
Received in revised form
15 January 2016
Accepted 9 February 2016

Myocardial fibrosis can arise from a range of pathological processes and its presence correlates with adverse clinical outcomes. Cardiac magnetic resonance (CMR) can provide a non-invasive assessment of cardiac structure, function, and tissue characteristics, which includes late gadolinium enhancement (LGE) techniques to identify focal irreversible replacement fibrosis with a high degree of accuracy and reproducibility. Importantly the presence of LGE is consistently associated with adverse outcomes in a range of common cardiac conditions; however, LGE techniques are qualitative and unable to detect diffuse myocardial fibrosis, which is an earlier form of fibrosis preceding replacement fibrosis that may be reversible. Novel T1 mapping techniques allow quantitative CMR assessment of diffuse myocardial fibrosis with the two most common measures being native T1 and extracellular volume (ECV) fraction. Native T1 differentiates normal from infarcted myocardium, is abnormal in hypertrophic cardiomyopathy, and may be particularly useful in the diagnosis of Anderson–Fabry disease and amyloidosis. ECV is a surrogate measure of the extracellular space and is equivalent to the myocardial volume of distribution of the gadolinium-based contrast medium. It is reproducible and correlates well with fibrosis on histology. ECV is abnormal in patients with cardiac failure and aortic stenosis, and is associated with functional impairment in these groups. T1 mapping techniques promise to allow earlier detection of disease, monitor disease progression, and inform prognosis; however, limitations remain. In particular, reference ranges are lacking for T1 mapping values as these are influenced by specific CMR techniques and magnetic field strength. In addition, there is significant overlap between T1 mapping values in healthy controls and most disease states, particularly using native T1, limiting the clinical application of these techniques at present.

Introduction

Myocardial fibrosis is integral to the pathology of a number local and systemic disease processes affecting the heart and its presence adversely predicts prognosis.[1–3] Myocardial fibrosis has traditionally been defined by histology of endomyocardial biopsies: the reference standard

* Guarantor and correspondent: R. J. Everett, British Heart Foundation/University Centre for Cardiovascular Science, Room SU 305 Chancellor's Building, University of Edinburgh, 49 Little France Crescent, Edinburgh EH16 4SB, UK. Tel.: +44 0131 242 6515; fax: +44 0131 242 6379.
E-mail address: Russell.everett@ed.ac.uk (R.J. Everett).

http://dx.doi.org/10.1016/j.crad.2016.02.013
0009-9260/

investigation for tissue characterisation of cardiomyopathies; however, this invasive technique brings with it a risk of serious complications (0.6–0.8%)[4] and is prone to sampling error. As such a non-invasive whole-heart method of assessing myocardial fibrosis is required.

Cardiac magnetic resonance imaging (CMR) is non-invasive and allows accurate assessment of cardiac structure and function. Most importantly, it provides detailed tissue characterisation, which is the key strength of CMR and is integral to its ability to aid diagnosis, prognosis, and treatment decisions. Over the last two decades, late gadolinium enhancement (LGE) imaging techniques have been developed that identify areas of focal replacement fibrosis in the myocardium. Their widespread clinical use is supported by expanding data showing that the presence of LGE is strongly associated with an adverse prognosis in several pathologies including myocardial infarction (MI),[5–8] dilated cardiomyopathy (DCM),[9] hypertrophic cardiomyopathy (HCM),[10,11] and aortic stenosis (AS).[1,12,13]

Although LGE is a useful imaging biomarker, it detects end-stage, irreversible tissue damage with replacement fibrosis. There is, therefore, considerable interest in developing novel techniques that allow earlier detection of potentially reversible diffuse fibrosis, frequently missed using LGE. Such early tissue characterisation can be achieved using MRI techniques that quantify myocardial T1 values and are starting to enter clinical practice. In this review, we will examine the novel imaging techniques used in the assessment of myocardial fibrosis, primarily focussing on the development of T1 mapping techniques, and discuss their clinical application.

LGE

This technique was first described in 1999[14] using the administration of gadolinium pentetate digmeglumine (Gd-DTPA). Following intravenous bolus administration, Gd-DTPA enters healthy myocardium down a concentration gradient (wash-in) within 1–3 minutes. As gadolinium is cleared from the blood pool by the kidneys, the contrast medium slowly exits the myocardium along the reverse concentration gradient (wash-out) over 10–30 minutes.

The large molecular size of gadolinium chelate prevents it from crossing cell membranes leading to accumulation in the extracellular space. Gadolinium potently shortens T1 related to its concentration in the tissue being imaged. Expansion of extracellular space will retain a higher concentration of gadolinium and therefore appear bright on inversion-recovery T1-weighted (T1W) sequence.[15] The inversion time (TI) can be manually adjusted to “null” the normal myocardium so that it appears black, providing the optimum visual contrasts for LGE detection. Newer phase-sensitive inversion recovery (PSIR) techniques use a background phase map, which is acquired at the same time as the image that can be used to produce intensity normalised images. This is less sensitive to TI selection, and so can avoid artefact. Although PSIR images have a lower spatial resolution, they also reduce background noise and improve the contrast-to-noise ratio[16] making them particularly useful in smaller volume centres.

Extracellular matrix (ECM) expansion and replacement fibrosis is seen in chronic MI leading to accumulation of gadolinium in these areas. In the acute setting of myocardial necrosis, there is a loss of cell membrane integrity leading to intracellular accumulation of gadolinium in the area of infarction. LGE sequences have shown excellent reproducibility and validation with histology in MI.[14] LGE imaging in the days following acute MI relates to acute cellular necrosis and myocardial oedema rather than scar and fibrosis, which usually occupies a smaller volume when it ultimately forms.[17] LGE is the reference-standard imaging technique to diagnose prior MI and offers important information on infarct size, myocardial salvage, and microvascular obstruction, all predictors of adverse outcome.[5–8,18] Importantly, these measures provide incremental prognostic information above clinical risk scores and left ventricular (LV) ejection fraction (LVEF).[8] In addition, LGE is present in a significant proportion of patients with DCM, HCM and advanced AS. Its presence in these conditions is also strongly linked with poor prognosis.[9]

LGE is essentially a difference test providing a binary assessment as to the presence or absence of LGE and requiring regions of normal myocardium to provide the necessary contrast; therefore, it has several major limitations. First, interpretation of LGE images requires a comparison between affected and unaffected myocardium and is therefore less able to detect diffuse pathological processes affecting the entire myocardium homogeneously. Second, the requirement to select manually an appropriate inversion time in order to “null” normal myocardium requires radiographer expertise and experience and introduces a potential source of error. Third, although quantification of fibrosis volume (FV) is possible, there is no universally accepted technique, and it has not been sufficiently validated for routine clinical use.[19] Finally, there is a small risk of nephrogenic systemic fibrosis with gadolinium administration, precluding its use in those with severe renal impairment,[20] although this is less of a concern with the newer cyclic agents.

T1 mapping technique

The most studied technique for assessment of diffuse myocardial fibrosis is assessment of T1 relaxation times, termed T1 mapping. A T1 map is a two-dimensional slice image where each voxel of the image displays the T1 relaxation time as signal intensity using a colour scheme for easier visual assessment. High T1 relaxation times are observed in diffuse fibrosis, protein deposition, and water in oedema. Low T1 values are seen in iron or lipid deposition.[21]

The multipoint approach to T1 sampling first described by Look and Locker (LL) in the 1970s involved continuous sampling of the T1 relaxation curve at multiple time points after an initial preparation pulse[22]; however, cardiac motion prevented the acquisition of a voxel-by-voxel T1 map and limited spatial resolution. Subsequently, the development

Please cite this article in press as: Everett RJ, et al., Assessment of myocardial fibrosis with T1 mapping MRI, Clinical Radiology (2016), http://dx.doi.org/10.1016/j.crad.2016.02.013

of the modified Look–Locker inversion (MOLLI) recovery sequence in 2004 allowed acquisition during a single breath-hold[23] by selectively acquiring data at a given time point in the cardiac cycle (using electrocardiogram [ECG] gating) and merging multiple LL sequences with varying inversion times into a single dataset (Fig 1); however, there are several limitations of the MOLLI technique. T1 values are consistently underestimated at high T1 values (>800 ms)[24] and higher heart rates, although newer MOLLI sequences have shown much less heart rate dependence.[25] In addition, the relatively long breath-hold required (over 17 cardiac cycles: roughly 15 seconds) may be challenging in some patients, particularly in the elderly or those with pulmonary disease or bradycardia.

The shortened MOLLI (ShMOLLI) recovery sequence was developed to address these limitations. Full recovery of longitudinal magnetisation is not achieved in ShMOLLI, but an algorithm allows conditional interpretation of T1 values to obtain precise measurements (Fig 2) with a consistent underestimation of T1 values, which can be corrected. This results in a halving of breath-hold times to approximately 7–9 seconds. Furthermore, the sequence is independent of heart rate, easier to post-process, and is accurate and reproducible over a wider range of T1 values.[24,26]

Several other variations of both inversion and saturation recovery techniques have been proposed. The saturation recovery single-shot acquisition (SASHA) pulse sequence consists of 10 single-shot balanced steady state free precession (bSSFP) images with ECG gating in diastasis. The sequence appeared to have good accuracy and to be both T1 and heart rate independent.[27] Several other novel techniques have been proposed but are beyond the scope of this article; the above techniques are the most common at the time of writing.

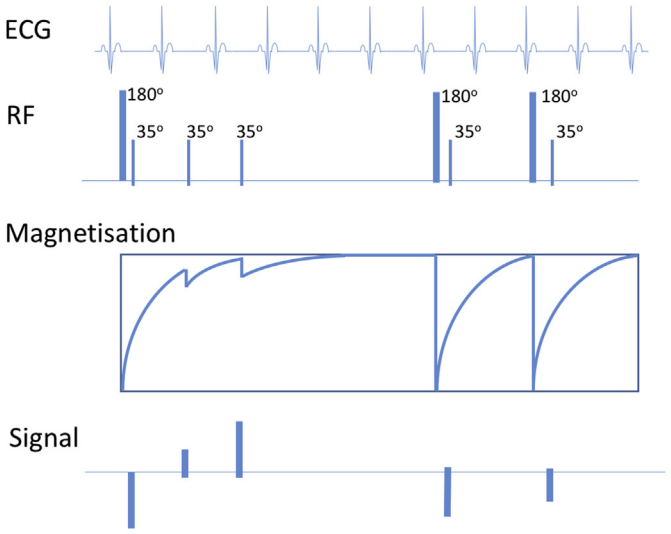

Figure 2 The ShMOLLI recovery sequence. Three inversions are still performed, however, five, one, and one images are acquired, but longitudinal magnetisation is not allowed to completely recover before the next inversion. A conditional algorithm is then applied leading to the creation of the final T1 map.

Following data acquisition, the images undergo post-processing. T1 maps are produced by combining data from 11 (MOLLI) or 5–7 (ShMOLLI) images. This may introduce errors due to through-plane motion. Position of source images may need to be corrected for misregistration caused by movement in between cardiac cycles due to a

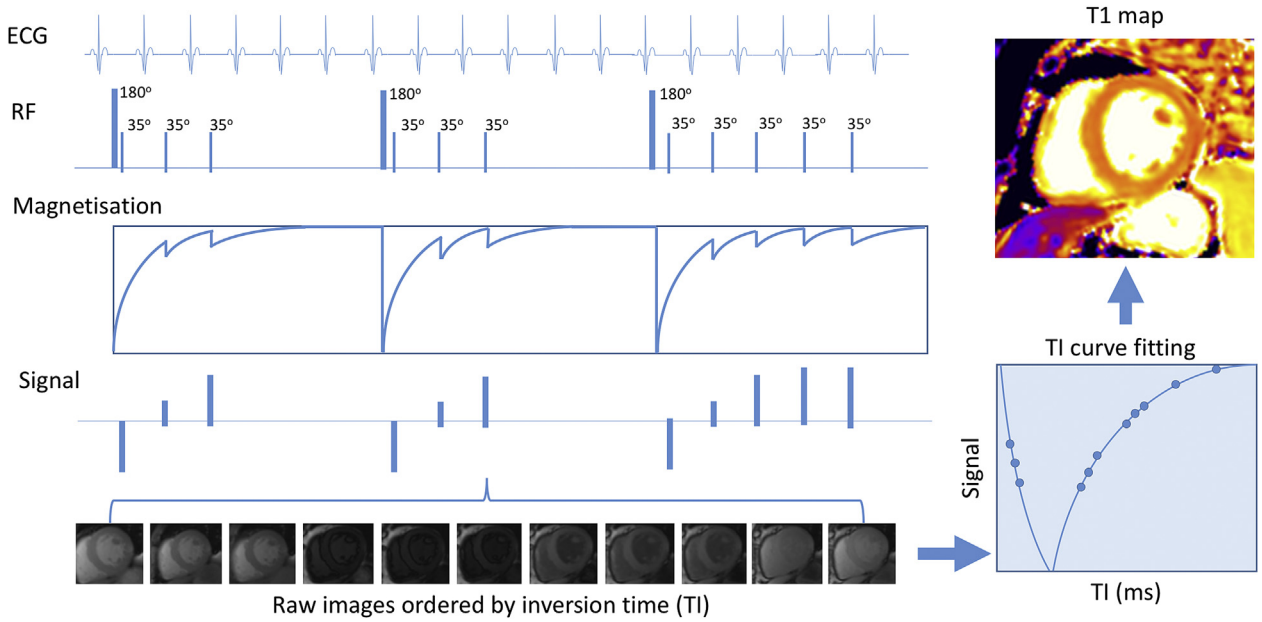

Figure 1 Use of MOLLI recovery sequence to calculate an estimate of T1 time. Three inversion recovery experiments are performed with three, three, and five images acquired. Images are ECG gated (acquired at consistent time delay from previous R wave to capture mid-diastole). The resulting raw images are then ordered by TI and signal values used to plot a T1 recovery curve, which is used to derive the T1 value. T1 values are then used to create a two-dimensional voxel map.

Please cite this article in press as: Everett RJ, et al., Assessment of myocardial fibrosis with T1 mapping MRI, Clinical Radiology (2016), http://dx.doi.org/10.1016/j.crad.2016.02.013

poor breath-hold,[28] which can be performed by automated non-rigid registration.

Gadolinium-based T1 measures

T1 mapping can also be performed after administration of gadolinium-based contrast medium administration, which shortens T1 relaxation times (Fig 3). Although providing increased signal, these post-contrast T1 values need to be corrected for a range of factors including individual variation in gadolinium kinetics and time from contrast medium administration to imaging. Gadolinium concentration has a strong non-linear relationship with the R1 relaxation rate (1/T1) and measuring the change in T1 in both the myocardium and blood pool following contrast medium administration allows the concentration of gadolinium in these compartments to be estimated. The ratio of myocardial contrast medium concentration to blood concentration is termed the partition coefficient (λ) and corrects for many of the above confounders. At contrast equilibrium, the gadolinium concentration will be equal in the myocardium and blood pool. Knowing the blood volume of distribution (1−haematocrit) allows the myocardial volume of distribution to be calculated as a surrogate for the extracellular space. This has been termed the extracellular volume (ECV) fraction. The absolute FV can then be calculated by multiplying the ECV by the myocardial volume.

Calculation of the ECV requires a steady state between myocardial and blood contrast agent, which was first achieved using a continuous contrast medium infusion. This approach, called equalisation-contrast CMR (EQ-CMR) was well validated against collagen volume fraction (CVF; the percentage of myocardial volume occupied by collagen on histological staining) but required an extra 10 minutes of scanning time plus 30−90 minutes of total patient time.[29] Alternative bolus techniques that are less cumbersome have been developed, such as dynamic-equilibrium CMR. This technique assumes that a dynamic equilibrium between the myocardium and blood pool is reached 15−20 minutes after the contrast medium bolus and so that the impact of gadolinium kinetic effects is negligible. This too has been histologically validated[30] with the optimal correlation observed using T1 measurements taken 15 minutes following contrast medium bolus.[31]

Reference values

There are a number of factors that influence the specific T1 values measured during scanning, including the image acquisition protocol, post-processing, scanner magnetic

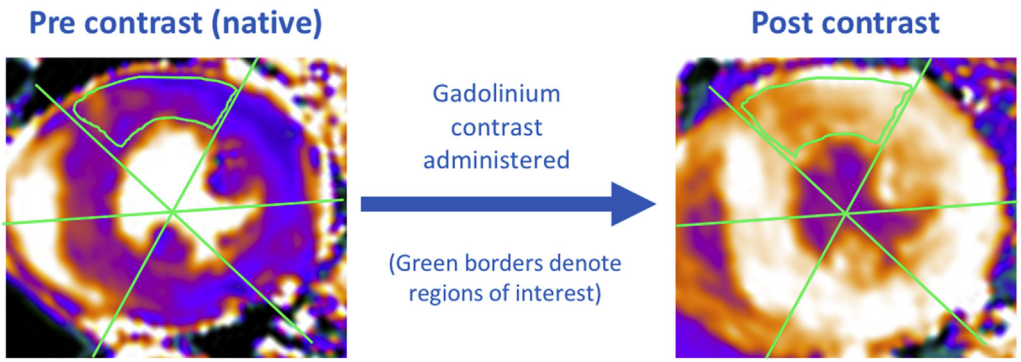

Measurement	Units	Calculation
Native T1	ms	Native T1 relaxation curve
Post-contrast T1	ms	Post-contrast relaxation curve
Partition coefficient (λ)	-	$[\Delta R1_{myocardium}/\Delta R1_{blood\text{-}pool}]$*
ECV	%	λ x (1 - haematocrit)
Fibrosis volume	ml	ECV x (LV mass / myocardial density)

*ΔR1 = (1/post-contrast T1 - 1/pre-contrast T1)
Myocardial density = 1.05g/ml

Figure 3 Common T1 mapping measurements are derived from regions of interest (ROI) drawn onto each myocardial segment and repeated following gadolinium administration.

Please cite this article in press as: Everett RJ, et al., Assessment of myocardial fibrosis with T1 mapping MRI, Clinical Radiology (2016), http://dx.doi.org/10.1016/j.crad.2016.02.013

field strength (T), contrast medium dose, and time delay to post-contrast imaging. The establishment of a normal range of values in healthy individuals is critical in order to use these quantitative techniques to diagnose disease states. These have, however, been delayed by the wide range of different approaches that are frequently site and vendor specific, and concentrated within a few specialist research centres. Although several small studies have been performed,[32,33] these have demonstrated a large overlap in values between healthy controls and most disease states, particularly with respect to native T1. Further research into new techniques or measures is required to address this key issue. Indeed a consensus statement from the Society of CMR (SCMR) has recently been produced to accelerate this development.[21] In particular, commercially available standardised sequences are awaited.

Histological validation

The myocardium can be divided conceptually into the cellular mass comprising myocytes and the extracellular interstitial space, containing the ECM. The ECM consists predominately of collagen (type I, 85% and type III, 11%), as well as basement membrane (including small amounts of collagen types IV and V), proteoglycans, glycosaminoglycans, and bioactive signalling molecules.[34]

ECV

The predominant change in myocardial fibrosis is the accumulation of excess type I collagen, which results in expansion of the ECM (and hence extracellular interstitial space) in relation to the total myocardial volume. Expansion of myocardial extracellular interstitial space is also seen with protein deposition in amyloidosis and acute myocardial oedema in MI, myocarditis, and Takotsubo cardiomyopathy.

No T1 mapping technique directly measures the extracellular matrix. The ECV, however, measures a useful surrogate; the extracellular space, which is occupied by the extracellular matrix, and therefore, is assumed to reflect diffuse myocardial fibrosis in the absence of protein deposition or oedema.

Several studies have been performed validating various T1 mapping measures against CVF determined by histological staining of myocardial biopsy samples in various cardiac pathologies (Table 1). A strong correlation was observed between native T1 and histological fibrosis in patients with severe AS as assessed on myocardial biopsy taken during aortic valve replacement (AVR).[35,36] Native T1 values were significantly different between these patients with AS and healthy controls,[36] and was also correlated with global longitudinal strain[35]; however, in a subsequent study of patients with less advance AS no difference was observed in native T1 values between age- and sex-matched control patients and those with AS.[37]

Isolated post-contrast T1 measurements have demonstrated mixed results. One study[31] demonstrated a poor correlation with histological fibrosis, whilst in AS this measurement had poor scan-rescan reproducibility and ability to differentiate disease states.[37] By contrast, other studies at 1.5 T observed a good correlation with histological fibrosis in patients with heart failure[38] and a mixture of pathologies including DCM, ischaemic cardiomyopathy, HCM, and amyloidosis.[39] Post-contrast T1 was also associated with ECM expansion in patients with heart failure with preserved ejection fraction, although this was thought to represent non-collagen ECM components.[40]

ECV is well validated against CVF. Excellent correlation has been shown at 1.5 T using EQ-CMR[29] and dynamic-equilibrium CMR[30] in patients with AS and intra-operative septal myocardial biopsy at the time of AVR. Comparable results were obtained in a similar patient group using a more contemporary ShMOLLI sequence.[41] Additional validation of ECV in whole-heart specimens explanted during cardiac transplantation showed strong correlation between ECV and CVF measured in 288 myocardial segments.[31] These patients comprised a mixture of ischaemic cardiomyopathy and DCM and were imaged at 1.5 T using a MOLLI dynamic contrast sequence.

Clinical application in specific myocardial pathologies

MI

Replacement myocardial fibrosis following MI starts in the subendocardium and extend transmurally towards the epicardium depending on the extent of infarction (Fig 4). Transmural infarction predicts a lack of functional recovery in the affected myocardial segment following coronary artery bypass grafting,[42,43] and increasing infarct size on LGE assessment correlates with reduced systolic LVEF and the risk of future cardiovascular events.[5–8]

The use of T1 mapping may allow more precise quantification of area of infarction. Native T1 is particularly attractive in the 20% of MI patients with severe renal impairment in whom gadolinium is contraindicated.[44] Native T1 relaxation times increase in both acute infarction and the scar that later forms.[24] Focal decreases in native T1 values can also be observed that are thought to relate to fat or iron deposition following haemorrhage into the infarcted area.

Native T1 is able to identify areas of acute infarction (<8 days, 1.5 T) with excellent sensitivity and specificity (96% and 91%, respectively) compared to LGE using a threshold-based approach (abnormal if T1 value of region >3 standard deviations [SD] above mean of healthy reference subjects). It is less useful at 1.5 T in the assessment of chronic infarction with a sensitivity of <50%[17] in this group; however, at 3 T both sensitivity (87–89%) and specificity (95–98%) are significantly improved. Interestingly, for this purpose a qualitative assessment performs less well (sensitivity 60–64%, specificity 86–91%) than the threshold based approach.[44] ECV is almost double in regions of prior MI (defined by the presence of LGE) compared to remote

Please cite this article in press as: Everett RJ, et al., Assessment of myocardial fibrosis with T1 mapping MRI, Clinical Radiology (2016), http://dx.doi.org/10.1016/j.crad.2016.02.013

Table 1
Histological validation of T1 mapping techniques.

Reference	Year	Area	Population	*N*	Measure	Method	Correlation
Iles *et al.*[38]	2008	Australia	DCM	25	Post-contrast T1	1.5 T, Inversion-recovery VAST sequence	$r=-0.7$, $p=0.03$
Flett *et al.*[29]	2010	UK	AS/HCM	26	ECV	1.5 T, EQ-CMR. Myocardial biopsy during AVR or septal myomectomy	$r2=0.80$, $p<0.001$
Fontana *et al.*[41]	2012	UK	AS	18	ECV	Multi-breath-hold T1 sequence ShMOLLI	$r2=0.589$ $r2=0.685$
Sibley *et al.*[39]	2012	USA	DCM/IHD/ HCM/amyloid	47	Post-contrast T1	1.5 T, inversion recovery Look Locker All patients who had undergone CMR and myocardial biopsy	$r=-0.57$, $p<0.0001$
Mascherbauer *et al.*[40]	2013	Austria	HFpEF	9	Post-contrast T1	1.5 T, inversion recovery FLASH	$r=0.98$, $p<0.01$
White *et al.*[30]	2013	UK	AS/HCM/IHD/ amyloid	18	ECV	1.5 T, EQ-CMR 1.5 T, DynEQ-CMR	$r2=0.69$. $p<0.01$ $r2=0.71$, $p<0.01$
Miller *et al.*[31]	2013	UK	DCM/IHD	6	ECV	1.5 T, DynEQ-CMR. Whole-heart explant, 288 segments analysed in total	$r2=0.555$, $p<0.001$
Bull *et al.*[36]	2013	UK	Severe AS (AVR)	19	Native T1	1.5 T, ShMOLLI	$r=0.65$, $p=0.002$
Lee *et al.*[35]	2015	South Korea	Severe AS (AVR)	20	Native T1	3 T, MOLLI	$r=0.777$, $p<0.001$

DCM, dilated cardiomyopathy; AS, aortic stenosis; HCM, hypertrophic cardiomyopathy; IHD, ischaemic heart disease; HFpEF, heart failure with preserved ejection fraction; AVR, aortic valve replacement; *n*, number of patients.

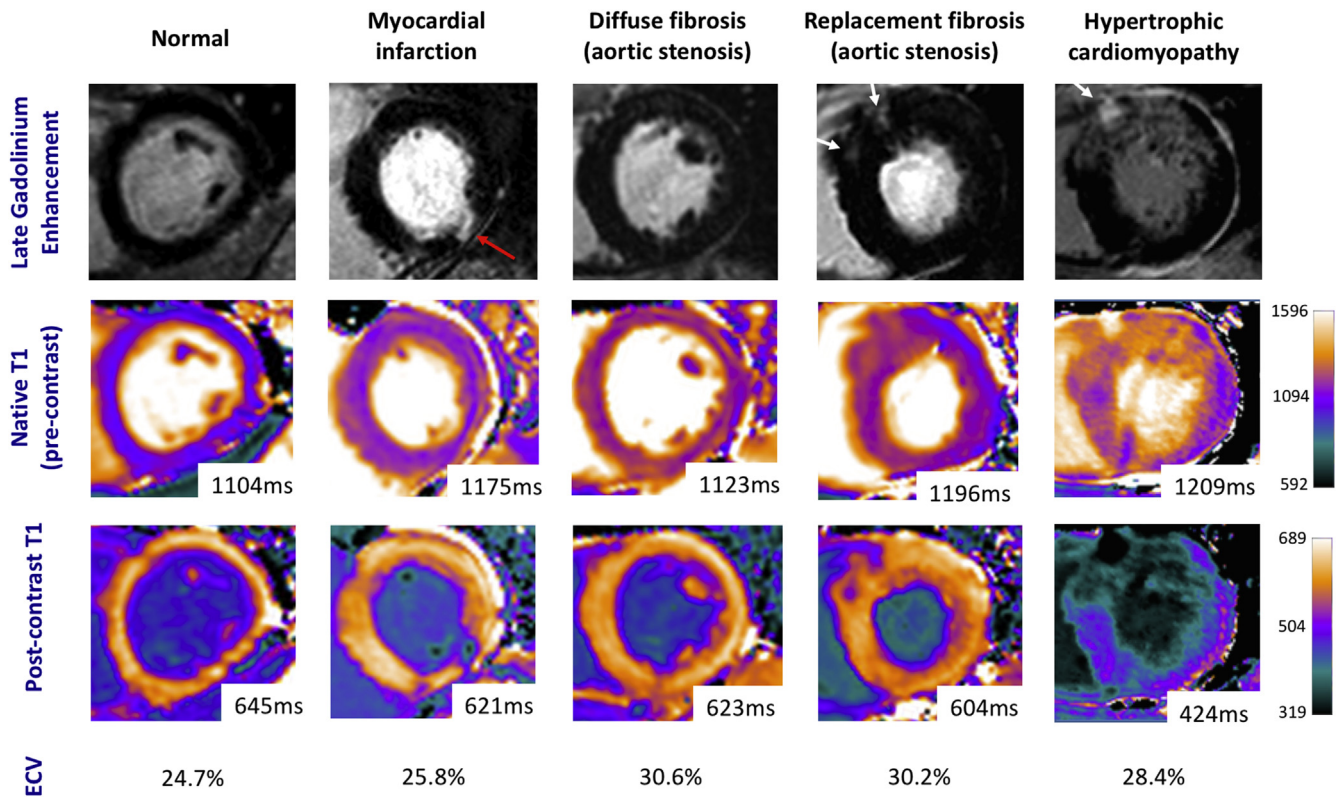

Figure 4 CMR short axis images with LGE and T1 mapping in different cardiac conditions. Areas of subendocardial (myocardial infarction, red arrow) and mid wall (AS and HCM, white arrows) late gadolinium enhancement are also identified visually with pre and post-contrast T1 maps. There is an increase in diffuse fibrosis in the AS patients as represented by higher ECV values. There is significant overlap between native T1 values in healthy controls and disease states.

Please cite this article in press as: Everett RJ, et al., Assessment of myocardial fibrosis with T1 mapping MRI, Clinical Radiology (2016), http://dx.doi.org/10.1016/j.crad.2016.02.013

normal myocardium (51 ± 8% versus 27 ± 3% respectively, $p<0.001$[45]).

Heart failure with reduced ejection fraction (HFrEF)

Myocardial fibrosis is a common end point in a range of cardiomyopathies and is identified in both systolic and diastolic heart failure.[46,47] Approximately 30% of patients with DCM have evidence of LGE in a mid-wall pattern that is associated with ventricular arrhythmias and cardiovascular mortality.[9,48] The identification of diffuse fibrosis using T1 mapping may be useful for further assessing prognosis and response to treatment.

The first study to validate post-contrast T1 measures against histological fibrosis in patients with heart failure showed that these values were lower in such patients compared to controls and correlated with diastolic function.[38] Abnormal post-contrast T1,[39,49,50] partition coefficient (λ)[51] and ECV[52] are associated with impaired ejection fraction (EF). Post-contrast T1 also correlates inversely with end-diastolic volume (EDV).[49] ECV is theoretically more sensitive in identifying early disease compared to EF and, as one would expect, increases in interstitial diffuse fibrosis appear to precede the onset of overt LV systolic impairment. Similar to LGE, ECV also appears to provide prognostic information on cardiovascular outcomes.[53,54]

Heart failure with preserved EF (HFpEF)

It has been estimated that 50% of individuals with the clinical syndrome of cardiac failure have a normal EF, with a similar prognosis to those with impaired systolic function.[55,56] These patients have abnormalities of LV relaxation rather than contraction, termed diastolic dysfunction, which is associated with increasing age, obesity, hypertension, diabetes mellitus, and atrial fibrillation. Echocardiography assessment using tissue Doppler, assessment of left atrial size and LV filling pattern is instrumental in making the diagnosis, but there is often clinical uncertainty. In addition, a proportion of the general population have some evidence of diastolic dysfunction on echocardiography.[55] ECM expansion and diffuse myocardial fibrosis are thought to be the key pathological processes underlying the development of this condition. CMR is, therefore, ideally placed to evaluate such patients although data in this ubiquitous population remains relatively sparse.

In one study, post-contrast T1 values were inversely associated with diastolic function, pulmonary vascular resistance, and adverse cardiac outcomes in 100 patients with HFpEF.[40] Another study demonstrated an increased ECV compared to healthy controls that was associated with reduced peak LV filling rate. ECV was higher still in patients with systolic heart failure, correlating inversely with EF, although there was significant overlap between these groups.[52] Focal replacement fibrosis is also common in HFpEF with 36% of 111 patients having evidence of LGE at 1.5 T (albeit using a relatively low threshold of 2 SD of signal intensity above remote myocardium to define presence of LGE). As with other conditions the presence of LGE was associated with an adverse prognosis in terms of cardiovascular death and heart failure admissions.[57]

Aortic stenosis and hypertension

Aortic stenosis is the most common valve disease in the Western world and responsible for significant morbidity. Valvular calcification and stenosis lead to progressive LV hypertrophy (LVH) and ultimately LV decompensation and heart failure unless AVR is performed. This decompensation is characterised by myocyte cell death and myocardial fibrosis.[58] Severity of valvular stenosis (as assessed on echocardiography) correlates poorly with the degree of LVH and LV impairment emphasising the importance of assessing both the valve and myocardium independently.[59] Contemporary guidelines advise AVR in the presence of symptoms (exertional angina, syncope, or dyspnoea) or reduction in LVEF. The poor prognosis following development of symptoms was described in 1968 in younger patients with bicuspid or rheumatic heart disease.[60] The demographics of AS have since shifted with most patients developing calcific disease of normal valves. Patients are now usually elderly with multiple comorbidities, which can make attributing symptoms to valve disease difficult. LV systolic impairment is recognised as an insensitive marker of LV dysfunction and often is irreversible following AVR.[61] In contrast diffuse myocardial fibrosis may regress following AVR.[62] There is therefore considerable interest in the use of CMR to assess fibrosis burden and to optimise the timing of AVR.

Diffuse fibrosis progresses to irreversible focal replacement fibrosis, which is detectable using LGE imaging,[63] and tends to be present in the LV mid-wall (Fig 4). LGE correlates with CVF on histology, myocardial injury,[64] appears irreversible post-AVR, predicts functional recovery following surgery and is an independent predictor of all-cause mortality.[1,12,13]

The assessment of diffuse fibrosis, while more challenging, may allow detection of LV decompensation before the development of irreversible replacement fibrosis or LV systolic impairment. T1 measures such as native T1[35,36] and ECV[65] are well validated against histology in populations with AS and can differentiate those patients from controls. Native T1 correlates with global longitudinal strain,[35] echo measures of AS severity, LV mass, and functional status[36]; however, native T1 lacked sensitivity to differentiate healthy controls from patients in a population with less severe AS.[37] Whilst uncorrected post-contrast T1 values lack reproducibility, both the partition co-efficient and ECV appear of promise in AS. In particular, ECV demonstrated the best intra- and interobserver and scan–rescan reproducibility,[37] and is associated with diastolic dysfunction and impaired functional status as measured by 6-minute walk test[65]; however, once again each of these T1 mapping techniques are limited by significant overlap in values between patients with AS and controls highlighting the need for novel techniques and measures.

Like AS, systolic hypertension is also associated with prolonged exposure of the LV to an increased afterload. The

Please cite this article in press as: Everett RJ, et al., Assessment of myocardial fibrosis with T1 mapping MRI, Clinical Radiology (2016), http://dx.doi.org/10.1016/j.crad.2016.02.013

myocardial response to this afterload is also similar, with LVH initially restoring wall stress but ultimately decompensating, driving the transition to heart failure and adverse events. Diffuse myocardial fibrosis is also seen on myocardial biopsy of hypertensive patients with LVH, with progressive fibrosis being associated with impairment in LVEF[66] and LV chamber stiffness.[67] Importantly, this diffuse fibrosis may regress with anti-hypertensive treatment,[67] and can be quantified with CMR T1 mapping. Indeed, ECV progressively increases moving from non-hypertensive controls, to hypertensive patients without LVH to hypertensive patients with evidence of LVH,[68,69] suggesting that ECM expansion could precede onset of overt LVH. Hypertensive patients with LVH also have higher native T1 compared to controls. ECV and native T1 are associated with reduced peak systolic and early diastolic strain rate[69] supporting their use as markers of early LV decompensation.

HCM

HCM refers to a heterogeneous group of genetic diseases characterised by LVH not explained by abnormal loading conditions (such as AS or systolic hypertension). The majority of cases involve mutations in genes encoding sarcomeric proteins but phenotypic expression and clinical manifestations are variable. The predominant pathology is myocyte hypertrophy with myofibril disarray but ECM abnormalities, such as diffuse interstitial and focal replacement fibrosis, are frequently present. HCM patients have an increased risk of heart failure, arrhythmias, and sudden cardiac death (SCD), although the risk factors for developing these complications are poorly characterised.

ECM remodelling and myocardial fibrosis is associated with stiffening of the ventricle leading to diastolic and systolic dysfunction, and can provide a substrate for dangerous re-entrant arrhythmias. Supporting this is the high prevalence of fibrosis demonstrated at post-mortem of patients with HCM who suffered SCD.[2,3] In addition, in the analysis of an explanted heart, CVF correlated inversely with segmental contractility on preoperative CMR in contrast to myocyte disarray.[70]

LGE identifies focal areas of replacement fibrosis in approximately two-thirds of patients with HCM (Fig 4).[10,11] It has been shown that LGE correlates well with myocardial fibrosis in an explanted heart[70] and predicts the development of heart failure, arrhythmia, and SCD.[10,11,71] In spite of growing evidence supporting the prognostic value of LGE, assessment is not currently recommended as part of risk stratification in clinical guidelines.

Given the high prevalence of replacement fibrosis in this population, T1 mapping measures may be of use in providing further risk stratification. Although the early data are somewhat limited and inconsistent, it hints at some exciting possibilities. Post-contrast T1 correlates inversely with CVF on histology, can distinguish HCM patients from normal individuals, and is associated with dyspnoea and diastolic dysfunction.[72] As discussed, there are, however, limitations and issues with reproducibility using this measure. ECV shows excellent spatial agreement with focal LGE in HCM[73] and can also differentiate patients from controls[74,75]; however, most early studies analysed ECV averaged across the whole heart, including areas of LGE. When ECV of non-LGE segments was analysed separately no change was observed compared to controls.[76] This is somewhat surprising and in contrast to the data using native T1,[26,77] which appears to provide the best discrimination between HCM and controls (97% specificity, 100% sensitivity, 99% diagnostic accuracy).[26,74,77] This may be because native T1 relaxation times are also influenced by the intracellular compartment which is also abnormal in patients with HCM. Although native T1 has not been validated against histology, it is associated with increasing LV mass[74] and strongly correlates with areas of LGE.[26] The use of T1 mapping (in particular native T1) in the identification of early phenotypes with subclinical fibrosis is an exciting area for future research.

Use of T1 mapping in assessment of non-fibrotic pathology

T1 mapping is also of potential benefit in the identification of several non-fibrotic cardiac diseases. Full exploration of these areas is beyond the scope of this review; however, we will discuss these conditions in brief.

AFD is an X-linked storage disorder characterised by accumulation of glycosphingolipid within lysosomes leading to heart failure, arrhythmia, stroke, and renal impairment. Importantly recombinant enzyme administration can lead to slowing or reversal of progression if initiated before end-stage disease is present. Native T1 (low values in areas of lipid) can readily distinguish AFD from other causes of LVH with no overlap.[78] This is one of the most compelling indications for T1 mapping assessment in an albeit rare clinical condition.

Cardiac involvement in amyloidosis is confirmed by the presence of LGE, although this is associated with late-stage disease and may not be sensitive in detecting earlier disease. Other techniques used to identify amyloid protein deposition, such as radiolabelled serum amyloid P and ^{99m}Tc-DPD scintigraphy are challenging in the heart due to cardiac motion. Native T1 is raised in those with suspected or confirmed cardiac amyloidosis, correlates with measures of systolic and diastolic dysfunction, and is raised compared to healthy controls in patients with no evidence of cardiac abnormality on echocardiography. It may, therefore, be of clinical use in detecting the early stages of cardiac amyloid involvement, although no validation with cardiac biopsy has been performed.[79]

Native T1 is decreased in iron overload, and there is evidence for superior inter-study reproducibility and increased sensitivity for mild iron loading compared to the conventionally used T2* sequence.[80] Myocardial oedema is traditionally best imaged with T2-weighed sequences, although acute oedema prolongs both T2 and T1 relaxation times (Fig 5). There is evidence that T1 mapping can differentiate acute from chronic MI and diagnose

Please cite this article in press as: Everett RJ, et al., Assessment of myocardial fibrosis with T1 mapping MRI, Clinical Radiology (2016), http://dx.doi.org/10.1016/j.crad.2016.02.013

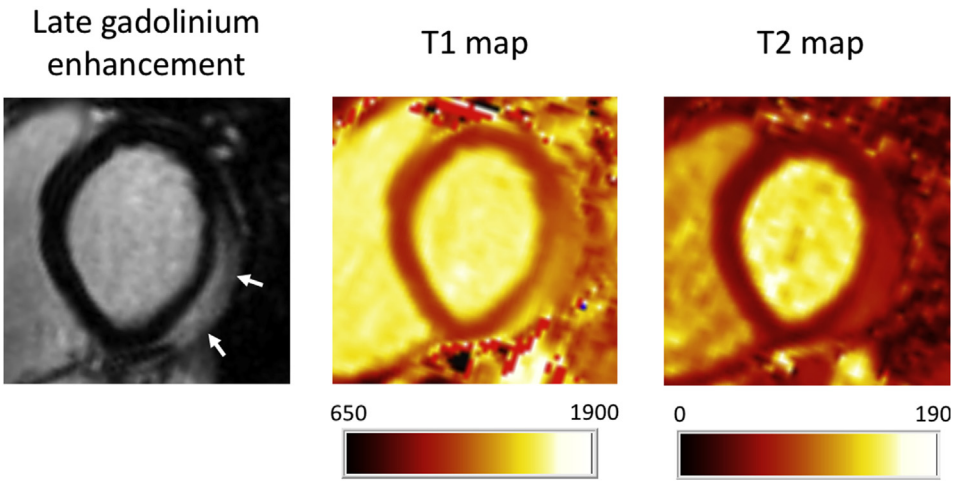

Figure 5 CMR images of a patient with myocarditis. A large area of myocardial oedema is visible in the lateral wall detectable on late gadolinium, T1 and T2 mapping.

myocarditis.[81] Although full review of T2 imaging is beyond the scope of this review, T1 mapping may be superior to T2W sequences as a reference region of interest (skeletal muscle or remote myocardium) is not required for comparison.

Summary of current status and future directions

T1 mapping is able to assess diffuse fibrosis in a non-invasive manner and offers significant advantages of LGE assessment; the technique is fully quantitative, able to detect earlier diffuse fibrosis and no inversion time needs to be set, reducing the likelihood of operator error. The two most promising T1 measures are native T1 and ECV; both correlate well with histological fibrosis in a number of cardiac pathologies. Native T1 is reproducible, able to differentiate patients from healthy volunteers in a number of conditions and most importantly does not require gadolinium contrast medium enabling its use in patients with renal dysfunction. It is likely to be most useful in identification and quantification of MI in patients with severe renal impairment for whom gadolinium is contraindicated. It has also found a compelling role in the diagnosis of rarer causes of LVH such as AFD and amyloidosis.

ECV has excellent reproducibility[37] and offers a measure of myocardial fibrosis relative to total LV volume, which is conceptually attractive to clinicians. It promises to be useful in patients with heart failure with either reduced or preserved EF as an additional method of disease staging and prognostication, although further research is required. In addition, the linear relationship between blood native T1 and haematocrit may enable estimation of ECV without requirement for venous blood sampling (so called "synthetic ECV").[82] The utility of ECV in pressure-overload states, such as AS, appears to be more limited. Our experience with AS patients shows that LV mass and diffuse fibrosis increase simultaneously with progressive disease, making ECV, a marker of relative fibrosis, insensitive in detecting an increase. We believe that the use of an absolute measure of whole-heart fibrosis, such as the FV (ECV $\times$ end-diastolic LV volume) may be more sensitive in tracking the progression of LV decompensation. This will need to be tested in future studies.

Important limitations persist, namely the overlap between healthy volunteers and disease states and the paucity of data on normal reference ranges, which are specific to manufacturer, acquisition technique, and magnetic field strength. Further research on these areas is keenly awaited.

Collagen- and elastin-specific contrast media

Whereas current gadolinium-based contrast media allow quantification of the ECV (a surrogate for the extracellular space), novel contrast agents that bind to specific components of the ECM could allow its composition to be assessed non-invasively. Both collagen- and elastin-specific MR contrast media have been developed and tested in a preclinical mouse model of MI. Collagen-specific gadolinium-based media bind to myocardial collagen and accordingly have a longer washout time from areas of replacement fibrosis leading to improved contrast-to-noise ratio on delayed CMR imaging.[83] Elastin-specific MR contrast agents (ESMA) bind to tropoelastin, which is involved in post-MI scar remodelling and thought to preserve elasticity in the infarcted heart. ESMA also displayed a greater contrast-to-noise ratio compared to current contrast media and correlated with increased synthesis of tropoelastin on histological analysis, which also correlated with improved LVEF.[84] ESMA may also be able to monitor the effects of novel therapies targeted at altering ECM composition and further clinical trials of both these agents are awaited.

Conclusion

Myocardial fibrosis is an important predictor of poor prognosis in many cardiac diseases. T1 mapping techniques continue to evolve allowing quantification of diffuse and

Please cite this article in press as: Everett RJ, et al., Assessment of myocardial fibrosis with T1 mapping MRI, Clinical Radiology (2016), http://dx.doi.org/10.1016/j.crad.2016.02.013

replacement fibrosis burden, and earlier detection and serial assessment of myocardial pathology. These novel techniques are clearly well placed to inform future clinical practice and help direct treatment strategies.

References

1. Azevedo CF, Nigri M, Higuchi ML, *et al*. Prognostic significance of myocardial fibrosis quantification by histopathology and magnetic resonance imaging in patients with severe aortic valve disease. *J Am Coll Cardiol* 2010;**56**(4):278–87.
2. Basso C, Thiene G, Corrado D, *et al*. Hypertrophic cardiomyopathy and sudden death in the young: pathologic evidence of myocardial ischemia. *Hum Pathol* 2000;**31**(8):988–98.
3. Shirani J, Pick R, Roberts WC, *et al*. Morphology and significance of the left ventricular collagen network in young patients with hypertrophic cardiomyopathy and sudden cardiac death. *J Am Coll Cardiol* 2000;**35**(1):36–44.
4. Yilmaz A, Kindermann I, Kindermann M, *et al*. Comparative evaluation of left and right ventricular endomyocardial biopsy: differences in complication rate and diagnostic performance. *Circulation* 2010;**122**(9):900–9.
5. Wu E, Ortiz JT, Tejedor P, *et al*. Infarct size by contrast enhanced cardiac magnetic resonance is a stronger predictor of outcomes than left ventricular ejection fraction or end-systolic volume index: prospective cohort study. *Heart* 2008;**94**(6):730–6.
6. Kelle S, Roes SD, Klein C, *et al*. Prognostic value of myocardial infarct size and contractile reserve using magnetic resonance imaging. *J Am Coll Cardiol* 2009;**54**(19):1770–7.
7. Roes SD, Kelle S, Kaandorp TAM, *et al*. Comparison of myocardial infarct size assessed with contrast-enhanced magnetic resonance imaging and left ventricular function and volumes to predict mortality in patients with healed myocardial infarction. *Am J Cardiol* 2007;**100**(6):930–6.
8. Eitel I, de Waha S, Wöhrle J, *et al*. Comprehensive prognosis assessment by CMR imaging after ST-segment elevation myocardial infarction. *J Am Coll Cardiol* 2014;**64**(12):1217–26.
9. Leyva F, Taylor RJ, Foley PWX, *et al*. Left ventricular midwall fibrosis as a predictor of mortality and morbidity after cardiac resynchronization therapy in patients with nonischemic cardiomyopathy. *J Am Coll Cardiol* 2012;**60**(17):1659–67.
10. Bruder O, Wagner A, Jensen CJ, *et al*. Myocardial scar visualized by cardiovascular magnetic resonance imaging predicts major adverse events in patients with hypertrophic cardiomyopathy. *J Am Coll Cardiol* 2010;**56**(11):875–87.
11. O'Hanlon R, Grasso A, Roughton M, *et al*. Prognostic significance of myocardial fibrosis in hypertrophic cardiomyopathy. *J Am Coll Cardiol* 2010;**56**(11):867–74.
12. Dweck MR, Joshi S, Murigu T, *et al*. Midwall fibrosis is an independent predictor of mortality in patients with aortic stenosis. *J Am Coll Cardiol* 2011;**58**(12):1271–9.
13. Barone-Rochette G, Piérard S, de Meester de Ravenstein C, *et al*. Prognostic significance of LGE by CMR in aortic stenosis patients undergoing valve replacement. *J Am Coll Cardiol* 2014;**64**(2):144–54.
14. Kim RJ, Fieno DS, Parrish TB, *et al*. Relationship of MRI delayed contrast enhancement to irreversible injury, infarct age, and contractile function. *Circulation* 1999;**100**(19):1992–2002.
15. Wu E, Judd RM, Vargas JD, *et al*. Visualisation of presence, location, and transmural extent of healed Q-wave and non-Q-wave myocardial infarction. *Lancet* 2001;**357**(9249):21–8.
16. Kellman P, Arai AE, McVeigh ER, *et al*. Phase-sensitive inversion recovery for detecting myocardial infarction using gadolinium-delayed hyperenhancement. *Magn Reson Med* 2002;**47**(2):372–83.
17. Messroghli DR, Walters K, Plein S, *et al*. Myocardial T1 mapping: application to patients with acute and chronic myocardial infarction. *Magn Reson Med* 2007;**58**(1):34–40.
18. van Kranenburg M, Magro M, Thiele H, *et al*. Prognostic value of microvascular obstruction and infarct size, as measured by CMR in STEMI patients. *JACC Cardiovasc Imaging* 2014;**7**(9):930–9.
19. Flett AS, Hasleton J, Cook C, *et al*. Evaluation of techniques for the quantification of myocardial scar of differing etiology using cardiac magnetic resonance. *JACC Cardiovasc Imaging* 2011;**4**(2):150–6.
20. Khawaja AZ, Cassidy DB, Shakarchi Al J, *et al*. Revisiting the risks of MRI with gadolinium based contrast agents-review of literature and guidelines. *Insights Imaging* 2015;**6**(5):553–8.
21. Moon JC, Messroghli DR, Kellman P, *et al*. Myocardial T1 mapping and extracellular volume quantification: a Society for Cardiovascular Magnetic Resonance (SCMR) and CMR Working Group of the European Society of Cardiology consensus statement. *J Cardiov Magn Reson* 2013;**15**(1):92.
22. Look DC, Locker DR. Time saving in measurement of NMR and EPR relaxation times. *Rev Sci Instrum* 1970;**41**(2):250–1.
23. Messroghli DR, Radjenovic A, Kozerke S, *et al*. Modified look-locker inversion recovery (MOLLI) for high-resolution T1 mapping of the heart. *Magn Reson Med* 2004;**52**(1):141–6.
24. Piechnik SK, Ferreira VM, Dall'Armellina E, *et al*. Shortened modified Look-Locker inversion recovery (ShMOLLI) for clinical myocardial T1-mapping at 1.5 and 3 T within a 9 heartbeat breathhold. *J Cardiov Magn Reson* 2010;**12**(1):69.
25. Kellman P, Hansen MS. T1-mapping in the heart: accuracy and precision. *J Cardiov Magn Reson* 2014;**16**(1):2.
26. Dass S, Suttie JJ, Piechnik SK, *et al*. Myocardial tissue characterization using magnetic resonance noncontrast t1 mapping in hypertrophic and dilated cardiomyopathy. *Circ Cardiovasc Imaging* 2012;**5**(6):726–33.
27. Chow K, Flewitt JA, Green JD, *et al*. Saturation recovery single-shot acquisition (SASHA) for myocardial T(1) mapping. *Magn Reson Med* 2014;**71**(6):2082–95.
28. Kellman P, Wilson JR, Xue H, *et al*. Extracellular volume fraction mapping in the myocardium, part 1: evaluation of an automated method. *J Cardiov Magn Reson* 2012;**14**(1):63.
29. Flett AS, Hayward MP, Ashworth MT, *et al*. Equilibrium contrast cardiovascular magnetic resonance for the measurement of diffuse myocardial fibrosis: preliminary validation in humans. *Circulation* 2010;**122**(2):138–44.
30. White SK, Sado DM, Fontana M, *et al*. T1 mapping for myocardial extracellular volume measurement by CMR: bolus only versus primed infusion technique. *JACC Cardiovasc Imaging* 2013;**6**(9):955–62.
31. Miller CA, Naish JH, Bishop P, *et al*. Comprehensive validation of cardiovascular magnetic resonance techniques for the assessment of myocardial extracellular volume. *Circ Cardiovasc Imaging* 2013;**6**(3):373–83.
32. Piechnik SK, Ferreira VM, Lewandowski AJ, *et al*. Normal variation of magnetic resonance T1 relaxation times in the human population at 1.5 T using ShMOLLI. *J Cardiov Magn Reson* 2013;**15**(1):13.
33. Dabir D, Child N, Kalra A, *et al*. Reference values for healthy human myocardium using a T1 mapping methodology: results from the International T1 Multicenter cardiovascular magnetic resonance study. *J Cardiov Magn Reson* 2014;**16**(1):69.
34. de Jong S, van Veen TAB, de Bakker JMT, *et al*. Biomarkers of myocardial fibrosis. *J Cardiovasc Pharmacol* 2011;**57**(5):522–35.
35. Lee S-P, Lee W, Lee JM, *et al*. Assessment of diffuse myocardial fibrosis by using MR imaging in asymptomatic patients with aortic stenosis. *Radiology* 2015;**274**(2):359–69.
36. Bull S, White SK, Piechnik SK, *et al*. Human non-contrast T1 values and correlation with histology in diffuse fibrosis. *Heart* 2013;**99**(13):932–7.
37. Chin CWL, Semple S, Malley T, *et al*. Optimization and comparison of myocardial T1 techniques at 3T in patients with aortic stenosis. *Eur Heart J Cardiovas Imaging* 2014;**15**(5):556–65.
38. Iles L, Pfluger H, Phrommintikul A, *et al*. Evaluation of diffuse myocardial fibrosis in heart failure with cardiac magnetic resonance contrast-enhanced T1 mapping. *J Am Coll Cardiol* 2008;**52**(19):1574–80.
39. Sibley CT, Noureldin RA, Gai N, *et al*. T1 Mapping in cardiomyopathy at cardiac mr: comparison with endomyocardial biopsy. *Radiology* 2012;**265**(3):724–32.
40. Mascherbauer J, Marzluf BA, Tufaro C, *et al*. Cardiac magnetic resonance post-contrast T1 time is associated with outcome in patients with heart failure and preserved ejection fraction. *Circ Cardiovasc Imaging* 2013;**6**(6):1056–65.
41. Fontana M, White SK, Banypersad SM. Comparison of T1 mapping techniques for ECV quantification. Histological validation and

Please cite this article in press as: Everett RJ, et al., Assessment of myocardial fibrosis with T1 mapping MRI, Clinical Radiology (2016), http://dx.doi.org/10.1016/j.crad.2016.02.013

reproducibility of ShMOLLI versus multibreath-hold T1 quantification. *J Cardiov Magn Reson* 2012;**14**:88.
42. Kim RJ, Wu E, Rafael A, *et al*. The use of contrast-enhanced magnetic resonance imaging to identify reversible myocardial dysfunction. *N Engl J Med* 2000;**343**(20):1445–53.
43. Pegg TJ, Selvanayagam JB, Jennifer J. Prediction of global left ventricular functional recovery in patients with heart failure undergoing surgical revascularisation, based on late gadolinium. *J Cardiov Magn Reson* 2010;**12**:56.
44. Kali A, Choi E-Y, Sharif B, *et al*. Native T1 mapping by 3-T CMR imaging for characterization of chronic myocardial infarctions. *JACC Cardiovasc Imaging* 2015;**8**(9):1019–30.
45. Ugander M, Oki AJ, Hsu L-Y, *et al*. Extracellular volume imaging by magnetic resonance imaging provides insights into overt and subclinical myocardial pathology. *Eur Heart J* 2012;**33**(10):1268–78.
46. Mann DL. Mechanisms and models in heart failure: a combinatorial approach. *Circulation* 1999;**100**(9):999–1008.
47. Heling A, Zimmermann R, Kostin S, *et al*. Increased expression of cytoskeletal, linkage, and extracellular proteins in failing human myocardium. *Circ Res* 2000;**86**(8):846–53.
48. Assomull RG, Prasad SK, Lyne J, *et al*. Cardiovascular magnetic resonance, fibrosis, and prognosis in dilated cardiomyopathy. *J Am Coll Cardiol* 2006;**48**(10):1977–85.
49. Tachi M, Amano Y, Inui K, *et al*. Relationship of postcontrast myocardial T1 value and delayed enhancement to reduced cardiac function and serious arrhythmia in dilated cardiomyopathy with left ventricular ejection fraction less than 35. *Acta Radiol* 2015.
50. Han Y, Peters DC, Dokhan B, *et al*. Shorter difference between myocardium and blood optimal inversion time suggests diffuse fibrosis in dilated cardiomyopathy. *J Magn Reson Imaging* 2009;**30**(5):967–72.
51. Hayashida T, Sueyoshi E, Nagayama H, *et al*. Comparison study on different quantification methods of diffuse myocardial fibrosis of dilated cardiomyopathy using myocardial T1 value. *Open J Radiol* 2013;**03**(03):117–23.
52. Su M-YM, Lin L-Y, Tseng Y-HE, *et al*. CMR-verified diffuse myocardial fibrosis is associated with diastolic dysfunction in HFpEF. *JACC Cardiovasc Imaging* 2014;**7**(10):991–7.
53. Wong TC, Piehler K, Meier CG, *et al*. Association between extracellular matrix expansion quantified by cardiovascular magnetic resonance and short term mortality. *Circulation* 2012;**126**(10):1206–16.
54. Wong TC, Piehler KM, Kang IA, *et al*. Myocardial extracellular volume fraction quantified by cardiovascular magnetic resonance is increased in diabetes and associated with mortality and incident heart failure admission. *Eur Heart J* 2014;**35**(10):657–64.
55. Hogg K, Swedberg K, McMurray J. Heart failure with preserved left ventricular systolic function: epidemiology, clinical characteristics, and prognosis. *J Am Coll Cardiol* 2004;**43**(3):317–27.
56. Bhatia RS, Tu JV, Lee DS, *et al*. Outcome of heart failure with preserved ejection fraction in a population-based study. *N Engl J Med* 2006;**355**(3):260–9.
57. Kato S, Saito N, Kirigaya H, *et al*. Prognostic significance of quantitative assessment of focal myocardial fibrosis in patients with heart failure with preserved ejection fraction. *Int J Cardiol* 2015;**191**:314–9.
58. Hein S, Arnon E, Kostin S, *et al*. Progression from compensated hypertrophy to failure in the pressure-overloaded human heart: structural deterioration and compensatory mechanisms. *Circulation* 2003;**107**(7):984–91.
59. Dweck MR, Boon NA, Newby DE. Calcific aortic stenosis. *J Am Coll Cardiol* 2012;**60**(19):1854–63.
60. Ross J, Braunwald E. Aortic stenosis. *Circulation* 1968;**38**(Suppl.):61–7.
61. Connolly HM, Oh JK, Orszulak TA, *et al*. Aortic valve replacement for aortic stenosis with severe left ventricular dysfunction. Prognostic indicators. *Circulation* 1997;**95**(10):2395–400.
62. Krayenbuehl HP, Hess OM, Monrad ES, *et al*. Left-ventricular myocardial structure in aortic-valve disease before, intermediate, and late after aortic-valve replacement. *Circulation* 1989;**79**(4):744–55.
63. Debl K, Djavidani B, Buchner S, *et al*. Delayed hyperenhancement in magnetic resonance imaging of left ventricular hypertrophy caused by aortic stenosis and hypertrophic cardiomyopathy: visualisation of focal fibrosis. *Heart* 2006;**92**(10):1447–51.
64. Chin CWL, Shah ASV, McAllister DA, *et al*. High-sensitivity troponin I concentrations are a marker of an advanced hypertrophic response and adverse outcomes in patients with aortic stenosis. *Eur Heart J* 2014;**35**(34):2312–21.
65. Flett AS, Sado DM, Quarta G, *et al*. Diffuse myocardial fibrosis in severe aortic stenosis: an equilibrium contrast cardiovascular magnetic resonance study. *Eur Heart J Cardiovasc Imaging* 2012;**13**(10). jes102–826.
66. Querejeta R, López B, González A, *et al*. Increased collagen type I synthesis in patients with heart failure of hypertensive origin: relation to myocardial fibrosis. *Circulation* 2004;**110**(10):1263–8.
67. Díez J, Querejeta R, López B, *et al*. Losartan-dependent regression of myocardial fibrosis is associated with reduction of left ventricular chamber stiffness in hypertensive patients. *Circulation* 2002;**105**(21):2512–7.
68. Coelho-Filho OR, Mongeon F-P, Mitchell R, *et al*. Role of transcytolemmal water-exchange in magnetic resonance measurements of diffuse myocardial fibrosis in hypertensive heart disease. *Circ Cardiovasc Imaging* 2013;**6**(1):134–41.
69. Kuruvilla S, Janardhanan R, Antkowiak P, *et al*. Increased extracellular volume and altered mechanics are associated with LVH in hypertensive heart disease, not hypertension alone. *JACC Cardiovasc Imaging* 2015;**8**(2):172–80.
70. Moon JCC, Reed E, Sheppard MN, *et al*. The histologic basis of late gadolinium enhancement cardiovascular magnetic resonance in hypertrophic cardiomyopathy. *J Am Coll Cardiol* 2004;**43**(12):2260–4.
71. Adabag AS, Maron BJ, Appelbaum E, *et al*. Occurrence and frequency of arrhythmias in hypertrophic cardiomyopathy in relation to delayed enhancement on cardiovascular magnetic resonance. *J Am Coll Cardiol* 2008;**51**(14):1369–74.
72. Ellims AH, Iles LM, Ling L-H, *et al*. A comprehensive evaluation of myocardial fibrosis in hypertrophic cardiomyopathy with cardiac magnetic resonance imaging: linking genotype with fibrotic phenotype. *Eur Heart J Cardiovasc Imaging* 2014;**15**(10):1108–16.
73. Kellman P, Wilson JR, Xue H. Extracellular volume fraction mapping in the myocardium, part 2: initial clinical experience. *J Cardiovasc Magn* 2012;**14**:64.
74. Puntmann VO, Voigt T, Chen Z, *et al*. Native T1 mapping in differentiation of normal myocardium from diffuse disease in hypertrophic and dilated cardiomyopathy. *JACC Cardiovasc Imaging* 2013;**6**(4):475–84.
75. Sado DM, Flett AS, Banypersad SM, *et al*. Cardiovascular magnetic resonance measurement of myocardial extracellular volume in health and disease. *Heart* 2012;**98**(19):1436–41.
76. Brouwer WP, Baars EN, Germans T, *et al*. *In-vivo* T1 cardiovascular magnetic resonance study of diffuse myocardial fibrosis in hypertrophic cardiomyopathy. *J Cardiov Magn Reson* 2014;**16**(1):28.
77. Małek ŁA, Werys K, Kłopotowski M, *et al*. Native T1-mapping for non-contrast assessment of myocardial fibrosis in patients with hypertrophic cardiomyopathy — comparison with late enhancement quantification. *Magn Reson Imaging* 2015;**33**(6):718–24.
78. Sado DM, White SK, Piechnik SK, *et al*. Identification and assessment of Anderson–Fabry disease by cardiovascular magnetic resonance noncontrast myocardial T1 mapping. *Circ Cardiovasc Imaging* 2013;**6**(3):392–8.
79. Karamitsos TD, Piechnik SK, Banypersad SM, *et al*. Noncontrast T1 mapping for the diagnosis of cardiac amyloidosis. *JACC Cardiovasc Imaging* 2013;**6**(4):488–97.
80. Sado DM, Maestrini V, Piechnik SK, *et al*. Noncontrast myocardial T1 mapping using cardiovascular magnetic resonance for iron overload. *J Magn Reson Im* 2015;**41**(6):1505–11.
81. Ferreira VM, Piechnik SK, Dall'Armellina E, *et al*. Non-contrast T1-mapping detects acute myocardial edema with high diagnostic accuracy: a comparison to T2-weighted cardiovascular magnetic resonance. *J Cardiov Magn Reson* 2012;**14**(1):42.
82. Treibel TA, Fontana M, Maestrini V, *et al*. Synthetic ECV — simplifying ECV quantification by deriving haematocrit from T1 blood. *Heart* 2015;**101**(Suppl. 2):A16–7.
83. Helm PA, Caravan P, French BA, *et al*. Postinfarction myocardial scarring in mice: molecular MR imaging with use of a collagen-targeting contrast agent. *Radiology* 2008;**247**(3):788–96.
84. Wildgruber M, Bielicki I, Aichler M, *et al*. Assessment of myocardial infarction and postinfarction scar remodeling with an elastin-specific magnetic resonance agent. *Circ Cardiovasc Imaging* 2014;**7**(2):321–9.

Please cite this article in press as: Everett RJ, et al., Assessment of myocardial fibrosis with T1 mapping MRI, Clinical Radiology (2016), http://dx.doi.org/10.1016/j.crad.2016.02.013

JACC: CARDIOVASCULAR IMAGING VOL. ■, NO. ■, 2016

ISSN 1936-878X
http://dx.doi.org/10.1016/j.jcmg.2016.10.007

Myocardial Fibrosis and Cardiac Decompensation in Aortic Stenosis

Calvin W.L. Chin, MD,[a,b] Russell J. Everett, MD,[a] Jacek Kwiecinski, MD,[a,c] Alex T. Vesey, MD, PhD,[a] Emily Yeung,[a] Gavin Esson,[a] William Jenkins, MD,[a] Maria Koo,[a] Saeed Mirsadraee, MD,[a] Audrey C. White,[a] Alan G. Japp, MD, PhD,[a] Sanjay K. Prasad, MD,[d] Scott Semple, PhD,[e] David E. Newby, MD, PhD,[a] Marc R. Dweck, MD, PhD[a]

ABSTRACT

OBJECTIVES Cardiac magnetic resonance (CMR) was used to investigate the extracellular compartment and myocardial fibrosis in patients with aortic stenosis, as well as their association with other measures of left ventricular decompensation and mortality.

BACKGROUND Progressive myocardial fibrosis drives the transition from hypertrophy to heart failure in aortic stenosis. Diffuse fibrosis is associated with extracellular volume expansion that is detectable by T1 mapping, whereas late gadolinium enhancement (LGE) detects replacement fibrosis.

METHODS In a prospective observational cohort study, 203 subjects (166 with aortic stenosis [69 years; 69% male]; 37 healthy volunteers [68 years; 65% male]) underwent comprehensive phenotypic characterization with clinical imaging and biomarker evaluation. On CMR, we quantified the total extracellular volume of the myocardium indexed to body surface area (iECV). The iECV upper limit of normal from the control group (22.5 ml/m^2) was used to define extracellular compartment expansion. Areas of replacement mid-wall LGE were also identified. All-cause mortality was determined during 2.9 $\pm$ 0.8 years of follow up.

RESULTS iECV demonstrated a good correlation with diffuse histological fibrosis on myocardial biopsies ($r = 0.87$; $p < 0.001$; $n = 11$) and was increased in patients with aortic stenosis (23.6 $\pm$ 7.2 ml/m^2 vs. 16.1 $\pm$ 3.2 ml/m^2 in control subjects; $p < 0.001$). iECV was used together with LGE to categorize patients with normal myocardium (iECV <22.5 ml/m^2; 51% of patients), extracellular expansion (iECV ≥22.5 ml/m^2; 22%), and replacement fibrosis (presence of mid-wall LGE, 27%). There was evidence of increasing hypertrophy, myocardial injury, diastolic dysfunction, and longitudinal systolic dysfunction consistent with progressive left ventricular decompensation (all $p < 0.05$) across these groups. Moreover, this categorization was of prognostic value with stepwise increases in unadjusted all-cause mortality (8 deaths/1,000 patient-years vs. 36 deaths/1,000 patient-years vs. 71 deaths/1,000 patient-years, respectively; $p = 0.009$).

CONCLUSIONS CMR detects ventricular decompensation in aortic stenosis through the identification of myocardial extracellular expansion and replacement fibrosis. This holds major promise in tracking myocardial health in valve disease and for optimizing the timing of valve replacement. (The Role of Myocardial Fibrosis in Patients With Aortic Stenosis; NCT01755936) (J Am Coll Cardiol Img 2016;■:■–■) © 2016 by the American College of Cardiology Foundation. Published by Elsevier. This is an open access article under the CC BY license (http://creativecommons.org/licenses/by/4.0/).

From the [a]BHF/Centre for Cardiovascular Science, University of Edinburgh, Edinburgh, United Kingdom; [b]Department of Cardiovascular Science, National Heart Center, Singapore; [c]First Department of Cardiology, Poznan University of Medical Sciences, Poznan, Poland; [d]Royal Brompton Hospital, London, United Kingdom; and the [e]Clinical Research Imaging Centre, University of Edinburgh, Edinburgh, United Kingdom. Dr. Chin was supported by the National Research Foundation, Ministry of Health, Singapore. Drs. Newby, Dweck, and Everett were supported by the British Heart Foundation (CH/09/002, FS/14/78/31020, and CH/09/002/26360, respectively). Dr. Dweck was also supported by the Sir Jules Thorn Biomedical Research Award 2015 (15/JTA). Dr. Newby was also supported by a Wellcome Trust Senior Investigator Award (WT103782AIA). Dr. Semple has been a consultant for GlaxoSmithKline. All other authors have reported that they have no relationships relevant to the contents of this paper to disclose. Drs. Chin and Everett contributed equally to this work.

Manuscript received June 21, 2016; revised manuscript received October 4, 2016, accepted October 5, 2016.

ABBREVIATIONS AND ACRONYMS

AVR = aortic valve replacement

BNP = brain natriuretic peptide

CMR = cardiac magnetic resonance

cTnI = cardiac troponin I

ECV = extracellular volume

ECG = electrocardiogram

iECV = indexed extracellular volume

IQR = interquartile range

LGE = late gadolinium enhancement

LV = left ventricular

LVH = left ventricular hypertrophy

Calcific aortic stenosis is the most common valvular heart condition in the western world and a major public health burden (1). In recent years, the role of left ventricular (LV) remodeling in disease progression, symptom development, and adverse cardiovascular events in aortic stenosis has been increasingly appreciated (2). In the initial phases, the increased afterload imposed by aortic valve narrowing induces adaptive left ventricular hypertrophy (LVH) that acts to maintain wall stress and cardiac output. Ultimately, this process decompensates, and patients transition from hypertrophy to heart failure and the development of symptoms and adverse cardiovascular events (2,3). This transition often correlates poorly with the severity of aortic valve narrowing and is predominantly driven by myocardial fibrosis and myocyte cell death (4), which is perhaps a consequence of supply-demand mismatch and myocardial ischemia in the hypertrophied myocardium (2). Therefore, there is considerable interest in developing novel biomarkers to detect the early signs of LV decompensation.

Cardiac magnetic resonance imaging (CMR) provides the noninvasive gold standard method for measuring LV wall thickness, mass, volumes, and ejection fraction. Moreover, it is able to detect structural changes in the LV myocardium, including replacement fibrosis with the late gadolinium technique and expansion of the extracellular volume using T1 mapping (5). The latter in part reflects increases in diffuse myocardial fibrosis (a reversible early form of fibrosis) (6) and potential changes in the intravascular compartment. Early studies have suggested that CMR-derived measures of LV mass and replacement myocardial fibrosis are of prognostic significance (7,8). However, these studies have largely been conducted in small cohorts of patients with end-stage aortic stenosis who were referred to CMR on clinical grounds. Therefore, these findings may have been confounded by referral bias, which limited their applicability and generalizability to the broad population of patients with aortic stenosis. Moreover, comparisons with age- and sex-matched control populations and prognostic T1 mapping studies have been lacking.

We report the largest prospective study to evaluate systematically the usefulness of CMR in patients with aortic stenosis. In particular, we investigated its ability to detect expansion of extracellular volume (ECV) and replacement myocardial fibrosis, and how these are related to other markers of LV decompensation, functional capacity, and clinical outcomes.

METHODS

STUDY POPULATION. All stable patients with at least mild aortic stenosis (aortic jet velocity ≥2 m/s) who attended the Edinburgh Heart Centre between March 2012 and August 2014 were invited to participate in this prospective observational cohort study. The exclusion criteria were other forms of valvular heart disease (≥ moderate severity), significant comorbidities with limited life expectancy, contraindications to gadolinium-enhanced CMR, and acquired or inherited nonischemic cardiomyopathies (as assessed by clinical history or ultimately by CMR). In addition, we recruited healthy volunteers from the community with similar demographic characteristics in terms of age and sex, but no history or clinical features consistent with current cardiovascular disease. The study was conducted in accordance with the Declaration of Helsinki and approved by the local research committee. Written informed consent was obtained from all participants.

SUBJECT CHARACTERIZATION. All subjects underwent detailed clinical evaluation including history, physical examination, and electrocardiography. In addition, venous blood samples were obtained for evaluation of biochemistry and cardiac biomarkers of interest.

Cardiac biomarkers. Plasma cardiac troponin I concentrations (cTnI) were determined by the ARCHITECT STAT high-sensitivity cTnI assay (Abbot Laboratories, Abbott Park, Illinois) (9). The brain natriuretic peptide (BNP) concentration was determined with Triage BNP assay (Biosite Inc., San Diego, California).

6-min walk test. A 6-min walk test was performed in 156 (94%) patients as an objective measure of functional capacity in our predominantly older adult cohort, many of whom could not perform an exercise tolerance test. Explicit instructions were given to patients asking them to walk as far as possible for 6 min.

Echocardiography. Comprehensive transthoracic echocardiography was performed in all patients (iE33, Philips Medical Systems, the Netherlands) by a dedicated research ultrasonographer (A.C.W.) and a cardiologist certified in echocardiography (C.W.L.C.). The severity of aortic stenosis and diastolic function were assessed according to American Society of Echocardiography (ASE) guidelines (Online Appendix).

Cardiac magnetic resonance. CMR was performed using a 3-T scanner (MAGNETOM Verio, Siemens AG, Erlangen, Germany). Short-axis cine images were acquired and used to calculate ventricular volumes,

mass, and function. Left ventricular hypertrophy (LVH) was defined as LV mass (indexed to body surface area using the Du Bois formula) >95th percentile using age- and sex-specific reference ranges (10). LV longitudinal function was determined by measuring the difference in mitral annular displacement between end-systole and end-diastole (Online Appendix).

Focal replacement fibrosis and ECV expansion were assessed in all patients using late gadolinium enhancement (LGE) and myocardial T1 mapping, respectively. LGE was performed 15 min after administration of 0.1 mmol/kg of gadobutrol (Gadovist, Bayer Pharma AG, Barmen, Germany). The presence of mid-wall myocardial fibrosis was determined qualitatively by 2 independent and experienced operators (M.R.D. and C.W.L.C.), and its distribution was recorded (7,9).

T1 mapping was performed using the Modified Look-Locker Inversion recovery (11) and a standardized image analysis approach (12). In the short-axis mid-cavity myocardium, 6 standard segments were defined on native T1 maps, and these regions were then copied onto the corresponding 20-min post-contrast maps (OsiriX version 4.1.1, Geneva, Switzerland). Analysis of mid-ventricle segments has been shown to correlate well with analysis of all 17 myocardial segments, is simpler to perform, and avoids partial volume effects in apical segments (12). Segments with mid-wall LGE present were included in this analysis, whereas segments that contained subendocardial, infarct-pattern LGE were excluded. Four commonly used T1 approaches were assessed: native and post-contrast myocardial T1, partition coefficient (lambda), and the ECV fraction. We recently reported the reproducibility of these measures at 3-T (12).

We also investigated a novel marker, the indexed extracellular volume (iECV), which modifies the ECV fraction to act as a measure of the total volume of the extracellular compartment in the left ventricle. It was derived using the formula: ECV fraction × LV end-diastolic myocardial volume normalized to the body surface area.

HISTOLOGICAL VALIDATION OF MYOCARDIAL FIBROSIS. All patients who underwent surgical aortic valve replacement were approached regarding intraoperative myocardial biopsy at the time of surgery. Biopsies were obtained from the basal muscular septum 2 cm below the outflow tract using a Tru-Cut needle (Carefusion, Vernon Hills, Illinois), and then were stained with picrosirius red and analyzed using an automated segmentation tool (Online Appendix). Two blinded and independent observers (A.T.V. and G.E.) analyzed all the specimens, and the interobserver reproducibility was 4.1 ± 2.6%.

CLINICAL OUTCOMES. We examined the prognostic value of the different patterns of fibrosis on all-cause mortality as our primary outcome. Patients were followed between March 2012 and September 2015. All deaths were identified through the General Register of Scotland. We also assessed aortic stenosis–related mortality. This was established from the official death certificate and defined as any death in which aortic stenosis was listed as either the primary cause or a contributing factor to that death by the clinical care team.

STATISTICAL ANALYSIS. We assessed the distribution of all continuous variables using the Shapiro-Wilk test and presented them as mean ± SD or median (interquartile range [IQR]). Comparisons were made using the 2-sample *t* test and the Mann-Whitney test where appropriate. We presented all categorical variables as percentages and used the chi-square test for comparison. The relationship between 2 continuous variables was assessed using either Pearson's r or Spearman's rho, as appropriate. Potential confounders were adjusted using multivariable linear regression analyses. Time-to-first event survival curves associated with the categories of LV decompensation were estimated using the Kaplan-Meier method and compared with the log-rank test. All statistical analyses were performed using SPSS version 20 (IBM, Armonk, New York) and GraphPad Prism version 6.0 (GraphPad, San Diego, California). A 2-sided $p < 0.05$ was considered statistically significant.

RESULTS

STUDY POPULATION. A total of 203 subjects were recruited: 166 patients with aortic stenosis (peak aortic valve velocity: 3.8 ± 0.90 m/s) and 37 healthy volunteers. These 2 groups were well matched for age, sex, chronic renal impairment, and diabetes. Although a history of hypertension was more common in the aortic stenosis group, blood pressure was well-controlled and similar between the 2 groups at enrollment (**Table 1**).

LEFT VENTRICULAR HYPERTROPHY. Although the severity of aortic stenosis correlated positively with LVH (LV mass index: $r = 0.48$; $p < 0.001$), it accounted for less than one-quarter ($r^2 = 0.23$) of the variance observed (**Figure 1**). Male sex and aortic stenosis severity were the only independent predictors of LV mass ($p < 0.001$ for both), independent of systolic blood pressure, age, and coronary artery disease status.

TABLE 1 Baseline Characteristics of Patients With Aortic Stenosis and Healthy Volunteers

	Healthy Volunteers (n = 37)	Aortic Stenosis (n = 166)	p Value
Age, yrs	68 (63–74)	69 (63–75)	0.44
Men	24 (65)	115 (69)	0.57
Hypertension	10 (27)	112 (67)	<0.001
Diabetes mellitus	0	25 (15)	–
Coronary artery disease	3 (8)	62 (37)	–
Coronary CTA assessment	13 (35)	21 (13)	–
Invasive coronary angiography	3 (8)	78 (47)	–
Previous PCI	2 (5)	11 (6)	–
Previous CABG	0	8 (5)	–
Atrial fibrillation	0	4 (2)	–
Body mass index, kg/m^2	27.0 ± 3.6	28.9 ± 4.8	0.02
Body surface area, m^2	1.86 ± 0.16	1.88 ± 0.19	0.54
NYHA functional class			
I	36 (97)	74 (45)	
II	1 (3)	56 (34)	<0.001
III	–	32 (19)	
IV	–	4 (2)	
6-min walk test, m	430 (400–475)	400 (340–450)	0.001
Systolic blood pressure, mm Hg	148 ± 16	151 ± 21	0.53
Biomarkers			
High sensitivity troponin I concentration, ng/l	3.1 (1.2–7.1)	6.6 (3.8–12.4)	<0.001
Brain natriuretic peptide concentration, pg/ml	9.5 (5.1–20.6)	26.1 (10.7–54.3)	0.001
Echocardiography			
Aortic valve area, cm^2	2.4 ± 0.6	1.0 ± 0.4	<0.001
Peak aortic jet velocity, m/s	1.4 ± 0.2	3.8 ± 0.9	<0.001
Mean pressure gradient, mm Hg	4.2 ± 1.4	35 ± 19	<0.001
Dimensionless index	0.71 (0.67–0.81)	0.26 (0.22–0.32)	<0.001
Valvulo-arterial impedance, mm Hg/ml/m^2	4.0 (3.6–4.7)	4.3 (3.6–5.1)	0.38
Mean e', cm/s	7.3 (6.2–8.1)	5.9 (4.9–7.5)	<0.001
Mean E/e' ratio	8.5 (7.0–10.4)	12.6 (10.3–16.9)	<0.001
Mean diastolic dysfunction grade	0.5 ± 0.8	2.0 ± 0.9	<0.001
Cardiac magnetic resonance			
EDVi, ml/m^2	66 (60–80)	69 (61–78)	0.52
End-systolic volume (indexed), ml/m^2	23 (19–29)	23 (18–27)	0.40
Stroke volume (indexed), ml/m^2	44 (40–50)	47 (40–54)	0.16
Systolic ejection fraction, %	65 (62–68)	67 (63–71)	0.02
Longitudinal function, mm	14.8 ± 2.7	12.2 ± 2.9	<0.001
LVMi, g/m^2	62 (54–71)	88 (73–99)	<0.001
LVMi/EDVi, g/ml	0.92 (0.84–0.99)	1.24 (1.04–1.44)	<0.001
Maximal myocardial wall thickness, mm	7.5 (6.8–8.7)	11.4 (8.8–14.2)	<0.001
Mean myocardial wall thickness, mm	5.6 (5.0–6.3)	7.4 (6.3–9.0)	<0.001
Indexed left atrial volume, ml/m^2	28 ± 11	36 ± 15	0.01
Mid-wall late gadolinium enhancement	0	44 (27)	–
Native myocardial T1, ms	1,166 ± 27	1,184 ± 42	0.02
20-min post-contrast myocardial T1, ms	645 ± 51	638 ± 46	0.47
Partition coefficient	0.45 ± 0.02	0.46 ± 0.04	0.06
Extracellular volume fraction, %	26.5 ± 1.3	27.7 ± 2.6	0.005
Fibrosis volume, ml	29.9 ± 7.3	44.4 ± 15.1	<0.0001
Indexed extracellular volume, ml/m^2	16.1 ± 3.2	23.6 ± 7.2	<0.0001

Values are median (interquartile range), n (%), or mean ± SD. Coronary artery disease was defined by previous myocardial infarction, clinical symptoms of angina with documented evidence of myocardial ischemia in the absence of severe aortic stenosis, a >50% luminal stenosis in a major epicardial coronary artery or previous coronary revascularization. All patients with clinical symptoms of angina underwent coronary angiography.

CABG = coronary artery bypass graft; CTA = computed tomography angiography; EDVi = end-diastolic volume (indexed); LVMi = left ventricular mass (index); NYHA = New York Heart Association; PCI = percutaneous coronary intervention.

FIGURE 1 Factors Governing the Magnitude of the Hypertrophic Response in Aortic Stenosis

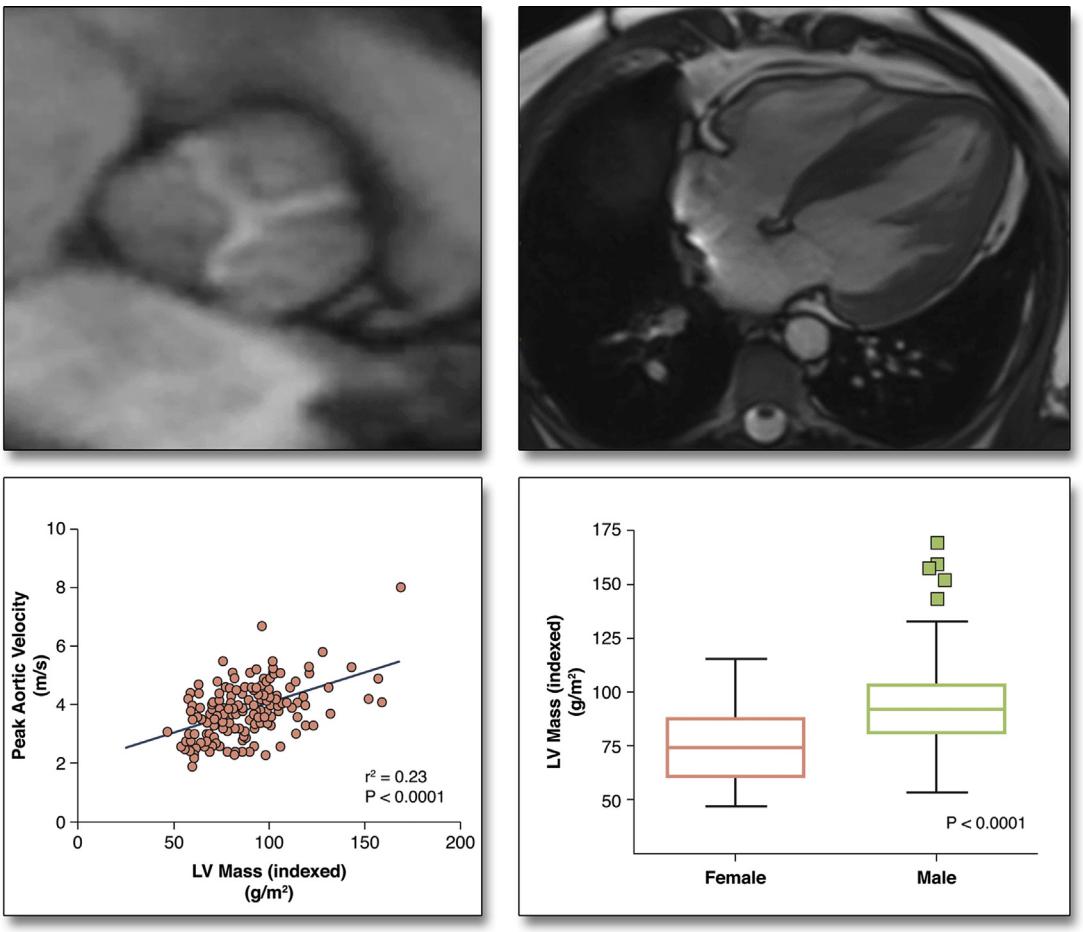

Only a modest correlation between the severity of valve narrowing and the magnitude of the hypertrophic response was observed. The other predictor of left ventricular (LV) mass index on multivariate analysis was sex, with men having more hypertrophy than women.

T1 MAPPING AND EXTRACELLULAR EXPANSION. Myocardial biopsies were obtained in 11 of 37 patients who underwent surgical aortic valve replacement. Strong correlations were observed between the amount of myocardial fibrosis on histology and T1 mapping parameters (native T1: $r = 0.76$; $p = 0.007$; lambda: $r = 0.82$; $p = 0.002$; ECV fraction: $r = 0.70$; $p = 0.016$; and iECV: $r = 0.87$; $p < 0.001$) (**Figure 2**), with the exception of post-contrast myocardial T1 ($r = 0.01$; $p = 0.98$). Indexed LV mass also correlated well with histological fibrosis ($r = 0.83$; $p < 0.001$).

Compared with the healthy volunteers, patients with aortic stenosis had increased diffuse myocardial fibrosis, with iECV providing the best discrimination between cases and control subjects (23.6 ± 7.2 ml/m^2 vs. 16.1 ± 3.2 ml/m^2; $p < 0.0001$) (**Table 1** and **Figure 2**). Moreover, of all the T1 measures, only the iECV demonstrated a progressive increase across patients with mild, moderate, and severe aortic stenosis (19.6 ± 4.6 ml/m^2 vs. 22.9 ± 5.4 ml/m^2 vs. 25.5 ± 8.1 ml/m^2, respectively; $p < 0.001$) (**Table 2**). Notably, the ECV fraction did not vary with aortic stenosis severity (as measured by peak aortic valve velocity; $p = 0.30$ (Online Table 1) and showed a high degree of overlap between cases and control subjects ($26.5 \pm 1.4\%$ vs. $27.7 \pm 2.6\%$; $p = 0.007$).

We explored iECV in greater detail, dividing our entire patient cohort into tertiles of iECV (**Table 3**). Using this approach, a steady increase across the tertiles was observed for each of the following markers of disease severity and LV decompensation: indexed LV mass, peak aortic valve velocity, plasma high-sensitivity cTnI concentrations, serum BNP concentrations, diastolic dysfunction, longitudinal systolic

FIGURE 2 iECV as a Marker of Extracellular Expansion in the Myocardium

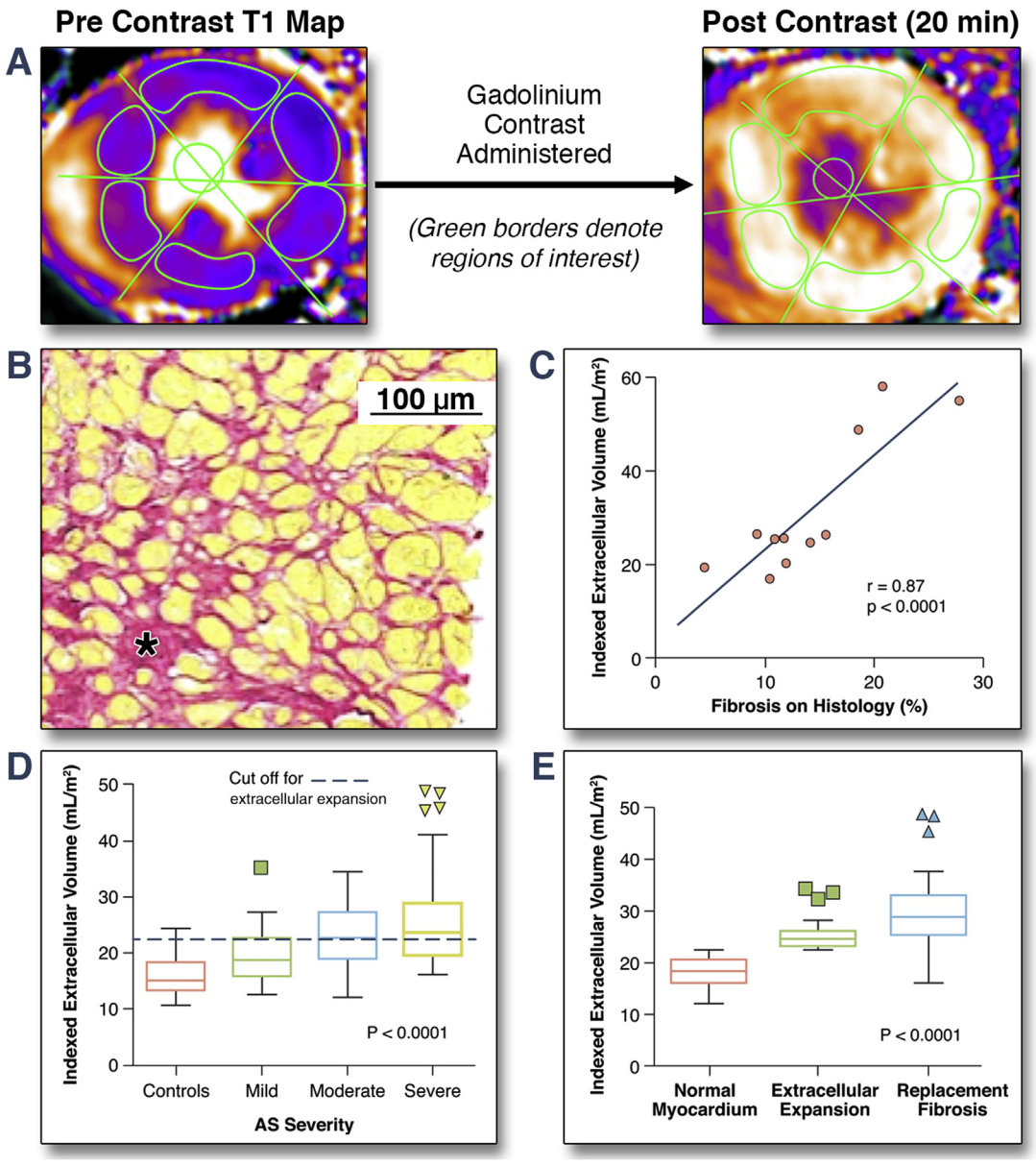

(A) Regions of interest manually drawn onto native and post-contrast T1 maps are used to calculate indexed extracellular volume (iECV). **(B)** Histology from a patient with aortic stenosis (AS) with areas of diffuse fibrosis stained with picrosirus red. **(C)** Excellent correlation between iECV and diffuse myocardial fibrosis on histology. **(D)** iECV provided good discrimination between disease states. **(E)** iECV values were higher in patients with replacement fibrosis than patients with normal myocardium or extracellular expansion.

dysfunction, and the proportion of patients with mid-wall fibrosis ($p < 0.05$ for all). Similar results were obtained using tertiles of the ECV fraction (Online Table 1), but by comparison, tertiles of LV mass index were less discriminatory, with no differences in diastolic function nor in serum BNP concentrations across these groups (both $p > 0.05$) (Online Table 2).

REPLACEMENT MYOCARDIAL FIBROSIS. Replacement mid-wall fibrosis, as assessed by LGE, was present in 44 (27%) patients with aortic stenosis but in none of the healthy volunteers. We examined the association between mid-wall myocardial fibrosis and the severity of aortic stenosis (**Table 2**). Although patients with mid-wall fibrosis had more severe aortic

TABLE 2 Cardiovascular Magnetic Resonance Measures of Myocardial Fibrosis and Functional Status by Severity of Aortic Stenosis

	Mild (n = 34)	Moderate (n = 45)	Severe (n = 87)	p Value
Age, yrs	67 (56–75)	72 (66–77)	71 (65–76)	0.048
Men	20 (59)	32 (71)	63 (72)	0.33
EDVi, ml/m^2	69 (60–77)	68 (64–81)	69 (61–79)	0.72
End-systolic volume (indexed), ml/m^2	24 (19–26)	23 (20–27)	22 (17–27)	0.87
Stroke volume (indexed), ml/m^2	47 (39–52)	47 (42–56)	47 (40–54)	0.56
Systolic ejection fraction, %	67 (63–69)	66 (63–70)	67 (63–72)	0.65
Longitudinal function, mm	13.6 ± 2.4	13.2 ± 2.9	11.2 ± 2.8	<0.001
LVMi, g/m^2	71 (61–86)	87 (74–98)	93 (80–104)	<0.001
LVMi/EDVi, g/ml	1.08 ± 0.20	1.21 ± 0.23	1.36 ± 0.28	<0.001
Maximal myocardial wall thickness, mm	8.2 ± 2.1	11.1 ± 3.3	13.4 ± 3.4	<0.001
Mean myocardial wall thickness, mm	5.9 ± 1.1	7.3 ± 1.6	8.7 ± 1.9	<0.001
Patients with LVH	6 (17)	24 (53)	59 (68)	<0.001
Native myocardial T1, ms	1,170 ± 30	1,180 ± 37	1,192 ± 46	0.02
20-min post-contrast myocardial T1, ms	637 ± 45	643 ± 48	636 ± 45	0.73
Partition coefficient	0.466 ± 0.03	0.466 ± 0.04	0.466 ± 0.05	0.07
ECV fraction, %	27.8 ± 2.5	27.5 ± 2.0	27.8 ± 3.0	0.79
iECV, ml/m^2	19.6 ± 4.6	22.9 ± 5.4	25.5 ± 8.1	<0.001
Extracellular expansion (iECV ≥22.5 ml/m^2)	9 (26)	23 (51)	47 (54)	0.021
Mid-wall late gadolinium enhancement	2 (5.9)	14 (31)	28 (32)	0.008
Diastolic function (E/e')	11.1 (8.0–14.2)	12.2 (10.1–16.4)	13.5 (11.4–18.6)	0.009
Natural log (hs troponin I)	1.25 (0.72–1.55)	1.76 (1.33–2.34)	2.16 (1.59–2.81)	<0.0001
6-min walk test, m	420 (363–448)	400 (340–450)	390 (320–440)	0.05

Values are median (interquartile range), n (%), or mean ± SD.
ECV = extracellular volume; LVH = left ventricular hypertrophy; other abbreviations as in Tables 1 and 2.

stenosis compared with those without (peak aortic valve velocity: 4.1 m/s; IQR: 3.7 to 4.6 m/s vs. 3.8 m/s; IQR: 3.4 to 4.6 m/s, respectively; p = 0.001), this difference was small and unlikely to be of any clinical significance. In contrast, patients with mid-wall fibrosis demonstrated a marked 30% increase in LV mass indicative of an advanced hypertrophic response (LV mass index 107 ± 24 g/m^2 vs. 82 ± 16 g/m^2, respectively; p < 0.001). LV mass index was independently associated with mid-wall myocardial fibrosis in those with hypertrophy (odds ratio: 1.09, 95% confidence interval: 1.04 to 1.14; p < 0.001) after adjusting for aortic stenosis severity, age, sex, and systolic blood pressure.

RELATIONSHIP BETWEEN MYOCARDIAL ECV AND REPLACEMENT FIBROSIS. It has been suggested that replacement fibrosis represents the irreversible final stage of diffuse interstitial fibrosis and extracellular expansion. Consistent with this hypothesis, patients with replacement mid-wall fibrosis had evidence of increased ECV on T1 mapping compared with patients without (iECV: 32.0 ml/m^2; IQR: 29.1 to 34.9 ml/m^2 vs. 21.5 ml/m^2; IQR: 20.6 to 22.4 ml/m^2; p < 0.0001; ECV fraction: 29.1 ± 2.4% vs. 26.9 ± 2.1%; p < 0.001). The iECV was independently associated with mid-wall fibrosis after adjusting for age, sex, severity of aortic stenosis, and even LV mass (odds ratio: 1.22; 95% confidence interval: 1.11 to 1.35; p < 0.001). Similar associations were observed using the ECV fraction.

CATEGORIZATION OF LV DECOMPENSATION. We proceeded to categorize patients into 3 groups according to our CMR measures of myocardial fibrosis: normal myocardium, extracellular expansion, and replacement mid-wall fibrosis (Figure 3). The upper limit of normal for iECV in the healthy volunteers (defined by 2 SDs above the mean, 22.5 ml/m^2) was used to define expansion of the extracellular myocardium. Values below this threshold defined normal myocardium. This categorization was then validated in the 11 patients who underwent myocardial biopsy, with the percentage fibrosis on histology increasing progressively across the 3 groups (normal myocardium: 8.9 ± 4.0% vs. extracellular expansion: 12.4 ± 2.5% vs. replacement fibrosis: 22.4 ± 4.9%; p < 0.004) (Table 4).

In the larger imaging cohort of patients with aortic stenosis (after exclusion of patients with an infarct pattern of LGE, n = 22, or incomplete T1 mapping data, n = 5), 71 patients had normal myocardium (iECV <22.5 ml/m^2). These patients had largely mild-to-moderate aortic stenosis, a mild hypertrophic response, minimal cardiac injury, and good

TABLE 3 Progressive Increase in Markers of LV Hypertrophy and Decompensation With Increasing iECV Stratified Into Tertiles

	Tertile 1 (n = 54)	Tertile 2 (n = 54)	Tertile 3 (n = 53)	p Value
Age, yrs	70 (63–75)	70 (65–70)	72 (64–78)	0.30
Men	27 (50)	42 (78)	43 (81)	0.0006
Echocardiography				
Peak aortic jet velocity, m/s	3.45 ± 0.78	3.77 ± 0.81	4.25 ± 0.96	<0.0001
Aortic valve area, cm^2	1.01 ± 0.37	0.95 ± 0.36	0.90 ± 0.35	0.32
Mean AV pressure gradient, mm Hg	27.6 ±12.7	32.7 ± 15.0	42.6 ± 23.7	<0.0001
Mild aortic stenosis	19	12	3	
Moderate aortic stenosis	13	17	15	
Severe aortic stenosis	22	25	35	
Valvulo-arterial impedance, mm Hg/ml/m^2	4.4 ± 1.1	4.0 ± 1.0	3.8 ± 1.0	0.019
Mean e', cm/s	6.9 ± 2.0	6.4 ± 1.7	5.4 ± 1.8	<0.0001
Mean E/e' ratio	11.6 (9.8–14.4)	12.4 (9.3–16.5)	14.3 (11.9–19.2)	0.02
Mean diastolic dysfunction grade	1.5 ± 1.0	2.0 ± 0.8	2.5 ± 0.7	<0.0001
CMR				
LVMi, g/m^2	68 ± 9	88 ± 9	110 ± 19	<0.0001
Ejection fraction, %	68 (63–71)	67 (64–73)	66 (61–71)	0.44
Longitudinal function, mm	13.0 ± 2.7	12.8 ± 2.7	11.0 ± 3.0	0.0004
Mid-wall fibrosis	2 (4)	6 (11)	36 (68)	0.0001
Indexed left atrial volume, ml/m^2	29 ± 13	36 ± 14	38 ± 13	0.004
Biomarkers				
Natural log (hs troponin I)	1.3 (0.8–1.6)	2.1 (1.5-2.4)	2.5 (1.9–3.3)	<0.0001
Natural log (BNP)	2.8 (1.9–3.5)	3.1 (2.4–3.9)	4.0 (2.8–4.7)	<0.0001
Functional status				
6-min walk test, m	410 (345–445)	410 (358–453)	385 (295–443)	0.09
NYHA functional class, %				
I	27 (50)	23 (43)	24 (45)	
II	20 (37)	19 (35)	15 (28)	
III	6 (11)	12 (22)	11 (21)	
IV	1 (2)	0 (0)	3 (6)	
Outcomes				
All-cause mortality	2	2	10	–
Mortality rate (per 1,000 patient-years)	12	12	72	0.005
Aortic stenosis–related mortality	0	2	8	–

Values are median (interquartile range), n (%), or mean ± SD. Five patients had insufficient data to calculate the indexed extracellular volume.
AV = aortic valve; BNP = brain natriuretic peptide; CMR = cardiac magnetic resonance; hs = high-sensitivity; other abbreviations as in Table 1.

LV performance (Table 4, Figures 3 and 4). Thirty-one patients had extracellular expansion (iECV ≥22.5 ml/m^2), with values for aortic stenosis severity, LV mass, myocardial injury, diastolic function, and longitudinal systolic function that were intermediate between patients with normal myocardium and replacement fibrosis. Finally, 37 patients had evidence of replacement myocardial fibrosis on LGE. These patients were confirmed as having the most severe aortic stenosis, LVH, myocardial injury, and impairment in LV performance (Table 4). Compared with patients with extracellular expansion, they had even higher iECV values (30.4 ± 8.2 ml/m^2 vs. 25.4 ± 3.1 ml/m^2; $p < 0.0001$) (Figure 2), whereas compared with patients with normal myocardium, they had increased serum BNP concentrations (16.7 pg/ml; IQR: 6.1 to 36.0 pg/ml vs. 34.4 pg/ml; IQR: 10.5 to 76.2 pg/ml, respectively, $p = 0.026$) and impaired functional capacity (6-min walk test: 405 ± 74 m vs. 359 ± 138 m, respectively; $p = 0.03$). Both mid-wall fibrosis and the ECV fraction were predictors of functional capacity independent of age, sex, LV mass, and peak velocity (Table 5). These findings were unchanged when patients with mild aortic stenosis were excluded from the analysis (Online Table 3).

CLINICAL OUTCOMES. Participants were followed up for an average of 2.9 ± 0.8 years during which a total of 14 patients with aortic stenosis died: 2 with normal myocardium, 4 with extracellular expansion and 8 with replacement fibrosis. Unadjusted all-cause mortality rates rose progressively across the groups (8 deaths/1,000 patient-years vs. 36 deaths/1,000 patient-years vs. 71 deaths/1,000 patient-years;

FIGURE 3 CMR Categorization of Myocardial Fibrosis in Aortic Stenosis

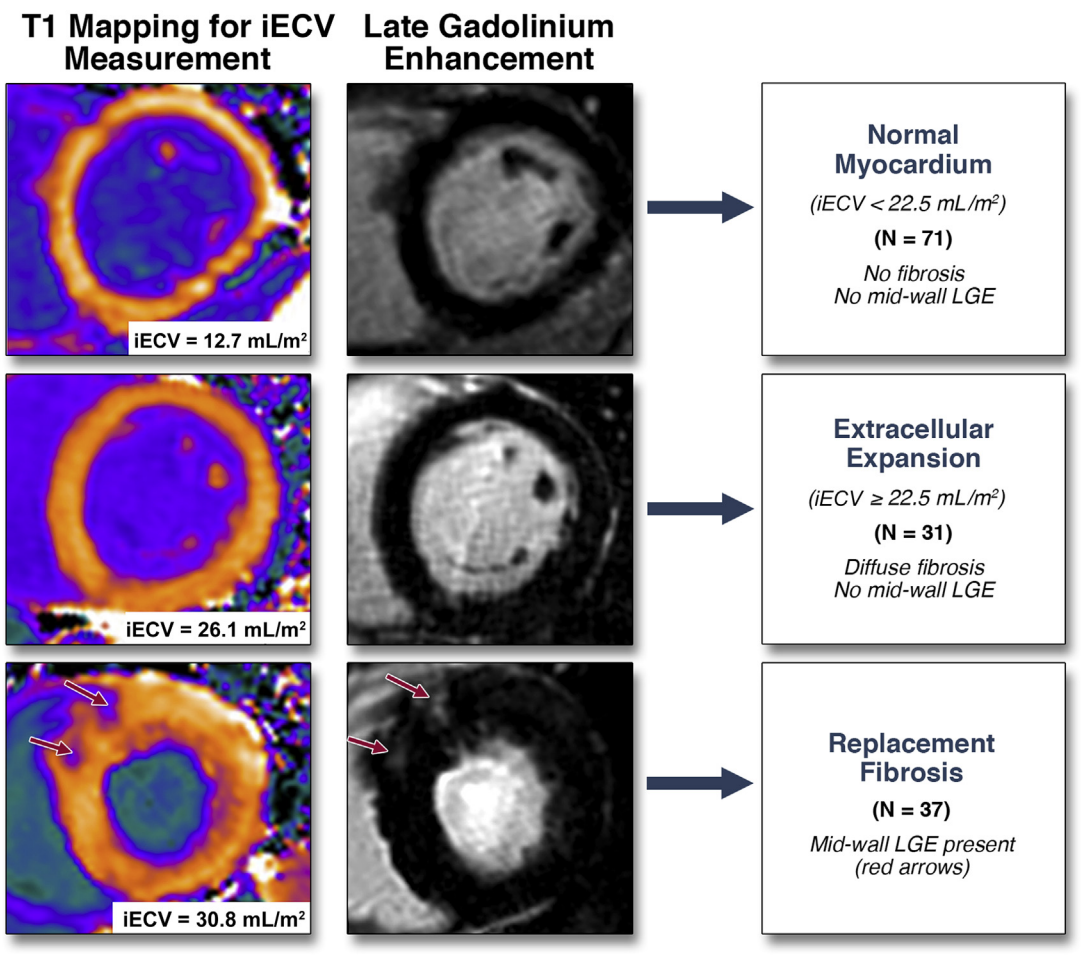

Patients with aortic stenosis were categorized into 3 groups based upon cardiac magnetic resonance (CMR) assessments of fibrosis. iECV = indexed extracellular volume; LGE = late gadolinium enhancement.

log-rank test: p = 0.009 (**Table 4**, **Figure 4**). AS-related mortality also increased in a stepwise fashion (0 deaths/1,000 patient-years vs. 36 deaths/1,000 patient-years vs. 52 deaths/1,000 patient-years; p = 0.0045) with no AS-related deaths in the normal myocardium group. Tertiles of ECV fraction (p = 0.0006) (Online Table 1) and iECV (p = 0.005) (**Table 3**) also displayed prognostic ability in this unadjusted analysis but no difference in mortality was observed across tertiles of the indexed LV mass (p = 0.23) (Online Table 2).

DISCUSSION

This is the largest prospective CMR study to systematically evaluate both extracellular expansion and replacement fibrosis in the myocardium of patients with aortic stenosis and healthy control subjects. Both measures are increased in aortic stenosis, but are only weakly associated with the severity of valve narrowing. In contrast, they demonstrate a close association with the magnitude of the hypertrophic response, the presence of LV dysfunction, the functional capacity of the patient, and, ultimately, clinical outcome. We believe these findings demonstrate that the structural changes in the LV myocardium are as important a consideration as the severity of the valvular disease itself. Based on these results, we propose that patients with aortic stenosis be categorized into 3 groups—those with normal myocardium, extracellular expansion, and replacement myocardial fibrosis. We believe this

TABLE 4 Characteristics of Patients Stratified According to iECV Thresholds and Presence of Mid-Wall Late Gadolinium Enhancement

	Normal Myocardium (n = 71)	Extracellular Expansion (n = 31)	Replacement Fibrosis (n = 37)	p Value
Age, yrs	70 (63–75)	70 (63–75)	71 (65–78)	0.59
Sex (male = 1)	0.56 (0.44–0.68)	0.81 (0.67–0.96)	0.76 (0.62–0.90)	0.023
Hypertension	48 (68)	20 (65)	22 (59)	0.70
Diabetes	8 (11)	7 (23)	2 (5)	0.09
Body mass index, kg/m^2	28.2 ± 4.5	28.9 ± 4.6	29.3 ± 4.3	0.44
Echocardiography				
Peak aortic jet velocity, m/s	3.53 ± 0.82	3.79 ± 1.0	4.23 ± 0.92	<0.001
Aortic valve area, cm^2	0.98 (0.73–1.18)	0.88 (1.2–0.7)	0.83 (0.73–0.91)	0.049
Mean AV pressure gradient, mm Hg	29.1 ± 14.2	34.8 ± 21.1	41.1 ± 23.5	0.007
Mild AS	24	7	2	
Moderate AS	18	10	11	
Severe AS	29	14	24	
Valvulo-arterial impedance, mm Hg/ml/m^2	4.1 ± 1.0	3.9 ± 0.9	4.0 ± 1.0	0.46
Mean e', cm/s	6.7 ± 2.0	6.5 ± 1.8	5.2 ± 1.4	0.0004
Mean E/e' ratio	13.1 ± 7.7	13.2 ± 4.8	16.5 ± 6.5	0.04
Mean diastolic dysfunction grade	1.5 ± 0.9	2.0 ± 0.9	2.7 ± 0.5	<0.0001
CMR				
LVMi, g/m^2	73 ± 11	96 ± 11	107 ± 25	<0.0001
Relative wall thickness	0.60 ± 0.12	0.61 ± 0.09	0.67 ± 0.11	0.018
ECVi, ml/m^2	18.3 ± 2.5	25.4 ± 3.1	30.4 ± 8.2	<0.0001
Ejection fraction, %	68 (63–71)	66 (64–71)	67 (64–72)	0.94
Longitudinal systolic function, mm	13.2 ± 2.6	12.5 ± 2.4	11.2 ± 3.1	0.002
Indexed left atrial volume, ml/m^2	31 ± 13	37 ± 11	38 ± 15	0.027
Biomarkers				
Natural log (hs troponin I)	1.43 ± 0.96	2.02 ± 0.93	2.60 ± 0.90	<0.0001
Natural log (BNP)	2.95 ± 1.00	3.06 ± 0.96	3.41 ± 1.10	0.12
Functional status				
6-min walk test, m	406 ± 74	385±95	359 ± 138	0.08
NYHA functional class				
I	33 (46)	18 (58)	17 (46)	
II	27 (38)	6 (19)	12 (32)	
III	11 (15)	7 (23)	5 (14)	
IV	0 (0)	0 (0)	3 (8)	
Outcomes				
All-cause mortality	2	4	8	–
All-cause mortality rate (per 1,000 patient- years)	8	36	71	0.009
AS-related mortality, n	0	4	6	–
AS-related mortality rate (per 1,000 patient-years)	0	36	52	0.0045

Patients Undergoing Myocardial Biopsy	Normal Myocardium on CMR (n = 3)	Extracellular Expansion on CMR (n = 5)	Replacement Fibrosis on CMR (n = 3)	p Value
Histological fibrosis, %	8.9 ± 4.0	12.4 ± 2.5	22.4 ± 4.9	0.004
Aortic valve area, cm^2	0.57 ± 0.10	0.94 ± 0.29	0.81 ± 0.44	0.29
Peak aortic jet velocity, m/s	4.6 (4.4–5.1)	4.5 (4.0–5.9)	4.9 (4.1–8.0)	0.63
LVMi, g/m^2	76 ± 15	98 ± 4	162 ± 6	<0.0001
Native myocardial T1, ms	1,189 ± 23	1,183 ± 16	1,277 ± 15	0.0002
Post-contrast myocardial T1, ms	676 ± 45	615 ± 24	672 ± 84	0.22
Partition coefficient	0.43 ± 0.05	0.47 ± 0.02	0.55 ± 0.02	0.008
ECV fraction, %	25.3 ± 3.1	27.3 ± 1.4	32.2 ± 1.9	0.019
iECV, ml/m^2	18.8 ± 1.9	25.6 ± 0.7	49.6 ± 4.8	<0.0001

Values are median (interquartile range), n (%), or mean ± SD.
Abbreviations as in Tables 1 to 3.

FIGURE 4 **Progressive LV Decompensation on Moving From Normal Myocardium to Extracellular Expansion to Replacement Fibrosis**

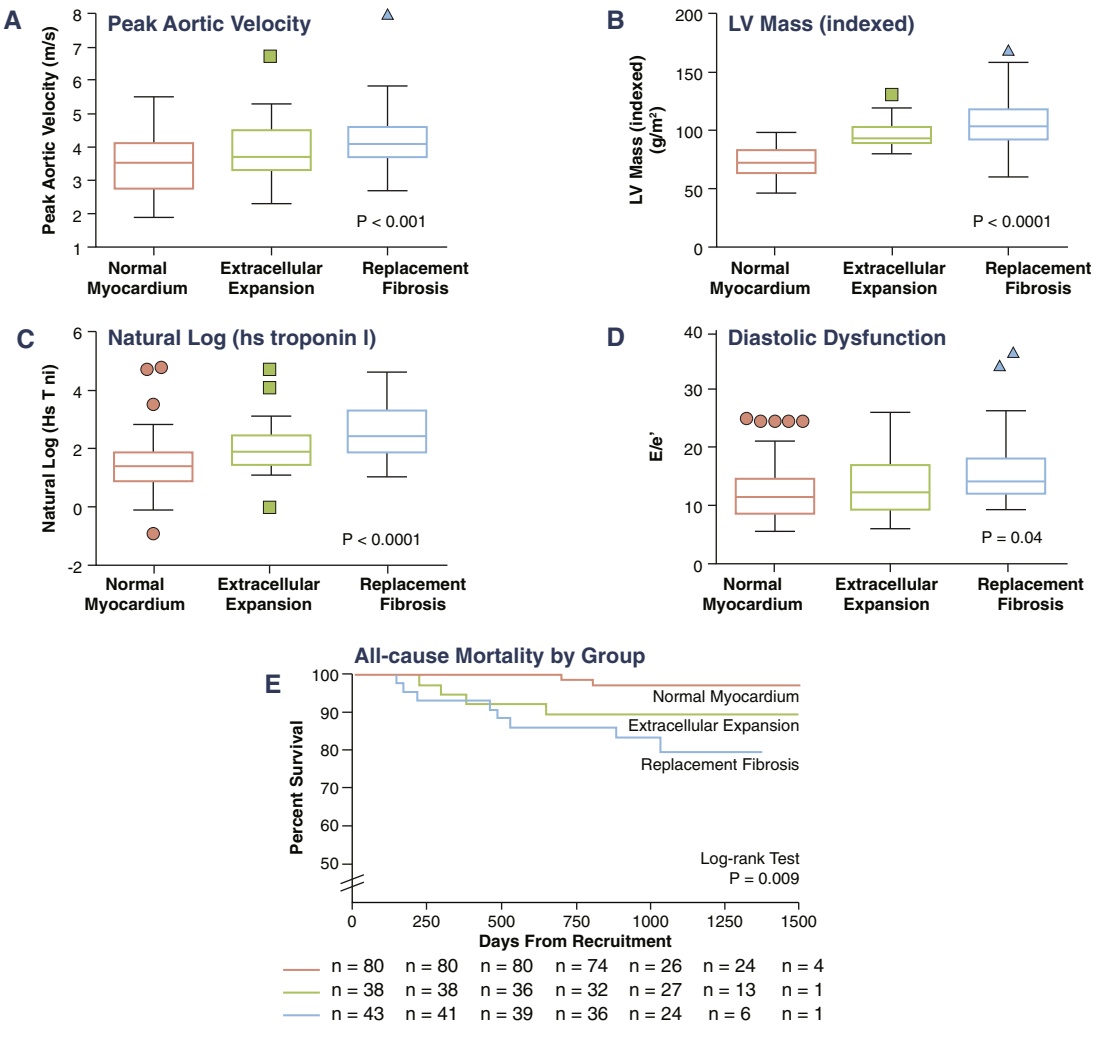

On moving from normal myocardium to extracellular expansion and then replacement fibrosis, there was a stepwise increase in the following measures: **(A)** the severity of valve narrowing; **(B)** the degree of hypertrophy; **(C)** myocardial injury; **(D)** left ventricular (LV) performance; and **(E)** all-cause-mortality. hsTni = high-sensitivity troponin I concentration.

classification has major potential in the early detection of subclinical ventricular decompensation in aortic stenosis and ultimately may be able to guide decisions regarding the timing of aortic valve replacement.

Our data demonstrated an association between the severity of valve narrowing and the degree of hypertrophy in aortic stenosis. However, this only explained approximately one-quarter of the observed variance in LV mass, confirming that the hypertrophic response in aortic stenosis cannot be accurately predicted from the degree of valve narrowing alone and should be assessed independently.

T1 mapping techniques (ECV fraction and iECV) can provide an assessment of myocardial ECV expansion. Potentially, this can reflect increased myocardial fibrosis, myocardial infiltration, or expansion in the intravascular compartment (13). In aortic stenosis, myocardial fibrosis has been established pathologically as a key process that drives the transition from hypertrophy to heart failure (4). Moreover, we and others have observed a close correlation between these parameters and histological assessments of myocardial fibrosis (5,14-16). However, there is some debate as to whether T1 mapping can provide direct assessment of the myocardium because of recent evidence that indicated that increased intravascular

TABLE 5 Univariable and Multivariable Linear Regression Analysis to Examine the Association of Fibrosis Assessments With Functional Status

	Univariable Analysis		Multivariable Analysis			
			Model 1 (ECV fraction)		Model 2 (mid-wall fibrosis)	
	Relative Change in 6-Min Walk (95% CI)	p Value	Relative Change in 6-Min Walk (95% CI)	p Value	Relative Change in 6-Min Walk (95% CI)	p Value
Age ≥70 yrs	−50.3 (−83.0 to −17.6)	0.003	−41.4 (−74.5 to −8.36)	0.01	−50.3 (−83.0 to −17.7)	0.003
Men	−0.81 (−37.7 to 36.1)	0.97	−19.9 (−61.3 to 21.6)	0.35	−8.88 (−48.5 to 30.7)	0.66
Peak aortic jet velocity, m/s	−12.25 (−30.6 to 6.14)	0.19	−14.9 (−35.4 to 5.73)	0.16	−11.9 (−32.4 to 8.64)	0.26
LVMi, g/m^2	−0.22 (−1.00 to 0.56)	0.57	0.62 (−0.44 to 1.68)	0.25	0.45 (−0.62 to 1.52)	0.41
ECV fraction, %	−9.09 (−15.4 to −2.81)	0.005	−9.77 (−17.0 to −2.58)	0.01	–	–
Presence of mid−wall fibrosis	−40.9 (−78.5 to −3.24)	0.03	–	–	−45.6 (−89.1 to −2.11)	0.04

CI = confidence interval; other abbreviations as in Tables 2 and 3.

volume may also influence native T1 values (17,18). Pressure overload conditions such as aortic stenosis are associated with reduced capillary density (19) and myocardial ischemia (20). Mahmod et al. (17) recently suggested that this ischemia might result in coronary vasodilatation and increased intravascular volume potentially contributing to increased native T1. Although confirmation of this interesting hypothesis is required, it may be that T1 values are also related to myocardial ischemia that is believed to trigger fibrosis and the transition from hypertrophy to heart failure. Regardless, T1 mapping remains at the very least a useful surrogate of myocardial fibrosis and LV decompensation in aortic stenosis.

Controversy remains as to the optimal T1 image analysis strategy (12,13,21). Consistent with previous research (12), both native T1 and the ECV fraction demonstrated major overlap with values in control groups and little difference among patients with mild, moderate, and severe aortic stenosis (**Table 2**). We sought to tackle this issue by developing a novel parameter, the iECV, which provides an assessment of the total ECV in the myocardium. This effectively combines the prognostic information provided by the ECV fraction with the improved discrimination between groups associated with indexed LV mass into a single measure (**Table 3**, Online Tables 1 and 2).

iECV demonstrated good correlation with histological assessment of fibrosis burden. Moreover, there was a clear stepwise increase across tertiles of iECV in each of the different clinical and imaging measures of LV decompensation, as well as clinical outcomes, supporting iECV as a marker of decompensation. Finally, iECV provided the best discrimination among disease states, being the only T1 measure to differentiate among patients with mild, moderate, and severe aortic stenosis. In combination, iECV would therefore appear to provide the most useful marker of LV decompensation in aortic stenosis with advantages compared with both the ECV fraction and LV mass in isolation.

How do extracellular expansion and diffuse fibrosis relate to the development of replacement fibrosis as detected using mid-wall LGE? In agreement with previous studies (7,8), regions of mid-wall LGE were observed in 27% of our patients, with approximately two-thirds with severe aortic stenosis and one-third with moderate aortic stenosis. Importantly, patients with mid-wall replacement fibrosis also had marked increases in iECV as a surrogate for diffuse fibrosis in their remote myocardium. Indeed, iECV was an independent predictor of the presence of mid-wall LGE. This was confirmed by our histological data and suggests that replacement fibrosis does not occur until the end stages of myocardial matrix remodeling and is preceded by an intermediate stage of extracellular expansion reflecting increasing diffuse fibrosis. Longitudinal studies using serial CMR imaging are required to confirm this hypothesis.

Using our CMR assessments, we categorized our patients into 3 stages of LV decompensation. We used iECV to differentiate patients with normal myocardium from those with extracellular expansion and then LGE to define replacement fibrosis (**Figure 3**). Across these groups, patients had advancing LVH, histological fibrosis, myocyte cell injury, diastolic dysfunction, and longitudinal systolic dysfunction, which suggested progressive, subclinical LV decompensation. Most importantly, there was a steady decline in prognosis, with unadjusted all-cause mortality rates quadrupling from the normal myocardium groups to the extracellular expansion groups and more than doubling again in those with replacement fibrosis. Moreover, these groups also predicted aortic stenosis–related deaths on unadjusted analysis, with no aortic stenosis–related deaths occurring in the normal myocardium group.

More simple categorization using LV mass was less discriminatory and not of prognostic value (Online Table 2).

Our categorization holds promise as a means of monitoring the development of LV decompensation and helping to optimize the timing of aortic valve replacement. Currently, the development of symptoms guides the need for surgery. However, symptoms are frequently difficult to assess in older adult patients with multiple co-morbidities. Objective imaging assessments that monitor the changes in myocardial structure that are themselves responsible for progressive LV decompensation are therefore potentially attractive (2,3). This is the first study to describe iECV in aortic stenosis, so that confirmation of our findings in larger studies with longer follow-up is required. However, we presented the fourth separate cohort to demonstrate the adverse prognosis associated with mid-wall LGE in aortic stenosis (7,8,22) and demonstrated its association with patient functional capacity, LV performance, and multiple other parameters of LV decompensation. These data have now led to the EVOLVED (Early Valve Replacement guided by Biomarkers of Left Ventricular Decompensation in Asymptomatic Patients with Advanced Aortic Stenosis) study. This multicenter, randomized controlled trial will begin enrollment next year and assess whether early valve intervention in patients with asymptomatic severe aortic stenosis and mid-wall fibrosis on CMR improves clinical outcomes compared with standard care.

STUDY LIMITATIONS. There were insufficient deaths to perform multivariate analysis. Studies with longer follow-up are required to confirm whether iECV is of independent prognostic value and to assess the contribution of the intravascular volume to T1 mapping values. Finally, although similar to previous studies (14–16), the number of patients who agreed to intraoperative myocardial biopsy was modest, which perhaps reflected the invasive nature of this assessment.

CONCLUSIONS

CMR can detect progressive fibrosis in aortic stenosis and can be used to categorize patients with normal myocardium, extracellular expansion, or replacement fibrosis. Across these groups, there was a stepwise increase in myocardial injury, fibrosis, LV dysfunction, and unadjusted mortality that was consistent with progressive ventricular decompensation. This categorization may be able to track the transition of hypertrophy to heart failure in patients with aortic stenosis.

ACKNOWLEDGEMENTS The authors thank Siemens Plc for the use of their T1 mapping work-in-progress software package. The Clinical Research Imaging Centre (Edinburgh) is supported by the National Health Service Research Scotland (NRS) through National Health Service Lothian Health Board.

REPRINT REQUESTS AND CORRESPONDENCE: Dr. Marc R. Dweck, BHF/Centre for Cardiovascular Science, Chancellor's Building, University of Edinburgh, 49 Little France Crescent, Edinburgh EH16 4SB, United Kingdom. E-mail: marc.dweck@ed.ac.uk.

PERSPECTIVES

COMPETENCY IN MEDICAL KNOWLEDGE: Decompensation of the hypertrophic response in aortic stenosis is driven by progressive myocardial fibrosis and the associated expansion in the ECV. Changes in the LV myocardium can be tracked using CMR, which can be used to categorize patients into 3 groups: normal myocardium, extracellular expansion, and replacement fibrosis. There is evidence of increasing myocyte injury, left ventricular dysfunction, functional impairment, and all-cause mortality across these groups.

TRANSLATIONAL OUTLOOK: This categorization holds promise in tracking the transition from hypertrophy to heart failure in aortic stenosis and in identifying the optimal timing of aortic valve replacement. Prospective randomized controlled studies are required to investigate this further.

REFERENCES

1. Nkomo VT, Gardin JM, Skelton TN, Gottdiener JS, Scott CG, Enriquez-Sarano M. Burden of valvular heart diseases: a population-based study. Lancet 2006;368:1005–11.

2. Dweck MR, Boon NA, Newby DE. Calcific aortic stenosis: a disease of the valve and the myocardium. J Am Coll Cardiol 2012;60:1854–63.

3. Chin CWL, Pawade TA, Newby DE, Dweck MR. Risk stratification in patients with aortic stenosis using novel imaging approaches. Circ Cardiovasc Imaging 2015;8:e003421.

4. Hein S, Arnon E, Kostin S, et al. Progression from compensated hypertrophy to failure in the pressure-overloaded human heart: structural deterioration and compensatory mechanisms. Circulation 2003;107:984–91.

5. Flett AS, Hayward MP, Ashworth MT, et al. Equilibrium contrast cardiovascular magnetic resonance for the measurement of diffuse myocardial fibrosis: preliminary validation in humans. Circulation 2010;122:138–44.

6. Krayenbeuhl HP, Hess OM, Monrad ES, Schneider J, Mall G, Turina M. Left-ventricular myocardial structure in aortic-valve disease before, intermediate, and late after aortic-valve replacement. Circulation 1989;79:744–55.

7. Dweck MR, Joshi S, Murigu T, et al. Midwall fibrosis is an independent predictor of mortality in patients with aortic stenosis. J Am Coll Cardiol 2011;58:1271–9.

8. Barone-Rochette G, Piérard S, de Meester de Ravenstein C, et al. Prognostic significance of LGE by CMR in aortic stenosis patients undergoing valve replacement. J Am Coll Cardiol 2014;64:144–54.

9. Chin CWL, Shah ASV, McAllister DA, et al. High-sensitivity troponin I concentrations are a marker of an advanced hypertrophic response and adverse outcomes in patients with aortic stenosis. Eur Heart J 2014;35:2312–21.

10. Maceira A, Prasad S, Khan M, Pennell D. Normalized left ventricular systolic and diastolic function by steady state free precession cardiovascular magnetic resonance. J Cardiovasc Magn Reson 2006;8:417–26.

11. Messroghli DR, Greiser A, Frohlich M, Fröhlich M, Dietz R, Schulz-Menger J. Optimization and validation of a fully-integrated pulse sequence for modified look-locker inversion-recovery (MOLLI) T1 mapping of the heart. J Magn Reson Imaging 2007;26:1081–6.

12. Chin CWL, Semple S, Malley T, et al. Optimization and comparison of myocardial T1 techniques at 3T in patients with aortic stenosis. Eur Heart J Cardiovasc Imaging 2014;15:556–65.

13. Moon JC, Messroghli DR, Kellman P, et al. Myocardial T1 mapping and extracellular volume quantification: a Society for Cardiovascular Magnetic Resonance (SCMR) and CMR Working Group of the European Society of Cardiology consensus statement. J Cardiovasc Magn Reson 2013;15:92.

14. Flett AS, Sado DM, Quarta G, et al. Diffuse myocardial fibrosis in severe aortic stenosis: an equilibrium contrast cardiovascular magnetic resonance study. Eur Heart J Cardiovasc Imaging 2012;13:819–26.

15. Bull S, White SK, Piechnik SK, et al. Human non-contrast T1 values and correlation with histology in diffuse fibrosis. Heart 2013;99:932–7.

16. Lee S-P, Lee W, Lee JM, et al. Assessment of diffuse myocardial fibrosis by using MR imaging in asymptomatic patients with aortic stenosis. Radiology 2015;274:359–69.

17. Mahmod M, Piechnik SK, Levelt E, et al. Adenosine stress native T1 mapping in severe aortic stenosis: evidence for a role of the intravascular compartment on myocardial T1 values. J Cardiovasc Magn Reson 2014;16:92.

18. Liu A, Wijesurendra RS, Francis JM, et al. Adenosine stress and rest T1 mapping can differentiate between ischemic, infarcted, remote, and normal myocardium without the need for gadolinium contrast agents. J Am Coll Cardiol Img 2016;9:27–36.

19. Rakusan K, Flanagan MF, Geva T, Southern J, Van Praagh R. Morphometry of human coronary capillaries during normal growth and the effect of age in left ventricular pressure-overload hypertrophy. Circulation 1992;86:38–46.

20. Galiuto L, Lotrionte M, Crea F, et al. Impaired coronary and myocardial flow in severe aortic stenosis is associated with increased apoptosis: a transthoracic Doppler and myocardial contrast echocardiography study. Heart 2006;92:208–12.

21. Everett RJ, Stirrat CG, Semple SIR, Newby DE, Dweck MR, Mirsadraee S. Assessment of myocardial fibrosis with T1 mapping MRI. Clin Radiol 2016;71:768–78.

22. Azevedo CF, Nigri M, Higuchi ML, et al. Prognostic significance of myocardial fibrosis quantification by histopathology and magnetic resonance imaging in patients with severe aortic valve disease. J Am Coll Cardiol 2010;56:278–87.

KEY WORDS aortic stenosis, fibrosis, hypertrophy, magnetic resonance imaging, myocardium, T1 mapping

APPENDIX For an expanded Methods section and supplemental tables, please see the online version of this paper.

Circulation: Cardiovascular Imaging

ORIGINAL ARTICLE

Progression of Hypertrophy and Myocardial Fibrosis in Aortic Stenosis

A Multicenter Cardiac Magnetic Resonance Study

See Editorial by Treibel et al

BACKGROUND: Aortic stenosis is accompanied by progressive left ventricular hypertrophy and fibrosis. We investigated the natural history of these processes in asymptomatic patients and their potential reversal post-aortic valve replacement (AVR).

METHODS: Asymptomatic and symptomatic patients with aortic stenosis underwent repeat echocardiography and magnetic resonance imaging. Changes in peak aortic-jet velocity, left ventricular mass index, diffuse fibrosis (indexed extracellular volume), and replacement fibrosis (late gadolinium enhancement [LGE]) were quantified.

RESULTS: In 61 asymptomatic patients (43% mild, 34% moderate, and 23% severe aortic stenosis), significant increases in peak aortic-jet velocity, left ventricular mass index, indexed extracellular volume, and LGE mass were observed after 2.1±0.7 years, with the most rapid progression observed in patients with most severe stenosis. Patients with baseline midwall LGE (n=16 [26%]; LGE mass, 2.5 g [0.8–4.8 g]) demonstrated particularly rapid increases in scar burden (78% [50%–158%] increase in LGE mass per year). In 38 symptomatic patients (age, 66±8 years; 76% men) who underwent AVR, there was a 19% (11%–25%) reduction in left ventricular mass index (P<0.0001) and an 11% (4%–16%) reduction in indexed extracellular volume (P=0.003) 0.9±0.3 years after surgery. By contrast midwall LGE (n=10 [26%]; mass, 3.3 g [2.6–8.0 g]) did not change post-AVR (n=10; 3.5 g [2.1–8.0 g]; P=0.23), with no evidence of regression even out to 2 years.

CONCLUSIONS: In patients with aortic stenosis, cellular hypertrophy and diffuse fibrosis progress in a rapid and balanced manner but are reversible after AVR. Once established, midwall LGE also accumulates rapidly but is irreversible post valve replacement. Given its adverse long-term prognosis, prompt AVR when midwall LGE is first identified may improve clinical outcomes.

CLINICAL TRIAL REGISTRATION: URL: https://www.clinicaltrials.gov. Unique identifiers: NCT01755936 and NCT01679431.

Russell J. Everett, MD, BSc*
Lionel Tastet, MSc*
Marie-Annick Clavel, DVM, PhD
Calvin W.L. Chin, MD, PhD
Romain Capoulade, PhD
Vassilios S. Vassiliou, MD
Jacek Kwiecinski, MD
Miquel Gomez, MD, PhD
Edwin J.R. van Beek, MD, PhD
Audrey C. White
Sanjay K. Prasad, MD
Eric Larose, DVM, MD
Christopher Tuck, BSc
Scott Semple, PhD
David E. Newby, MD, DSc, PhD
Philippe Pibarot, DVM, PhD†
Marc R. Dweck, MD, PhD†

*Dr Everett and L. Tastet are joint first authors.

†Drs Pibarot and Dweck are joint senior authors.

Key Words: aortic valve stenosis ■ fibrosis ■ gadolinium ■ hypertrophy ■ magnetic resonance imaging

http://circimaging.ahajournals.org

CLINICAL PERSPECTIVE

Left ventricular hypertrophy and myocardial fibrosis are key processes in aortic stenosis that can be assessed by cardiovascular magnetic resonance. However, longitudinal changes in myocardial hypertrophy and fibrosis before and after aortic valve replacement are not well studied. We performed a multicenter prospective cohort study of 99 subjects who underwent serial echocardiography and cardiovascular magnetic resonance with assessment of left ventricular mass, diffuse fibrosis (T1 mapping), and replacement fibrosis (late gadolinium enhancement). Sixty-one subjects were asymptomatic allowing us to assess the natural history of hypertrophy and fibrosis for 2.1±0.7 years. Thirty-eight symptomatic subjects underwent aortic valve replacement with repeat imaging after 1 year allowing us to assess the left ventricular remodeling response to surgery. Our data demonstrate that in patients with aortic stenosis, cellular hypertrophy and diffuse interstitial fibrosis increase in a balanced and exponential manner before reversing (at different rates) after aortic valve replacement. Midwall replacement fibrosis also accumulates rapidly once established in the ventricle but crucially seems irreversible after aortic valve replacement. The myocardial scar burden that patients develop while waiting for surgery, therefore, persists into the long term. This is an important observation because midwall fibrosis has consistently demonstrated an association with adverse outcome in a proportionate manner across multiple patient cohorts. Our data, therefore, suggest that prompt valve replacement as soon as midwall fibrosis develops may hold promise in improving clinical outcomes in patients with aortic stenosis, and this hypothesis will be examined in the currently-recruiting EVOLVED trial (Early Valve Replacement guided by Biomarkers of Left Ventricular Decompensation in Asymptomatic Patients with Severe Aortic Stenosis).

Aortic stenosis (AS) is the most common valve disease requiring operative intervention in high-income countries.[1] Traditional assessments of AS severity focus on the degree of hemodynamic obstruction in the valve. However, the importance of the myocardial response to pressure overload has been increasingly appreciated, especially when considering the development of symptoms and long-term prognosis after valve intervention.[2] Left ventricular hypertrophy (LVH) initially normalizes wall stress and maintains cardiac output for many years, if not decades. However, with time, the left ventricle (LV) decompensates and the patient transitions toward heart failure, symptoms, and adverse events.

Pathological studies have suggested that this transition from hypertrophy to heart failure is driven by a combination of myocyte cell death and myocardial fibrosis.[3] Magnetic resonance imaging (MRI) can detect focal myocardial fibrosis using late gadolinium enhancement (LGE) and estimates diffuse interstitial fibrosis with T1 mapping. A midwall pattern of LGE observed in AS acts as a marker of LV decompensation and is associated with an adverse prognosis after surgery.[4–8] However, to date, we have lacked longitudinal studies to assess how LVH and fibrosis progress with time and how aortic valve replacement (AVR) affects these processes. The aims of this prospective multicenter study were to assess the time course of LVH and fibrosis in patients with asymptomatic AS and to determine how they are affected in symptomatic patients who undergo AVR.

METHODS

Study Population

Patients were recruited from 2 large prospective observational MRI studies investigating the natural history of AS (NCT01755936, Edinburgh Heart Centre, United Kingdom,[7] and NCT01679431, Quebec Heart and Lung Institute, Canada[9]). In both studies, patients underwent comprehensive clinical and echocardiographic assessment including repeat MRI. Eligible participants had undergone at least 2 serial MRI scans. Symptomatic patients had AVR shortly after baseline MRI allowing us to assess the reverse remodeling effect of surgery on repeat scans. The study was conducted in accordance with the Declaration of Helsinki and approved by the local research committees. Written informed consent was obtained from all participants. Study data can be made available to other researchers on request to the corresponding author.

Echocardiography

Comprehensive transthoracic echocardiography was performed in all patients to assess AS severity as per clinical guidelines (Data Supplement).

Cardiac Magnetic Resonance

MRI was performed using both 1.5T and 3T scanners, and standard cine images of the LV were acquired. LGE was performed 15 minutes after administration of gadobutrol. T1 mapping was performed using the Modified Look-Locker Inversion-recovery sequence[10] before and 15 to 20 minutes after gadolinium contrast administration. Although there was variation in the scanners used at the different centers, all patients underwent standardized baseline and repeat imaging within their respective institutions (Data Supplement). To account for potential interscanner variation in T1 measurements,[11] extracellular volume (ECV)–derived T1 mapping measures were obtained to normalize myocardial T1 values to blood-pool measurements.

Image Analysis

Analysis of all MRI scans from both centers was performed at the Edinburgh Core Lab using CVI42 (Circle Cardiovascular Imaging Inc, Calgary, Canada) by a single reporter (R.J.E.) blinded to the scan time point (Data Supplement). Short-axis cine images were used to calculate ventricular volumes, mass, and function. The presence of midwall LGE was determined both qualitatively and quantitatively by 2 experienced operators (R.J.E. and M.R.D.), and its distribution recorded. LGE was quantified in a semiautomated manner using a signal intensity threshold of >3 SDs above the mean value in a region of normal myocardium.[12] Although segments with midwall late enhancement were included in the overall T1 calculation, segments with subendocardial infarct pattern LGE were excluded. ECV fraction (ECV%) and indexed ECV (iECV: ECV%× LV end-diastolic myocardial volume normalized to body surface area) were calculated using the motion-corrected native and postcontrast T1 maps (Data Supplement). We have previously reported the reproducibility of these measures at 3T[13] and demonstrated that iECV acts as a marker of LV decompensation in AS, correlates with the burden of diffuse fibrosis on histology, and is associated with future clinical events.[7] Other groups have also recently used the same parameter.[14]

Statistical Analysis

All statistical analyses were performed using GraphPad Prism version 7.0 and SPSS version 23. A 2-sided $P<0.05$ was considered statistically significant. Given heterogeneity in timing of follow-up imaging, changes in the LV remodeling variables were annualized. Annualized change was calculated as the difference between the baseline and final follow-up MRI scans, divided by the number of days in between time points and multiplied by 365. This approach assumes that progression is linear. In a sensitivity analysis, we restricted analysis of progression and reverse remodeling in those patients who had repeat imaging at the same time interval (2 years in the natural history cohort and 1 year in the AVR cohort) and examined absolute change in the LV remodeling variables.

We assessed the distribution of all continuous variables using the Shapiro–Wilk test and presented them as appropriate using mean±SD or median (interquartile range). Annualized change was assessed using a 1 sample *t* test or Wilcoxon signed-rank test where appropriate to compare with a hypothetical mean (or median) of 0. Other comparisons were made using the Kruskal–Wallis test where appropriate. We presented all categorical variables as percentages and used the χ^2 test for comparison. Absolute change in the sensitivity analysis was analyzed using the paired *t* test or Wilcoxon-matched pairs signed-rank test. Univariate linear regression was performed on both cohorts to investigate the change in indexed LV mass (LVMi) using variables known or suspected to influence LVM change (including age, sex, history of hypertension, and valvuloarterial impedance). Multivariable linear regression analysis was then performed with change in LVMi as the dependent variable, and the same relevant clinical variables included as covariates. R.J.E. had full access to study data and is responsible for data integrity and analysis.

RESULTS

Repeat MRI was performed in a total of 99 patients (n=63 from United Kingdom, n=36 from Canada; Table 1), 38 underwent AVR (AVR cohort: age, 66±8 years; 76% men; peak aortic-jet velocity, 4.70±0.83 m/s) and 61 remained under medical surveillance without intervention (natural history cohort: age, 61±12 years; 66% men; peak aortic-jet velocity, 3.24±0.76 m/s).

Natural History Cohort (LV Remodeling)

At baseline, AS was graded as mild in half of the cohort, with the remainder split between moderate (34%) and severe (23%; Table 1). No patient had symptoms attributable to valve disease. Follow-up MRI was performed at 2.1±0.7 years after baseline scan.

As expected, AS severity increased (peak aortic-jet velocity, 0.15 m/s per year [0–0.29 m/s per year]; mean gradient, 3 mm Hg/y [1–5 mm Hg/y]; aortic valve area: –0.05 cm²/y [–0.08 to –0.01 cm²/y]; $P<0.001$ for all; Table 2) with concurrent increases in both LVMi (3 g/m² per year [1–5 g/m² per year]; $P<0.001$) and maximum LV wall thickness (0.5 mm/y [0–1 mm/y]; $P<0.001$). These changes were accompanied by a reduction in longitudinal systolic function (–0.5 mm/y [–1.5 to 0.3 mm/y];

Table 1. Baseline Characteristics of Patients in the Natural History and AVR Cohorts

	Natural History Cohort, n=61	AVR Cohort, n=38
Age, y	61±12	66±8
Male sex, n (%)	40 (66)	29 (76)
Body mass index, kg/m²	28.3±5.6	27.3±3.6
Body surface area, m²	1.88±0.21	1.86±0.16
Past medical history		
Hypertension, n (%)	35 (58)	23 (61)
Diabetes mellitus, n (%)	21 (34)	6 (16)
Hyperlipidemia, n (%)	17 (28)	19 (50)
Obstructive coronary artery disease, n (%)	15 (25)	16 (42)
Previous percutaneous coronary intervention, n (%)	9 (15)	6 (16)
Previous coronary artery bypass graft, n (%)	3 (5)	0 (0)
Systolic blood pressure, mm Hg	139±22	146±22
Diastolic blood pressure, mm Hg	82±11	85±13
Echocardiography		
Aortic stenosis severity, n (%)		
Mild	26 (43)	0
Moderate	21 (34)	0
Asymptomatic severe	14 (23)	0
Symptomatic severe	0	38 (100)

AVR indicates aortic valve replacement.

Table 2. Baseline and Annualized Change in Markers of Left Ventricular Remodeling Among Patients in the Natural History and AVR Groups

LV Assessment	Natural History Group, n=61 (2.1±0.7 y Follow-Up)			AVR Group, n=38 (0.9±0.3 y Follow-Up)			
	Baseline Values	Annualized Absolute Change, units/y	*P* Value	Baseline Values	Absolute Change	Annualized Absolute Change, units/y	*P* Value
Indexed left ventricular end-diastolic volume, mL/m²	70±12	−1 (−4, 2)	0.015	67±15	…	−3 (−9, 2)	0.009
Indexed left ventricular end-systolic volume, mL/m²	18±7	−1 (−3, 1)	0.03	19±13	…	−2 (−5, 1)	0.19
Indexed stroke volume, mL/m²	52±9	0 (−3, 2)	0.31	49±8	…	−3 (−7, 1)	0.009
Ejection fraction, %	75±8	0 (−2, 4)	0.23	74±8	…	0 (−4, 4)	0.78
Left ventricular mass index, g/m²	75±20	3 (1, 5)	<0.0001	93±21	…	−10 (−19, −5)	<0.0001
Maximum left ventricular wall thickness, mm	12±3	0.5 (0, 1)	<0.0001	15±3	…	−2 (−2, −1)	<0.0001
Mass/volume, g/mL	1.09±0.28	0.08 (0.02, 0.14)	<0.0001	1.43±0.32	…	−0.08 (−0.19, 0.02)	0.003
Longitudinal systolic function, mm	14±3	−0.5 (−1.5, 0.3)	0.0003	12±3	…	1 (−1, 3)	0.10
Indexed left atrial volume, mL/m²	37±12	0 (−3, 3)	0.99	37±11	…	−1 (−8, 4)	0.33
Infarct late gadolinium enhancement, n (%)	8 (13)	…	…	5 (13)	…	…	…
Infarct late gadolinium enhancement mass, g	7.6±4.5	−0.1 (−1.4, 0.7)	0.56	4.8±2.8	…	0 (−0.7, 1.7)	0.72
Midwall late gadolinium enhancement, n (%)	16 (26)	…	…	10 (26)	…	…	…
Midwall late gadolinium enhancement mass, g	2.5 (0.8, 4.8)	1.6 (0.4, 4.1)	<0.0001	3.3 (2.6, 8.0)	…	−0.9 (−1.2, 0.5)	0.22
T1 mapping measures							
Extracellular volume fraction, %	26.6±3.1	0 (−1, 1)	0.80	27.2±2.8	…	1.2 (0.4, 2.2)	0.003
Total extracellular volume, mL	40±13	0.8 (0.1, 4.0)	<0.0001	47±18	…	−3 (−12, −1)	<0.0001
Indexed extracellular volume, mL/m²	21±6	0.5 (0, 2.3)	<0.0001	25±8	…	−2 (−3, −1)	<0.0001
Echocardiography							
Peak aortic-jet velocity, m/s	3.24±0.76	0.15 (0, 0.29)	<0.0001	4.70±0.83	−2.05 (−2.70, 1.56)	…	<0.0001
Mean aortic valve gradient, mm Hg	24±12	3 (1, 5)	<0.0001	52±22	−32 (−44, −26)	…	<0.0001
Aortic valve area, cm²	1.08±0.31	−0.05 (−0.08, −0.01)	<0.0001	0.79±0.20	0.73 (0.46, 0.91)	…	<0.0001
Indexed stroke volume, mL/m²	42±7	0 (−1, 2)	0.31	48±10	…	−1 (−9, 4)	0.13
Mean systolic blood pressure, mm Hg	139±22	−1 (−6, 2)	0.011	146±22	…	−2 (−22, 11)	0.46
Valvuloarterial impedance (Zva), mm Hg/mL per m²	4.06±0.99	−0.01 (−0.15, 0.20)	0.86	4.29±1.05	−0.60 (−1.19, 0.08)	…	<0.0001
E/A ratio	1.1±0.3	0 (−0.1, 0.1)	0.71	1.0±0.3	…	0.16 (−0.06, 0.42)	0.004
Mean e′, cm/s	7.47±2.34	−0.10 (−0.59, 0.42)	0.20	6.15±2.04	…	1.35 (0.26, 2.91)	0.0004
E/e′ ratio	10.9 (8.7, 12.8)	0.6 (−0.4, 1.3)	0.006	12.9 (10.2, 18.0)	…	−1.3 (−4.3, 1.1)	0.02

Variables are expressed as mean±SD or median (IQR) as appropriate. For the annualized changes, the unit is the unit mentioned after the name of the variable per year: for example, for indexed left ventricular volumes (mL/m²), the unit for the annualized change is mL/m² per year. AVR indicates aortic valve replacement; and IQR, interquartile range.

P=0.003) and an increase in LV filling pressures (E/e′, 0.6 /y [−0.4 to 1.3 /y]; *P*=0.006; Table 3). There was no significant change in LV stroke volume or ejection fraction over time (both *P*≥0.20).

When classified by baseline AS severity, there was a stepwise increase in the progression of both the valve stenosis severity (change in peak aortic-jet velocity: mild AS, 0.05 m/s per year [−0.03 to 0.20 m/s per year]; moderate AS, 0.16 m/s per year [−0.04 to 0.29 m/s per year]; and severe AS, 0.33 m/s per year [0.16–0.42 m/s per year]; *P*=0.002) and the hypertrophic response (change in LVMi: mild AS, 2 g/m² per year [1–4 g/m² per year]; moderate AS, 3 g/m² per year [2–5 g/m² per year]; and severe AS, 5 g/

Table 3. Diastolic Function Grade at Baseline and Follow-Up in the Natural History and AVR Groups

Diastolic Function Grade, n (%)	Natural History Group, n=61 (2.1±0.7 y Follow-Up)		AVR Group, n=38 (0.9±0.3 y Follow-Up)	
	Baseline	Follow-Up	Baseline	Follow-Up
0	5 (8)	0	0	0
1	34 (56)	39 (64)	23 (61)	24 (63)
2	22 (36)	21 (34)	15 (39)	13 (34)
3	0	1 (2)	0	1 (3)

AVR indicates aortic valve replacement.

m^2 per year [2–9 g/m^2 per year]; *P*=0.07; Table 4; Figure 1). Indeed, a moderate correlation was observed between the rate of peak aortic-jet velocity progression and the rate of LVMi progression (*r*=0.41; *P*=0.001) with both baseline and annualized peak aortic-jet velocity change being predictors of the rate of LVMi progression on univariable analysis. Annualized change in peak aortic-jet velocity was the only independent predictor of LVMi progression on multivariable analysis (*P*=0.02; Table 5).

Myocardial Fibrosis

iECV increased over time (0.5 mL/m^2 per year [0–2.3 mL/m^2 per year]; *P*<0.0001; Table 2; Figure 1), with progression again appearing to increase in a stepwise

Table 4. Annualized Change in Markers of Progression and Left Ventricular Remodeling According to Aortic Stenosis Severity in the Natural History Group

LV Assessment	Aortic Valve Stenosis Severity			*P* Value
	Mild, n=26	Moderate, n=21	Severe, n=14	
Indexed left ventricular end-diastolic volume, mL/m^2 per year	−1 (−5, 3)	−1 (−4, 2)	−2 (−5, 3)	0.93
Indexed left ventricular end-systolic volume, mL/m^2 per year	−1 (−5, 4)	−1 (−7, 2)	−3 (−5, 3)	0.43
Indexed stroke volume, mL/m^2 per year	−1 (−3, 1)	0 (−3, 3)	0 (−3, 2)	0.55
Ejection fraction, %/y	0 (−3, 2)	0 (−1, 4)	2 (−2, 4)	0.26
Left ventricular mass index, g/m^2 per year	2 (1, 4)	3 (2, 5)	5 (2, 9)	0.07
Maximum left ventricular wall thickness, mm/y	0.5 (0.0, 1.0)	0.5 (−0.3, 1.2)	0.5 (0.0, 1.0)	0.91
Mass/volume, g/mL per year	0.06 (−0.01, 0.11)	0.06 (0.02, 0.12)	0.14 (0.08, 0.27)	0.01
Longitudinal systolic function, mm/y	−0.5 (−1.1, 0.3)	−1.2 (−2.0, −0.3)	−0.1 (−1.5, 0.5)	0.08
Indexed left atrial volume, mL/m^2 per year	−1 (−3, 2)	1 (−2, 5)	0 (−5, 2)	0.30
Infarct late gadolinium enhancement, n (%)	2 (8)	3 (14)	3 (21)	…
Midwall late gadolinium enhancement, n (%)	1 (4)	10 (48)	5 (36)	…
Midwall late gadolinium enhancement mass, g/y	0	1.2 (0.3, 2.4)	4.1 (2.8, 7.2)	0.02
T1 mapping measures				
Extracellular volume fraction, %/y	0 (−1.9, 0.8)	0 (−0.8. 1.7)	0 (0.5, 0.9)	0.61
Total extracellular volume, mL/y	0.7 (0.0, 1.0)	1.5 (−0.2, 6.8)	3.7 (0.4, 6.0)	0.08
Indexed extracellular volume, mL/m^2 per year	0.3 (−0.1, 0.6)	0.8 (−0.1, 2.9)	2.0 (0.2, 2.9)	0.07
Echocardiography				
Peak aortic-jet velocity, m/s per year	0.05 (−0.03, 0.20)	0.16 (−0.04, 0.29)	0.33 (0.16, 0.42)	0.002
Mean aortic valve gradient, mm Hg/y	2 (0, 3)	2 (0, 5)	7 (3, 10)	<0.001
Aortic valve area, cm^2/y	−0.05 (−0.12, −0.02)	−0.03 (−0.07, 0.00)	−0.06 (−0.09, 0.00)	0.47
Indexed stroke volume, mL/m^2 per year	−1 (−2, 1)	0 (−1, 2)	3 (−2, 5)	0.06
Mean systolic blood pressure, mm Hg/y	−2 (−6, 1)	−1 (−7, 3)	−5 (−15, 1)	0.65
Valvuloarterial impedance, mm Hg/mL per m^2 per year	0 (−0.15, 0.28)	0 (−0.15, 0.49)	0.36 (−0.32, 1.19)	0.50
E/A ratio	0 (−0.1, 0.1)	0 (−0.1, 0.2)	0 (−0.2, 0.1)	0.91
Mean e′, cm/s per year	−0.17 (−0.56, 0.18)	−0.04 (−0.73, 0.58)	−0.15 (−0.78, 0.51)	0.82
E/e′ ratio	0.6 (−0.4, 1.2)	−0.1 (−0.9, 1.1)	1.6 (0.9, 2.3)	<0.001

Results expressed as median (IQR). IQR indicates interquartile range; and LV, left ventricle.

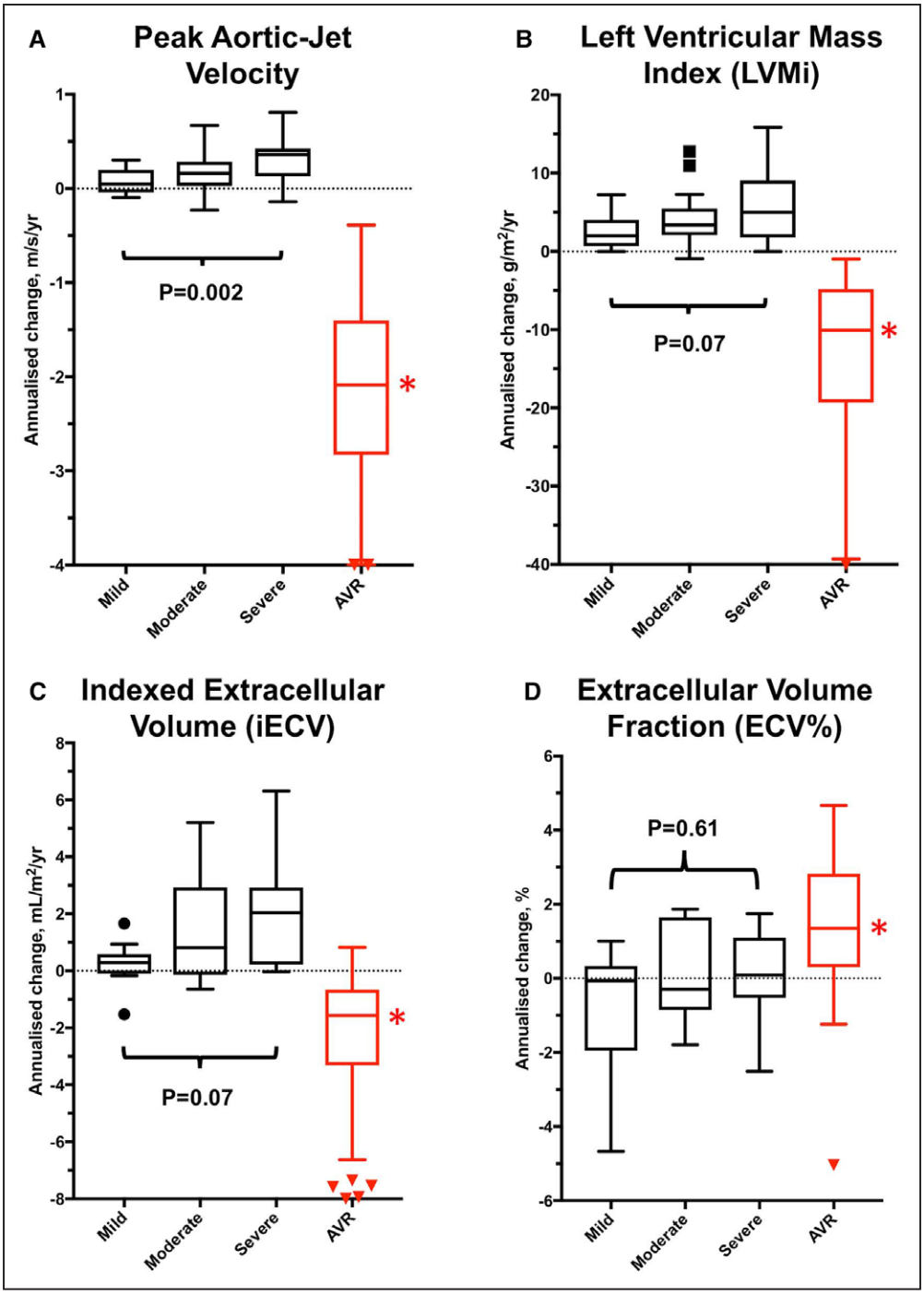

Figure 1. Annualized changes in aortic valve obstruction, left ventricular hypertrophy, and diffuse fibrosis in the natural history and aortic valve replacement (AVR) groups. Annualized progression in peak aortic-jet velocity (**A**), left ventricular mass (**B**), and diffuse fibrosis (indexed extracellular volume [iECV], **C**) increased in a stepwise fashion with severity of aortic stenosis. The slowest progression for each parameter was observed in patients with mild aortic stenosis and the fastest progression in those with severe stenosis. Extracellular volume fraction (ECV%) did not change (**D**), suggesting balanced progression in cellular hypertrophy and interstitial fibrosis. After AVR, there was significant regression in valve obstruction (**A**), left ventricular mass index (LVMi; **B**), and iECV (diffuse fibrosis, **C**). ECV% increased (**D**) suggesting more rapid regression in cellular hypertrophy than interstitial diffuse fibrosis (all $P<0.005$). *Significant ($P<0.005$) annualized change comparing pre- and post-AVR values for each measure.

manner across patients with mild (0.3 mL/m^2 [–0.1 to 0.6 mL/m^2]), moderate (0.8 mL/m^2 [–0.1 to 2.9 mL/m^2]), and severe (2.0 mL/m^2 [0.2–2.9 mL/m^2]) AS (P=0.07; Table 4). Indeed, iECV increased ≈7-fold faster in those with severe versus mild AS (P=0.01; Figure 1). By contrast, no progression in ECV% was observed over time either across the cohort as a whole (0% [–1% to 1%); P=0.80) or within severity subgroups (P=0.61).

Midwall LGE was present at baseline in 16 patients (26%) and progressed rapidly with time (change in LGE mass, 1.6 g/y [0.4–4.1 g/y]; $P<0.0001$; Table 2), equivalent to a relative annual progression of 78% (50%–158%).

Table 5. Univariable and Multivariable Linear Regression Analysis to Examine the Predictors of Annualized Progression and Regression of Left Ventricular Mass Over Time

	Univariable Analysis		Multivariable Analysis	
	Change in Left Ventricular Mass Index, β (95% CI), g/m² per Year	*P* Value	Change in Left Ventricular Mass Index, β (95% CI), g/m² per Year	*P* Value
Natural history group: factors influencing left ventricular mass progression				
Age, y	0.03 (–0.05 to 0.10)	0.50	0.05 (–0.04 to 0.13)	0.30
Men	0.66 (–1.33 to 2.64)	0.51	0.95 (–1.16 to 3.05)	0.37
Hypertension	–1.38 (–3.25 to 0.49)	0.14	–1.75 (–3.95 to 0.44)	0.12
Valvuloarterial impedance	–0.24 (–1.49 to 1.01)	0.70	–0.08 (–1.35 to 1.20)	0.91
Baseline peak aortic-jet velocity, m/s	1.44 (0.26 to 2.63)	0.02	0.67 (–0.73 to 2.07)	0.34
Annualized peak aortic-jet velocity change, m/s per year	7.10 (2.90 to 11.30)	0.001	4.98 (0.53 to 9.91)	0.048
Presence midwall late gadolinium enhancement	0.45 (–1.67 to 2.56)	0.68	–0.17 (–2.28 to 1.95)	0.88
AVR group: factors influencing left ventricular mass regression				
Age, y	0.45 (0.01 to 0.90)	0.047	–0.11 (–0.46 to 0.24)	0.53
Men	–3.0 (–12.1 to 6.1)	0.50	5.23 (–1.10 to 11.55)	0.10
Hypertension	10.4 (3.9 to 16.8)	0.002	5.52 (0.29 to 10.75)	0.04
Valvuloarterial impedance	1.9 (–1.4 to 5.2)	0.26	–0.69 (–3.18 to 1.79)	0.57
Pre-AVR left ventricular mass index, g/m²	–0.37 (–0.49 to –0.25)	<0.001	–0.39 (–0.53 to –0.26)	<0.001
Peak aortic-jet velocity at 1 y post-AVR, m/s	2.2 (–4.3 to 8.8)	0.49	4.33 (–0.27 to 8.93)	0.06
Presence midwall late gadolinium enhancement	–9.3 (–17.5 to –1.1)	0.027	–4.7 (–10.5 to 1.12)	0.11

AVR indicates aortic valve replacement; and CI, confidence interval.

This occurred both at the sites of existing LGE and, in a quarter of patients, at remote sites with the development of new areas of midwall LGE (Figures 2 and 3). Again faster rates of progression were observed in patients with more advanced valve stenosis (*P*=0.02) and greater levels of diffuse fibrosis (*P*=0.019, by tertiles of iECV; Figure 2). Moreover, patients with the most midwall LGE at baseline demonstrated the fastest subsequent progression (tertile 1 baseline LGE, 0.3 g/y [0.1–0.9 g/y]; tertile 2, 1.6 g/y [1.0–3.8 g/y]; and tertile 3, 4.1 g/y [3.4–7.2 g/y]; *P*=0.007; Figure 2). Eight patients (13%) had a subendocardial pattern of LGE at baseline. On repeat MRI, there were no new areas of subendocardial LGE and no change in the subendocardial LGE mass (*P*=0.56; Table 2), consistent with these areas representing previous myocardial infarction.

AVR Cohort (Reverse Remodeling)

Patients underwent AVR for a guideline-based indication 32 days (13–66 days) after baseline imaging with repeat imaging performed 0.9±0.3 years after AVR. Twenty-nine patients received a bioprosthetic AVR, and in 9 patients, a mechanical prosthesis was used. No patient underwent transcatheter valve replacement. As expected, echocardiographic assessments of aortic valve obstruction improved after surgery (change in peak aortic-jet velocity, –2.05 m/s [–2.70 to 1.56 m/s]; change in mean gradient, –32 mm Hg [–44 to –26 mm Hg]; change in aortic valve area, 0.73 cm² [0.46–0.91 cm²]; change in valvuloarterial impedance, –0.60 [–1.19 to 0.08]; all *P*<0.0001; Table 2).

There was a 19% reduction in LVMi (–10 g/m² per year [–19 to –5 g/m² per year]; *P*<0.0001; Table 2) after AVR, accompanied by a corresponding reduction in maximal LV wall thickness (–2 mm/y [–2 to –1 mm/y]; *P*<0.0001). A moderate correlation was observed between the magnitude of LVM regression and the reduction in peak aortic-jet velocity after valve intervention (ρ=0.35; *P*=0.03). On multivariable regression analysis, a high pre-AVR LVMi and the absence of hypertension were both associated with greater LVM regression (Table 5) as was a lower post-AVR V_{max} although this last variable did not reach statistical significance (*P*=0.06).

Measures of LV relaxation and filling pressure improved after AVR (mean e′, 1.35 [0.26–2.91]; *P*=0.0004; E/e′, –1.3 [–4.3 to 1.1]; *P*=0.02), and there was an apparent trend toward improved longitudinal LV systolic function (1 mm/y [–1 to 3 mm/y]; *P*=0.10). No change in ejection fraction was observed (*P*=0.78) although the indexed end-diastolic LV volume did decrease modestly (–3 mL/m² per year [–9 to 2 mL/m² per year]; *P*=0.009).

Myocardial Fibrosis

There was a 11% reduction in iECV on repeat imaging after AVR (–2 mL/m² per year [–3 to –1 mL/m²

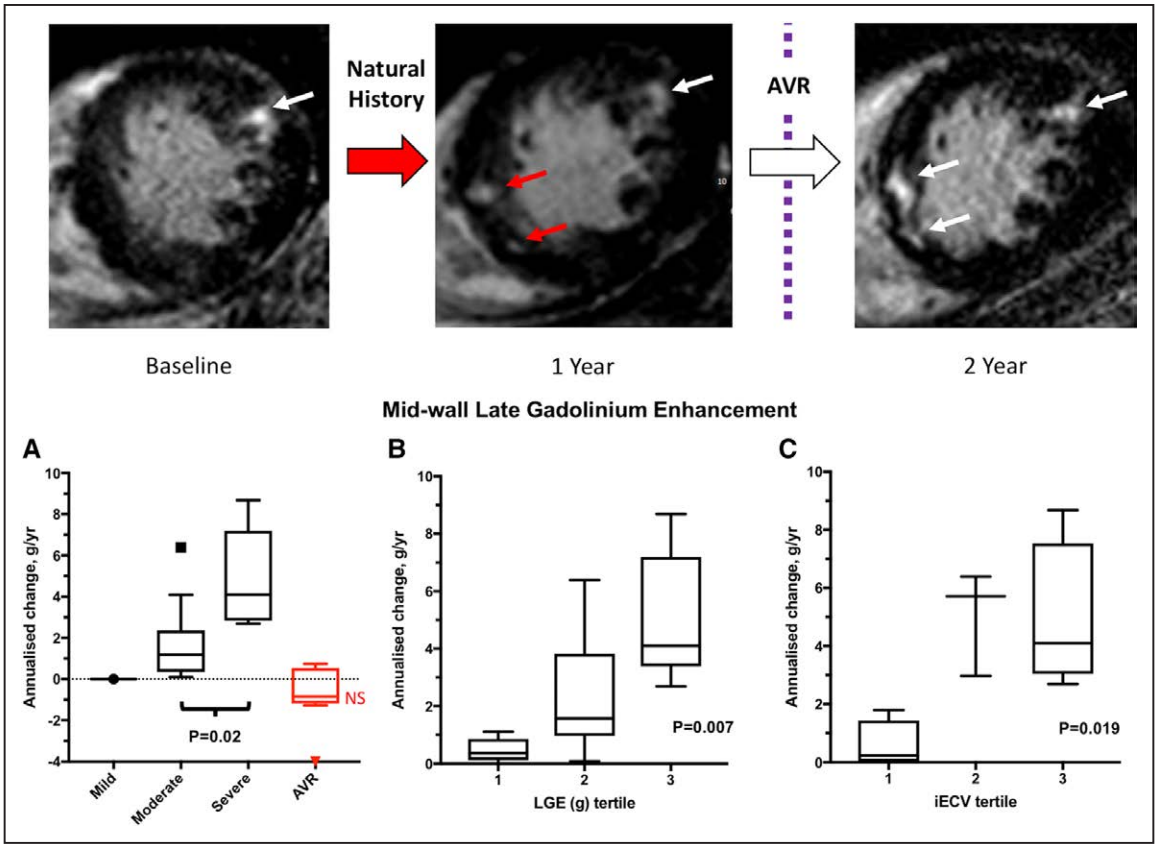

Figure 2. Serial magnetic resonance images in a patient with severe aortic stenosis and progression of replacement fibrosis. **Top** row, Midwall late gadolinium enhancement (LGE) is present baseline magnetic resonance imaging (MRI; white arrow, baseline image). New areas of LGE can be seen on follow-up MRI after 1 y (red arrows). The patient subsequently developed exertional breathlessness and underwent aortic valve replacement (AVR). Repeat imaging 1 y after AVR demonstrated no change in the pattern or volume of LGE. In patients with established midwall LGE, rapid accumulation of further LGE was observed with the fastest progression in those with the most severe aortic stenosis (**A**), the highest baseline burden of LGE (**B**), and the most advanced indexed extracellular volume (iECV; **C**). After AVR, there was no change in LGE burden (**A**). NS indicates no significant annualized change in AVR group compared with baseline values.

per year]; *P*<0.001; Table 2; Figure 1). In contrast, the ECV% increased (1.2% /y [0.4%–2.2% /y]; *P*=0.003; Figure 1) consistent with faster regression of LVM than diffuse fibrosis. The type of replacement valve implanted did not influence the degree of LVM (*P*=0.61) or iECV (*P*=0.97) regression.

On visual assessment, midwall LGE was present in 10 patients (26%) at baseline. No patient went on to develop new areas of LGE on repeat imaging nor did any patient with existing LGE demonstrate resolution of any established areas post-AVR (Figure 3). Quantitatively, there was no significant change in LGE mass after AVR (*P*=0.22; Table 2) even in patients rescanned after 2 years. Infarct pattern LGE was observed at baseline in 5 patients (13%). One new infarct was detected on repeat imaging, but overall no change was observed in LGE mass in these patients (*P*=0.72).

Sensitivity analysis was performed in patients who underwent repeat imaging at the same time interval (2 years in the natural history cohort, n=50; 1 year in the AVR cohort, n=27). Our findings were unchanged from those made across the cohort as a whole (Figure I and Table I in the Data Supplement).

DISCUSSION

This is the first study to characterize how LVH and fibrosis progress in AS and how these processes then reverse remodel after AVR. Using a multicenter multimodality imaging approach with serial echocardiography and MRI, we have demonstrated that both hypertrophy and fibrosis progress in an increasingly rapid manner as AS severity advances. Once midwall patterns of replacement fibrosis (LGE) have become established, further scarring seems to accumulate rapidly. Although LVH and diffuse fibrosis reverse after AVR, midwall LGE does not and seems to be irreversible. Given the adverse prognosis associated with midwall fibrosis burden, our data suggest prompt AVR at the first sign of midwall LGE or just before its development might improve long-term patient outcomes.

In the natural history cohort, we observed a slow and steady progression in each of the echocardiographic measures of valvular stenosis as anticipated.[15] This valve progression was strongly influenced by baseline AS severity, with the slowest progression in patients with mild stenosis and the most rapid progression in

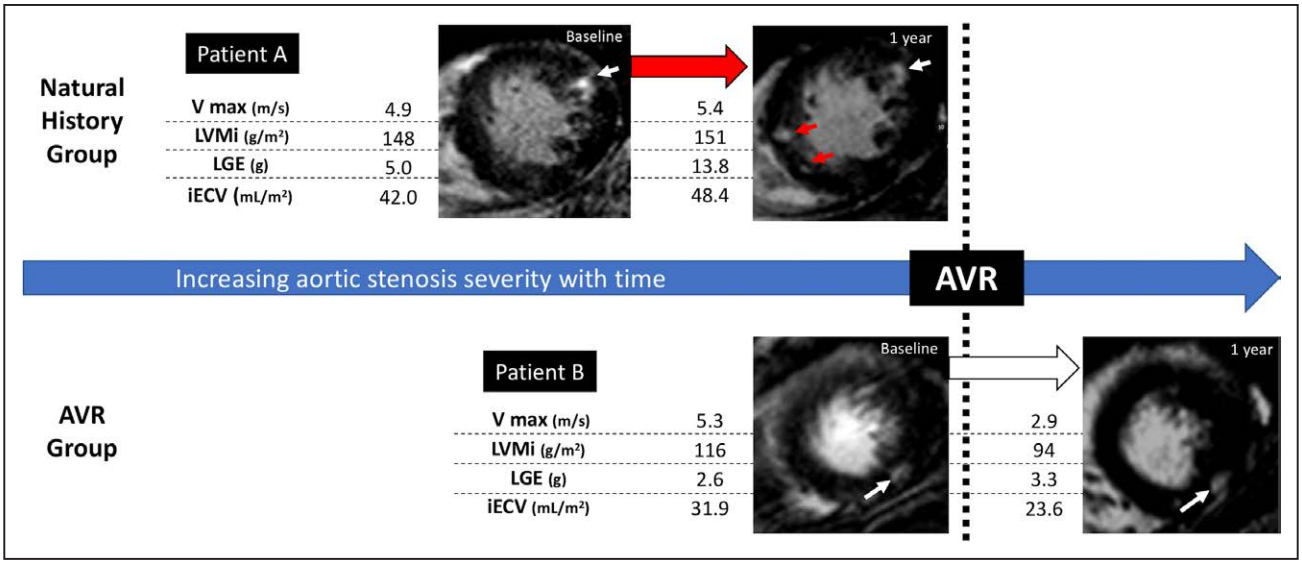

Figure 3. Changes in left ventricular mass (LVM), diffuse fibrosis, and replacement fibrosis in aortic stenosis before and after valve replacement. Longitudinal changes in LVM index (LVMi), diffuse fibrosis (indexed extracellular volume [iECV]), and replacement fibrosis (late gadolinium enhancement [LGE]) before and after valve replacement (AVR) are illustrated with 2 example patients (A and B). All 3 measures increase exponentially as stenosis severity increases (patient **A**, natural history cohort), and new areas of LGE are seen on follow-up imaging (red arrows). However, after AVR, cellular hypertrophy regresses more quickly than diffuse fibrosis, and replacement fibrosis seems unchanged (patient **B**, white arrows). AVR indicates aortic valve replacement; and V_{max}, peak aortic-jet velocity.

those with severe obstruction. This was mirrored by a similar pattern of increasing LVM progression. Indeed, a moderate correlation was observed between valve stenosis progression and LVM progression, with the annualized increase in peak aortic-jet velocity, the only independent predictor of LVM progression on multivariable analysis. Consistent with this, AVR resulted in a substantial reduction in aortic valve obstruction that was accompanied by a ≈20% reduction in the LVM. Again, there was a strong correlation between the reduction in transvalvular gradient and LVM regression, with the former emerging as an independent predictor of reverse remodeling on multivariable analysis. One surprising finding was a small but significant reduction in stroke volume after AVR. This may relate to accompanying reductions in LV end-diastolic volume but requires further study.

What about myocardial fibrosis? MRI is the only noninvasive imaging technique capable of assessing both diffuse interstitial (T1 mapping techniques) and replacement fibrosis (LGE). T1 mapping provides multiple different measurements that demonstrate close agreement with collagen volume fraction on histology and therefore act as surrogates of interstitial myocardial fibrosis.[7,16] We here investigated the ECV% and iECV because of the advantages these measures hold when comparing values acquired in a multicenter setting on different scanners and at different field strengths. Although ECV% gives an indication of the proportion of the myocardium made up of fibrosis, iECV is a surrogate of the total fibrosis burden in the LV. Together these 2 measures can provide unique insights into how the extracellular and intracellular compartments of the myocardium change in AS and in response to AVR. Like peak aortic-jet velocity and LVMi, the iECV increased with time suggesting progressive expansion of the extracellular compartment and diffuse interstitial fibrosis. Once again, this progression appeared to occur quickest in those with the most advanced valvular stenosis. By comparison, ECV% did not demonstrate any evidence of progression, suggesting balanced increases in the size of the cellular and extracellular compartments as LV remodeling advances.

After AVR, reductions in iECV were observed similar to those observed in peak aortic-jet velocity and LVM, confirming that diffuse interstitial fibrosis is indeed reversible. However, the accompanying rise in ECV% suggests that regression in cellular hypertrophy occurs faster and to a greater degree than this reduction in diffuse fibrosis. These novel imaging findings are in keeping with historical data from myocardial biopsies performed after AVR showing an initial increase of percentage interstitial fibrosis on histology at 18 months.[17]

Midwall LGE represents a more advanced stage of focal replacement fibrosis[18] in the myocardium and has been described in numerous AS populations.[4,6,19] Midwall LGE is a marker of LV decompensation demonstrating a close association with myocardial injury, LV diastolic function, LV systolic function, and exercise capacity.[7] Moreover, multiple different studies from multiple centers have confirmed midwall LGE as a powerful prognostic marker of long-term all-cause and cardiovascular mortality.[4–7] Most of these adverse events occur after AVR,[20] and there seems to be a proportionate relationship: the more myocardial LGE, the worse the clinical outcomes.[4,5]

For the first time, we have demonstrated that the burden of midwall LGE increases while asymptomatic patients are being monitored in the clinic. Indeed, once midwall LGE has become established, then further accumulation of such scarring is relatively rapid, increasing on average by 75% each year especially in patients with a high baseline fibrosis burden. Importantly, we go on to demonstrate that although this progressive scarring is arrested by AVR, it does not reverse even out to 2 years after AVR. This is consistent with smaller short-term studies and implies that the scar that patients develop while waiting for surgery remains with them for the rest of their life, contributing to their poorer long-term prognosis. These findings could have important clinical implications for optimizing patient care and the timing of AVR. For example, based on our data, prompt AVR could be undertaken when midwall LGE is first identified to prevent the accumulation of further scarring and to improve long-term patient outcomes. This strategy requires prospective confirmation and is currently being tested in the EVOLVED (Early Valve Replacement guided by Biomarkers of Left Ventricular Decompensation in Asymptomatic Patients with Severe Aortic Stenosis) randomized controlled trial (NCT03094143).

Our study does have some limitations. Given the heterogeneity in the timing of follow-up imaging, we used annualized change for our primary analysis. This assumes linear progression or regression of variables which may not be the case. In the sensitivity analysis, we repeated our analysis of the data using absolute change in the subgroup of patients who underwent repeat imaging after the same time interval (2 years in the natural history cohort [n=50] and 1 year in the AVR cohort [n=27]). Our results were consistent with the annualized analysis. Further studies are still required to investigate how LV remodeling and reverse remodeling progress over multiple time points in individual patients. The ECV measurements (ECV%, iECV) reflect the size of the extracellular compartment and therefore potentially represent multiple different factors, including the intravascular space and myocardial infiltration. However, in patients with AS (and in the absence of associated cardiac amyloidosis), there is a close association between these ECV measurements and histological markers of interstitial fibrosis, confirming that they provide a useful surrogate measure of interstitial fibrosis, as here presented.

CONCLUSIONS

We have used echocardiography and MRI to characterize the structural changes in the myocardium that occur in patients with AS both during routine surveillance and after AVR. In patients with AS, cellular hypertrophy and diffuse interstitial fibrosis increase in a balanced and exponential manner before reversing at different rates after AVR. Once established, midwall replacement fibrosis accumulates rapidly but seems irreversible after AVR. The myocardial scar burden that patients develop while waiting for surgery, therefore, persists into the long term along with prognostic implications that this entails. Prompt valve replacement as soon as midwall fibrosis develops holds promise in improving clinical outcomes in patients with AS.

ARTICLE INFORMATION

Received December 10, 2017; accepted April 23, 2018.

The Data Supplement is available at http://circimaging.ahajournals.org/lookup/suppl/doi:10.1161/CIRCIMAGING.117.007451/-/DC1.

Correspondence

Russell J. Everett, MD, BSc, British Heart Foundation Centre for Cardiovascular Science, Chancellor's Bldg, University of Edinburgh, 49 Little France Crescent, Edinburgh, EH16 4SB, United Kingdom. E-mail Russell.everett@ed.ac.uk

Affiliations

British Heart Foundation Centre for Cardiovascular Science (R.J.E., J.K., M.G., E.J.R.v.B., C.W., S.S., D.E.N., M.R.D.), Edinburgh Imaging Queen's Medical Research Institute Facility (E.J.R.v.B., S.S.), and Edinburgh Clinical Trials Unit, Usher Institute of Population Health Sciences and Informatics (C.T.), University of Edinburgh, United Kingdom. Department of Medicine, Quebec Heart and Lung Institute, Canada (L.T., M.-A.C., R.C., E.L., P.P.). Department of Cardiovascular Science, National Heart Center Singapore (C.W.L.C.). Cardiovascular Magnetic Resonance Unit, Royal Brompton Hospital, London, United Kingdom (V.S.V., S.K.P.). Norwich Medical School, Norfolk and Norwich University Hospital, United Kingdom (V.S.V.). First Department of Cardiology, Poznan University of Medical Sciences, Poland (J.K.). Hospital del Mar Medical Research Institute, Universitat Pompeu Fabra, Barcelona, Spain (M.G.).

Sources of Funding

The work was supported by the British Heart Foundation (CH/09/002/26360 to Dr Newby RE/13/3/30183 to Dr Prasad FS/14/78/31020 to Dr Dweck), the Wellcome Trust (WT103782AIA to Dr Newby), the Sir Jules Thorn Charitable Trust (15/JTA to Dr Dweck), the Québec Heart and Lung Institute Foundation, and Canadian Institutes of Health Research (FDN-143225 and MOP-114997 to Drs Pibarot and Clavel).

Disclosures

None.

REFERENCES

1. Iung B, Baron G, Butchart EG, Delahaye F, Gohlke-Bärwolf C, Levang OW, Tornos P, Vanoverschelde JL, Vermeer F, Boersma E, Ravaud P, Vahanian A. A prospective survey of patients with valvular heart disease in Europe: the Euro Heart Survey on Valvular Heart Disease. *Eur Heart J*. 2003;24:1231–1243.
2. Dweck MR, Boon NA, Newby DE. Calcific aortic stenosis: a disease of the valve and the myocardium. *J Am Coll Cardiol*. 2012;60:1854–1863. doi: 10.1016/j.jacc.2012.02.093.
3. Hein S, Arnon E, Kostin S, Schönburg M, Elsässer A, Polyakova V, Bauer EP, Klövekorn WP, Schaper J. Progression from compensated hypertrophy to failure in the pressure-overloaded human heart: structural deterioration and compensatory mechanisms. *Circulation*. 2003;107:984–991.
4. Dweck MR, Joshi S, Murigu T, Alpendurada F, Jabbour A, Melina G, Banya W, Gulati A, Roussin I, Raza S, Prasad NA, Wage R, Quarto C, Angeloni E, Refice S, Sheppard M, Cook SA, Kilner PJ, Pennell DJ, Newby DE, Mohiaddin RH, Pepper J, Prasad SK. Midwall fibrosis is an independent predictor of mortality in patients with aortic stenosis. *J Am Coll Cardiol*. 2011;58:1271–1279. doi: 10.1016/j.jacc.2011.03.064.

5. Azevedo CF, Nigri M, Higuchi ML, Pomerantzeff PM, Spina GS, Sampaio RO, Tarasoutchi F, Grinberg M, Rochitte CE. Prognostic significance of myocardial fibrosis quantification by histopathology and magnetic resonance imaging in patients with severe aortic valve disease. *J Am Coll Cardiol*. 2010;56:278–287. doi: 10.1016/j.jacc.2009.12.074.
6. Barone-Rochette G, Piérard S, De Meester de Ravenstein C, Seldrum S, Melchior J, Maes F, Pouleur AC, Vancraeynest D, Pasquet A, Vanoverschelde JL, Gerber BL. Prognostic significance of LGE by CMR in aortic stenosis patients undergoing valve replacement. *J Am Coll Cardiol*. 2014;64:144–154. doi: 10.1016/j.jacc.2014.02.612.
7. Chin CWL, Everett RJ, Kwiecinski J, Vesey AT, Yeung E, Esson G, Jenkins W, Koo M, Mirsadraee S, White AC, Japp AG, Prasad SK, Semple S, Newby DE, Dweck MR. Myocardial fibrosis and cardiac decompensation in aortic stenosis. *JACC Cardiovasc Imaging*. 2017;10:1320–1333. doi: 10.1016/j.jcmg.2016.10.007.
8. Vassiliou VS, Perperoglou A, Raphael CE, Joshi S, Malley T, Everett R, Halliday B, Pennell DJ, Dweck MR, Prasad SK. Midwall fibrosis and 5-year outcome in moderate and severe aortic stenosis. *J Am Coll Cardiol*. 2017;69:1755–1756. doi: 10.1016/j.jacc.2017.01.034.
9. Capoulade R, Mahmut A, Tastet L, Arsenault M, Bédard É, Dumesnil JG, Després JP, Larose É, Arsenault BJ, Bossé Y, Mathieu P, Pibarot P. Impact of plasma Lp-PLA2 activity on the progression of aortic stenosis: the PROGRESSA study. *JACC Cardiovasc Imaging*. 2015;8:26–33. doi: 10.1016/j.jcmg.2014.09.016.
10. Messroghli DR, Greiser A, Fröhlich M, Dietz R, Schulz-Menger J. Optimization and validation of a fully-integrated pulse sequence for Modified Look-Locker Inversion-recovery (MOLLI) T1 mapping of the heart. *J Magn Reson Imaging*. 2007;26:1081–1086. doi: 10.1002/jmri.21119.
11. Lee JJ, Liu S, Nacif MS, Ugander M, Han J, Kawel N, Sibley CT, Kellman P, Arai AE, Bluemke DA. Myocardial T1 and extracellular volume fraction mapping at 3 tesla. *J Cardiovasc Magn Reson*. 2011;13:75. doi: 10.1186/1532-429X-13-75.
12. Mikami Y, Kolman L, Joncas SX, Stirrat J, Scholl D, Rajchl M, Lydell CP, Weeks SG, Howarth AG, White JA. Accuracy and reproducibility of semi-automated late gadolinium enhancement quantification techniques in patients with hypertrophic cardiomyopathy. *J Cardiovasc Magn Reson*. 2014;16:85. doi: 10.1186/s12968-014-0085-x.
13. Chin CW, Semple S, Malley T, White AC, Mirsadraee S, Weale PJ, Prasad S, Newby DE, Dweck MR. Optimization and comparison of myocardial T1 techniques at 3T in patients with aortic stenosis. *Eur Heart J Cardiovasc Imaging*. 2014;15:556–565. doi: 10.1093/ehjci/jet245.
14. Treibel TA, Kozor R, Schofield R, Benedetti G, Fontana M, Bhuva AN, Sheikh A, López B, González A, Manisty C, Lloyd G, Kellman P, Díez J, Moon JC. Reverse myocardial remodeling following valve replacement in patients with aortic stenosis. *J Am Coll Cardiol*. 2018;71:860–871. doi: 10.1016/j.jacc.2017.12.035.
15. Otto CM, Burwash IG, Legget ME, Munt BI, Fujioka M, Healy NL, Kraft CD, Miyake-Hull CY, Schwaegler RG. Prospective study of asymptomatic valvular aortic stenosis. Clinical, echocardiographic, and exercise predictors of outcome. *Circulation*. 1997;95:2262–2270.
16. Flett AS, Hayward MP, Ashworth MT, Hansen MS, Taylor AM, Elliott PM, McGregor C, Moon JC. Equilibrium contrast cardiovascular magnetic resonance for the measurement of diffuse myocardial fibrosis: preliminary validation in humans. *Circulation*. 2010;122:138–144. doi: 10.1161/CIRCULATIONAHA.109.930636.
17. Krayenbuehl HP, Hess OM, Monrad ES, Schneider J, Mall G, Turina M. Left ventricular myocardial structure in aortic valve disease before, intermediate, and late after aortic valve replacement. *Circulation*. 1989;79:744–755.
18. Treibel TA, López B, González A, Menacho K, Schofield RS, Ravassa S, Fontana M, White SK, DiSalvo C, Roberts N, Ashworth MT, Díez J, Moon JC. Reappraising myocardial fibrosis in severe aortic stenosis: an invasive and non-invasive study in 133 patients. *Eur Heart J*. 2018;39:699–709. doi: 10.1093/eurheartj/ehx353.
19. Rudolph A, Abdel-Aty H, Bohl S, Boyé P, Zagrosek A, Dietz R, Schulz-Menger J. Noninvasive detection of fibrosis applying contrast-enhanced cardiac magnetic resonance in different forms of left ventricular hypertrophy relation to remodeling. *J Am Coll Cardiol*. 2009;53:284–291. doi: 10.1016/j.jacc.2008.08.064.
20. Quarto C, Dweck MR, Murigu T, Joshi S, Melina G, Angeloni E, Prasad SK, Pepper JR. Late gadolinium enhancement as a potential marker of increased perioperative risk in aortic valve replacement. *Interact Cardiovasc Thorac Surg*. 2012;15:45–50. doi: 10.1093/icvts/ivs098.